



# Espectrometria de masses d'alta resolució i mesura de massa exacta. Caracterització de la matèria orgànica dissolta en masses d'aigua naturals i tractades

Nuria Cortés Francisco

**ADVERTIMENT.** La consulta d'aquesta tesi queda condicionada a l'acceptació de les següents condicions d'ús: La difusió d'aquesta tesi per mitjà del servei TDX ([www.tdx.cat](http://www.tdx.cat)) i a través del Dipòsit Digital de la UB ([diposit.ub.edu](http://diposit.ub.edu)) ha estat autoritzada pels titulars dels drets de propietat intel·lectual únicament per a usos privats emmarcats en activitats d'investigació i docència. No s'autoritza la seva reproducció amb finalitats de lucre ni la seva difusió i posada a disposició des d'un lloc aliè al servei TDX ni al Dipòsit Digital de la UB. No s'autoritza la presentació del seu contingut en una finestra o marc aliè a TDX o al Dipòsit Digital de la UB (framing). Aquesta reserva de drets afecta tant al resum de presentació de la tesi com als seus continguts. En la utilització o cita de parts de la tesi és obligat indicar el nom de la persona autora.

**ADVERTENCIA.** La consulta de esta tesis queda condicionada a la aceptación de las siguientes condiciones de uso: La difusión de esta tesis por medio del servicio TDR ([www.tdx.cat](http://www.tdx.cat)) y a través del Repositorio Digital de la UB ([diposit.ub.edu](http://diposit.ub.edu)) ha sido autorizada por los titulares de los derechos de propiedad intelectual únicamente para usos privados enmarcados en actividades de investigación y docencia. No se autoriza su reproducción con finalidades de lucro ni su difusión y puesta a disposición desde un sitio ajeno al servicio TDR o al Repositorio Digital de la UB. No se autoriza la presentación de su contenido en una ventana o marco ajeno a TDR o al Repositorio Digital de la UB (framing). Esta reserva de derechos afecta tanto al resumen de presentación de la tesis como a sus contenidos. En la utilización o cita de partes de la tesis es obligado indicar el nombre de la persona autora.

**WARNING.** On having consulted this thesis you're accepting the following use conditions: Spreading this thesis by the TDX ([www.tdx.cat](http://www.tdx.cat)) service and by the UB Digital Repository ([diposit.ub.edu](http://diposit.ub.edu)) has been authorized by the titular of the intellectual property rights only for private uses placed in investigation and teaching activities. Reproduction with lucrative aims is not authorized nor its spreading and availability from a site foreign to the TDX service or to the UB Digital Repository. Introducing its content in a window or frame foreign to the TDX service or to the UB Digital Repository is not authorized (framing). Those rights affect to the presentation summary of the thesis as well as to its contents. In the using or citation of parts of the thesis it's obliged to indicate the name of the author.

## **DEPARTAMENT de QUÍMICA ANALÍTICA**

Programa de Doctorat: Química Analítica del Medi Ambient i la Pol·lució

# **Espectrometria de masses d'alta resolució i mesura de massa exacta. Caracterització de la matèria orgànica dissolta en masses d'aigua naturals i tractades.**

Memòria presentada per optar al títol de Doctora  
per la Universitat de Barcelona per

**NURIA CORTÉS FRANCISCO**

**Director de la Tesi:**

**Dr. Josep Caixach Gamisans**  
Investigador Científic i Director del  
Laboratori d' Espectrometria de Masses /  
Contaminants Orgànics del Consell Superior  
d'Investigacions Científiques

**Tutora de la Tesi:**

**Dra. Encarnación Moyano Morcillo**  
Professora Titular del Departament de  
Química Analítica de la Universitat de  
Barcelona

Barcelona, Setembre del 2014



El Dr. Josep Caixach Gamisans, Investigador Científic i Director del Laboratori d'Espectrometria de Masses / Contaminants Orgànics del Consell Superior d'Investigacions Científiques,

FA CONSTAR,

Que la present memòria titulada "Espectrometria de masses d'alta resolució i mesura de massa exacta. Caracterització de la matèria orgànica dissolta en masses d'aigua naturals i tractades", ha estat realitzada sota la meua direcció per la Sra. Nuria Cortés Francisco en el Laboratori d'Espectrometria de Masses / Contaminants Orgànics del Consell Superior d'Investigacions Científiques i que tots els resultats presentats són fruit de les experiències realitzades per la citada doctoranda.

I per a que així es faci constar, expedixo i firmo el present certificat.

Barcelona, Setembre del 2014

Dr. Josep Caixach Gamisans



**Espectrometria de Masses d'Alta Resolució i  
Mesura de Massa Exacta. Caracterització de  
la Matèria Orgànica Dissolta en Masses  
d'Aigua Naturals i Tractades.**

**High Resolution Mass Spectrometry and  
Accurate Mass Measurements.  
Characterization of Dissolved Organic Matter  
in Natural and Affected Water Bodies.**



"...the world is open for play,  
everything and everybody is  
mockable in a wonderful way"

Robin Williams



Als meus pares, a la meva germana i a l'Héctor,  
perquè sense vosaltres res seria possible.



## Agraïments / Acknowledgments

Una de les coses positives que m'emporto dels anys que he estat treballant en la realització d'aquesta tesi són les persones a les que he tingut el plaer de conèixer i redescobrir, per bé i per mal. A molts de vosaltres ja us tenia vistos, però és en els moments en que el teu món gira al voltant de jornades infinites de laboratori i ordinador, quan aprens qui val la pena tenir ben a prop teu. Per això vull agrair a moltíssimes persones (i espero no deixar-me'n cap) l'ajuda, el suport, la confiança i l'estima rebuda durant tots aquests anys.

En primer lloc m'agradaria agrair al meu director de tesi, el Dr. Josep Caixach la confiança dipositada en mi durant tots aquests anys: primer en les pràctiques, després amb el màster i finalment en la realització d'aquesta tesi. Gràcies, perquè m'has donat llibertat d'acció; així és com se n'aprèn i es deixa créixer a les persones.

También quiero agradecer a mi tutora, la Dra. Encarnación Moyano los buenos consejos que me ha dado, su implicación y sus ánimos, especialmente durante la redacción de esta memoria.

I would like to thank Dr. Philippe Schmitt-Kopplin of the Research Unit Analytical Biogeochemistry, Helmholtz Zentrum München and specially Dr. Hertkorn, Dr. Harir, Dra. Lucio, Mrs. Silvia Thaller and Mrs. Eva Holzmann for their help and implication on the work during my stays, as well as all the members of the team for welcoming me to the group.

My special thanks to Norbert: Ich werde nie all die Dinge, die du für mich während meines Aufenthaltes in München getan hast vergessen, und ich beziehe mich dabei nicht nur auf die Forschung, sondern auch im Besonderen auf unsere persönliche Beziehung. München war für 6 Monate wie mein Zuhause und ich werde Euch alle für immer in meinem Herzen behalten.

Part d'aquest treball es va fer en el marc del conveni que el Laboratori mantenia amb Degremont i durant la realització del Projecte Sostaqua. Per això vull agrair la col·laboració, suport econòmic i suport científic a l'empresa Degremont i els grups del Departament d'Enginyeria Química de la Universitat de Barcelona que hi van participar. Molt especialment a la Dra. Sylvie Baig de Degremont i la Dra. Andrea Guastalli de la Universitat de Barcelona.

Al Dr. Santi Esplugas i al seu equip, especialment a la Mireia, perquè sempre ha sigut interessant aprendre del món dels tractaments avançats de la seva mà i compartir amb ells els nostres coneixements.

Al Dr. Miquel Rovira, al Dr. Xavier Martinez-Lladó i a la Dra. Gemma Ribera del Centre Tecnològic de Manresa per la seva fantàstica col·laboració en diverses etapes d'aquesta tesi. Ha sigut un plaer treballar amb vosaltres i ho vull agrair molt especialment a la Gemma, que s'ha bolcat en la correcció d'alguns dels treballs d'aquesta tesi, com si fos la seva pròpia.

A tota la gent de la Universitat, del CSIC, del Parc, dels Serveis i d'altres empreses que en un moment o altre m'han ajudat a fer funcionar l'ATR, a aconseguir rebliments per SPE, a fer funcionar alguns masses, a calibrar equips, a fer comandes, a aconseguir mostres, a trobar "papers", a mostrejar, a enviar paquets...Penso en el Dr. Alluè, la Dra. Jauregui, el Sr. Jordi Martín, la Dra. Fernández i molts i molts altres. Gràcies!

A l' Arantxa, a la Stefania, a la Montse, a l'Óscar, al Julià, a la Cintia, a la Núria, a la Maria, al Carles, al Dani, a la Mar, a la Bárbara, a la Mónica, al Dr. Josep Rivera, a la Laura, al Joan, al Karell, al Jordi Sauló, al Miquel Angel, a la Gene, al Jordi Parera, a l'Esteban i a la Manoli. Tots heu tingut sempre una paraula amable amb mi i m'heu fet més agradables aquests anys al Laboratori. Molt especialment ho vull agrair:

A Oscar y su buen humor, pase lo que pase: nadie ameniza la hora de comer como tú y tus quesos. Al Julià, gràcies per les teves crítiques "des-constructives" i els teus bons consells. A la Cintia, per "liar-me" a quedar-me al Laboratori i per la seva ambició contagiosa. A la Núria, perquè sempre sempre has estat disposada a ajudar-me. A la Mar i al Dani, perquè va ser divertit tenir-vos per aquí i us he trobat a faltar. A la Laura, perquè ets l'alegria i l'optimisme en persona.

A la Montse, perquè t'agrada cuidar-me i a mi m'agrada que em cuidis. Gràcies perquè sempre has intentat ajudar-me amb el que podies i m'has posat en un "pedestal". Et trobaré a faltar.

A l'Arantxu, perquè sempre has confiat en mi més que jo mateixa. Perquè m'has ajudat, m'has animat i m'has esbronat quan m'ha calgut; i això és el que fa una bona amiga. Moltes gràcies per tot.

A Stefania: que suerte que hemos tenido de que se hayan cruzado nuestros caminos! Trabajar contigo es siempre un placer y un reto. Que nada ni nadie te quite esta energía, pasión, dedicación, perseverancia y talento que tienes. Me he intentado impregnar durante estos años de un poquito de todo eso. Gracias por compartirlo conmigo.

Liebe Silke und Marianna. You "chicas" are the most amazing people I had the pleasure to meet in München. You made me feel home and I hope we will keep in touch. Ihr seid alle jederzeit herzlich bei mir in Barcelona willkommen und ich würde mich sehr freuen, wenn ihr mich besuchen würdet. Grazie mille!

A Porlados, porque todos hemos sufrido en nuestras carnes lo que es hacer la tesis, por propia experiencia o por los que teníamos al lado. Porque podamos compartir muchas más cosas, aunque si pueden ser más viajes, más fiestas y más bodas, pues mejor!

A Joaquín, porque sin pedirlo mi hermana y yo hemos tenido un hermano mayor, que siempre ha presumido de nosotras de una manera que hasta nos hace sonrojar. Eres la fiesta!

A la Marta "d'Igualada", perquè passen els anys, i tot hi el dia a dia i la distància, seguim fent l'esforç de cuidar l'una de l'altra. Ets molt especial per mi. Gràcies.

A les Nenes. Perquè ja fa tant que ens coneixem que hi penso i no recordo l'escola, les tardes de divendres, les festes...sense vosaltres. Gràcies, perquè m'heu mirat emocionades quan us explicava que m'havien acceptat el meu primer article (i el segon i el tercer) com si fos alguna cosa excepcional; i us heu ofert més d'una i de dues vegades a ajudar-me. Heu superat les meves expectatives i espero haver estat a l'alçada. Perquè no tots els amics, s'ofereixen a corregir l'anglès o dissenyar la portada d'aquesta tesi en plena Diada. M'ha fet molta il·lusió perquè volia fer-vos partícips també d'aquesta part de la meva vida. Gràcies Julz, Anni i Geminis.

I finalment i molt especialment ho vull agrair:

A Marisa, Manolo, Iván, Mónica y mi sobri que está a punto de nacer!! Porque me hacéis sentir como en casa. Gracias.

A mis tíos, tías, primos y primas porque somos pocos pero más o menos bien avenidos...y sino siempre estamos a tiempo de montar una cena en el chiringuito, una fiesta sorpresa (o dos o tres), un viaje a München, una comida en el Montmar, una partida de pádel, un SingStar o un paseo en tractor amarillo.

Muy muy especialmente a mi tía Chus y mi tío Alberto. Ya veis, vuestra Rubia de Verano ya es doctora! Teneros lejos, me hacer tener más ganas de veros para poder celebrar este momento juntos...como cuando colgabais las notas del cole en la nevera. Gracias por quererme tanto. Yo también os quiero mucho.

Al meu pare i a la meva mare. Perquè per la Meritxell i per mi sempre heu estat i sou un exemple a seguir. Perquè us heu sacrificat per nosaltres molt més del que s'espera de qualsevol pare o mare i ho heu fet sense demanar res a canvi. Som conscients de la sort que hem tingut de tenir la nostra petita família tan unida i no hi ha manera humana de demostrar-vos quant us estimem. Però ho intentem i cada dia volem donar-vos les gràcies amb petits gestos, com aquesta tesi que és per vosaltres i gràcies a vosaltres. Us estimo molt, sou la meva vida.

A la meva germana gran Meritxell, la meva inspiració. Perquè no en va, mentre estava escrivint aquesta tesi he tingut sempre i en tot moment la teva tesi com a referència. Perquè no sé que menjar primer si les olives o les patates. Sempre m'has obert camí i has fet que tot fos més natural i menys transcendental. T'estimo moltíssim.

I finalment a l'Héctor, que no només ha patit de ben a prop la redacció d'aquesta memòria, sinó que ha confiat en mi i m'ha animat, fins i tot a contracor, a seguir treballant, a marxar fóra, a escriure els articles...Que ha contribuït activament fins hi tot amb hores de feina durant els caps de setmana i festius a la realització d'aquesta tesi. Perquè saps que ho estàs fent bé, quan una de les persones a les qui més estimes, queda bocabadat en escoltar-te exposant la teva feina en una conferència a milers de quilòmetres de casa. I això t'anima a seguir i ha pensar que casi tots els sacrificis han valgut la pena. Te quiero mucho amore. Gracias por todo.



# Table of Contents

Acronyms.....	xix
Objectives and Organization of the Thesis .....	xxiii
<b>1. Introduction .....</b>	<b>1</b>
1.1. Natural Organic Matter .....	3
1.2. Methods of Analysis of Dissolved Organic Matter .....	6
<b>2. High Resolution Mass Spectrometry and Accurate Mass Measurements....</b>	<b>13</b>
2.1. Introduction .....	15
2.2. Experimental Procedure and Results .....	19
2.2.1. <b>Book Chapter</b> .....	21
High Resolution Mass Spectrometric Techniques for Structural Characterization and Determination of Organic Pollutants in the Environment. Chapter 6 in <i>Chromatographic Analysis of the Environment: Spectrometry Based Approaches, 4<sup>th</sup> Edition</i> .	
2.2.2. <b>Research Article N° 1</b> .....	75
Accurate Mass Measurements and Ultrahigh-Resolution: Evaluation of Different Mass Spectrometers for Daily Routine Analysis of Small Molecules in Negative Electrospray Ionization Mode. <i>Analytical and Bioanalytical Chemistry</i> <b>2011</b> , 400, (10), 3595-3606.	
2.3. Discussion.....	89
<b>3. Analysis of Dissolved Organic Matter by High Resolution Mass Spectrometry .....</b>	<b>93</b>
3.1. Introduction .....	95

3.1.1. Dissolved Organic Matter Isolation of Water Bodies .....	95
3.1.2. High Resolution Mass Spectrometry.....	96
3.1.3. Formula Determination, Data Analysis and Representation.....	104
3.1.4. Structural Characterization.....	106
3.2. Experimental Procedure and Results.....	107
3.2.1. <b>Direct Analysis of Dissolved Organic Matter</b> .....	108
3.2.1.1. Isolation of Dissolved Organic Matter.....	108
3.2.1.2. Sample Introduction and Ion Source .....	112
3.2.1.3. Performance of Fourier Transform Mass Analyzers .....	114
3.2.2. <b>Research Article N° 2</b> .....	125
Structural Characterization of Marine Dissolved Organic Matter. Fragmentation Studies. <i>Analytical and Bioanalytical Chemistry, (submitted).</i>	
3.3. Discussion .....	141
<b>4. Dissolved Organic Matter Characterization through Water Treatment Plants .....</b>	<b>145</b>
4.1. Introduction.....	147
4.1.1. Drinking Water Treatment Plants .....	148
4.1.2. Desalination .....	150
4.1.3. Relevance of Dissolved Organic Matter for Drinking Water Supply .....	151
4.1.4. Membrane Technology .....	152
4.1.5. Membrane Fouling .....	154
4.2. Experimental Procedure and Results.....	156
4.2.1. <b>Research Article N° 3</b> .....	159

Molecular Characterization of Dissolved Organic Matter through a Desalination Process by High Resolution Mass Spectrometry. <i>Environmental Science &amp; Technology</i> <b>2013</b> , 47, (17), 9619-9627.	
<b>4.2.2. Research Article N° 4</b> .....	171
High-field FT-ICR Mass Spectrometry and NMR Spectroscopy to Characterize DOM Removal through a Nanofiltration Pilot Plant. <i>Water Research</i> <b>2014</b> , DOI: 10.1016/j.watres.2014.08.046.	
<b>4.2.3. Research Article N° 5</b> .....	203
Molecular Characterization of DOM causing Fouling to NF Membranes by High-field FT-ICR Mass Spectrometry and NMR Spectroscopy. <i>Environmental Science &amp; Technology</i> , (submitted).	
<b>4.3. Discussion</b> .....	229
<b>5. Conclusions</b> .....	<b>235</b>
<b>References</b> .....	<b>239</b>
<b>Appendix A.</b> Supporting Information <b>Research Article N° 3</b> .....	255
<b>Appendix B.</b> Supporting Information <b>Research Article N° 4</b> .....	265
<b>Appendix C.</b> Supporting Information <b>Research Article N° 5</b> .....	293
<b>Appendix D.</b> Summary in Catalan - Resum en Català.....	321



# Acronyms

<b>AGC</b>	Automatic gain control
<b>AM</b>	Accurate mass
<b>APCI</b>	Atmospheric pressure chemical ionization
<b>API</b>	Atmospheric pressure ionization
<b>APPI</b>	Atmospheric pressure photo ionization
<b>BAC</b>	Biologically activated carbon
<b>C18</b>	Octadecil sílica
<b>CDOM</b>	Chromophoric dissolved organic matter
<b>CE</b>	Capillary electrophoresis
<b>DBE</b>	Double bond equivalents
<b>DBE/C</b>	Ratio between double bond equivalents and number of carbons
<b>DBE-O</b>	Double bond equivalents minus number of oxygens
<b>DBPs</b>	Disinfection by products
<b>DIE</b>	Direct infusion electrospray
<b>DOC</b>	Dissolved organic carbon
<b>DOM</b>	Dissolved organic matter
<b>DWTP</b>	Drinking water treatment plant
<b>ESI</b>	Electrospray ionization
<b>ESI-HRMS</b>	Electrospray ionization-high resolution mass spectrometry
<b>FA</b>	Fulvic acids
<b>FIA</b>	Flow injection electrospray
<b>FIE</b>	Flow injection analysis
<b>FT</b>	Fourier transform
<b>FT-ICR</b>	Fourier transform ion cyclotron resonance
<b>FWHM</b>	Full width at half maximum
<b>GAC</b>	Granulated activated carbon
<b>GC</b>	Gas chromatography
<b>GC-HRMS</b>	Gas chromatography-high resolution mass spectrometry
<b>GC-MS/MS</b>	Gas chromatography-tandem mass spectrometry
<b>HA</b>	Humic acids
<b>HCA</b>	Hierarchal cluster analysis
<b>HCD</b>	High collision dissociation
<b>HR</b>	High resolution

<b>HRMS</b>	High resolution mass spectrometry
<b>HRMS/MS</b>	High resolution tandem mass spectrometry
<b>ICR</b>	Ion cyclotron resonance
<b>IHSS</b>	International humic substance society
<b>IT</b>	Ion trap
<b>KMD</b>	Kendrik mass deffect
<b>LAS</b>	Linear alkylbenzene sulfonate
<b>LC</b>	Liquid chromatography
<b>LC-HRMS</b>	Liquid chromatography-high resolution mass spectrometry
<b>LIT</b>	Linear ion trap
<b>LLE</b>	Liquid-liquid extraction
<b>MF</b>	Microfiltration
<b>MS</b>	Mass spectrometry
<b>MS/MS</b>	Tandem mass spectrometry
<b>NF</b>	Nanofiltration
<b>NMR</b>	Nuclear magnetic resonance
<b>NOM</b>	Natural organic matter
<b>NPOC</b>	Non-purgable organic carbon
<b>PPL</b>	Styrene-divinylbenzene polymer
<b>Q</b>	Quadrupole
<b>QqQ</b>	Triple quadrupole
<b>Q-TOF</b>	Quadrupole -Time of flight
<b>RDBE</b>	Ring plus double bond equivalent
<b>RO</b>	Reverse osmosis
<b>SD</b>	Standard deviation
<b>SDI</b>	Silt density index
<b>SEC</b>	Size exclusion chromatography
<b>SIM</b>	Selected ion monitoring
<b>SPE</b>	Solid phase extraction
<b>SRFA</b>	Suwannee river fulvic acids
<b>SUVA</b>	Specific ultraviolet-visible spectroscopy absorbance
<b>THM</b>	Trihalomethanes
<b>TIC</b>	Total inorganic carbon
<b>TN</b>	Total nitrogen
<b>TOC</b>	Total organic carbon
<b>TOF</b>	Time of flight

<b>TOX</b>	Total organic halogen
<b>UF</b>	Ultrafiltration
<b>UF-NF</b>	Ultrafiltration-nanofiltration
<b>UV</b>	Ultraviolet–visible spectroscopy



# Objectives and Organization of the Thesis

This thesis mainly focuses on the use of high resolution mass spectrometry (HRMS) for the characterization of dissolved organic matter (DOM) in natural and affected environments. HRMS is one of the techniques that has given more information about DOM, providing information about the molecular formula of the organic compounds in these complex mixtures.

The specific objectives raised in this thesis are:

- To investigate the advantages of HRMS for the identification and characterization of compounds in the environment. The study is conducted to assess how different parameters can affect the final formula assignment, with special attention to mass accuracy and resolution. The final aim is to design a procedure for the characterization of unknown compounds in complex samples.
- To evaluate the performance of different mass analyzers: triple quadrupole (QqQ), time of flight (TOF), Fourier transform ion cyclotron (FT-ICR) and FT-orbitrap when acquiring high resolution (HR) data. New technologies and great advances have been developed in the recent years and the capabilities of these mass analyzers should be evaluated with regard to: calibration protocols, mass accuracy, resolution, sensitivity and spectral accuracy.
- To apply HRMS to characterize aquatic DOM in both natural and affected environments. The main interest is to evaluate DOM changes at molecular level through different water treatment plants to describe which effects each treatment step has on DOM, with special focus on advanced treatments based on membrane technology.

The present thesis is organized as follows:

- Chapter 1 consists of a brief description of natural organic matter (NOM). It includes the state-of-the-art of the different analytical techniques used so far for the analysis of DOM with special focus on HRMS and the significance of DOM in water treatment plants.

- Chapter 2 starts with a discussion of some parameters influencing accurate mass (AM) measurements and the identification of organic compounds when using HRMS. Some environmental applications are discussed. The results are included in a book chapter entitled "*High Resolution Mass Spectrometric Techniques for Structural Characterization and Determination of Organic Pollutants in the Environment*" included in the book "*Chromatographic Analysis of the Environment: Spectrometry Based Approaches*" and in a research article entitled "*Accurate Mass Measurements and Ultrahigh-Resolution: Evaluation of Different Mass Spectrometers for Daily Routine Analysis of Small Molecules in Negative Electrospray Ionization Mode*" published in *Analytical and Bioanalytical Chemistry* **2011**, 400, (10), 3595-3606.
  
- In Chapter 3, the methodology used for the characterization of DOM is described. New approaches have been developed based on FT-orbitrap mass analyzer in comparison to FT-ICR and some limitations of the main techniques (i.e. DOM isolation, data processing, structural information) have been discussed. In addition, the structural characterization of marine DOM has been studied using high resolution tandem mass spectrometry (HRMS/MS) and it is included in the research article "*Structural Characterization of Marine Dissolved Organic Matter. Fragmentation Studies*" submitted to *Analytical and Bioanalytical Chemistry*.
  
- A new application of DOM characterization when using HR spectrometric techniques is presented in chapter 4: Dissolved Organic Matter Characterization through Water Treatment Plants. The results are included in three research articles: "*Molecular Characterization of Dissolved Organic Matter through a Desalination Process by High Resolution Mass Spectrometry*" published in *Environmental Science & Technology* **2013**, 47, (17), 9619-9627; "*High-field FT-ICR Mass Spectrometry and NMR Spectroscopy to Characterize DOM Removal through a Nanofiltration Pilot Plant*" published in *Water Research* **2014**, DOI: 10.1016/j.watres.2014.08.046 and "*Molecular Characterization of DOM causing Fouling to NF Membranes by High-field FT-ICR Mass Spectrometry and NMR Spectroscopy*" submitted to *Environmental Science & Technology*.
  
- Finally, Chapter 5 briefly summarizes the main conclusions drawn in this research.

This thesis has been developed in the Mass Spectrometry Laboratory / Organic Pollutants in the Institute of Environmental Assessment and Water Research of the Spanish Council for Scientific Research under the supervision of Dr. Josep Caixach. Dra. Encarnación Moyano from the University of Barcelona has also supervised the arrangement and content of the present thesis. Part of this thesis was carried out in the Research Unit Analytical Biogeochemistry (BGC), Helmholtz Zentrum München, Deutsches Forschungszentrum für Gesundheit und Umwelt (GmbH) under the supervision of Dr. Norbert Hertkorn and Dr. Philippe Schmitt-Kopplin, during two research stays of three months each.



# **Chapter 1.**

## **Introduction**

---



## 1.1. Natural Organic Matter

All living matter in the environment eventually dies and decomposes into what is known as natural organic matter (NOM). NOM is a complex mixture of organic compounds, formed from a variety of sources that has been degraded (chemically or biologically) and it is composed mainly of carbon, hydrogen, oxygen, nitrogen, sulfur and phosphorus (Nebbioso et al., 2013; Sleighter et al., 2011). This definition is so wide that with the effort to define NOM in a more concise way, it has been said to comprehend what is called: non-humic (i.e. lipids, proteins, carbohydrates) and humic substances. Another way to define NOM is by means of three operationally defined fractions termed: fulvic acids (FA), humic acids (HA) and humin. This classification is based on solubility: HA are the fraction of humic substances that are insoluble in water at pH 1, FA are the fraction soluble at all pH conditions and humin is insoluble under all pH conditions (Tremblay 2006).

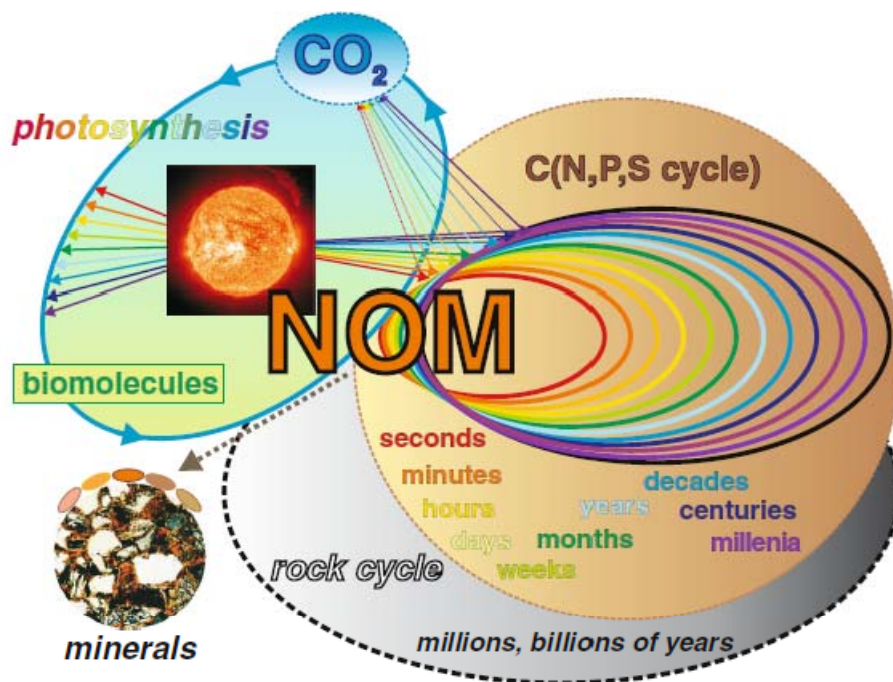


**Figure 1.1.** Representation of the reactivity and interaction of NOM with the environment (Hertkorn et al., 2007).

NOM has a very important role in many environmental processes as it is present in all natural waters, soils, sediments and air. The reactivity and interaction of NOM with terrestrial, limnic and marine ecosystems is continuous, but not fully understood. The

dynamic equilibrium of NOM generation and decomposition spans timescales of many different orders of magnitude (from microseconds to hundreds of thousands of years), and it results from a combined action of biotic and abiotic reactions. For instance, photochemical degradation is one of the most significant abiotic reactions of NOM, often results in small molecules like CO<sub>2</sub>, which are mobile and are easily distributed within various ecosystems (Hertkorn et al., 2007) (Figure 1.1).

Dissolved organic matter (DOM) is usually defined as the aquatic NOM (Mopper et al., 2007, Perdue et al., 2003). Some authors have also operationally defined DOM as the portion of NOM that can go through a 0.45 µm filter (Nebbioso et al., 2013), although in several other studies reporting DOM characterization the filtration step is carried out through filters of 0.1 µm to 0.7 µm (Sleighter et al., 2008; Koch et al., 2005; Schmidt et al., 2009). This discrimination is not so clear and for this reason many researchers use these terms interchangeably. In any case, DOM cannot be correctly regarded as a chemical solution, it is rather a very fine colloidal suspension (Mopper et al., 2007). It has been reported that DOM in the aquatic media is only formed by FA and HA (<http://www.humicsubstances.org/>), but as said before, this definition is based on an operational procedure and we prefer to use the term DOM along the present thesis.

The molecular composition, molecular weight and structural composition of DOM is still under investigation. As it is a natural complex mixture, no synthetic standards are available and as far as we know, the International Humic Substance Society (IHSS) is the only organization providing standards and reference materials of FA, HA or NOM from the aquatic media (and other environments). This scientific organization fractionates DOM following different isolation procedures (i.e., XAD resins, reverse osmosis-RO). The procedures used by the IHSS to isolate standard and reference HA and FA are simply the methods chosen by a working group of scientists in 1981. On the basis of information that was available at that time, these methods were considered as being most suitable for the specific purpose of establishing a collection of standard and reference samples from the selected bulk source materials. IHSS does not endorse or recommend these methods as the best methods for extracting DOM. However, these standards are very well characterized, as they have been used in several studies and are very useful for comparison. The elemental composition of some standards are included in Table 1.1. as an example.

**Table 1.1.** Elemental analysis of humic acids and fulvic acids standards and natural organic matter reference material from International Humic Substance Society (adapted from <http://www.humicsubstances.org/>).

Standard	C	H	O	N	S	P	Total	H <sub>2</sub> O	Ash
HA Suwannee River II, 2S101H	52.63	4.28	42.04	1.17	0.54	0.013	100.6		1.04
FA Suwannee River, 1S101F	52.44	4.31	42.20	0.72	0.44	<0.01	100.1	8.8	0.46
NOM Suwannee River, 1R101N	48.8	3.9	39.7	1.02	0.6	0.02	101	8.15	7.0

DOM in the aquatic media (e.g. oceans, rivers, groundwater) represents one of the largest active carbon reservoirs (represents 50-75 % of the dissolved organic carbon (DOC) in waters) and the amount of DOC in the oceans is comparable to the amount of CO<sub>2</sub> in the atmosphere (see Table 1.2.) (Hertkorn et al., 2002; Nebbioso et al., 2013).

**Table 1.2.** Concentration of organic carbon in freshwaters and marine waters (Perdue et al., 2003; Hertkorn et al., 2013; Koch et al., 2005).

Water Type	µmol C /L
Groundwater	60
River	580
Marsh	1420
Bog	2750
Ocean	64
Mangrove pore water	2760
Sea	62

DOM is not toxic by definition, however the presence of DOM in water can influence the solubility and fate of anthropogenic pollutants in the aquatic media. For instance, DOM can significantly affect the drinking water quality in terms of taste, color and odor, transportation of organic pollutants and water treatment process (Murphy et al., 1990; Frimmel et al., 1996; Kaiya et al., 1996; Camper, 2004; Eikebrokk et al., 2004). DOM has been reported as disturbing the good performance of the water treatments and it is said to be a precursor of disinfection by products (DBPs) formation. For these reasons, knowledge of DOM is of importance in drinking water treatment process operations. Further implications and consequences of DOM are discussed more in depth in 4.1. *Introduction* from Chapter 4.

## 1.2. Methods of Analysis of Dissolved Organic Matter

Different techniques have been used for the analysis of DOM and in fact, several techniques combined together are often necessary to solve a particular problem, due to the complexity of DOM.

In general, the concentration of DOM in aquatic media is very low and powerful techniques with high sensitivity are necessary (Stenson et al., 2003). In the table below (Table 1.3), there is a summary of the main analytical techniques used so far for the characterization of DOM. For each technique the information that can be obtained and the most outstanding findings have been summarized and cited. We can differentiate between techniques: i) to measure bulk parameters: aromaticity, % of elemental composition; ii) to obtain molecular information: molecular mass distribution and identification of individual compounds and iii) to obtain structural information: functional groups and chemical environments.

Different separation techniques: liquid chromatography (LC), gas chromatography (GC), size exclusion chromatography (SEC), capillary electrophoresis (CE) as well as thermal degradation techniques (i.e. pyrolysis), have also been used coupled to different detectors (i.e. flame ionization detection, photodiode array detection, organic carbon detection) or different mass analyzers, such as triple quadrupole (QqQ), quadrupole-time of flight (Q-TOF) or Fourier transform ion cyclotron resonance (FT-ICR) (Allpike et al., 2005; van Heemst et al., 1999; Mawhinney et al., 2009). For instance, SEC has been coupled to organic carbon detector or ultraviolet–visible spectroscopy (UV) to study the molecular weight of DOM. However, depending on the detector used, different molecular weight distributions have been found. The main problem of this separation technique is that there are no representative standards to calibrate the column (Reemtsma et al., 2001). Moreover, when coupled to FT-ICR, resolution in the mass analyzer has to be below 100,000 to gain sufficient sensitivity and so peaks in the spectra are not completely resolved (Reemtsma et al., 2008).

Some of these techniques can be directly used without the necessity of any pre-concentration or isolation of DOM, such as UV or fluorescence. However, depending on the salinity of the water and / or the concentration of DOM, some modifications of the standard methods should be carried out. For instance, for UV a *cuvette* of 10 cm instead of 1 cm might be used to obtain lower detection limits (i.e. when measuring UV for marine DOM) or in the case of Fourier transform-infrared spectroscopy, an additional sampling technique named attenuated total reflection can be used to measure liquid

samples directly. Generally speaking, for the methods based on nuclear magnetic resonance (NMR) and mass spectrometry (MS) an extraction step prior to instrumental analysis is necessary. The method more widely used nowadays is based on solid phase extraction (SPE) with different sorbents. Further information about isolation procedures is included in 3.1.1. *Dissolved Organic Matter Isolation of Water Bodies* in the introduction section of Chapter 3.

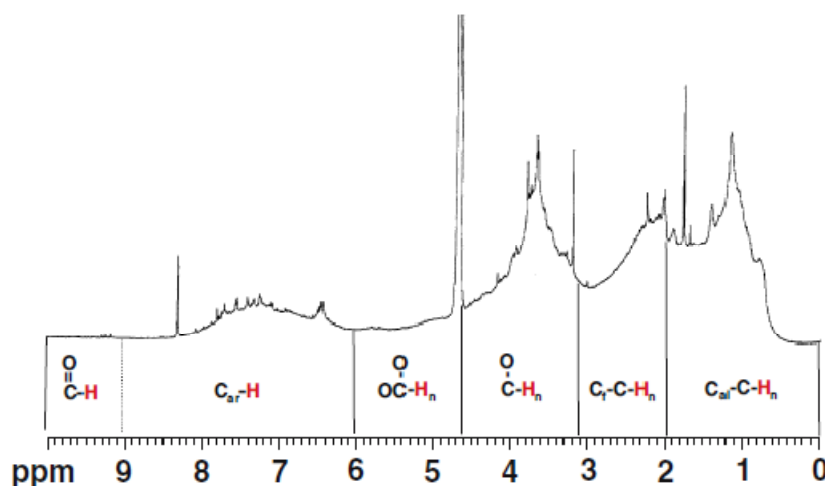


**Figure 1.2.** 500 MHz  $^1\text{H}$  NMR spectrum of a complex sample (terrestrial organic matter) showing the overlap of the individual NMR resonances and showing the integral areas of each key substructures (adapted from Hertkorn et al., 2007).

Regarding structural information, NMR is undoubtedly the most widely used technique for structural characterization of molecules (Mopper et al., 2007). For DOM samples, when one-dimensional  $^1\text{H}$  NMR or  $^{13}\text{C}$  NMR is applied, a spectra with broad and unresolved peaks is obtained, due to the vast diversity of major functional groups present in DOM. However, the areas under the peaks corresponding to the various chemical shift ranges are integrated to obtain estimates of the relative contributions made by the corresponding functional group to the entire spectrum (see Figure 1.2). To date, the  $^1\text{H}$  NMR has been the most acquired spectra for liquid state NMR studies of DOM. This technique has received some criticism, due to lack of sensitivity. For this reason and similar to other techniques (i.e. MS), a pre-concentration or isolation step is necessary, although substantial improvements in the NMR signal-to-noise ratio and sensitivity have been achieved by the modern high-field instrumentation (i.e., 500 and 800 MHz). An alternative to one-dimensional overlapping chemical shifts spectra are the two-dimensional liquid-state NMR studies (Hertkorn et al., 2007).

**Table 1.3.** The main analytical techniques used for the characterization of DOM. For each technique the information that can be obtained and the most outstanding findings have been summarized.

Analytical Technique	Information obtained	Outstanding findings	References <sup>a</sup>
Elemental Analysis	Elemental composition	Different composition from FA and HA.	Sparks et al., 1995
Ultraviolet–Visible Spectroscopy	Aromaticity	Study of degradation processes of NOM. Chromophoric DOM (CDOM).	Amery et al., 2008 Jaffé et al., 2008 Tipping et al., 2009
Fluorescence	Aromaticity	Condensed aromatic rings. Unsaturated aliphatic chains. Minor components of NOM.	Hudson et al., 2007
Excitation-Emission Matrix Fluorescence	Aromaticity	Distinguish between protein-, humic- and fulvic- like CDOM. Optical properties of DOM.	Boheme et al., 2006 Burdige et al., 2004 Herzprung et al., 2012
Fourier Transform - Infrared Spectroscopy	Functional groups	Presence of aromatic, aliphatic and carboxylic groups.	Tanaka et al., 2001
Nuclear Magnetic Resonance (NMR)	Functional groups	NOM molecules are composed of partially degraded plant component. Fulvic acids are different from humic acids. Phenolic carbons are not the major components of humics.	Blondeau 1986 Wershaw et al., 1990 Hertkorn et al., 2006 Lam et al., 2007 Hertkorn et al., 2013
2D-NMR	Structural information	Link NOM to well known biopolymer classes.	
Mass Spectrometry	Molecular mass distribution	Single charged ions every 2 Da. Series of peaks separated by 14 Da.	McIntyre et al., 1997 Persson et al., 2000
High Resolution Mass Spectrometry	Resolution and identification of individual elemental compositions from DOM.	Regular patterns with mass difference 0.0364 Da. Elemental formulas of DOM.	Stenson et al., 2003 Altieri et al., 2009 D'Andrilli et al., 2010
Tandem Mass Spectrometry	Structural information	44 Da and 18 Da neutral losses. Carboxyl and hydroxyl functional groups.	Leenheer et al., 2001 Witt et al., 2009

<sup>a</sup> The references included are only examples of the work done in DOM characterization highlighting the most outstanding results, using the different analytical techniques and it is far from being an extensive bibliographic review.

The advent of atmospheric pressure ionization (API) sources and high resolution mass spectrometry (HRMS) revolutionized the ability to analyze DOM (Mopper et al., 2007; Reemtsma 2009; Hertkorn et al., 2008). HRMS for the characterization of DOM has been used for more than 20 years now. The most remarkable findings achieved so far with regard to molecular information are:

- DOM spectra revealed thousands of peaks between  $m/z$  100 and 1000.
- Each nominal mass showed several individual peaks.
- Regular mass spacing patterns of (see Figure 1.3):
  - 14.0156 Da corresponding to  $\text{CH}_2$  groups
  - 2.0157 Da corresponding to variations in double bond equivalents (DBE) and  $\text{H}_2$  content
  - 1.0034 Da corresponding to the mass difference between  $^{13}\text{C}$  and  $^{12}\text{C}$
  - 0.0364 Da corresponding to exchange  $\text{CH}_4$  versus oxygen.
- All resolved peaks seemed to be singularly charged.
- Each peak represents a unique elemental formula and more likely numerous compounds with different structures.

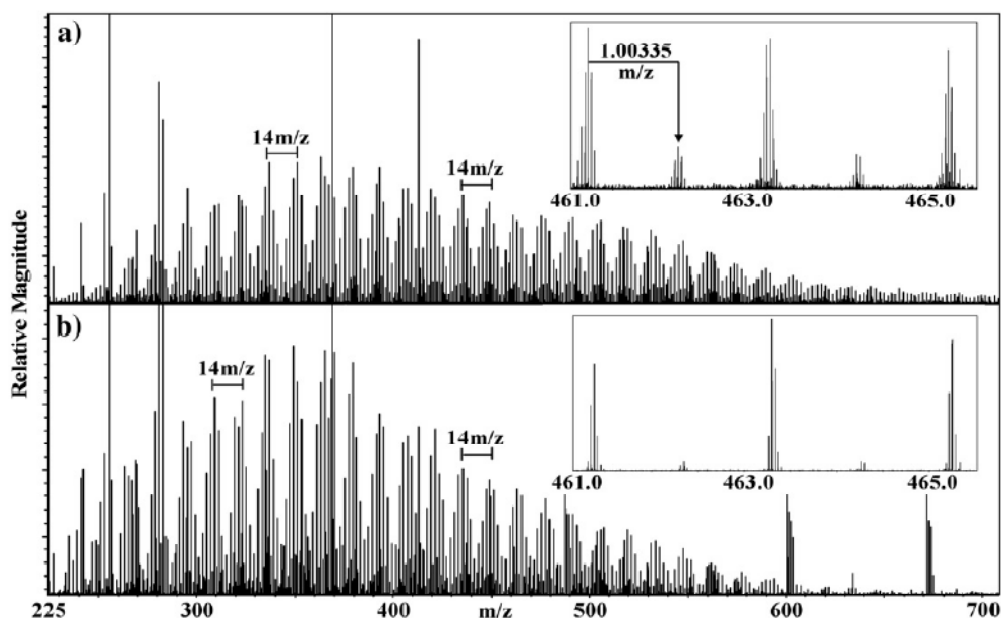


**Figure 1.3.** a) Negative ion mass spectrum ( $m/z$  225–700) of extracted Dismal Swamp water. b) Negative ion mass spectrum ( $m/z$  225–700) of extracted offshore coastal water. The insets are an expanded region of 461.0–465.5, to highlight the complexity at each nominal mass and to show that the analytes are singly charged (Sleighter et al., 2008).

Most of these studies have been conducted to discover the insights of the composition and functioning of DOM from different origins to understand the carbon cycle, the transportation of DOM from rivers to the ocean or to compare DOM reactivity / degradation from different natural or affected environments (see Figure 1.4) (Schmidt et al., 2009; Sleighter et al., 2008; Hertkorn et al., 2013; Koch et al., 2005; Herzprung et al., 2010; Kujawinski et al., 2009; D'Andrilli et al., 2010; Gonsior et al., 2011a; Zhang et al., 2014).

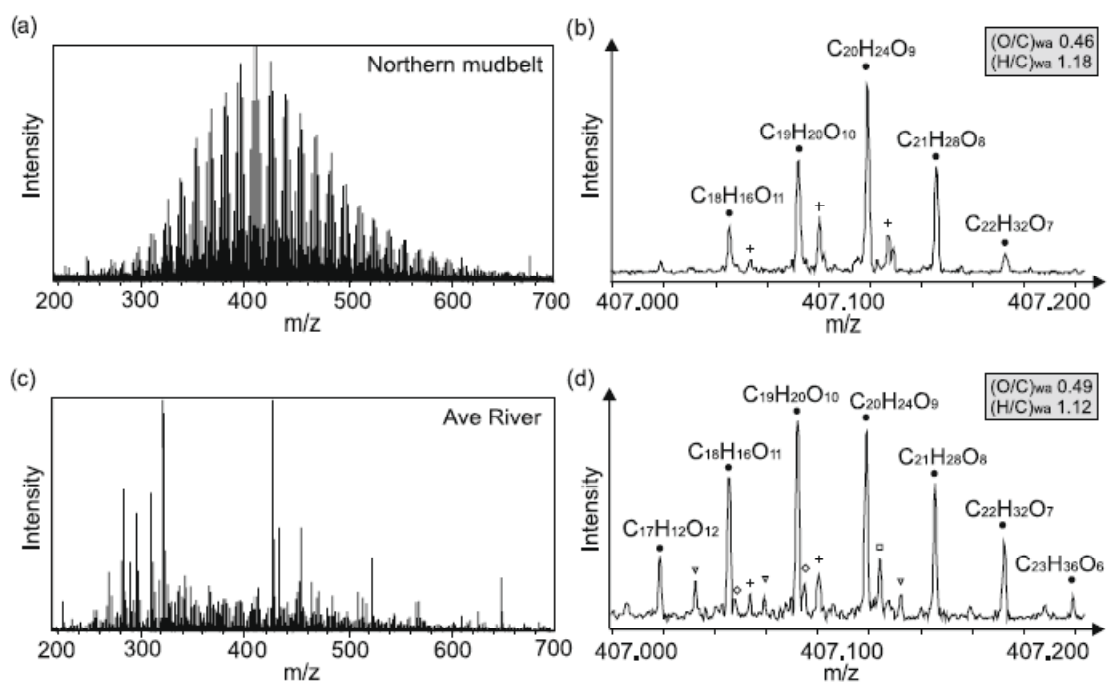


**Figure 1.4.** Electrospray negative FT-ICR mass spectra and expanded sections of mass spectra at nominal mass 407 of: (a and b) northern mudbelt-derived sediment pore water DOM and (c and d) Ave River DOM. The different series characterized by the replacement of O by CH<sub>4</sub>, nitrogen-bearing and sulfur-bearing series are indicated. (O/C)<sub>wa</sub> and (H/C)<sub>wa</sub> refer to CHO-compounds in the presented mass range and reflect a lower relative O content and a higher relative H content in the pore water DOM (Schmidt et al., 2009).

However, as it has been discussed before, apart from the environmental relevance of DOM, it also affects the production of drinkable water and it has been pointed out as a precursor for DBPs formation (Richardson et al., 2007). Only recently and in very few studies this technology has been applied to discover the real role of DOM along water treatment plants (Zhang et al., 2012a; Zhang et al., 2012b; Lavonen et al., 2013) and as far as we know, no attempts have been made to evaluate advanced water treatments based on membrane technology. As has been commented before one of the aims of the thesis is to evaluate DOM changes at molecular level through different water treatment plants.

HRMS has been the mass spectrometric technique chosen to study these changes, as the use of FT-ICR and more recently FT-orbitrap mass analyzers has provided details about DOM composition, where the other techniques and other mass spectrometers failed to resolve the numerous constituents. However, there are still some limitations and challenges that have to be considered when using HRMS for the characterization of DOM:

- i) HRMS is mandatory to resolve all the signals in the spectrum.
- ii) Very accurate mass (AM) measurements are necessary to obtain reliable formula assignment.
- iii) Very sensitive method and / or pre-isolation treatments are essential to concentrate DOM and remove salts.
- iv) Data processing methods should be designed so that restrictive criteria and / or filtering strategies can be applied to extract the information contained in a high resolution (HR) spectrum.
- v) Strategies based on MS or other technologies (i.e. NMR) are basic to obtain structural information of individual compounds from DOM.



## **Chapter 2.**

# **High Resolution Mass Spectrometry and Accurate Mass Measurements**

---



## 2.1. Introduction

MS has become one of the most important analytical tools nowadays. Since its origins, when J.J. Thomson constructed the first mass spectrometer (Borman et al., 2003) several scientific achievements have been reached. Some of the last developments are described in Cole 2012 and Cross 2011, such as the new mass analyzer FT-orbitrap (or simply orbitrap) or the new direct analysis ion sources: desorption electrospray ionization and direct analysis in real time. In Table 2.1., there is a summary of the most outstanding developments in mass spectrometry, related to environmental analysis and HRMS.

**Table 2.1.** Historical developments in mass spectrometry mainly related to environmental analysis and high resolution mass spectrometry (adapted from Borman S. et al., 2003; <http://masspec.scripps.edu>).

Researcher(s)	Year	Contribution
J. J. Thomson	1897	First mass spectrometer ( <i>Parabola Spectrograph</i> )
F. W. Aston	1919	Atomic weight using mass spectrometry
A. J. Dempster	1920	Electron ionization source
J. Mattauch and F.K. Herzog	1934	Double-focusing analyzer
W. E. Stephens	1946	Time of flight mass analyzer
J.A. Hipple et al.	1949	Ion cyclotron resonance
A.O. Nier and E.G. Johnson	1953	Reverse geometry double-focusing instruments
W. Paul	1953	Quadrupole mass analyzer
J.H. Beynon	1956	Identification of organic compounds with high resolution mass spectrometry
J.H. Futrell and C.D. Miller	1966	Tandem mass spectrometry
M. Dole / J.B. Fenn	1968	Electrospray Ionization
M. B. Comisarow and A. G. Marshall	1974	Fourier transform ion cyclotron resonance
R.A. Yost and C.G. Enke	1978	Triple quadrupole mass analyzer
G.L. Glish and D.E. Goeringer	1984	Quadrupole-Time of flight mass analyzer
A. Makarov	2000	FT-Orbitrap
Z. Takats et al. (R.G. Cooks)	2004	Desorption electrospray ionization
R.B. Cody et al.	2005	Direct analysis in real time

As shown in Table 2.1., almost all the mass analyzers known and used nowadays were developed in the last century: quadrupole (Q), time of flight (TOF), FT-ICR, magnetic sector and any combination of them. However, instrumentation has evolved significantly in the last years and an image is worth a thousand words (Figure 2.1.). In 1987, Brunnée in his search for the ideal mass analyzer ended up with the map of the *Treasure Island*, concluding that there is no final solution and so the perfect mass analyzer does not exist.

At that time, Brunnée defined the ion cyclotron resonance (ICR) principle as listening to a musician striking many keys of a piano at once and HRMS was mainly restricted to magnetic sectors (Brunnée 1987). In the *Treasure Island* proposed by Makarov in 2009, the scenario is completely different. The mass spectrometers based on QqQ technology are the main instrumentation of analytical laboratories with high work load, magnetic sectors are being replaced and they are basically restricted to some specific applications and the new generation of Q-TOF mass analyzers and the new mass analyzer orbitrap are gaining adepts.

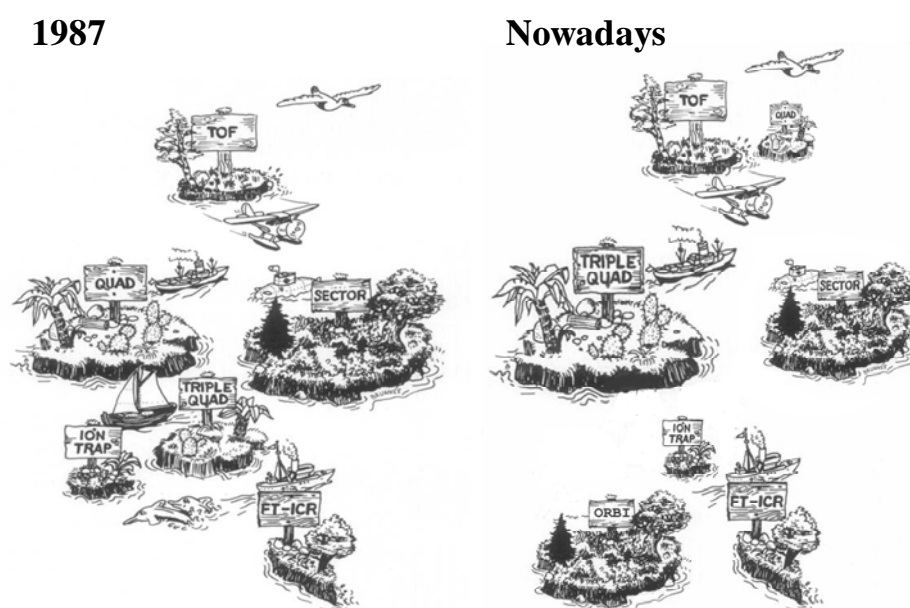


**Figure 2.1.** (Left) The *Treasure Island* from Brunnée illustrating the different mass analyzers in use in 1987. (Right) The *Treasure Island* proposed by Makarov (adapted from the Makarov conference in the International Mass Spectrometry Conference in Bremen 2009), which corresponds to the situation nowadays.

With regard to HRMS, the mass analyzers available nowadays to perform HR analysis are: magnetic sectors (usually coupled to GC), TOF, orbitrap and FT-ICR (see Figure 2.2.). Generally speaking, TOF, orbitrap and FT-ICR mass analyzers have usually been used coupled to LC to perform AM measurements. However, each mass spectrometer is conceptually different. TOF mass analyzers are based on measurements of time of transit, whereas in orbitrap and FT-ICR, ions describe harmonic oscillations confined in an electrostatic and magnetic field, respectively (Marshall et al., 2008).

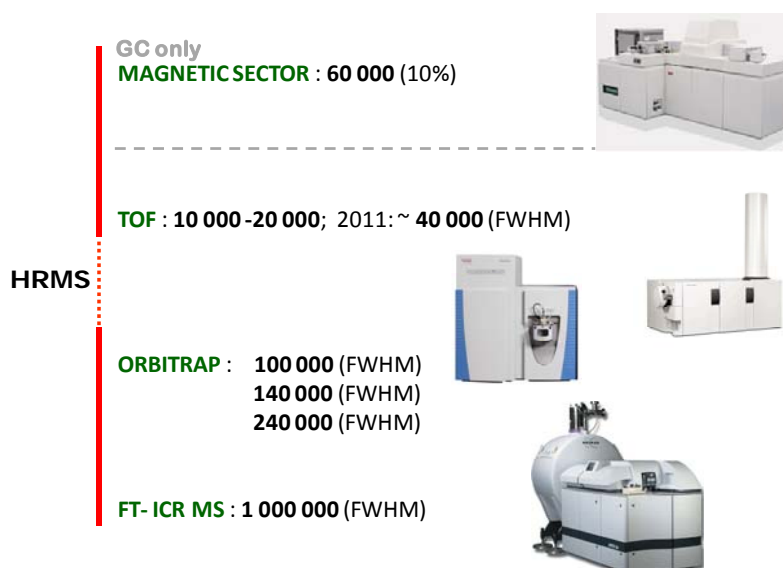


**Figure 2.2.** High resolution mass analyzers in use nowadays capable of acquiring accurate data. The maximum resolution (full width at half maximum - FWHM) achievable for each mass analyzer is displayed.

Brunnée (Brunnée 1987) was judging the different mass analyzes technologies based on: mass range, resolution, exact mass determination, sensitivity, all ion detection, ion storage, scanning speed, dynamic range, quantitation, tandem mass capabilities, sample introduction, simplicity and relation of performance/cost (see Figure 2.3.). Not surprisingly, nowadays the capabilities of the new mass spectrometers are also judged based on these criteria. Guidance based on the different mass analyzers has been done before (Bristow et al., 2003). Since then, new instrumentation such as the orbitrap has appeared and TOF analyzers have reached an unprecedented level of resolution and mass accuracy. For this reason, an update of the topic was necessary and in this thesis a comparison has been carried out between different modern mass analyzers.

The use of MS has spread to many different fields and it is increasing every day (Gelpí 2008, Gelpí 2009). To date, several applications are being developed in many laboratories on a research and / or routine base (Forcisi et al., 2013; Bijlsma et al., 2013; Kaufmann 2012; Vichi et al., 2013; Kumar et al., 2013). Not surprisingly, the number of publications from 2004 to 2013 has raised by more than 200 % (Figure 2.4.). One of the uses of MS is the structural characterization and determination of organic compounds by HRMS. It was first applied by John Beynon in the 1950s, who used a single magnetic sector for the identification of a wide variety of molecules based on AM measurements (Beynon 1954; Beynon 1960). In environmental studies, the aim of any AM measurement is to elucidate the elemental formulas of a compound and / or quantify the presence of organic compounds in the environment (Hernández et al., 2012; Krauss et

al., 2010). In this thesis, some applications have been tested to evaluate the advantages of using AM measurements in front of low/medium MS in environmental analysis.

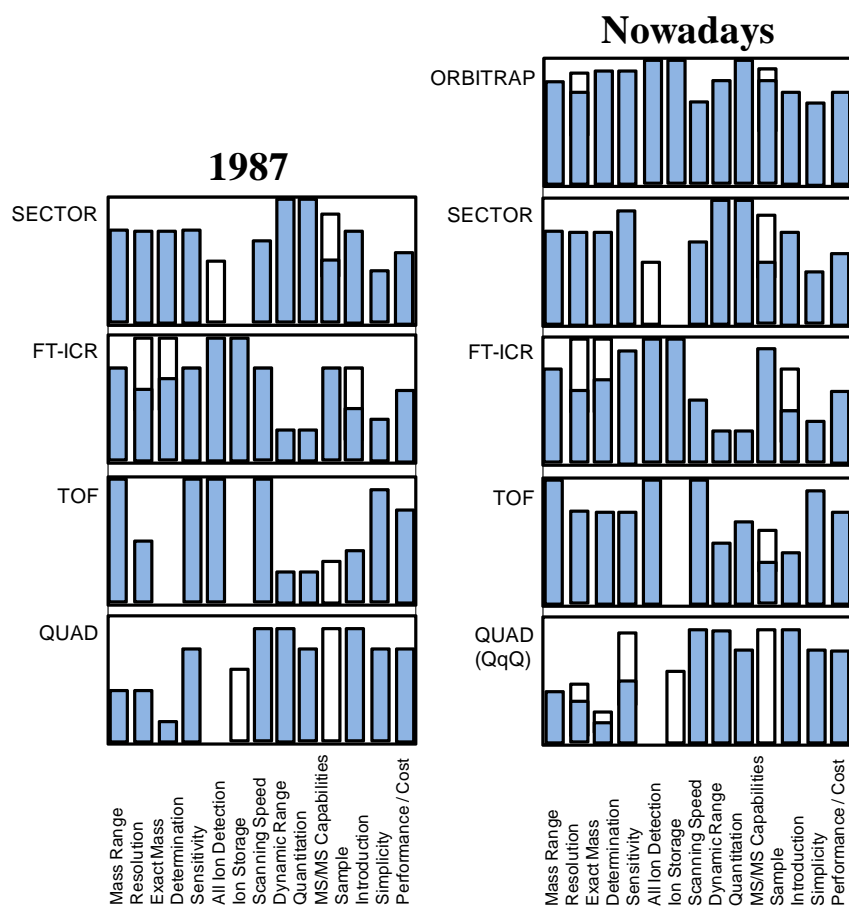


**Figure 2.3.** Characteristics of the mass analyzers in 1987 (adapted from Brunnée 1987) and characteristics of the mass analyzers nowadays, including the new mass analyzer orbitrap.

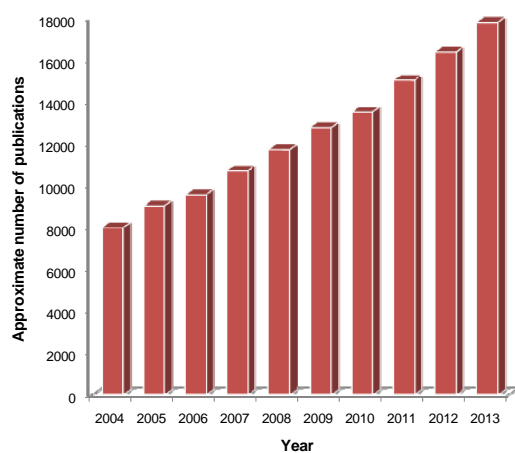


**Figure 2.4.** Approximate number of publications on the topic mass spectrometry in the last 10 years. Search conducted in [www.scopus.com](http://www.scopus.com) in September 2014.

## 2.2. Experimental Procedure and Results

The experimental part and results in this chapter are included as two publications. Firstly, the research study entitled *High Resolution Mass Spectrometric Techniques for Structural Characterization and Determination of Organic Pollutants in the Environment*, which will be chapter 6 in the coming book *Chromatographic Analysis of the Environment: Mass Spectrometry Based Approaches*, 4<sup>th</sup> edition. In this work, the main terminology, parameters influencing the AM measurements and instrumentation have been described. Furthermore, specific merits and limitations of HR mass spectrometers have also been discussed. Experience gained through the use of different mass spectrometers and dealing with complex matrixes has enabled us to draw some strategies that can help to determine the elemental formula of a compound. Some applications from the literature, but also some experimental work developed during the thesis, have been included to point out the advantages and need of using HRMS in front of other techniques.

Additionally, to evaluate the capabilities of new mass spectrometers a comparison was carried out. Different mass analyzers technologies were tested during a single day of work for the analysis of small molecules in negative electrospray (ESI) mode. The procedure and the results of this comparison study are included in the research article entitled *Accurate Mass Measurements and Ultrahigh-Resolution: Evaluation of Different Mass Spectrometers for Daily Routine Analysis of Small Molecules in Negative Electrospray Ionization Mode* published in *Analytical and Bioanalytical Chemistry*. This study was necessary in terms of a timely update on the topic, as other comparative studies had been carried out some years before (Bristow et al., 2003). Furthermore, the present study focuses on a wider mass range (not only a single  $m/z$ ). In addition, the negative ESI was tested as there were almost no data on AM measurements in this mode. Moreover, the analysis of DOM is usually preferentially acquired in negative mode. Some of the main features were compared, i.e. resolution, exact mass determination, sensitivity, simplicity and calibration protocol.



### **2.2.1. Book Chapter**

Nuria Cortés-Francisco and Josep Caixach

High Resolution Mass Spectrometric Techniques for Structural Characterization and Determination of Organic Pollutants in the Environment.

Chapter 6 in *Chromatographic Analysis of the Environment: Mass Spectrometry Based Approaches*, 4<sup>th</sup> edition.

Leo M.L. Nollet & D. Lambropoulou (Editors)

CRC Press Boca Raton, Florida, USA (Taylor and Francis Group)



## **6. High resolution mass spectrometric techniques for structural characterization and determination of organic pollutants in the environment.**

Nuria Cortés-Francisco and Josep Caixach

### **I. Introduction**

### **II. High Resolution Mass Spectrometry Terminology**

### **III. Factors influencing the accuracy and precision of an accurate mass measurement**

- A. Resolution
- B. Tuning, Peak shape and Ion Abundance
- C. Calibration protocols

### **IV. Elemental formula determination**

- A. Mass Measurement accuracy and precision: Uncertainty of the data
- B. Elements to consider
- C. Restrictions of elements number
- D. Ion type, adduct formation and charge. RDBE and Nitrogen Rule
- E. Isotopic pattern and isotope ion ratio
- F. Valences (LEWIS and SENIOR rules)
- G. Element ratios and Element probability check
- H. Complementary techniques to obtain structural information
- I. Any additional information
- J. Database and Automatic Data Processing

### **V. Instrumentation**

- A. Double-focusing electric/magnetic sector mass analyzer
- B. Fourier transform ion cyclotron resonance mass analyzer
- C. Time of flight mass analyzer
- D. Fourier transform Orbitrap mass analyzer
- E. Hybrid Mass Spectrometers

### **VI. Environmental applications**

- A. GC-HRMS applications
- B. LC-HRMS applications

### **VIII. References**

## I. Introduction

Mass spectrometry (MS) has a dynamic history with a continually progressing technology that has made significant advances into different fields and specially in environmental analysis (Gelpí 2008; Gelpí 2009). Since Aston (1927), magnetic sectors were the mass analyzers dominating the scene of high resolution (HR) and accurate mass measurements.

The use of high resolution mass spectrometry (HRMS) for structural characterization and determination of organic compounds was first applied by John Beynon in the 1950s. Beynon used a single magnetic sector for the identification of a wide variety of molecules based on accurate mass measurements. Beynon explained for the first time that, if the mass of an ion from a chemical compound was determined with sufficient accuracy, the elemental composition of this compound could be determined (Beynon 1954; Beynon 1960). In his work entitled "Mass Spectrometry and its Applications to Organic Chemistry", Beynon highlighted the importance of carrying out very accurate mass measurements to distinguish between different possible candidates, when structural characterization and determination of an organic compounds should be carried out. Based on his experience, Beynon already pointed out in his work different rules (e.g. isotopic pattern, ring plus double bond equivalents - RDBE) that could be applied to identify one molecule from a list of several candidates. Some of these assumptions are still in use nowadays.

At that moment, the availability of such measurements was limited due to the cost and complexity of instrumentation (Bristow 2006). However, the panorama of MS early described by Brunnée in 1987 (Brunnée 1987) has been substantially modified (Makarov 2009a). HRMS is no longer restricted to magnetic sectors, and a wide variety of mass analyzers have been designed and improved for this purpose (Bristow 2006).

The use of high resolution presents several advantages with regard to low or tandem mass spectrometry (MS/MS). In environmental analysis the number of potential organic pollutants might be huge. These contaminants can be at very low concentrations and can be unknown or occur as a result of the degradation of the original contaminant (Hernández et al., 2012). High resolution helps to trace contaminants, as well as to identify analogs for which standards are not available (Krauss et al., 2010).

The chapter starts with a review of HRMS terminology, followed by the discussion of some parameters influencing accurate mass measurements and the identification of organic compounds when using HRMS. Section V focuses on the main mass analyzers capable of acquiring HR mass data. Finally, some environmental applications are discussed. We have chosen only few examples that illustrate the main advantages and/or requirements of using HR, more than just giving a list of recent studies using HRMS applied to environmental analysis, which are available in some recent reviews (Hernández et al., 2012; Krauss et al., 2010).

## II. High Resolution Mass Spectrometry Terminology

As can be seen in the literature, there are many applications for which accurate mass measurement is used. However, in a study from Bristow (Bristow et al., 2003), a lack of understanding (particularly amongst newer users) has been detected. For this reason, guidance on undertaking key aspects of the methodology in order to obtain robust measurements and traceable data has been reported (Webb et al., 2004; Bristow 2006). Moreover, concerning the number of publications quoting accurate mass data, in which some terms are used inconsistently, guidance for terminology and treatment of data has also been described in detail (Brenton et al., 2010) and the main definitions are summarized below. Also, the IUPAC recommendations have recently been published (Murray et al., 2013). An example is given in Figure 6.1. to illustrate the main definitions.

- **Nominal mass**

The mass of an ion or molecule calculated using the mass of the most abundant isotope of each element rounded to the nearest integer value and multiplied by the number of atoms of each element.

- **Accurate mass**

The experimentally determined mass of an ion measured to an appropriate degree of accuracy and precision used to determine, or limit the possibilities for, the elemental formula of the ion.

- **Exact mass**

The calculated mass of an ion whose elemental formula, isotopic composition, charge state are known i.e. the theoretical mass. The IUPAC definition constricts the definition to

using one isotope of each atom involved, usually the lightest isotope, but generalizes the definition to cover an ion or neutral molecule. The charge state is relevant as the mass of the electron (0.00055Da) or multiple charges, may not be negligible in the context of mass measurement.

- **Monoisotopic mass**

The exact mass of an ion or molecule calculated using the mass of the most abundant isotope of each element.

- **Mass Measurement accuracy**

The difference between the measured value (accurate mass) and the true value (exact mass) is the “accuracy” of the “accurate mass measurement” and it is suggested that the term “mass measurement accuracy” should be used to denote this difference (Brenton et al., 2010).

The mass measurement error (or accuracy) of a single reading will be:

$$\begin{aligned} \Delta m &= (m_{\text{Theoretical}} - m_{\text{Experimental}}) && \text{in Da} \\ \text{Equation 6.1.} \quad &= (m_{\text{Theoretical}} - m_{\text{Experimental}}) \times 10^3 && \text{in mDa} \\ &= \left( \frac{m_{\text{Theoretical}} - m_{\text{Experimental}}}{m_{\text{Theoretical}}} \right) \times 10^6 && \text{in parts per million (ppm)} \end{aligned}$$

If several measurements are recorded and an average result should be calculated, it is usually expressed as the root-mean-square (RMS) to prevent negative and positive values cancelling each other. Another option is to calculate the average absolute mass measurement accuracy (Brenton et al., 2010).

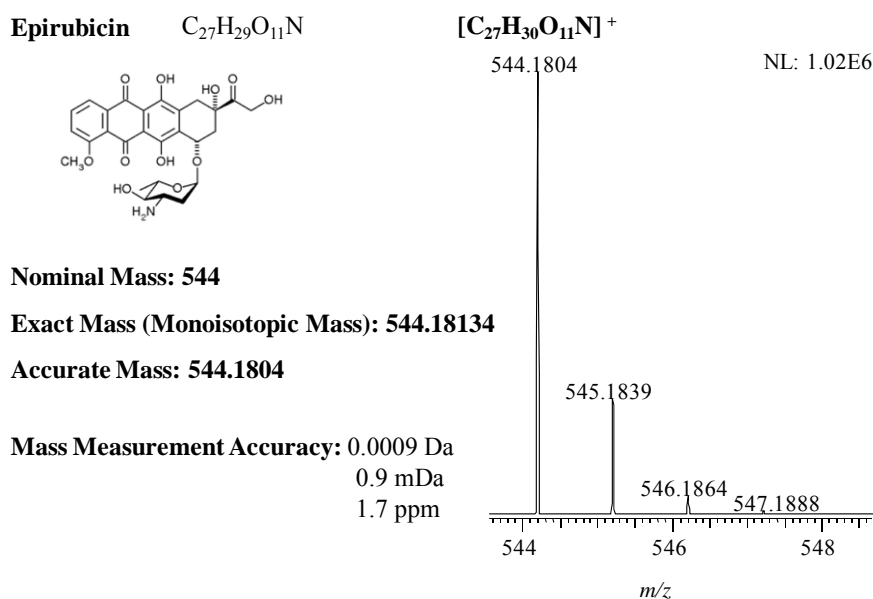


**Figure 6.1.** Nominal mass, Exact Mass, Accurate Mass and Mass Measurement Accuracy for the ion  $C_{27}H_{30}O_{11}N^+$  of the neutral compound Epirubicin. The mass spectra is also shown.

- **Mass Measurement precision**

The repeatability of the measurement reflecting random errors. Random errors cause measurements to fall on either side of the average experimental measurement and affect the precision of the set of measurements. Although it is not usually reported in accurate mass measurements, precision is very important to know the uncertainty (U) of the mass measurement. Standard deviation may be used to quote the precision of the data set.

- **Mass Resolution and Mass Resolving Power**

It should be pointed out that the definition of resolution and resolving power has been a subject of controversy. In the last recommendations from IUPAC resolution (R) is defined as:

**Equation 6.2.** 
$$R = \frac{m}{\Delta m}$$

The  $m/z$  value at which the measurement was made should be reported as well as the definition and method of measurement of  $\Delta(m/z)$ . For instance, for magnetic sector instruments, two peaks of equal intensity are considered to be resolved when they are

separated by a valley, which is 10% of the height of each peak. The definition used with quadrupole, Fourier transform ion cyclotron resonance (FT-ICR), ion trap (IT), time of flight (TOF) and FT orbitrap mass spectrometers is based on a peak width measured at 50% peak height (full width half maximum - FWHM), producing a value approximately double that calculated using the 10% valley definition (see Figure 6.2.) (Bristow 2006). The resolving power is the ability of an instrument or measurement procedure to distinguish between two peaks at  $m/z$  values differing by a small amount and expressed as the peak width in mass units (Murray et al., 2013).

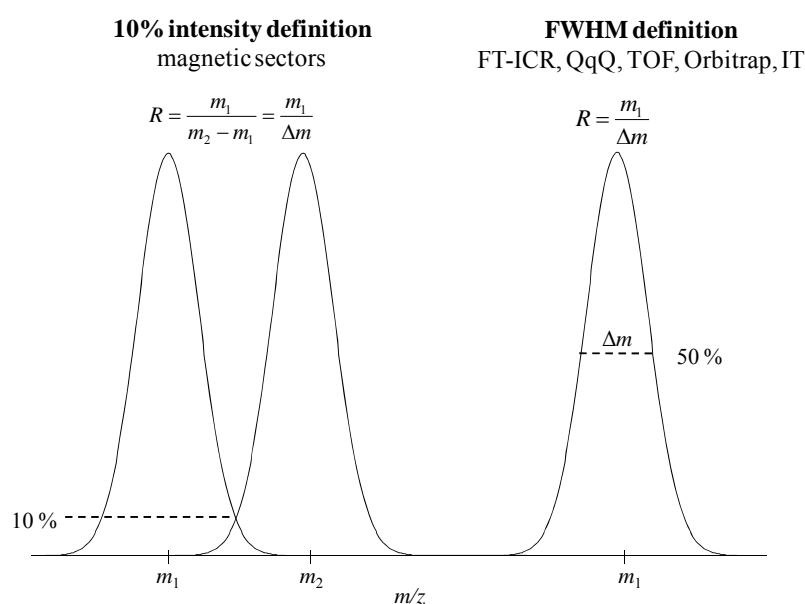


**Figure 6.2.** Definitions of resolution.

### III. Factors influencing the accuracy and precision of an accurate mass measurement

Ideally, we would like to obtain the best accuracy and precision, due to the fact that depending on the mass measurement accuracy (mDa or ppm) achieved, there will be a higher or lower number of potential elemental formulas for a compound. The better the accuracy the less the ambiguity. But can we measure the mass of a compound with such a great accuracy and precision?

The accuracy and precision achieved depends on several factors as shown in Figure 6.3. such as resolution, interferences of the matrix, the mass analyzer, calibration protocol and some operational factors, such as room temperature.

Webb et al. (Webb et al., 2004) wrote a practice guide to provide users and suppliers of accurate mass instrumentation the essential steps in obtaining reliable data. They highlighted that in order to achieve high accuracy and precision a number of key considerations when carrying out accurate mass measurements must be understood and optimized. Those included tuning and peak shape, ion abundance, resolution, calibration, sample introduction, data manipulation, validation and quality control checks. Some of these considerations should be general to any method development when using MS. The parameters that we have considered to be crucial for accurate mass measurements are discussed below or in the next sections.

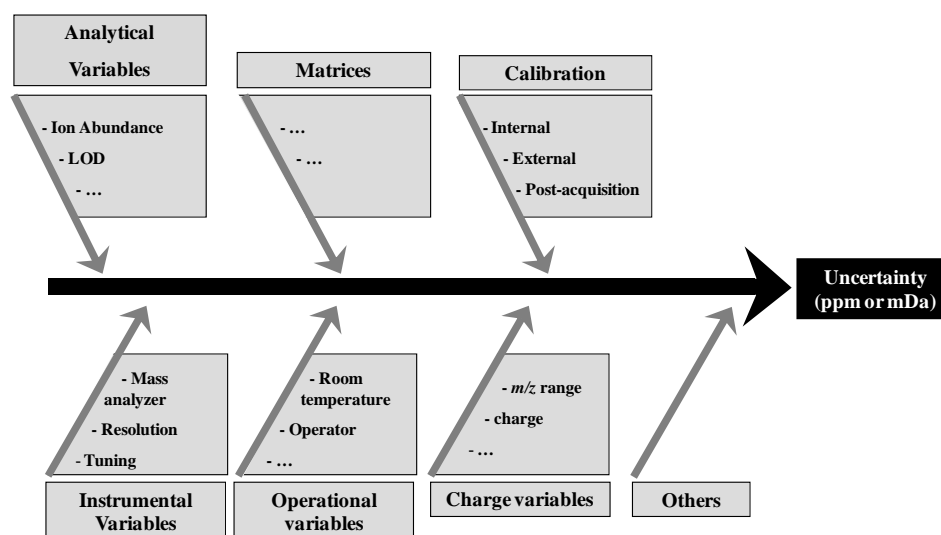


**Figure 6.3.** Factors that can influence the uncertainty (accuracy and precision) of a measurement.

### A. Resolution

Regarding mass measurement accuracy, it should be taken care when linking these ideas with HR. Low resolution instruments have not traditionally been employed to record accurate mass measurements, but some very good results (accurate and precise measurements) have been obtained (Bristow 2003; Balogh 2004). These results showed that when there are no unresolved isobaric ions and a strict experimental protocol is used, accurate mass measurements can be independent from resolution. However, in every-day

analysis when analyzing complex matrixes, such as in the field of environmental analysis, HR can help preventing false assignments. Moreover, HR is mandatory for the identification of non-target compounds (transformation products of known compounds) or screening of unknowns. Definition of what is considered to be high resolution is difficult. Legislation applying to method development (European Commission 2002) is still not updated. At the moment, we only have the old definition based on magnetic sector instruments (HR is 10,000 at 10% valley) which translates to 20,000 - 25,000 (FWHM). Fixing a value is always a controversial issue, due to commercial interests. Some reference guides state that resolution higher than 20,000 in all the mass range should be considered HR (European Commission 2012), however in complex mixtures such as natural organic matter (NOM) this is not enough, as shown in Figure 6.4. Even when R: 20,000 or 50,000 (FWHM) is used (Figure 6.4.b and c) all the signals are not resolved and the main consequence is that the elemental compositions that would be obtained by the accurate masses displayed in Figure 6.4.b, c and d would be wrong and would never correspond to the real ones. This is an extreme case, but this is the effect that any interference can have on the accurate mass measurement of a compound. One may think that working in the highest resolution mode will solve all the problems, however it should be taken into account that resolution has two major effects on the mass spectra of compound: the width of the signal and the intensity. The ion abundance (or intensity) may also have an effect on accuracy and precision, and in addition, the scan rate would be slow when higher resolution is achieved (see section V. Instrumentation).

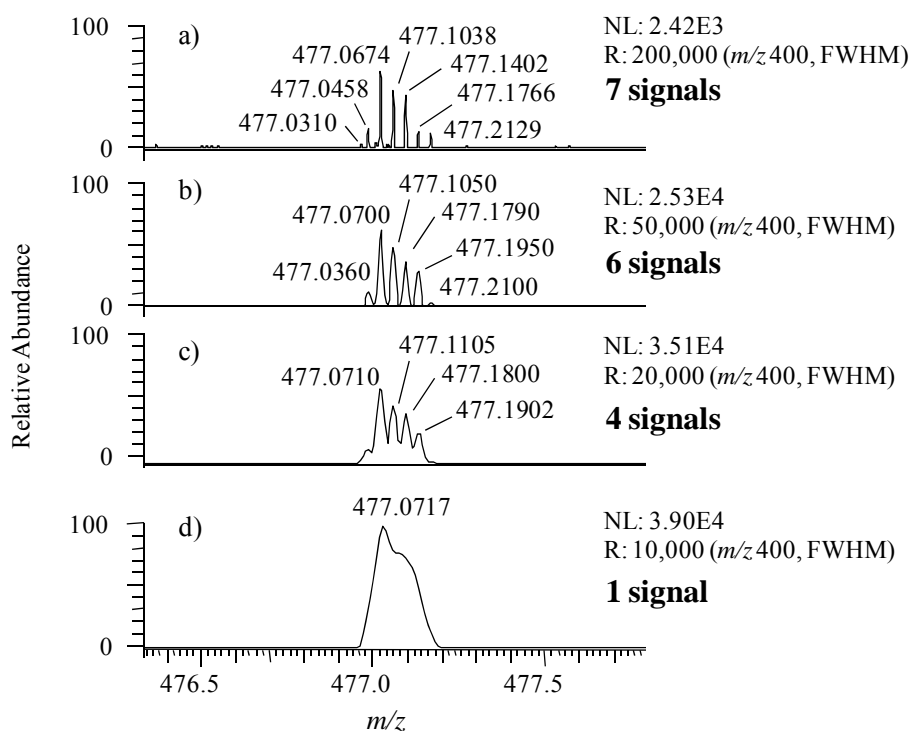


**Figure 6.4.** Mass spectrum of fulvic acids (zoom at  $m/z$  477) from International Humic Substance Society obtained at different resolution (R) acquired with an FT-ICR mass analyzer.

## B. Tuning, Peak shape and Ion Abundance

The tuning of the instrument should be good enough to be sure that the peak shape is symmetric and we have enough ion abundance. If the optimization of the ion source (e.g. type of ion source, temperatures, voltages) and the mass analyzer (e.g. scan rate, resolution, ion accumulation) is not properly done, it may result in a low ion abundance and therefore in a worse mass accuracy. We strongly discourage to acquire data in centroid mode, instead of profile mode. Despite the inconvenience of memory that profile raw files may have, the peak shape can give us a clue of how properly or badly we are performing the accurate mass measurements. For instance the peak shape can reveal if there is more than one compound under the envelope (Figure 6.4.d).

## C. Calibration protocols

There are a number of methods for accurate mass measurement, which involve different approaches and instrumentation, but all involve calibration of the mass scale (Brenton, 2010). Mass calibration consists of fitting the observed mass measurements to the exact

mass of two or more different ions. The calibration process is crucial to achieve highly accurate mass measurements. Calibration may be external (i.e., reference masses from a mass spectrum of another analyte acquired under similar conditions) and / or internal (i.e., the reference masses are for ions of known elemental composition in the same mass spectrum as the analyte) (Marshall et al., 2008).

In all the mass spectrometers external calibration is done automatically, with the infusion of a standard. The corrections to the mass axis are stored by the instrument and frozen in memory. A good external calibration is required to obtain good mass accuracy and it only works satisfactorily if the instrument is stable (Webb et al., 2004). For some HR mass spectrometers such as, FT-ICR and FT-orbitrap, external calibration is very stable and no other calibration protocols might be applied. For TOF and magnetic sectors mass analyzers an additional internal calibration have usually been required, to prevent calibration drift (Cortés-Francisco et al., 2011).

In internal calibration, the  $m/z$  scale is calibrated using ions of known  $m/z$ , usually called lock masses, which are scanned during the same experiment as the compounds of interest. The lock masses can be introduced into the mass spectrometer mixed in the sample solution, infused from a separate source into the mass spectrometer or teed in at the same time as the analytes. The main problem is that ion suppression and chemical interferences might be created between lock masses and analytes (Webb et al., 2004). With internal calibration, the mass range can be constantly recalibrated during acquisition, but an internal calibration can be also done a posteriori of the data acquisition, which is called post-processing or post-acquisition calibration. In post-acquisition mode, no mass corrections are made to the peak in the scan; only external calibration stored in the instrument memory is used. The main purpose is to recalculate the data acquired with respect to the exact masses of a reference compound which was present in the ion source during the measurement. The reference compound serves as a “ruler” in calculating the accurate masses of the unknowns that are adjacent to the known compounds. The main advantage of post-acquisition calibration is that the mass analyzers do not waste acquisition time looking for the lock mass and constantly recalibrating during acquisition, and more points per peak can be obtained in the analysis. Moreover, accuracy and precision are as good as with the common internal calibration (Cortés-Francisco et al., 2011). Internal calibration is typically twice accurate as external calibration (Marshall et al., 2008).

## IV. Elemental formula determination

Once the accurate mass measurement of the ion has been recorded, the value is used to generate a list of elemental formulae. In most of the commercial software controlling the instruments the elemental formula determination can be carried out manually. The user has to set a few minimum parameters to obtain a list of candidates: uncertainty of the data (mass tolerance), elements to be used, number of elements and charge. Although these restrictions are set, the final list will contain many possible elemental formulae and therefore a number of key strategies should be employed to refine the list. Portolés et al. (Portolés et al., 2011) claimed that elucidation of unknowns cannot be achieved by following a standardized procedure, as both expertise and creativity are necessary in the process. We partially agree with this statement, however a minimum of information should be included when reporting analysis of unknowns or simply when using HRMS. No one would ever submit a study for quantification without the quantification limits. Strict criteria should also be applied when judging a HRMS determination. However, with no doubt HRMS is one of the areas of MS where expertise is specially needed.

### A. Mass Measurement accuracy and precision: Uncertainty of the data

As required by the Journal of the American Society for Mass Spectrometry setting fixed acceptable error limits for accurate mass measurement is not recommended. It should be highlighted that it has always given more importance to accuracy rather than to precision. Precision has received limited coverage in the literature, but it is important, and both accuracy and precision should be considered when talking about uncertainty in the measurement and evaluation of mass spectrometers. As far as possible, it is necessary to know the uncertainty associated to an accurate mass measurement, as it is the limit of quantification associated to quantify. Only this way can the list of theoretical candidates that should be taken into account be known.

It is important to understand the degree of accuracy and precision required relative to: i) the  $m/z$  of the ion that is measured ii) the intended use of the mass measurement: target and non-target analysis (it is not the same confirming and identity from a known compound or looking for unknowns) iii) previous information we have from the sample or the pollutants.

**i) the  $m/z$  of the ion that is measured**

With increasing  $m/z$ , the number of formulas which will fit a measured molecular mass increases, therefore an unambiguous result becomes impossible to obtain (Quenzer et al., 2002). In a previous study (Cortés-Francisco et al., 2011) considering mass range between  $m/z$  100 and 600, it has been observed that there is less accuracy in mass measurements for higher  $m/z$  compounds than for lower ones, for several mass analyzers tested and different calibration protocols applied. Regarding precision, the same behavior as for accuracy has been detected; precision of the measurements is worse at higher  $m/z$  values. It can be concluded that the uncertainty in the measurements is in all cases worse for higher  $m/z$  values. In contrast, a better mass measurement, in accuracy and precision terms, is needed for higher masses in order to have less candidates and the correct molecular formula (Webb et al., 2004).

**ii) the intended use of the mass measurement: target or non-target analysis**

It is not the same confirming and identity from a known compound (where standards are available) or looking for unknowns. In some cases sub-ppm or milidalton accuracy and precision for daily routine analysis have been considered adequate to discriminate between possible candidates, taking into account the nature of the compounds ( $m/z$  100–600) (Cortés-Francisco et al., 2011). In many cases, additional information other than just the accurate mass measurement will be needed to obtain the correct elemental composition. This includes, restrictions for the number of elements, isotopic pattern, RDBE, nitrogen rule, which are discussed in the next section. The correct determination of the elemental formula will be definitively related to **iii) the previous information we have from the sample or the pollutants.**

**B. Elements to consider**

For the formula generation, if we have no information of the kind of compound we are looking for, we should consider all the possible elements in an organic compound. This is a lot and nobody is doing so. For example, in the seven golden rules study (Kind et al., 2007) Kind et al. consider in general the following elements: C, H, N, O, P, S, F, Cl, Br and Si. Logically, in the examples, they usually reduce the elements, for instance C, H, N, O, S, P and Si. That's what people usually do, based on previous information. Some

studies report screening of unknowns, but the screening is focused on some derivatives of well-known compounds. In these cases, the term non-target would apply better.

### C. Restrictions of elements number

The restriction of element numbers is important to obtain a number of reasonable candidates that we can afterwards analyze based on other strategies (e.g. isotopic pattern). The easy one is the calculation of maximum carbons: dividing the mass range (maximum nominal  $m/z$  of the spectra) through the element mass (12 for carbon). For the rest of elements, Kind et al. (Kind et al., 2007), recommend some restrictions. However, any previous information about the sample will help to set these restrictions in a more appropriate way. This is especially important for the analysis of tandem mass spectra, where no selection of the precursor is carried out ("All Ion Fragmentation" - AIF mode in orbitrap or MS<sup>E</sup> in TOF). Filtering the fragments of the spectra coming from the molecule in front of the rest coming from the matrix is easy if restrictions in elements and number of elements is done. For instance, if we assume that the molecular ion could be [C<sub>27</sub>H<sub>30</sub>NO<sub>11</sub>]<sup>+</sup>, we are going to restrict the elements as follows: C ≤ 27, H ≤ 30, N ≤ 1, O ≤ 11.

### D. Ion type, adduct formation and charge. RDBE and Nitrogen Rule.

If the ion type, the adducts formed in the ion source and the charge are known (which we usually do); any formula giving an inappropriate RDBE value (meaning integer or non-integer) should give enough evidence to ignore incorrect formulas (Table 6.1.) (Webb et al., 2004).

#### Equation 6.3.

$$RDBE = C + Si - \frac{1}{2}(H + F + Cl + Br + I) + \frac{1}{2}(N + P) + 1$$

**Table 6.1.** Ion type and RDBE value expected, based on Equation 6.3.

Ion type	RDBE value
Even electron ion, e.g. [M+H] <sup>+</sup> [M-H] <sup>-</sup>	Non-integer
Odd electron ion, e.g. M <sup>+</sup>	Integer

It is true that the RDBE formula considers only the lowest valence state for each element and sometimes the true RDBE values are not calculated correctly. It is also suggested (Kind et al., 2007) to use it to detect formulas with an extremely high RDBE value, due to the fact that most of the compounds were found to have a RDBE < 40 (exception of fullerenes).

The nitrogen rule (Table 6.2.) is suggested for some authors (Webb et al., 2004; Bristow et al., 2006) to know if the molecule have an odd, even or zero number of nitrogen atoms, based on the odd or even  $m/z$ . It has been shown that this assumption can be done only with nominal masses and when using accurate mass measurements for  $m/z < 500$ .

**Table 6.2.** Nitrogen Rule.

Odd $m/z$	Even $m/z$	Number of nitrogen atoms
Even electron ion, e.g. $[M+H]^+$ $[M-H]^-$	Odd electron ion, e.g. $M^+$	$N_0, N_2, N_4 \dots$
Odd electron ion, e.g. $M^+$	Even electron ion, e.g. $[M+H]^+$ $[M-H]^-$	$N_1, N_3, N_5 \dots$

### E. Isotopic pattern and isotope ion ratio

From a list of feasible candidates, the isotopic pattern could help to eliminate the less probable formulas, especially for halogenated compounds, but also for Si and S-compounds. This process is not easily done automatically by the software, and if it is done, the scientist should be skeptic on how the software is comparing the isotopic pattern and giving this % of similarity or isotopic fit. First question that should be considered is how many isotopic peaks ( $M+1$ ,  $M+2$ ,  $M+3$ ) are taken into account for the comparison? How is the theoretical isotopic pattern simulated? Sensitivity and resolution can change dramatically the theoretical isotopic pattern. An example is shown in Figure 6.5. If very high resolution is used (e.g. R: 300,000 FWHM) for the *in silico* isotopic pattern, the  $M+1$  can be so well resolved that the different contributions of the natural abundant isotopes can show a isotopic pattern very different from the experimental one. Simulation should be carried out under the same conditions that the experimental pattern is obtained.

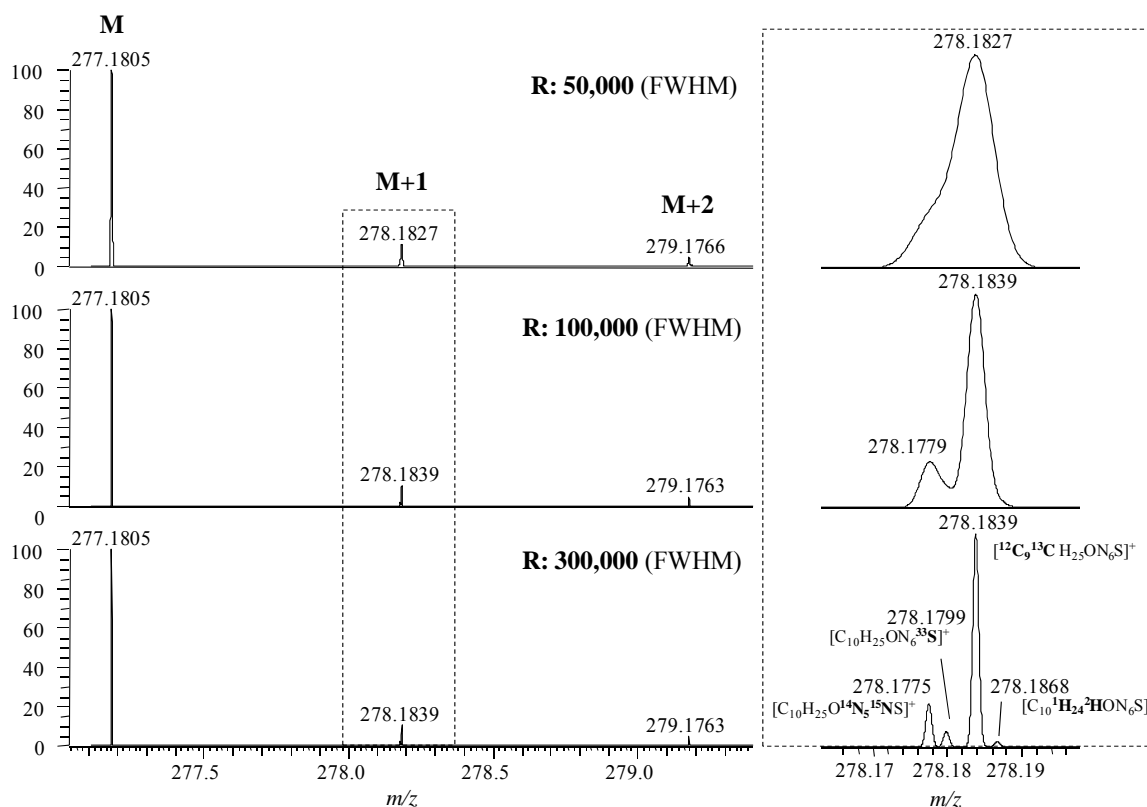


**Figure 6.5.** (Left) Isotopic pattern simulation at R: 50,000, R: 100,000 and R: 300,000 (FWHM) of the ion  $[\text{C}_{10}\text{H}_{25}\text{ON}_6\text{S}]^+$ , where the molecular ion (M) and the isotopic ion (M+1) and (M+2) are shown. (Right) Zoom of the M+1 (nominal mass 278), showing the different contributions of the natural abundant isotopes.

If possible, an alternative to *in silico* isotopic pattern comparison, will be the comparison of the isotopic pattern of standards (analyzed under identical experimental conditions) to the  $m/z$  of interest. This can be done calculating the isotope ion ratio. The ratio is calculated as the ratio between the monoisotope ion (diagnostic ion) and the isotope ion (M+1, corresponding to the natural isotope  $^{13}\text{C}$ ). It is more easy to perform it, when the molecular ion has relatively high  $m/z$  ( $m/z \geq 500$ ) and so M+1 is around 50%. The calculation of the isotope ion ratio can be easily and automatically done by any software (Domènech et al., 2013).

## F. Valences (LEWIS and SENIOR rules)

The LEWIS and SENIOR rules measure the occupancy of s and p orbitals. The LEWIS rule is based on the octet rule (elements share electrons with total occupancy). The

SENIOR rule add some criteria, so that the maximum and mixed valence states for each element are taken into account (Kind et al., 2007).

### **G. Element ratios and Element probability check**

When thousands of elemental formulas can be extracted from a spectra, it is very useful to filter less probable candidates based on elemental ratios and element probability check. This protocol is usually applied in the characterization of NOM (Herzprung et al., 2010) or metabolomics. A list of common element ratios are described in the study from Kind et al., (Kind et al., 2007), which can be very useful, especially for H/C ratio.

### **H. Complementary techniques to obtain structural information**

HR and high accuracy are powerful tools to confirm an identity, but they are insufficient for obtaining a unique structure of an unknown yet. Structural information is needed, and it can be complemented with MS/MS experiments and/or nuclear magnetic resonance (NMR), if possible (Webb et al., 2004; Cortés-Francisco et al., 2011).

### **I. Any additional information**

Kind et al. (Kind et al. 2007) suggested the subtraction of the TMS derivatization agent used for the analysis of some molecules by GC/MS to distinguish between candidates (rule 7). Generally speaking, any information we can have from the sample or the pre-treatment (derivatization step, pH extraction, purification, solubility) can help to restrict the parameters described in sections B to G to obtain a shorter list of reasonable candidates. An example is given by Vichi et al. in a recent study applied for the determination of volatile thiols in lipid matrix (Vichi et al., 2013). Due to the fact that a very specific derivatization agent was used (Ebselen) which contains Selenium, restrictive criteria were set to generate reliable elemental formulas:  $C \geq 13$ ,  $O \geq 1$ ,  $N=1$ ,  $Se=1$ ,  $S=1$ ,  $Na \leq 1$  and  $RDBE \geq 8.5$ . It was known that in this case any non-targeted thiol will react with this agent and so, a minimum of number of elements and RDBE could be set. In addition, Selenium has a characteristic isotopic pattern, so in this case it was also very helpful for ranking candidates.

In some fields, the determination of the molecular formulae can be confirmed if any regular pattern between the different compounds of the sample is known. Such is the case for marine NOM, where regular patterns with mass differences of 14.0156 Da, which spanned the entire spectra, are the result of ions that differ from each other in number of CH<sub>2</sub> groups. Other typical repeated spacing of 2.0156 Da are a result of ions that differ from each other in number of 2H and moreover, mass distances arose from a replacement of CH<sub>4</sub> by O with a mass difference of 0.0364 Da. Van Krevelen plots and Kendrick Mass Deffect (KMD) diagrams have been, until the moment, the best way adopted for marine chemistries and petroleomic analyzers to face this problem (Kim et al., 2003; Stenson et al., 2003). Van Krevelen diagrams are useful to classify substance classes in a first approach and KMD is used to sort out homologous series of organic compounds.

For some other applications, such as metabolomics, small subset of the mass spectrum signals can be used to built a mass difference network, based on metabolic pathways and reactions. This way, any  $m/z$  in the spectrum that cannot be part of this compositional space map could be considered to be not well assigned or not significant (Forcisi et al., 2013).

An example is given in the following lines to illustrate the different strategies that can be used to obtain an elemental formula from an accurate mass measurement.

**Example:**

LC-HRMS analysis (R: 50,000 FWHM) and accurate mass measurements of a wastewater sample after liquid-liquid extraction have been carried out. We want to identify a signal in the spectra (Figure 6.6.) with accurate mass  $m/z$  498.9302. We assume no previous information is available (real unknown) and for this reason we generate the list of candidates based on the parameters described in Table 6.3. When no additional information is available, it has been shown that setting very restrictive criteria will lead to an erroneous candidate (Cortés-Francisco et al., 2011).

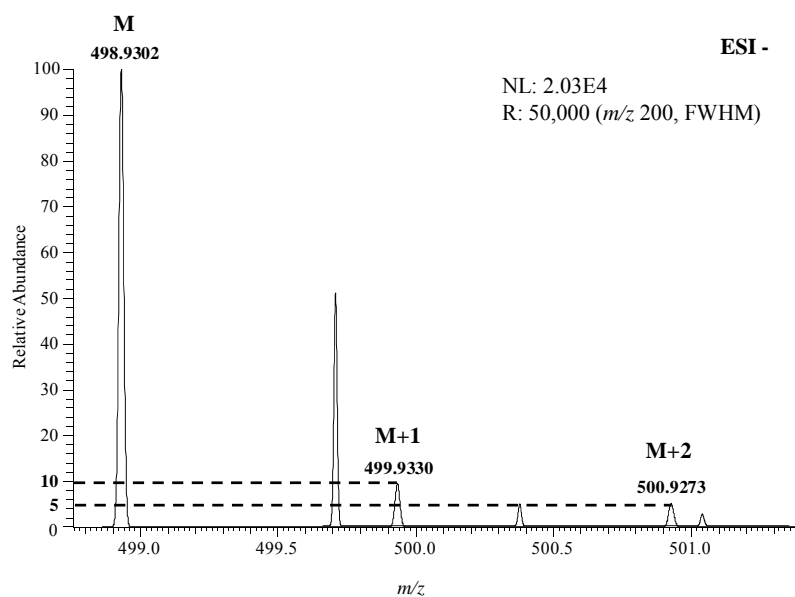


**Figure 6.6.** Experimental spectrum obtained from the analysis of a wastewater sample after liquid-liquid extraction, showing the signal that should be identified ( $m/z$  498.9302) and the isotopic pattern (M+1 and M+2) and the intensities.

**Table 6.3.** Parameters used to generate the list of candidates for the identification of  $m/z$  498.9302.

Parameter		Comment	
Uncertainty (Accuracy and Precision)	< 2ppm	Accuracy and precision obtained with $n=7$ replicates of the calibration levels.	
Ion type / Adduct Formation / Charge	$M^-$ , charge = -1	Negative ESI mode.	
RDBE	Maximum 40	No fullerenes.	
Elements to consider	CHNOPSFCIBrSi	A priori, if no additional information available.	
Restrictions of Elements	Carbon	Maximum: $499 / 12 = 42$ Minimum: 1	Maximum limit for a hypothetical molecule that consists exclusively of carbon.
	Rest	Seven Gold Rules restrictions	A priori, if no additional information available.

If looking for unknowns very general parameters have to be set and restrictions have to be done step by step, after careful observation of the spectra. The main drawback of setting so general parameters is that a large list of candidates is usually obtained. In this example, we get **more than 400 candidates** and the **correct hit is ranked in position 120**. Based on the parameters defined in the text, we can work to refine the list and try to reduce the list (see Table 6.4.).

**Table 6.4.** Parameters used to refine the list of candidates for the identification of  $m/z$  498.9302 (see text).

Parameters	Comment	Reset Parameters		Number of Candidates	Correct hit in position
		Elements to consider			
Nitrogen Rule	$m/z$ 499 $\rightarrow$ N=0 or even number of N atoms. Hypothesis: N=0	Elements to consider	CHOPSFCIBrSi	> 400	22nd
Isotopic pattern	No characteristic isotopic pattern from halogenated atoms	Elements to consider	CHOPSFSi	> 400	9th
Isotopic pattern	Isotopic pattern Si: M+1 and M+2 more intense	Elements to consider	CHOPSF	97	3rd
Isotopic Pattern: M+1	M+1 intensity: principally contribution of $^{13}\text{C}$	Restrictions of Elements	Maximum number of carbons: 10	73	1st
Isotopic Pattern: M+2	M+2 intensity: principally contribution of $^{34}\text{S}$ and $^{18}\text{O}$	Restrictions of Elements	S = 2 and O = 0	No candidates	--
		Restrictions of Elements	S = 1 and O = 1-5	2 candidates	1st
		Restrictions of Elements	S = 0 and O = 22-27	1 candidate	Not the correct one
LEWIS and SENIOR rules	Evaluate the three candidates	The 3 candidates fulfill the rules		3 candidates	--
Database	Search the three candidates	Only 1 candidate found		1 candidate	1st

In this case, detailed observation of the **isotopic pattern** helps to reduce the number of candidates. Halogenated compounds (containing Cl and Br) have a very characteristic pattern, but something similar happens with Si, due to the fact that  $^{29}\text{Si}$  and  $^{30}\text{Si}$  have a natural abundance 4.6 % and 3.1 %, respectively. These significant abundances will definitely contribute to the intensity of M+1 and M+2. Since for the compound of interest M+1 is less than 10% and M+2 is around 5% (Figure 6.6.), the isotopic pattern presents no especial features. That is the reason why the principal hypothesis is that the main contribution for M+1 is due to  $^{13}\text{C}$ . Without taking into consideration the halogenated compounds and Si, we reduce the number of candidates from more than 400 to 97. If we assume that M+1 is principally due to  $^{13}\text{C}$ , we can recalculate the maximum number of carbons, reducing from 42 to 10 the number of carbon atoms.

With the elements in use (CHOPSF) and if we focus in M+2, we can see that the only elements that can contribute to M+2 are S and O (isotope natural abundances,  $^{34}\text{S}$ : 4.5 % and  $^{18}\text{O}$ : 2 %). Based on the fact that M+2 is around 5%, we can have three different scenarios, as shown in Table 6.4. With this three options we end up with 3 candidates (Figure 6.7.).

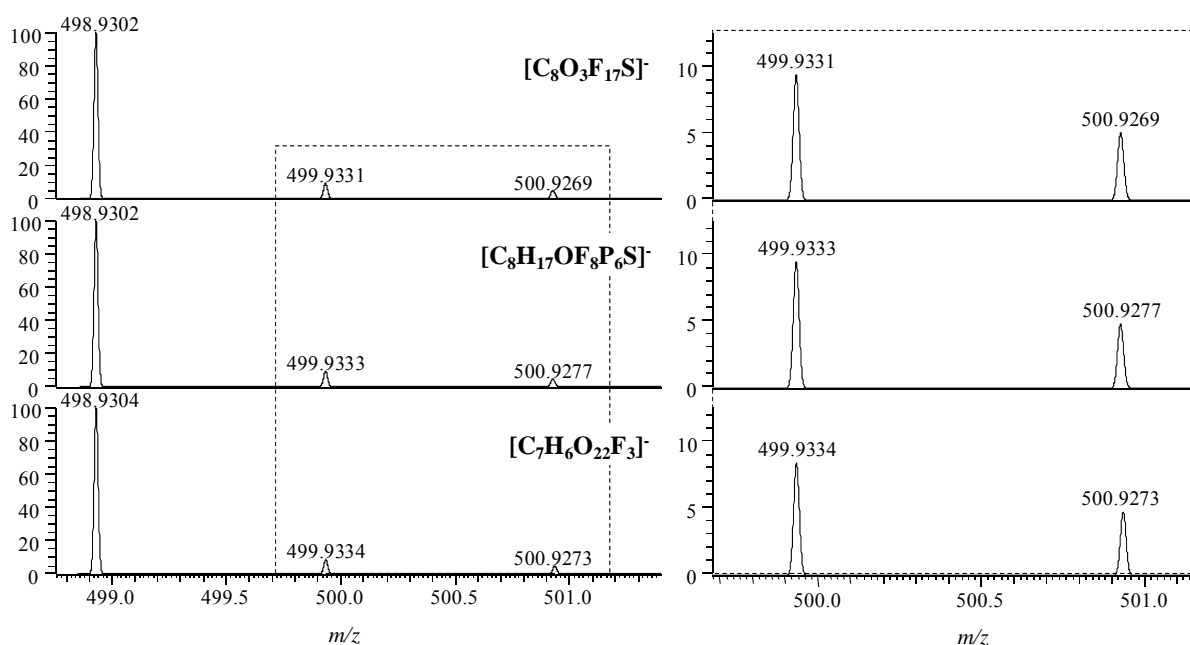


**Figure 6.7.** (Left) Isotopic pattern simulation of the three final candidates. (Right) Zoom of the M+1 and M+2 (nominal mass 500) to show that no difference between the three molecules can be observed.

The isotopic pattern of these compounds show very little differences and there is no easy way to distinguish which is the correct option. At this point, we can check for the SENIOR and LEWIS rules, as well as search in databases. Applying the software developed by Kind et al., (Kind et al., 2007), we checked that both the LEWIS and SENIOR rules are fulfilled. **However, when searching in databases, only the [C8O3F17S] candidate is found. This formula corresponds to the perfluorooctane sulfonate, which is an emerging pollutant that can be for sure present in a wastewater sample. This is the correct hit.**

## **J. Database and Automatic Data Processing**

Using HRMS enables the extraction of thousands of features from environmental samples. However, as it has been demonstrated above, the identification of discriminating signals is the most laborious and time consuming step of accurate mass measurements. It still remains unsolved how to process all the information contained in a high resolved mass spectrum in an automatic and fast way.

One of the reasons why GC/MS has dominated in environmental applications (for quantification and screening purpose) is due to the successful use of mass spectral libraries, such as NIST. Few attempts have been done to have the same for LC/MS. It has been a challenge due to solvent, voltage and temperature effects in adduct formation and ionization efficiencies. Moreover, LC-MS/MS libraries have also been designed, but again the different voltages applied for fragmentation in the cell, change from one instrument to the other. Nowadays, MassBank is one of the free largest tandem mass spectra database available. Apart from these spectral libraries, there are also compound database such as PubChem, Reaxys, Chempidier and KEGG, but usually they do not have spectral information.

At the moment, screening of HRMS fragments with several peaks within a reasonable time frame for automated batch processing and fast database queries is not available, although work is being done in this direction. For instance, MetFrag was designed to generate all possible topological fragments of a candidate compound in order to match the fragment mass with measured peaks (Wolf et al., 2010). More recently, MetFusion has been created to integrate the results from MassBank and MetFrag, so that the

identification can be carried out with the combination of experimental spectral libraries and *in silico* fragmentation (Gerlich et al., 2012).

## V. Instrumentation

Identification and quantification of compounds requires of an appropriate sample preparation (extraction, enrichment, purification) followed by the instrumental analysis, generally coupling gas chromatography (GC), and/or liquid chromatography (LC) to MS, depending on the nature of the compounds. Reasonably, GC or LC play an important role in separation and consequent organic pollutants identification.

Apart from the chromatographic separation, the optimal ionization source should be also identified. There are many different commercially available ion sources for environmental analysis: electron ionization (EI), chemical ionization (CI), negative ion chemical ionization (NICI) and more recently atmospheric pressure chemical ionization (APCI) are used for volatile and semi-volatile compounds eluting from GC; electrospray ionization (ESI), APCI and atmospheric pressure photo ionization (APPI) are used for thermally labile polar and non-polar compounds eluting from LC. Each source varies in its ionization mechanism and consequently the analytical window for each is quite different.

The state of the art in the majority of GC-MS studies is the EI interface. EI is a positive hard ionization source which is highly reproducible. Fragmented spectra are usually obtained and the identification of compounds is based on the use of libraries. However, the extensive fragmentation of the molecule provides no information about the molecular ion ( $M^+$ ), so screening of non-target compounds should be carried out based on the main fragment ion and the availability of the spectra in commercial libraries. Mass spectrometrists have ever been searching for ionization methods softer than EI, because molecular weight determination is of key importance for structure elucidation. The recent use of APCI with eluting compounds from GC, permits to keep the molecular ion intact and facilitates the screening of unknowns based on their accurate mass measurement and molecular formula (Portolés et al., 2011). For LC-MS, ESI is now the ionization method of choice. With this ionization technique the analysis of non-volatile intact molecules can be performed (Kind et al., 2010). Compared to the other interfaces (APCI and APPI), ESI covers with great sensitivity the efficient ionization of a wide variety of chemical

compounds. Moreover, as it is a soft ionization source usually molecular ions ( $[M+H]^+$  /  $[M-H]^-$ ) are obtained, as no or little fragmentation occurs in the ion source. ESI is sensitive to changes in solvent composition and so molecular ions resulting from clusters with sodium or ammonium can occur. Moreover, multiple charged ions can also be formed, which enables the analysis of larger molecules such as peptides or polymers (Cole 1997; Cech et al., 2001; Kebarle et al., 2000).

Moreover, in the last decade new approaches designed for the direct analysis without chromatographic separation have been introduced (Cooks et al., 2006). These approaches, pioneered by Cooks, enable fast analysis without any or minimum sample preparation, which increases the sample throughput. Some of these new ionization techniques are desorption ESI (DESI) (Takáts et al., 2004; Takáts et al., 2005), direct analysis in real time (DART) (Gross 2014), desorption APCI (DAPCI) (Chen et al., 2007) and desorption APPI (DAPPI) (Haapala et al., 2007).

In general, the choice of the ion source has no significant effect on mass measurement accuracy. However, it should be taken into account when selecting the ion source that mass measurement accuracy is directly proportional to mass spectral peak height-to-noise ratio (Chen et al., 1986). As a consequence, any improvement in ionization efficiency should translate into improved mass accuracy.

Once the best ion source has been determined and so ions are to be produced, those are guided through different mechanisms to the mass analyzer. The mass analyzer is the heart of the mass spectrometer and is the place where ions are separated based on their different  $m/z$  ratio.

This chapter focuses on the high resolution mass analyzers (those capable of routine resolution  $> 20,000$  FWHM) for structural characterization and determination of organic pollutants in the environment. Those are double focusing electrostatic/magnetic sector, FT-ICR, TOF and FT-orbitrap mass analyzers. Double focusing electrostatic/magnetic sector instruments have been traditionally used coupled to GC with EI interface. TOF mass analyzers have been coupled to both GC and LC, with several different interfaces. The rest are usually coupled to LC with ESI source or eventually with any other atmospheric pressure ionization interfaces mentioned above (Holčapek et al., 2012). Other analytical mass analyzers, such as quadrupole mass filter, IT and triple quads have

important uses in environmental analysis, but are not optimal for the highest resolution of complex matrixes.

The aim of this section is to give an overview of the main performance characteristics of the mass analyzers used in environmental analysis and complete technical details of all the mass analyzers are out of the scope of this chapter. For this reason, no equations of motion will be included, as they can be found in articles and reviews dedicated exclusively to instrumentation (Marshall et al., 2008; Xian et al., 2012).

### **A. Double-focusing electric/magnetic sector instruments mass analyzer**

Double-focusing electric/magnetic sector instruments, usually named magnetic sectors, are based on measurements of ion deflection (Marshall et al., 2008). The term "double-focusing" refers to the fact that the combination of electrostatic and magnetic sectors focuses ions according to both direction and energy to provide higher resolution. The magnetic sector (B) exerts a force perpendicular to the ion motion to deflect ions according to their momentum. Higher mass ions are deflected less than lower mass ions, so ions are separated only by their masses. To obtain a spectrum of good resolution, the electrostatic sector (E) creates an electric field that exerts a force perpendicular to the ion motion to deflect ions according to their kinetic energy. Two geometries exist from these mass analyzers, depending on the order of the different sectors: EB or BE. Moreover, different combination of magnetic and electrostatic sectors (multi-sectors) as well as combinations with some other mass analyzers (quadrupole, linear IT) were the first hybrid instruments that existed (Gross 2011). Those instruments were replaced, due to space and technical requirements and nowadays the EBE configuration is the one that is most used.

Based on the sectors in the instrument, there are a number of different ways to acquire accurate mass measurements: peak matching, dynamic voltage scanning and magnet scanning (Bristow 2006). Briefly, the different scan modes differ whether the magnetic field is hold constant (peak matching and dynamic voltage scanning) or the magnetic sector is scanned over a wide  $m/z$  range (magnet scanning). As observed in previous studies (Bristow et al., 2003) the accuracy is better when peak matching or dynamic voltage scanning are used, however the  $m/z$  range in these modes are very narrow and lock mass reference is absolutely indispensable.

The coupling of HRGC to HRMS has been an extraordinary tool due to its sensitivity, selectivity, specificity and robustness. It has been for several years the reference instrumentation for analysis of many persistent organic pollutants, especially for dioxins, furans and brominated diphenyl ethers (PBDEs), due to the demand for sensitivity as a consequence of strict regulations and extremely low levels of these compounds in different matrixes. As noted in several reviews the evolution of magnetic sector in the last 10 years has been modest. Some improvements have been done on the amount of sample injected (Li et al., 2009) and/or the simultaneous GC analysis (Medeiros et al., 2007), however no improvements have been achieved on the mass analyzer itself. This technique need very expertise operator, expensive maintenance for optimum performance, large space and complementary accessories. For these reasons, magnetic sectors are no longer attractive to laboratories and users tend to replace this instrumentation for alternative techniques, such as TOF and triple quads (Hernández et al., 2012).

### **B. Fourier transform ion cyclotron resonance mass analyzer**

Introduced in 1974 (Comisarow et al., 1974), FT-ICR MS has evolved (Marshall 2000; Marshall et al., 2002) to become the highest resolution broadband mass analysis technique (Marshall et al., 1998; Marshall et al., 2008).

The principle of the FT-ICR analyzer is based on the circular oscillation that charged ions exhibit in the ICR cell once they are introduced into a homogeneous magnetic field. The circular motion defined by a cyclotron frequency is specific to each  $m/z$ . Linearity of detection and very high fidelity in the determination of frequency are inherent to FT instruments and allow very high mass accuracy (Scigelova et al., 2011). The cyclotron frequency varies as  $(m/z)^{-1}$ , (Marshall et al., 1998) and as a result the ICR mass resolution varies as  $(m/z)^{-1}$ .

FT-ICR mass analyzer is a pulsed detector. Because ion introduction is often temporally continuous (e.g. ESI), ions are typically accumulated externally during detection of ions from the preceding accumulation period (Senko et al., 1997). In FTICR, ions are externally accumulated in a multipole electric ion trap and simultaneously ejected toward the ICR cell. Ions should enter the ICR cell at low kinetic energies, so that they can be confined. Afterwards ions are coherently excited to a larger radius for a signal to be detected. The detection is carried out in the ICR cell-wall where the detector plates are

placed, in order to induce a measurable image current and transformed into mass spectra using fast FT (Perry et al., 2008).

Resolution, mass accuracy, scan rate,  $m/z$  range and dynamic range are proportional to magnetic field (B) strength. ICR mass resolution and scan rate increases proportional to B, whereas mass accuracy, dynamic range, and upper  $m/z$  limit increases as  $B^2$  (Marshall 1996; Schaub et al., 2008).

As a consequence, FT-ICR instruments with stronger magnetic field would increase resolution. Vacuum of  $10^{-9}$  to  $10^{-10}$  Torr is required to achieve HR, vacuum requirements being more stringent for higher-field magnets. Another way to increase the resolution is to allow for longer transient acquisitions. However, longer acquisitions times might not be always practical, particularly in the case of coupling to LC. The magnetic field strength in commercially available FT-ICR instruments range from 7 to 15 Tesla (T) and 21 T systems are under construction at the USA National High Magnetic Field Laboratory and Pacific Northwest National Laboratory (Xian et al., 2012).

Although FT-ICR instruments detect ions of a wide  $m/z$  range simultaneously, they present a limitation for the lower masses. Compared to modern TOF instruments that can detect ions starting from  $m/z$  20 or the orbitrap that can detect ions starting from  $m/z$  50, modern FT-ICR instruments are confined to lower mass limit of  $m/z$  125. As explained above, the cyclotron frequency has an inverse non linear relationship with  $m/z$ , so very low masses are not easily excited for detection in the ICR cell. Moreover, in order to maintain the superior mass accuracy and resolution of FT-ICR mass analyzers, sampling rates  $> 1.6$  scans /second are shown to be necessary (Forcisi et al., 2013), which makes it incompatible to UHPLC or even HPLC. As a consequence the coupling of LC to FT-ICR cannot be optimally performed.

The stored waveform inverse Fourier transform (SWIFT) mode is used to excite the ions in the ICR cell for detection, as well as to perform ion isolation before MS/MS analysis in the ICR cell. To perform MS/MS experiments and carry out fragmentation in the ICR cell, gas has to be admitted and pressure in the cell has to be raised. However, for the accurate mass measurements, enough time needs to be allowed for the gas to be dissipated and the ICR cell to return to the low pressure required for excitation and detection. It is much more practical to carry out collision-induced dissociation (CID) outside of the ultra-high vacuum region in an external analyzer or collision cell. In fact,

the commercially available FT-ICR instruments are presented as an hybrid that consists of a linear IT or a quadrupole coupled to a FT-ICR mass analyzer. Progress is expected in the direction of higher field magnets for FT-ICR, which will allow to significantly increase resolution at a given acquisition time.

FT-ICR mass analyzer presents an unsurpassed high accuracy and resolution. However, the large size, complexity, maintenance and cost restrict the laboratory settings where it can be used. In many cases, their applications have involved extremely complex samples, such as molecular characterization of NOM (Koch et al., 2008, Hertkorn et al., 2008; Hertkorn et al., 2013), aerosols (Schmitt-Kopplin et al., 2010), diesel fuel (Hughey et al., 2001), the analysis of samples without pre-treatment such as wine (Cooper et al., 2001), and the application in areas such as metabolomics and proteomics (Witt et al., 2001).

### **C. Time of flight mass analyzer**

TOF mass analyzers are conceptually simple and are based on measurements of time of transit. Ions of the same initial position and velocity can be simultaneously accelerated (by a pulsed direct-current electric field), and then allowed to fly freely (i.e., no external electric or magnetic fields) to a detector located some meters away, along the tube of flight (Marshall et al., 2008). It will take different time for each ion to reach the detector, depending on their  $m/z$ . Based on the way it works, TOF mass analyzers are inherently fast and sensitive because all masses are measured simultaneously (i.e., the multiplex advantage), compared to scanning instruments (e.g. sectors and quadrupoles) that sequentially focus only one ion mass on the detector while all others are lost (Marshall et al., 2008).

The TOF mass analyzer, initially projected by Stephan in 1946 (Mirsaleh-Kohan et al., 2008) and reduced to practice in 1948 (Cameron et al., 1948) has evolved in the last twenty years and since then TOF has been considered a high resolution mass analyzer and has been used for accurate mass measurements. For TOF, mass resolution is related to time of flight, so increasing the flight time, permitted to improve resolution. Delayed ion extraction, orthogonal ion introduction and kinetic energy focusing by use of a reflectron introduced by Mamyryn in 1973 (Mamyryn 2001; Guilhaus 1995), were some of the main improvements carried out in TOF technology. Nowadays, manufacturers claim that with high field pusher and dual stage reflectrons, commercial TOF mass analyzers can reach

mass resolution of 40,000 (FWHM) (Pringle et al., 2007; Ow et al., 2010). Recent advances described TOF mass analyzers capable of attaining mass resolution of 50,000 or higher, with the multipass (Toyoda et al., 2003; Shchepunov et al., 2010; Ioanoviciu 2010; Verentchikov et al., 2011) and spiral (Sato et al., 2007) designs (Xian et al., 2012). The great speed of mass spectral acquisition is one of the main advantages of TOF analyzers, especially when coupled to GC and UHPLC. In fact, these fast scanning rates is what makes this mass analyzer at the eyes of some researchers and vendors as suitable as higher resolution mass analyzers, such as FT-ICR or orbitrap. In fact, TOF mass analyzers may have more stable characteristics (better sensitivity and similar mass accuracy) than FT-ICR at high sampling rates (Forcisi et al., 2013).

For daily routine analysis, broadband mass resolution of 10,000 - 40,000 and RMS mass accuracy of 1-10 ppm may be attained. However, it should be highlighted that the mass accuracy may differ depending on the improved calibration routines. In most of the studies, internal calibration of mass spectrometers based on TOF technology has been reported (Wu et al., 2003; Stroh et al., 2007; Mol et al., 2008; Orтели et al., 2009; Kaufmann et al., 2008; Wang et al., 2009). The drift in the mass measurements in these mass analyzers may be important, mainly due to environmental factors, which lead to instability of the calibration. However, as instrumentation evolves extremely fast, new TOFs utilize advanced temperature compensation systems leading to better routine mass measurement accuracy.

Based on TOF technology, the development of the hybrid Q-TOF and TOF-TOF mass spectrometer has also revolutionized the application of TOF to accurate mass measurement with the possibility to perform MS/MS experiments (Wolff et al., 2001; Ibañez et al., 2005; Wang et al., 2009). Although the hybrid models provide additional versatility, the analytical performance and fundamental principles of operation of TOF are the same. TOF-TOF is restricted to metabolomics and proteomics applications and it is not so widely used in environmental analysis. Following the coherence of the present chapter this hybrid mass spectrometer will not be described. Both TOF and Q-TOF have been widely used for target analysis and screening purposes in environmental field (Hayward et al., 2009; Hernández et al., 2007; Portolés et al., 2011; Lebedev et al., 2013). However, Q-TOF permits the integration of MS/MS or MS<sup>E</sup> experiments (acquisition is carried out at low and high collision energies within the same chromatographic run). The main advantage of Q-TOF are high sensitivity, mass resolution and mass accuracy of the

resulting tandem mass spectra in both precursor (MS) and product ion (MS/MS) modes (Chernushevich et al., 2001).

#### **D. Fourier transform Orbitrap mass analyzer**

The orbitrap, the newest FT mass analyzer, invented in 1999 (Makarov 2000) has been widely distributed since its commercial introduction in 2005, with the launching of the LTQ-Orbitrap tandem mass spectrometer at the ASMS Conference in San Antonio (Hu et al., 2005).

The original roots of the orbitrap stem from the principle of orbital trapping, the ability to trap charged particles in electrostatic fields, defined by Kingdon in 1923 (Kingdon 1923) and bears a similarity to two types of ion-trapping mass analyzers, the Paul trap (quadrupole ion trap), and the FT-ICR (Hu et al., 2005). Alexander Makarov used the term “Orbitrap” to describe the harmonic oscillations of the ions in this new mass analyzer.

The orbitrap confines ions in an electrostatic quadrol logarithmic potential well created between carefully shaped coaxial central and outer electrodes. In the absence of superconducting magnet (Ham 2008; Perry et al., 2008), ion stability is achieved only due to ions orbiting around an axial electrode. Orbiting ions perform harmonic oscillations along the electrode with frequency proportional to  $(m/z)^{-1/2}$ . As a result, the mass resolution in orbitrap is proportional to  $(m/z)^{-1/2}$  (Perry et al., 2008). In the orbitrap, the axial frequency is used to derive the  $m/z$  ratio, since it is independent of the initial properties of the ions. It is this independence that is responsible for the high resolution and mass accuracy of the orbitrap (Makarov 2000). These oscillations are detected using image current detection and are transformed into mass spectra using fast FT, similarly to FT ICR.

Like FT-ICR, orbitrap mass analyzer is a pulsed detector, but in this case ions are collected in a “C” trap, and injected simultaneously toward the orbitrap (Perry et al., 2008). This method provides fast and uniform injection for large ion populations. Automatic gain control (AGC) target and maximum injection time are parameters typically found in ITs, that should be also appropriately selected in the orbitrap (Kaufmann et al., 2010). AGC target and maximum ion time is used to control the number of ions and maximum time taken to fill the "C" trap, respectively.

The orbitrap mass analyzer affords outstanding performance with respect to mass accuracy, resolution, sensitivity and dynamic range. The orbitrap has proven to be a robust mass analyzer that can routinely deliver HR and mass accuracy. Mass inaccuracy is typically < 5 ppm for externally calibrated mass spectra and < 2 ppm for internally calibrated mass spectra (Marshall et al., 2008), but demonstrated to be as low as 0.2 ppm under favorable conditions (Perry et al., 2008). In the commercial orbitrap instruments, resolution can be switched in discrete steps. The resolution is controlled by varying the transient acquisition time (which changes the overall scan cycle time). To yield higher resolution values, higher scan times should be employed, such as for resolution of 100,000 ( $m/z$  400 FWHM) employs 1.9 sec scan cycle time, whereas for a resolution of 60,000 uses 1 sec.

As a result, some applications restricted until the moment to FT-ICR can be transferred to orbitrap analyzers, such as proteomics, metabolomics and NOM characterization. The main advantage is that orbitrap does not need such an expensive and delicate maintenance compared with FT-ICR (Cortés-Francisco, 2011).

Since the first commercial LTQ-Orbitrap, different orbitrap based mass spectrometers have been designed. For simplicity, it can be said that three different configurations can be found. The single-stage Orbitrap HCD mass spectrometer, the hybrid quadrupole-Orbitrap HCD mass spectrometer and the hybrid linear ion trap-Orbitrap HCD mass spectrometer. Although the hybrid models provide additional versatility to MS/MS experiments, the analytical performance and fundamental principles of operation of the orbitrap analyzers in all the instruments are identical (Perry et al., 2008). Currently, there are several commercial orbitrap instruments and even instruments with the same configuration present different technical specifications (resolution, fragmentation techniques, accuracy) depending on the specific model. Recent design of orbitrap mass analyzer consisted in increased field strength inside the orbitrap that has allowed to significantly increase resolution at a given acquisition time (Makarov et al., 2009b). As described elsewhere (Forcisi et al., 2013), the orbitrap is a formidable alternative to TOF and FT-ICR mass analyzers as it closes the gap between the two mass analyzers.

Although the orbitrap is coupled to LC a study presented a modification of a LTQ-orbitrap hybrid instrument for high-mass accuracy and GC/HRMS. With the development of a new scan sequence (the nested scan), mass accuracy less than 1 ppm with internal calibration and resolution exceeding 100,000 were routinely achievable. In combination

with isotopic distribution information, the GC-orbitrap facilitates the unambiguous determination of small molecule elemental compositions and meets the mass spectral requirements of challenging EPA methods (Peterson et al., 2010). The GC-orbitrap will represent a significant step forward in the field of GC/HRMS, at the moment basically dominated by magnetic sectors and TOF analyzers.

### **E. Hybrid Mass Spectrometers**

There have been enormous advances in HR instrumentation in recent years, including hybrid mass spectrometers. Readers can refer to an in-depth review surrounding the development of hybrid instruments over the last 30 years (Glish et al., 2008). However, some last models may be missing, such is the case for the hybrid quadrupole-Orbitrap HCD mass spectrometer, as it was first commercially available in 2011. The technique requires two mass analyzers in series (or a single mass analyzer that can be used sequentially) to analyze the precursor and product ions (Kind et al., 2010).

Generally speaking, the hybrid instruments provide the possibility to acquire data with different modes of operation, which include precursor ion scans, product ion scans, neutral loss scans and selected reaction monitoring. The different modes of operation, are discussed in De Hoffmann (De Hoffmann 1996). It should be highlighted that the final and quality of information obtained in each case, may differ depending on the mass analyzers forming the hybrid instrument. CID is the most common technique to obtain tandem mass spectra. Precursor ion stability and internal energy under CID have also been previously discussed (Kertesz et al., 2009).

Ideally, last generation hybrid TOF and orbitrap mass analyzers have to obtain accurate masses at  $MS^n$  level (Fjeldsted 2009; Glish et al., 2008), without losing sensitivity, acquisition rate, resolution and mass accuracy. Nowadays with UHPLC, chromatographic peaks can be around 30s or lower and it may be difficult to obtain full scan spectra and tandem mass spectra (MS/MS) or  $MS^n$  scans (Bedair et al., 2008; Staack et al., 2007) with enough points-per-peak.

Data-dependent acquisition mode can help to have enough time to perform additional MS/MS scans. The mass analyzers operate at full scan (or SIM) and by data-dependant, a fixed number of peaks selected from a survey scan using predetermined rules are selected and the corresponding ions are subjected to MS/MS analysis (Murray, 2010). The

predetermined rules may include a list of  $m/z$  precursors, reject list, dynamic exclusion, signal-to-noise threshold, loop count and multiplex (Kumar et al., 2013; Michalski et al., 2011). The data-dependent mode may seem a semi-automatic way of performing MS/MS spectra. However, meticulous optimization of some parameters is crucial, to prevent the mass analyzer to perform MS/MS spectra of a solvent or contaminant ion, especially when ions are co-eluting.

## **VI. Environmental applications**

In environmental analysis, usually the main goal of any target analysis is the identification and quantification of pollutants, and so the main benefit of using HRMS is to have better detection limits and less interferences. Basically the gain of a HRMS-based method compared to a triple quad is the fact that one is so much more sure of the fact that the compound is really "the compound".

However, for some applications is not only an advantage but a real need. This is the case for the analysis of toxins, for which there are so many varieties and no standards, NOM characterization, metabolites and transformation products (DBPs, ozone derivative compounds).

The examples given below using GC-HRMS or LC-HRMS have been chosen to illustrate the advantages and need of using HRMS in front of other techniques.

### **A. GC-HRMS applications**

One of the reasons why GC/MS has dominated in environmental applications is due to the successful use of mass spectral libraries (Lebedev et al., 2013). Moreover, working in selected ion monitoring (SIM) mode high sensitivity can be obtained. However, some analysis required lower detection limits and mass resolution, due to co-elution in chromatography. Such is the case for PBDEs, chlorinated biphenyl congeners (PCBs), dioxins and furans. The Environmental Protection Agency (EPA) methods for the analysis of these compounds require the use of double-focusing electric/magnetic sector instruments (US EPA 1994; US EPA 2007; US EPA 2008). Apart from some legal requirements, double-focusing electric/magnetic sector instruments have been used to solve some other environmental issues. Due to chromatographic co-elution of some

congeners of polychlorinated terphenyls the use of HR was mandatory to resolve interferences in the detection and measurement (Caixach et al., 1994). With more than 670 compounds, toxaphene analysis was difficult due to the complexity of the mixture. No complete chromatographic resolution was achieved and HRMS better than 10,000 (at 10% valley) was necessary (Santos et al., 1997). Another application in which double-focusing electric/magnetic sector instruments were used is the analysis of nitrosamines (Ontario Ministry of Environment 2007; Planas et al., 2008). However, in this case compare to dioxins the use of magnetic sector is not required and in fact EPA proposed a new approach using GC-MS/MS and CI (US EPA 2004) as well as some others that have been recently published (Yoon et al., 2012). Similar method detection limits have been achieved in the methods using HRMS and MS/MS. The fact that GC-MS/MS is more available than magnetic sectors will increase the number of methods quoting MS/MS, when similar performance methods can be achieved, as in this case.

Despite its low dynamic range and sensitivity, GC-TOF have also been reported for the quantitative analysis of pesticides, PBDEs and PCBs (Hayward et al., 2009; Hernández et al., 2007) trying to be a substitute to magnetic sectors. The main advantage of developing a quantitative method for organic pollutants using GC-TOF is that full scan data is acquired and the same injection can be used for screening purposes and elucidation of non-target compounds. In this sense, GC-TOF can be a real alternative to double-focusing electric/magnetic sector instruments (Hernández et al., 2012). Several studies reported the use of TOF and Q-TOF analyzers for identifying contaminants and degradation products in the environment (Hernández et al., 2007; Portolés et al., 2011). In the study from Lebedev et al., (Lebedev et al., 2013) for target and non-target analysis of semi-volatile compounds in snow samples, the use of GC-TOF compared to GC/MS identification (only based on mass spectral libraries) prevent from carrying out a false assignment. In the examples cited above, the identification of the compounds is based on the elemental formula of several ions, in combination with the previous mass spectral list obtained from libraries or using any other software, except for Portolés et al., which introduced several other rules (e.g. carbon filtering, maximum mass error based on previous experience, isotopic pattern for some halogens). The resolution that can be reached by the instruments used ranged from 7,000 to 25,000 (FWHM), although it varies along the mass range and for the moment any resolution below 20,000 (FWHM) should not be considered HR. As the readers will notice these references are older than the ones reported for LC-MS

applications (see below) and in general for the last 10 years HRMS coupled to GC has offered less innovation. Although TOF technology have improved in the last years, HRMS applications are always more related to LC than GC, also due to the fact that for the moment orbitrap has been basically coupled to LC (except for the study from Peterson et al., (Peterson et al., 2010).

### **B. LC-HRMS applications**

Contrary to what happens with GC-HRMS, in general sensitivity has been criticize when using LC-HRMS in front of LC-MS/MS. Many studies claimed the limitations for instruments such as TOF and Q-TOF to achieve as good detection limits and linearity as those achieved by triple quads (Hernández et al., 2004; Krauss et al., 2010). However, with the new Q-TOF and orbitrap mass analyzers, these deficiencies have been overcome and detection limits are equal or better when using HRMS. For instance, the target analysis of cytostatic compounds in wastewater treatment plants has been carried out using both HRMS and MS/MS. In this case, the orbitrap mass analyzer in full scan and AIF modes have been used, acquiring at 2 spectra/second working with HR (R: 50,000  $m/z$  200, FWHM). Compared to a triple quad, we have obtained very good linearity and as good instrument detection limits, but better specificity, because both precursor and fragment ions are measured using HRMS (Gómez-Canela et al., 2013). In fact, hidden interferences from the matrices will contribute to the integrated peak for the target compound and there is a serious risk of having a case of overquantitation or false assignment (Scigelova et al., 2011; Kumar et al., 2013). Some readers will disagree with the statements proposed above and will claim that better specificity in MS/MS can be obtained when monitoring more transitions per compound, without the necessity to buy new HRMS instrumentation. In many cases HRMS is not absolutely mandatory, although it is of no doubt that when using HRMS for target analysis, interferences are better resolved and quantification can be carried out easily. In contrast, there are some environmental applications in which HR is much more essential.

One of these fields that can take advantage of using HRMS is the determination of toxins. In a recent study, the determination of marine toxins using HRMS has been carried out (Domènech et al., 2013). Quantification and confirmation criteria have been proposed and discussed, due to the fact that legislation has not been updated and several different

strategies are found in literature (Mol et al., 2012), compared to MS/MS (Pitarch et al., 2007; Gerssen et al., 2010). Apart from the sensitivity of the developed method, it should be highlighted that the specificity of the technique permitted to resolve matrix interferences as shown in Figure 6.8.

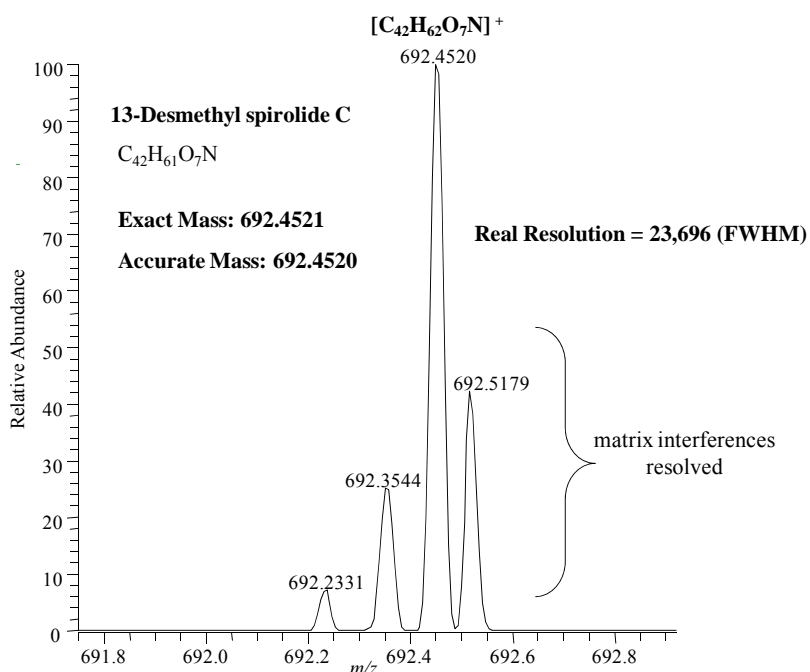


**Figure 6.8.** 13-Desmethylspirolide C spectrum ( $m/z$  692.4521) at 0.18 pg/L in mussel.

Apart from sensitivity and selectivity, one of the main advantages of using HRMS is the fact that data acquisition is carried out in full scan mode. We obtain the complete mass spectra of the molecular and fragment ions, when working in AIF with orbitrap or  $MS^E$  with TOF, because no precursor selection is done. From these data, retrospective analysis can be conducted and compounds chemically related to the target analytes can be found.

The potential of using HRMS and the possibility to work in full scan mode instead of MS/MS is given with an "in-house" example of algae extracts. A routine method was developed and validated using LC-MS/MS for the analysis of the toxin cylindrospermopsin (CYN) in algae bloom (Guzmán-Guillén et al., 2012). The same samples used in the study by Guzmán-Guillén et al., were voluntarily supplied by Dra. Ana Cameán and were analyzed using HRMS. Essentially, we received the extracts and worked on the optimization of the instrumental conditions. After LC separation with an Hypercarb column, MS analyses were carried out with an Orbitrap-Exactive HCD equipped with an ESI source. CYN is ionized in positive or negative mode, but during

method development better limits of quantification in negative mode were obtained. Thus, the molecular ion ( $m/z$  414.1090) for quantification and two fragment ions ( $m/z$  272.0710 and  $m/z$  96.9601) for confirmation were chosen (Figure 6.9.). Two scan events were defined: full scan and AIF (HCD 50eV) working in high resolution ( $R$ : 50,000  $m/z$  200, FWHM) with mass accuracy and precision better than 2 ppm.

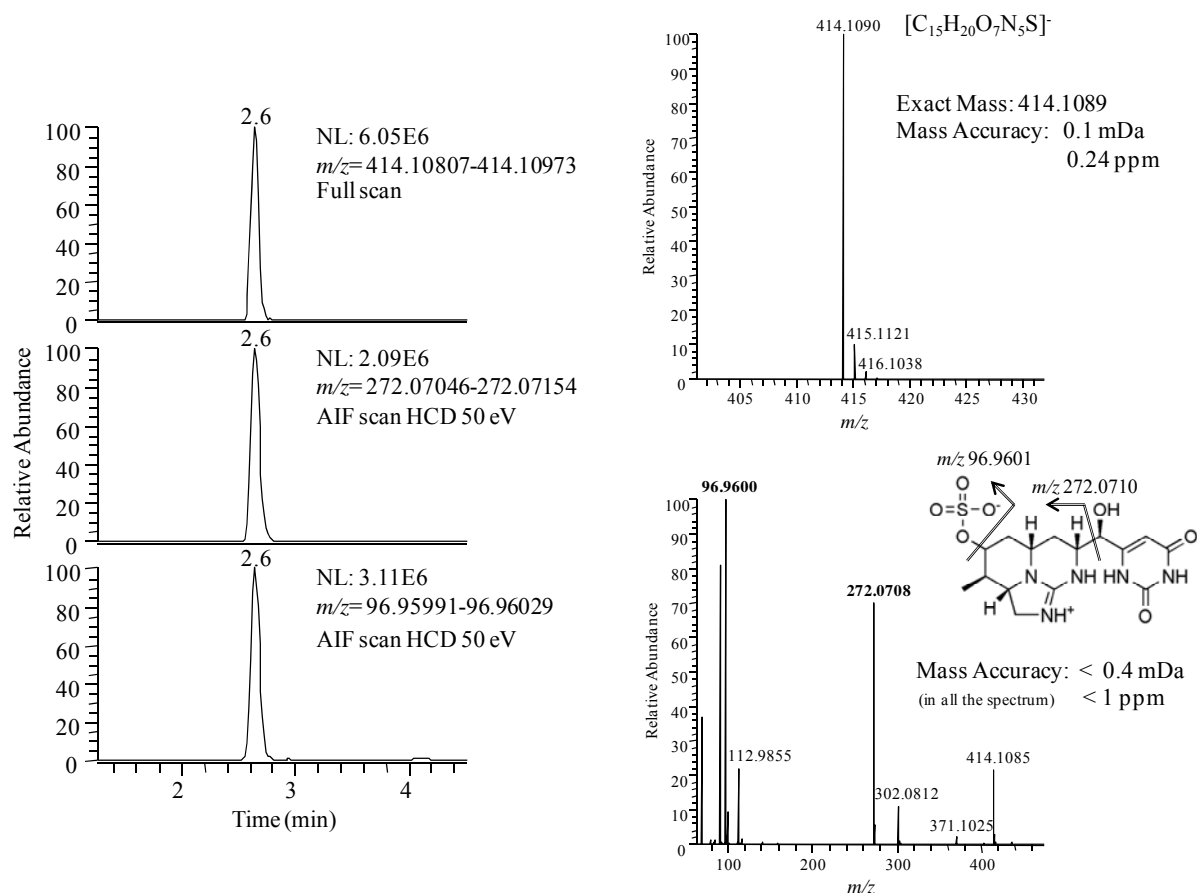


**Figure 6.9.** (Left) Extracted ion chromatogram for the molecular ion  $m/z$  414.1090 and two fragment ions ( $m/z$  272.0710 and  $m/z$  96.9601) of CYN (0.1  $\mu\text{g/L}$  standard) with mass tolerance of 2 ppm (based on uncertainty of the measurements). (Right) Full scan spectrum and AIF spectrum showing the different fragments on the molecule for CYN.

CYN was detected and confirmed in the samples, due to presence of the molecular ion and two fragment ions in the retention time ( $t_R$ : 2.6 min) of the standard (Figure 6.10.). In addition, a chromatographic peak coming after the CYN ( $t_R$ : 2.9 min) was detected in the AIF scan event. The unknown compound presented the two fragment ions characteristic of CYN, so we assumed that it might be a chemically related compound. Retrospective analysis of the full scan event revealed a molecular ion with  $m/z$  398.1142.

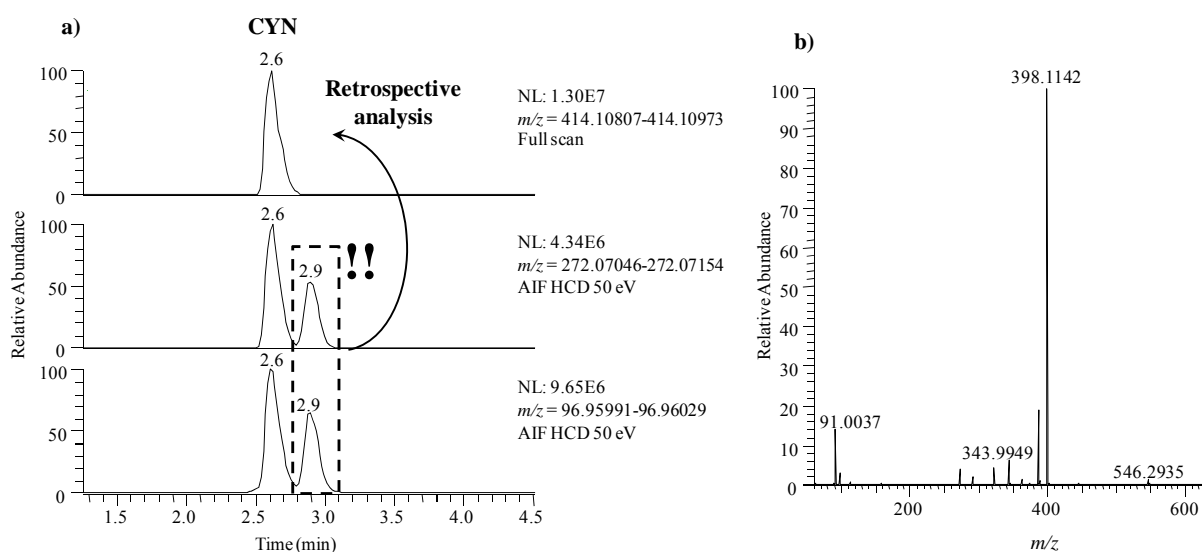


**Figure 6.10.** a) Extracted ion chromatogram for the molecular ion  $m/z$  414.1090 and two fragment ions ( $m/z$  272.0710 and  $m/z$  96.9601) of CYN (sample A) with mass tolerance of 2 ppm (based on uncertainty of the measurements). A chromatographic peak coming after the CYN ( $t_R$ : 2.9 min) was detected in the AIF scan event. The unknown compound presented the two fragment ions characteristic of CYN. b) Full scan mass spectrum showing the molecular ion obtained from the retrospective analysis of the full scan event. This peak was identified as deoxy-CYN.

This peak in the full scan event corresponded to the  $m/z$  of CYN with a mass difference of 15.9948, which matched with an O atom. Based on the accurate mass measurement ( $m/z$  398.1142) and the two fragment ions that corresponded to the same fragments as for CYN ( $m/z$  96.9601 [ $\text{HO}_4\text{S}^-$ ] and  $m/z$  272.0710 [ $\text{C}_{10}\text{H}_{14}\text{O}_4\text{N}_3\text{S}^-$ ]) the new compound was identified as deoxy-cylindrospermopsin, a variety of cyanobacterial toxin already described in the literature (Dell'Aversano et al., 2004). A false negative result was avoided, and not only CYN but also deoxy-CYN were found and quantified in several samples, as standards for CYN and deoxy-CYN are available (Figure 6.11.). However, there are several toxins that have been reported, but there are not standards available. In this sense, HRMS is essential for preliminary identification.

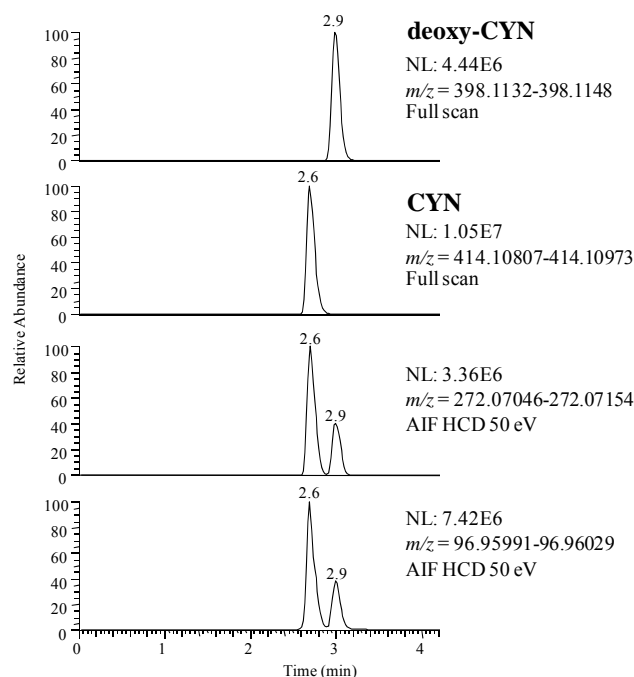


**Figure 6.11.** Extracted ion chromatogram for the molecular ion  $m/z$  398.1142 (deoxy-CYN) and  $m/z$  414.1090 (CYN) and the two characteristic fragment ions ( $m/z$  272.0710 and  $m/z$  96.9601) from a real sample. Mass tolerance of 2 ppm (based on uncertainty of the measurements).

In this example a huge peak was easily detected in the AIF spectrum, so the elemental formula determination of this single compound was fast. As mentioned above, the main bottleneck in the screening experiments is the identification of unknown compounds. This is the case in fields such as metabolomics and proteomics (and all the "omics" science), but we also have a similar challenge in environmental analysis with NOM characterization. Not surprisingly, the characterization of NOM has been one of the fields that has significantly progressed in the last years, thanks to the evolution of HRMS. NOM characterization can consist on bulk parameters such as total organic carbon, dissolved organic carbon and spectroscopy techniques such as, ultraviolet and visible absorption spectroscopy, specific UV-absorbance and excitation emission matrix fluorescence spectroscopy (Matilainen et al., 2011). However, high-field NMR spectroscopy and FT-ICR MS have been powerful discovery tools (Hertkorn et al., 2013). Based on these techniques, molecular level NOM composition and structure exhibit far more variance than anticipated from more uniform bulk parameters, which are subjected to intrinsic averaging (Hertkorn et al., 2007).

The properties and amount of dissolved organic matter (DOM) in natural waters can significantly affect the production of drinking water as it may cause adverse aesthetic qualities such as color, taste and odor. The use of HRMS have shown the effect of water treatment processes on DOM, such as activated carbon adsorption, ozonation or membrane treatments (Herzprung et al., 2012; Zhang et al., 2012a; Zhang et al., 2012b; Cortés-Francisco, et al., 2013). Based on HRMS, it has been shown that DOM can serve as main precursor of disinfection by-products (DBPs) during chlorination (Hua et al., 2007; Richardson et al., 2007), as DOM molecules with a low degree of oxidation (low O/C) were found to be more reactive toward chlorine (Zhang et al., 2012b, Lavonen et al., 2013) and new DBPs have been characterized. Identification and formula determination is based on ultrahigh resolution ( $R > 100,000$  FWHM), sub-ppm accuracy on accurate mass measurements and posterior strategies to filter the list of candidates obtained, i.e. elements in use, isotopic pattern and element ratios. Due to the amount of information obtained from each analysis, the representation of the data is usually done based on van Krevelen diagrams, as mentioned above. More recently, statistical analysis have been applied to compare the data obtained by FT-ICR and bring out hidden correlations (Sleighter et al., 2010).

## VIII. References

1. Balogh, M. P. (2004) Debating resolution and mass accuracy. *LCGC Europe* 17(3), 152–159.
2. Bedair, M., Sumner, L.W. (2008) Current and emerging mass spectrometry technologies for metabolomics. *Trends in Analytical Chemistry* 27(3):238–250.
3. Beynon, J.H. (1954). Qualitative analysis of organic compounds by mass spectrometry. *Nature* 174, 735–37.
4. Beynon, J.H. (1960) *Mass Spectrometry and Its Applications to Organic Chemistry*, 1st edn. Elsevier, London.
5. Brenton, A., Godfrey, A., (2010) Accurate mass measurement: Terminology and treatment of data. *Journal of The American Society for Mass Spectrometry* 21(11), 1821-1835.

6. Bristow, A. W. T.; Webb, K. S. (2003) Intercomparison study on accurate mass measurement of small molecules in mass spectrometry. *Journal of the American Society for Mass Spectrometry* 14(10), 1086-1098.
7. Bristow, A.W.T. (2006) Accurate mass measurement for the determination of elemental formula—A tutorial. *Mass Spectrometry Reviews* 25(1), 99-111.
8. Brunnée, C. (1987) The ideal mass analyzer: Fact or fiction? *International Journal of Mass Spectrometry and Ion Processes* 76(2), 125-237.
9. Caixach, J., Rivera, J., Galceran, M.T., Santos, F.J. (1994) Homologue distributions of polychlorinated terphenyls by high-resolution gas chromatography and high-resolution mass spectrometry. *Journal of Chromatography A* 675, 205-211.
10. Cameron, A. E.; Eggers, D. F. (1948) Ion velocitron. *Review of Scientific Instruments* 19, 605–607.
11. Cech, N. B., Enke, C. G. (2001) Practical implications of some recent studies in electrospray ionization fundamentals. *Mass Spectrometry Reviews* 20(6), 362-387.
12. Chen, L., Cottrell, C.E. and Marshall, A.G. (1986) Effect of signal-to-noise ratio and number of data points upon precision in measurement of peak amplitude, position and width in fourier transform spectrometry. *Chemometrics and Intelligent Laboratory Systems* 1(1), 51-58.
13. Chen, H.; Zheng, J.; Zhang, X.; Luo, M.; Wang, Z.; Qiao, X. (2007) Surface desorption atmospheric pressure chemical ionization mass spectrometry for direct ambient sample analysis without toxic chemical contamination. *Journal of Mass Spectrometry* 42, 1045-1056.
14. Chernushevich, I. V., Loboda, A. V., Thomson, B. A. (2001) An introduction to quadrupole–time-of-flight mass spectrometry. *Journal of Mass Spectrometry* 36(8), 849-865.
15. Cole B. R. (1997) *Electrospray ionization mass spectrometry. Fundamentals, Instrumentation and Applications.* Wiley Interscience.
16. Comisarow, M.B. and Marshall, A.G. (1974) Fourier transform ion cyclotron resonance spectroscopy. *Chemical Physics Letters* 25(2), 282-283.

17. Cooks, R.G., Ouyang, Z., Takáts, Z., Wiseman, J.M. (2006) Ambient mass spectrometry. *Science* 311, 1566.
18. Cooper, H.J. and Marshall, A.G. (2001) Electrospray Ionization Fourier Transform Mass Spectrometric Analysis of Wine. *Journal of Agricultural and Food Chemistry* 49(12), 5710-5718.
19. Cortés-Francisco, N., Flores, C., Moyano, E. and Caixach, J. (2011) Accurate mass measurements and ultrahigh-resolution: evaluation of different mass spectrometers for daily routine analysis of small molecules in negative electrospray ionization mode. *Analytical and Bioanalytical Chemistry* 400(10), 3595-3606.
20. Cortés-Francisco, N., Caixach, J. (2013) Molecular Characterization of Dissolved Organic Matter through a Desalination Process by High Resolution Mass Spectrometry. *Environmental Science & Technology* 47(17), 9619-9627.
21. De Hoffmann, E. (1996) Tandem mass spectrometry: a primer. *Journal of Mass Spectrometry* 31(2), 129–137.
22. Dell'Aversano, C.; Eaglesham, G.K.; Quilliam, M.A. (2004) Analysis of cyanobacterial toxins by hydrophilic interaction liquid chromatography–mass spectrometry. *Journal of Chromatography A* 1028, 155-164.
23. Domènech, A., Cortés-Francisco, N., Palacios, O., Franco, J.M., Riobó, P., Llerena, J.J., Stefania Vichi and Caixach, J. (2013) Determination of lipophilic marine toxins in mussels. Quantification and confirmation criteria using high resolution mass spectrometry. *Journal of Chromatography A*. doi: 10.1016/j.chroma.2013.12.071
24. European Commission, (2002) Decision 2002/657/EC, *Off. J. Eur. Commun.* 221, 8.
25. European Commission, (2012) Directorate General Health and Consumer Protection, SANCO/12495/2011.
26. Fjeldsted, J.C. (2009) Accurate mass measurements with orthogonal axis time-of-flight mass spectrometry. In: Ferrer I, Thurman EM (eds) *Liquid chromatography time-of-flight mass spectrometry*. Wiley, New York.
27. Forcisi, S., Moritz, F., Kanawati, B., Tziotis, D., Lehmann, R. and Schmitt-Kopplin, P. (2013) Liquid chromatography-mass spectrometry in metabolomics research: Mass analyzers in ultra high pressure liquid chromatography coupling. *Journal of Chromatography A* 1292(0), 51-65.

28. Gelpí E (2008) From large analogical instruments to small digital black boxes: 40 years of progress in mass spectrometry and its role in proteomics. Part I 1965–1984. *Journal of Mass Spectrometry* 43(4), 419–435.
29. Gelpí, E. (2009) From large analogical instruments to small digital black boxes: 40 years of progress in mass spectrometry and its role in proteomics. Part II 1985–2000. *Journal of Mass Spectrometry* 44(8), 1137-1161.
30. Gerlich, M. and Neumann, S. (2012) MetFusion: integration of compound identification strategies. *Journal of Mass Spectrometry* 48(3), 291-298.
31. Gerssen, A., van Olst, E.H., Mulder, P.P., de Boer, J. (2010) In-house validation of a liquid chromatography tandem mass spectrometry method for the analysis of lipophilic marine toxins in shellfish using matrix-matched calibration. *Analytical and Bioanalytical Chemistry* 397, 3079-3088.
32. Glish, G.L., Burinsky, D.J. (2008) Hybrid mass spectrometers for tandem mass spectrometry. *Journal of the American Society for Mass Spectrometry* 19(2), 161–172.
33. Godfrey, A. and Brenton, A. (2012) Accurate mass measurements and their appropriate use for reliable analyte identification. *Analytical and Bioanalytical Chemistry* 404(4), 1159-1164.
34. Gómez-Canela, C., Cortés-Francisco, N., Ventura, F., Caixach, J. and Lacorte, S. (2013) Liquid chromatography coupled to tandem mass spectrometry and high resolution mass spectrometry as analytical tools to characterize multi-class cytostatic compounds. *Journal of Chromatography A* 1276(0), 78-94.
35. Gross, J.H. (2011) *Mass Spectrometry*. 2nd Edition Springer. Heidelberg, Germany.
36. Gross, J.H. (2014) Direct analysis in real time-a critical review on DART-MS. *Analytical and Bioanalytical Chemistry* 406(1), 63-80.
37. Guilhaus, M. (1995) Principles and Instrumentation in Time-of-flight Mass Spectrometry. *Journal of Mass Spectrometry* 30, 1519-1532.
38. Guzmán-Guillén, R., Prieto, A.I., Gustavo, A., Soria-Díaz, M.E., Cameán, A.M. (2012) Cylindrospermopsin determination in water by LC-MS/MS: Optimization and validation of the method and application to real samples. *Environmental Toxicology and Chemistry* 31, 2233–2238.

39. Haapala, M., Pól, J., Saarela, V., Arvola, V., Kotiaho, T., Ketola, R.A., Franssila, S., Kauppila, T.J. and Kostianen, R. (2007) Desorption Atmospheric Pressure Photoionization. *Analytical Chemistry* 79(20), 7867-7872.
40. Ham, B.M. (2008) *Even Electron Mass Spectrometry with Biomolecule Applications*, 1st edn. Wiley Interscience, United States of America.
41. Hayward, D.G., Wong, J.W. (2009) Organohalogen and Organophosphorous Pesticide Method for Ginseng Root — A Comparison of Gas Chromatography-Single Quadrupole Mass Spectrometry with High Resolution Time-of-Flight Mass Spectrometry. *Analytical Chemistry* 81(14), 5716-5723.
42. Hernández, F., Ibáñez, M., Sancho, J.V., Pozo, O.J. (2004) Comparison of Different Mass Spectrometric Techniques combined with Liquid Chromatography for Confirmation of Pesticides in Environmental Water Based on the Use of Identification Points. *Analytical Chemistry* 76, 4349-4357.
43. Hernández, F., Portolés, T., Pitarch, E., López, F.J. (2007) Target and Nontarget Screening of Organic Micropollutants in Water by Solid-Phase Microextraction Combined with Gas Chromatography/High-Resolution Time-of-Flight Mass Spectrometry. *Analytical Chemistry* 79(24), 9494-9504.
44. Hernández, F., Sancho, J.V., Ibáñez, M., Abad, E., Portolés, T. and Mattioli, L. (2012) Current use of high-resolution mass spectrometry in the environmental sciences. *Analytical and Bioanalytical Chemistry* 403(5), 1251-1264.
45. Herniman, J.M., Langley, G.J., Bristow, T.W.T. and O'Connor, G. (2005) The Validation of Exact Mass Measurements for Small Molecules Using FT-ICRMS for Improved Confidence in the Selection of Elemental Formulas. *Journal of the American Society for Mass Spectrometry* 16(7), 1100-1108.
46. Hertkorn, N., Ruecker, C., Meringer, M., Gugisch, R., Frommberger, M., Perdue, E., Witt, M. and Schmitt-Kopplin, P. (2007) High-precision frequency measurements: indispensable tools at the core of the molecular-level analysis of complex systems. *Analytical and Bioanalytical Chemistry* 389(5), 1311-1327.
47. Hertkorn, N., Frommberger, M., Witt, M., Koch, B.P., Schmitt-Kopplin, P. and Perdue, E.M. (2008) Natural Organic Matter and the Event Horizon of Mass Spectrometry. *Analytical Chemistry* 80(23), 8908-8919.

48. Hertkorn, N., Harir, M., Koch, B.P., Michalke, B. and Schmitt-Kopplin, P. (2013) High-field NMR spectroscopy and FTICR mass spectrometry: powerful discovery tools for the molecular level characterization of marine dissolved organic matter. *Biogeosciences* 10(3), 1583-1624.
49. Herzsprung, P., Hertkorn, N., Friese, K. and Schmitt-Kopplin, P. (2010) Photochemical degradation of natural organic sulfur compounds (CHOS) from iron-rich mine pit lake pore waters – an initial understanding from evaluation of single-elemental formulae using ultra-high-resolution mass spectrometry. *Rapid Communications in Mass Spectrometry* 24(19), 2909-2924.
50. Herzsprung, P.; von Tümpling, W.; Hertkorn, N.; Harir, M.; Büttner, O.; Bravidor, J.; Friese, K.; Schmitt-Kopplin, P., (2012) Variations of DOM Quality in Inflows of a Drinking Water Reservoir: Linking of van Krevelen Diagrams with EEMF Spectra by Rank Correlation. *Environmental Science & Technology* 46(10), 5511-5518.
51. Holčapek, M., Jirásko, R. and Lída, M. (2012) Recent developments in liquid chromatography-mass spectrometry and related techniques. *Journal of Chromatography A* 1259(0), 3-15.
52. Hu, Q., Noll, R. J., Li, H., Makarov, A., Hardman, M., Cooks, R.G. (2005) The Orbitrap: a new mass spectrometer. *Journal of Mass Spectrometry* 40(4), 430–443.
53. Hua, G.; Reckhow, D. A. (2007) Characterization of disinfection byproduct precursors based on hydrophobicity and molecular size. *Environmental Science & Technology* 41, 3309–3315.
54. Hughey CA, Hendrickson CL, Rodgers RP, Marshall AG (2001) Elemental composition analysis of processed and unprocessed diesel fuel by electrospray ionization Fourier transform ion cyclotron resonance mass spectrometry. *Energy Fuels* 15(5), 1186–1193.
55. Ioanoviciu, D. (2010) The spiral main path electric deflector as a time-of-flight mass analyzer. *International Journal of Mass Spectrometry* 290, 145–147.
56. Ibañez, M., Sancho, J.V., Pozo, O.J., Niessen, W., Hernández, F. (2005) Use of quadrupole time-of-flight mass spectrometry in the elucidation of unknown compounds present in environmental water. *Rapid Communications in Mass Spectrometry* 19, 169–178.

57. Kaufmann, A., Butcher, P., Maden, K., Widmer, M. (2008) Quantitative multiresidue method for about 100 veterinary drugs in different meat matrices by sub 2- $\mu$ m particulate high-performance liquid chromatography coupled to time of flight mass spectrometry. *Journal of Chromatography A* 1194, 66-79.
58. Kaufmann, A., Widmer, M., Maden, K., (2010) Post-interface signal suppression, a phenomenon observed in a single-stage Orbitrap mass spectrometer coupled to an electrospray interfaced liquid chromatography. *Rapid Communications in Mass Spectrometry* 24(14), 2162-2170.
59. Kaufmann, A., (2012) The current role of high-resolution mass spectrometry in food analysis. *Analytical and Bioanalytical Chemistry*, 403, (5), 1233-1249.
60. Kebarle, P. and Peschke, M. (2000) On the mechanisms by which the charged droplets produced by electrospray lead to gas phase ions. *Analytica Chimica Acta* 406(1), 11-35.
61. Kertesz, T.M., Hall, L.H., Hill, D.W., Grant, D.F. (2009) CE50: quantifying collision induced dissociation energy for small molecule characterization and identification. *Journal of the American Society for Mass Spectrometry* 20(9), 1759–1767.
62. Kim, S., Kramer, R.W., Hatcher, P.G. (2003) Graphical method for analysis of ultrahigh-resolution broadband mass spectra of natural organic matter, the Van Krevelen Diagram. *Analytical Chemistry* 75, 5336–5344.
63. Kind, T. and Fiehn, O. (2007) Seven Golden Rules for heuristic filtering of molecular formulas obtained by accurate mass spectrometry. *BMC Bioinformatics* 8(1), 105.
64. Kind, T. and Fiehn, O. (2010) Advances in structure elucidation of small molecules using mass spectrometry. *Bioanalytical Reviews* 2(1), 23-60.
65. Kingdon, K.H. (1923) A method for the neutralization of electron space charge by positive ionization at very low gas pressures. *Physical Review* 21, 408–418.
66. Koch, B.P., Ludwichowski, K.-U., Kattner, G., Dittmar, T. and Witt, M. (2008) Advanced characterization of marine dissolved organic matter by combining reversed-phase liquid chromatography and FT-ICR-MS. *Marine Chemistry* 111(3-4), 233-241.
67. Krauss, M., Singer, H. and Hollender, J. (2010) LC-high resolution MS in environmental analysis: from target screening to the identification of unknowns. *Analytical and Bioanalytical Chemistry* 397(3), 943-951.

68. Kumar, P., Rúbies, A., Centrich, F., Granados, M., Cortés-Francisco, N., Caixach, J., Companyó, R. (2013) Targeted analysis with benchtop quadrupole-orbitrap hybrid mass spectrometer: Application to determination of synthetic hormones in animal urine. *Analytica Chimica Acta* 780, 65-73.
69. Lebedev, A.T., Polyakova, O.V., Mazur, D.M. and Artaev, V.B. (2013) The benefits of high resolution mass spectrometry in environmental analysis. *Analyst* 138(22), 6946-6953.
70. Li, Y., Whitaker, J.S., McCarty, C.L. (2009) New Advances in Large-Volume Injection Gas Chromatography-Mass Spectrometry. *Journal of Liquid Chromatography & Related Technologies*, 32:11-12, 1644-1671.
71. Makarov, A. (2000) Electrostatic Axially Harmonic Orbital Trapping: A High-Performance Technique of Mass Analysis. *Analytical Chemistry* 72(6), 1156.
72. Makarov A. (2009a) Invited Presentation, 18th International Mass Spectrometry Conference, Bremen.
73. Makarov, A., Denisov, E., Lange, O. (2009b) Performance Evaluation of a High-field Orbitrap Mass Analyzer. *Journal of the American Society for Mass Spectrometry* 20(8), 1391-1396.
74. Mamyurin, B.A. (2001) Time-of-flight mass spectrometry (concepts, achievements, and prospects). *International Journal of Mass Spectrometry* 206(3), 251-266.
75. Marshall, A.G. (1996) Ion Cyclotron Resonance and Nuclear Magnetic Resonance Spectroscopies: Magnetic Partners for Elucidation of Molecular Structure and Reactivity. *Accounts of Chemical Research* 29(7), 307-316.
76. Marshall, A.G., Hendrickson, C.L. and Jackson, G.S. (1998) Fourier transform ion cyclotron resonance mass spectrometry: A primer. *Mass Spectrometry Reviews* 17(1), 1-35.
77. Marshall, A.G. (2000) Milestones in fourier transform ion cyclotron resonance mass spectrometry technique development. *International Journal of Mass Spectrometry* 200 (1-3), 331-356.
78. Marshall, A.G. and Hendrickson, C.L. (2002) Fourier transform ion cyclotron resonance detection: principles and experimental configurations. *International Journal of Mass Spectrometry* 215(1-3), 59-75.

79. Marshall, A.G. and Hendrickson, C.L. (2008) High-Resolution Mass Spectrometers. *Annual Review of Analytical Chemistry* 1(1), 579-599.
80. Matilainen, A.; Gjessing, E. T.; Lahtinen, T.; Hed, L.; Bhatnagar, A.; Sillanpää, M. (2011) An overview of the methods used in the characterization of natural organic matter (NOM) in relation to drinking water treatment. *Chemosphere* 83(11), 1431-1442.
81. Medeiros, P.M., Simoneit, B.R.T. (2007) Gas chromatography coupled to mass spectrometry for analyses of organic compounds and biomarkers as tracers for geological, environmental, and forensic research. *Journal of Separation Science* 30 (10), 1516–1536.
82. Michalski, A., Damoc, E., Hauschild, J.-P., Lange, O., Wiegand, A., Makarov, A., Nagaraj, N., Cox, J., Mann, M., Horning, S. (2011) Mass spectrometry-based proteomics using Q Exactive, a high-performance benchtop quadrupole Orbitrap mass spectrometer. *Molecular & Cellular Proteomics* 10.9.
83. Mirsaleh-Kohan, N., Robertson, W.D., Compton, R.N. (2008) Electron ionization time-of-flight mass spectrometry: Historical review and current applications. *Mass Spectrometry Reviews* 27, 237-285.
84. Mol, H.G.J., Plaza-Bolaños, P., Zomer, P., de Rijk, T.C., Stolker, A.A.M., Mulder, P.P.J. (2008) Toward a Generic Extraction Method for Simultaneous Determination of Pesticides, Mycotoxins, Plant Toxins, and Veterinary Drugs in Feed and Food Matrixes. *Analytical Chemistry* 80(24), 9450-9459.
85. Mol, H.J., Zomer, P., Koning, M. (2012) Qualitative aspects and validation of a screening method for pesticides in vegetables and fruits based on liquid chromatography coupled to full scan high resolution (Orbitrap) mass spectrometry. *Analytical and Bioanalytical Chemistry* 403, 2891-2908.
86. Murray, K. K. (2010) Glossary of terms for separations coupled to mass spectrometry. *Journal of Chromatography A* 1217(25), 3922-3928.
87. Murray, K. K., Boyd, R. K., Eberlin, M. N., Langley, G. J., Li, L., Naito, Y. (2013) Definitions of terms relating to mass spectrometry (IUPAC Recommendations 2013). *Pure and Applied Chemistry (IUPAC)*, 85 (7), 1515-1609.
88. Ontario Ministry of Environment (2007) The Determination of N-nitrosamines in Water by Gas Chromatography-High Resolution Mass Spectrometry (GC/HRMS), NITROSO-E3388, Toronto, Canada.

89. Ortelli, D., Cognard, E., Jan, P., Edder, P. (2009) Comprehensive fast multiresidue screening of 150 veterinary drugs in milk by ultra-performance liquid chromatography coupled to time of flight mass spectrometry. *Journal of Chromatography B* 877, 2363-2374.
90. Ow, S.Y., Noirel, J., Salim, M., Evans, C., Watson, R., Wright, P.C. (2010) Balancing robust quantification and identification for iTRAQ: application of UHR-ToF MS. *Proteomics* 10(11), 2205–2213.
91. Perry, R.H., Cooks, R.G. and Noll, R.J. (2008) Orbitrap mass spectrometry: Instrumentation, ion motion and applications. *Mass Spectrometry Reviews* 27(6), 661-699.
92. Peterson, A.C., McAlister, G.C., Quarmby, S.T., Griep-Raming, J. and Coon, J.J. (2010) Development and Characterization of a GC-Enabled QLT-Orbitrap for High-Resolution and High-Mass Accuracy GC/MS. *Analytical Chemistry* 82(20), 8618-8628.
93. Pitarch, E., Medina, C., Portolés, T., López, F.J., Hernández, F. (2007) Determination of priority organic micro-pollutants in water by gas chromatography coupled to triple quadrupole mass spectrometry. *Analytical ChimicaActa* 583(2), 246-58.
94. Planas, C., Palacios, Ó., Ventura, F., Rivera, J. and Caixach, J. (2008) Analysis of nitrosamines in water by automated SPE and isotope dilution GC/HRMS: Occurrence in the different steps of a drinking water treatment plant, and in chlorinated samples from a reservoir and a sewage treatment plant effluent. *Talanta* 76(4), 906-913.
95. Portolés, T., Pitarch, E., López, F.J., Hernández, F. and Niessen, W.M.A. (2011) Use of soft and hard ionization techniques for elucidation of unknown compounds by gas chromatography/time-of-flight mass spectrometry. *Rapid Communications in Mass Spectrometry* 25(11), 1589-1599.
96. Pringle, S.D., Giles, K., Wildgoose, J.L., Williams, J.P., Slade, S.E., Thalassinos, K., Bateman, R.H., Bowers, M.T., Scrivens, J.H. (2007) An investigations of the mobility separation of some peptide and protein ions using a new hybrid quadrupole/travelling wave IMS/oa-TOF instrument. *International Journal of Mass Spectrometry* 261, 1–12.
97. Quenzer, T.L., Robinson, J.M. Bolanios, B., Milgram, E. and Greig, M.J. (2002) Automated accurate mass analysis using FT-ICR mass spectrometry. *Proceedings of the 50<sup>th</sup> Annual Conference on Mass Spectrometry and Allied Topics*, Orlando, FL.

98. Richardson, S. D.; Plewa, M. J.; Wagner, E. D.; Schoeny, R.; DeMarini, D. M. (2007) Occurrence, genotoxicity, and carcinogenicity of regulated and emerging disinfection by-products in drinking water: A review and roadmap for research. *Mutation Research/Reviews in Mutation Research* 636(1-3), 178-242.
99. Santos, F.J., Galceran, M.T., Caixach, J., Rivera, J., Huguet, X. (1997) Characterization of Toxaphene by High Resolution Gas Chromatography Combined with High Resolution Mass Spectrometry and Tandem Mass Spectrometry. *Rapid Communications in Mass Spectrometry* 11, 341-348.
100. Satoh, T., Sato, T., Tamura, J. (2007) Development of a High-Performance MALDI-TOF Mass Spectrometer Utilizing a Spiral Ion Trajectory. *Journal of the American Society for Mass Spectrometry* 18, 1318–1323.
101. Schaub, T.M., Hendrickson, C.L., Horning, S., Quinn, J.P., Senko, M.W. and Marshall, A.G. (2008) High-Performance Mass Spectrometry: Fourier Transform Ion Cyclotron Resonance at 14.5 Tesla. *Analytical Chemistry* 80(11), 3985-3990.
102. Schmitt-Kopplin, P., Gelencsér, A., Dabek-Zlotorzynska, E., Kiss, G., Hertkorn, N., Harir, M., Hong, Y. and Gebefügi, I. (2010) Analysis of the Unresolved Organic Fraction in Atmospheric Aerosols with Ultrahigh-Resolution Mass Spectrometry and Nuclear Magnetic Resonance Spectroscopy: Organosulfates As Photochemical Smog Constituents. *Analytical Chemistry* 82(19), 8017-8026.
103. Scigelova, M., Hornshaw, M., Giannakopoulos, A. and Makarov, A. (2011) Fourier Transform Mass Spectrometry. *Molecular & Cellular Proteomics* 10(7).
104. Senko, M.W., Hendrickson, C.L., Emmett, M.R., Shi, S.D.H. and Marshall, A.G. (1997) External Accumulation of Ions for Enhanced Electrospray Ionization Fourier Transform Ion Cyclotron Resonance Mass Spectrometry. *Journal of the American Society for Mass Spectrometry* 8(9), 970-976.
105. Shchepunov, V., Berdnikov, A., Lzumi, H., Giles, R., Gall, N. (2010) Proceedings of the 58th ASMS Conference on Mass Spectrometry & Allied Topics, Salt Lake City, UT, May 23–27.
106. Sleighter, R.L., Liu, Z., Xue, J. and Hatcher, P.G. (2010) Multivariate Statistical Approaches for the Characterization of Dissolved Organic Matter Analyzed by Ultrahigh

- Resolution Mass Spectrometry. *Environmental Science & Technology* 44(19), 7576-7582.
107. Staack, R.F., Hopfgartner, G. (2007) New analytical strategies in studying drug metabolism. *Analytical and Bioanalytical Chemistry* 388(7), 1365–1380.
108. Stenson, A. C., Marshall, A. G., Cooper, W. T. (2003) Exact Masses and Chemical Formulas of Individual Suwannee River Fulvic Acids from Ultrahigh Resolution Electrospray Ionization Fourier Transform Ion Cyclotron Resonance Mass Spectra. *Analytical Chemistry* 75(6), 1275-1284.
109. Stroh, J.G., Petucci, C.J., Brecker, S.J., Huang, N., Lau, J.M. (2007) Automated sub-ppm mass accuracy on an ESI-TOF for use with drug discovery compound libraries. *Journal of the American Society for Mass Spectrometry* 18(9), 1612–1616.
110. Takáts Z, Wiseman JM, Gologan B, Cooks RG. (2004) Mass spectrometry sampling under ambient conditions with desorption electrospray ionization. *Science* 306, 471.
111. Takáts, Z., Wiseman, J.M. and Cooks, R.G. (2005) Ambient mass spectrometry using desorption electrospray ionization (DESI): instrumentation, mechanisms and applications in forensics, chemistry, and biology. *Journal of Mass Spectrometry* 40(10), 1261-1275.
112. Toyoda, M., Okumura, D., Ishihara, M., Katakuse, I. (2003) Multi-turn time-of-flight mass spectrometers with electrostatic sectors. *Journal of Mass Spectrometry* 38, 1125–1142.
113. U.S. EPA. (1994) Method 1613: Tetra- through Octa-Chlorinated Dioxins and Furans by Isotopic Dilution HRGC/HRMS. EPA: Washington, DC.
114. U.S. EPA. (2004) Method 521. Determination of Nitrosamines in Drinking Water by Solid Phase Extraction and Capillary Column Gas Chromatography with Large Volume Injection and Chemical Ionization Tandem Mass Spectrometry (MS/MS). EPA/600/R-05/054, Cincinnati.
115. U.S. EPA. (2007) Method 1614: Brominated Diphenyl Ethers in Water, Soil, Sediment, and Tissue by HRGC/HRMS. EPA: Washington, DC.
116. U.S. EPA. (2008) Method 1668, Revision B: Method 1668B Chlorinated Biphenyl Congeners in Water, Soil, Sediment, Biosolids, and Tissue by HRGC/HRMS. EPA: Washington, DC.

117. Verentchikov, A. N., Yavor, M. I. (2011) Quasi-Planar Multi-Reflecting Time-of-Flight Mass Spectrometer. United States Patent, US 2011/ 01086729 A1.
118. Vichi, S., Cortés-Francisco, N. and Caixach, J. (2013) Determination of volatile thiols in lipid matrix by simultaneous derivatization/extraction and liquid chromatography-high resolution mass spectrometric analysis. Application to virgin olive oil. *Journal of Chromatography A* 1318(0), 180-188.
119. Wang, J., Leung, D. (2009) Applications of Ultra-performance Liquid Chromatography Electrospray Ionization Quadrupole Time-of-Flight Mass Spectrometry on Analysis of 138 Pesticides in Fruit- and Vegetable-Based Infant Foods. *Journal of Agricultural and Food Chemistry* 57, 2162-2173.
120. Webb K., B.T., Sargent M., Stein B. (2004) Methodology for Accurate Mass Measurement of Small Molecules. Best Practice Guide. LGC Ltd, London.
121. Witt M, Fuchser J, Baykut G (2001) Fourier transform ion cyclotron resonance mass spectrometry with nanolc/microelectrospray ionization and matrix-assisted laser desorption/ionization: analytical performance in peptide mass fingerprint analysis. *Journal of the American Society for Mass Spectrometry* 1, 553–561.
122. Wolf, S., Schmidt, S., Muller-Hannemann, M. and Neumann, S. (2010) In silico fragmentation for computer assisted identification of metabolite mass spectra. *BMC Bioinformatics* 11(1), 148.
123. Wolff, J.C., Eckers, C., Sage, A.B., Giles, K., Bateman, R. (2001) Accurate mass liquid chromatography/mass spectrometry on quadrupole orthogonal acceleration time-of-flight mass analyzers using switching between separate sample and reference sprays. 2. Applications using the dual-electrospray ion source. *Analytical Chemistry* 73, 2605–2612.
124. Wu, J., McAllister, H. (2003) Exact mass measurement on an electrospray ionization time-of-flight mass spectrometer: error distribution and selective averaging. *Journal of Mass Spectrometry* 38(10), 1043–1053.
125. Xian, F., Hendrickson, C.L. and Marshall, A.G. (2012) High Resolution Mass Spectrometry. *Analytical Chemistry* 84(2), 708-719.

126. Yoon, S., Nakada, N. and Tanaka, H. (2012) A new method for quantifying N-nitrosamines in wastewater samples by gas chromatography-triple quadrupole mass spectrometry. *Talanta* 97(0), 256-261.
127. Zhang, H.; Zhang, Y.; Shi, Q.; Ren, S.; Yu, J.; Ji, F.; Luo, W.; Yang, M. (2012a) Characterization of low molecular weight dissolved natural organic matter along the treatment trait of a waterworks using Fourier transform ion cyclotron resonance mass spectrometry. *Water Research* 46(16), 5197-5204.
128. Zhang, H.; Zhang, Y.; Shi, Q.; Hu, J.; Chu, M.; Yu, J.; Yang, M. (2012b) Study on Transformation of Natural Organic Matter in Source Water during Chlorination and Its Chlorinated Products using Ultrahigh Resolution Mass Spectrometry. *Environmental Science & Technology* 46(8), 4396-4402.

### **2.2.2. Research Article Nº 1**

Nuria Cortés-Francisco, Cintia Flores, Encarnación Moyano and Josep Caixach

Accurate Mass Measurements and Ultrahigh-Resolution: Evaluation of Different Mass Spectrometers for Daily Routine Analysis of Small Molecules in Negative Electrospray Ionization Mode.

*Analytical and Bioanalytical Chemistry* **2011**, 400, (10), 3595-3606.



# Accurate mass measurements and ultrahigh-resolution: evaluation of different mass spectrometers for daily routine analysis of small molecules in negative electrospray ionization mode

Nuria Cortés-Francisco · Cintia Flores · Encarnación Moyano · Josep Caixach

Received: 11 February 2011 / Revised: 16 April 2011 / Accepted: 19 April 2011 / Published online: 8 May 2011  
© Springer-Verlag 2011

**Abstract** Six mass spectrometers based on different mass analyzer technologies, such as time-of-flight (TOF), hybrid quadrupole-TOF (Q-TOF), orbitrap, Fourier transform ion cyclotron resonance (FT-ICR), and triple quadrupole (QqQ), installed at independent laboratories have been tested during a single day of work for the analysis of small molecules in negative electrospray ionization (ESI) mode. The uncertainty in the mass measurements obtained from each mass spectrometer has been determined by taking the precision and accuracy of replicate measurements into account. The present study is focused on calibration processes (before, after, and during the mass measurement), the resolving power of the mass spectrometers, and the data processing for obtaining elemental formulae. The mass range between  $m/z$  100 and 600 has been evaluated with a mix of four standards. This mass range includes small molecules usually detected in food and environmental samples. Negative ESI has been tested as there is almost no data on accurate mass (AM) measurements in this mode. Moreover, it has been used because it is the ESI mode for analysis of many compounds, such as pharmaceutical, herbicides, and fluorinated compounds. Natural organic matter has been used to demonstrate the significance of ultrahigh-resolution in complex mixtures. Sub-millidalton accuracy and precision have been obtained with Q-TOF,

FT-ICR, and orbitrap achieving equivalent results. Poorer accuracy and precision have been obtained with the QqQ used: 11 mDa root-mean-square error and 6–11 mDa standard deviation. Some advice and requirements for daily AM routine analysis are also discussed here.

**Keywords** Ultrahigh-resolution · Accurate mass measurements · Molecular formulae determination · Small organic compounds · TOF · Orbitrap

## Introduction

The determination of accurate mass (AM) is used to confirm elemental formulae of compounds. Since Aston (1927), magnetic sectors have been the mass analyzers dominating the scene of AM measurements. In the 1950s, John Beynon explained for the first time that, if the mass of an ion from a chemical compound was determined with sufficient accuracy, the elemental composition of this compound could be determined [1]. At that moment, the availability of such measurements was limited due to the cost and complexity of the instrumentation [2, 3].

However, AM measurements are no longer restricted to magnetic sectors, and a wide variety of mass analyzers have been designed and improved for this purpose [2]. Currently, time-of-flight (TOF), hybrid quadrupole-TOF (Q-TOF), Fourier transform ion cyclotron resonance (FT-ICR), and recently introduced orbitrap are instruments capable of performing better accuracy and providing higher resolving power.

TOF is an attractive instrument due to its potentially unlimited  $m/z$  range and high-speed acquisition capabilities [2]. Moreover, with the latest TOF mass spectrometers, mass resolving power as high as 40,000 (full width at half

N. Cortés-Francisco · C. Flores · J. Caixach (✉)  
Mass Spectrometry Laboratory/Organic Pollutants, IDAEA-CSIC,  
Jordi Girona 18,  
08034 Barcelona, Spain  
e-mail: josep.caixach@idaea.csic.es

E. Moyano  
Department of Analytical Chemistry, University of Barcelona,  
Martí i Franquès 1–11, Diagonal 647,  
08028 Barcelona, Spain

maximum (FWHM),  $m/z$  922) and accuracy of <1 ppm are possible [4, 5]. Based on TOF technology, the development of the hybrid Q-TOF mass spectrometer has also revolutionized the application of TOF to AM measurement with the possibility to perform tandem mass experiments [6–8]. In most of the studies, internal calibration of TOF and Q-TOF mass analyzers has been reported, as the drift in the mass measurements in these mass analyzers is important. This is mainly due to environmental factors, which lead to instability of the calibration and the necessity to daily recalibrate the mass spectrometer [9]. However, as instrumentation evolves extremely fast, last-generation TOFs utilize new generations of detectors and thermal expansion-corrected analyzer tubes leading to better routine mass measurement accuracy.

FT-ICR presents an unsurpassed high accuracy and resolving power. However, the large size, complexity, maintenance, and cost of this mass analyzer restrict the laboratory setting where it can be used. In many cases, their applications have involved extremely complex samples, such as raw seawater, which contains natural organic matter (NOM) at a very low concentration. In these samples, more than 1,000 different compounds were resolved in the range from  $m/z$  100 to 700, with as many as six resolved ions at each nominal mass [10–12]. Some other complex analytical problems would be diesel fuel [13], the analysis of samples without pre-treatment such as wine [14], and the application in areas such as metabolomics and proteomics [15].

Usually, QqQ mass analyzers are defined as low-resolution mass spectrometers and thus not usually considered as tools for AM measurement. However, quadrupole mass analyzers have been used some times [2], and in fact, they have obtained really good results in AM measurement intercomparison [16]. Last-generation triple quadrupoles with hyperbolic rods have been designed to be capable of recording AM measurements and performing enhanced resolution.

A more recent mass analyzer has been introduced to the market: the orbitrap. This mass analyzer achieves very high mass resolution without the need of a superconducting magnet [17, 18]. As a result, some applications restricted until the moment to FT-ICR (TOF analyzers have not been used, due to lack of resolving power) can be transferred to orbitrap analyzers, such as proteomics, metabolomics, and NOM characterization. The main advantage is that orbitrap does not need such an expensive and delicate maintenance compared with FT-ICR.

As can be seen in the literature, there are many applications for which AM measurement is required. However, in a previous study [16], a lack of understanding (particularly amongst newer users) has been detected. More recently, guidance for terminology and treatment of data has been also published [19] concerning the number of

publications quoting AM data, in which some terms are used inconsistently.

The aim of this study was to evaluate the AM measurement carried out by instruments based on different mass analyzer technologies during a single day of work for routine analysis of small molecules in negative ESI mode. Other studies have been carried out before, comparing different instrumentation [20, 21]. Those previous reports pay special attention to AM measurement of a single mass. In this current study, the AM measurement in a range of masses ( $m/z$  100–600) has been evaluated, taking into account the calibration processes (before, after, and during the mass measurement), the resolving power of the mass spectrometer and the data processing for obtaining elemental formulae [20].

## Experimental section

### Instrumentation

Different mass spectrometers have been used during the present study, but two common characteristics are found in all the instruments—the possibility of performing AM measurements and the option of working in enhanced resolving power.

As TOF analyzers, two available mass spectrometers have been used—the Agilent G3250AA LC/MSD TOF (Agilent Technologies, Inc., Santa Clara, USA) and the Q-STAR Elite Hybrid (AB Sciex, Toronto, Canada)—referred along the manuscript as TOF 1 and TOF 2, respectively. As a QqQ, the model Finnigan TSQ Quantum Ultra AM (Thermo Electron, San José, USA) has been used (QqQ). Two different models of orbitrap (Thermo Electron, Bremen, Germany) analyzers have also been used—LTQ-Orbitrap XL (Orbitrap 1) and Exactive-Orbitrap (Orbitrap 2). FT-ICR data have been performed on a Thermo Electron (Bremen, Germany) model Finnigan LTQ-FT hybrid MS system equipped with a 7.0 Tesla magnet (FT-ICR). In all cases, ESI ion source has been used in negative mode.

Firstly, TOF 1 mass analyzer can reach an accuracy of 5 ppm at  $m/z$  609.2807 (3 mDa) with internal calibration and a resolving power greater than 13,000 (FWHM,  $m/z$  2722). It is provided with an internal calibration solution which permits the entrance of standard into the ion source. The orthogonal ion source has two independent probes.

Another TOF analyzer (TOF 2) based on Q-TOF hybrid technology has been tested. The technical characteristics of this analyzer are accuracy better than 5 ppm in the mass range between  $m/z$  500–800 (2.5–4 mDa) and resolving power of 10,000 (FWHM,  $m/z$  829). For this mass analyzer, the ion source is a Turbo IonSpray, so heated nitrogen

currents favor the ionization of the compounds. To perform internal calibration, a calibration solution can be used in.

Moreover, the QqQ used in the study has hyperbolic rods, and it is capable of improving peak-shape to assure a better calculation of centroid. With an expected accuracy of 5 mDa in the mass range  $m/z$  168–400 (29.8–12.5 ppm) and 5 ppm at  $m/z$  400–1226 (2–6 mDa) and a constant resolution in all the mass range of 0.04 (equivalent to resolving power of TOF 1 used in the study), it is designed to perform enhanced resolution.

FT-ICR device has been, up to the moment, the mass analyzer capable of providing better accuracy and highest resolving power. The hybrid FT-ICR used in the present study consists of a linear ion trap coupled to a FT-ICR mass analyzer. In this case, an accuracy of 1.2 ppm with external calibration and less than 1 ppm with internal calibration can be reached in all the mass range (sub-millidalton accuracy in all the mass range). The everyday working resolving power is set to 100,000 (FWHM,  $m/z$  400) at a scan rate of 1 Hz and up to 1,000,000 (FWHM,  $m/z$  400) at a slower scan rate.

A more recent technology known as orbitrap has also been used. Orbitrap 1 is a hybrid mass spectrometer that consists of a linear ion trap coupled to a FT-Orbitrap mass analyzer. It can achieve accuracy about 3 ppm (0.3–1.8 mDa, in the mass range of the study) with external calibration and 1 ppm with internal calibration (sub-millidalton in the mass range of the study). It can work at 60,000 (FWHM,  $m/z$  400) at a scan rate of 1 Hz and with maximum resolving power of 100,000 (FWHM,  $m/z$  400) at a slower scan rate. Besides, Orbitrap 2 mass spectrometer used in the study does not have a linear ion trap before the orbitrap mass analyzer, although the orbitrap analyzer itself is identical. It can produce AM measurements with less than 5 ppm error with external calibration (0.5–3 mDa, in the mass range of the study) and less than 2 ppm error using internal calibration (less than 1.2 mDa error in the mass range of the study). It can reach a resolving power of 100,000 (FWHM,  $m/z$  200) at a scan rate of 1 Hz.

Although during the experiments hybrid systems have been used, only full scan results have been included in the present manuscript.

## Chemicals

A mix of four standards of mass-to-charge ratios between 93.0346 and 542.7457 has been used to evaluate the mass measurements of the mass spectrometers described above. The mix consisted of acetyl salicylic acid (purity >99.0%, Fluka, Germany),  $d_{25}$ -dodecylsulphate sodium (98.9% atom D, CDN Isotopes, Canada), perfluorooctane sulphonate potassium (high-performance liquid chromatography-grade, Sigma-Aldrich, Germany) and tetrabromo bisphenol A

(high-performance liquid chromatography-grade, Sigma-Aldrich, Germany). In all cases, the mass of the electron has been taken into account as 0.00055 Da [20].

Fulvic acids standards (1S101F) and natural organic matter standards (1R101N) from International Humic Substance Society (MN, USA) have been used as real low-concentrated water samples to confirm the results obtained with the mix of four standards with the different mass spectrometers.

The compounds have been dissolved in methanol (Suprasolv, Merck, Germany). Mix solution has been injected with no previous separation into the mass spectrometers. Methanol (Suprasolv, Merck, Germany) and water (Ultra pure MilliQ water) with a proportion of 80:20, respectively, at 50  $\mu$ L/min flow rate have been used as mobile phase. Nitrogen (Alphagaz N<sub>2</sub>, purity 99.999%, Air Liquid) has been used in all the mass spectrometers as nebulization gas. In the case of FT-ICR, helium (purity 99.999%, Air Liquid) has been used.

## Procedures

Six mass spectrometers have been tested, which translates to well over 60 individual data sets, as ten replicates have been carried out for each mass spectrometer during a single day of work. In Table 1, the compounds and the diagnostic ions for each  $m/z$  ratio have been included, and the mass accuracy has been quoted as root-mean-square error (RMS error) and precision as the standard deviation (SD). Moreover, the drift of the measurement during few hours (Fig. 1) has been studied. In the case of FT-ICR, accuracy and precision of the mass measurement were tested at different resolving powers, in order to observe different behaviors (Fig. 2).

For the different mass spectrometers, the data processing when looking for the correct formulae has been evaluated. Xcalibur 2.0.7. software (Thermo Fisher Scientific) has been used in all cases. Restrictive criteria have been described and tested in some specific examples of the study.

## Results and discussion

Depending on the mass accuracy (millidaltons or parts per million) obtained, there will be a higher or lower number of potential elemental formulae for a compound. Thus, the degree of accuracy required relative to the  $m/z$  of the ion that is measured has to be taken into account. The *Journal of the American Society for Mass Spectrometry* advice that setting fixed acceptable error limits for exact molecular mass measurement is not recommended [22]. It should be highlighted that it has always given more importance to accuracy rather than to precision. Precision has received

**Table 1** Accuracy and precision in the mass range of study, for the different mass spectrometers with external calibration

Compound	Diagnostic ion	Theoretical mass/ instruments	TOF 1	TOF 2	QqQ <sup>a</sup>	Orbitrap 1	Orbitrap 2	FT-ICR
Acetyl salicylic acid	[C <sub>6</sub> H <sub>5</sub> O <sub>1</sub> ] <sup>+</sup>	93.0346	0.8 (±0.4)	0.7 (±0.2)	–	0.13 (±0.04)	0.16 (±0.05)	–
	[C <sub>7</sub> H <sub>5</sub> O <sub>3</sub> ] <sup>+</sup>	137.0244	0.97 (±0.7)	0.97 (±0.2)	–	0.28 (±0.04)	0.13 (±0.04)	0.09 (±0.04)
d <sub>25</sub> -Dodecylsulphate sodium	[C <sub>12</sub> D <sub>25</sub> O <sub>4</sub> S] <sup>+</sup>	290.3048	2 (±1.6)	2.1 (±0.4)	11 (±11)	0.9 (±0.1)	0.22 (±0.06)	0.3 (±0.1)
Perfluorooctane sulphonate potassium	[C <sub>8</sub> F <sub>17</sub> O <sub>3</sub> S] <sup>+</sup>	498.9302	3 (±3)	2.6 (±0.7)	11 (±6)	1.5 (±0.2)	0.9 (±0.3)	0.6 (±0.15)
Tetrabromo bisphenol A	[C <sub>15</sub> H <sub>11</sub> O <sub>2</sub> <sup>79</sup> Br <sub>2</sub> <sup>81</sup> Br <sub>2</sub> ] <sup>+</sup>	542.7457	3 (±3)	2.8 (±0.8)	–	1.6 (±0.2)	0.9 (±0.3)	0.9 (±0.1)

The mean of  $n=10$  replicates expressed as root-mean-square error (RMS error) and in *brackets* the standard deviation (SD), both in millidaltons

<sup>a</sup> Mass range had to be modified because of analyzer limitations

limited coverage in the literature, but it is important, and both accuracy and precision should be considered when talking about uncertainty in the measurement and evaluation of mass spectrometers [22]. In the present manuscript, accuracy and precision expressed as millidaltons will be used.

In the present study, the uncertainty in the mass measurements obtained from each mass spectrometer has been determined by taking the precision and accuracy of various replicate measurements into account. In general, for the mass range of study, there is less accuracy in mass measurements for higher masses in our experiment ( $m/z$  542.7457) than for lower ones (Table 1). Regarding precision, the same behavior as for accuracy has been detected; precision of the measurements is worse at higher  $m/z$  values. It can be concluded that the uncertainty in the measurements is in all cases worse for higher  $m/z$  values. In contrast, a better mass measurement, in accuracy and

precision terms, is needed for higher masses in order to have less candidates and the correct molecular formula [20].

In the present study, sub-millidalton accuracy and precision for daily routine analysis have been considered adequate to discriminate between possible candidates, taking into account the nature of the compounds ( $m/z$  100–600). As will be discussed in the next few lines, different mass spectrometers reached this good precision and accuracy (FT-ICR, TOF 2, Orbitrap 1, and Orbitrap 2); however, different calibration protocols should be applied in each case.

#### Calibration modes

The calibration process is crucial to achieving highly AM measurements. In mass spectrometers, external calibration is needed, and depending on the mass analyzer, this process

**Fig. 1** Mass errors obtained with TOF 1 mass spectrometer. In **a** five replicates were carried out at  $t=0$  h and five were carried out at  $t=5$  h. In **b** the same replicates after all the mass measurements were corrected with post-acquisition calibration

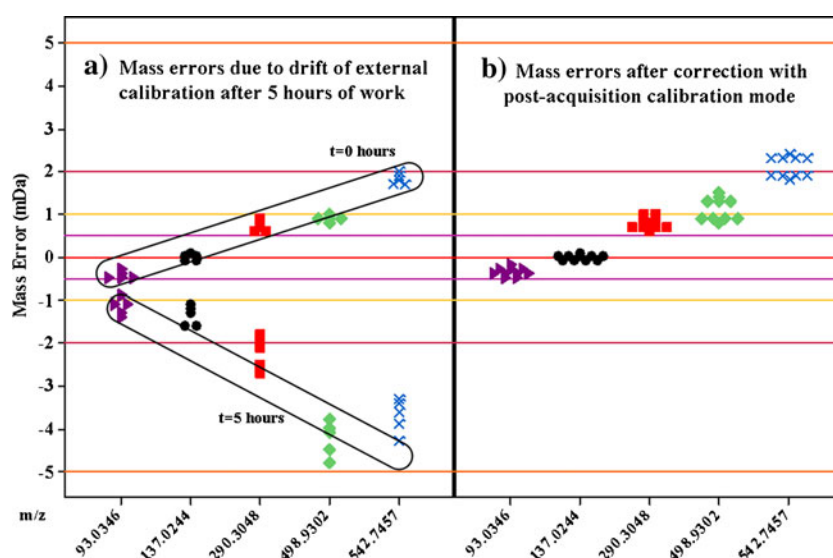
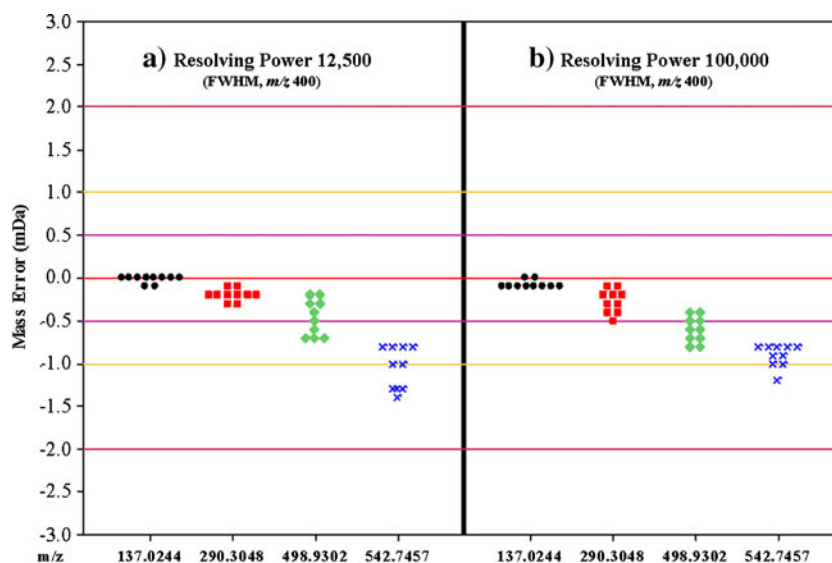


**Fig. 2** Mass errors obtained with FT-ICR mass spectrometer of the study, at different resolving power



should be done daily. In some mass spectrometers, other calibration processes are possible, such as internal and post-acquisition calibration, in order to achieve even better results. In the current study, different calibration approaches have been applied, according to the specifications of the instruments and their software.

#### External calibration

In all the mass spectrometers external calibration is done automatically, with the infusion of a standard. The corrections to the mass axis are stored by the instrument and frozen in memory. The evaluation of the performance of the external calibration for each mass spectrometer during a single day of work for  $m/z$  100–600 has been carried out analyzing the standard mix solution.

In all the mass spectrometers of the study, external calibration has been done the same day of the experiments, following the protocols established in the different laboratories. For TOF 1 and TOF 2, that was necessary because the drift was considerable after only a few hours of work (see Fig. 1 and explanation below). For QqQ, it was essential as the calibration protocol is different when low-resolution and enhanced resolution experiments are being performed [23, 24].

No extra external calibration had been performed during the same day in none of the mass spectrometers of the study, in order to better evaluate the drift of these mass spectrometers during a whole day of work.

For TOF 1, the results obtained revealed that accuracy of the measurements was within specifications, with higher error values for higher  $m/z$  values (Table 1). However, the precision of the instrument is doubtful, as it presented high dispersion with SD values between 0.4 and 3 mDa along the mass range, as can be observed in Table 1. As a result,

the mass spectrometer presented an uncertainty in the AM measurements of even 3 mDa RMS  $\pm$ 3 mDa SD (for  $m/z$  542.7457 value), presenting mass measurements with errors at the third decimal.

Taking accuracy into account, similar results are obtained with TOF 2, with RMS errors between 0.7 and 2.8 mDa. However, far better precision is achieved (0.2–0.8 mDa SD), and as a result, less uncertainty is associated to the mass measurements (Table 1). It is well known that mass spectrometers of the same type often achieve equivalent mass measurement accuracy but with significant differences in precision.

As has been described before, the QqQ used in the study is designed to perform enhanced resolution and obtain acceptable accuracy. However, important limitations have been faced during the study, and the instrument presented poor results in comparison with what was expected. Specifications around 5 mDa were desirable in the mass range of study; however, only an RMS error of 11 mDa has been obtained (Table 1). The main handicap was that mass range had to be modified because it was only capable of performing enhanced resolution experiments and AM measurements with a narrow window of about 200 Da. For that reason, only  $m/z$  290.3048 and  $m/z$  498.9302 could be evaluated. Very low accuracy and precision have been achieved with external calibration, with errors about 11 mDa RMS  $\pm$ 6 mDa SD ( $m/z$  498.9302). External calibration has demonstrated not to be stable enough. Compared with TOF 1 and TOF 2, QqQ is far from achieving as accurate and precise results as those for daily routine analysis. It demonstrates that, although in the literature, quadrupole analyzers have achieved high mass accuracies, such devices are not capable of performing high accurate daily screening analysis and can only obtain high mass accuracies in extremely good conditions. However,

for specific applications, the enhanced resolution mode could help separate isobaric interferences and confirm some identities. It should be applied to a single compound each time, as the accuracy in the mass range is limited.

For Orbitrap 1, the accuracy of the mass measurements ranged from 0.13 to 1.6 mDa RMS error, and the precision ranged from 0.04 to 0.2 mDa. The error of the measurement for the lower molecular compounds is presented at the fourth decimal. Moreover, for Orbitrap 2, better accuracy (0.16–0.9 mDa RMS error) and equivalent precision have been observed. As a consequence, the error of the measurement in all the mass range for Orbitrap 2 is presented at the fourth decimal. The better stability of the mass measurement for Orbitrap 1 and Orbitrap 2 compared with TOF 1 and TOF 2 is due to the temperature-compensated electronics that the orbitraps have. New generations of TOF analyzers have also recently introduced new technology to correct the drift properties due to the expansion of the TOF analyzers [5] to perform long-term accuracy experiments.

As expected, the best results of the whole study with external calibration have been achieved with the FT-ICR. Considering accuracy less than 1 mDa RMS error was observed in all the mass ranges. The error of the measurement for the compounds in all the mass ranges are presented at the fourth decimal (Table 1). It should be noticed that close results to FT-ICR have been achieved with Orbitrap 2. Concerning accuracy, some applications restricted until the moment to FT-ICR can be transferred to orbitrap analyzers because they can achieve as good results as FT-ICR analyzers. However, taking resolution into account, FT-ICR mass analyzers still dominate the scene of ultrahigh-resolution.

#### *Internal calibration*

In internal calibration, lock masses are scanned during the same mass spectrometry experiment as the compounds of interest, and with the lock masses, the mass range is constantly recalibrated during acquisition. The lock masses can be mixed in the sample solution, infused from a separate source into the mass spectrometer or teed in. The main problem is that ion suppression and chemical interferences can be created between lock masses and analytes. During several experiments performed with the different mass spectrometers of the study, some of these handicaps have been detected.

TOF 1 has an orthogonal ion source with two independent probes, one for the ionization of the sample and one for the ionization of the calibration solution, to permit constant recalibration of mass range. The high response of calibration solution in the mass spectrometer produces chemical interferences, as well as important carryover.

Dilution of the calibration solution is not recommended by the manufacturer, as the solution is prepared taking into account the optimum intensity that the lock mass must have in the spectra to be used as internal calibration solution. Apart from intensity, TOF 1 requires special characteristics of the lock masses (first lock mass with  $m/z \leq 330$  Da and the second lock mass at 500 Da from the first one used). If the lock mass does not fulfill these requirements, the mass range will not be continuously recalibrated.

At that point, working with a more concentrated mix of standards for the AM experiments would have solved the problem, but chemical interferences were especially significant with low-concentration samples, such as water containing fulvic acids or natural organic matter. This calibration mode presented limited applicability for samples where low concentration of unknown compounds may be expected.

For internal calibration with QqQ, two lock masses of the same intensity should be present in the sample. When acquiring in this mode, narrow mass range should be set because the scan rate permitted is very low. This calibration mode is only suitable when applied to a single compound each time, as the accuracy in the mass range is limited. Previous studies [25] published that used hyperbolic quadrupole to perform AM measurements with internal calibration reported mass errors between 1.5 and 10 mDa and precision around 2–5 mDa, confirming our results and the instability of mass accuracy with this mass analyzer, even when internal calibration is performed. As described in the study by H.Gallart-Ayala et al., confirmation of compounds is possible with this mass error; however, non-target screening may be not possible. Moreover, enhanced resolution and AM measurements with internal calibration can be performed in selected ion monitoring with this mass spectrometer. However, this scan mode is not useful for screening of unknowns.

Several experiments were carried out with TOF 2 with internal calibration. In this case, the ion source only has one probe, so the internal calibration solution must be teed in and it influences the ionization of the mix of the standards used, causing ion suppression. This effect was even worse in some of the samples tested (fulvic acids), losing almost completely the ionization of the sample. Other calibration protocols have been considered to improve accuracy and precision.

The same phenomenon was observed with Orbitrap 1. Nevertheless, in order to force the mass spectrometer to perform internal calibration, extra experiments were performed with Orbitrap 1. Internal standards and recovery standards, already added in the real samples during pre-treatment, have been used as internal lock masses. The main trick was that those were added in the correct concentration to make sure the intensity was adequate to

be used as internal lock masses. This way, it was made sure that the mass spectrometer could find the ions and that internal calibration was done, without completely losing the signals of our compounds.

With  $m/z$  290.3048 and 498.9302, the best results were obtained. As an example, the uncertainty decreases from 1.6 mDa RMS  $\pm$  0.2 mDa SD to 0.2 mDa RMS  $\pm$  0.1 mDa SD ( $m/z$  542.7457). As expected and reported before [26], internal calibration is typically at least twice as accurate as external calibration. However, chemical interferences and ion suppression should be solved out when unknown compounds are present in the sample in low concentration.

For Orbitrap 2 and FT-ICR used in the study, as very good results were obtained (sub-millidalton accuracy and precision), due to such recent calibration (same day), experiments with internal calibration have not been carried out.

#### *Post-acquisition calibration*

Apart from external and internal calibration, post-acquisition calibration has been considered. In post-acquisition mode, no lock masses are applied during acquisition and, therefore, no mass corrections are made to the peak in the scan, only external calibration stored in the instrument memory is used. The main purpose is to recalculate the data acquired with respect to the exact masses of a reference compound which was present in the ion source during the measurement. The reference compound serves as a “ruler” in calculating the accurate masses of the unknowns that are adjacent to the known compounds. The idea was to find an alternative tool, to obtain better AM measurements than with external calibration in a fast easy way.

For QqQ, many experiments were performed with the *post-processing* mode. However, the experiment could not be completed because the commercial software is still not available. Many other data treatment software have been tested; however the incompatibility with types of files has not made the post-correction of the axis possible.

For TOF 1 and TOF 2, post-acquisition was easy and fast. The software is already operable and integrated, and the lock mass that is used to recalibrate spectra requires only some specific characteristics. In both cases, replicate measurements were performed immediately after external calibration ( $t=0$  h) and after a few hours of work ( $t=5$  h; Fig. 1a). At that point, the drift in the measurement was, in both cases, significant, and external calibration should have been done again. Different post-acquisition calibration protocols were tested in each case considering one and two lock masses present in the sample or in the ion source. In both mass spectrometers, the best results were obtained when two lock masses were used, and those are the results shown in the manuscript. For TOF 1, recalibration had to be

performed using two ions of the calibration solution remaining in the spectra (as a consequence to carryover), as TOF 1 requires special characteristics of the lock masses. With post-acquisition calibration, no problems with intensity of lock mass were detected, so the remaining intensity of these ions was enough for them to be used as recalibration lock masses. For TOF 2, two of the compounds in the standard solution used during the study ( $m/z$  137.0244 and  $m/z$  498.9302) were used as lock masses for recalibration, as it does not specify any requirements.

With recalibration, TOF 1 can achieve greater accuracy and precision, obtaining AM measurements as accurate and precise as those obtained with recent external calibration (Fig. 1b). Two data groups could not be distinguished because both experiments at  $t=0$  h and  $t=5$  h had similar behavior, and the drift in the measurement had been corrected.

It should be highlighted that TOF 2 mass spectrometer after post-acquisition calibration improves ten times the accuracy of the measurements and four times the precision. As an example, for  $m/z$  542.7457, an uncertainty of the measurement improves from 2.8 mDa RMS  $\pm$  0.8 mDa SD to 0.2 mDa RMS  $\pm$  0.2 mDa SD.

For Orbitrap 1, better results were also desirable (sub-millidalton errors), so post-acquisition calibration was performed using the software coming with the instrument. Applying the same protocol as with TOF 2, two of the compounds in the standard solution were used for recalibration. Orbitrap 1 mass spectrometer after post-acquisition calibration improves five times the accuracy of the measurements and two times the precision. As an example, for  $m/z$  542.7457, an uncertainty of the measurement improves from 1.6 mDa RMS  $\pm$  0.2 mDa SD to 0.3 mDa RMS  $\pm$  0.1 mDa SD.

Considering these experiments, the results obtained after recalibration with TOF 2 and Orbitrap 1 are as accurate and precise as those with internal calibration. The main advantage is that one can decide after the run, whether accuracy and precision are or are not adequate for the nature of the compounds. For example, with TOF 2, the experiments performed immediately after the everyday external calibration were highly accurate and precise (sub-millidalton); however, during the day, the uncertainty of the measurement became worse. When a long run of samples is being performed, worse results for the last samples injected might be expected. At that point, internal standards and recovery standards already added in the sample during pre-treatment can be used to perform (only if necessary) recalibration after the run.

Post-acquisition calibration is a powerful methodology for achieving more AM measurements (when necessary) and especially useful when the mass spectrometer tends to have unstable external calibration.

## Resolving power

There has been a great controversy between the resolving power and resolution terms. In fact, some authors used to talk about resolution [27], and they have recently changed to using resolving power instead [28]. In the current study, the later definition will be applied [29].

Resolving power differs depending on the mass analyzer and the mass spectrometer, and it depends in each case of some parameters such as time, voltage, or frequency. The resolving power and resolution along the mass range change depending on the mass analyzer. It is necessary to have not only the resolving power but also the  $m/z$  at which it is defined and at which height it has been measured (5%, 10%, or 50% of the valley) [26]. For example, TOF 1 with 13,000 resolving power (FWHM,  $m/z$  2,722) but a real resolution of 0.21 Da cannot separate isobaric compounds better than QqQ (used also in the study) with a real resolution of 0.04 Da.

As it is well known, resolving power has two major effects on the mass spectra of compounds—the width of the signal and the intensity. Regarding accuracy and precision, it should be taken care when linking these ideas with ultrahigh-resolution. In most cases, with higher resolving power, more AM measurement will be obtained. In fact, ultrahigh-resolving power is absolutely necessary when analyzing complex mixtures such as fulvic acids, humic acids, and NOM [12], as shown in the fulvic acids spectra analyzed during the present study with FT-ICR (Fig. 3). During the last few years, TOF analyzers have been related to high resolving power and AM measurements, when coupled to liquid chromatography in daily routine. Actually, TOF analyzers' common resolving power cannot resolve peaks, in these cases, as can be seen in Fig. 3b. The shape of the peak reveals that there is more than one compound under the envelope, but the reality is that more than six different compounds with the same nominal mass are hidden. This can only be detected by applying ultrahigh-resolving power (Fig. 3a). As a consequence, the elemental composition that would be obtained by the AM displayed in Fig. 3b ( $m/z$  547.0767) would be wrong and would never correspond to the real ones.

However, when no isobaric interferences are present, such as in the standard mix solution of the current study, resolving power does not affect the accuracy and precision of the measurement, as shown in Fig. 2. The standard was analyzed at resolving power 12,500 (FWHM,  $m/z$  400) and 100,000 (FWHM,  $m/z$  400) with external calibration in both cases. The mass errors for each measurement at different resolving power are equivalent, with higher dispersion and less accuracy for higher  $m/z$  ratio compounds, as has been commented before. That is the reason why, in many studies published before [2, 16, 30, 31], low-resolution mass

spectrometers, such as QqQ, have obtained as good results in AM measurements as TOF or FT-ICR analyzers.

## Data processing for elemental formulae determination

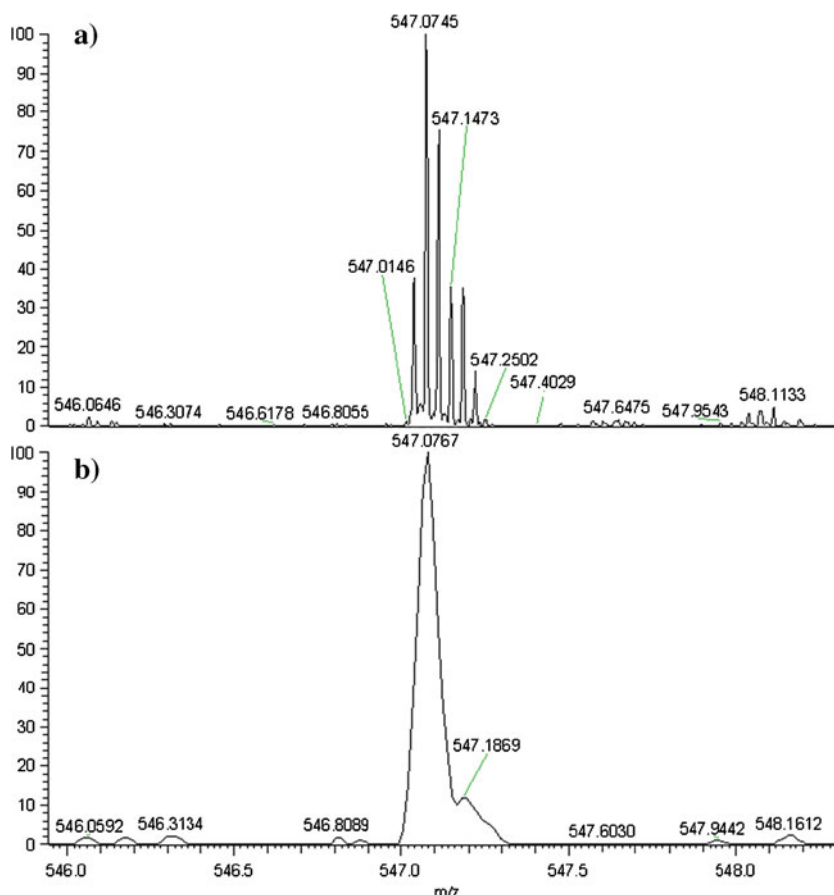
The aim of an AM measurement is to confirm the molecular formula of a compound. The capabilities of the software when looking for the correct formulae have been evaluated [20, 32].

Ultrahigh-resolution will not be useful when there is no previous information about what is being looked for. Some studies use TOF analyzers and report screening of unknown compounds. In most cases, the unknown term is loosely used, as the screening is focused on some metabolites and derivatives of well-known compounds. In these cases, the term non-target would apply better. Ultrahigh-resolving power and high accuracy are powerful tools to confirm an identity, but they are insufficient for obtaining a unique structure of an unknown yet [22]. Structural information is needed, and it can be complemented with tandem mass (MS/MS) experiments and/or nuclear magnetic resonance, if possible.

In order to obtain a limited list of possible candidate formulae from a mass measurement, heuristic criteria based on uncertainty in mass measurement (accuracy and precision), the number of ring plus double bond (RDB) equivalents, the charge, the adducts formed, the isotopic pattern in the mass spectra, and the elements in use can be applied.

As far as possible, it is necessary to know the uncertainty associated to an AM measurement, as it is the limit of quantification associated to quantify. Only in this way can the list of theoretical candidates that should be taken into account be known. In the data system used, a parameter called *mass tolerance* is defined as how close a measured mass must be to the theoretical mass to be considered the same mass. For that reason, from the results obtained in the present study, the *mass tolerance* should be different in each case. For Orbitrap 2 with external calibration, a *mass tolerance* of even less than 1.5 mDa can be fixed because the uncertainty expected from this mass spectrometer is better than that (see Table 1). Elemental formulae, the theoretical mass of which differs more than 1.5 mDa from the mass measured, should be ruled out as not-possible candidates. In contrast, for TOF 1, the *mass tolerance* should be fixed at almost 6 mDa when external calibration is used, so it is likely to obtain a longer list of candidates in this case (even nine candidates should be considered). That would make more difficult the identification and/or confirmation of a compound. As has been discussed before, for TOF 1, it is possible to improve the uncertainty in the measurements by post-acquisition calibration. This way, the *mass tolerance* could also be fixed in a lower value (around 3 mDa), decreasing the amount of candidates from nine to five.

**Fig. 3** Mass spectrum of fulvic acids from International Humic Substance Society obtained at different resolving power: **a** resolving power, 100,000 (FWHM,  $m/z$  400). **b** Resolving power, 12,500 (FWHM,  $m/z$  400) with FT-ICR



To illustrate the importance of uncertainty in building the list of candidates, some experiments with the AM data of the study and the software have been performed. Taking into account SD, the number of replicates ( $n$ ), and the percentage of confidence set as 90%, the confidence interval has been calculated. The confidence interval generates lower and upper limits for the mean, the confidence limits [33]. As the confidence interval is the likely range of the true value, the confidence limits have been considered to be the most distant mass measurement from the AM value that can be achieved in each case. These mass limit values have been tested in the software to see at which position the correct formula could be obtained. In the manuscript, only the results from TOF 1 and FT-ICR for  $m/z$  value 542.7457, with external calibration, have been included, as an example.

For TOF 1, the confidence limits calculated have been 542.7448 and 542.7485 (Table 2), so all the AM measurements performed with this mass spectrometer may be between these two values. When selecting the elements in use (C, H, O,  $^{79}\text{Br}$ ,  $^{81}\text{Br}$ ), the charge as  $-1$  and *mass tolerance* as 6 mDa (Table 1), a list of candidates has been obtained but only the first three candidates have been included in Table 2. For  $m/z$  542.7448, the correct formula was obtained in the third position, but for  $m/z$  542.7485,

none of these top three formulae were correct. In fact, the correct formula was in eighth position. However, for FT-ICR, as better accuracy and precision have been obtained, the confidence limits have been 542.7465 and 542.7467; the confidence interval in this case is narrower. With the same restrictive criteria as before but with a *mass tolerance* of 1 mDa (Table 1), a shorter list of three candidates has been obtained and included in Table 2. For FT-ICR's confidence limits, the correct formula was obtained at third position. At that point, the isotopic pattern will permit to ignore the false candidates and obtain the correct formula from this short list. For TOF 1, as the list of candidates is longer, the comparison of the isotopic pattern will be more difficult and extra data evaluation will be necessary.

Apart from uncertainty, if the ion type, the adducts formed in the ion source and the charge are known; any formulae giving an inappropriate RDB value should give enough evidence to ignore incorrect formulae [20]. In the present study, soft ionization technique ESI in negative mode leads to  $[\text{M}-\text{H}]^-$  adduct ions, which means charge  $-1$  and a fractional RDB.

Nevertheless, previous information regarding the nature of the compounds is basic for the correct determination of the elemental formulae. As the number of elements increases (C, H, O, N, S, F...), less uncertainty in the

**Table 2** Determination of molecular formulae for TOF 1 and FT-ICR mass spectrometers

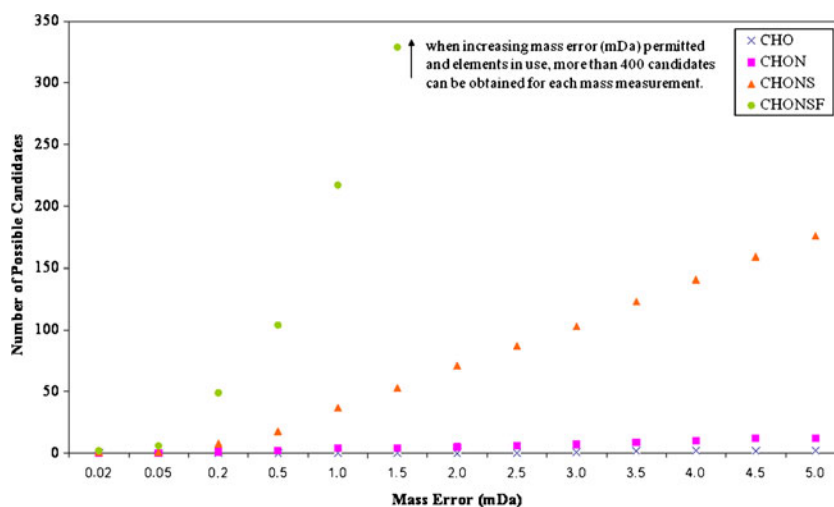
Theoretical mass	Mass spectrometer	Confidence limits	List of candidates	RDB	Mass error (mDa)	
542.7457	TOF 1	542.7448	1	$C_{14}H_{11}O_3^{79}Br_4^-$	7.5	-0.08
			2	$C_6H_8O_{14}^{79}Br_2^{81}Br_2^-$	1.5	-0.12
			<b>3</b>	<b><math>C_{15}H_{11}O_2^{79}Br_2^{81}Br_2^-</math></b>	<b>8.5</b>	<b>-0.91</b>
		542.7485	1	$C_{24}O^{79}Br_2^{81}Br^-$	23.5	0.07
			2	$C_{11}H_{13}O_5^{79}Br_3^{81}Br^-$	3.5	0.35
			3	$C_{12}H_{13}O_4^{79}Br^{81}Br_3^-$	4.5	-0.64
	FT-ICR	542.7465	1	$C_{16}H_{11}O^{81}Br_4^-$	9.5	-0.20
			2	$C_7H_8O_{13}^{81}Br_3^-$	2.5	0.59
			<b>3</b>	<b><math>C_{15}H_{11}O_2^{79}Br_2^{81}Br_2^-</math></b>	<b>8.5</b>	<b>0.99</b>
		542.7467	1	$C_{16}H_{11}O^{81}Br_4^-$	9.5	0.00
			2	$C_7H_8O_{13}^{81}Br_3^-$	2.5	0.79
			<b>3</b>	<b><math>C_{15}H_{11}O_2^{79}Br_2^{81}Br_2^-</math></b>	<b>8.5</b>	<b>0.99</b>

measure should be permitted because, if not, the number of candidates rises exponentially [34]. One of the compounds present in the mix solution ( $C_8F_{17}O_3SK$ ) has been used to demonstrate this. It has been treated as a real unknown (no previous data of elemental composition, only spectra information), although the exact mass ( $m/z$  498.9302) has been considered. Different elements have been defined each time, beginning with elements which are present in most of organic compounds (C, H, O). At that point, few candidates have been obtained, even with the *mass tolerance* of 5 mDa. However, none of the elemental formulae obtained was the correct one, although no error in the mass measurement has been committed. Erroneous previous data would have lead to error formulae. In Fig. 4, it can be observed how, when increasing the elements in use (apart from C, H, O also N and S, also present in many organic compounds), the number of possible candidates increases exponentially, taking into account the same *mass tolerance*. In fact, with

the best results obtained in the present study with external calibration (uncertainty around 1 mDa for **FT-ICR**), it would not have been enough to have one unique candidate. In this case, if we had not initially known some halogenated compounds such as fluorine is present, the first hypothesis of formulae would have been wrong. Isotopic pattern would then once again be helpful to discriminate between potential candidates.

As it has been demonstrated above, the identification of discriminating signals is the most laborious and time-consuming step of the AM measurement experiments. It still remains unsolved how to process all the information contained in an ultrahigh resolved mass spectrum in an automatic and fast way. As for example, with NOM mass spectra that contain over thousands of signals, only statistical approaches are suitable to analyze all the data. Van Krevelen plots and Kendrick Mass Deffect have been, until the moment, the best way adopted for marine chemistries and petroleomic analyzers to face this problem [35, 36].

**Fig. 4** For mass measurement ( $m/z$  498.9302), the number of candidates, depending on initial information given to the software (elemental composition) has been tested, taking into account the degree of accuracy permitted (millidaltons)



## Conclusions

A wide variety of mass analyzers are used daily for routine AM measurements: TOF, Q-TOF, FT-ICR, Orbitraps, and QqQ. Six mass spectrometers based on these mass analyzers have been tested in the mass range  $m/z$  100–600, during a single day of work in negative ionization mode.

It has been observed that, for the mass range of study, there is better accuracy and precision in mass measurements for lower masses ( $m/z$  93.0346) than for higher ones, for all the mass analyzers. In contrast, a better accuracy and precision is needed for higher masses in order to have fewer candidates to obtain the correct molecular formulae. However, when external calibration is well-fixed and low mass errors are performed, even at high masses, only few candidates (two or three) would be obtained, making it easier to discriminate between them.

Different calibration modes have been used: internal, external, and post-acquisition. Concerning external calibration, the best results have been obtained with FT-ICR and Orbitrap 2. For TOF mass analyzers currently used in many laboratories, the drift of mass measurements remains unsolved. Last-generation TOF mass spectrometers would contradict this statement, as manufacturers claim more stable accuracies for these mass analyzers. Apart from fixing external calibration properly, other calibration protocols may be taken into account internal and/or post-acquisition calibrations. The good results obtained with post-acquisition calibration and the possibility of performing it only when necessary (when mass drift is observed) makes it the best option to obtain greater accuracy and precision (as good as with the common internal calibration). Concerning accuracy and precision, the new orbitraps can compete with the simpler FT-ICR (7 Tesla). However, taking resolution into account, FT-ICR mass analyzers still dominate the scene of ultrahigh-resolution.

As it has been demonstrated, ultrahigh-resolution is mandatory in some applications, such as characterization of NOM, because isobaric interferences are present. It should be highlighted that, in most cases, ultrahigh-resolution is necessary but not sufficient, as a stable calibration is one of the main factors to take into account.

The data processing for obtaining possible formulae of a non-targeted compound is the final goal of each AM measurement. To obtain a reliable list of candidate formulae, it is necessary to know the uncertainty associated to an AM measurement (as it is the limit of quantification associated to quantify). Apart from that, previous information/hypothesis regarding the nature of the compounds is basic for the correct determination of the elemental formulae. In the recent years, there has been a revolution in “accurate” mass spectrometers, but it still remains unsolved how to process all the information contained in an ultrahigh resolved mass spectrum in an automatic and fast way.

**Acknowledgment** The authors of this work would like to thank Dra. M. Vilaseca from Institute for Research in Biomedicine-UB, Dra. I. Fernández, Dra. O. Jáuregui and Dr. I. Casals from Serveis Científicotècnics-Universitat de Barcelona, Dr. J.A. Allué from Araclon Biotech, and Dr. E. Genin from Thermo Fisher Scientific for technical support. This work has been partially financed within the framework of the project CENIT: Desarrollos Tecnológicos hacia el Ciclo Urbano del Agua Autosostenible (SOSTAQUA), CEN20071039.

## References

- Beynon JH (1960) *Mass Spectrometry and Its Applications to Organic Chemistry*, 1st edn. Elsevier, London
- Bristow AWT (2006) Accurate mass measurement for the determination of elemental formula-A tutorial. *Mass Spectrom Rev* 25:99–111
- Brunnée C (1987) The ideal mass analyzer: fact or fiction? *Int J Mass Spectrom Ion Process* 76:125–237
- Ow SY, Noirel J, Salim M, Evans C, Watson R, Wright PC (2010) Balancing robust quantification and identification for iTRAQ: application of UHR-ToF MS. *Proteomics* 10:1–9
- Bruker Daltonics (2010) UHR-TOF maXis Brochure. December
- Wolff JC, Eckers C, Sage AB, Giles K, Bateman R (2001) Accurate mass liquid chromatography/mass spectrometry on quadrupole orthogonal acceleration time-of-flight mass analyzers using switching between separate sample and reference sprays. 2. Applications using the dual-electrospray ion source. *Anal Chem* 73:2605–2612
- Richards D (2001) Proceedings of the 25th Annual Meeting of the British Mass Spectrometry Society, University of Southampton: 78
- Ibañez M, Sancho JV, Pozo OJ, Niessen W, Hernández F (2005) Use of quadrupole time-of-flight mass spectrometry in the elucidation of unknown compounds present in environmental water. *Rapid Commun Mass Spectrom* 19:169–178
- Wu J, McAllister H (2003) Exact mass measurement on an electrospray ionization time-of-flight mass spectrometer: error distribution and selective averaging. *J Mass Spectrom* 38(10):1043–1053
- Koch BP, Dittmar T (2006) From mass to structure: an aromaticity index for high-resolution mass data of natural organic matter. *Rapid Commun Mass Spectrom* 20:926–932
- Kujawinski EB, Hatcher PG, Freitas MA (2002) High resolution Fourier transform ion cyclotron resonance mass spectrometry of humic and fulvic acids: improvements and comparisons. *Anal Chem* 74:413–419
- Koch BP, Ludwiczowski KU, Kattner G, Dittmar T, Witt M (2008) Advanced characterization of marine dissolved organic matter by combining reversed-phase liquid chromatography and FT-ICR-MS. *Mar Chem* 111:233–241
- Hughey CA, Hendrickson CL, Rodgers RP, Marshall AG (2001) Elemental composition analysis of processed and unprocessed diesel fuel by electrospray ionization Fourier transform ion cyclotron resonance mass spectrometry. *Energy Fuels* 15(5):1186–1193
- Cooper HJ, Marshall AG (2001) Electrospray ionization fourier transform mass spectrometric analysis of wine. *J Agric Food Chem* 49:5710–5718
- Witt M, Fuchser J, Baykut G (2001) Fourier transform ion cyclotron resonance mass spectrometry with nanolc/microelectrospray ionization and matrix-assisted laser desorption/ionization: analytical performance in peptide mass fingerprint analysis. *J Am Soc Mass Spectrom* 1:553–561
- Bristow AWT, Webb KS (2003) Intercomparison study on accurate mass measurement of small molecules in mass spectrometry. *J Am Soc Mass Spectrom* 14:1086–1098

17. Ham BM (2008) *Even Electron Mass Spectrometry with Biomolecule Applications*, 1st edn. Wiley Interscience, United States of America
18. Perry RH, Cooks RG, Noll RJ (2008) Orbitrap mass spectrometry: instrumentation, ion motion and applications. *Mass Spectrom Rev* 27:661–699
19. Gareth Brenton A, Ruth Godfrey A (2010) Accurate mass measurement: terminology and treatment of data. *J Am Soc Mass Spectrom* 21:1821–1835
20. Webb K, Bristow AWT, Sargent M, Stein BK (2004) *Methodology for Accurate Mass Measurement of Small Molecules*. Best Practice Guide. LGC Ltd, London
21. Sargent M, O'Connor G. Feasibility study: Mass spectrometry techniques for accurate molecular weight determinations of large molecules. LGC/VAM/2001/026
22. "Guide for Authors" *J. Am. Soc. Mass. Spectrom*
23. Hughes N, Winnik W, Dunyach J, Amad M, Splendore M, Paul G (2003) High-sensitivity quantitation of cabergoline and pergolide using a triple-quadrupole mass spectrometer with enhanced mass-resolution capabilities. *J Mass Spectrom* 38:743–751
24. Paul G, Winnik W, Hughes N, Schweingruber H, Heller R, Schoen A (2003) Accurate mass measurement at enhanced mass-resolution on a triple quadrupole mass-spectrometer for the identification of a reaction impurity and collisionally-induced fragment ions of cabergoline. *Rapid Commun Mass Spectrom* 17:561–568
25. Gallart-Ayala H, Moyano E, Galceran MT (2010) Multiple-stage mass spectrometry analysis of bisphenol A diglycidyl ether, bisphenol F diglycidyl ether and their derivatives. *Rapid Commun Mass Spectrom* 24:3469–3477
26. Marshall AG, Hendrickson CL (2008) High-Resolution Mass Spectrometers. *Annu Rev Anal Chem* 1:579–599
27. Makarov A (2000) Electrostatic axially harmonic orbital trapping: a high-performance technique of mass analysis. *Anal Chem* 72:1156–1162
28. Makarov A, Denisov E, Lange O, Horning S (2006) Dynamic range of mass accuracy in Itq orbitrap hybrid mass spectrometer. *J Am Soc Mass Spectrom* 17:977–982
29. Marshall AG, Hendrickson CL (2002) Fourier transform ion cyclotron resonance detection: principles and experimental configurations. *Int J Mass Spectrom* 215:59–75
30. Balogh MP (2004) Debating resolution and mass accuracy. *LCGC Europe* 17(3):152–159
31. Tyler AN, Clayton E, Green BN (1996) Exact mass measurement of polar organic molecules at low resolution using electrospray ionization and a quadrupole mass spectrometer. *Anal Chem* 68:3561–3569
32. Kind T, Fiehn O (2007) Seven Golden Rules for heuristic filtering of molecular formulas obtained by accurate mass spectrometry. *BMC Bioinform* 8:105
33. Snedecor GW, Cochran WG (1989) *Statistical Methods*, 8th edn. Iowa State University Press, Iowa
34. Herniman JM, Langley GJ, Bristow AWT, O'Connor G (2005) The validation of exact mass measurements for small molecules using FT-ICRMS for improved confidence in the selection of elemental formulas. *J Am Soc Mass Spectrom* 16:1100–1108
35. Kim S, Kramer RW, Hatcher PG (2003) Graphical method for analysis of ultrahigh-resolution broadband mass spectra of natural organic matter, the Van Krevelen Diagram. *Anal Chem* 75:5336–5344
36. Schmidt F, Koch BP, Elvert M, Witt M, Haag K, Hinrichs K (2008) Poster. ASMS Conference on Mass Spectrometry. ASMS, Denver, CO, USA

## 2.3. Discussion

MS is a fast changing field that has experienced significant development of new instrumentation along with increasing applications in the area of environmental analysis, especially when talking about HR.

HR mass analyzers are expected to provide AM measurements. From the studies performed in section 2.2.1. and 2.2.2., we have seen that some parameters (see Figure 6.3. section 2.2.1. page 29) are very much influencing the accuracy and precision of an AM measurement: resolution, calibration protocols, tuning, peak shape and ion abundance.

Using HRMS for the analysis of complex samples can help to prevent false assignments. If signals are not resolved, the elemental compositions obtained by the accurate masses measured will be wrong, as was shown in Figure 6.4.b, c and d from Section 2.2.1. page 31. Trying to recommend a minimum resolution value to ensure complete resolution of interferences is highly dependent of the matrix and compounds. Moreover, fixing a value is always a controversial issue, due to commercial interests. Besides, legislation applying to method development is still not updated (European Commission 2002). Some reference guides (European Commission 2012) are starting to recommend resolution higher than 20,000 (full width at half maximum - FWHM), however as shown in complex samples such as DOM, this is not enough. We can make out if we are acquiring our data with enough resolution by having a look at the peak shape. In fact, peak shape can reveal if there is more than one compound under the envelope (Figure 6.4.d in Section 2.2.1. page 31). That is the reason why acquiring in profile is highly advisable. In addition, the tuning of the instrument should be good enough to be sure that the peak shape is symmetric and we have enough ion abundance.

Apart from these factors influencing the accurate mass, calibration protocols are crucial in achieving high accuracy and precision. External calibration is always mandatory but an additional internal calibration might be necessary to obtain sub-ppm or sub-mDa accuracy. For FT-ICR and FT-orbitrap the external calibration is so stable that in some cases it may be accurate enough. In fact, it has been shown that concerning accuracy and precision, the new orbitraps can compete with the simpler FT-ICR (see Table 1 in Section 2.2.2. page 80). Post-acquisition calibration should be considered as a very good option to improve the results, in contrast to conventional internal calibration. This option should be seriously considered to correct the drift in the measurements for mass analyzers especially sensible to ambient conditions (see Figure 1 section 2.2.2. page

80). However, as observed and explained in the study presented in section 2.2.2, not all instruments have the required software ready for use.

The aim of any AM measurement is to obtain the elemental formula, to confirm the identity of a compound or carry out a screening of unknowns. If looking for real unknowns very general parameters have to be set and restrictions have to be done step by step, after careful observation of the spectra (see example in Table 6.3 and Table 6.4 Section 2.2.1. pages 40-41). Setting very restrictive criteria will lead to an erroneous candidate as obtained from the simulations carried out in the study included in section 2.2.2. page 86. Several strategies may help to reduce the number of possible candidates, such as: accuracy and precision of the measurements, ion type and adduct formation, charge, ring plus double bond equivalents (RDBE), elements to consider and restrictions of elements, isotopic pattern and isotopic ion ratio.

The degree of accuracy and precision required to obtain a list of theoretical candidates is one of the main parameters that should be set. Generally speaking, the better the accuracy the less the ambiguity (less possible candidates), as shown in Figure 4 (Section 2.2.2. page 86). Moreover, it has been shown that better accuracy and precision are needed for higher masses in order to have a reduced number of candidates to obtain the molecular formulae. In the study comparing the capabilities of the different mass analyzers, it was shown that accuracy and precision achieved are better for lower masses than for higher ones (considering mass range  $m/z$  100-600) (see Table 1 in Section 2.2.2. page 80).

Once a list of candidates has been obtained, applying filters to identify the compounds of interest is the most time-consuming step and for this reason any additional information from the samples or compounds is quite helpful. For instance, one of the strategies adopted for the characterization of DOM is to filter the less probable candidates based on the elemental ratios. However, processing and representing all the information contained in a HR spectrum in an automatic and fast way is still not completely solved. Automated batch processing and fast databases are being developed including fragmentation studies, such as MetFrag (Wolf et al., 2010) and MetFusion (Gerlich et al., 2012).

Several examples have been developed to exemplify the advantages and need of using HRMS and high resolution tandem mass spectrometry (HRMS/MS) better than selected ion monitoring (SIM) or tandem mass spectrometry (MS/MS) (see page 54). Generally speaking, gas chromatography-high resolution mass spectrometry (GC-HRMS) has experienced less innovation in the last 10 years in comparison to liquid chromatography-high resolution mass spectrometry (LC-HRMS). While GC-HRMS is slowly being replaced by gas chromatography-tandem mass spectrometry (GC-MS/MS), LC-HRMS for environmental applications is becoming more necessary and in some cases essential, especially when no standards are available. One of the fields that has gone through outstanding progress in the recent years has been DOM characterization. In the present thesis, HR for the analysis of DOM characterization has been the main technique used.



# **Chapter 3.**

## **Analysis of Dissolved Organic Matter by High Resolution Mass Spectrometry**

---



## 3.1. Introduction

The molecular characterization of DOM has become a primary research environmental topic. Despite the significant progress in the last few years, it continues to be a daunting task. Direct analysis of DOM by electrospray-high resolution mass spectrometry (ESI-HRMS) is the technique that provides the most information, but there are several considerations that have to be taken into account.

Firstly, sample preparation for DOM is an important consideration, as it can be difficult to separate DOM from water or inorganic matter without losing or altering it. Furthermore, DOM is not amenable to most instrumental analysis, because it is a low concentration of highly functionalized polymeric substances that do not behave uniformly. Besides, data analysis and structural information from a HRMS spectrum provide such an amount of data that it makes the data processing and evaluation of results extremely time-consuming.

### 3.1.1. Dissolved Organic Matter Isolation of Water Bodies

There is constant research to determine the best method for isolation and concentration of DOM for posterior analysis by MS. Traditionally DOM was extracted depending on the pH at which it was soluble and categorized as FA, HA and humin, based on XAD resins (Aiken et al., 1992). Nowadays the methods most commonly employed to isolate DOM from the aquatic media are SPE, ultrafiltration (UF), RO, electro dialysis and / or some combinations of them (Green et al., 2014, Koprivnjak et al., 2009).

All methods are biased by the chemical and physical properties that regulate the extraction procedure and as a consequence DOM characteristics may vary (Simjouw et al., 2005; Green et al., 2014). Each methodology presents pros and cons, and far from being standardized, some other new procedures, such as membrane dialysis, extraction with different solvents and carbon nanotubes are emerging (Remucal et al., 2012; Fleurs et al., 2011; Sánchez-González et al., 2012).

Moreover, although DOM from different origins (e.g. freshwater, marine, groundwater DOM) presents some similarities, the extraction protocol efficiency might change depending on the water body. For instance, SPE (C<sub>18</sub> or PPL) is said to be not so effective when dealing with marine DOM (22-32 % recovery) in comparison to freshwater (42-60 % recovery) (Sleighter et al., 2008). Furthermore, there is almost nothing in the literature about the changes at molecular level that these different procedures may cause (Simjouw et al., 2005). So, further research should be carried out in this direction.

Besides, all the above mentioned methods require a filtration step before extraction, to ensure better performance of the method. Not all the studies perform the filtration stage under the same conditions (material of the filter, filter pore size). These factors might also alter DOM. In the present study, to avoid filtration an alternative methodology was used: the liquid-liquid extraction (LLE).

### 3.1.2. High Resolution Mass Spectrometry

#### *Sample Introduction and Ion Source*

First consideration that should be taken into account for the analysis of DOM with API source coupled to HRMS is that only ionizable compounds are susceptible to be analyzed (Nebbioso et al., 2013). Fortunately, there are many different commercially available API sources that can be coupled to HRMS. ESI, atmospheric pressure chemical ionization (APCI) and atmospheric pressure photo ionization (APPI) are used for thermally labile polar and non-polar compounds. Each source varies in its ionization mechanism and consequently the analytical window for each is quite different (see Figure 3.1.).

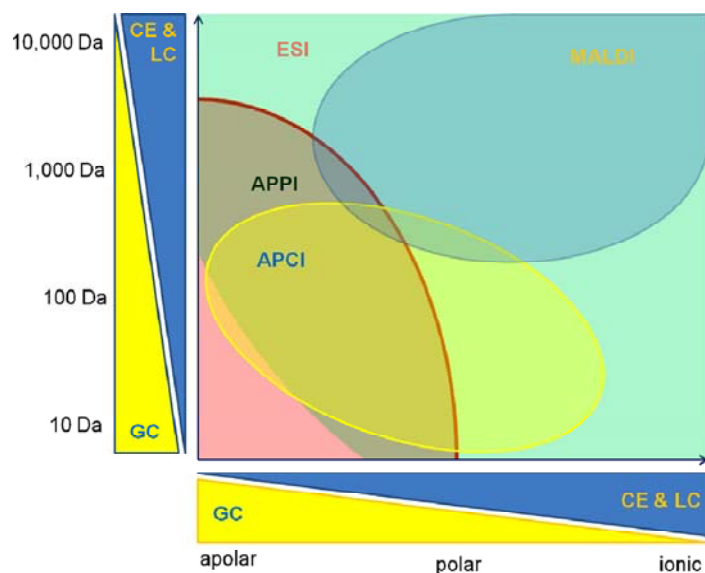


**Figure 3.1.** Diagram showing the mass range and polarity range covered by different ionization mechanisms (Forcisi et al., 2013).

Compared to the other interfaces (APCI and APPI), ESI covers with great sensitivity the efficient ionization of a wide variety of chemical compounds. With this soft ionization technique, the analysis of non-volatile intact molecules can be performed and for this

reason is now the ionization method of choice for the characterization of DOM. However, other ionization sources have also been tested (Hertkorn et al., 2008; D'Andrilli et al., 2010). In these previous studies, more assignable formulas were identified by ESI than by APPI or APCI, for DOM of different origins (see Figure 3.2.).

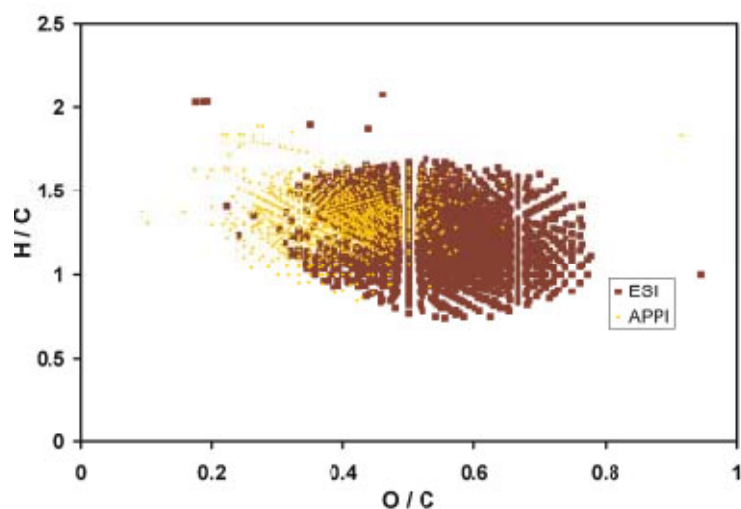


**Figure 3.2.** Van Krevelen diagram (see below) for all formulas observed in marine DOM by APPI and ESI (D'Andrilli et al., 2010).

Moreover, as it is a soft ionization source, usually molecular ions ( $[M+H]^+$  /  $[M-H]^-$ ) are obtained and no or little fragmentation occurs in the ion source. ESI is sensitive to changes in solvent composition and so molecular ions resulting from clusters with i.e. sodium and ammonium can occur (Bruins, 1998). For this reason, negative electrospray is usually the ionization mode used and  $[M-H]^-$  are the ions formed. This way the compounds are not ionized in alternative routes forming several adducts at a time and making the resulting spectra more complex.

The use of ESI for direct analysis without chromatographic separation has been applied using different strategies. These include: flow injection analysis (FIA) or flow injection electrospray (FIE) and direct-infusion electrospray (DIE). In FIA (or FIE) an amount of extracted sample is introduced to the ion source in solution as the flow from LC, whilst in DIE the extract diluted in a solvent is delivered directly to the ion source (Beckmann et al., 2008). Although applying these approaches for the analysis of real samples might cause ion suppression (huge differences between concentration ranges and chemical environments), it is worth using it, as a "global" overview sample composition can be obtained (Beckmann et al., 2008; Draper et al., 2013; Donegan et al., 2012). In fact, it has been successfully used in several studies from different disciplines even with

quantification purposes (Gao et al., 2013; Beißmann et al., 2013; Bhandari et al., 2012; Drapet et al., 2013).

Home-made FIA and DIE can be used, as only few common laboratory instruments are necessary, i.e. syringe, HPLC pump and syringe pump. More sophisticated liquid handling robots, such as Triversa NanoMate (Advion, USA) can be used. Moreover, in the last decade other improved approaches designed for the direct analysis (of extracts and samples) have been introduced creating a whole new group of desorption/ionization techniques (Cooks et al., 2006; Gross et al., 2014).

### Mass Analyzer

Due to the complexity of DOM, only mass analyzers capable of acquiring HRMS data are suitable for the characterization of DOM. As described in section 2.2.1. *Book Chapter: High Resolution Mass Spectrometric Techniques for Structural Characterization and Determination of Organic Pollutants in the Environment*, TOF, FT-orbitrap and FT-ICR are the mass analyzers capable of acquiring HR data for non-volatile compounds. However, TOF mass analyzers have presented some resolution limitations at low mass ( $m/z < 1000$ ) and drift from mass accuracy can occur (see also section 2.2.2. *Research Article N° 1: Accurate Mass Measurements and Ultrahigh-Resolution: Evaluation of Different Mass Spectrometers for Daily Routine Analysis of Small Molecules in Negative Electrospray Ionization Mode*). For such a complex mixture as DOM, TOF analyzers present limited resolution and peaks are not completely resolved, as shown in Figure 3.3.

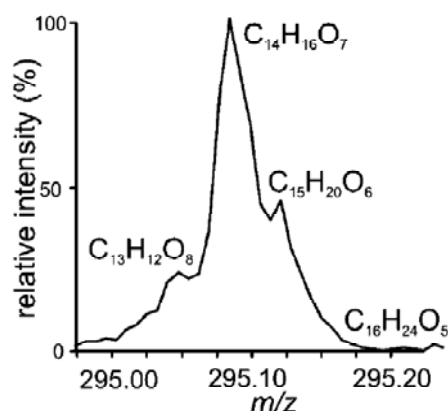


**Figure 3.3.** TOF spectra of the mass range  $m/z$  295.0-295.2 for a DOM sample (adapted from These et al., 2005).

For these reasons, the mass analyzers used in the present study were FT-orbitrap and FT-ICR. These are the mass analyzers capable of routine resolution  $\geq 100,000$  (FWHM). The key performance characteristics of Fourier transform (FT) mass spectrometers, including the theory and principles of operation, are described below.

### **Fourier Transform Ion Cyclotron Resonance Mass Analyzer**

The FT-ICR mass analyzer is a trapped-ion technique. The principle of operation is based on the ion motion in a magnetic field. The measurement of an ion by FT-ICR mass analyzer consists of different stages:

- 1) External Ion accumulation: the ion source generates ions continuously, but the FT-ICR mass analyzer is a pulsed detector. For this reason, ions are accumulated (externally to the ICR cell) in a multipole electric ion trap, while the ICR cell is full with ions from the preceding accumulation period (Senko et al., 1997; Xian et al., 2012).
- 2) Injection into the ICR cell: ions should be simultaneously ejected toward the ICR cell, minimizing spatial spreading of ions of a single  $m/z$ . It is achieved by applying 10–30 V to tilted wires placed between the rods of the multipole electric ion trap. Ions should enter the ICR cell at low kinetic energies, so that they can be confined and preferably located in the center of the cell (Scigelova et al., 2011).

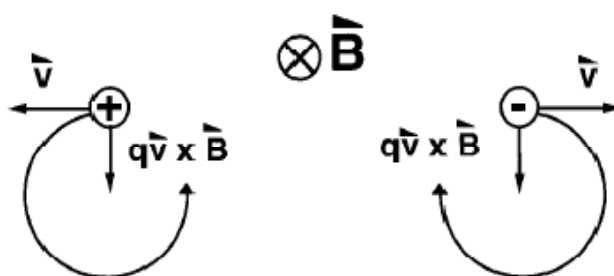


**Figure 3.4.** Ion cyclotron motion, in which  $B$  is the magnetic field,  $q$  is charge and  $v$  is velocity. The path of an ion moving in the plane of the paper is bent into a circle by the magnetic force produced by a magnetic field directed perpendicular to the plane of the paper. Positive and negative ions orbit in opposite senses. (Marshall et al., 1991).

- 3) Ion motion inside the ICR cell: when an ion enters a magnetic field, a force affects this charged particle and as a consequence the ion is trapped by the magnetic field on a circular trajectory. The ion moves perpendicular to the magnetic field with a rotation frequency ( $\omega$ ) (see Figure 3.4.). This frequency is characteristic for each mass and magnetic field and it is not dependant on initial coordinates and velocity of the ion

(Scigelova et al., 2011). To maintain ion spatial coherence also parallel to the magnetic field, an electrostatic field is applied.

4) Excitation of ions in the ICR cell: The cyclotron motion that ions have in the ICR cell is too small to generate a detectable image current. Ions should be excited to a larger radius for a signal to be detected (see Figure 3.5.). This can be achieved by several different methods, but basically an electric field has to be applied.

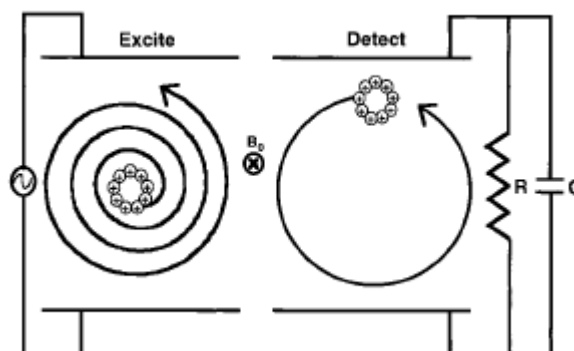


**Figure 3.5.** Ions are excited in the ICR cell with the application of an electric field. Therefore, the ion motion changes and ions are detectable by the detector plates (Marshall et al., 1998).

5) Detection of the signals and FT operation: The detection is carried out in the ICR cell-wall where the detector plates are placed, in order to induce a measurable image current which is transformed into a mass spectrum using fast FT (Perry et al., 2008). The FT tool converts the time domain signal into frequencies. With the calibration of the instrument, the frequencies are transformed to  $m/z$  and this way the mass spectrum is obtained (see Figure 3.7.).

### **Fourier Transform Orbitrap Mass Analyzer**

The orbitrap is the newest FT mass analyzer, invented in 1999 (Makarov 2000). The original roots of the orbitrap stem from the ability to trap charged particles in electrostatic fields, defined by Kingdon in 1923 (Kingdon 1923) and bears a similarity to the FT-ICR (Hu et al., 2005). As happens with FT-ICR mass analyzers, the mass spectrum obtained from the orbitrap is preceded by several steps:

1) External Ion accumulation: Like FT-ICR, orbitrap mass analyzer is a pulsed detector, but in this case ions are collected in a “C” trap and injected simultaneously toward the orbitrap (Perry et al., 2008). This method provides fast and uniform injection for large ion populations. Automatic gain control (AGC) target and maximum injection time are

parameters typically found in ion traps (IT), that should be also appropriately selected in the orbitrap (Kaufmann et al., 2010). AGC target and maximum injection time are used to control the number of ions and maximum time taken to fill the "C" trap.

2) Injection into the orbitrap: The ions enter the orbitrap through a small hole in one of the outer electrodes, due to a pulsed extraction from the "C" trap. The high voltage of the central electrode causes an attractive force to the ions, so that they cannot escape.

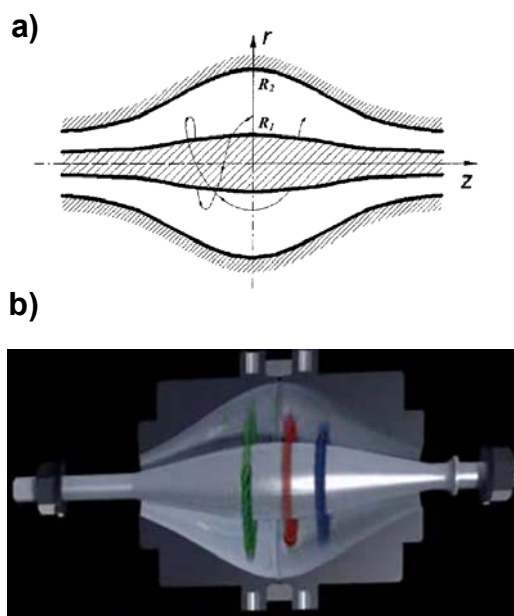


**Figure 3.6.** a) Example of a stable ion trajectory in an orbitrap mass analyzer (Makarov 2000); b) Representation of the ion motion of different  $m/z$  ions inside the orbitrap (adapted from [www.thermoscientific.com](http://www.thermoscientific.com)).

3) Ion motion inside the orbitrap: The orbitrap confines ions in an electrostatic field created between shaped coaxial central and outer electrodes. In the absence of a superconducting magnet, ion stability is achieved only due to ions orbiting around the axial electrode (Figure 3.6.) (Ham 2008; Perry et al., 2008). The field inside the orbitrap is not static and by increasing the voltage the ions are forced to initiate axial oscillations. Different to FT-ICR, no excitation stage is necessary. Orbiting ions perform harmonic oscillations along the electrode with frequency proportional to  $(m/z)^{-1/2}$ .

4) Detection of the signals and FT operation: The oscillations from the ions along the central electrode are detected using image current detection by the outer orbitrap electrodes and are transformed into mass spectra using fast FT, similarly to FT-ICR.

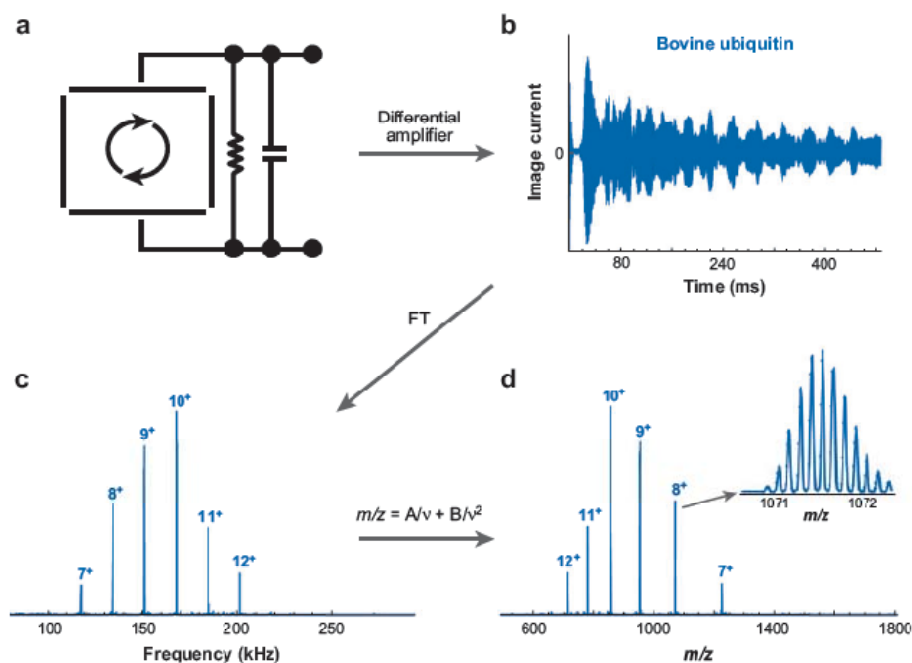


**Figure 3.7.** a) Schematic representation of excited ion cyclotron rotation, b) time-domain image-current signal from opposed detection electrodes, c) frequency-domain spectrum obtained by fast Fourier transform and d) mass spectrum obtained by calibrated frequency-to- $m/z$  conversion (Marshall et al., 1998).

### ***FT Mass Analyzers Commercially Available***

The main components of an FT-ICR mass analyzer are: a high-field magnet, an ion cyclotron resonance cell and a vacuum system capable of achieving  $10^{-9}$  to  $10^{-10}$  Torr. The main components of an FT-orbitrap are: a "C" trap, an orbitrap and a vacuum system capable of similar vacuum values. Based on these basic configurations, several instruments are available, presenting different performance characteristics (see Table 3.1.).

The commercially available FT-ICR instruments are presented as an hybrid that consists of a linear ion trap (LIT) or a Q coupled to a FT-ICR mass analyzer. Currently, there are several instruments that even with the same configuration present different technical specifications (resolution, fragmentation techniques, accuracy) depending on the specific model.

Since the first commercial LIT-Orbitrap, different orbitrap based mass spectrometers have been designed. It can be said that three different configurations can be found. The single-stage Orbitrap high collision dissociation (HCD) mass spectrometer, the hybrid Q-Orbitrap HCD mass spectrometer and the hybrid LIT-Orbitrap HCD mass spectrometer. Although the hybrid models provide additional versatility to MS/MS experiments, the

analytical performance and fundamental principles of operation of the orbitrap analyzers in all the instruments are identical (Perry et al., 2008).

**Table 3.1.** Overview of Fourier Transform mass analyzers commercially available with their technical specifications. In bold the mass spectrometers used during the present study (see below 3.2.1.3. Performance of Fourier Transform Mass Analyzers) (adapted from Holčapek et al., 2012).

Mass analyzer	Instrument name, manufacturer	Resolution, $m/\Delta m$ (FWHM)	Mass Accuracy		$m/z$ range	Acquisition speed
			External	Internal		
Q-ICR	Solarix 15T, Bruker Daltonics	2,500,000 ( $m/z$ 400)	< 0.6	< 0.25	100-10,000	-
	<b>Solarix 12T, Bruker Daltonics</b>	1,000,000 ( $m/z$ 400)	< 0.6	< 0.25	100-10,000	-
LIT-ICR	<b>LTQ FT Ultra 7T, Thermo Scientific</b>	1,000,000 ( $m/z$ 400)	< 1.2	< 1	50-4000	1 Hz at R: 100,000
LIT-Orbitrap	Orbitrap Elite, Thermo Scientific	240,000 ( $m/z$ 400)	< 3	< 1	50-2000; 200-4000	4 Hz at R: 60,000 1 Hz at R: 240,000
	<b>LTQ Orbitrap XL, Thermo Scientific</b>	100,000 ( $m/z$ 400)	< 3	< 1	50-2000; 200-4000	1 Hz at R: 60,000 0.6 Hz at R: 100,000
Q-Orbitrap	Q Exactive Plus, Thermo Scientific	280,000 ( $m/z$ 200)	< 3	< 1	50-4000	1 Hz at R: 280,000
Orbitrap	Exactive Plus, Thermo Scientific	140,000 ( $m/z$ 200)	< 3	< 1	50-6000	1 Hz at R: 140,000
	<b>Exactive, Thermo Scientific</b>	100,000 ( $m/z$ 200)	< 5	< 2	50-4000	1 Hz at R: 100,000

### 3.1.3. Formula Determination, Data Analysis and Representation

As discussed above, the final goal of any AM measurement is the determination of the elemental formula. For DOM, identification and formula determination is based on ultrahigh resolution ( $R > 100,000$  FWHM), sub-ppm accuracy on accurate mass measurements and posterior strategies to filter the list of candidates obtained, i.e. elements in use, isotopic pattern and element ratios.

It can be difficult, tedious and labor-intensive to compare the thousands of assigned molecular formulas for a single DOM sample. One method of depicting large data sets of elemental formulas is by mean of van Krevelen diagrams, which are useful to classify substance classes in a first approach (Kujawinski et al., 2006). Since major chemical classes typically found in DOM have characteristic H/C and O/C ratios, they cluster within specific regions of the van Krevelen diagram (see Figure 3.8.). Further, van Krevelen plots are used to evaluate the degree of alkylation, hydrogenation, hydration, and oxidation of DOM (Kim et al., 2003).

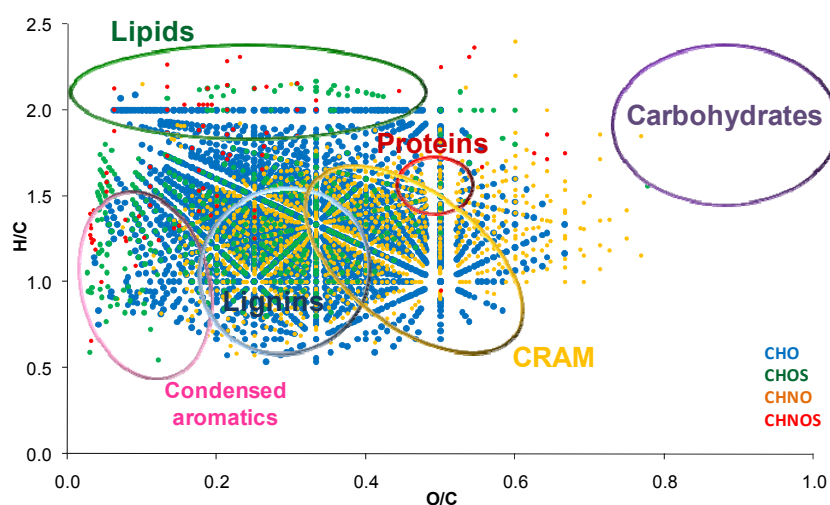


**Figure 3.8.** Van Krevelen diagram for a DOM sample. The colored circles show the theoretical areas to classify substance classes, described in the NOM literature (Hertkorn et al., 2006; Hertkorn et al., 2008; Sleighter et al., 2008).

Van Krevelen diagrams can be built taking into account the different composition of the elemental formulas assigned and also on color-coded analyte relative abundance plots or intensity bubble plots. Although intensity in an ESI-HRMS spectrum does not translate directly into relative concentration for analytes of very diverse chemical composition, a qualitative comparison of isolates on the basis of signal intensities can be performed

when the samples have been analyzed with identical instrumental conditions (Reemtsma et al., 2009).

Moreover, Kendrick Mass Deffect (KMD) is another diagram that is often used for the characterization of DOM and it is used to sort out homologous series of organic compounds (see Figure 3.9.) (Hertkorn et al., 2006). KMD has also been used for some researchers as an strategy to determine the most probable formula, when assignment of formulas at higher masses was not unequivocal (Stenson et al., 2003).

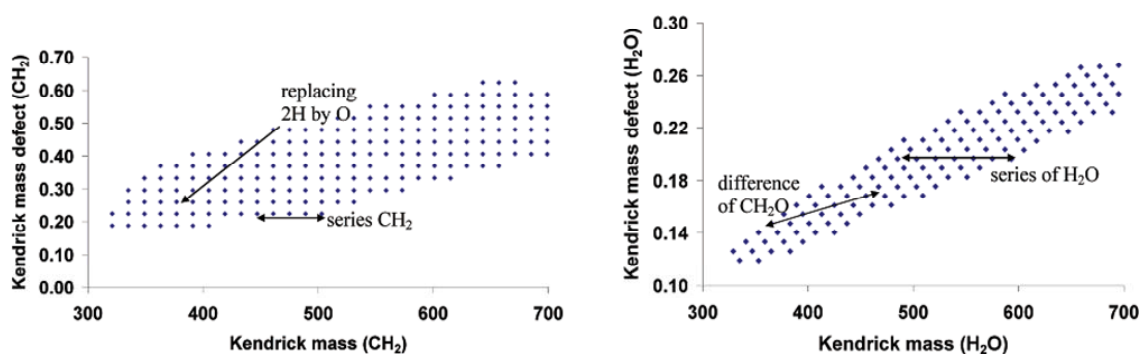


**Figure 3.9.** Kendrick Mass Deffect analysis based on CH<sub>2</sub> group (left) and based on H<sub>2</sub>O (right) (adapted from Kim et al., 2003).

Useful parameters in the characterization of the unsaturation and aromaticity of molecular formulas are the DBE, the ratio between DBE and carbon (DBE/C), and the double bond equivalents minus oxygen (DBE-O) (Gonsior et al., 2009; Tfaily et al., 2013). Although scientists are more familiar with DBE, the DBE/C parameter is better to be used since bigger molecules can have higher DBE but lower “true” carbon unsaturation. On the other hand, the DBE-O parameter has also been described as a better indicator for the unsaturation of the carbon skeleton compared to the DBE, since most oxygen atoms in DOM molecules are a part of carboxyl group that is counted as one DBE. In the present study, DBE-O has been used to better understand the changes of unsaturation and aromaticity along the treatment.

More recently, multivariate statistical analysis in combination with visualization diagrams have been utilized to evaluate relationships among sample sets. Hierarchical cluster analysis (HCA) illustrates in a dendrogram the correlations between samples (Sleighter et al., 2010). While HCA is useful for grouping samples based on their similarity, it does not indicate the reasons why the samples are similar or different. Non-metric multidimensional scaling, indicator species analysis, principal component analysis and orthogonal partial least squares have been used to define trends on the data,

discriminate between experimental groups and export the  $m/z$  values that define each group (Kujawinski et al., 2009; Sleighter et al., 2010; Xu et al., 2012).

In the present study some of these representations have been used to process and organize HRMS data.

### 3.1.4. Structural Characterization

Even though data analysis of HR mass spectra of DOM can provide accurate molecular formulas, structural information is still unknown. MS cannot distinguish structural isomers of an elemental composition, so the same molecular formula in multiple samples does not necessarily mean that their molecular structure also correspond.

As described in chapter 1 subsection 1.2. *Methods of Analysis of Dissolved Organic Matter* some complementary techniques have given information at structural level about DOM. The most in use nowadays is high-field NMR (Hertkorn et al., 2013). However, also based on HRMS, some tandem experiments have been performed in few studies. Tandem mass experiments have been carried out in low resolution mass spectrometers, in FT-ICR and more recently in FT-orbitrap. Most of the studies have shown neutral losses corresponding to H<sub>2</sub>O, CO<sub>2</sub>, CO and OCH<sub>2</sub> and are focused on DOM standards (i.e. Suwannee River FA (SRFA) standard).

In the present study, tandem mass experiments have been carried out with an FT-orbitrap to obtain structural information from marine DOM (sample) and compare the fragmentation pathways with the fragments obtained under the same conditions for the SRFA standard.

## 3.2. Experimental Procedure and Results

As has been perviously mentioned, in this chapter we describe the methodology used for the characterization of DOM in the aquatic media and it can be divided in two subsections: 3.2.1. *Direct Analysis of Dissolved Organic Matter* and 3.2.2. *Research Article N° 2: Structural Characterization of Marine Dissolved Organic Matter. Fragmentation Studies.*

Firstly, a new approach for DOM isolation based on LLE has been successfully applied in comparison to the most usual one based on SPE (3.2.1.1. *Isolation of Dissolved Organic Matter*). Further information about molecular changes of DOM isolated by these techniques is under investigation.

Moreover, new approaches have been tested based on FT-orbitrap mass analyzer in comparison to FT-ICR, to confirm the capabilities of the new mass analyzer. Comparisons were carried out analyzing the SRFA standard and are included and discussed in the section 3.2.1.3. *Performance of Fourier Transform Mass Analyzers.* Figures of merit such as resolution, sensitivity, mass accuracy and spectral accuracy of each type of instrument are evaluated.

All these results are not included as an article, due to the fact that some of the studies comprehend several other experimental data and contributions that have to be fully processed in the future to be published. However, it is a very important and successful part of the work developed during the realization of this thesis and for this reason we have considered it to be essential to be included.

In addition, structural information is important to fully elucidate the characteristics of DOM. In the second part, an approach based on HRMS/MS has been applied to obtain information about the functional groups present in marine DOM. Experimental details, results and discussion are included as a research article entitled *Structural Characterization of Marine Dissolved Organic Matter. Fragmentation Studies* submitted to *Analytical and Bioanalytical Chemistry*.

### 3.2.1. Direct Analysis of Dissolved Organic Matter

#### 3.2.1.1. Isolation of Dissolved Organic Matter

From the different extraction procedures available in the literature, SPE is in general the easiest, most achievable and popular nowadays. Some other methodologies (e.g. UF, XAD) although also quite used, require specific instrumentation (i.e. pumps, membranes) or present problems with blanks due to resin leaching (Sleighter et al., 2011). However, the main drawback of the SPE method is that a previous filtration step is necessary to assure good performance of the SPE cartridge. As the aim of these studies was to see the evolution of DOM along advanced treatments, we did not want to add any further filtration step, which does not correspond to the treatment. For that reason, LLE was used to avoid sample filtering and analyze the whole water.

LLE has been used and is still used for screening purposes in other applications (Barco et al., 2003; Cabaleiro et al., 2013; Gure et al., 2014; Wei et al., 2014). The main advantage is that the analysis of whole water can be performed and the contact with plastics or teflon tubes is minimized; so in general the sample contamination is less probable. Only muffled glass material and high-performance liquid chromatographic grade solvents are used. However, it has been generally substituted by SPE methods, due to the amount of solvent used and the impossibility of automation. As said before, SPE with different cartridges is frequently used in the literature for DOM analysis. However, in order to know how the LLE method was performing for the isolation of DOM, several tests were carried out.

Briefly the extraction protocols used were:

**DOM extraction by LLE.** 1L of each sample was acidified with 10% hydrochloric acid to pH 2 and extracted with 2 x 100 mL of dichloromethane/isopropyl alcohol (90:10 v/v) using separatory funnel techniques. The extracts were concentrated down to 250  $\mu$ L at 40 °C under nitrogen.

**DOM extraction by SPE-PPL.** 1 L of each sample was filtered (0.45  $\mu$ m Millipore) and acidified with 10% hydrochloric acid to pH 2. According to the manufacturers guidelines and references in the literature (Dittmar et al., 2008), the cartridges (Bond Elut PPL, 500 mg, 6mL) were rinsed with 1 cartridge filling of methanol immediately before

use. For the DOM adsorption, the samples were passed through the cartridges with the help of a peristaltic pump at flow rates not exceeding 10 mL/min. Before elution of DOM, the cartridges were rinsed with at least 2 cartridge volumes of 0.01 M HCl for complete removal of salt. Sorbents were dried and DOM was immediately eluted with 1 cartridge volume methanol at a flow rate of <2 mL/min into a muffled turbovap. The extracts were concentrated down to 250  $\mu$ L at 40 °C under nitrogen.

### **Extraction Efficiencies**

Extraction efficiency as sometimes reported by measuring the non-purgable organic carbon (NPOC) before and after the sample going through the SPE cartridge was not performed with LLE, just in case any small contribution of organic solvents will distort the measurements. For this reason, the yield of DOM recovery on extraction using organic solvents (dichloromethane/isopropyl alcohol) was tested comparing the amount of dry DOM extracted with SPE (PPL cartridge) and LLE extraction, obtaining a relative DOM recovery:

$$\text{Equation 3.1.} \quad \% \text{ rDOM recovery} = \frac{\text{mg of dry DOM extracted by LLE}}{\text{mg of dry DOM extracted by SPE}} \times 100$$

As discussed before, the different mechanisms involved in each isolation protocol may modify the characteristics of DOM extracted. However, the same way round, the characteristics of DOM from different origins as well as other compounds present in the water, may modify the efficiency of each isolation protocol. For this reason, the extractions (SPE-PPL and LLE) were tested in different water types: ultrapure water, SRFA dissolved in ultrapure water, pristine water, surface water from a river, coastal seawater, deep seawater and wastewater. The water samples were from different origins and presented very different characteristics (Table 3.2.). All the extractions were carried out in duplicate. An aliquot of each extraction was concentrated to dryness (until constant weight) under nitrogen in a vial, so that the amount of dry sample could be weighted.

The LLE method presented acceptable recoveries with respect to the SPE-PPL method (see Table 3.3.). As a result, the yield of rDOM recovery (LLE in front of SPE) was between 34-49%, for marine DOM. That was the worst case for LLE; however, for the

rest of water bodies, the extraction efficiencies were equivalent or in the case of wastewater the recovery was better for the LLE (258 % recovery with respect to SPE extraction).

**Table 3.2.** Summary of some complementary analysis performed on the samples. The mean value and the standard deviation (in brackets) of n:4 is shown.

Water Samples	pH	Conductivity (mS/cm)	NPOC (mg/L)	TIC (mg/L)	TN (mg/L)	UV (254nm m <sup>-1</sup> )
Ultrapure water	6.68 (0.02)	0 (0)	0.2 (0.08)	0.009 (0.006)	0.47 (0.09)	0.12 (0.03)
SRFA in ultrapure water	8.84 (0.03)	51 (1)	1.9 (0.2)	10.6 (0.1)	0.5 (0.1)	4.15 (0.02)
Pristine Water	8.22 (0.08)	0.191 (0.001)	0.79 (0.09)	16.3 (0.1)	0.57 (0.5)	0.28 (0.02)
Surface Water	8.38 (0.01)	0.284 (0.001)	3.08 (0.08)	12.2 (0.1)	2.4 (0.2)	7.0 (0.1)
Coastal Seawater	8.19 (0.01)	38.19 (0.01)	0.98 (0.02)	13.1 (0.1)	0.8 (0.3)	2.8 (0.1)
Deep Seawater	8.02 (0.02)	119 (1)	0.72 (0.01)	18.8 (0.1)	0.4 (0.05)	0.8 (0.3)
Wastewater	8.32 (0.03)	1.29 (0.01)	337 (5)	41.4 (0.4)	41.5 (0.05)	67.7 (0.6)

**Table 3.3.** Yield of rDOM recovery (LLE in front of SPE) for the samples of the study. The mean and the standard deviation (in brackets) of n:2 is shown.

Water Samples	% rDOM recovery
Ultrapure water	98 (1)
SRFA in ultrapure water	102 (5)
Pristine Water	114 (7)
Surface Water	85 (10)
Coastal Seawater	49 (6)
Deep Seawater	34 (10)
Wastewater	258 (20)

### Characteristics of DOM-LLE

SRFA is usually used for comparison with other DOM samples (freshwater or marine DOM), although the isolation procedure for SRFA is carried out with XAD resins ([www.humicsubstances.org](http://www.humicsubstances.org)). As it is a reference standard in many studies, LLE was initially tested using SRFA dissolved in ultrapure water (2 mg C/L). As can be seen in Figure 3.10., after extraction the typical regular patterns observed for SRFA standard are still visible.

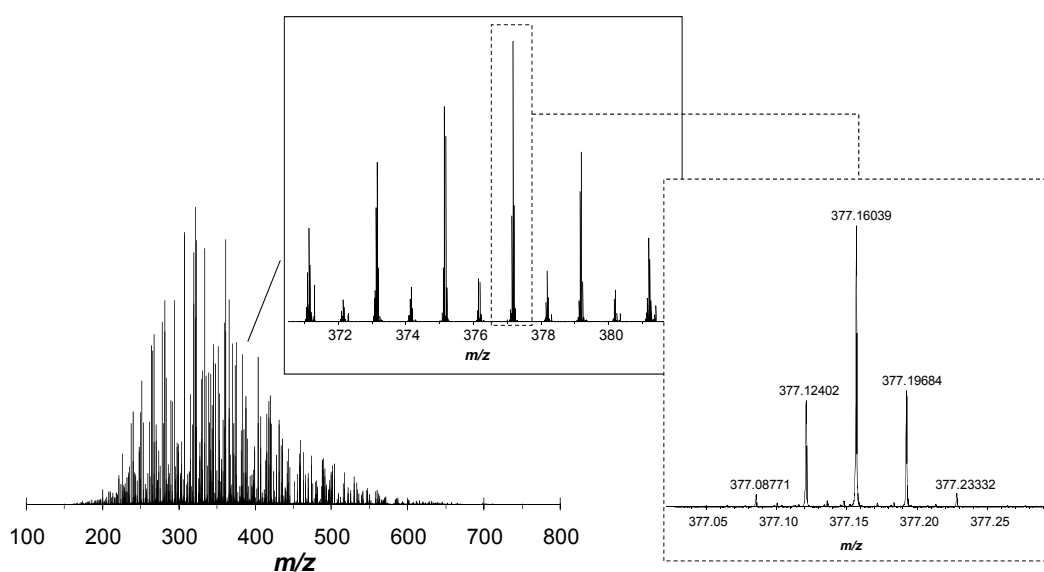


**Figure 3.10.** (Left) SRFA analysis with FT-orbitrap (R:100,000,  $m/z$  400) after LLE. (Middle) Zoom of the mass range  $m/z$  372-380. (Right) Zoom of the nominal mass  $m/z$  377, showing the regular patterns typical of DOM.

Furthermore, first analysis of surface seawater showed also comparable results with the data in the literature. In Table 3.4, the main DOM characteristics ( $H/C_{av}$ ,  $O/C_{av}$ ,  $DBE_{av}$ ) are summarized for comparison with other studies of marine DOM characterization. It is shown that equivalent results can be obtained with both methodologies, LLE and SPE (with different sorbents). For the LLE extract, only the  $DBE_{av}$  value seems to be a little bit lower than the rest. As described elsewhere, fractionation occurs in any extraction procedure and we can expect that fractionation occurs in LLE too (Sleighter et al., 2008; Green et al., 2014).

From the results of the study, more saturated compounds (more hydrogen content) might be enriched in DOM-LLE (lower number of DBE). Similar phenomenon has been observed in other methods. For instance, it has been described that  $C_{18}$  has a higher selectivity for N-poor compounds because organic nitrogen is often charged, specially at

pH=2. Therefore N-containing compounds are not retained by the apolar C<sub>18</sub> phase (Koch et al., 2005). Further research should be carried out with respect to individual compounds being extracted with all the methodologies in use. For instance, the effect of different SPE sorbents and different organic solvents for the LLE should be tested at molecular level.

**Table 3.4.** Characteristics of the formulas identified of marine DOM by different extraction protocols.

Sampling Site	Extraction protocol	O/C <sub>av</sub>	H/C <sub>av</sub>	DBE <sub>av</sub>	References
Surface Sea - 30 m	LLE	0.32	1.43	6.2	This study
Surface Sea - 30 m	SPE - C18	0.37	1.29	9.3	Koch et al., 2005
Surface Ocean - N/A	SPE - C18	0.35	1.30	9.4	Kujawinski et al., 2009
Surface Ocean - 48 m	SPE - PPL	0.53	1.62	N/A	Hertkorn et al., 2013
Coastal Sea	SPE - C18	0.33	1.43	7.2	Sleighter et al., 2008
Coastal Sea	SPE - PPL	0.49	1.25	9.3	Lechtenfeld et al., 2013
Deep Ocean - 1000 m	SPE - C18	0.33	1.12	8.9	Kujawinski et al., 2009
Deep Ocean - N/A	SPE - PPL	0.50	1.24	9.14	Schmidt et al., 2009
Deep Ocean - 5446 m	SPE - PPL	0.67	1.74	N/A	Hertkorn et al., 2013

N/A: no data available

### 3.2.1.2. Sample introduction and Ion Source

As described above, the coupling of LC to HRMS for the analysis of DOM is unsolved. In fact with conventional C<sub>18</sub> columns, the structural information and regular patterns of DOM are lost (Mawhinney et al., 2009; Green et al., 2014). This is a drawback because these homologous series are usually used to confirm an assigned formula (i.e. KMD). Furthermore, SEC is said to form adducts or colloids, changing the real nature of DOM (Koch et al., 2005). In any case, reversed-phase and SEC chromatography are usually used as preparative techniques rather than a technique to introduce the DOM sample into the mass spectrometer (Koch et al., 2008). The main reason is that scan speed for high resolution acquisition (R>100,000) is too slow. Some couplings have been carried

out between LC and TOF mass analyzers due to the fact that TOF presents faster scan speed, but then this mass analyzer presents some limitations with regard to resolution (Mawhinney et al., 2009). Due to the difficulties that liquid chromatography may present, most of the studies use direct analysis of DOM extracts (Drapet et al., 2013).

In the present study, FIE (or FIA) and DIE have been used for the introduction of the sample into the mass spectrometer. Briefly,

**FIE analysis.** The FIE (or FIA) analysis consisted in the injection of 10 $\mu$ L of DOM extract into a stream of solvent (MeOH:H<sub>2</sub>O, 80:20) entering the ionization chamber at a steady rate (50  $\mu$ L/min). A typical infusion profile lasted around 1 min rising sharply and then tailing off more gradually. A delay of 3 minutes before the next sample is infused into the solvent stream was set to avoid any 'carry over' between consecutive injections. Moreover, a region of signal 'noise' is obtained, which can be used for background subtraction. The resulting spectra is the combine spectra of the scans comprising approximately the center of the major infusion peak (see Figure 3.11.).

**DIE analysis.** For the DIE analysis diluted DOM extracts (in methanol) were injected into the electrospray source using a micro-liter pump at a flow rate of 120  $\mu$ L $\cdot$ h<sup>-1</sup>. Infusion lasted for 20 minutes, giving the mass analyzer (FT-ICR in this case) time to acquire 500 scans. Between injections a washing step was necessary (20 extra minutes) to prevent contamination from the previous sample.

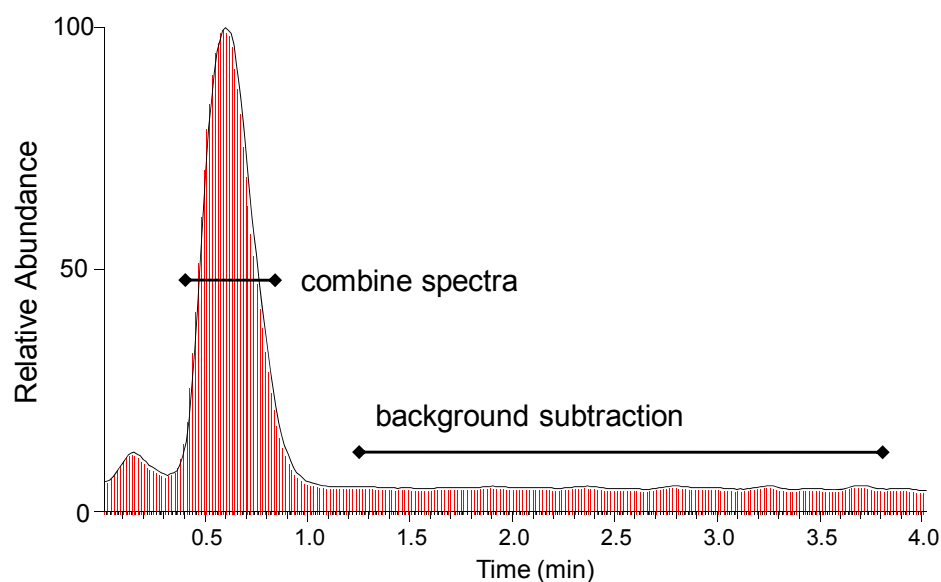


**Figure 3.11.** Flow injection analysis of an ESI-HRMS experiment with a single peak containing all DOM compounds in the absence of a chromatographic column. The vertical red lines are the scans performed.

Using FIE or DIE mode of sample introduction presents different characteristics with regard to time of analysis, carry over, number of scans and scan speed (see Table 3.5.). FIE presents two main advantages in front of direct infusion: analysis time and carry over. However, limitations due to scan speed of the instrument will determine the sample introduction mode. Furthermore, if more than one experiment should be carried out, such as MS/MS fragmentation, DIE will be more suitable, as higher number of scans can be acquired.

With regard to ion source, ESI was chosen to carry out all the analysis. As explained above, other studies have shown that ESI is the ion source with which more assigned formulas have been obtained. All the analysis were carried out in negative and positive mode, although only negative data is included in the thesis. The simplicity of the spectra in negative mode makes it more suitable to export the most outstanding results.

**Table 3.5.** Characteristics when using flow injection or direct infusion for the analysis of DOM with HRMS.

	<b>Flow injection</b>	<b>Direct infusion</b>
<b>Time of analysis</b>	short (e.g. 2 minutes)	long (e.g. 20 minutes)
<b>Carry over - contamination</b>	less	more
<b>Scan speed of the mass analyzer</b>	should be fast	not necessary fast
<b>Number of scans</b>	few	as many as you want
<b>Number of experiments</b>	one (i.e. full scan)	several (i.e. full scan + MS/MS)

### 3.2.1.3. Performance of Fourier Transform Mass Analyzers

Linearity of detection and very high fidelity in the determination of frequency are inherent to FT instruments and allow very high mass accuracy (Scigelova et al., 2011, Makarov 2000). The main reason is that frequency can be measured more accurately than any other experimental parameter (i.e. voltage, time of flight), due to the fact that it is independent of the initial ion properties (initial position and/or velocity of the ion). In the FT-ICR and FT-orbitrap, the rotation frequency and the axial frequency, respectively are used to derive the  $m/z$  ratio (see Table 3.6.).

**Table 3.6.** Fundamental and resolution equations for FT-ICR and FT-orbitrap mass analyzers.

	<b>Fundamental Equation</b>	<b>Resolution Equation</b>
<b>FT-ICR</b>	$\omega = \frac{z}{m}B$	$R = \frac{m}{\Delta m} = \frac{rB^2z}{2\epsilon m}$
<b>FT-Orbitrap</b>	$\omega = \left(\frac{kz}{m}\right)^{1/2}$	$R = \frac{m}{\Delta m} = \frac{1}{2\Delta\omega_{50\%}}\left(\frac{kz}{m}\right)^{1/2}$

FT-ICR has proved to be capable of molecular DOM characterization. FT-orbitrap has been less used and as any new technique has received some criticism. In the present study, FT-ICR and FT-orbitrap have been used for DOM characterization. For the two mass analyzers of the study, different commercially available instruments have been used:

- a Q-ICR (Solarix 12T, Bruker Daltonics), from now on 12T FT-ICR
- a LIT-ICR (LTQ FT Ultra 7T, Thermo Scientific), from now on 7T FT-ICR
- a LIT-Orbitrap (LTQ-Orbitrap XL, Thermo Scientific), from now on standard Orbitrap
- an Orbitrap (Exactive, Thermo Scientific), from now on compact Orbitrap

Experimental comparison has been carried out between them to visualize the different effects that the mass analyzer, acquisition time and magnetic field may have on resolution. Moreover, resolution is going to have some effect on mass accuracy, spectral accuracy and peak height (sensitivity). These effects have been studied. SRFA standard from the IHSS, diluted in methanol (1 mg / L) has been used for the comparison. Triplicates have been carried out for each case (each instrument and operational condition) and the results are the mean of these replicates. The technical specifications of the different mass spectrometers used are highlighted in bold and described in Table 3.1. The instruments were externally calibrated and eventually internal calibration (post-acquisition correction) was also carried out.

### **Resolution**

One of the most important characteristics of FT-ICR and FT-orbitrap is resolution, as they are capable of routine resolution  $\geq 100,000$ . As it has been discussed before, resolution has two major effects on the mass spectra of compounds: the width of the signal and the intensity (section 2.2.2.). When increasing resolution, peaks in the spectrum become thinner, so interferences will not disturb. Nevertheless, the loss in

intensity of the signal is significant. Resolution differs depending on the mass analyzer and the mass spectrometer. For FT-ICR, resolution varies as  $(m/z)^{-1}$  which means that for a fixed magnetic field strength and acquisition time, we are going to have worse resolution at higher masses. Similar to FT-ICR, for the orbitrap the mass resolution is proportional to  $(m/z)^{-1/2}$  (Perry et al., 2008).

To evaluate the resolution of the different models of the mass analyzers, an acquisition time of 1 second was set and analysis of SRFA by direct injection were carried out. As expected and as it is shown in Figure 3.12., FT-ICR (no matter the field strength, i.e. 12T or 7T) can achieve higher resolution in all the mass range of the study ( $m/z$  200-800).

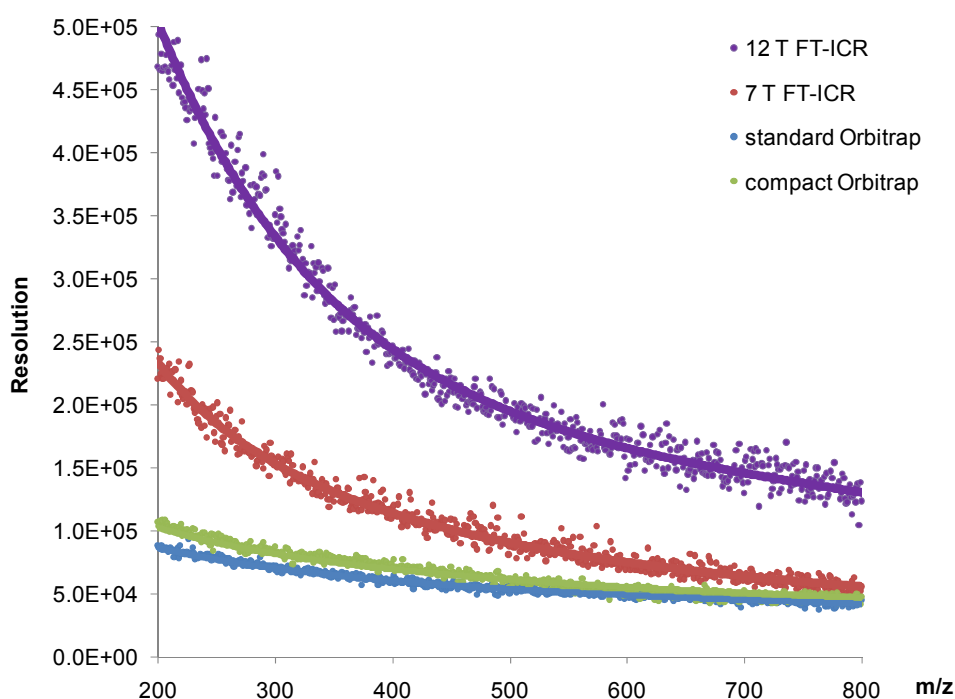


**Figure 3.12.** Resolution achievable with FT-ICR and FT-Orbitrap mass analyzers. An acquisition time of 1 second has been considered for FT-ICR with field strength 12 and 7 T and for two models of FT-Orbitrap, standard and compact.

For the mass range  $m/z$  200-800, where most of DOM signals are found, resolution with FT-ICR is higher, whereas for higher  $m/z$  ( $m/z > 1100$ ) resolution of the different instruments used is more similar (Perry et al., 2008). However, it is important to highlight that for FT-ICR resolution diminishes faster than for FT-orbitrap with respect to  $m/z$ , as can be observed in Figure 3.12. and as it can be deduced from the resolution equation in Table 3.6. For FT-ICR resolution diminishes inversely proportional to  $m/z$ , whereas for FT-orbitrap the resolution diminishes inversely proportional to the square of the  $m/z$ .

In complex samples, maximum resolution is desirable in order to be sure to resolve all the compounds. One way to increase resolution is to allow for longer transient acquisitions (Scigelova et al., 2011; Perry et al., 2008). As can be seen in Figure 3.13., using 1 second or 2 seconds acquisition time per spectra, double resolution can be obtained. The same effect is observed in both FT-ICR and FT-orbitrap, no matter the instrument model.

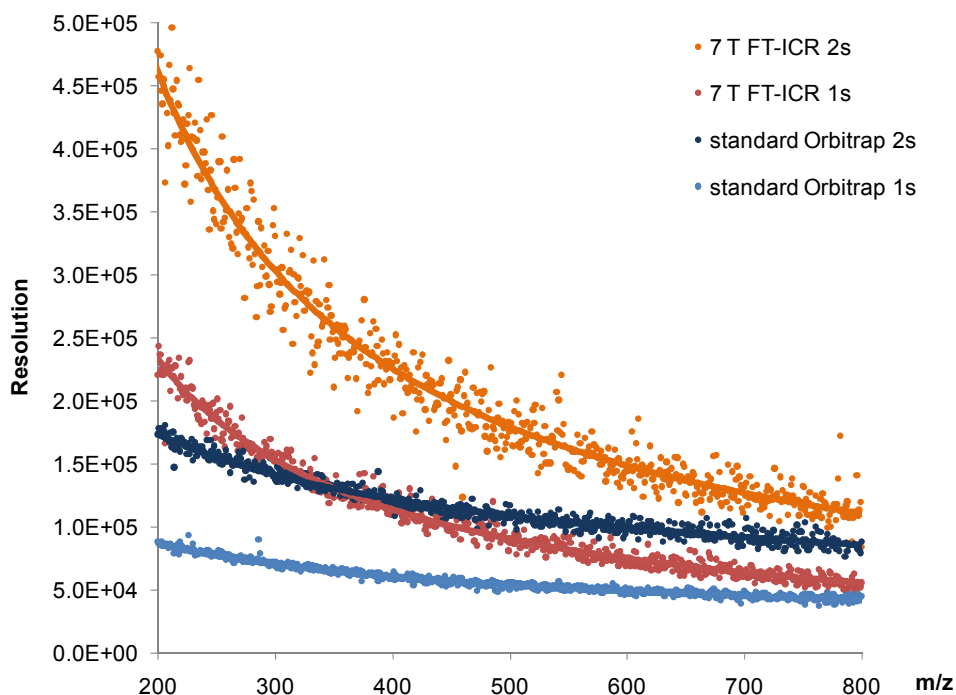


**Figure 3.13.** Effect of transient acquisition time on resolution. Resolution achieved with 7 T FT-ICR and standard FT-Orbitrap mass analyzers at different transient acquisitions time of 1 second and 2 seconds.

As has been described before (Scigelova et al., 2011) and is also observed in the present data, the standard FT-Orbitrap can achieve better resolution for  $m/z > 500$  if the acquisition time is longer. However, the acquisition time for the FT-orbitrap mass analyzer is more limited: maximum 2 seconds (3 seconds in the last improved prototypes) and so it is the resolution achievable (Makarov et al., 2009).

Furthermore, for FT-ICR mass analyzers resolution is proportional to magnetic field ( $B$ ) strength and as a consequence, FT-ICR instruments with stronger magnetic field would achieve higher resolution (see equation in Table 3.6.). An example is shown in Figure 3.14. For orbitrap, the last designs showed that decreasing the gap between the inner and outer orbitrap electrodes, allowed higher frequencies of ion oscillations and hence higher resolution over fixed acquisition time (Makarov et al., 2009).

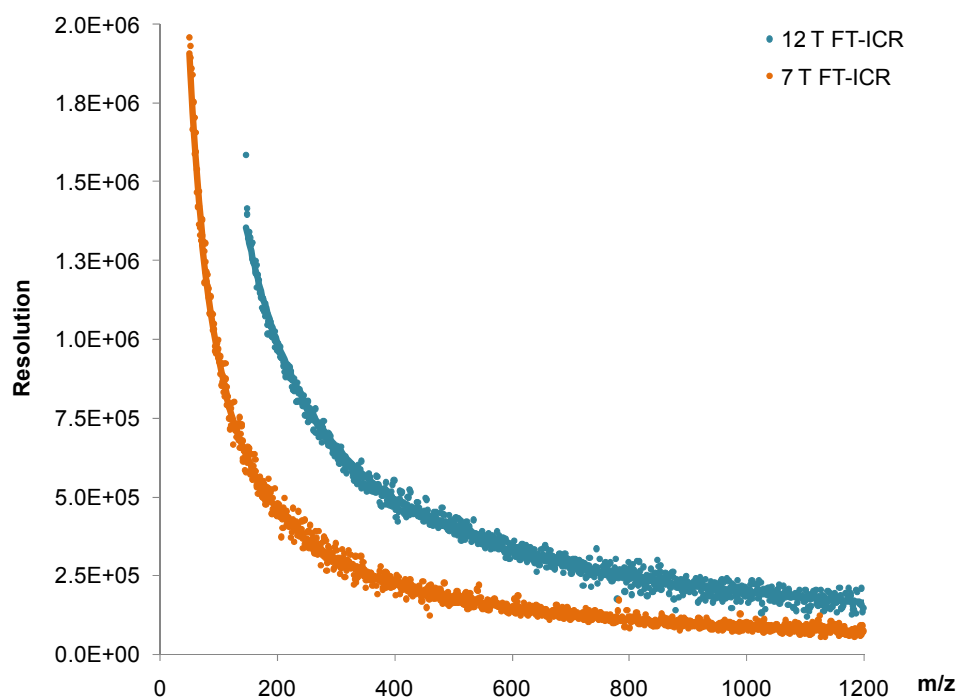


**Figure 3.14.** Effect of magnetic field strength on resolution. Resolution achieved with 7 and 12 T FT-ICR mass analyzers at acquisition time of 2 seconds.

### **Sensitivity**

FT-ICR and FT-orbitrap present high sensitivity with respect to some other mass analyzers where ions are lost during the transfer into the orthogonal TOF or during scanning in QqQ. However, the increase of resolution may lead to decrease of sensitivity. In Figure 3.15., the loss in intensity of the signals versus the resolution used in each case has been plotted for 7T FT-ICR and the standard Orbitrap.

It is shown that both standard Orbitrap and 7T FT-ICR have a great loss in peak height. It is especially important for 7T FT-ICR when resolution of 1,000,000 (FWHM,  $m/z$  400) has been used. It should be noticed that standard Orbitrap is far more sensitive than 7T FT-ICR when working at medium resolution (12,500 FWHM  $m/z$  400), but maximum resolution is lower than for FT-ICR.

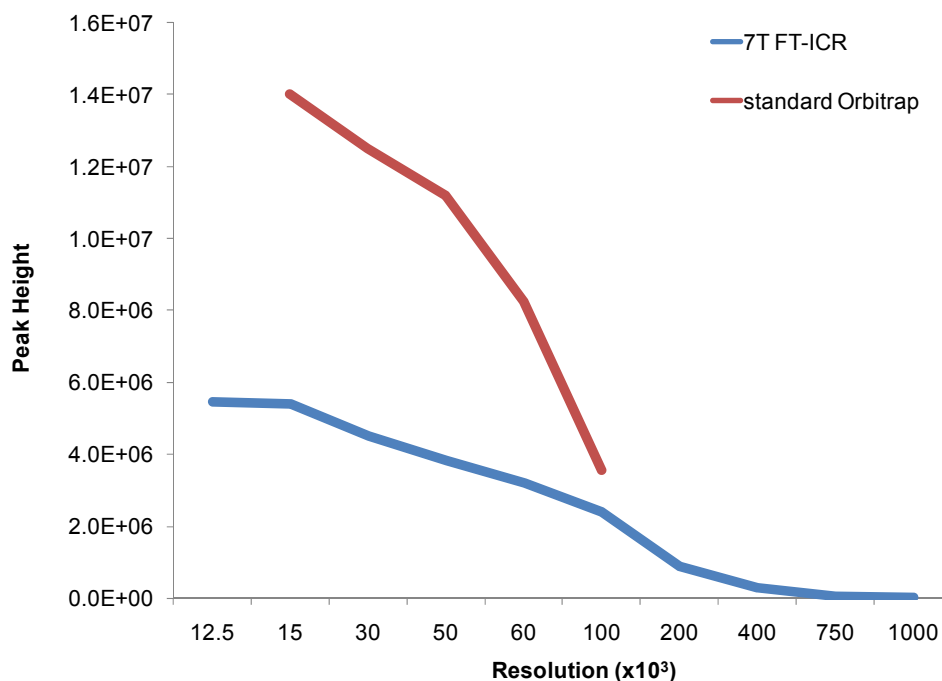


**Figure 3.15.** Sensitivity expressed as peak height vs resolution for two of the mass analyzers used in the study: standard Orbitrap and 7 T FT-ICR.

### **Mass Accuracy**

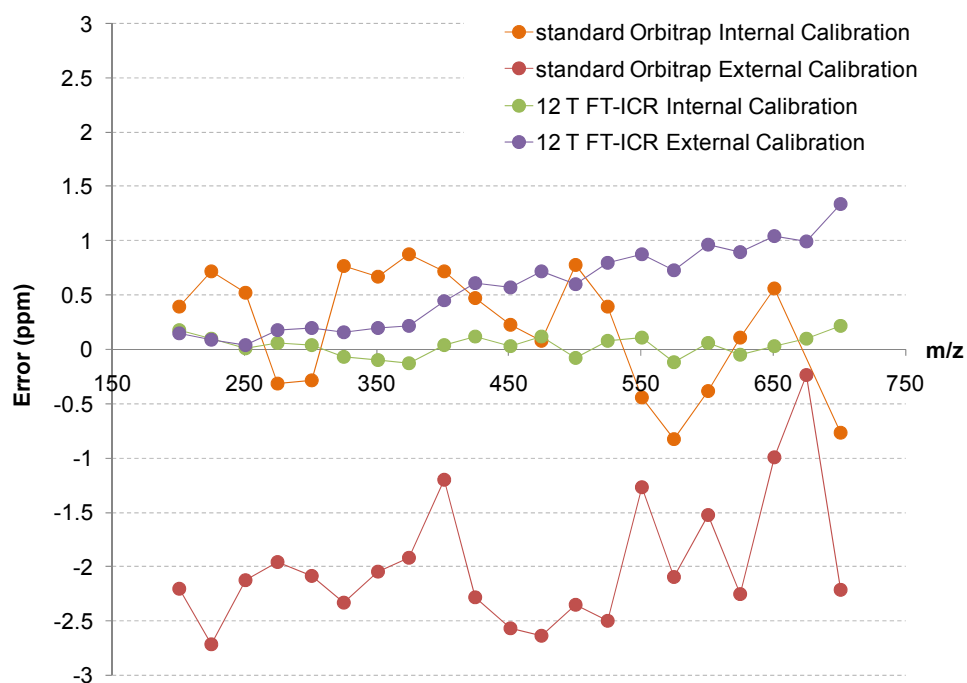
To evaluate the mass accuracy, well-known series described for SRFA in the mass range  $m/z$  200-800 (see Table 3.7.) were searched in each acquisition and the mass error for each elemental formula was calculated.

As has been discussed before (see Chapter 2 section 2.2.1.), mass accuracy depends on several factors. In a previous study, it was shown that when no interferences are present, FT-orbitrap can be as accurate as FT-ICR (Chapter 2 section 2.2.2.). However, when a complex sample such as SRFA is analyzed, it is shown that FT-ICR instruments can achieve better results (see Figure 3.16.).

The higher resolution in FT-ICR makes here the difference and with external calibration FT-ICR mass accuracy is always below 1 ppm, whereas FT-orbitrap mass accuracy is below 3 ppm. In any case, if sub-ppm mass errors had to be achieved, some post-acquisition corrections might be carried out. As has been shown before, for these mass analyzers and some others, post acquisition calibration will improve twice or three times the accuracy of the measurements (Chapter 2 section 2.2.2.). After post-acquisition calibration the mass accuracy is better than 1 ppm for FT-orbitrap and better than 0.5 ppm for FT-ICR (see Figure 3.16.).

**Table 3.7.** Suwannee river fulvic acids series already described in the literature.

Theo. Mass	RDBE	Composition
201.04046	4.5	C8 H9 O6
225.04046	6.5	C10 H9 O6
251.01973	8.5	C11 H7 O7
275.05611	9.5	C14 H11 O6
301.03538	11.5	C15 H9 O7
325.09289	7.5	C15 H17 O8
351.10854	8.5	C17 H19 O8
375.07216	11.5	C18 H15 O9
401.05142	13.5	C19 H13 O10
425.10893	9.5	C19 H21 O11
451.12458	10.5	C21 H23 O11
475.08820	13.5	C22 H19 O12
501.06746	15.5	C23 H17 O13
525.06746	17.5	C25 H17 O13
551.08311	18.5	C27 H19 O13
575.10424	15.5	C26 H23 O15
601.08351	17.5	C27 H21 O16
625.08351	19.5	C29 H21 O16
651.09916	20.5	C31 H23 O16
675.09916	22.5	C33 H23 O16
701.09955	19.5	C31 H25 O19

**Figure 3.16.** Effect of mass analyzer, resolution and calibration protocol on mass accuracy.

### **Spectral Accuracy**

Ideally, any formula determination may be confirmed comparing the isotopic pattern (M+1, M+2, M+3...)(Chapter 2 section 2.2.1.). This is feasible if few unknown compounds are to be analyzed. However, in DOM analysis, the isotopic pattern information is usually reduced to detecting the M+1 isotopic ion, corresponding to  $^{13}\text{C}$ . The rest of the isotopic distribution (M+2, M+3...) is usually not detected. Even when looking for the most abundant isotopic ion (i.e. M+1), two main problems can occur: i) the ion abundance of M+1 isotopic ion is low (usually <50 % of relative abundance) and ii) due to the complexity of DOM spectra, the isotopic ions might be interfered (not completely resolved).

FT-ICR has been widely used for DOM characterization and the capabilities of detecting the M+1 isotopic ion have been tested and used for formula assignment (Stoll et al., 2006; He et al., 2011; Miura et al., 2010). However, FT-orbitrap performance has been less investigated. Spectral accuracy for FT-orbitrap mass analyzer has been studied (sometimes in comparison to FT-ICR), but the previous studies have focused on individual compounds (sulfur-containing compounds), far from the scenario of DOM complexity (Blake et al., 2011; Erve et al., 2009).

For these reasons, spectral accuracy has been tested in the standard FT-Orbitrap working at resolution 100,000 (FWHM,  $m/z$  400) and after post-acquisition correction of the mass range (internal calibration). Some ions of the SRFA series used to evaluate mass accuracy (see above) have been used to compare the experimental isotopic pattern with the theoretical one. Ions have been selected along the mass range, from nominal mass 201 to 601. Simulation of the theoretical isotopic pattern has been carried out following the suggestions included in Chapter 2 section 2.2.1. The peak height expressed as relative intensity (with respect to the monoisotopic peak, M) has been used for comparison between the theoretical and the experimental isotopic pattern. Mass accuracy has been also evaluated for M+1.

As shown in Table 3.8., the M+1 isotopic peak corresponding to  $^{13}\text{C}$  was detected for all the  $m/z$  along the mass range (nominal masses 201, 301, 401, 501, 601). However, the rest of the isotopic pattern was not detectable (M+2). Comparing the experimental relative intensity of M+1 with the theoretical one, a deviation lower than 30 % was observed for all the cases. Although this value is higher than others reported in the literature (Blake et al., 2011; Erve et al., 2009), the rest of the studies were not dealing with such a complex sample. Spectral inaccuracy is probably due to interferences caused by the same sample (resolution was not enough) or due to lack of sensitivity

(M+1 abundance is in all the cases <30%). Moreover, as can be seen in all the  $m/z$ , the mass accuracy for M+1 is worse than for monoisotopic peak. Some examples are included in Figure 3.17 and Figure 3.18. For instance, for the  $m/z$  201.04384 assigned as  $C_8H_9O_6^-$  only the M+1 corresponding to  $C_7^{13}CH_9O_6^-$  was detected. The other isotopic ion in M+1 and the two isotopic ions for M+2 were not detected. Some other peaks corresponding to other compounds are detected very close to the  $m/z$ , but all of them look quite resolved. Resolution at this nominal mass is around 200,000 (FWHM). However, in the example in Figure 3.18, the experimental M+1 peak (from monoisotopic ion  $m/z$  601.0835) looks pretty thick. Probably, two or more peaks are not resolved. Experimental resolution at nominal mass 601 is < 100,000 (FWHM).

**Table 3.8.** Comparison between the theoretical and the experimental isotopic pattern based on the relative intensity of the different isotopic peaks (M+1 and M+2). The error (in ppm), the resolution for each ion and the elemental composition are included.

Isotopic pattern	Theoretical $m/z$	Theoretical relative intensity	Experimental $m/z$	Experimental relative intensity (SD) <sup>a</sup>	Error (SD) <sup>a</sup>	Resolution <sup>b</sup>	Ion composition [M-H] <sup>-</sup>
M	201.0405	100	201.0405	100	0.4 (0.1)	184,970	$C_8H_9O_6$
M+1	202.0438	8.7	202.0443	10.1 (0.4)	2.2 (0.3)	201,652	$C_7^{13}CH_9O_6$
	202.0468	0.4	N.D.				
M+2	203.0447	1.2	N.D.				
	203.0473	0.3	N.D.				
M	301.0354	100	301.0353	100	0.3 (0.1)	157,452	$C_{15}H_9O_7$
M+1	302.0387	16.3	302.0385	19.7 (0.9)	0.8 (0.2)	123,299	$C_{14}^{13}CH_9O_7$
	303.0396	1.4	N.D.				
M+2	303.0422	1.3	N.D.				
M	401.0514	100	401.0517	100	0.7 (0.1)	124,450	$C_{19}H_{13}O_{10}$
M+1	402.0549	20.8	402.0545	27 (2)	1.0 (0.5)	110,450	$C_{18}^{13}CH_{13}O_{10}$
	403.0570	2.7	N.D.				
M+2							
M	501.0675	100	501.0683	100	0.8 (0.1)	110,110	$C_{23}H_{17}O_{13}$
M+1	502.0708	25.4	502.0721	20.2 (0.8)	2.6 (0.4)	122,520	$C_{22}^{13}CH_{17}O_{13}$
	503.0732	4.7	N.D.				
M+2							
M	601.0835	100	601.0828	100	0.4 (0.2)	97,946	$C_{27}H_{21}O_{16}$
M+1	602.0869	29.4	602.0889	23 (2)	3.4 (0.5)	55,052	$C_{26}^{13}CH_{21}O_{16}$
	603.0892	6.8	N.D.				

N.D.: not detected

<sup>a</sup>: all the measurements were carried in triplicate, so the mean and the standard deviation (SD) are included.

<sup>b</sup>: experimental resolution (mean for three acquisitions) and resolution used for the isotopic pattern simulation.

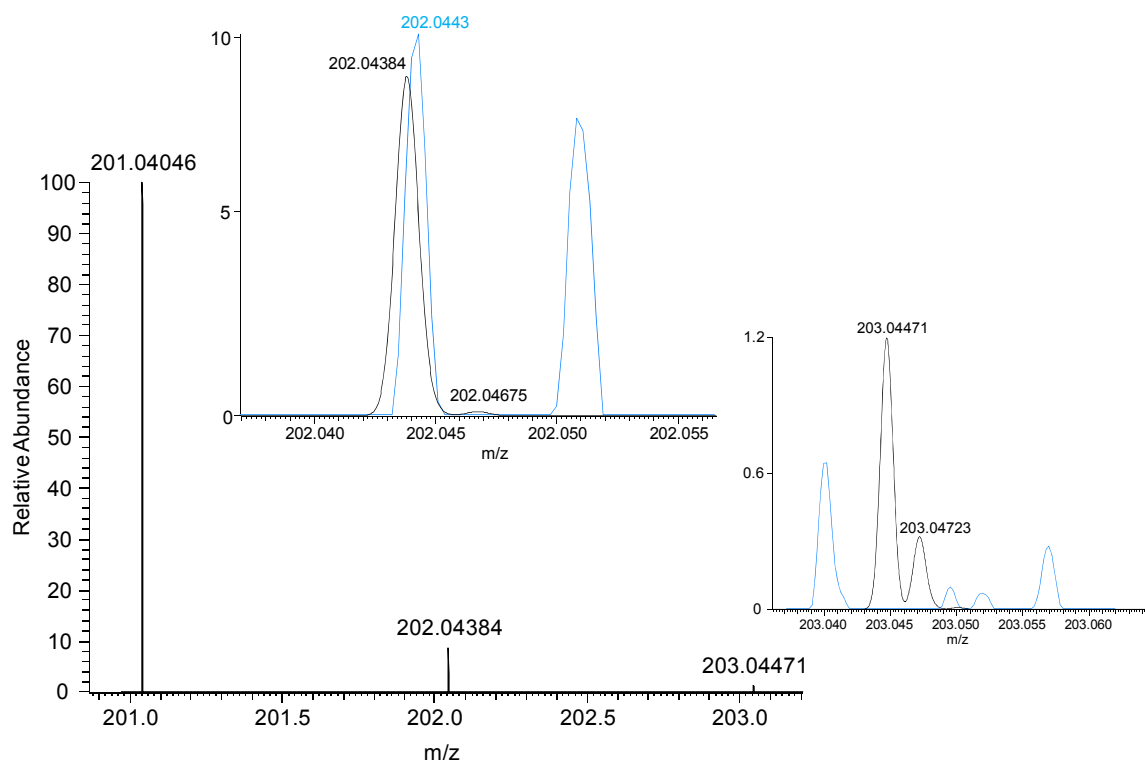


**Figure 3.17.** Isotopic pattern simulation for  $m/z$  201.0405 ( $C_8H_9O_6^-$ ) at R: 184,970 (FWHM). The zoom showing M+1 and M+2 are also included. In blue the isotopic peaks for the experimental SRFA spectra are superposed. Peaks assigned as other elemental formulas, not corresponding to any isotopic peak of the  $C_8H_9O_6^-$  ion are marked with an \*.

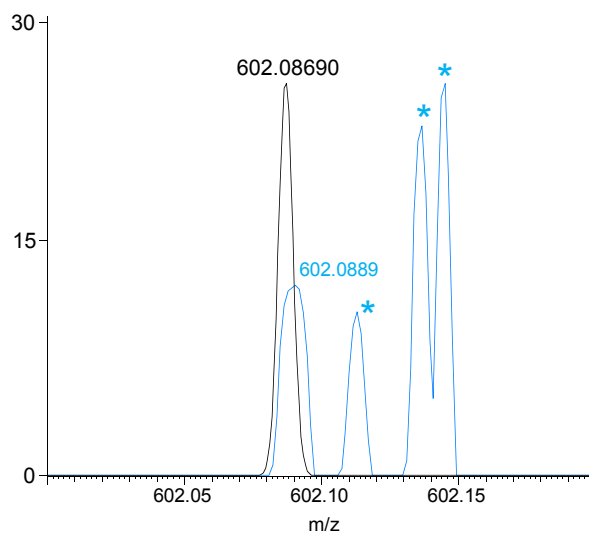


**Figure 3.18.** M+1 isotopic ion simulation for  $m/z$  602.0869 ( $C_{26}^{13}CH_{21}O_{16}^-$ ) at R: 55,052 (FWHM). In blue the experimental SRFA spectra is superposed. Peaks assigned as other elemental formulas, not corresponding to any isotopic peak of the  $C_{27}H_{21}O_{16}^-$  ion are marked with an \*.



### **3.2.2. Research Article N° 2**

Nuria Cortés-Francisco and Josep Caixach

Structural Characterization of Marine Dissolved Organic Matter. Fragmentation Studies.

*Analytical and Bioanalytical Chemistry*, (submitted).



# Structural characterization of marine dissolved organic matter. Fragmentation studies.

*Nuria Cortés-Francisco<sup>1</sup> and Josep Caixach<sup>1\*</sup>*

<sup>1</sup>Mass Spectrometry Laboratory / Organic Pollutants, IDAEA-CSIC, Jordi Girona 18, 08034 Barcelona, Spain. Tel: (+34) 93 400 61 00. Fax: (+34) 93 204 59 04

E-mail address: josep.caixach@cid.csic.es

**Keywords:** high resolution mass spectrometry, marine DOM, product ion spectra, fragmentation studies, Orbitrap.

## ABSTRACT

High resolution tandem mass spectrometry by collision induced dissociation with a linear ion trap-Orbitrap has been performed on marine dissolved organic matter (DOM). Product ion spectra of selected precursor ions ( $m/z$  359-375) have been acquired to obtain structural information, after optimization of instrumental parameters. Several fragments were assigned to the different precursor ions indicating the presence of carboxyl, hydroxyl, lactones, quinones, esters and structures more similar to lignin-degraded molecules. On the basis of these findings coastal marine DOM molecules, although structurally homogeneous might be more rich in diversity of functional groups than previously described. Moreover, to evaluate the performance of the method the Suwannee river fulvic acids (SRFA) reference standard was also analyzed under identical conditions. Some common features and differences have been described between marine DOM and SRFA. Searching in databases failed to assign or find similarities to any known compound.

## INTRODUCTION

The application of electrospray ionization high resolution mass spectrometry has transformed the comprehension of dissolved organic matter (DOM) at molecular level. Several studies has assigned molecular formulas to DOM extracts from different origins providing information on natural or affected environments and degradation/transformation processes. However, DOM is very complex and each elemental formula could represent millions or more constitutional isomers depending on the mass [1].

Nowadays, structural information from DOM is still missing, due to the fact that DOM separation into individual compounds by conventional techniques such as liquid chromatography

or electrophoresis is impossible. Several attempts have been done to obtain structural information using different techniques such as nuclear magnetic resonance (NMR), Fourier transform-infrared spectroscopy (FT-IR) and tandem mass spectrometry. For instance, NMR analysis have revealed that phenolic carbons are not the major components of humic substances [2] and FT-IR analysis have shown presence of aromatic, aliphatic and carboxylic groups [3]. Mass spectrometry has also been successfully applied. Low resolution tandem mass spectrometry has been applied in most of the studies and it has been used to analyze Suwannee river fulvic acids (SRFA) standard, deep ocean DOM and freshwater fulvic acids. Few studies have used high resolution tandem mass spectrometry for the characterization of SRFA and organosulfates in particulate organic matter (see Table 1) [4-13]. The presence of carboxyl and hydroxyl groups have been confirmed by several of these studies. Tandem mass spectrometry has been successfully applied to elucidate the structure of some of the molecular formulas assigned and some tentative structures have been proposed.

In this respect, the introduction of hybrid linear ion trap-Orbitrap has provided a new approach for structural characterization of DOM with enhanced sensitivity and resolution, thus providing improved selectivity and mass measurement accuracy for tandem mass spectrometry data. The purpose of this study was to develop a method to acquire product ion spectra of marine DOM to obtain structural information. The method has been based on the use of high resolution tandem mass spectrometry by collision induced dissociation (CID) experiments with an LTQ-Orbitrap. High resolved product ion spectra and good mass accuracies in accurate mass measurements have been used to find similarities / differences with SRFA, a well studied reference material.

**Table 1.** Previous studies (from the last 15 years) where fragmentation studies of DOM from different origins have been performed.

<b>Dissolved Organic Matter analyzed</b>	<b>References</b>
Deep Ocean DOM	Reemtsma et al., 2008 [4]
Suwannee River standards (IHSS)	Stenson et al., 2002; Stenson et al., 2003 [5,6]
Acidic metabolites in fulvic acids from groundwater	Jobelius et al., 2014 [7]
Fulvic acids from different origins	Plancque et al., 2001 [8]
SRFA standard (IHSS)	Witt et al., 2009 [9]
River and Ocean DOM	Liu et al., 2011 [10]
SRFA (IHSS)	Leenher et al., 2001 [11]
Standard soil and peat fulvic acids standards (IHSS)	McIntyre et al., 2002 [12]
Organosulfates in aerosols	Lin et al., 2012 [13]

## MATERIALS AND METHODS

### Chemicals.

All reagents were of analytical or high-performance liquid chromatographic grade. Dichloromethane, methanol and hydrochloric acid were purchased from Merck (Darmstadt, Germany). Isopropyl alcohol was from Carlo Erba (Milan, Italy) and formic acid was from Panreac (Barcelona, Spain). Highpurity water produced with a Milli-Q Organex-Q System Millipore (Millipore Corp., Bedford, MA) was used. Suwannee River Fulvic Acid (SRFA) (1S101F) standard from International Humic Substance Society (Minnesota, United States) has been diluted in methanol and analyzed to find common components between the real sample and the standard.

### Sample collection and preparation.

A composite water sample from the seawater intake system of a pilot desalination plant installed in the coast of Barcelona (Spain) was collected in Pyrex borosilicate amber glass bottles. The seawater has been previously characterized as part of a whole study [14]. Briefly, 1.5L from the sample was acidified with 10% hydrochloric acid to pH 2 and extracted with 2 x 100 mL of dichloromethane/isopropyl alcohol (90:10 v/v) and the extract was concentrated down to 250  $\mu$ L at 40 °C under nitrogen.

### LTQ-Orbitrap Mass Spectrometry.

The analysis of the standard and the sample were carried out with a LTQ-Orbitrap XL (Thermo Fisher Scientific, Bremen, Germany) equipped with a nano-ESI source (Nanospray Flex Ion Source, Thermo Fisher Scientific, Bremen, Germany). Optimization was carried out analyzing an SRFA standard by infusion in the Orbitrap in full scan negative ionization mode.

Optimized parameters were spray voltage, capillary voltage, skimmer voltage, tube lens voltage and capillary temperature. Finally, all mass spectra were acquired in negative ionization mode produced by capillary voltage -35V, tube lens -90V and capillary temperature of 300°C. The automatic gain control was used to consistently full fill the C-trap and gain mass accuracy and resolution [15]. High resolution defined as R: 100,000 ( $m/z$  400, full width at half maximum) was set.

For tandem mass experiments, ions in the mass range between  $m/z$  359-375 (Figure 1) have been selected in the LTQ before they were pulsed through the trap to the collision cell where they were fragmented by CID, using increasing voltage increments up to 30 eV. It was only possible to

isolate ions in 0.7 Da mass window, and therefore tandem mass experiments include several precursor ions. The same masses were selected for both SRFA standard and marine DOM extracts to compare the fragmentation patterns.

Post-acquisition calibration had to be performed using reference homologous series described in DOM before by the RecalOffline Xcalibur application. The accuracy of the precursor and product ions was always better than 2 ppm.

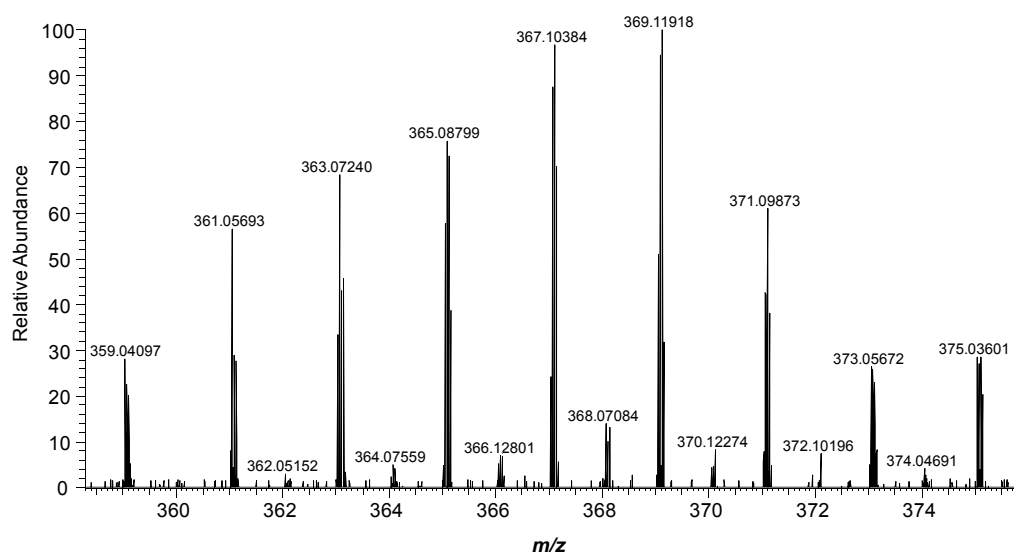


**Figure 1.** Suwannee river fulvic acids full scan spectra of the precursor ions chosen for the posterior fragmentation experiments.

### Data Analysis.

The mass peaks were exported to peak lists and from these lists feasible elemental formulas were generated. Different restrictive criteria were set to generate reliable elemental formulas, depending on the precursor ion selected (Table 2). This way the possible assignments for each product ion were not so numerous and the assignment of the product ions were more easy and reliable. The molecular formula calculation was performed with Xcalibur 2.1 (Thermo Fisher Scientific, Bremen, Germany) and the posterior analysis of the data was done using our own developed excel macros. Data filtering of the assigned formulas was done applying exact mass differences / neutral losses (Table 3), to correlate each precursor ion with the possible ion fragments. The methodology developed for fragment assignment rely on a not broken fragmentation pathway, where the differences between fragment ions could be attributable to a known neutral loss or functional group fragmentation.

**In-silico fragmentation.**

In order to build the puzzle obtained from the tandem experiments for the marine DOM and the SRFA, the different HR product ion spectra obtained after data filtering were used in MetFrag application [16] to relate the neutral losses and product ions obtained to a known structure from databases. The search was performed in PubChem and Chemspider databases.

**Table 2.** Restrictive criteria defined to generate reliable elemental formulas.

Parameter		Comment	
Mass accuracy	< 2ppm	Recalibration (post-acquisition) performed.	
Ion type / Adduct Formation / Charge	M <sup>-</sup> , charge = -1	Negative ESI mode.	
Double bond equivalents	Maximum 40	No fullerenes.	
Elements to consider	CHNOS	Prior information from full scan analysis.	
Restrictions of Elements	Carbon	Maximum: nominal mass of the precursor ion / 12 Minimum: 1	e.g. for $m/z$ 359, maximum number of C = $359/12=30$
	Hydrogen	H/C ratio	H/C: 0.3 - 2.5 Maximum O/C: 1 Maximum N/C: 1
	Oxygen	O/C ratio	
	Nitrogen	N/C ratios	
	Sulfur	Max.: 1 ; Min.: 0	

**RESULTS AND DISCUSSION****Method development.**

In addition to optimizing the experimental parameters for efficient DOM ionization, in the development of the method the collision energy for each precursor ion had to be optimized. It was interesting to observe that the collision energy had to be increase from lower  $m/z$  ( $m/z$  359) to higher ones ( $m/z$  375) by 15 eV. The precursor ions were fragmented maintaining > 20 % of the ion intensity in the product ion spectra. However, as one precursor ion selected is in reality several different compounds (see Figure 2), not for all the ions was possible to maintain a peak intensity > 20 %, but always higher than 5 %.

**Table 3.** Recurring mass differences, neutral losses and fragments identified from previous studies and / or searched in the present work base on the accurate mass.

<b>Recurring Mass Differences</b>	<b><math>\Delta m/z</math> theoretical</b>	<b>References</b>
CO vs N <sub>2</sub>	0.0112	Reemtsma et al., 2008 [4]
O <sub>2</sub> vs S	0.0178	Searched in the present study
CH <sub>4</sub> vs O	0.0364	Stenson et al., 2002; Stenson et al., 2003; Reemtsma et al., 2008 [4-6]
CH vs N	0.9953	Stenson et al., 2002; Stenson et al., 2003 [5, 6]
<sup>12</sup> C vs <sup>13</sup> C	1.0034	Stenson et al., 2002; Stenson et al., 2003 [5, 6]
H <sub>2</sub> vs double bond / ring	2.0157	Stenson et al., 2002; Stenson et al., 2003 [5, 6]
longer CH <sub>2</sub> backbone	14.0157	Stenson et al., 2002; Stenson et al., 2003; Jobelius et al., 2014 [5-7]
<b>Fragments / Neutral Losses</b>	<b><math>m/z</math> fragment / mass loss (Da)</b>	<b>References</b>
O	15.9949	Plancque et al., 2001 [8]
CH <sub>4</sub>	16.0313	Witt et al., 2009 [9]
H <sub>2</sub> O	18.0106	Reemtsma et al., 2008; Plancque et al., 2001; Witt et al., 2009; Liu et al., 2011; Leenher et al., 2001; Jobelius et al., 2014; Stenson et al., 2003 [4, 6-11]
CO	27.9949	Reemtsma et al., 2008; Witt et al., 2009; Leenher et al., 2001 [4, 9, 11]
CH <sub>2</sub> CH <sub>2</sub>	28.0313	Jobelius et al., 2014 [7]
CHO	29.0027	Searched in the present study
CH <sub>2</sub> O	30.0106	Liu et al., 2011; Jobelius et al., 2014 [7, 10]
CH <sub>2</sub> CH <sub>2</sub> CH <sub>2</sub>	42.0470	Searched in the present study
CO <sub>2</sub>	43.9898	Reemtsma et al., 2008; Plancque et al., 2001; Witt et al., 2009; Liu et al., 2011; Leenher et al., 2001; Jobelius et al., 2014; McIntyre et al., 2002; Stenson et al., 2003 [4, 6-12]
C <sub>2</sub> H <sub>4</sub> O	44.0262	Searched in the present study
C <sub>4</sub> H <sub>8</sub>	56.0626	Plancque et al., 2001 [8]
NO <sub>3</sub> <sup>-</sup>	61.9884	Reemtsma et al., 2008; Lin et al., 2012 [4, 13]
HNO <sub>3</sub>	62.9956	Reemtsma et al., 2008; Lin et al., 2012 [4, 13]
SO <sub>3</sub> <sup>-</sup>	79.9574	Searched in the present study
CO <sub>2</sub> (x2)	87.9797	Plancque et al., 2001; Liu et al., 2011; Jobelius et al., 2014 [7,8,10]
·SO <sub>4</sub> <sup>-</sup>	95.9523	Lin et al., 2012 [13]
HSO <sub>4</sub> <sup>-</sup>	96.9601	Lin et al., 2012 [13]

Once the mass spectra were acquired, the hard task was to assign to each precursor the corresponding fragments. Due to the fact that soft fragmentation was applied (collision energy < 30 eV) the zoom of the different fragments showed similar regular patterns as the once typically described in DOM full scan spectra (see Figure 2). This way all the fragments presented a reasonable peak height in the spectra, so that they could be assigned following the data analysis process described. The non-assigned peaks were removed from the spectrum list and only the assigned peaks with mass accuracy better than 2 ppm were considered in the study. Mass difference between the experimental  $m/z$  of the ions in the spectra were calculated in order to attribute the mass difference to a neutral loss (Table 3). The same mass difference was also calculated between the theoretical  $m/z$  assigned. This was done using our own developed excel macros, so that all the ions in the spectra are included and the reiterative mass difference calculation could be done systematically. Due to high mass accuracy in formulas assignment, the accuracy in mass difference was always very good and the error was found in the fourth decimal. The resulting excel spreadsheet are included as supplementary material.

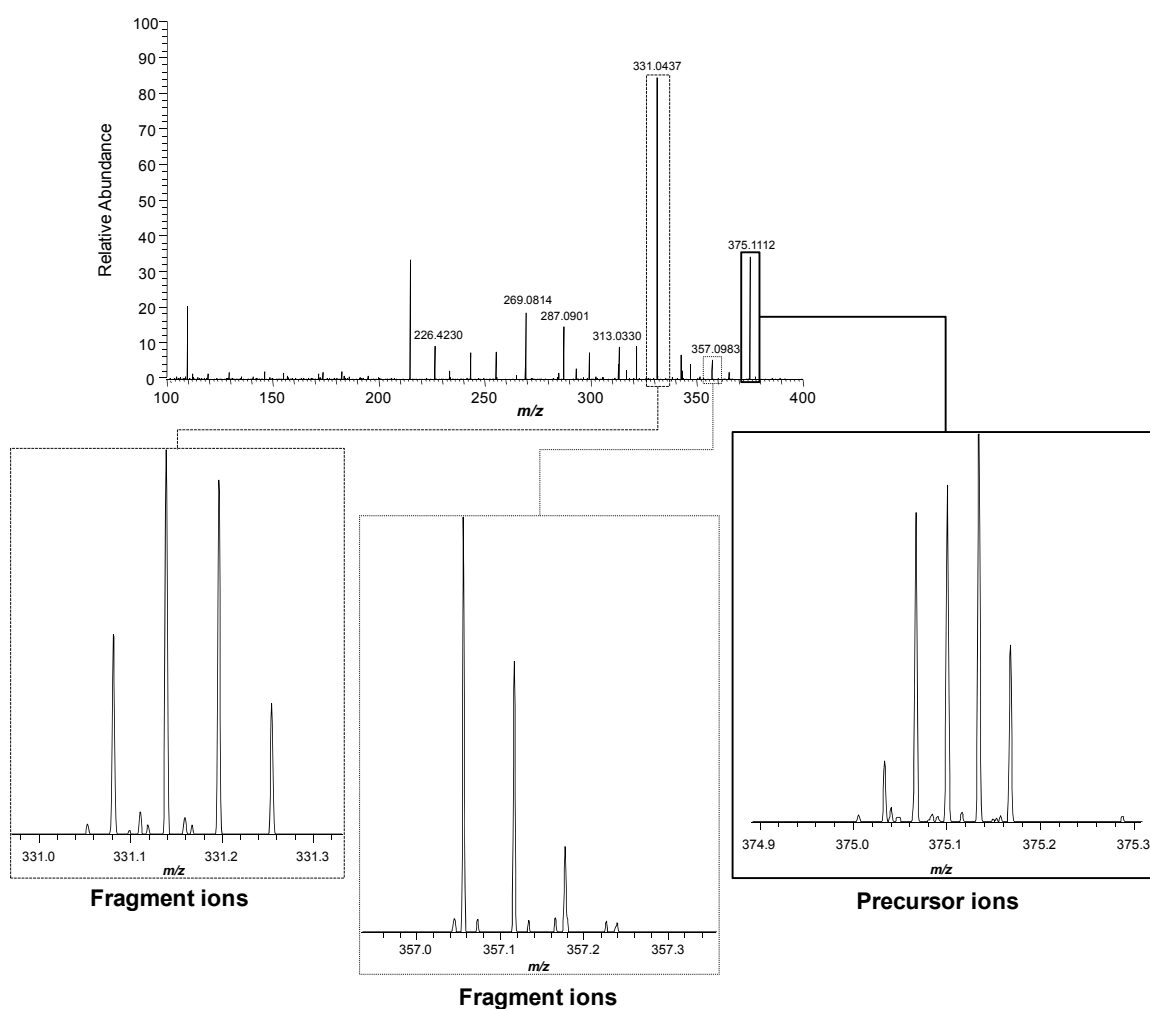


**Figure 2.** Product ion spectra of the selected  $m/z$  375 of marine DOM. (Below) the zoom of the precursor ions as well as two of the fragment ions, showing also regular spacing typical from DOM.

### SRFA tandem mass spectrometry.

SRFA is a reference standard in many studies and several fragmentation studies in low or high resolution tandem mass spectrometry have been carried out using it (see Table 1), for this reason it has been used to test the present method. Moreover, SRFA is usually used for comparison with other DOM samples (freshwater or marine DOM), although it should be highlighted that the isolation procedure for SRFA is carried out with XAD resins [17].

Regarding structural information, carboxyl and in less degree the hydroxyl groups are said to be the major functional groups in SRFA. From the product ion spectra acquired in the present study several neutral losses in tandem mass spectrometry experiments have been assigned to  $\text{CO}_2$ ,  $\text{CO}$  and  $\text{H}_2\text{O}$  losses (Figure 3). These results are in accordance with previous studies [5,6,9,11] and confirmed the suitability of the method.

In previous studies using full scan high resolution mass spectrometry it has been shown that fulvic acids and marine DOM present different molecular characteristics, although they can experience some molecular formulas overlap. In fact, this marine DOM extract has shown that the marine DOM of the study presents CHO compounds with lower DBE and at the same time, lower content of oxygen [14] when compared with SRFA. As described below, in addition to the described neutral losses of water and  $\text{CO}_2$ , some other differences have been found.

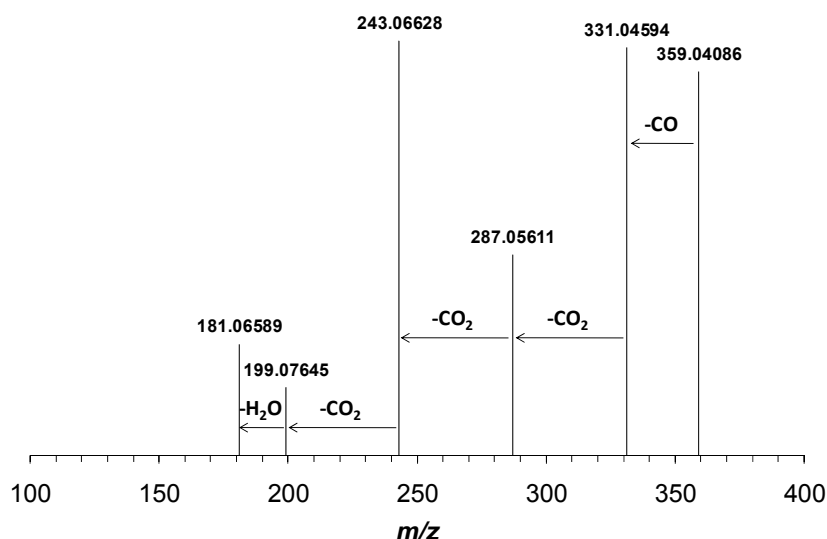


**Figure 3.** Product ion spectra of SRFA for one of the precursor ions with nominal mass 359, showing the different neutral losses and fragments assigned.

**Marine DOM. Structural information.**

Product ion spectra of CHO-compounds confirmed successive neutral losses of 18.0106 Da corresponding to a water molecule in parallel with losses of 43.9898 Da corresponding to a CO<sub>2</sub> group. These findings have been described before in DOM from different origins [4,6-12]. Previous studies using low resolution triple quadrupole mass analysis or high resolution tandem mass spectrometry using Q-TOF or FT-ICR have been applied to Suwannee river standards, fulvic acids from different origins and deep ocean DOM, among others (see Table 1). In the marine DOM of the study and the precursor ions selected, up to 3 losses of 43.9898 Da and up to 3 losses of 18.0106 Da have been observed. The neutral loss of 44 Da has been always attributable to CO<sub>2</sub> group, because it is the most usual one in negative mode when decarboxylation occurs. In fact, a major component of marine DOM are carboxyl-rich alicyclic molecules (CRAM) which usually experience several CO<sub>2</sub> losses [2]. Some ions found in the product ion spectra and with an assigned molecular formula showed a mass difference of 44.0262 Da with some other fragments. The systematic recalibration done in all the spectra and rules and restrictive criteria used for mass assignment confirmed that it was not a false assignment. Besides, any combination to assign the product ion to any other fragmentation pathway failed. The neutral loss exact mass corresponds to a loss of (OC<sub>2</sub>H<sub>4</sub>) which has not been described before in DOM (Figure 4). However, this finding is in accordance with some more recent studies. Liu et al., already reported that a fraction of coastal marine DOM may exist as lignin-type molecules that have undergone degradation. These lignin-degraded molecules may exhibit different fragmentation patterns, as the ones shown in the present study, due to different chemical structures [10]. Moreover, Kostyukevich et al. using hydrogen/deuterium exchange FT ion cyclotron resonance MS come to the conclusion that not all the oxygen present in the fulvic acids molecules should be carboxyl or hydroxyl groups, but some other functionalities [18]. Other fragmentation studies from marine DOM done before has been done using low resolution mass spectrometry and so the neutral loss 44 Da has been mainly assigned to CO<sub>2</sub> groups [4]. Thus, on the basis of these findings coastal marine DOM molecules, although structurally homogeneous might be more rich in diversity of functional groups than previously described [4]. Moreover, a loss of 27.9949 Da (CO - methoxy group) indicative of lactones, quinones or esters have been also identified, although in less occurrence than the hydroxyl or carboxyl group. This loss in negative electrospray mode was only described before by Leenheer et al. and Witt et al., for the SRFA demonstrating some similarities between fulvic acids from surface water (Suwannee River) and marine DOM [9,11]. In none of the other studies this loss has been reported. This might indicate differences in structural composition in DOM from different origins, apart from some differences in molecular formulas already described in some other studies [19,20].

As described above, most of the precursor ions showed successive losses (see Figure 4). However, few others showed less fragmentation (one or two fragments). This was the case for some of the precursor ions classified as lipid like in the full scan spectra (low DBE, high H/C ratio, low O/C ratio) [14]. It is interesting to highlight that these compounds experience only a neutral loss (18.0106 Da) probably corresponding to one water molecule. This fragmentation has been observed for some fatty acids, such as palmitic or stearic. Although this coincidence in the fragmentation pattern does not mean that we are talking about the same exact structure it gives a clue, that as hypothesized by the assigned formula from full scan analysis and the location into de van Krevelen diagram, these compounds probably have a long aliphatic chain with few (one or two) functional groups, such as one carboxylic acid or / and one hydroxyl group.

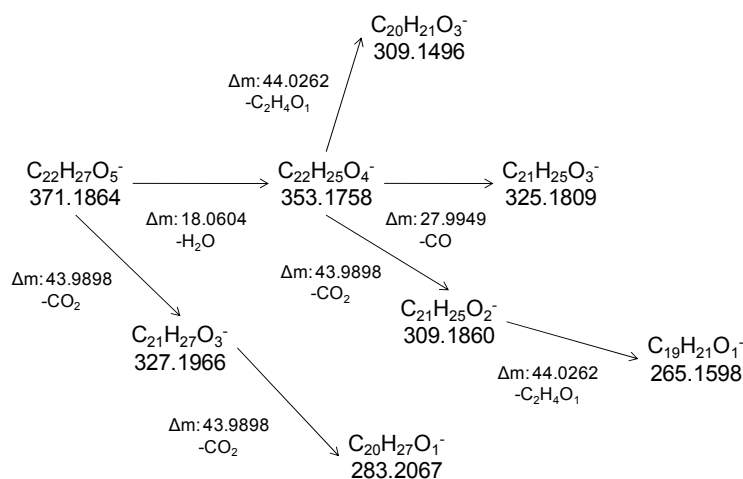


**Figure 4.** Fragmentation pathway of one of the precursor ions with nominal mass 371, showing the different fragments generated and neutral losses.

Although they are minor components, compounds containing nitrogen and/or sulfur have been also identified in marine DOM [21]. Product ion spectra of CHON-compounds suggested that the nitrogen atoms in these molecules were included in the backbone of these molecules. Compared to other studies, where the oxidized nitrogen in atmospheric aerosols showed the presence of nitrate esters clearly indicated by the loss of 63 Da and the formation of  $m/z$  62 in the negative ion mode [22]. Regarding the CHOS compounds, a loss of 79.9574 Da and the formation of  $m/z$  95.9523 or 96.9601 were expected to confirm the presence of sulfite or sulfate functional groups connected to some organic moieties [13], as shown in DOM from aerosols. However, none of these ions / neutral losses were detected here, probably due to the little abundance of these compounds in the sample of the study. Neutral losses imputable to  $\text{CO}_2$  and  $\text{H}_2\text{O}$  were the only ones recorded.

### **Searching in databases.**

The tandem mass spectra obtained for marine DOM and SRFA were used to search in the Metfrag application, similar compounds that can be listed in databases. From the trials performed several hits were found based on exact mass (4 to 165, depending on the  $m/z$ ). However, each time only one fragment of the whole mass spectra could be explained with the structures proposed. The rest (up to 4 fragments) were not explained. As the structure of DOM is under investigation and so far the synthesis/isolation of individual compounds have not been achieved, DOM individual compounds are not considered in databases. Besides, none of the compounds (natural or synthesized) already characterized in databases can assimilate to any of the described functionalities from DOM. This gives an idea of how unique and complex is DOM structure.

### **ACKNOWLEDGMENT**

The authors thank Dr. J.A. Allué from Araclon Biotech for MS technical support and P. Eng. H. Constenla for developing the excel macros for data treatment.

### **ELECTRONIC SUPPLEMENTARY MATERIAL**

A spread sheet data base in excel format include all the assigned formulas for the precursor ions and fragments ions of marine DOM.

### **REFERENCES**

1. Hertkorn N, Frommberger M, Witt M, Koch BP, Schmitt-Kopplin P, Perdue EM (2008) Natural Organic Matter and the Event Horizon of Mass Spectrometry. *Analytical Chemistry* 80 (23):8908-8919.
2. Hertkorn N, Benner R, Frommberger M, Schmitt-Kopplin P, Witt M, Kaiser K, Kettrup A, Hedges JI (2006) Characterization of a major refractory component of marine dissolved organic matter. *Geochimica et Cosmochimica Acta* 70 (12):2990-3010.
3. Tanaka, T, Nagao S, Ogawa H (2001) Attenuated Total Reflection Fourier Transform Infrared (ATR-FTIR) Spectroscopy of Functional Groups of Humic Acid Dissolving in Aqueous Solution. *Analytical Sciences* 17: i1081 – i1084.
4. Reemtsma T, These A, Linscheid M, Leenheer J, Spitzy A (2008) Molecular and Structural Characterization of Dissolved Organic Matter from the Deep Ocean by FTICR-MS, Including

- Hydrophilic Nitrogenous Organic Molecules. *Environmental Science & Technology* 42 (5):1430-1437.
5. Stenson AC, Landing WM, Marshall AG, Cooper WT (2002) Ionization and Fragmentation of Humic Substances in Electrospray Ionization Fourier Transform-Ion Cyclotron Resonance Mass Spectrometry. *Analytical Chemistry* 74 (17) : 4397-4409.
  6. Stenson AC, Marshall AG, Cooper WT (2003) Exact Masses and Chemical Formulas of Individual Suwannee River Fulvic Acids from Ultrahigh Resolution Electrospray Ionization Fourier Transform Ion Cyclotron Resonance Mass Spectra. *Analytical Chemistry* 75 (6):1275-1284.
  7. Jobelius C, Frimmel FH, Zwiener C (2014) Mass spectrometric screening and identification of acidic metabolites in fulvic acid fractions of contaminated groundwater. *Analytical and Bioanalytical Chemistry* 406 (14):3415-3429
  8. Planque G, Amekraz B, Moulin V, Toulhoat P, Moulin C (2001) Molecular structure of fulvic acids by electrospray with quadrupole time-of-flight mass spectrometry. *Rapid Communications in Mass Spectrometry* 15 (10):827-835.
  9. Witt M, Fuchser J, Koch BP (2009) Fragmentation Studies of Fulvic Acids Using Collision Induced Dissociation Fourier Transform Ion Cyclotron Resonance Mass Spectrometry. *Analytical Chemistry* 81 (7):2688-2694.
  10. Liu Z, Sleighter RL, Zhong J, Hatcher PG (2011) The chemical changes of DOM from black waters to coastal marine waters by HPLC combined with ultrahigh resolution mass spectrometry. *Estuarine, Coastal and Shelf Science* 92 (2):205-216.
  11. Leenheer JA, Rostad CE, Gates PM, Furlong ET, Ferrer I (2001) Molecular Resolution and Fragmentation of Fulvic Acid by Electrospray Ionization/Multistage Tandem Mass Spectrometry. *Analytical Chemistry* 73 (7):1461-1471.
  12. McIntyre C, McRae C, Jardine D, Batts BD (2002) Identification of compound classes in soil and peat fulvic acids as observed by electrospray ionization tandem mass spectrometry. *Rapid Communications in Mass Spectrometry* 16 (16):1604-1609.
  13. Lin P, Yu JZ, Engling G, Kalberer M (2012) Organosulfates in Humic-like Substance Fraction Isolated from Aerosols at Seven Locations in East Asia: A Study by Ultra-High-Resolution Mass Spectrometry. *Environmental Science & Technology* 46 (24):13118-13127.
  14. Cortés-Francisco N, Caixach J (2013) Molecular Characterization of Dissolved Organic Matter through a Desalination Process by High Resolution Mass Spectrometry. *Environmental Science & Technology* 47 (17):9619-9627.

15. Blake S, Walker SH, Muddiman D, Hinks D, Beck K (2011) Spectral Accuracy and Sulfur Counting Capabilities of the LTQ-FT-ICR and the LTQ-Orbitrap XL for Small Molecule Analysis. *Journal of The American Society for Mass Spectrometry* 22 (12):2269-2275.
16. Wolf S, Schmidt S, Muller-Hannemann M, Neumann S (2010) In silico fragmentation for computer assisted identification of metabolite mass spectra. *BMC Bioinformatics* 11 (1):148
17. [www.humicsubstances.org](http://www.humicsubstances.org)
18. Kostyukevich Y, Kononikhin A, Popov I, Kharybin O, Perminova I, Konstantinov A, Nikolaev E (2013) Enumeration of Labile Hydrogens in Natural Organic Matter by Use of Hydrogen/Deuterium Exchange Fourier Transform Ion Cyclotron Resonance Mass Spectrometry. *Analytical Chemistry* 85 (22):11007-11013.
19. Koch BP, Witt M, Engbrodt R, Dittmar T, Kattner G (2005) Molecular formulae of marine and terrigenous dissolved organic matter detected by electrospray ionization Fourier transform ion cyclotron resonance mass spectrometry. *Geochimica et Cosmochimica Acta* 69 (13):3299-3308.
20. Sleighter RL, Chen H, Wozniak AS, Willoughby AS, Caricasole P, Hatcher PG (2012) Establishing a Measure of Reproducibility of Ultrahigh-Resolution Mass Spectra for Complex Mixtures of Natural Organic Matter. *Analytical Chemistry* 84 (21):9184-9191.
21. Hertkorn N, Harir M, Koch BP, Michalke B, Schmitt-Kopplin P (2013) High-field NMR spectroscopy and FTICR mass spectrometry: powerful discovery tools for the molecular level characterization of marine dissolved organic matter. *Biogeosciences* 10 (3):1583-1624.
22. Reemtsma T, These A, Venkatachari P, Xia X, Hopke PK, Springer A, Linscheid M (2006) Identification of Fulvic Acids and Sulfated and Nitrated Analogues in Atmospheric Aerosol by Electrospray Ionization Fourier Transform Ion Cyclotron Resonance Mass Spectrometry. *Analytical Chemistry* 78 (24):8299-8304.



### 3.3. Discussion

HRMS coupled to API source is clearly a powerful technique for the examination of the complex composition of DOM. Although a lot of research is being done in this field, there are still several difficulties that have to be overcome. From the results included in this thesis we can conclude that isolation of DOM and structural information are the fields where larger improvements should be made.

The state-of-the-art of DOM characterization shows that several different methods are used in parallel for DOM isolation (see section 3.1.1. *Dissolved Organic Matter Isolation of Water Bodies* page 95). We have shown that very similar results with regard to DOM features ( $H/C_{av}$ ,  $O/C_{av}$  and  $DBE_{av}$ ) can be obtained with LLE. Moreover, DOM recovery has shown to be acceptable, in comparison to most used methods. For these reasons, the LLE method can also be used for DOM extraction, without the necessity of prior filtration unlike most of the other methods in the literature. The effect of SPE and LLE on individual compounds is under investigation because very little is known at molecular level even for the most used methods. This lack of information makes the comparison between studies more difficult. Some researchers advise that the least invasive sample preparation or combination of several methodologies will lead to a more extensive characterization of any DOM (Sleighter et al., 2008; Green et al., 2014). This is especially important when general characterization of the media is desired to be obtained. In the present thesis, we were looking for differences (or lack of differences) in DOM along treatment plants. From our point of view, this can be done using SPE, LLE or any other methodology as long as all the samples are treated the same way.

Apart from sample treatment, the instrumental analysis can distort the data obtained. Strict protocols and tests are carried out to ensure reliable results. Only mass analyzers with outstanding specifications can deal with such a complex sample and for this reason in the last years FT-ICR has been the mass analyzer providing the most information of DOM at molecular level. However, in the last years the FT-orbitrap has shown promising results. SRFA analysis in different instruments based on FT-ICR and FT-orbitrap technology have shown with regard to resolution, sensitivity, mass accuracy and spectral accuracy, that FT-orbitrap can be used for characterization of DOM (see section 3.2.1.3. *Performance of Fourier Transform Mass Analyzers* page 114). In Table 3.9., the main advantages and disadvantages of each mass analyzer encountered through the development of this thesis have been summarized.

**Table 3.9.** Advantages and limitations of the two mass analyzers used in the present thesis.

	FT-ICR	FT-Orbitrap
<b>Mass range</b>	wide $m/z$ range	wide $m/z$ range
	limitation for lower $m/z$	low mass: $m/z$ 50
<b>Resolution</b>	unsurpassed resolution, $R > 1,000,000$ faster decrease with $m/z$	high resolution, maximum 240,000 ( $m/z$ 400, FWHM) limited due to shorter acquisition time
<b>Acquisition time</b>	long acquisition time	fast acquisition speed (compared to FT-ICR)
	20 minutes / sample	5 minutes / sample
<b>Sample introduction</b>	difficult coupling to UHPLC or HPLC	at maximum resolution: difficult coupling to UHPLC or HPLC
	Direct injection	Direct injection or Flow injection
<b>Exact Mass</b>	high mass accuracy	high mass accuracy
	1 ppm external calibration	3 ppm external calibration
	< 0.5 ppm post-acquisition calibration	< 1 ppm post-acquisition calibration
<b>Calibration</b>	mass calibration stability	mass calibration stability
<b>Sensitivity</b>	high sensitivity (more time needed per run)	high sensitivity high dynamic range
<b>MS/MS Capabilities</b>	possibility of working in tandem mass ( $MS^n$ )	possibility of working in tandem mass ( $MS^n$ ) but only with hybrid models
	single ion selection with very small mass difference in the ICR cell	
<b>Simplicity</b>	expertise operator	expertise operator
<b>Cost</b>	high cost	medium cost
	large size	medium size
	expensive maintenance	moderate maintenance

FT-ICR and FT-orbitrap present several similar features with respect to principle of operation (see section 3.1.2. *High Resolution Mass Spectrometry* page 96) as well as the main technical specifications (Table 3.9): wide  $m/z$  range, mass calibration stability,

high sensitivity, possibility of working in tandem mass and expertise operator needed. However, they also present some differences.

As shown above (Figure 3.12 page 116) the FT-ICR can achieve higher resolution in the mass range of interest for DOM analysis ( $m/z$  200-800). As has been discussed (see Figure 3.13. page 117), the acquisition time will determine the resolution achievable. Moreover, the acquisition time necessary to obtain 1 spectra conditionates the sample introduction as has been shown in section 3.2.1.2. (page 112). For this reason, the analysis of DOM carried out using FT-ICR mass analyzers has been used with direct infusion, because resolution was  $R > 400,000$  and acquisition time  $\sim 4$  seconds. However, for orbitrap using  $R: 100,000$  and acquisition time of  $\sim 1$  second, FIE introduction was tested.

Regarding the formula determination, the mass accuracy (see Figure 3.16 page 120) and spectral accuracy (see page 121) are only slightly better for FT-ICR (spectral accuracy compared based on other studies found in the literature). Moreover, it has been shown that FT-orbitrap is capable of DOM characterization, as tested with the analysis of SRFA. Although the outstanding performance of FT-ICR is not completely achieved by FT-orbitrap, and probably signals with less peak intensity are not resolved and higher mass errors are obtained, it should be considered as a quite good alternative to FT-ICR.

Structural information is missing for DOM characterization. Although outstanding findings have been carried out with different techniques as described in chapter 1, the complexity of DOM makes very difficult the elucidation of any structure. The fragmentation studies performed in marine DOM and SRFA standards confirmed that carboxyl and hydroxyl groups are the major functionalities in DOM. However, high resolution tandem mass spectrometry of marine DOM has shown for the first time that the neutral loss 44 cannot be only imputable to  $\text{CO}_2$ , but also to  $\text{C}_2\text{H}_4\text{O}$ . This neutral loss is more related to lignin-like structures, as described more recently in coastal marine DOM (Liu et al., 2010). The tandem mass spectra of the study were evaluated investing a lot of time and effort. For each sample only a reduced group of precursor ions could be studied. It can be concluded that structural information using fragmentation studies should be carried out in selected samples and precursor ions, otherwise the amount of signals to analyze will lead to a never-ending process.

As described before (*1.2. Methods of Analysis of Dissolved Organic Matter* and *3.1. Introduction* subsection *3.1.4. Structural Characterization*, pages 6 and 106, respectively) there are some other techniques that have given information at structural level. NMR is

one of the techniques that has given more evidences. For this reason, in the present thesis,  $^1\text{H}$  NMR was also used to obtain structural information in a more straightforward way for a larger set of samples ( $n=22$ ) analyzed from different drinking water treatment plants (DWTP) (see Chapter 4).

# **Chapter 4.**

## **Dissolved Organic Matter Characterization through Water Treatment Plants**

---



## 4.1. Introduction

In the last years, there has been a shortage of freshwater due to overuse and misuse, and as a consequence the largest sources of freshwater are under increasing pressure (www.unep.org). It is clear that in order to meet rising demand for a decreasing resource, water providers must find new sources of supply to increase capacity while remaining environmentally sensitive. There are many treatment options available and the characteristics of source water will dictate the type of treatment required:

- **Freshwater** is usually drawn from two natural sources: surface and ground water. Usually surface water is derived from areas open to the atmosphere and so it requires more intensive treatment.
- **Seawater** and saline aquifers account for 97.5% of the Earth's water resources and represent a potential source of drinking water. Thus, desalination techniques involving seawater RO have emerged as important candidates (Greenlee et al., 2009).
- **Wastewater** reuse consists of total or partial treatment of the water, in order to obtain recycled water with the quality it had, before it had been used. There are two main types of reuse, depending on the quality of recycled water, one known as non-potable and one known as potable. The potable use is related to drinkable water. The non-potable use includes the irrigation of some parks and golf courses, some industrial uses, such as cooling water, and urban uses, as for example the water used to wash the streets.

Regulations are more strict every day, due to high concern on organic contaminants in the drinking water effluents (European Union 2008/105/CE and 2013/39/UE). Moreover, an increase in the content of NOM has been observed in several water bodies (Eikebrokk et al., 2004), as well as changes in some important characteristics such as color and specific UV absorbance (SUVA). These changes in raw water quality increase the required removal capacity in water treatment. Somehow, none of this is possible without advanced treatment lines.

### 4.1.1. Drinking Water Treatment Plants

Conventional treatments for drinking water are usually based on four main steps: predisinfection, coagulation, filtration and final disinfection (see Figure 4.1).

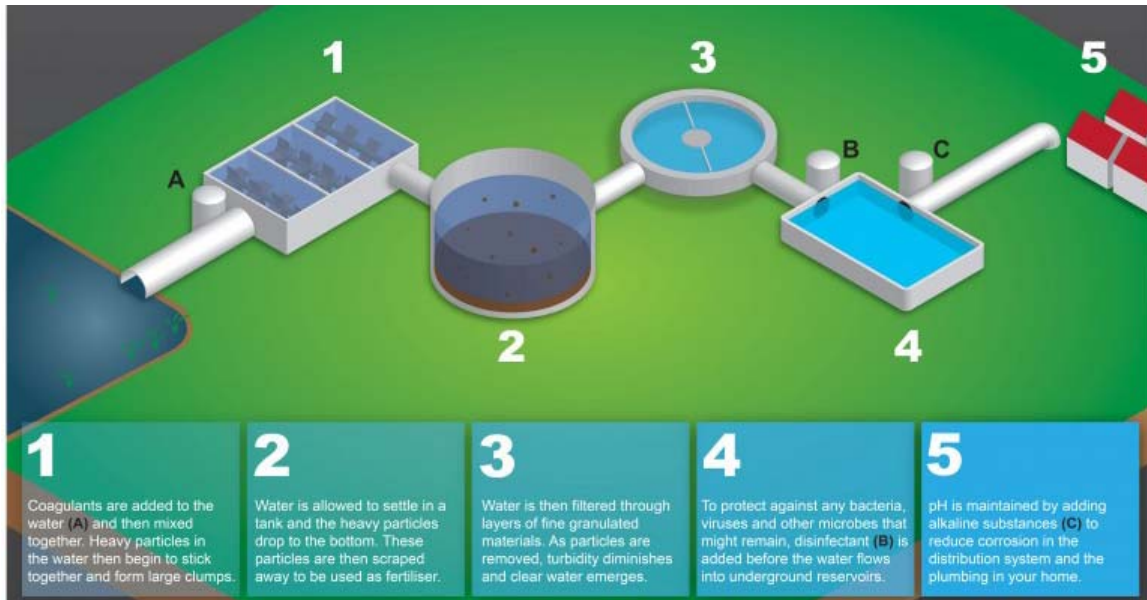


**Figure 4.1.** Water treatment process from a conventional DWTP ([www.grahamscutt.co.uk](http://www.grahamscutt.co.uk)).

In the disinfection process chemical disinfectants such as chlorine and ozone are used to eliminate microorganisms, such as viruses and bacteria. The coagulation entails the use of aluminum and iron salts as sticky particles to attract the suspended matter in water. This way the particles are so heavy that they settle out of the water. During filtration particles such as clay, silts, iron and microorganisms are removed.

Variations and combinations of different treatment processes are common due to the changeability of water quality (see Figure 4.1). Alternatively to coagulation and filtration, other separation techniques might be applied, such as activated carbon or membrane technology (Table 4.1). For instance, membranes have been added at the end of the train to further reduce turbidity and to remove other contaminants (Baruth 2004; Verliefde et al., 2007; Verliefde et al., 2009b). A good example is the DWTP of Sant Joan Despí. After disinfection, flocculation/decanting and sand filtration two treatment lines are working in parallel: i) conventional: combining ozonation and granular activated carbon filtering and ii) ultrafiltration (UF) and RO treatment. At the end, the water filtered through the activated carbon is mixed with the water coming from the membranes. This technology combination makes it possible to guarantee the health standards for trihalomethanes (THMs) ([www.aiguesdebarcelona.cat](http://www.aiguesdebarcelona.cat)).

**Table 4.1.** The most common drinking water treatment processes (adapted from Baruth 2004). In bold the process components regarding the use of membrane filtration and the main water quality parameter affected.

<b>Water Quality Parameter</b>	<b>Treatment / Action</b>	<b>Process Components</b>
<b>Turbidity-particulate reduction</b>	Filtration	Sand Filtration Coagulation Flocculation Clarification <b>Membrane filtration</b>
Bacteria and Viruses	Filtration	(see above)
	Disinfection	Chlorine Chloramine Chlorine dioxide Ozone UV
<b>Color</b>	Filtration / Coagulation	(see above)
	Adsorption	Granulated Activated Carbon (GAC) Powdered Activated Carbon Ion exchange resins
	Oxidation	Ozone Chlorine Potassium permanganate Chlorine dioxide
	Advanced filtration	<b>Nanofiltration</b>
Taste and color control	Oxidation	Ozone Chlorine Potassium permanganate Chlorine dioxide
	Adsorption	Biologically Activated Carbon (BAC)
Volatile organic reduction	Air stripping	GAC adsorption Combination of the above
<b>Disinfection by-product control</b>	Precursor reduction	Enhanced coagulation GAC adsorption BAC -preozonation <b>Nanofiltration</b>
	Disinfection by-product	GAC adsorption Air stripping
Iron, manganese reduction	Preoxidation and filtration	
<b>Hardness Reduction</b>	Lime softening	Ion exchange <b>Nanofiltration</b>
<b>Inorganic, organic chemical reduction</b>	Reduction	Ion exchange
	Adsorption	BAC
	Advanced filtration	<b>Reverse Osmosis</b>
Corrosion control	Post-treatment	pH adjustment inhibitors

### 4.1.2. Desalination

The growing demand for freshwater is partially satisfied by desalination plants. The desalination process is usually based on membrane treatments and the most commonly used is RO.

Prior to RO treatment, particles and other compounds must be removed from the water to prolong membrane life. Pretreatment usually consists of chemical coagulation, fine filtration, microfiltration (MF) and / or UF, scaling control. From the RO stage, two effluents result from this process: the permeate and the brine. The permeate is the clean drinking water, which should undergo a post-treatment disinfection and stabilization process before being delivered to customers for consumption. The brine is a leftover concentrate of salty water (twice as salty) which should be diluted prior to discharge (at least in Europe and USA) (Greenlee et al., 2009; Malaeb, et al., 2011; Pérez-Gonzalez, et al., 2012).

The largest RO-based desalination plant in Europe is located in Barcelona. With a drinking water output of 200,000 m<sup>3</sup>/day the desalination plant is supplying drinkable water to the city since 2009. An scheme of the process is included in Figure 4.2. In this case the pretreatment consists on a flotation/flocculation, gravity filtration and closed filtration. In the RO for each 100 liters of seawater, 45 liters of permeate are obtained. The permeate water is then remineralized. The 55 % of brine produced is mixed with the effluent of the wastewater treatment plant of Baix Llobregat to reduce the salinity and to be discharged into the sea (www.atll.cat).

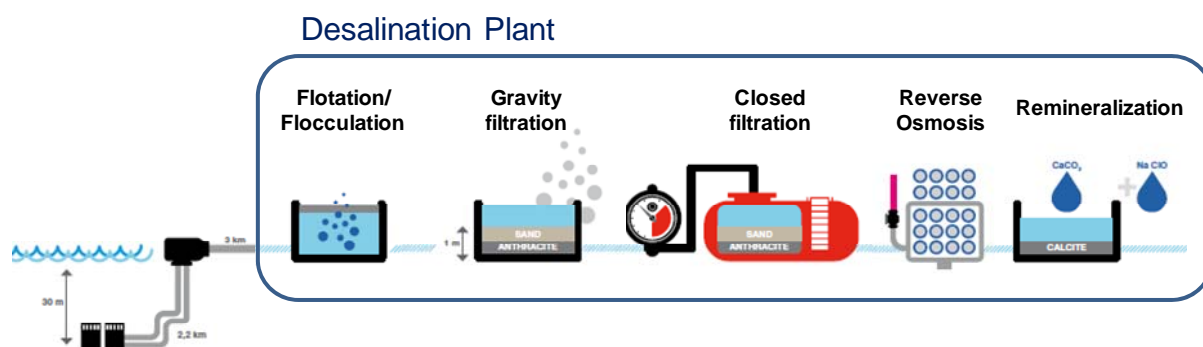


**Figure 4.2.** Desalination plant from Barcelona based on reverse osmosis treatment, showing the different steps of the treatment: seawater intake; pretreatment: flotation/flocculation, gravity filtration, closed filtration; RO membranes and remineralization (adapted from www.atll.cat).

### 4.1.3. Relevance of Dissolved Organic Matter for Drinking Water Supply

The properties and amount of DOM in natural waters can significantly affect the drinking water quality in different terms: i) taste, color and odor, ii) transportation of organic pollutants and iii) water treatment process (Murphy et al., 1990; Frimmel et al., 1996; Kaiya et al., 1996; Camper et al., 2004; Eikebrokk et al., 2004).

A common drinking water goal is to remove DOM, as it is a precursor for unwanted DBPs during chemical disinfection with chlorine. It has been shown that the choice of disinfectant has a large impact on DBP formation (Lavonen et al., 2013) and the levels of some emerging DBPs (see Figure 4.3) are increased by alternative disinfectants, such as ozone or chloramines (Richardson et al., 2007). In Europe, there are four legislated THMs (European Communities, 2007). However, other DBPs are included in lists from previous studies due to their toxicological importance and occurrence (Krasner et al., 2006; Richardson et al., 2007). Decreasing the amount of DOM may lead to a decrease in the potential formation of DBPs.

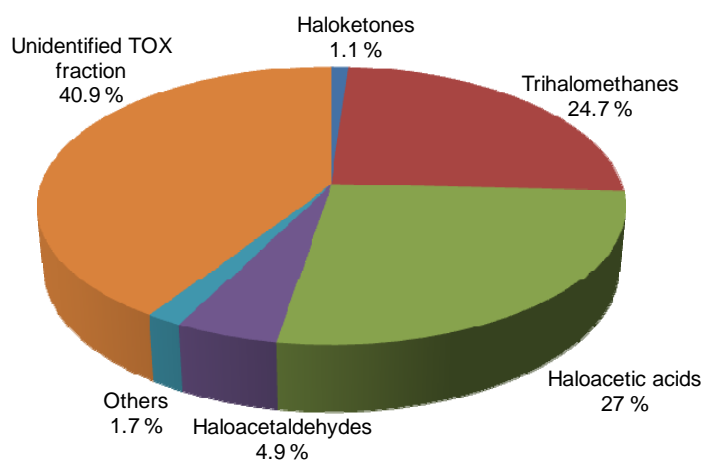


**Figure 4.3.** Types of DBPs formed and their contribution to the overall total organic halogen (TOX) in drinking water (adapted from Pressman et al., 2010).

DOM can also affect the performance of water treatment processes including coagulation, activated carbon adsorption and membrane filtration. For instance, it has been reported that an increase of raw water color, increased the required coagulant dose, sludge production and number of backwashes per day (Eikebrokk et al., 2004). In membrane filtration, membrane fouling curtails the viability of UF, nanofiltration (NF) or RO processes (Xu et al., 2010; Jeong et al., 2013).

#### 4.1.4. Membrane Technology

Membranes are able to separate molecules from a solution as a result of their differences in size, shape, chemical structure or electric charge. All membrane processes separate feed water into two streams, the permeate (for UF, NF and RO) and the concentrate or brine (Figure 4.4).

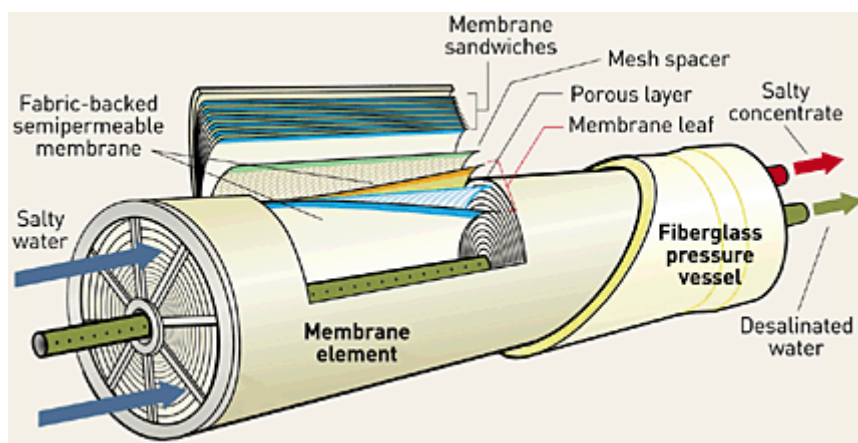


**Figure 4.4.** Scheme of a RO membrane, showing the main parts of a membrane module and the way the feed water (salty water) is separated into two streams: permeate (desalinated water) and brine (salty concentrate) ([www.membrane.ces.utexas.edu](http://www.membrane.ces.utexas.edu)).

There are several different processes in the drinking water industry that use membrane technology: desalting, softening, dissolved organics and color removal, particle and microbial elimination (Verliefde et al., 2007; Verliefde et al., 2009b).

Depending on the water quality and goal of the treatment, there are several types of membranes with regard to selectivity range, properties (e.g. configuration, material, porosity, weight cut-off, roughness, Z-potential, isoelectric point) and performances (e.g. % conductivity rejection, clean water permeability, water recovery) that can be used (see Figure 4.5).

Most membrane treatment systems require some pretreatment. The type of pretreatment system required depends on raw water quality and membrane type. The pretreatment should condition the feed water to allow the membrane treatment to be effective (i.e. using coagulants to enlarge the particles so that they can be removed by MF) or should modify the feed water to prolong membrane life.

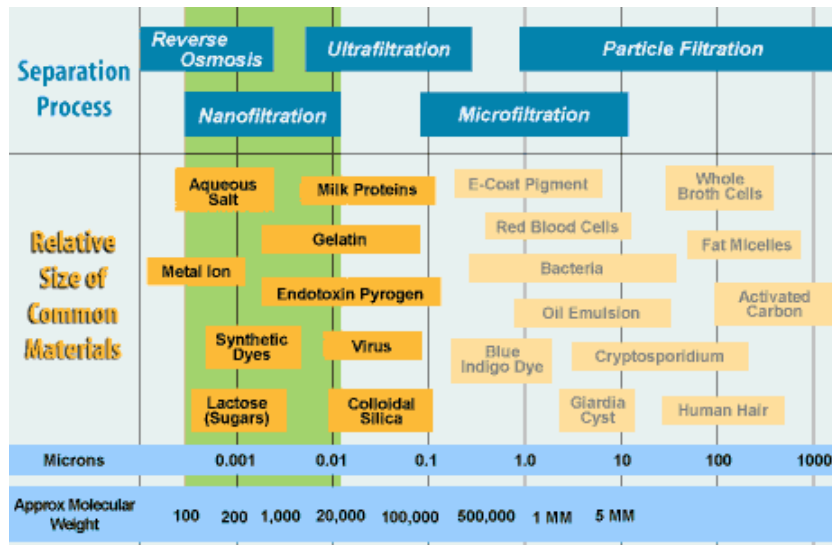


Figure 4.5. Membrane classification regarding selectivity range (www.eco-web.com).

The main problems of membrane technology are the high energy requirements in comparison to conventional processes and fouling tendency of membranes which increase flux decline, decreasing membrane performance (see Table 4.2).

Table 4.2. Advantages and drawbacks of membrane technology (from Ribera 2013).

Advantages	Drawbacks
Separation can be carried out continuously	Energy consumption
Flexibility to be combined with other processes (hybrid processing)	Membrane Fouling
Separation can be carried out under mild conditions	Membrane lifetime
Easy scaling-up	Low selectivity
Reduction of steps in some treatments processes	
Variability in membrane properties to adjust correctly for each use	
Chemical addition is not playing the main role	

### 4.1.5. Membrane Fouling

Membrane fouling is a phenomena that can occur on membranes and that involves a reduction of permeate flow at constant operational pressure or an increase of operational pressure when membranes are operating at constant permeate flow. The research developed in this area is trying to find out preventive measures and corrective actions for each fouling case. Fouling can be classified as inorganic, organic or biofouling, taking into account the constituents causing it. It may consist in particles deposition, pore blocking, physical and chemical interactions between compounds and membrane or the development of biofilm.

**Table 4.3.** Foulants and their control strategies in NF and RO processes (Schäfer et al., 2005)

Foulant	Fouling Control
	Operate below solubility limit
	Pre-treatment
Scaling / Silica	Acid Addition (pH=4-6)
	Low recovery
	Antiscalants addition
Colloids	Pretreatment using: coagulation-filtration, MF or UF
Organics	Pretreatment using: biological process, activated carbon, ion exchange, ozone or enhanced coagulation
Biological solids	Pretreatment using disinfection, filtration, coagulation, MF or UF

At the end of the life of the membranes, some elements may be sacrificed to carry out what is called membrane autopsy. Membrane autopsy is a destructive analysis to identify the major causes of fouling (Schäfer et al., 2005). The characterization usually consists on visual inspection, measuring membrane properties such as zeta-potential, contact angle and elemental composition of the membrane surface, membrane scanning electron microscopy images, attenuated total reflection-Fourier transform infrared spectrometry and microbiological analysis (Xu et al., 2010; Verfliefde et al., 2009b; Jeong et al., 2013).

Regarding organic fouling, naturally occurring dissolved organics cause fouling in RO and NF systems. There is no definitive correlation between the quantity of organics

(measured as total organic carbon-TOC) and the performance decline of RO and NF systems (Baruth 2004). In some studies different techniques such as UV, SUVA, excitation emission matrix fluorescence spectroscopy, liquid chromatography-organic carbon detection and molecular weight distribution have been used to characterize the organic fouling (Verliefde 2009b; Jeong et al., 2013). However, no information is available concerning the molecular characterization. Knowing the type of molecules (i.e. elemental compositions and main functional groups) better actions could be carried out to prevent or at least remove organic fouling from the membranes to enlarge lifetime. In this sense, the molecular characterization of the fouling caused in two different NF membranes was carried out.

## 4.2. Experimental Procedure and Results

Understanding the evolution of DOM in water treatment plants is necessary to determine the effect of each treatment step and try to improve their efficiency. Pilot testing is often used to determine the effects of dissolved organics on membranes. In the present study, research has been carried out in this direction and the effluent water from two different water pilot treatment plants with advanced membrane treatments has been analyzed (see Figure 4.6).

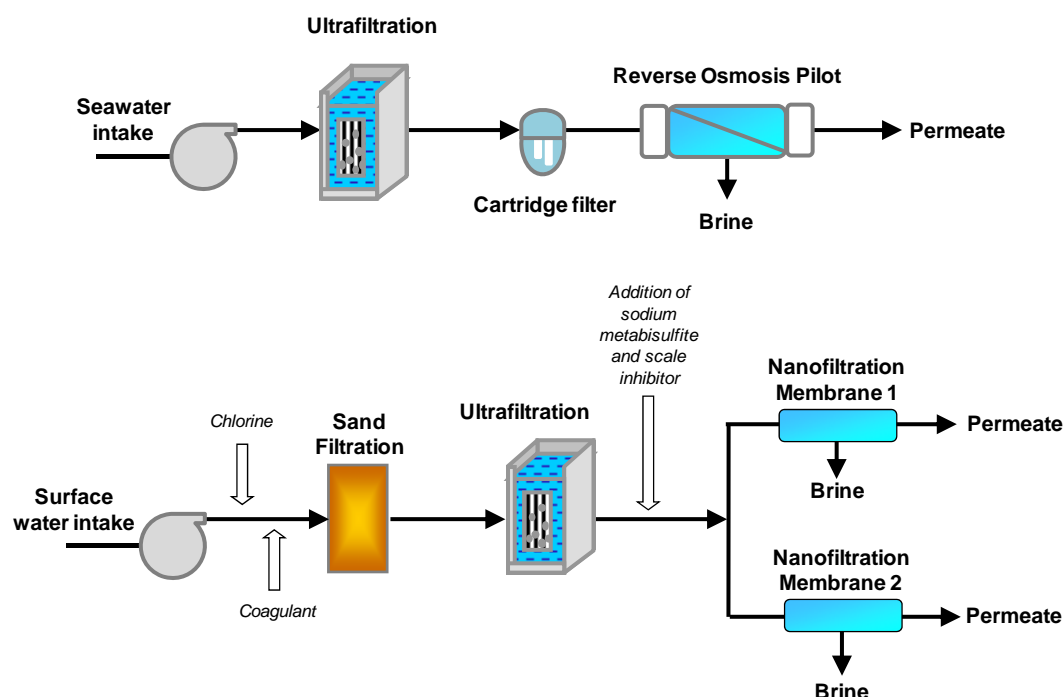


**Figure 4.6.** Scheme of the two pilot plants of the study: (above) Desalination Plant and (below) Drinking water treatment plant.

In a first study, the water going through the different steps of a desalination treatment plant was analyzed. The method development and results obtained are included in the Research Article N° 3: *Molecular Characterization of Dissolved Organic Matter through a Desalination Process by High Resolution Mass Spectrometry* published in *Environmental Science and Technology* included in section 4.2.1. This study was developed within the framework of the SOSTAQUA project (CEN20071039).

In a second study, we have evaluated the molecular changes of DOM through an ultrafiltration-nanofiltration (UF-NF) pilot plant, using two dissimilar NF membranes tested in parallel. The Research Article N° 4: *High-field FT-ICR Mass Spectrometry and*

*NMR Spectroscopy to Characterize DOM Removal through a Nanofiltration Pilot Plant* published in *Water Research* and included in section 4.2.2. summarizes the procedure and results. This pilot plant was in operation during 6 months in the DWTP of Aigües de Manresa under the supervision of the researchers of the Centre Tecnològic de Manresa (CTM). The FT-ICR MS and NMR measurements were carried out during my stay in the Helmholtz Zentrum Muenchen, German Research Center for Environmental Health, Research Unit Analytical Biogeochemistry (BGC).

Regarding the fouling of the membranes, the aim was to develop a new method to study the adsorption of DOM on membrane surfaces, in order to obtain molecular information of DOM susceptible to cause fouling on different membranes. Results and discussion are included in the submitted Research Article N° 5: *Molecular Characterization of DOM causing Fouling to NF Membranes by High-field FT-ICR Mass Spectrometry and NMR Spectroscopy* included in section 4.2.3.



### **4.2.1. Research Article Nº 3**

Nuria Cortés-Francisco and Josep Caixach

Molecular Characterization of Dissolved Organic Matter through a Desalination Process by High Resolution Mass Spectrometry.

*Environmental Science & Technology* **2013**, 47, (17), 9619-9627.



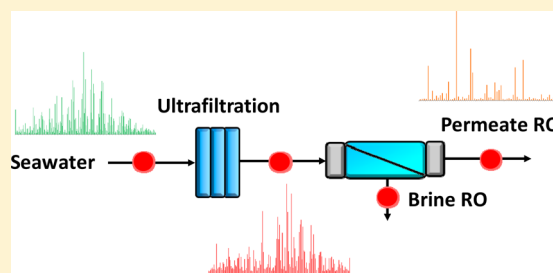
## Molecular Characterization of Dissolved Organic Matter through a Desalination Process by High Resolution Mass Spectrometry

Nuria Cortés-Francisco and Josep Caixach\*

Mass Spectrometry Laboratory/Organic Pollutants, IDAEA-CSIC, Jordi Girona 18, 08034 Barcelona, Spain

### S Supporting Information

**ABSTRACT:** The effect of different water treatments such as ultrafiltration (UF) and reverse osmosis (RO) on dissolved organic matter (DOM) is still unknown. Electrospray ionization Fourier transform orbitrap mass spectrometry has been used to provide valuable information of marine DOM evolution through a desalination process on a molecular scale. In the present manuscript, the characterization of four real composite water samples from a desalination pilot plant installed in the coast of Barcelona (Spain) has been carried out. The sampling was performed on each point of the pilot plant: raw seawater (RSW), UF effluent, brine RO and permeate RO. The mass spectra of the different samples show several thousand peaks, however for the present screening study, only the mass range  $m/z$  200–500 and the main signals in this mass range (relative intensities  $\geq 1\%$ ) have been considered. The analysis of RSW and UF samples reveal that there is little effect on DOM by the UF pilot. However, when the water is treated on the RO an important change on DOM has been observed. The recurring periodical patterns found in RSW and UF are lost in Permeate RO sample. Compounds with more aliphatic character, with higher H/C ratio ( $H/C_{av}$  1.72) are present in the Permeate and some of them have been tentatively identified as fatty acids.



### INTRODUCTION

In the last years, there has been a shortage of fresh water, due to overuse and misuse. Seawater and saline aquifers account for 97.5% of the Earth's water resources and represent a potential source of drinking water. Thus, desalination techniques involving seawater reverse osmosis (RO) have emerged as important candidates.<sup>1</sup> The properties and amount of dissolved organic matter (DOM) in natural waters can significantly affect the production of drinking water.<sup>2–4</sup> It may cause adverse aesthetic qualities such as color, taste, and odor, but also it can affect the performance of water treatment processes, such as activated carbon adsorption, ozonation, or membrane treatments. Moreover, DOM can serve as main precursor of disinfection byproducts (DBPs) during chlorination.<sup>5,6</sup>

DOM is an extremely complex mixture of organic compounds and the amount and characteristics of it depends on climate, geology, and topography.<sup>7</sup> Marine DOM is found at very low concentrations in comparison to huge amounts of inorganic salts, so the removal of DOM and salts to obtain fresh water from seawater represents a real challenge. In order to improve and optimize removal processes of this organic matter, the characterization of DOM at different purification and treatment processes stages is important.<sup>2</sup> In treatment lines, the characterization usually consists on bulk parameters such as total organic carbon (TOC), dissolved organic carbon, and spectroscopy techniques such as, ultraviolet and visible absorption spectroscopy, specific UV-absorbance, and excitation emission matrix fluorescence spectroscopy.<sup>8</sup>

In the last years, a desalination treatment plant which takes the water from the Mediterranean Sea and supplies fresh water to the city of Barcelona has been built.<sup>9</sup> In parallel to the construction of the desalination plant there was a desalination pilot plant installed, in order to investigate in the pretreatments and the reverse osmosis processes with the same real water intake.

Our goal was to characterize the molecular composition of water-soluble organic matter from Mediterranean seawater and see the evolution of DOM through a desalination pilot plant. In this study, DOM has been studied by use of electrospray ionization high-resolution Fourier transform orbitrap mass spectrometry (ESI LTQ-FT-Orbitrap-MS), due to the fact that high resolution mass spectrometry (HRMS) is one of the techniques that has given more information of the molecular species, exact masses and molecular formulas of DOM.<sup>8</sup> Due to the difficulty of data interpretation and limitations of the technique (lacking ability for identification of isomers, limited resolution) a strict protocol has been applied to ensure reliable results. To the best of our knowledge, no studies have evaluated this evolution to understand the changes in DOM through a desalination process, which is a critical aspect to better describe pretreatment and reverse osmosis processes.

Received: January 3, 2013

Revised: July 17, 2013

Accepted: July 24, 2013

Published: July 24, 2013

## ■ EXPERIMENTAL SECTION

**Chemicals.** All reagents were of analytical or high-performance liquid chromatographic grade. Dichloromethane, methanol, and hydrochloric acid were purchased from Merck (Darmstadt, Germany). Isopropyl alcohol was from Carlo Erba (Milan, Italy), and formic acid was from Panreac (Barcelona, Spain). Highpurity water produced with a Milli-Q Organex-Q System Millipore (Millipore Corp., Bedford, MA) was used. The internal standards sodium dodecyl- $d_{25}$  sulfate was purchased from CDN Isotopes (Quebec, Canada) and the dioctyl sodium sulfosuccinate was purchased from Sigma-Aldrich (Schnellendorf, Germany). Suwannee River Fulvic Acid (SRFA) (1S101F) and Suwannee River Natural Organic Matter (SRNOM) (1R101N) standards from International Humic Substance Society (Minnesota, United States) have been diluted in methanol and analyzed to find common components between the real samples and the standards.

**Sample collection and preparation.** Four real composite water samples from a pilot desalination plant installed in the coast of Barcelona (Spain) were collected in Pyrex borosilicate amber glass bottles. The seawater intake system is located 2200 m from the shoreline and 31 m below sea level in the Mediterranean Sea.<sup>9</sup> Raw seawater (RSW) is passed through an out/in ultrafiltration (UF) hollow fiber membrane (polyvinylidene fluoride; 0.02  $\mu\text{m}$  nominal pore size). The UF effluent is then passed through 5  $\mu\text{m}$  security cartridge filters and fed through a RO module (thin film composite membrane operating at 14  $\text{L m}^{-2} \text{h}^{-1}$  and 45% of recovery). The sampling was performed on each point of the pilot treatment plant: RSW, UF effluent, brine RO, and permeate RO. Samples were stored at 4 °C and analyzed within 48 h. We acidified 1.5 L from each sample with 10% hydrochloric acid to pH 2 and extracted with 2  $\times$  100 mL of dichloromethane/isopropyl alcohol (90:10 v/v) and the extracts were concentrated down to 250  $\mu\text{L}$  at 40 °C under nitrogen. 100 fold dilution and reanalysis was performed to the brine RO sample. Sodium dodecyl- $d_{25}$  sulfate and dioctyl sodium sulfosuccinate were added as internal standards used as lock mass for internal calibration of the spectra. This extraction protocol was chosen in order to manipulate as less as possible the real nature of the water, and analyze the whole water without prior filtration, as well as to eliminate any remaining salts which would suppress the ion generation within electrospray.

**LTQ-Orbitrap Mass Spectrometry.** Flow injection analysis (FIA)<sup>10</sup> of 10  $\mu\text{L}$  of the standards and the samples has been carried out with a LTQ-Orbitrap XL (Thermo Fisher Scientific, Bremen, Germany) equipped with an ESI source. The LC system consists of a Surveyor MS Plus pump and a Micro As autosampler (Thermo Fisher Scientific, San Jose, California). The mobil phase was methanol:water (80:20) at 50  $\mu\text{L}/\text{min}$ .

All mass spectra were acquired in negative ionization mode produced by an ESI source voltage of 3.00 kV, capillary voltage -35 V and tube lens -90 V, after ion source parameters optimization. The sheath gas flow was set at 20 and aux gas flow 5, both arbitrary units and capillary temperature of 300 °C. Negative ionization was used, because it has been reported to produce more ions from marine DOM samples<sup>11,12</sup> and we were not specifically searching for compounds containing nitrogen, which then positive mode would have been more appropriated. The mass range was  $m/z$  50–1200, because prior analysis showed no signals in a higher  $m/z$  range.

A protocol has been developed to better evaluate the uncertainty of the accurate mass measurements and to build the van Krevelen plots in a systematic way, so that the different data from each sample can be comparable. The first step was to evaluate the uncertainty of the accurate mass measurements of the mass spectrometer, based on prior experience.<sup>13</sup> Internal and external calibration experiments were performed taking into account the internal standards added (data not shown). Finally, the spectra were internally calibrated using as lock masses sodium dodecyl- $d_{25}$  sulfate ( $m/z$  290.3048) and dioctyl sodium sulfosuccinate ( $m/z$  421.2265) added during the sample treatment. This way, the accuracy and precision in the relevant mass range ( $m/z$  200–500) was always <1 ppm. The automatic gain control was used to consistently full fill the C-trap and gain mass accuracy and resolution.<sup>14</sup> High resolving power defined as  $R$ : 100 000 ( $m/z$  400, full width at half-maximum) was set. However, as resolving power and resolution change along the mass range, experimental resolving power much better than 150 000 was found in part of the relevant mass range ( $m/z$  200–350). This resolution might be limited for signals with low signal-to-noise ratio and for this reason the mass peaks used to evaluate the molecular composition all represent single negatively charged molecular ions with relative intensities  $\geq 1\%$ .

These peaks were exported to peak lists and from these lists feasible elemental formulas were generated. Different restrictive criteria were set to generate reliable elemental formulas:  $C \leq 60$ ,  $H \leq 120$ ,  $O \leq 60$ ,  $N \leq 3$ ,  $S \leq 1$ . It was assumed that some percentage of the total observed peaks remain unidentified. Possibly they contain additional elements or more heteroatoms than permitted in the calculations. Data filtering of the assigned formulas was done applying rules and assumptions as described in Herzsprung and colleagues<sup>15</sup> and Koch et. al.<sup>16</sup> The molecular formulas calculation was performed with Xcalibur 2.1 (Thermo Fisher Scientific, Bremen, Germany) and the posterior analysis of the data was done using our own developed excel macros. For each negative ion observed, the elemental formulas reported is the corresponding neutral whose mass is the mass of the negative ion plus a proton (1.007276 Da). Moreover, it should be noticed that each elemental formulas could represent millions or more constitutional isomers depending on the mass.<sup>7</sup>

### van Krevelen and Kendrick Mass Defect Analysis.

One method of depicting large data sets of elemental formulas is by mean of van Krevelen diagrams, which are useful to classify substance classes in a first approach.<sup>17</sup> Since major chemical classes typically found in DOM have characteristic H/C and O/C ratios, they cluster within specific regions of the Van Krevelen diagram.<sup>18</sup> Further, van Krevelen plots are used to evaluate the degree of alkylation, hydrogenation, hydration, and oxidation of NOM.<sup>20</sup> In the present study, van Krevelen diagrams were built taking into account the different composition of the elemental formulas assigned and also on color-coded analyte relative abundance plots. Although intensity in an ESI-MS spectrum does not translate directly into relative concentration for analytes of very diverse chemical composition, a qualitative comparison of isolates on the basis of signal intensities can be performed when the samples have been analyzed with identical instrumental conditions.<sup>21</sup> For that reason, all the standards and samples are analyzed using identical measurement conditions and data evaluation protocols. Moreover, useful parameters in the characterization of the unsaturation and aromaticity of molecular formulas are the

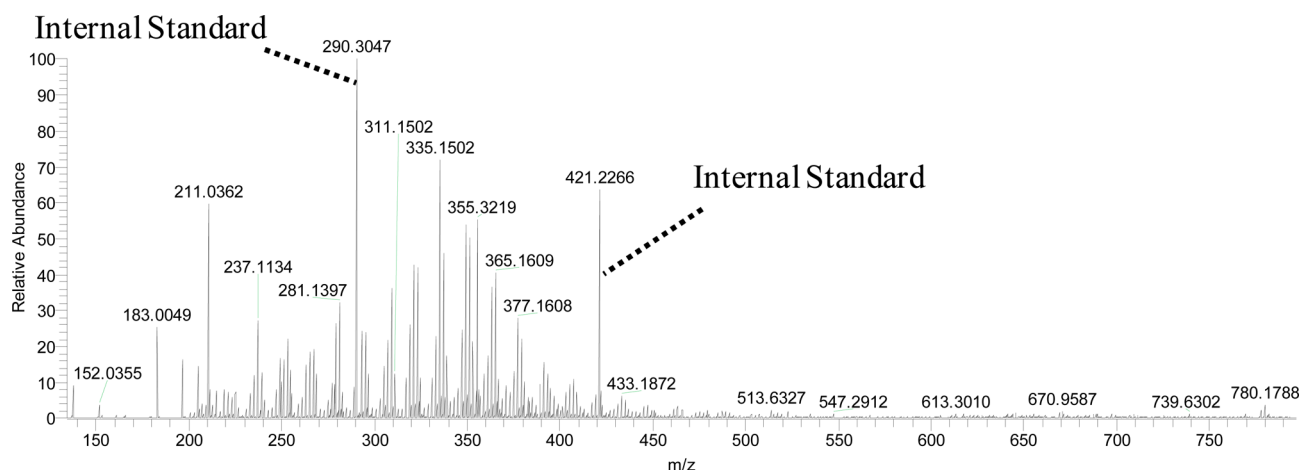


Figure 1. Mass spectrum of RSW sample obtained by negative ESI-LTQ-FT-Orbitrap-MS.

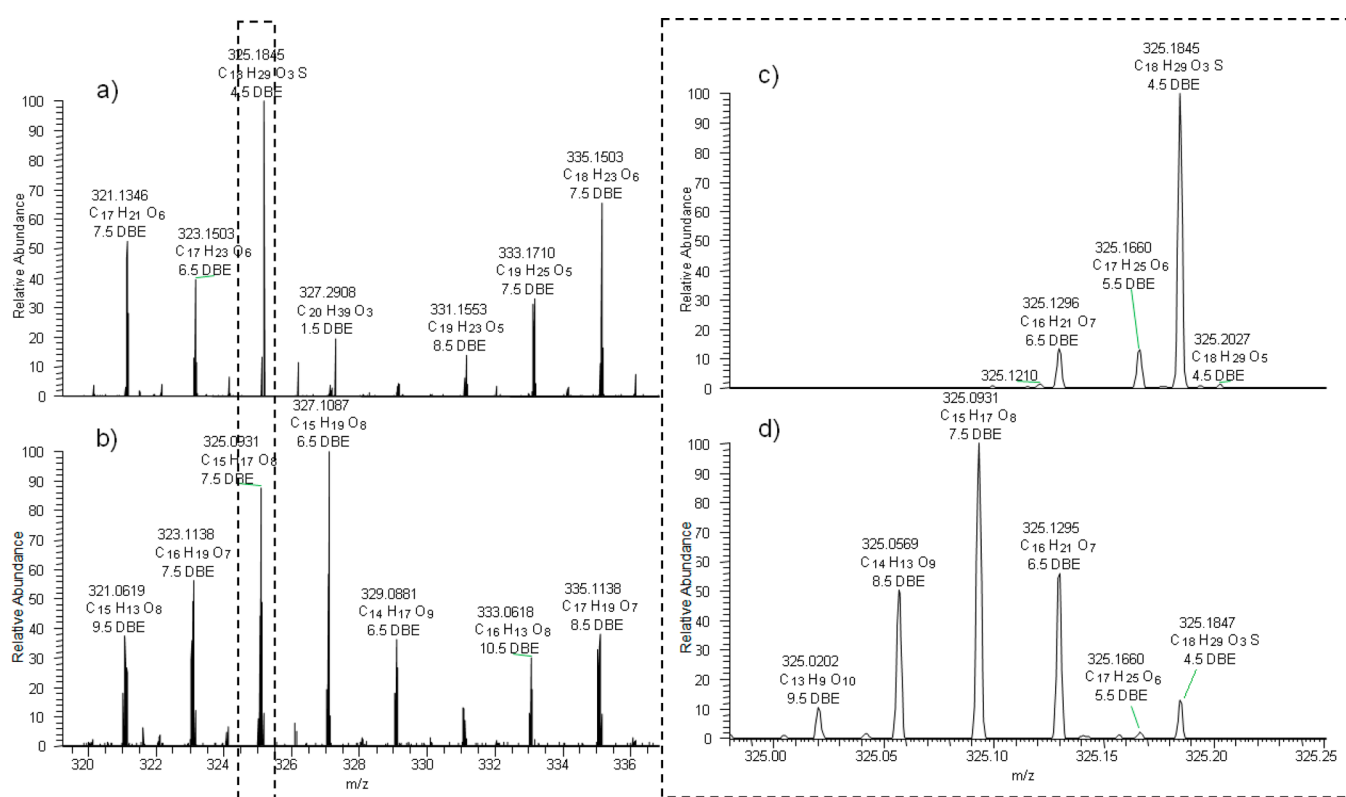


Figure 2. Mass spectra of (a) RSW sample and (b) SRFA standard, showing assigned elemental formulas and DBE in the mass range  $m/z$  320–336. The nominal mass 325 expansion of LTQ-Orbitrap mass spectra of (c) RSW and (d) SRFA show series of compounds related by a formal exchange of  $\text{CH}_4$  vs oxygen. The depicted elemental formulas represent negative singly charged molecular ions.

double bond equivalents (DBE), the ratio between DBE and carbon (DBE/C), and the double bond equivalents minus oxygen (DBE-O).<sup>18,19</sup> Although scientists are more familiar with DBE, the DBE/C parameter is better to be used since bigger molecules can have higher DBE but lower “true” carbon unsaturation. Along the manuscript the two values have been included. On the other hand, the DBE-O parameter has been also described as a better indicator for the unsaturation of the carbon skeleton compared to the DBE, since most oxygen atoms in DOM molecules are a part of carboxyl group that is counted as one DBE. In the present study, DBE-O has been used to better understand the changes of unsaturation and aromaticity along the treatment. Moreover, Kendrick Mass

Defect (KMD) is used to sort out homologous series of organic compounds. In the present study, it has been applied to the data sets for interpretation.<sup>12</sup>

**Complementary Analysis.** Supporting Information (SI) Table S1 summarizes the data for some complementary analysis performed on the samples. pH, conductivity, nonpurgable organic carbon (NPOC), salinity, silt density index (SDI) measurements, and enumeration of phytoplankton were recorded on each sample. These conventional analysis were performed by laboratory of Aigües de Barcelona (AGBAR), Degrémont-Suez employers in charge of the pilot plant and Instituto de Ciencias del Mar (ICM-CSIC) in Barcelona.

**Table 1. Characteristics of the Formulae Identified by Negative ESI-LTQ-FT-Orbitrap-MS Comparing the Standards and the Samples Analyzed<sup>a</sup>**

	assigned formulas	% CHO formulas	carbon range	oxygen range	O/C <sub>av</sub>	H/C <sub>av</sub>	DBE <sub>av</sub>	DBE/C <sub>av</sub>	reference
SRFA standard	817	68	5–34	1–15	0.45	1.03	9.9	0.56	experimental data
SRNOM standard	844	77	7–34	1–16	0.5	1.04	9.5	0.55	experimental data
RSW	279	83	7–32	1–10	0.32	1.43	6.2	0.35	experimental data
UF effluent	183	86	8–32	1–10	0.29	1.46	5.8	0.33	experimental data
permeate RO	63	73	9–32	1–7	0.18	1.72	3.6	0.21	experimental data
brine RO	251	80	8–31	1–10	0.29	1.34	7.2	0.39	experimental data
SRFA standard					0.42	1.05	11.4		Koch, B.P. et al. <sup>22</sup>
Weddell Sea (30 m depth - C18 extracted)					0.37	1.29	9.3		Koch, B.P. et al. <sup>22</sup>
offshore coastal water (C18 extracted)					0.33	1.43	7.2		Sleighter, R.L. et al. <sup>24</sup>

<sup>a</sup>Some characteristics of marine samples and standards from the literature are included to compare with the nature of the samples analyzed in the present study.

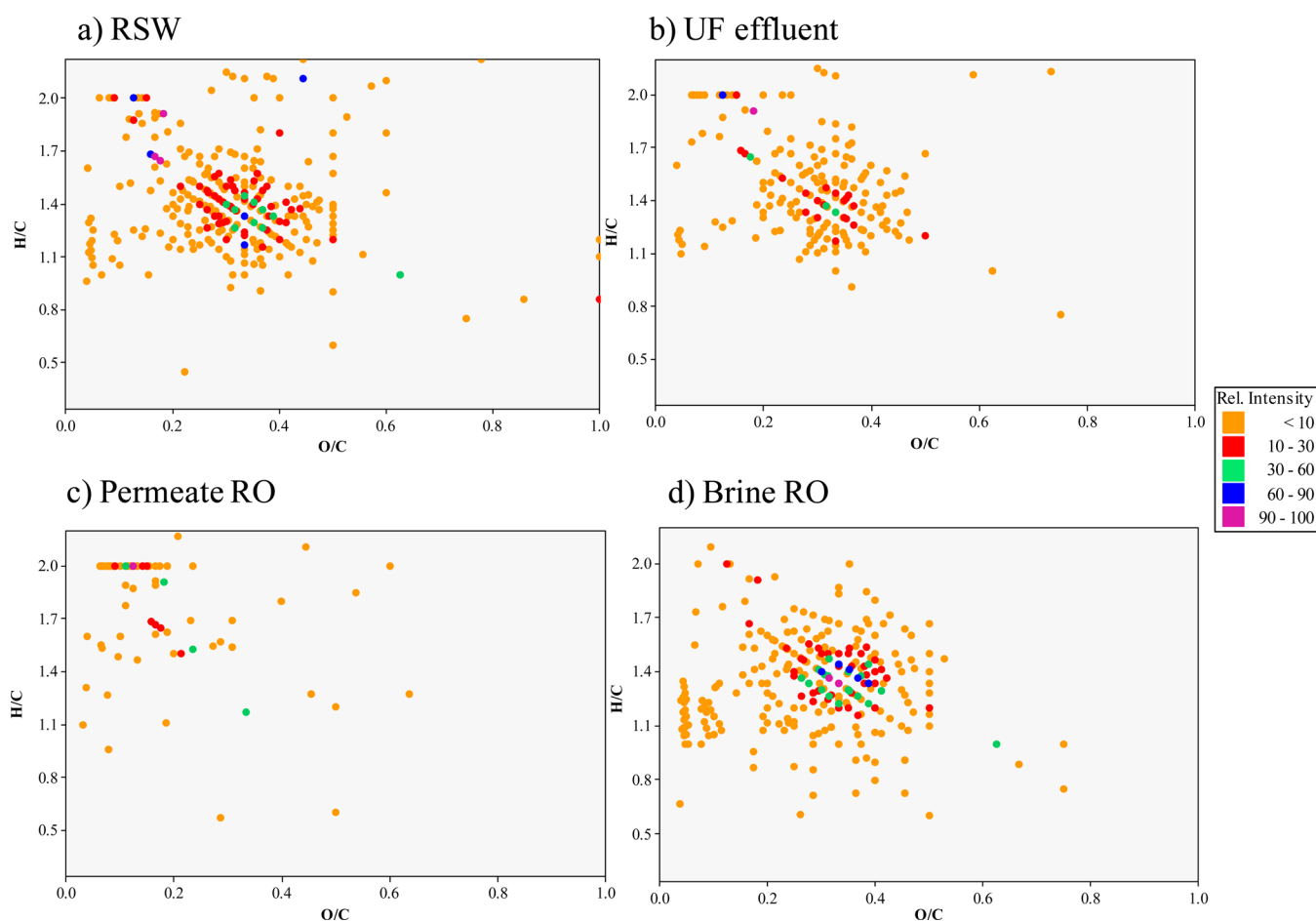


**Figure 3.** Van Krevelen diagrams for all formulae assigned of (a) RSW, (b) UF effluent, (c) Permeate RO, and (d) Brine RO samples on color-coded analyte relative abundance plots.

## RESULTS AND DISCUSSION

**Raw Seawater Characterization.** In seawater the amount of DOM quantified as TOC is very low, always under 1 mg C/L (SI Table S1). Compared to other aquatic environments (freshwater, wastewater), the low concentration of DOM and the high salinity (31200 mg NaCl/L) makes the analysis more difficult.

The mass spectra of the RSW sample (Figure 1) show several thousand peaks between  $m/z$  150–800, however for the present screening study, only the mass range  $m/z$  200–500 and

the main signals in this mass range (relative intensities  $\geq 1\%$ ) have been considered. With a maximum of the peak distribution around  $m/z$  350, a total of 231 of the exact mass measurements could be assigned to elemental compositions containing only CHO. The rest of the assigned peaks represents a little part of all the signals (17%) and includes compounds containing CHON, CHOS and CHONS (see SI). This low contribution of compounds containing atoms different from CHO could be explained, due to the threshold at 1% of the relative intensities performed, that makes that some small

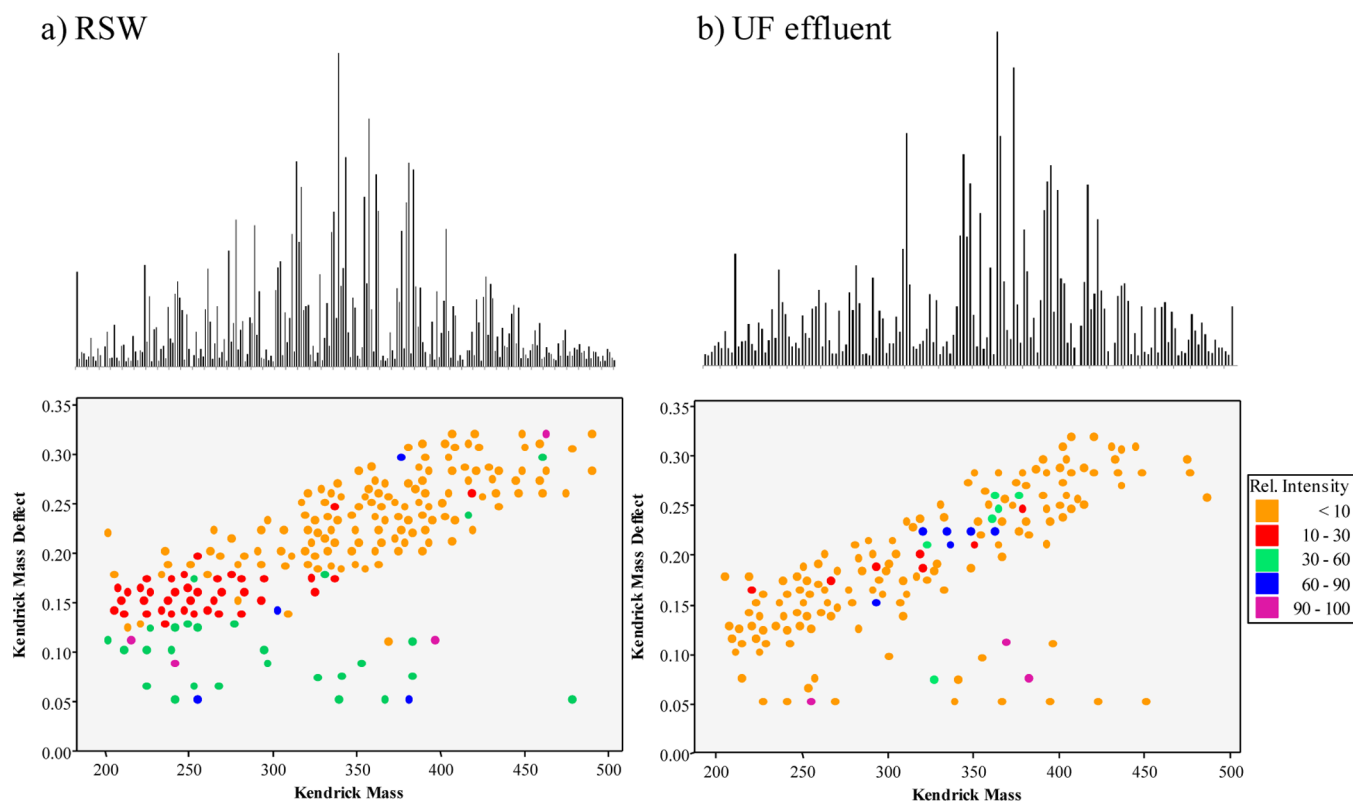


**Figure 4.** The Kendrick Mass defect ( $\text{CH}_2$ ) vs Kendrick nominal mass for the assigned formulas of (a) RSW and (b) UF effluent samples, on color-coded analyte relative abundance plots. Above the corresponding reconstructed mass spectra.

signals corresponding to molecules with heteroatoms have not been considered in the final assigned list.

As described elsewhere,<sup>22,24</sup> DOM from RSW is a complex mixture of compounds with regular patterns that span the entire spectrum (Figure 2). Analysis of the DBE/C from the neutral chemical formulas suggests, that the RSW sample analyzed is significantly saturated, which translates to low DBE/C values, with a  $\text{DBE}/\text{C}_{\text{av}}$  of 0.35 ( $\text{DBE}_{\text{av}}$ : 6.2). When compared to the SRFA standard (SI Figure S1a and Figure 2d), it can be seen that the signals are not identical and the RSW sample presents CHO compounds with lower DBE and at the same time, lower content of oxygen. These differences are present along the spectrum. As a consequence, the observed O/C ratios are lower than for SRFA and SRNOM with an average O/C ratio of 0.32 and an average H/C ratio of 1.43 (Table 1).

These higher H/C ratios could be explained due to selective fractionation of DOM as a consequence of the different extraction protocols used for the samples (LLE extraction) and SRFA (XAD resins) and SRNOM (reverse osmosis), as pointed out before by Gonsior et al.<sup>23</sup> However, compared to other studies where marine DOM has been analyzed using different extraction protocols (SPE-C18 and SPE-PPL), similar values has been obtained (Table 1), showing that DOM from seawater origin presents always higher H/C ratios and lower O/C ratios, with lower  $\text{DBE}_{\text{av}}$ .<sup>22,24</sup> These conclusions make sense as far as lignins are not present in marine DOM, which are the main contributor to oxygen in terrestrial DOM.

This high degree of order and saturation (high H/C ratio) of RSW can be observed in SI Figure S2, the van Krevelen diagram of RSW built taking into account the different composition of the elemental formulas assigned. In the present study, the CHO compounds are the major component of the

fraction of DOM analyzed (83% of assigned formulas) and present the higher relative intensity in the spectrum (see Figure 3a). These compounds present regular patterns as described before and they can be sorted out into homologous mass series based on Kendrick Mass Defect diagram<sup>7,22,24–26</sup> (Figure 4a).

Thus, it is known that DOM may be multifunctional with a combination of hydroxyl, carbonyl, carboxyl, ester, nitrate, and sulfate functional groups.<sup>22,24</sup> However, these compounds containing nitrogen (CHON and CHONS) are not significant, regarding the low level of organic nitrogen in seawater that has been reported previously.<sup>27–29</sup> For instance, only two series containing  $-\text{ON}_3\text{S}$  and  $-\text{O}_2\text{N}_3\text{S}$  have been identified and it should be taken into account that these molecules present low relative intensity (between 1 and 6%).

Moreover, during the extraction samples are acidified to pH 2 prior to extraction, in order to protonate any sites with a negative charge, but it also protonates nitrogen atoms, leading to the formation of a water-soluble cationic species. On the other hand, the ionization of compounds containing nitrogen in negative electrospray mode it is known to be less efficient in front of compounds containing sulfonated groups and/or negatively charged groups like fatty acids.<sup>11,24</sup>

Apart from the background of DOM, some influence of anthropogenic compounds has been detected in the RSW sample, due to the fact that the water intake of the desalination plant is influenced by the proximity of the metropolitan area of Barcelona (population of 3 000 000). The four most prominent individual peaks in the CHOS group are  $m/z$  297.1530, 311.1686, 325.1843, 339.1999 which have been identified as anthropogenic linear alkyl benzene sulfonates (SI Table S2).<sup>23,30</sup> The rest of CHOS compounds have number of

**Table 2. Accurate Mass Measurements and Elemental Compositions of Tentatively Identified Lipid-Like Compounds Found in RSW and Permeate RO**

experimental $m/z$ from single negatively charged molecular ion <sup>a</sup>	delta (ppm) <sup>a</sup>	theoretical mass of the neutral chemical formulas	neutral chemical formulas	DBE	H/C	O/C	tentative identification
241.2175	0.66	242.2246	C <sub>15</sub> H <sub>30</sub> O <sub>2</sub>	1	2.000	0.133	pentadecanoic acid
255.2330	0.29	256.2402	C <sub>16</sub> H <sub>32</sub> O <sub>2</sub>	1	2.000	0.125	palmitic acid
339.3270	0.35	340.3341	C <sub>22</sub> H <sub>44</sub> O <sub>2</sub>	1	2.000	0.091	behenic acid
367.3583	0.27	368.3654	C <sub>24</sub> H <sub>48</sub> O <sub>2</sub>	1	2.000	0.083	lignoceric acid
383.3531	0.06	384.3603	C <sub>24</sub> H <sub>48</sub> O <sub>3</sub>	1	2.000	0.125	lignoceric acid oxidation product
327.2906	0.50	328.2977	C <sub>20</sub> H <sub>40</sub> O <sub>3</sub>	1	2.000	0.150	arachidic acid oxidation product
253.2174	0.58	253.2168	C <sub>16</sub> H <sub>30</sub> O <sub>2</sub>	2	1.875	0.125	plamitoleic acid
297.2438	0.86	298.2508	C <sub>18</sub> H <sub>34</sub> O <sub>3</sub>	2	1.889	0.167	oleic acid oxidation product
279.2332	0.99	280.2402	C <sub>18</sub> H <sub>32</sub> O <sub>2</sub>	3	1.778	0.111	linoleic acid

<sup>a</sup>Experimental  $m/z$  from single negatively charged molecular ion and Delta (ppm) from the Permeate RO sample.

oxygen between 4 and 7, suggesting that most of them are multifunctional with possibly sulfate or sulfonate groups.

**DOM Evolution through Desalination Line.** No effect on TOC (measured as NPOC) was found through the treatment line, except for permeate RO sample, where a huge decrease on TOC (98%) and conductivity (99%) has been observed (see SI Table S1). The decrease on the bulk of TOC alone, does not indicate whether individual compounds are partially or completely removed. However, some effect on DOM can be observed at molecular level during the treatment when high resolution mass spectrometry is used for the analysis.

Pretreatment is required to remove mineral, particulate, organic, and biological contaminants from seawater that negatively affect the performance of the RO membranes and which would otherwise accumulate onto the membrane surfaces. In the desalination pilot plant of the study, UF pretreatment was chosen in order to treat seawater to obtain high quality water to feed the RO pilot. In terms of membrane manufacturers, good quality water means having SDI value lower than 3%/min. This surrogate parameter is still widely used, however as stated by numerous researchers the SDI measurement has several limitations.<sup>31,32</sup>

Comparing the conventional parameters (SI Table S1) of RSW sample in front of UF sample can be observed that the SDI parameter and the enumeration of phytoplankton are the only ones changing considerably. Both parameters are more related to particulate content than to DOM, giving the idea that the UF has a great effect on the particulate fraction.

With HRMS, small changes at molecular level of the organic matter has been observed, however, there is not a huge change in bulk DOM composition as can be seen by this high-abundance cluster spanning  $0.2 < O/C < 0.5$  and  $1.0 < H/C < 1.75$ , as shown in Figure 3b and SI Figure S3b. The high degree of order of DOM in RSW can still be observed in UF sample, with several CH<sub>2</sub> series spanning along the mass range (Figure 4). Analysis of the DBE/C from the neutral chemical formula suggests, that the UF sample analyzed is also significantly saturated with an average H/C ratio 1.46, which translates to low DBE/C values, with a DBE/C<sub>av</sub> of 0.33 (DBE<sub>av</sub> of 5.8) (Table 1). In general, it can be concluded that there is no significant change regarding the nature of DOM at molecular nature, as observed analyzing the different characteristics of Table 1. In fact, most of the elemental formulas obtained in RSW are still present in the UF sample (see Figure 3b and SI

Figure S3b), the only difference is the relative intensity of some of them in the mass spectrum (see SI) and as can be seen in SI Figure S6 there is no cut off regarding the mass-to-charge ratio. The fact that, some elemental formulas from RSW are missing in the UF sample, is probably because they were present at very low intensity in RSW and the signal is lost. Few molecules remain with relative intensity higher than 10% and most of the molecules are found between 1 and 10% relative intensity in UF. It should be highlighted that the S-containing compounds tentatively identified as anthropogenic linear alkyl benzene sulfonates are still present in the UF effluent.

As expected, when the water is treated on the reverse osmosis an important change on the DOM has been observed. The recurring periodical patterns found in RSW and UF are lost, and the major signals in the Permeate RO spectrum correspond to compounds with less atoms of oxygen and more atoms of hydrogen. The DOM of RSW and UF samples have a more unsaturated character because most of the compounds present H/C ratio between 1 and 1.5, and in average H/C ratio 1.43 and 1.46, respectively. Likewise, major signals observed in the present study for Permeate RO sample present more aliphatic character with higher H/C ratio of an average ratio 1.72. Of course the transfer mechanisms through a RO membrane are very different from those occurring through a UF membrane<sup>27</sup> and there is a huge removal of dissolved compounds coming from the UF effluent to the permeate. As can be seen in Figure 3c and SI Figure S3c, the molecules that remain on the Permeate could be classified as *lipid-like* (SI Figure S4).<sup>20,33</sup> Some of the signals assigned have been tentatively identified as fatty acids and as described elsewhere,<sup>24,34</sup> they are found in many aquatic media (Table 2.). This high relative intensity of fatty acids on the Permeate can be explained due to the pH of the water when entering the reverse osmosis module (pH higher than the pK<sub>a</sub> of the fatty acids) and the negatively charged nature of the membranes used in the present plant. Other components present in the inlet reverse osmosis water (inorganic compounds, quelants....) can influence this factor.<sup>34</sup> Similar effect is observed with the anthropogenic linear alkyl benzene sulfonates. These anionic surfactants pass also through the membrane and it can be seen that they are still present in the van Krevelen diagram of Permeate RO sample. The anionic and polar character of these compounds could explain the fact that they go through the membranes to the Permeate.

As shown in Figure 5, there are remarkable differences on DBE-O distributions from UF effluent sample and Permeate

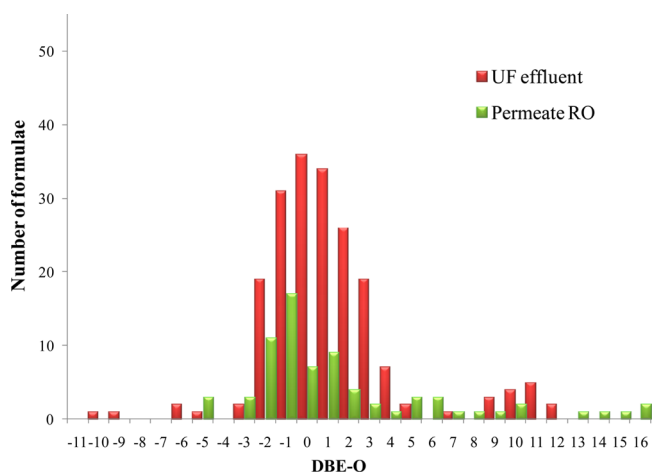


**Figure 5.** Number of formulas as a function of DBE-O value for UF effluent and permeate RO samples.

RO sample. The DBE-O distribution shift to more negative values for Permeate RO sample suggests that more highly saturated compounds pass through the membranes in the reverse osmosis. Moreover, if we have a look to the DBE-O distribution along the treatment plant (SI Figure S5), it can be observed that the Brine RO sample presents DBE-O values shifted to more positive (maximum at 1), compared to the RSW sample.

At molecular level, there are two changes well visible in the van Krevelen diagrams shown in Figure 3, when comparing the Permeate RO sample and the Brine RO sample: (1) the recurring DOM patterns from UF sample are present again in the Brine RO sample; (2) the *lipid-like* compounds are not present in the Brine RO sample. These differences are due to the effect of the membrane treatment on DOM and not due to concentration effect (Brine TOC 100 fold more concentrated, see SI Table S1). It has been corroborated by reanalyzing the Brine RO sample diluted by 100 (SI Figure S7).

Moreover, the relative intensity of the formulas in the Brine RO sample compared to UF is again higher, due to the fact that there is a concentration factor of 1.6–2.5 times, between the water inlet (UF effluent) at the RO module and the Brine.<sup>35,36</sup> This effect is especially important for compounds containing nitrogen. For instance, the relative intensity of the two series containing  $-\text{ON}_3\text{S}$  and  $-\text{O}_2\text{N}_3\text{S}$  in Brine is equivalent to the relative intensity of the same series in the RSW sample. In Brine, compounds containing CHON and CHONS present higher relative intensity (between 1 and 10%). With the exploration of the present data, it seems as compounds containing nitrogen and with less saturated structures (DBE: 7.2 and  $\text{DBE}/C_{\text{av}}: 0.39$ ) are not capable of going through the membrane and these compounds are rejected into the Brine. Further research should be carried out in this topic.

**Drinking Water Processing.** High-resolution and accurate mass measurements have been widely used to characterize natural organic matter of different environments (freshwater, seawater, pore water, groundwater, ice cores, soils, aerosols)<sup>22–24,33,37,38</sup> and also recently to have an overview of how DOM changed along a conventional water treatment line and after chlorination.<sup>3,4</sup> This study demonstrates that this

technique is also selective to evaluate the evolution of a desalination treatment, characterizing which effects have each step treatment in the DOM. To some extent, this study as well as some others completed before,<sup>3,4</sup> allow the water supply industry to employ more effective water treatment strategies. For instance, as huge removal of DOM is achieved by RO,<sup>36</sup> the permeate RO can be expected to be better quality drinking water, producing less DBPs compared to the coagulation effluent which was investigated by Zhang et al.<sup>3</sup> Complementary to conventional parameters, with this method, molecular behavior of the DOM along advanced treatments could be performed, giving information about how is each treatment working. These data sets provide a foundation for understanding the effect that desalination process has on DOM, with respect to molecular composition.

## ■ ASSOCIATED CONTENT

### 📄 Supporting Information

Additional figures and tables as noted in the text can be found. These include complementary analysis (Table S1); elemental formulas of some compounds identified (Table S2); SRFA and SRNOM mass spectra (Figure S1); van Krevelen diagrams (Figure S2, S3, S4, and S7) and other additional plots (Figure S5 and S6). Moreover, a spread sheet database in excel format include all the elemental formulas. This material is available free of charge via the Internet at <http://pubs.acs.org>.

## ■ AUTHOR INFORMATION

### ✉ Corresponding Author

\*Phone: +34 93 400 61 00; fax: +34 93 204 59 04; e-mail: [josep.caixach@idaea.csic.es](mailto:josep.caixach@idaea.csic.es).

### Notes

The authors declare no competing financial interest.

## ■ ACKNOWLEDGMENTS

We thank Dr. J.A. Allué from Araclon Biotech for MS technical support, Dra. A. Guastalli for her help during sampling and P.Eng H. Constenla to help developing excel macros for data treatment. This work has been partially financed within the framework of the project CENIT: Desarrollos Tecnológicos hacia el Ciclo Urbano del Agua Autosostenible (SOSTAQUA), CEN20071039. Part of this work was presented as an oral presentation in the Fourth IWA Specialty Conference on: Natural Organic Matter: From Source to Tap and Beyond (Costa Mesa, CA, July 2011). We are grateful to some suggestions and comments coming from the audience and the chairman, specially related to the graphics and representation of the data.

## ■ REFERENCES

- (1) Greenlee, L. F.; Lawler, D. F.; Freeman, B. D.; Marrot, B.; Moulin, P. Reverse osmosis desalination: Water sources, technology, and today's challenges. *Water Res.* **2009**, *43*, 2317–2348.
- (2) Herzsprung, P.; von Tümpling, W.; Hertkorn, N.; Harir, M.; Büttner, O.; Bravidor, J.; Friese, K.; Schmitt-Kopplin, P. Variations of DOM quality in inflows of a drinking water reservoir: Linking of van Krevelen diagrams with EEMF spectra by rank correlation. *Environ. Sci. Technol.* **2012**, *46* (10), 5511–5518.
- (3) Zhang, H.; Zhang, Y.; Shi, Q.; Ren, S.; Yu, J.; Ji, F.; Luo, W.; Yang, M. Characterization of low molecular weight dissolved natural organic matter along the treatment trait of a waterworks using Fourier transform ion cyclotron resonance mass spectrometry. *Water Res.* **2012**, *46* (16), 5197–5204.

- (4) Zhang, H.; Zhang, Y.; Shi, Q.; Hu, J.; Chu, M.; Yu, J.; Yang, M. Study on transformation of natural organic matter in source water during chlorination and its chlorinated products using ultrahigh resolution mass spectrometry. *Environ. Sci. Technol.* **2012**, *46* (8), 4396–4402.
- (5) Hua, G.; Reckhow, D. A. Characterization of disinfection byproduct precursors based on hydrophobicity and molecular size. *Environ. Sci. Technol.* **2007**, *41*, 3309–3315.
- (6) Richardson, S. D.; Plewa, M. J.; Wagner, E. D.; Schoeny, R.; DeMarini, D. M. Occurrence, genotoxicity, and carcinogenicity of regulated and emerging disinfection by-products in drinking water: A review and roadmap for research. *Mutat. Res.-Rev. Mutat. Res.* **2007**, *636*, 178–242.
- (7) Hertkorn, N.; Frommberger, M.; Witt, M.; Koch, B. P.; Schmitt-Kopplin, P.; Perdue, E. M. Natural organic matter and the event horizon of mass spectrometry. *Anal. Chem.* **2008**, *80* (23), 8908–8919.
- (8) Matilainen, A.; Gjessing, E. T.; Lahtinen, T.; Hed, L.; Bhatnagar, A.; Sillanpää, M. An overview of the methods used in the characterisation of natural organic matter (NOM) in relation to drinking water treatment. *Chemosphere* **2011**, *83* (11), 1431–1442.
- (9) <http://www.water-technology.net/projects/barcelonadesalinatio> (accessed May 2012).
- (10) Beckmann, M.; Parker, D.; Enot, D. P.; Duval, E.; Draper, J. High-throughput, nontargeted metabolite fingerprinting using nominal mass flow injection electrospray mass spectrometry. *Nat. Protocols* **2008**, *3* (3), 486–504.
- (11) D'Andrilli, J.; Dittmar, T.; Koch, B. P.; Purcell, J. M.; Marshall, A. G.; Cooper, W. T. Comprehensive characterization of marine dissolved organic matter by Fourier transform ion cyclotron resonance mass spectrometry with electrospray and atmospheric pressure photoionization. *Rapid Commun. Mass Spectrom.* **2010**, *24* (5), 643–650.
- (12) Stenson, A. C.; Marshall, A. G.; Cooper, W. T. Exact masses and chemical formulas of individual suwannee river fulvic acids from ultrahigh resolution electrospray ionization fourier transform ion cyclotron resonance mass spectra. *Anal. Chem.* **2003**, *75* (6), 1275–1284.
- (13) Cortés-Francisco, N.; Flores, C.; Moyano, E.; Caixach, J. Accurate mass measurements and ultrahigh-resolution: evaluation of different mass spectrometers for daily routine analysis of small molecules in negative electrospray ionization mode. *Anal. Bioanal. Chem.* **2011**, *400* (10), 3595–3606.
- (14) Blake, S.; Walker, S. H.; Muddiman, D.; Hinks, D.; Beck, K. Spectral accuracy and sulfur counting capabilities of the LTQ-FT-ICR and the LTQ-orbitrap XL for small molecule analysis. *Journal of The American Society for Mass Spectrometry* **2011**, *22* (12), 2269–2275.
- (15) Herzsprung, P.; Hertkorn, N.; Friese, K.; Schmitt-Kopplin, P. Photochemical degradation of natural organic sulfur compounds (CHOS) from iron-rich mine pit lake pore waters—An initial understanding from evaluation of single-elemental formulae using ultra-high-resolution mass spectrometry. *Rapid Commun. Mass Spectrom.* **2010**, *24* (19), 2909–2924.
- (16) Koch, B. P.; Dittmar, T.; Witt, M.; Kattner, G. Fundamentals of molecular formula assignment to ultrahigh resolution mass data of natural organic matter. *Anal. Chem.* **2007**, *79* (4), 1758–1763.
- (17) Kujawinski, E. B.; Behn, M. D. Automated analysis of electrospray ionization fourier transform ion cyclotron resonance mass spectra of natural organic matter. *Anal. Chem.* **2006**, *78* (13), 4363–4373.
- (18) Gonsior, M.; Peake, B. M.; Cooper, W. T.; Podgorski, D.; D'Andrilli, J.; Cooper, W. J. Photochemically induced changes in dissolved organic matter identified by ultrahigh resolution fourier transform ion cyclotron resonance mass spectrometry. *Environ. Sci. Technol.* **2009**, *43*, 698–703.
- (19) Tfaily, M. M.; Hamdan, R.; Corbett, J. E.; Chanton, J. P.; Glaser, P. H.; Cooper, W. T. Investigating dissolved organic matter decomposition in northern peatlands using complimentary analytical techniques. *Geochim. Cosmochim. Acta* **2013**, *112*, 116–129.
- (20) Kim, S.; Kramer, R. W.; Hatcher, P. G. Graphical method for analysis of ultrahigh-resolution broadband mass spectra of natural organic matter, the Van Krevelen diagram. *Anal. Chem.* **2003**, *75* (20), 5336–5344.
- (21) Reemtsma, T. The carbon versus mass diagram to visualize and exploit FTICR-MS data of natural organic matter. *J. Mass Spectrom.* **2009**, *45* (4), 382–390.
- (22) Koch, B. P.; Witt, M.; Engbrodt, R.; Dittmar, T.; Kattner, G. Molecular formulae of marine and terrigenous dissolved organic matter detected by electrospray ionization Fourier transform ion cyclotron resonance mass spectrometry. *Geochim. Cosmochim. Acta* **2005**, *69* (13), 3299–3308.
- (23) Gonsior, M.; Zwartjes, M.; Cooper, W. J.; Song, W.; Ishida, K. P.; Tseng, L. Y.; Jeung, M. K.; Rosso, D.; Hertkorn, N.; Schmitt-Kopplin, P. Molecular characterization of effluent organic matter identified by ultrahigh resolution mass spectrometry. *Water Res.* **2011**, *45* (9), 2943–2953.
- (24) Sleighter, R. L.; Hatcher, P. G. Molecular characterization of dissolved organic matter (DOM) along a river to ocean transect of the lower Chesapeake Bay by ultrahigh resolution electrospray ionization Fourier transform ion cyclotron resonance mass spectrometry. *Mar. Chem.* **2008**, *110*, 140–152.
- (25) Mazzoleni, L. R.; Ehrmann, B. M.; Shen, X.; Marshall, A. G.; Collett, J. L. Water-soluble atmospheric organic matter in fog: Exact masses and chemical formula identification by ultrahigh-resolution fourier transform ion cyclotron resonance mass spectrometry. *Environ. Sci. Technol.* **2010**, *44* (10), 3690–3697.
- (26) Chang, S. Hsu. Definition of hydrogen deficiency for hydrocarbons with functional groups. *Energy Fuels* **2010**, *24*, 4097–4098.
- (27) Leparç, J.; Rapenne, S.; Courties, C.; Lebaron, P.; Croué, J. P.; Jacquemet, V.; Turner, G. Water quality and performance evaluation at seawater reverse osmosis plants through the use of advanced analytical tools. *Desalination* **2007**, *203* (1–3), 243–255.
- (28) Doval, M. D.; Pérez, F. F.; Berdalet, E. Dissolved and particulate organic carbon and nitrogen in the Northwestern Mediterranean. *Deep Sea Res., Part I* **1999**, *46* (3), 511–527.
- (29) Aminot, A.; Kérouel, R. Dissolved organic carbon, nitrogen and phosphorus in the N-E Atlantic and the N-W Mediterranean with particular reference to non-refractory fractions and degradation. *Deep Sea Res., Part I* **2004**, *51* (12), 1975–1999.
- (30) Barco, M.; Planas, C.; Palacios, O.; Ventura, F.; Rivera, J.; Caixach, J. Simultaneous quantitative analysis of anionic, cationic, and nonionic surfactants in water by electrospray ionization mass spectrometry with flow injection analysis. *Anal. Chem.* **2003**, *75* (19), 5129–5136.
- (31) Karabelas, A. J. Critical assessment of fouling indices. MEDRC Report, Project #98-BS-034, 2003.
- (32) Boerlage, S. F. E.; Kennedy, M.; Tarawnwh, Z.; De Faber, R.; Schippers, J. C. Development of the MFI-UF in constant flux filtration. *Desalination* **2003**, *161*, 103–113.
- (33) Schmitt-Kopplin, P.; Gelencsér, A.; Dabek-Zlotorzynska, E.; Kiss, G.; Hertkorn, N.; Harir, M.; Hong, Y.; Gebefügi, I. Analysis of the unresolved organic fraction in atmospheric aerosols with ultrahigh-resolution mass spectrometry and nuclear magnetic resonance spectroscopy: Organosulfates as photochemical smog constituents. *Anal. Chem.* **2010**, *82* (19), 8017–8026.
- (34) Ang, W. S.; Elimelech, M. Fatty acid fouling of reverse osmosis membranes: Implications for wastewater reclamation. *Water Res.* **2008**, *42* (16), 4393–4403.
- (35) Taniguchi, Y.; Ohya, H.; Reverse osmosis process and system design. Membrane processes. In *Encyclopedia of Desalination and Water Resources*. <http://www.desware.net/Membrane-Processes.aspx>.
- (36) Koprivnjak, J. F.; Pfromm, P. H.; Ingall, E.; Vetter, T. A.; Schmitt-Kopplin, P.; Hertkorn, N.; Frommberger, M.; Knicker, H.; Perdue, E. M. Chemical and spectroscopic characterization of marine dissolved organic matter isolated using coupled reverse osmosis–electrodialysis. *Geochim. Cosmochim. Acta* **2009**, *73* (14), 4215–4231.

(37) Schmidt, F.; Elvert, M.; Koch, B. P.; Witt, M.; Hinrichs, K.-U. Molecular characterization of dissolved organic matter in pore water of continental shelf sediments. *Geochim. Cosmochim. Acta* **2009**, *73* (11), 3337–3358.

(38) Gonsior, M.; Peake, B. M.; Cooper, W. T.; Podgorski, D. C.; D'Andrilli, J.; Dittmar, T.; Cooper, W. J. Characterization of dissolved organic matter across the Subtropical Convergence off the South Island, New Zealand. *Mar. Chem.* **2011**, *123* (1–4), 99–110.



#### 4.2.2. Research Article Nº 4

Nuria Cortés-Francisco, Mourad Harir, Marianna Lucio, Gemma Ribera, Xavier Martinez-Lladó, Miquel Rovira, Philippe Schmitt-Kopplin, Norbert Hertkorn and Josep Caixach

High-field FT-ICR Mass Spectrometry and NMR Spectroscopy to Characterize DOM Removal through a Nanofiltration Pilot Plant.

*Water Research* **2014**, DOI: 10.1016/j.watres.2014.08.046.



# High-field FT-ICR mass spectrometry and NMR spectroscopy to characterize DOM removal through a nanofiltration pilot plant

Nuria Cortés-Francisco <sup>1\*</sup>, Mourad Harir <sup>2</sup>, Marianna Lucio <sup>2</sup>, Gemma Ribera <sup>3</sup>, Xavier Martínez-Lladó <sup>3</sup>, Miquel Rovira <sup>3</sup>, Philippe Schmitt-Kopplin <sup>2,4</sup>, Norbert Hertkorn <sup>2\*</sup> and Josep Caixach <sup>1</sup>

<sup>1</sup> Mass Spectrometry Laboratory / Organic Pollutants, IDAEA-CSIC; Jordi Girona 18-26, 08034 Barcelona, Spain. Tel: (+34) 93 400 61 00. Fax: (+34) 93 204 59 04.

<sup>2</sup> Helmholtz Zentrum Muenchen, German Research Center for Environmental Health, Research Unit Analytical Biogeochemistry (BGC), Ingolstaedter Landstrasse 1, D-85764 Neuherberg, Germany.

<sup>3</sup> Fundació CTM Centre Tecnològic; Plaça de la Ciència, 2, 08243 Manresa, Spain.

<sup>4</sup> Chair of Analytical Food Chemistry, Technische Universität München, Alte Akademie 10, 85354, Freising-Weihenstephan, Germany

E-mail addresses: [nuria.cortes@cid.csic.es](mailto:nuria.cortes@cid.csic.es) & [hertkorn@helmholtz-muenchen.de](mailto:hertkorn@helmholtz-muenchen.de)

## Abstract

Ultrahigh resolution Fourier transform ion cyclotron mass spectrometry and nuclear magnetic resonance spectroscopy were combined to evaluate the molecular changes of dissolved organic matter (DOM) through an ultrafiltration-nanofiltration (UF-NF) pilot plant, using two dissimilar NF membranes tested in parallel. The sampling was performed on seven key locations within the pilot plant: pretreated water, UF effluent, UF effluent after addition of reagents, permeate NF 1, permeate NF 2, brine NF 1 and brine NF 2, during two sampling campaigns. The study showed that there is no significant change in the nature of DOM at molecular level, when the water was treated with UF and / or with the addition of sodium metabisulfite and antiscaling agents. However, enormous decrease of DOM concentration was observed when the water was treated on the NF membranes.

The NF process preferentially removed compounds with higher oxygen and nitrogen content (more hydrophilic compounds), whereas molecules with longer pure aliphatic chains and less content of oxygen were the ones capable of passing through the membranes. Moreover, slight molecular selectivity between the two NF membranes was also observed.

**Keywords:** FT-ICR mass spectrometry, NMR spectroscopy, dissolved organic matter, nanofiltration, drinking water treatment plant, DBPs.

## 1. Introduction

Among others, a common goal for drinking water treatment plants (DWTP) is to remove natural organic matter (NOM) as it is a precursor for unwanted disinfection by-products (DBPs) during chemical disinfection processes, such as chlorination (Hua et al., 2007; Richardson et al., 2007). Moreover, NOM has been shown to contribute to the production of biologically unstable water and other unwanted water quality issues; such as color, taste and odor (Herzprung et al., 2012; Zhang et al., 2012a and 2012b) and to some extent, it can also affect the performance of water treatment processes (Lamsal et al., 2011). Accordingly, nanofiltration (NF) has been gradually implemented in DWTP as a result of its effectiveness in removing NOM and contaminants such as pharmaceuticals, heavy metals or pesticides (Ribera et al., 2014; Verliefde et al., 2009b; Ates et al., 2009; de la Rubia et al., 2008; Bellona et al., 2004), obtaining a high degree of water quality (Moons et al., 2006; Verliefde et al., 2007). Rejection of organic solutes by NF processes depends on feed water quality, operating conditions, module and system design as well as solute-membrane physicochemical interactions. In general, three major solute-membrane interactions are distinguished: steric exclusion (molecular size), charge interactions and solute-membrane affinity (hydrophobic attraction, hydrogen bonding, dielectric effects, etc.) (Braeken et al., 2005; Her et al., 2000; Verliefde et al. 2009a).

Knowledge of dissolved organic matter (DOM) behavior along different water treatment steps is of importance to improve and optimize the different treatments (Herzprung et al., 2012). To date, no studies have evaluated this evolution to understand the changes in DOM through a NF pilot plant from a molecular level; as in treatment plants, the characterization usually consists on bulk parameters (Matilainen et al., 2011). Molecular

level DOM composition and structure often exhibit far more variance than anticipated from bulk parameters, which are subjected to intrinsic averaging (Ritchie et al., 2008; Kelleher et al., 2006; Hertkorn et al., 2007). High resolution mass spectrometry (HRMS) is one of the techniques that has given more information of the molecular species, exact masses and molecular formulas of DOM (Matilainen et al., 2011). HRMS allows for an unprecedented resolution of thousands of molecular formulas from DOM mixture, however with considerable selectivity depending on sample handling and ionization method applied (Hertkorn et al., 2008; Stenson et al., 2003). Nuclear magnetic resonance (NMR) spectroscopy on the other hand evaluates atomic environments of DOM molecules, however at less sensitivity. For instance, one dimensional NMR spectra can provide reliable relationships between NMR chemical shift and extended substructures in a quantitative way, if carefully acquired (Hertkorn et al., 2013).

The aim of this study was to use ultrahigh resolution Fourier transform ion cyclotron mass spectrometry (FT-ICR MS) and high-field NMR spectroscopy to evaluate the changes of DOM through a NF pilot plant from a molecular level. Statistical analysis were applied to compare the data obtained by FT-ICR MS and NMR, bring out hidden correlations and see if there was any significant difference on DOM quality along the treatment.

## **2. Materials and methods**

### **2.1. Feed water type**

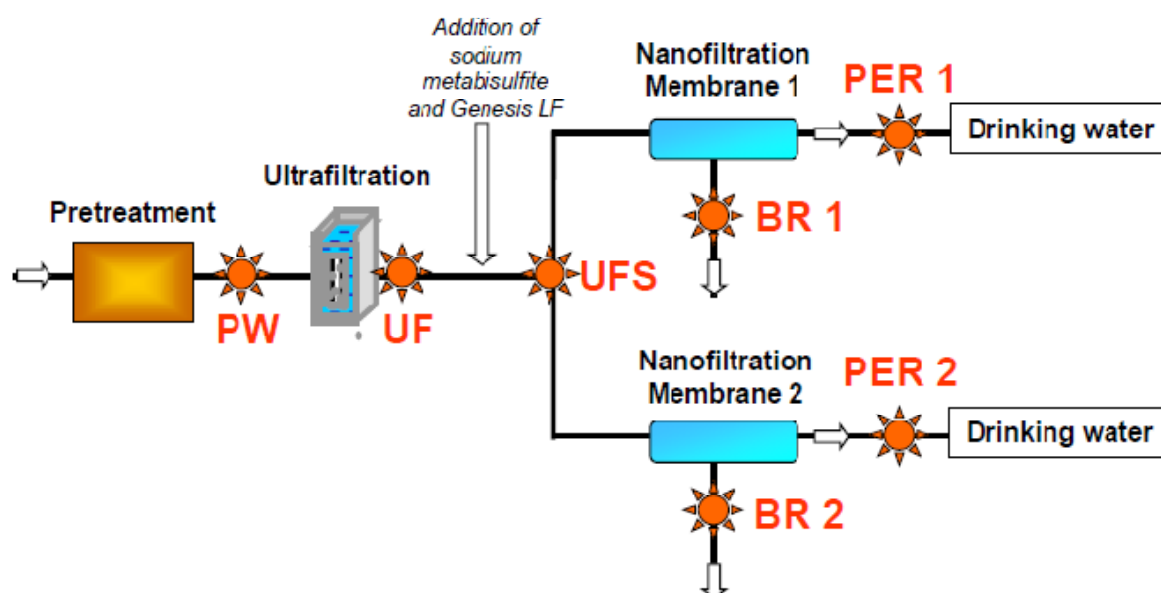
A small reservoir (Agulla's Lake; 0.2 Hm<sup>3</sup>) fed with superficial water from Llobregat River, provides a potable source water for the city of Manresa (Catalonia, Spain). This water is pre-disinfected in the drinking water treatment plant (DWTP) using chlorine and coagulated with aluminum polychloride, prior to sand filtration (pretreated water). To assure water quality, current installation has a final disinfection step based on a final chlorination to distribute biologically safe water to 70,000 inhabitants, approximately. In order to represent the behavior of a full-scale NF process, a pilot plant was fed with pretreated water (PW) from the output of the sand filtration stage, prior to final chlorination.

## 2.2. Pilot plant set-up and membranes used

A NF pilot plant, which includes a UF module as pretreatment, was designed and installed in the DWTP in order to study the filtration performance of two NF commercial membranes (Ribera et al., 2013; Ribera et al., 2014) and to study the evolution of DOM through a NF process.

The membranes of the study (ESNA1LF2-4040-membrane 1 and NF270-4040-membrane 2) were selected from the results of laboratory tests, because they had demonstrated high water permeability and beneficial partial inorganic salt rejection, as described elsewhere (Ribera et al., 2013). The schematic diagram of the experimental set-up for the NF pilot plant is shown in Figure 1. Further details about the pilot plant set-up can be found in Supplementary Information (SI). Also in SI, Table A1 provides the main suppliers specifications of UF and NF membranes used and Table A2 indicates some specific NF membrane properties obtained from previous studies.

**Figure 1.** Scheme of the pilot plant, showing the main treatment stages: ultrafiltration and nanofiltration (NF) membranes modules. The sampling locations are also shown in the picture: pretreated water (PW), ultrafiltration effluent (UF), ultrafiltration effluent after adding antiscalant (UFS), NF permeate 1 (PER1), NF permeate 2 (PER2), NF brine 1 (BR1) and NF brine 2 (BR2).



### 2.3. Sampling campaigns

Two sampling campaigns were carried out: June and October 2011. In that period from June to beginning of October feed water showed higher trihalomethane formation potential (THMFP) due to higher temperature, biological activity and DOM concentration, as it is expected in the warm period. That worse scenario was the one that was chosen to evaluate the membranes performance using FT-ICR MS and NMR spectroscopy.

The sampling was performed on seven key locations within the pilot treatment plant (Figure 1): PW, UF effluent, UF effluent after chemical products dosage (UFS), permeate NF 1 (PER1) and permeate NF 2 (PER2), brine NF 1 (BR1) and brine NF 2 (BR2). Samples were stored at 4 °C and extracted within 48 h.

### 2.4. DOM extraction

1.5 L from each sample was acidified with 10% hydrochloric acid (Merck, Darmstadt, Germany) to pH 2 and extracted with 2 x 100 mL of dichloromethane/isopropyl alcohol (90:10 v/v) (Merck, Darmstadt, Germany / Carlo Erba, Italy). The extracts were redissolved in methanol (Merck, Darmstadt, Germany) and they were concentrated down to 250 µL at 40 °C under nitrogen. Extended protocol details can be found in SI.

### 2.5. Fourier transform ion cyclotron mass spectrometry

Ultrahigh-resolution Fourier transform ion cyclotron (FT-ICR) mass spectra were acquired using a 12 T Bruker Solarix mass spectrometer (Bruker Daltonics, Bremen, Germany) and an electrospray ionization source in negative mode. The spectra were acquired with a time domain of 4 megawords and 500 scans were accumulated for each spectrum. Further details are described in SI.

Calculation of elemental formulas for each peak was done in a batch mode by an in-house written software tool. The generated formulas were validated by setting sensible chemical constraints [signal-to-noise (S/N)>4, N rule, O/C ratio  $\leq 1$ , H/C ratio  $\leq 2n + 2$  ( $C_nH_{2n+2}$ ), element counts: C  $\leq 100$ , H  $\leq 200$ , O  $\leq 80$ , N  $\leq 3$ , S  $\leq 2$  and mass accuracy window (set at  $\pm 500$ ppb)]. Final assigned formulas were generated and categorized using homemade

software into groups containing CHO, CHNO, CHOS or CHNOS type of molecules which were used to reconstruct the group-selective mass spectra (Schmitt-Kopplin et al., 2010). For each negative ion observed, the elemental formula reported is the corresponding neutral whose mass is the mass of the negative ion plus a proton (1.007276 Da). Furthermore, the given computed average values of H, C, N, O and S (atom %) and the H/C, O/C, C/N and C/S ratios as well as DBE, DBE/C and mass-to-charge ( $m/z$ ) ratio were based upon intensity-weighted averages of mass peaks with assigned molecular formulas (Table 1). It should be highlighted that the intensity depends on the ionization potential and different components may influence the ionization yield of each other (Hertkorn et al. 2008).

## 2.6. NMR analysis

All proton detected NMR spectra were acquired immediately after sample preparation with a Bruker Avance III NMR spectrometer operating at 800.13 MHz ( $B_0 = 18.8$  T) and TopSpin 3.0/PL3 software with samples from redissolved solids (1.2-6.2 mg solid DOM in typically 43-123  $\mu$ L methanol- $d_4$  (Table A3) in sealed 1.7 mm Bruker Match tubes. Further details are given in SI.

For data analysis of the NMR acquisitions, spectra were all normalized to identical areas of total integral from  $\delta_H \sim 0.5$ -9.5 ppm (excluding residual water, methanol and formic acid) and the spectra were divided into 0.001 ppm width buckets and exported using Amix version 3.9.4 (Bruker BioSpin, Rheinstetten, Germany).  $^1\text{H}$  NMR section integrals were defined in Table 2 based on key substructures from DOM (Hertkorn et al., 2006; Lam et al., 2007; Hertkorn et al., 2013).

## 2.7. Complementary analysis

Different complementary analyses were carried out regularly during the six months of operation of the plant, as well as for the samples of the present study (see Table A4, Table A5 and Table A6). These analyses included: inorganic composition, pH, conductivity, ultraviolet light adsorption (UVA), silt density index (SDI), non-purgable organic carbon (NPOC), THMFP, regulated trihalomethanes (THMs), total inorganic carbon (TIC), total nitrogen (TN).

Moreover, for the screening of unregulated DBPs, 1 L of the samples: UF effluent, Permeate NF 1 and Permeate NF 2 (from June and October 2011) were chlorinated off-line. Each sample after chlorination were extracted by closed-loop stripping analysis and analyzed by gas chromatography coupled to mass spectrometry.

All these analysis were carried out as described in SI.

## **2.8. Statistical analysis**

Due to the fact that analyzing samples using FT-ICR MS and NMR spectroscopy deal with huge amounts of data, we applied different multivariate statistical analysis (principal component analysis - PCA, hierarchical clustering - HCA, orthogonal partial least squares - OPLS/O2PLS-DA) to compare the results with any significant difference on DOM along the treatment (Sleighter et al., 2010). Expanded description of the statistical analysis is included in SI.

## **3. Results and Discussion**

### **3.1. DOM in source water**

#### **3.1.1. Seasonal variation**

It is known that DOM composition in water can be affected as a result of seasonal variations (Stedmon et al., 2006; Jaffé et al., 2008; Her et al., 2000; Herzprung et al., 2012; Zhang et al., 2014), such as warm and drought periods, insulation time on water reservoirs or water consumption. The period here compressed (June to beginning of October 2011) presented similar climate conditions, and no major difference were found between samples. For instance, inorganic solutes were considered practically invariant during the experimental period; and some bulk parameters such as UVA, NPOC and conductivity were not significantly different during the sampling periods. Moreover, no differences on DOM composition could be observed in the mass spectra of PW for the two sampling campaigns. Barely any difference between the two different samples could be found when assigned elemental compositions were compared. More than 85% (October) and 91% (June) of the assigned elemental compositions were common in both PW samples. The small amount of non-common signals generally presented very low

intensity, close to S/N threshold. Last but not least, structural information obtained from  $^1\text{H-NMR}$  spectra also showed no major difference between the two sampling campaigns.

Moreover, we confirmed with OPLS/O2PLS-DA score scatter plot (data not shown) and HCA (Figure A1) that the samples presented no evidence of a possible significant distinction between the two sampling periods, being very close each other in terms of DOM composition. So here on, the samples will be described together, only highlighting differences with regard to the different treatment steps (UF and NF).

### 3.1.2. Pretreated water

Superficial water from Llobregat River after pretreatment (predisinfection, coagulation and sand filtration) was feeding the NF pilot plant of the study (the so called PW). The reconstructed mass spectra of the PW samples (Figure A2) show several thousand peaks between  $m/z$  150–800. Expanded mass spectra at the nominal mass  $m/z$  361 is shown as an example in Figure A3, showing typical mass spacing patterns, that have been described before for aquatic DOM (Stenson et al., 2003; Sleighter et al., 2008; Hertkorn et al., 2008; Schmidt et al., 2009). These regular patterns are also clearly identified in the van Krevelen plots of PW samples, taking into account the different composition of the elemental formulas assigned (Figure 2 and Figure A4). With more than 4000 assigned mass peaks, the CHO compounds are the major component of the fraction of DOM analyzed (58% of assigned formulas) and present the higher relative intensity in the spectrum (see Table 1, Figure 2, Figure A4 and Figure A5). The numbers of CHNO compounds represent almost 30% and the CHOS compounds range around 11-13%. Compounds containing nitrogen are significant here, regarding the level of nitrogen in the PW (see in SI Table A6.). However, these molecules present lower intensity than CHO or CHOS compounds, as the ionization of compounds containing nitrogen in negative electrospray mode it is known to be less efficient compared with compounds containing sulfonated groups and/or negatively charged groups like fatty acids (D'Andrilli et al., 2010; Sleighter et al., 2008). Thus, it is known that aquatic DOM may be multifunctional with a combination of hydroxyl, carbonyl, carboxyl, ester, nitrate, amines, amides, N-heterocycles and sulfate functional groups (Stenson et al., 2003; Sleighter et al., 2008; Hertkorn et al., 2008; Schmidt et al., 2009), and moreover freshwater DOM, which is currently described as plant-derived products such as lipids, carbohydrates, carboxyl-rich

alicyclic materials (CRAM) and other terpene derivatives, aromatic condensed structures and lignin-derived compound (Nebbioso et al., 2013). Further FT-ICR MS data analysis showed that the PW samples analyzed presented higher H/C ratios (1.36 -1.38), when compared to previous studies (Kim et al., 2004; Sleighter et al., 2008; Schmidt et al., 2009; Minor et al., 2012), which translates to lower DBE/ $C_{av}$  values of 0.37-0.36 (DBE<sub>av</sub>: 7.8-7.6).

Regarding the structural information obtained from  $^1\text{H}$  NMR spectra, the PW samples (Figure A6) showed smooth bulk envelopes, reflecting intrinsic averaging from massive signal overlap, typical from DOM of other environments (Hertkorn et al., 2006; Lam et al., 2007; Hertkorn et al., 2013). In Figure A6, the spectra have been normalized to 100% intensity for the polymethylene group ( $\delta_{\text{H}} \sim 1.28$  ppm). Moreover, spectra were all normalized to identical areas of total integral from  $\delta_{\text{H}} \sim 0.5$ -9.5 ppm (excluding residual water, methanol and formic acid) (see NMR section integrals in Table 2) showing the fundamental substructures from higher to lower field (from right to left): pure aliphatic  $\delta_{\text{H}} \sim 0.5$ -1.25 ppm,  $\underline{\text{H}}_3\text{C-C-C}$ ; polymethylene group  $\delta_{\text{H}} \sim 1.25$ -1.35 ppm,  $(\underline{\text{C}}\underline{\text{H}}_2)_n$ ; functionalized aliphatics  $\delta_{\text{H}} \sim 1.35$ -1.9 ppm,  $\underline{\text{H}}\text{-C-C-CO}$ ; “acetate-analogue” and CRAM  $\delta_{\text{H}} \sim 1.9$ -3.1 ppm,  $\underline{\text{H}}\text{-C-C-O}$ ; “carbohydrate-like” and methoxy  $\delta_{\text{H}} \sim 3.1$ -4.9 ppm,  $\underline{\text{H}}\text{CO}$ ; olefins  $\delta_{\text{H}} \sim 5.3$ -7.0 ppm  $\underline{\text{H}}\text{C}=\text{C}$ ,  $\underline{\text{H}}\text{CO}_2$ ; and aromatic  $\delta_{\text{H}} \sim 7.0$ -9.5 ppm,  $\underline{\text{H}}_{\text{ar}}$  NMR resonances.

The total aliphatic section ( $\delta_{\text{H}} \sim 0.5$ -1.9 ppm) is the most predominant in PW, with more than 60%, followed by the section for “acetate-analogue” and CRAM ( $\delta_{\text{H}} \sim 1.9$ -3.1 ppm) and “carbohydrate-like” and methoxy ( $\delta_{\text{H}} \sim 3.1$ -4.9 ppm). Compared to previous studies, considering freshwater and marine DOM (Hertkorn et al., 2006; Lam et al., 2007; Hertkorn et al., 2013), the freshwater of the study presents an important aliphatic signature. For instance, in Lam et al. (Lam et al., 2007), sections involving oxygen atoms (carbohydrate and CRAM) accounted for almost 79% of the proton signals, showing similarities with marine DOM from Hertkorn et al. (Hertkorn et al., 2006). Moreover, olefins ( $\delta_{\text{H}} \sim 5.3$ -7.0 ppm) and aromatics ( $\delta_{\text{H}} \sim 7.0$ -9.5 ppm) represent less than 5% of the total proton signals. These observations are in accordance with UVA values obtained from PW. The UVA values are low, so aromatic compounds are less representative than aliphatic compounds (Ates et al., 2009).

These higher H/C ratios (lower DBE/ $C_{av}$ ) and the fact that the aliphatic section is the most predominant in the PW of the study, could be explained due to the fact that the freshwater

has gone through pretreatment (predisinfection, coagulation and sand filtration). As Zhang et al. pointed out, oxygenated compounds (high O/C ratios) are preferentially removed by coagulation (Zhang et al., 2012a).

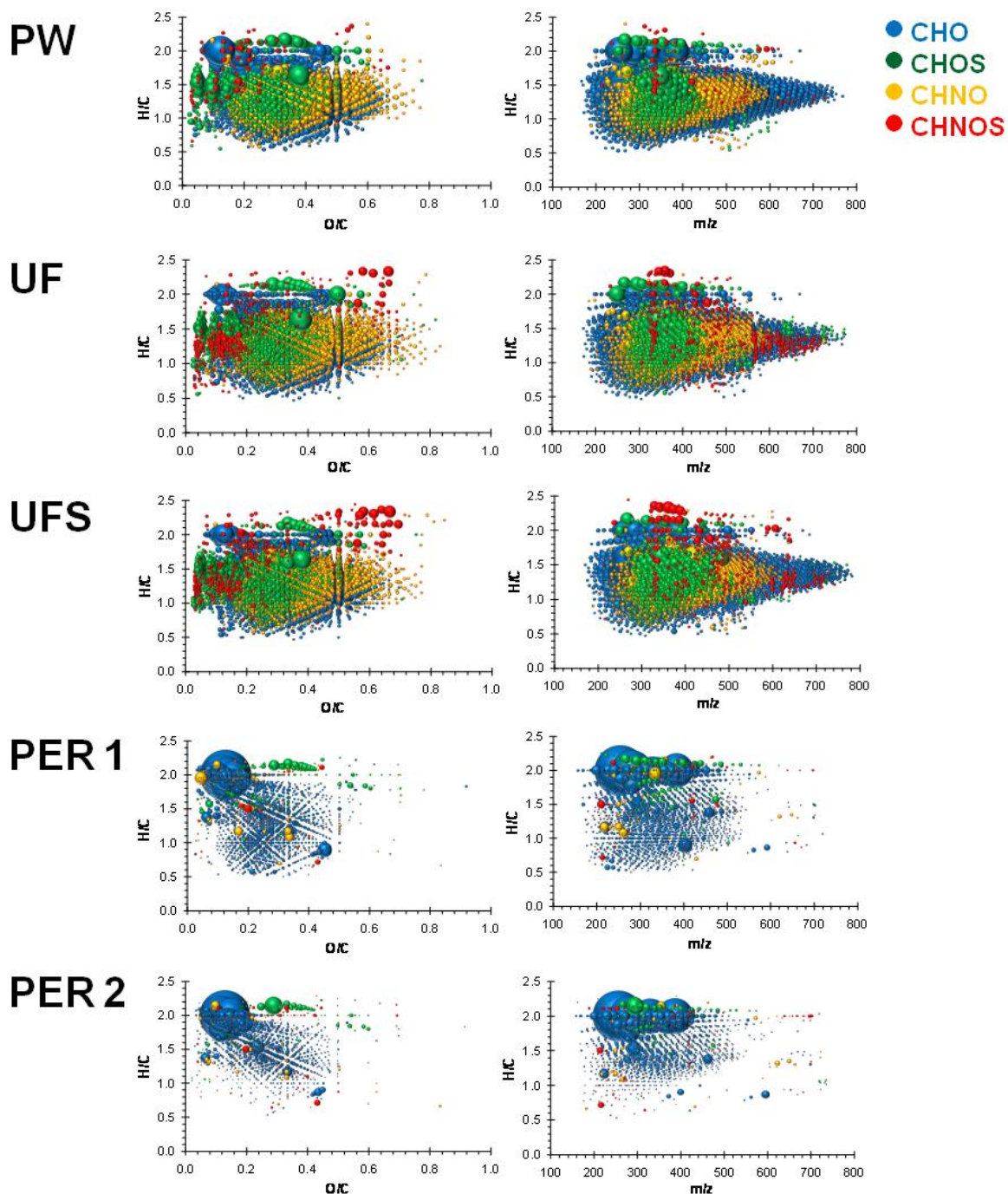


**Figure 2.** (Left) Van Krevelen diagrams for all formulas assigned of the June samples (see Figure A4 for October): pretreated water (PW), ultrafiltration effluent (UF), ultrafiltration effluent after adding antiscalant (UFS), NF permeate 1 (PER1), NF permeate 2 (PER2), on color-coded composition: CHO (blue), CHOS (green), CHNO (orange), CHNOS (red). (Right) H/C ratio vs mass-to-charge ( $m/z$ ) plot for all formulas assigned of the samples: PW, UF, UFS, PER1, PER2; with the same color-coded composition. Circular areas indicate relative mass peak intensity.

### 3.2. DOM evolution through treatment line

No effect on TOC (measured as NPOC) was found through the treatment line, except for permeate NF samples, where a decrease on TOC (between 91 and 97 %) and conductivity (between 53 and 84%) was observed (see SI Table A6). The decrease on the bulk of TOC alone, does not indicate whether individual organic compounds are partially or completely removed. However, some effect on DOM can be observed at molecular level during the treatment when ultrahigh resolution FT-ICR MS and NMR spectroscopy are used.

#### 3.2.1. UF and scaling inhibitor

Due to the high SDI observed in the feed water an UF step was added to improve the quality of NF feed water. Moreover, metabisulfite and antiscalant (Genesys LF) addition was required to remove free chlorine and to avoid inorganic and colloidal scaling.

With FT-ICR MS, almost no changes at molecular level of the organic matter were observed. In Figure A2 and Figure A7a and b, it is shown that the majority of signals from PW are present in the mass spectra of UF and UFS samples. As a consequence, the high degree of order of DOM in PW can still be observed in UF and UFS samples, as can be seen by the high-abundance cluster spanning  $0.2 < O/C < 0.5$  and  $1.0 < H/C < 1.75$ , as shown in Figure 2 and Figure A4. Around 50% of the formulas assigned for the UF and UFS samples corresponded to compounds containing CHO, whereas the CHNO compounds represent around 30% and the CHOS are almost 15% (see Table 1). Analysis of the DBE/C from the neutral chemical formula suggests, that the UF and UFS samples analyzed have also significant high  $H/C_{av}$  ratio between 1.34 and 1.38, which translates to  $DBE/C_{av}$  between 0.36 and 0.38 ( $DBE_{av}$  between 7.6 and 8.2) (Table 1). In fact, more than 85% of the elemental formulas obtained in PW are still present in the UF and UFS samples and as can be seen in Figure 2 and Figure A4, there is no cut off regarding the  $m/z$ . These results can be confirmed when observing the NMR section integrals in Table 2 (Figure A8). As observed with the PW samples, the total aliphatic section ( $\delta_H \sim 0.5$ -1.9 ppm) is the most predominant in UF and UFS samples, with more than 60%, followed by the CRAM section ( $\delta_H \sim 1.9$ -3.1 ppm) and "carbohydrate-like" and methoxy ( $\delta_H \sim 3.1$ -4.9 ppm).

The conclusions from the detailed observation of FT-ICR mass spectra and  $^1\text{H}$  NMR spectra already obtained, have been confirmed when applying statistical analysis. It is shown in Figure A1, that there are no significant differences between the PW samples and the UF and UFS samples. Indeed, the two dendrograms (Ward distance) disclose high similarities between PW, UF, UFS and moreover BR. They both yield only two clusters: the first containing the permeate samples (PER1 and PER2) and the second one containing the rest of the samples (PW, UF, UFS and BR).

These observations are in accordance with some previous studies, where they have evaluated the performance of UF processes (Verliefde et al., 2009a; Cortés-Francisco et al., 2013). UF pretreatment is affecting rather the particulate as can be seen with the decrease of SDI parameter. Moreover, antiscalants directly have no effect on DOM, although they can control calcium and magnesium salts from precipitation and their concentration in water can affect the organic matter rejection or fouling process on the membranes (Her et al., 2000; Nghiem et al., 2008).

**Table 1.** Counts of mass peaks as computed from negative electrospray 12T FT-ICR mass spectra for singly charged ions with nitrogen rule check and 500 ppb tolerance.

Members of molecular series	Pretreated Water		UF effluent		UF effluent + antiscaling		Permeate NF 1		Permeate NF 2		Brine NF 1		Brine NF 2	
	June	Oct	June	Oct	June	Oct	June	Oct	June	Oct	June	Oct	June	Oct
CHO compounds	2452 (58%)	2623 (58%)	2421 (47%)	2413 (57%)	2605 (50%)	2572 (56%)	1499 (83%)	1314 (77%)	1057 (78%)	1204 (78%)	2461 (52%)	2674 (57%)	2461 (57%)	1411 (44%)
CHOS compounds	452 (11%)	602 (13%)	702 (14%)	526 (13%)	777 (15%)	686 (15%)	143 (8%)	124 (7%)	97 (7%)	115 (7%)	821 (17%)	690 (15%)	496 (11%)	794 (25%)
CHNO compounds	1243 (29%)	1226 (27%)	1691 (33%)	1199 (29%)	1542 (29%)	1208 (26%)	125 (7%)	209 (12%)	135 (10%)	197 (13%)	1314 (28%)	1194 (26%)	1253 (29%)	879 (28%)
CHNOS compounds	84 (2%)	79 (2%)	318 (6%)	54 (1%)	316 (6%)	131 (3%)	38 (2%)	53 (4%)	61 (5%)	26 (2%)	131 (3%)	90 (2%)	119 (3%)	109 (3%)
Number of assigned mass peaks	4231 (20%)	4530 (20%)	5132 (19%)	4192 (19%)	5240 (20%)	4597 (23%)	1805 (13%)	1700 (12%)	1350 (11%)	1542 (11%)	4727 (21%)	4648 (21%)	4329 (20%)	3193 (16%)
total number of mass peaks	22104	22765	26632	22089	26701	20236	13661	14255	12833	13533	22845	22089	22097	20435
average H [%]	7.38	7.58	7.24	7.52	7.32	7.45	10.2	10.4	10.9	10.2	7.23	7.28	7.22	7.30
average C [%]	65.2	66.1	64.9	65.8	65.5	65.6	71.5	70.1	71.8	70.5	64.5	65.1	64.8	65.2
average O [%]	26.6	25.5	26.7	25.8	26.1	26.0	17.1	18.3	16.1	18.0	27.1	26.7	27.1	24.7
average N [%]	0.36	0.30	0.53	0.35	0.45	0.30	0.36	0.37	0.32	0.29	0.38	0.28	0.36	0.47

Members of molecular series	Pretreated Water		UF effluent		UF effluent + antiscaling		Permeate NF 1		Permeate NF 2		Brine NF 1		Brine NF 2	
	June	Oct	June	Oct	June	Oct	June	Oct	June	Oct	June	Oct	June	Oct
average S [%]	0.45	0.52	0.63	0.52	0.64	0.65	0.83	0.83	0.78	1.06	0.75	0.59	0.49	0.92
computed H/C ratio from FTICR mass peaks	1.36	1.38	1.34	1.37	1.34	1.36	1.70	1.78	1.84	1.73	1.35	1.34	1.34	1.34
computed O/C ratio from FTICR mass peaks	0.31	0.29	0.31	0.29	0.30	0.30	0.18	0.20	0.17	0.19	0.32	0.31	0.31	0.30
computed C/N ratio from FTICR mass peaks	16.2	16.5	14.7	16.4	14.6	16.7	10.9	12.9	11.4	13.4	15.6	16.6	15.7	14.2
computed C/S ratio from FTICR mass peaks	14.2	14.6	16.4	14.6	16.2	15.1	14.5	14.8	13.2	14.5	14.5	14.5	14.7	17.9
Average DBE, intensity weighted	7.8	7.6	8.0	7.6	8.2	7.7	3.9	3.2	2.6	3.6	7.9	7.9	8.0	7.8
Average DBE/C, intensity weighted	0.37	0.36	0.38	0.37	0.38	0.37	0.21	0.17	0.14	0.19	0.38	0.38	0.38	0.38
Average mass, intensity weighted	384.5	378.4	387.2	377.3	393.8	381.8	327.2	325.4	325.5	322.8	386.0	385.9	386.8	378.0

**Table 2.**  $^1\text{H}$  NMR section integrals (percent of non-exchangeable protons) and key substructures from DOM samples (exclusion of residual water, methanol and formic acid).

$\delta(^1\text{H})$ [ppm]		9.5 - 7.0	7.0 - 5.3	4.9 - 3.1	3.1 - 1.9	1.9 - 1.35	1.35-1.25	1.25-0.5	Sum 1.9-0.5	$\text{H}_{\text{olefinic}} / \text{H}_{\text{aromatic}}$	$\text{H}_3\text{C} / (\text{CH}_2)_n$
Key substructures		$\underline{\text{H}}_{\text{ar}}$	$\underline{\text{H}}\text{C}=\text{C}, \underline{\text{H}}\text{CO}_2$	$\underline{\text{H}}\text{CO}$	$\underline{\text{H}}\text{-C-C-O}$	$\underline{\text{H}}\text{-C-C-C-O}$	$(\underline{\text{C}}\text{H}_2)_n$	$\underline{\text{H}}_3\text{C-C-C}$			
<b>Pretreated Water</b>	June	2.3	1.5	9.3	22.8	23.6	15.3	25.2	64.0	0.7	1.7
	Oct	2.1	1.5	9.9	24.2	23.6	15.5	23.4	62.4	0.7	1.5
<b>UF effluent</b>	June	2.8	1.3	7.2	20.5	23.6	15.3	29.3	68.3	0.5	1.9
	Oct	2.7	1.3	8.7	21.6	23.7	12.3	29.8	65.8	0.5	2.4
<b>UF effluent + antiscaling</b>	June	3.1	1.1	13.6	17.8	20.4	19.5	24.5	64.4	0.4	1.3
	Oct	2.4	1.2	7.4	21.1	24.0	14.8	29.1	67.9	0.5	2.0
<b>Permeate NF 1</b>	June	4.7	3.3	10.1	9.4	17.7	36.9	18.0	72.6	0.7	0.5
	Oct	2.4	1.5	7.5	8.0	17.8	48.0	15.0	80.7	0.6	0.3
<b>Permeate NF 2</b>	June	4.2	3.0	9.8	8.7	17.5	39.1	17.8	74.4	0.7	0.5
	Oct	3.6	1.7	10.6	9.4	18.3	35.0	21.4	74.7	0.5	0.6
<b>Brine NF 1</b>	June	1.8	1.5	10.7	26.1	24.7	10.9	24.3	59.9	0.8	2.2
	Oct	2.2	2.2	7.1	25.6	25.6	9.2	28.1	62.9	1.0	3.1

$\delta(^1\text{H})$ [ppm]		9.5 - 7.0	7.0 - 5.3	4.9 - 3.1	3.1 - 1.9	1.9 - 1.35	1.35-1.25	1.25-0.5	Sum 1.9-0.5	$H_{\text{olefinic}} / H_{\text{aromatic}}$	$\underline{\text{H}}_3\text{C} / (\underline{\text{C}}\underline{\text{H}}_2)_n$
Key substructures		$\underline{\text{H}}_{\text{ar}}$	$\underline{\text{H}}\text{C}=\text{C}, \underline{\text{H}}\text{CO}_2$	$\underline{\text{H}}\text{CO}$	$\underline{\text{H}}\text{-C-C-O}$	$\underline{\text{H}}\text{-C-C-C-O}$	$(\underline{\text{C}}\underline{\text{H}}_2)_n$	$\underline{\text{H}}_3\text{C-C-C}$			
<b>Brine NF 2</b>	June	1.9	1.1	8.4	22.5	23.4	13.5	29.2	66.2	0.6	2.2
	Oct	2.2	1.8	7.8	25.9	25.4	9.4	27.6	62.4	0.8	2.9

### 3.2.2. Nanofiltration membranes

Water treatment by the NF membranes showed a large effect on DOM that could already be observed from the analysis of bulk parameters. In a previous study, it was shown that the low molecular weight fraction of DOM is permeable in both membranes studied, resulting in a residual THMFP in the permeate water. Moreover, as similar NPOC values and THMPF were obtained, the performances of the two membranes had to be very similar with regard to DOM rejection (Ribera et al., 2013). However, adding structural and molecular information to the conclusions already raised from NPOC and UVA analysis, would help to design better strategies to improve and/or ideally completely remove DOM.

With FT-ICR MS, a huge attenuation of DOM is observed when the water is treated on the NF membranes and few signals can be observed in the mass spectra (Figure A2 and Figure A7c and d). The main group of signals in Permeate samples correspond to compounds with less atoms of oxygen and more atoms of hydrogen. This is also shown in Figure 2 and Figure A4 where most of the signals missing in the van Krevelen plot, when comparing UFS samples to Permeate samples, are between  $0.1 < O/C < 0.8$  and  $0.5 < H/C < 1.75$  ratios. It can be also observed in Table 1 how the percentage of hydrogen is increased from something around 7 % (for UFS samples) to 10 % (for Permeate samples), whereas the percentage of oxygen is reduced from something around 26 % (for the UFS samples) to 16-18 % (for Permeate samples). As a consequence, the Permeate samples present lower  $DBE_{av}$  and  $DBE/C_{av}$  values.

Apart from the important decrease of compounds containing oxygen, also compounds containing nitrogen are drastically removed by NF. Whereas in the UFS samples feeding the NF membranes, the CHNO compounds represent around the 30% of the assigned formulas, in the Permeate samples these compounds represent only around the 10%. It can be concluded that compounds more functionalized with higher content of oxygen and other heteroatoms such as nitrogen, are preferably removed by NF membranes. This effect has been also observed before with different water treatments: in the study from Zhang et al., after coagulation (Zhang et al., 2012a) or in a previous study with reverse osmosis membranes (Cortés-Francisco et al., 2013).

Further analysis of the FT-ICR MS data showed that in the Permeate samples a decrease of average mass had occurred due to NF process, going from  $m/z$  384.5 and 378.4 (June

and October, respectively) to somewhat higher than  $m/z$  320 Da (see Table 1). Moreover, when observing the H/C vs  $m/z$  plot (Figure 2 and Figure A4), it can be seen that almost all molecules with  $m/z$  higher than 500 are gone after NF. However, this cut-off of the NF membranes with regard to  $m/z$ , does not relate only to molecular size (meaning that all kind of small molecules can pass through the membranes, whereas larger molecules cannot). As observed before, the molecules containing more oxygen and nitrogen cannot go through the membranes and as a consequence the decrease of  $m/z$  is mostly due to depletion of number of oxygen (and nitrogen) atoms. This leads to the conclusion, that different mechanisms of solute transport in NF membranes may play a role here. As mentioned above, three major solute-membrane interactions are distinguished: steric exclusion (size exclusion-molecular size), charge interactions and solute-membrane affinity (Braeken et al., 2005; Her et al., 2000; Verliefe et al. 2009a). Molecular size understood as molecular weight (Braeken et al., 2005; Verliefe et al., 2007) does not explain alone the behavior of DOM through the NF process. As the NF membranes of the study present nominal molecular weight cut off between 175 and 270 (see Table A2), one would have expected that higher molecular compounds ( $> 300$  Da) have been drastically removed. However, compounds with less content of oxygen and nitrogen can pass through the membranes, even with molecular weights higher than 400 Da. While compounds with more oxygen and nitrogen content and so more polar are well rejected by the NF membranes, compounds described as more hydrophobic present more affinity for the membranes, and so are found in the Permeate samples (PER1 and PER2). Moreover, polar compounds might have a hydration shell and so by this effect these molecules may have a larger molecular size, making more effective their removal. With the data shown here, it can be concluded that hydrophobic interactions influence the rejection of DOM by NF processes.

These results can be confirmed when observing the NMR section integrals in Table 2 (see also Figure A9). The integrals from sections involving oxygen atoms ( $\delta_H \sim 1.9-3.1$  ppm for CRAM and  $\delta_H \sim 1.35-1.9$  ppm for functionalized aliphatics) are much lower for the Permeate samples, declined in some cases by more than 50%. On the contrary, the polymethylene section ( $\delta_H \sim 1.25-1.35$  ppm) is increased in Permeate samples and the pure aliphatic section ( $\delta_H \sim 0.9-1.25$  ppm) is slightly decreased. As a consequence, the  $H_3C/(CH_2)_n$  ratio for the four Permeate samples is significantly attenuated in comparison to the water feeding the NF modules (UFS samples). If the discrimination in the NF

membranes would be only due to molecular size, then the  $H_3C/(CH_2)_n$  ratio should have been higher in the Permeate samples. It can be concluded that NF process preferentially removed compounds with higher oxygen and nitrogen content (more hydrophilic compounds), whereas molecules with longer pure aliphatic chains and less content of oxygen are the ones capable of going through the membranes.

With HCA analysis (Figure A1), we infer that in both data sets (FT-ICR MS and NMR data) there are two main groups (Permeate vs PW, UF, UFS and BR), distinguished also in the PCA scores scatter plot (data not shown). In FT-ICR MS, they have been investigated through a multivariate classification model in order to describe the separation. Once we found a valid model for the classification, we studied which are the main characteristic of each group. For this purpose, we built up an OPLS/O2PLS-DA model, in which X matrix contains all the  $m/z$  variables and Y the class. This is a powerful method able to separate the predictive variation (what in the X is related to Y) from the orthogonal variation (what in X is uncorrelated to Y). Once checked the robustness of the model ( $R^2Y(\text{cum})=0.98$ ,  $Q^2(\text{cum})=0.93$  with  $p=3.57e^{-5}$ , applying Anova on the Cross validated predictive residuals) we examined the S-Plot (Figure 3). It provides information of the main factors responsible for the differences among the samples. The extreme right part is related more with the Permeate samples (PER 1 and PER 2), whereas the left one with PW, UF, UFS and BR. The most significant elemental formulas of each group are visualized in the van Krevelen diagrams as well as H/C ratio vs  $m/z$  plots (Figure 3). The most representative elemental formulas in Permeate samples can be classified as "lipids-like": these compounds present very low content of oxygen and high content of hydrogen (van Krevelen region  $0.05 < O/C < 0.2$  and  $1.5 < H/C < 2.25$ ).

The multiblock PCA analysis (Xu et al., 2012) has been applied to NMR data. The different blocks stand for the most significant integrals regions (and so key substructures). It underlines the relation between the most significant integrals regions and sample classes (Permeate vs PW, UF, UFS and BR). For instance, it can be seen in Figure 4 and Table 3 that the polymethylene section ( $\delta_H \sim 1.25-1.35$  ppm) is defined with 5 components (t). The first component ( $(CH_2)_n$ , t1) already explains 0.94 variance for the Permeate samples. However, the sections involving oxygen atoms ( $\delta_H \sim 1.9-3.1$  ppm for CRAM and  $\delta_H \sim 1.35-1.9$  ppm for functionalized aliphatics) are explained by 0.93 and 0.85 variance for the rest of the samples (RW, UF, UFS and BR) (Figure 4 and Table 3). It confirms that

substructures such as CRAM and functionalized aliphatics are more significant in the RW,UF,UFS and BR, whereas the polymethylene groups are more significant in the Permeate samples.

**Figure 3.**a) S-Plot obtained from FT-ICR MS data analysis using OPLS/O2PLS-DA model. It provides information of the main  $m/z$  responsible for the differences among the two group of samples. The extreme right part is related more with the permeate NF samples (deep-red dots), whereas the left one is more related with PW, UF, UFS and BR (grey dots). The elemental formulas of the most related masses for each group are visualized in the van Krevelen diagrams and the H/C ratio vs  $m/z$  plots: b)  $m/z$  more significant in Permeate Samples and c)  $m/z$  more significant in PW, UF, UFS and BR samples. Circular areas indicate relative mass peak intensity, obtained from the average mass peak intensity considering for b) the four Permeate samples together and for c) the rest of the samples (PW, UF, UFS and BR for June and October).

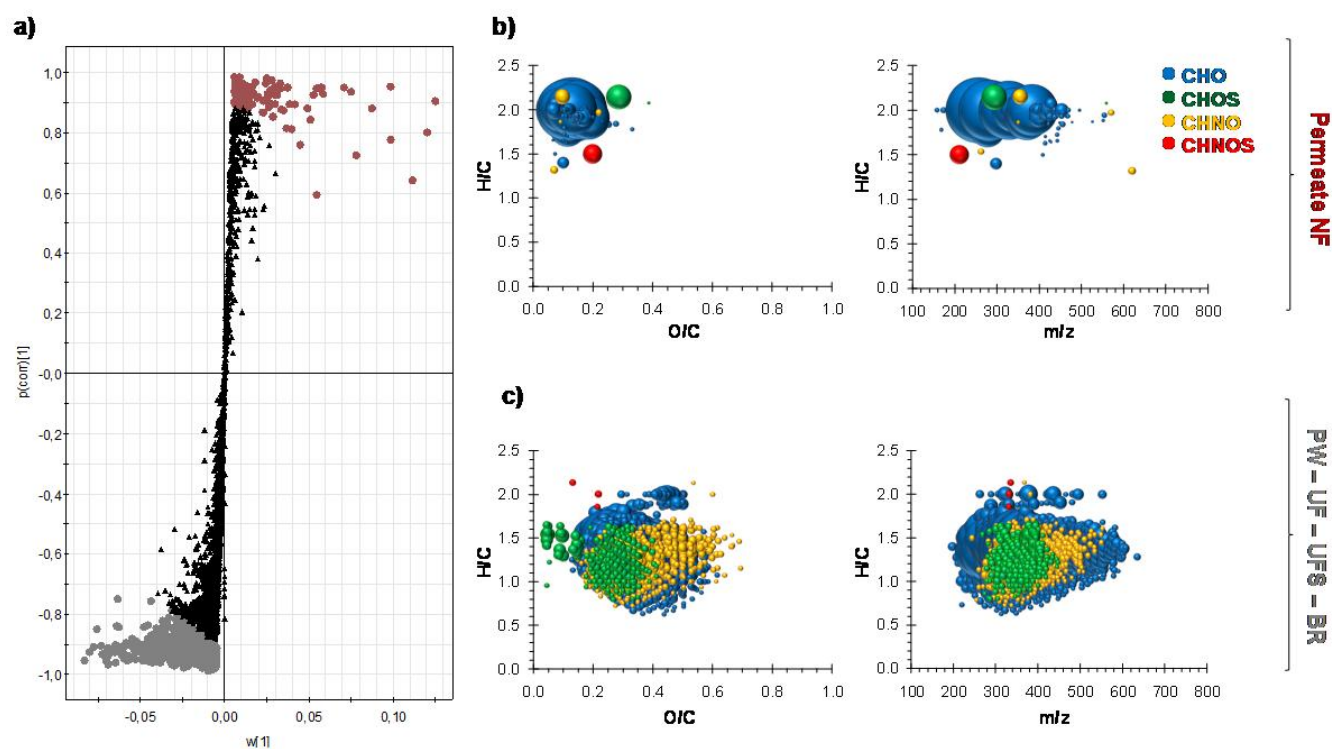


**Figure 4.** Multiblock PCA analysis applied to NMR data. The different blocks stand for the most significant integrals regions (and so key substructures). It underlines the relation between the most significant integrals regions and sample classes (Permeate samples vs PW, UF, UFS and BR). The components in the upper part of the graph are more significant for the Permeate samples, whereas the components from each integral region in the low half part of the graph are more significant for the rest of the samples (see also Table 3).

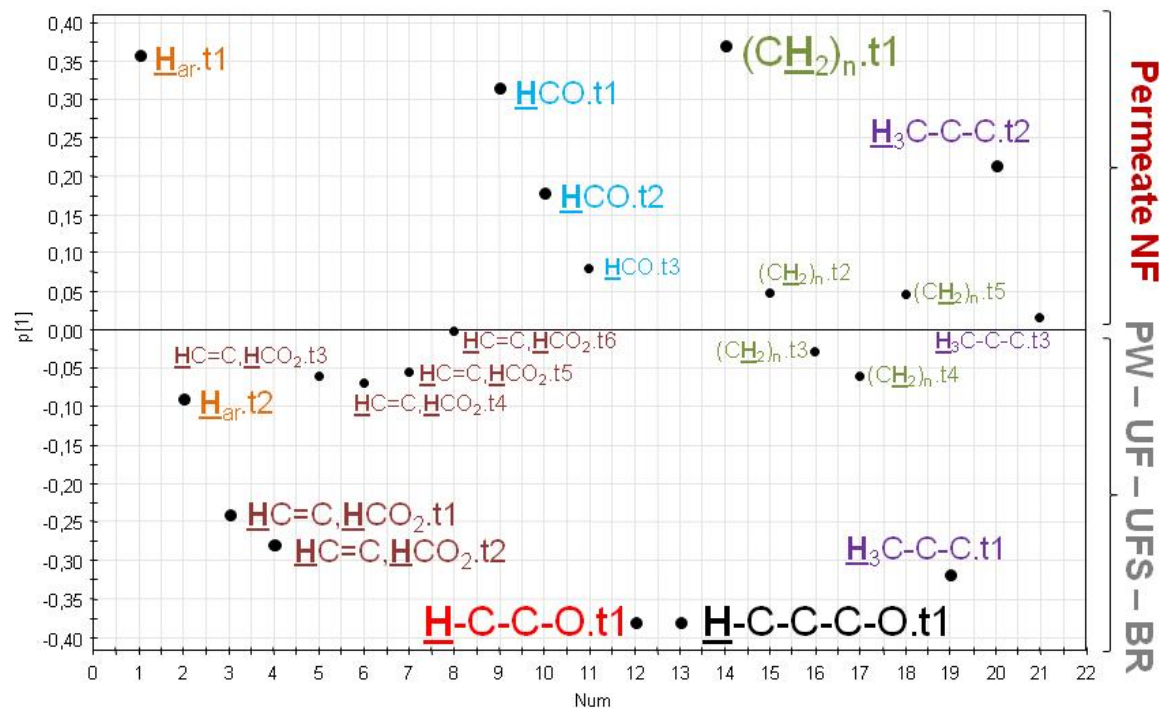


**Table 3.** Variance of each block (key substructures) of the Multiblock PCA analysis applied to NMR data. The values are the variance explained with different number of components (t) represented in Figure 4.

$\delta(^1\text{H})$ [ppm]	9.5 - 7.0	7.0 - 5.3	4.9 - 3.1	3.1 - 1.9	1.9 - 1.35	1.35-1.25	1.25-0.5
Key substructures or blocks	<u>H</u> <sub>ar</sub>	<u>H</u> C=C, <u>H</u> CO <sub>2</sub>	<u>H</u> CO	<u>H</u> -C-C-O	<u>H</u> -C-C-C-O	( <u>C</u> H <sub>2</sub> ) <sub>n</sub>	<u>H</u> <sub>3</sub> C-C-C
Variance explained by each component	0.48	0.44	0.47	0.93	0.85	0.94	0.67
		0.22					
		0.12	0.18				
	0.07						
	0.04	0.12				0.01	0.06
	0.03		0.002				

### 3.2.2.1. Different performance between membranes

The design of the pilot plant allows comparing the performance of the two NF membranes, due to the fact that the same water (UFS sample) is feeding the NF modules.

From the FT-ICR MS data, when comparing absence/presence of theoretical  $m/z$  (within 0.1 ppm mass accuracy window) of the assigned formulas for each sample (PER 1 vs PER 2), we obtained that in PER 1 there are 34% and 30% of unique  $m/z$  (June and October, respectively), compared to PER 2. Considering June and October together, the extracted  $m/z$  that commonly occurred in PER 1 and PER 2 were compared, in order to determine if some of these  $m/z$  presented an increase/decrease of intensity in PER 1 relative to PER 2. It is shown in Figure A10, that there is a slight enrichment in PER 1 with respect to PER 2. In Figure A11, the  $m/z$  unique and the intensity enriched in PER 1 have been plotted in van Krevelen diagram and H/C ratio vs  $m/z$  plot, as well as the  $m/z$  unique for PER 2. In Figure A11a there are two slight areas of the van Krevelen diagram that seem to be more enriched for PER 1: compounds with high H/C ratio (H/C~ 2.0) and H/C ratio < 1.0 (aromatic compounds). Although FT-ICR MS is not a quantitative technique, it seems that membrane 2 removes a higher number of organic compounds. From an analytical point of view, it is interesting to point out, that these trends are not apparent from aggregate parameters such as: i) conventional analysis, UV and TOC, ii) average values for H, C, N, O and S (atom %), DBE and the DBE/C, H/C, O/C, C/N and C/S ratios or iii) integrals regions from  $^1\text{H}$  NMR.

Despite this slight difference of DOM removal, no major differences were found with relation to the levels from regulated THMs, THMFP and some other DBPs (Table A5 and Figure A12). As explained elsewhere (Ribera et al., 2013) the THMFP removal capacity of the two membranes tested in laboratory scale were very similar (more than 90%). In fact, permeability and salt rejection (84% for membrane 1 and 53% for membrane 2) were the main criteria for selection of ESNA1LF2-4040 (membrane 1) and NF270-4040 (membrane 2) membranes for the pilot-scale study.

### 3.2.2.2. Brine samples

As described above, the Brine samples disclose high similarities between PW, UF and UFS, as shown in the two dendrograms (Figure A1). As shown in Table 1, the average values for H, C, N, O and S (atom %), DBE and the DBE/C, H/C, O/C, C/N and C/S

ratios are similar to PW. Data from NMR gives similar structures as in the PW (Table 2). The mass spectra, the van Krevelen diagram, the H/C vs  $m/z$  plot and the  $^1\text{H}$  NMR spectra of BR 1 and BR 2 from June are shown as an example in Figure A13 and Figure A14.

### 3.3. Impact on drinking quality

DOM molecules with a low degree of oxidation (low O/C) were found to be more reactive toward chlorine as described in other studies (Zhang et al., 2012b, Lavonen et al., 2013). The NF process of the study does not remove compounds with low content of oxygen, as a consequence the molecules that remain in the permeate effluent are still more susceptible to chlorination. Moreover, it is said that the precursor materials for THMs tend to be aromatic whereas HAAs precursor materials are aliphatic as discussed in Bond et al. (Bond et al., 2009) and Hong et al. (Hong et al., 2009). As a consequence, applying NF process to water treatment plants would lead to diminution of THMs, but maybe not to a decrease of HAAs. It is important to highlight, that this effect of DOM by NF process has been also observed in other different treatments (Zhang et al., 2012a, Cortés-Francisco et al., 2013) and as proposed by Zhang et al., the efficiency of DOM removal by NF process may be improved by some other pretreatments, such as ozone preoxidation. However, it has been also shown that the choice of disinfectant has a large impact on DBP formation (Lavonen et al., 2013) and the levels of some emerging DBPs are increased by alternative disinfectants, such as ozone or chloramines (Richardson et al., 2007). On the other hand, UV spectroscopy and stoichiometry studies have suggested that nitrogen in NOM might play a significant role in the chlorine consumption reaction. With the use of NF process nitrogenated compounds are highly removed and concerning the formation of some other DBPs containing nitrogen, such as nitrosamines, their occurrence in final drinking water may be reduced.

To study the effect that the final disinfection step can have on the permeate water coming from the NF process, strong chlorination simulating the final disinfection step (5710-B Standard Method) was applied to the Permeate samples. Although very low levels of TOC are found in the Permeate samples (522-79  $\mu\text{g C / L}$ ), a variety of DBPs were still found after chlorination. Two of the four regulated THMs (chloroform and bromodichloromethane) were systematically detected at  $\mu\text{g/L}$  levels in the Permeate samples (during the six months), below the European legislation limits (European

Communities, 2007) (Table A5). Other DBPs, included in lists from previous studies due to their toxicological importance and occurrence (Krasner et al., 2006; Richardson et al., 2007) were also detected in the Permeate samples (PER 1 and PER 2, considering both sampling campaigns together) at low ng/L levels (Figure A12). Although the levels for the regulated THMs and the other unregulated DBPs are low, it is an issue that has to be taken into account, as the permeate water from the NF process is supposed to be the final drinking water. The HAAs were not analyzed in the present samples, as their determination required a more specific analysis, apart from the fact that the HAAs are not still regulated in Europe and so the DWTP do not pay special attention to them. However, further studies should be carried out with relation to HAAs.

#### **4. Conclusions**

The present study illustrated the differences in the character of DOM that was removed along a NF pilot plant and moreover, the slight differences between two different NF membranes. These data sets provide a foundation for understanding the effect that NF processes has on DOM, with respect to molecular composition. The study showed that there is no significant change regarding the nature of DOM at molecular nature, when the water is treated with UF and / or with the addition of antiscaling agents. However, huge decrease of DOM is observed when the water is treated on the NF membranes. The NF process preferentially removes compounds with higher oxygen and nitrogen content (more hydrophilic compounds), whereas molecules with longer pure aliphatic chains and less content of oxygen are the ones capable of going through the membranes. This study demonstrates that combining NMR and HRMS it is possible to characterize which effects have each step treatment in DOM. To some extent, this study as well as some others completed before (Zhang et al., 2012a; Zhang et al., 2012b; Lavonen et al., 2013; Cortés-Francisco et al., 2013) may advice the water industry to improve water treatments.

#### **Acknowledgements**

The authors are grateful to the International Humic Substance Society for the Training Grant that has enabled the collaboration between the Mass Spectrometry Laboratory / Organic Pollutants (IDAEA-CSIC) and Helmholtz Zentrum München, German Research Center for Environmental Health, Research Unit Analytical Biogeochemistry (BGC). The

authors would also like to thank Aigües de Manresa S.A. for providing the facilities required to install and operate the pilot plant. The authors gratefully acknowledge Montse Cortina (LEM/CO-CSIC) for the unregulated DBPs analysis.

### **Author contributions**

N.C.-F. and J.C. designed research. G.R., X.M.-L. and M.R. designed and were in charge of the pilot plant, supplied the samples and performed most of the complementary analysis. FT-ICR MS and NMR measurements were realized by N.C.-F., M. H., P.S.-K. and N.H. in the Helmholtz Zentrum München, German Research Center for Environmental Health, Research Unit Analytical Biogeochemistry (BGC). N.C.-F., M.H. and N.H. analyzed data. N.C.-F. wrote the paper. M.L. performed the statistical analysis. All the authors contributed significantly in the correction and improvement of the last version of the manuscript.

### **Appendix A. Supplementary Information**

Supplementary data as noted in the text can be found in the online version. This include additional materials and methods details, tables and figures. Moreover, a spread sheet data base in excel format include all the elemental formulas of the samples.

### **References**

1. Ates, N., Yilmaz, L., Kitis, M. and Yetis, U. (2009) Removal of disinfection by-product precursors by UF and NF membranes in low-SUVA waters. *Journal of Membrane Science* 328, 104-112.
2. Bellona, C., Drewes, J.E., Xu, P. and Amy, G. (2004) Factors affecting the rejection of organic solutes during NF/RO treatment - a literature review. *Water Research* 38(12), 2795-2809.
3. Bond, T., Henriot, O., Goslan, E.H., Parsons, S.A. and Jefferson, B. (2009) Disinfection Byproduct Formation and Fractionation Behavior of Natural Organic Matter Surrogates. *Environmental Science & Technology* 43(15), 5982-5989.
4. Braeken, L., Ramaekers, R., Zhang, Y., Maes, G., Bruggen, B.V.d. and Vandecasteele, C. (2005) Influence of hydrophobicity on retention in nanofiltration of

- aqueous solutions containing organic compounds. *Journal of Membrane Science* 252, 195-203.
5. Cortés-Francisco, N. and Caixach, J. (2013) Molecular Characterization of Dissolved Organic Matter through a Desalination Process by High Resolution Mass Spectrometry. *Environmental Science & Technology* 47(17), 9619-9627.
  6. D'Andrilli, J., Dittmar, T., Koch, B.P., Purcell, J.M., Marshall, A.G. and Cooper, W.T. (2010) Comprehensive characterization of marine dissolved organic matter by Fourier transform ion cyclotron resonance mass spectrometry with electrospray and atmospheric pressure photoionization. *Rapid Communications in Mass Spectrometry* 24(5), 643-650.
  7. de la Rubia, À., Rodríguez, M., León, V.M. and Prats, D. (2008) Removal of natural organic matter and THM formation potential by ultra- and nanofiltration of surface water. *Water Research* 42(3), 714-722.
  8. European Communities (Drinking Water) (No. 2) Regulations. SI. No. 278 of 2007. (<http://www.irishstatutebook.ie/2007/en/si/0278.html>) Accessed 12/12/2013.
  9. Her, N., Amy, G. and Jarusutthirak, C. (2000) Seasonal variations of nanofiltration (NF) foulants: identification and control. *Desalination* 132(1-3), 143-160.
  10. Hertkorn, N., Benner, R., Frommberger, M., Schmitt-Kopplin, P., Witt, M., Kaiser, K., Kettrup, A. and Hedges, J.I. (2006) Characterization of a major refractory component of marine dissolved organic matter. *Geochimica et Cosmochimica Acta* 70(12), 2990-3010.
  11. Hertkorn, N., Ruecker, C., Meringer, M., Gugisch, R., Frommberger, M., Perdue, E., Witt, M. and Schmitt-Kopplin, P. (2007) High-precision frequency measurements: indispensable tools at the core of the molecular-level analysis of complex systems. *Analytical and Bioanalytical Chemistry* 389(5), 1311-1327
  12. Hertkorn, N., Frommberger, M., Witt, M., Koch, B.P., Schmitt-Kopplin, P. and Perdue, E.M. (2008) Natural Organic Matter and the Event Horizon of Mass Spectrometry. *Analytical Chemistry* 80(23), 8908-8919.
  13. Hertkorn, N., Harir, M., Koch, B.P., Michalke, B. and Schmitt-Kopplin, P. (2013) High-field NMR spectroscopy and FTICR mass spectrometry: powerful discovery tools for the molecular level characterization of marine dissolved organic matter. *Biogeosciences* 10(3), 1583-1624.
  14. Herzsprung, P., von Tümpling, W., Hertkorn, N., Harir, M., Büttner, O., Bravidor, J., Friese, K. and Schmitt-Kopplin, P. (2012) Variations of DOM Quality in Inflows of a

- Drinking Water Reservoir: Linking of van Krevelen Diagrams with EEMF Spectra by Rank Correlation. *Environmental Science & Technology* 46(10), 5511-5518.
15. Hong, H.C., Wong, M.H. and Liang, Y. (2009) Amino Acids as Precursors of Trihalomethane and Haloacetic Acid Formation During Chlorination. *Archives of Environmental Contamination and Toxicology* 56(4), 638-645.
  16. Hua, G. and Reckhow, D.A. (2007) Characterization of Disinfection Byproduct Precursors Based on Hydrophobicity and Molecular Size. *Environmental Science & Technology* 41(9), 3309-3315.
  17. Jaffé, R., McKnight, D., Maie, N., Cory, R., McDowell, W.H. and Campbell, J.L. (2008) Spatial and temporal variations in DOM composition in ecosystems: The importance of long-term monitoring of optical properties. *Journal of Geophysical Research: Biogeosciences* 113(G4), G04032.
  18. Kelleher, B.P. and Simpson, A.J. (2006) Humic Substances in Soils: Are They Really Chemically Distinct? *Environmental Science & Technology* 40(15), 4605-4611.
  19. Kim, S., Kaplan, L.A., Benner, R. and Hatcher, P.G. (2004) Hydrogen-deficient molecules in natural riverine water samples - evidence for the existence of black carbon in DOM. *Marine Chemistry* 92(1-4), 225-234.
  20. Krasner, S.W., Weinberg, H.S., Richardson, S.D., Pastor, S.J., Chinn, R., Scilimenti, M.J., Onstad, G.D. and Thruston, A.D. (2006) Occurrence of a New Generation of Disinfection Byproducts. *Environmental Science & Technology* 40(23), 7175-7185.
  21. Lam, B., Baer, A., Alae, M., Lefebvre, B., Moser, A., Williams, A. and Simpson, A.J. (2007) Major Structural Components in Freshwater Dissolved Organic Matter. *Environmental Science & Technology* 41(24), 8240-8247.
  22. Lamsal, R., Walsh, M.E. and Gagnon, G.A. (2011) Comparison of advanced oxidation processes for the removal of natural organic matter. *Water Research* 45(10), 3263-3269.
  23. Lavonen, E.E., Gonsior, M., Tranvik, L.J., Schmitt-Kopplin, P. and Köhler, S.J. (2013) Selective Chlorination of Natural Organic Matter: Identification of Previously Unknown Disinfection Byproducts. *Environmental Science & Technology* 47(5), 2264-2271.
  24. Matilainen, A., Gjessing, E.T., Lahtinen, T., Hed, L., Bhatnagar, A. and Sillanpää, M. (2011) An overview of the methods used in the characterisation of natural organic matter (NOM) in relation to drinking water treatment. *Chemosphere* 83(11), 1431-1442.

25. Minor, E.C., Steinbring, C.J., Longnecker, K. and Kujawinski, E.B. (2012) Characterization of dissolved organic matter in Lake Superior and its watershed using ultrahigh resolution mass spectrometry. *Organic Geochemistry* 43(0), 1-11.
26. Moons, K. and Van der Bruggen, B. (2006) Removal of micropollutants during drinking water production from surface water with nanofiltration. *Desalination* 199, 245-247.
27. Nebbioso, A. and Piccolo, A. (2013) Molecular characterization of dissolved organic matter (DOM): a critical review. *Analytical and Bioanalytical Chemistry* 405(1), 109-124.
28. Nghiem, L.D., Vogel, D. and Khan, S. (2008) Characterising humic acid fouling of nanofiltration membranes using bisphenol A as a molecular indicator. *Water Research* 42(15), 4049-4058.
29. Ribera, G., Llenas, L., Rovira, M., de Pablo, J. and Martinez-Llado, X. (2013) Pilot plant comparison study of two commercial nanofiltration membranes in a drinking water treatment plant. *Desalination and Water Treatment* 51(1-3), 448-457.
30. Ribera, G., Clarens, F., Martinez-Lladó, X., Jubany, I., Martí, V., Rovira, M. (2014) Life cycle and human health risk assessments as tools for decision making in the design and implementation of nanofiltration in drinking water treatment plants. *Science of the Total Environment* 466-467 (1), 377-386.
31. Richardson, S.D., Plewa, M.J., Wagner, E.D., Schoeny, R. and DeMarini, D.M. (2007) Occurrence, genotoxicity, and carcinogenicity of regulated and emerging disinfection by-products in drinking water: A review and roadmap for research. *Mutation Research/Reviews in Mutation Research* 636(1-3), 178-242.
32. Ritchie, J.D. and Perdue, E.M. (2008) Analytical constraints on acidic functional groups in humic substances. *Organic Geochemistry* 39(6), 783-799.
33. Schmidt, F., Elvert, M., Koch, B.P., Witt, M. and Hinrichs, K.-U. (2009) Molecular characterization of dissolved organic matter in pore water of continental shelf sediments. *Geochimica et Cosmochimica Acta* 73(11), 3337-3358.
34. Schmitt-Kopplin, P., Gelencsér, A., Dabek-Zlotorzynska, E., Kiss, G., Hertkorn, N., Harir, M., Hong, Y. and Gebefügi, I. (2010) Analysis of the Unresolved Organic Fraction in Atmospheric Aerosols with Ultrahigh-Resolution Mass Spectrometry and Nuclear Magnetic Resonance Spectroscopy: Organosulfates As Photochemical Smog Constituents. *Analytical Chemistry* 82(19), 8017-8026.

35. Sleighter, R.L. and Hatcher, P.G. (2008) Molecular characterization of dissolved organic matter (DOM) along a river to ocean transect of the lower Chesapeake Bay by ultrahigh resolution electrospray ionization Fourier transform ion cyclotron resonance mass spectrometry. *Marine Chemistry* 110(3–4), 140-152.
36. Sleighter, R.L., Liu, Z., Xue, J. and Hatcher, P.G. (2010) Multivariate Statistical Approaches for the Characterization of Dissolved Organic Matter Analyzed by Ultrahigh Resolution Mass Spectrometry. *Environmental Science & Technology* 44(19), 7576-7582.
37. Stedmon, C., Markager, S., SØndergaard, M., Vang, T., Laubel, A., Borch, N. and Windelin, A. (2006) Dissolved organic matter (DOM) export to a temperate estuary: seasonal variations and implications of land use. *Estuaries and Coasts* 29(3), 388-400.
38. Stenson, A.C., Marshall, A.G. and Cooper, W.T. (2003) Exact Masses and Chemical Formulas of Individual Suwannee River Fulvic Acids from Ultrahigh Resolution Electrospray Ionization Fourier Transform Ion Cyclotron Resonance Mass Spectra. *Analytical Chemistry* 75(6), 1275-1284.
39. Verliefe, A., Cornelissen, E., Amy, G., Van der Bruggen, B. and van Dijk, H. (2007) Priority organic micropollutants in water sources in Flanders and the Netherlands and assessment of removal possibilities with nanofiltration. *Environmental Pollution* 146(1), 281-289.
40. Verliefe, A.R.D., Cornelissen, E.R., Heijman, S.G.J., Hoek, E.M.V., Amy, G.L., Bruggen, B.V.d. and van Dijk, J.C. (2009a) Influence of Solute–Membrane Affinity on Rejection of Uncharged Organic Solutes by Nanofiltration Membranes. *Environmental Science & Technology* 43(7), 2400-2406.
41. Verliefe, A.R.D., Cornelissen, E.R., Heijman, S.G.J., Petrinic, I., Luxbacher, T., Amy, G.L., Van der Bruggen, B. and van Dijk, J.C. (2009b) Influence of membrane fouling by (pretreated) surface water on rejection of pharmaceutically active compounds (PhACs) by nanofiltration membranes. *Journal of Membrane Science* 330, 90-103.
42. Xu, Y. and Goodacre, R. (2012) Multiblock principal component analysis: an efficient tool for analyzing metabolomics data which contain two influential factors. *Metabolomics* 8(1), 37-51.
43. Zhang, H., Zhang, Y., Shi, Q., Ren, S., Yu, J., Ji, F., Luo, W. and Yang, M. (2012a) Characterization of low molecular weight dissolved natural organic matter along the

treatment trait of a waterworks using Fourier transform ion cyclotron resonance mass spectrometry. *Water Research* 46(16), 5197-5204.

44. Zhang, H., Zhang, Y., Shi, Q., Hu, J., Chu, M., Yu, J. and Yang, M. (2012b) Study on Transformation of Natural Organic Matter in Source Water during Chlorination and Its Chlorinated Products using Ultrahigh Resolution Mass Spectrometry. *Environmental Science & Technology* 46(8), 4396-4402.
45. Zhang, F., Harir, M., Moritz, F., Zhang, J., Witting, M., Wu, Y., Schmitt-Kopplin, P., Fekete, A., Gaspar, A. and Hertkorn, N. (2014) Molecular and structural characterization of dissolved organic matter during and post cyanobacterial bloom in Taihu by combination of NMR spectroscopy and FTICR mass spectrometry. *Water Research* 57(0), 280-294.

### **4.2.3. Research Article N° 5**

Nuria Cortés-Francisco, Mourad Harir, Gemma Ribera, Xavier Martinez-Lladó, Miquel Rovira, Philippe Schmitt-Kopplin, Norbert Hertkorn and Josep Caixach

Molecular Characterization of DOM causing Fouling to NF Membranes by High-field FT-ICR Mass Spectrometry and NMR spectroscopy.

*Environmental Science & Technology, (submitted)*



## **Molecular characterization of DOM causing fouling to NF membranes by high-field FT-ICR mass spectrometry and NMR spectroscopy.**

Nuria Cortés-Francisco <sup>1</sup>, Mourad Harir <sup>2</sup>, Gemma Ribera <sup>3</sup>, Xavier Martinez-Llado <sup>3</sup>, Miquel Rovira <sup>3</sup>, Philippe Schmitt-Kopplin <sup>2,4</sup>, Norbert Hertkorn <sup>\*,2</sup>, and Josep Caixach <sup>1</sup>

<sup>1</sup> Mass Spectrometry Laboratory / Organic Pollutants, IDAEA-CSIC; Jordi Girona 18-26, 08034 Barcelona, Spain. Tel: (+34) 93 400 61 00. Fax: (+34) 93 204 59 04.

<sup>2</sup> Helmholtz Zentrum Muenchen, German Research Center for Environmental Health, Research Unit Analytical Biogeochemistry (BGC), Ingolstaedter Landstrasse 1, D-85764 Neuherberg, Germany. Tel: (+49) 089 3187 2834. Fax: (+49) 089 3187 3358.

<sup>3</sup> Fundació CTM Centre Tecnològic; Plaça de la Ciència, 2, 08243 Manresa, Spain.

<sup>4</sup> Chair of Analytical Food Chemistry, Technische Universität München, Alte Akademie 10, 85354, Freising-Weihenstephan, Germany

E-mail addresses: hertkorn@helmholtz-muenchen.de

### **ABSTRACT**

Ultrahigh resolution Fourier transform ion cyclotron mass spectrometry was used for the molecular characterization of dissolved organic matter (DOM) which had caused fouling to two different NF membranes. These membranes have been sacrificed and analyzed after six months operation in a ultrafiltration-nanofiltration (UF-NF) pilot plant installed in a drinking water treatment plant. The design of the pilot plant had allowed to feed both NF membrane modules with identical raw water (UF effluent after addition of reagents) and later to compare the DOM adsorbed on the two NF membranes. The extraction of DOM from the membranes was optimized testing different proportions of membrane, temperature and alkaline solutions. Moreover, nuclear magnetic resonance spectroscopy has been applied to obtain structural information of DOM extracted from the NF membranes. DOM presented a high content of nitrogen, sulfur and oxygen, comparable to brine effluents. Functionalized molecules with more heteroatoms were preferentially adsorbed onto the membranes. Molecular

differences between the DOM adsorbed on the two dissimilar NF membranes were also observed.

## INTRODUCTION

Membrane technology is widely used in water treatment plants because of its effectiveness in removing natural organic matter and contaminants such as pharmaceuticals, heavy metals or pesticides<sup>1-5</sup>, and a high degree of water quality<sup>6</sup> is obtained at reasonable expenditure.

Membrane fouling continues to be the key impediment for successful application of membrane processes because it causes increased energy demand and decrease of membrane lifetime<sup>7</sup>. Dissolved compounds presented in feed water can absorb, accumulate or precipitate on the membrane leading to fouling and causing membrane problems. Usually, membranes should be cleaned with specific protocols when a continuous output loss is experienced. At the end of the membrane life of installation, certain elements may be sacrificed to carry out what is called membrane autopsy. Membrane autopsy is a destructive analysis to characterize the major causes of fouling<sup>8</sup> and/or identify the causes of the poor performance of the membranes. The characterization usually consists of visual inspection, measuring membrane properties such as zeta-potential, contact angle and elemental composition of the membrane surface, membrane scanning electron microscopy images, attenuated total reflection-Fourier transform infrared spectrometry and microbiological analysis<sup>7,9,10</sup>. These techniques are used to identify deposits on membrane surfaces and relate those to inorganic fouling (caused by alumino-silicates, calcium and carbonates), or to organic fouling and biofilms (caused by micro organisms)<sup>8</sup>.

As described elsewhere, low molecular organic matter is prone to adsorb onto the membrane surface and to initiate organic fouling and subsequent biofouling<sup>7,8</sup>. In several studies, various techniques such as ultraviolet, visible absorption (UVA) spectroscopy and excitation emission matrix fluorescence spectroscopy, liquid chromatography-organic carbon detection and molecular weight distribution have been used to characterize the organic fouling<sup>9,10</sup>. However, little is still known of molecular level composition and structure of DOM which might initiate and exacerbate membrane fouling processes.

In the present study, the extraction of DOM from NF membranes was optimized in order to improve the recovery of DOM while keeping the damage to the membranes as limited as feasible. The following factors were evaluated: amount of membrane, extraction temperatures and the effect of different alkaline solutions as extraction solvents. Regarding the analytical techniques, ultrahigh resolution ion cyclotron Fourier transform (FT-ICR/MS) mass spectrometry and nuclear magnetic resonance spectroscopy (NMR) have been used to obtain molecular details of DOM causing fouling on the two NF membranes. Here, FT-ICR mass spectrometry provides sensitive information of the molecular formulas composing DOM and NMR spectroscopy supplies quantitative relationships between NMR parameters and extended carbon-based substructures<sup>11,12</sup>.

## MATERIALS AND METHODS

**Nanofiltration Pilot plant and Feed Water.** The drinking water treatment plant (DWTP) of Manresa (Catalonia, Spain) takes the water from a small reservoir (Agulla's Lake; 0.2 Hm<sup>3</sup>) fed with superficial water from Llobregat River. The water is predisinfected using chlorine and coagulated with aluminum polychloride, prior to slow sand filtration (pretreated water). To assure disinfection, the current installation has a final chlorination step.

A ultrafiltration-nanofiltration (UF-NF) pilot plant fed with pretreated water from the output of the sand filtration stage, prior to final chlorination was installed for six months. The schematic diagram of the experimental set-up for the pilot plant is shown in SI Figure S1. The water feeding the NF membranes was the UF effluent after addition of reagents as follows: sodium metabisulfite (1 - 2 ppm) to remove free chlorine and scale inhibitor (1.5 ppm of Genesys LF) to avoid inorganic scaling. In a previous study, two sampling campaigns have been carried out to characterize the molecular evolution of DOM in water along the pilot plant<sup>13</sup>. A review of the main characteristics: i) complementary analysis: conductivity, pH, non-purgable organic carbon (NPOC), UVA, total inorganic carbon (TIC), total nitrogen (TN), major inorganic cations (calcium, magnesium, potassium and sodium) and anions (chloride, nitrates, sulphates); ii) FT-ICR MS data and iii) <sup>1</sup>H NMR derived structural information of the DOM in water feeding the membranes can be found in the Table S1, Table 1 and Table 2, respectively.

**Nanofiltration Membranes.** In the NF process step, two different membranes were contained in separated trains of each six 4" spiral wound modules: ESNA1LF2-4040 (membrane 1 - M1) and NF270-4040 (membrane 2 - M2). They were operating at the same recovery (50 %) and permeate flux (28 l/mh), to represent the operational conditions of an industrial full-scale NF plant. The design allowed the simultaneous comparison of the two selected commercial membranes. SI Table S2 provides the main suppliers specifications of UF and NF membranes used as well as some relevant NF membrane properties obtained from previous studies.

Three chemical cleanings using NaOH and sodium dodecylsulfate (SDS) were carried out in order to recover the permeate flow (25/5/2011, 12/7/2011 and 01/8/2011). At the end of the pilot plant experimentation, the first modules of each type of membrane were sacrificed in order to analyze the cause of permeability decrease and any fouling on the membranes.

Preliminary observations of the modules were carried out before its opening. Each sheet of membrane was numbered and divided in sample areas, which then were numbered following the direction of water flow during the operation in the pilot plant. Sample conservation of membranes for consecutive analysis consisted in rinsing with milli-Q water and its wet conservation in the fridge, at 4°C.

Moreover, blank membranes: ESNA1LF2-4040 (B1) and NF270-4040 (B2) were also analyzed and cleaned with milli-Q water before extraction.

**Scanning electron microscopy-energy dispersive X-ray spectroscopy analysis.** To determine the sort of membrane deposits, scanning electron microscopy-energy dispersive X-ray spectroscopy (SEM-EDX) analyses were carried out. Membrane samples were prepared as small pieces of 0.5\*1 cm and dried at room temperature. Afterwards, the small pieces of membrane were metalized with Au-Pd to capture images and spectra using an scanning electronic coupled to electron ray X diffraction microscopy (SUPRA<sup>TM</sup> Field Emission SEM, Carl Zeiss, with a Microanalysis X-Max EDX, Oxford Instruments).

**DOM extraction.** A DIN A-4 piece (A 20 x 30 cm section) of each used membrane (M1 and M2) and blank membrane (B1 and B2) were cut into small pieces (0.5 x 1 cm)

and extracted in two different alkaline solutions (0.1 % NaOH with pH = 12.9; 0.35 M NH<sub>4</sub>OH with pH = 11.7) as follows: 40 mL of the alkaline solution was added into a screw cap-tube with the pieces of membrane and mildly sonicated in an ultrasonic bath at room temperature during 5 minutes. After sonication, the solution was acidified to pH = 2 with formic acid (98 %, Sigma-Aldrich) for subsequent solid phase extraction using SPE-PPL cartridges (200 mg, 3 mL, Bond Elut, Agilent). The cartridges were conditioned with 1 mL methanol and 1 mL of water acidified with formic acid (1 mL water and 50  $\mu$ L 25% formic acid) before sample application. The compounds were eluted with 1 mL methanol and ready for infusion analysis for FT-ICR mass spectrometry.

For NMR spectroscopy, aliquots of CH<sub>3</sub>OH extracts of the samples were evaporated in vacuum to dryness and CD<sub>3</sub>OD (99.95 % <sup>2</sup>H, Aldrich, Steinheim, Germany) was added; this cycle was repeated three times to largely exchange methanol-h<sub>4</sub> by methanol-d<sub>4</sub>.

**FT-ICR mass spectrometry.** Ultrahigh-resolution Fourier transform ion cyclotron (FT-ICR) mass spectra were acquired using a 12 T Bruker Solarix mass spectrometer (Bruker Daltonics, Bremen, Germany) and an electrospray ionization source in negative mode. DOM extracts were injected into the electrospray source using a micro-liter pump at a flow rate of 120  $\mu$ L·h<sup>-1</sup> with a nebulizer gas pressure of 138 kPa and a drying gas pressure of 103 kPa. A source heater temperature of 200°C was maintained to ensure rapid desolvation in the ionized droplets. Spectra were first externally calibrated on clusters of arginine (0.57  $\mu$ mol·L<sup>-1</sup> in methanol) and internal calibration was systematically done using appropriate reference mass list reaching accuracy values lower than 500 ppb. The spectra were acquired with a time domain of 4 megawords and 500 scans were accumulated for each spectrum.

Calculation of elemental formulas for each peak was done in a batch mode by an in-house written software tool. The generated formulas were validated by setting sensible chemical constraints [signal-to-noise (S/N) >3, N rule, O/C ratio  $\leq$  1, H/C ratio  $\leq$  2n + 2 (C<sub>n</sub>H<sub>2n+2</sub>), element counts: C  $\leq$  100, H  $\leq$  200, O  $\leq$  80, N  $\leq$  3, S  $\leq$  2 and mass accuracy window (set at  $\pm$  500 ppb)]. Final assigned formulas were generated and categorized into groups containing CHO, CHNO, CHOS or CHNOS type of molecules<sup>14</sup>. For each negative ion observed, the elemental formula reported is the corresponding neutral whose mass is the mass of the negative ion plus a proton (1.007276 Da). Furthermore,

the given computed average values of H, C, N, O and S (atom %) and the H/C, O/C, C/N and C/S atomic ratios as well as double bond equivalents (DBE) and DBE to carbon (DBE/C) and mass-to-charge ( $m/z$ ) ratios were based upon intensity-weighted averages of mass peaks with assigned molecular formulas (Table 1).

**Data Analysis.** A scheme of the data evaluation procedure is included in SI Figure S2. Briefly, the formulas assigned from the FT-ICR data of the eight extracts have been compared based on presence/absence of the assigned formulas (comparison based on computed exact  $m/z$  theoretical and mass window  $\Delta m : \pm 0.1$  ppm) using an in-house written software tool.

For comparative analysis (see below and SI Figure S2), the Unique Assigned Formulas were extracted and the given computed average values of H, C, N, O and S (atom %) and the H/C, O/C, C/N and C/S ratios as well as DBE and carbon (DBE/C) and mass-to-charge ( $m/z$ ) ratios were recalculated based upon intensity-weighted averages of mass peaks.

Considering the interference that mass peaks originating from the blanks (B1 and B2) may cause on the attribution of mass peaks of DOM adsorbed onto the membranes (M1 and M2), any  $m/z$  present in the blanks was removed and the Unique Assigned Formulas present in M1 and M2 were named DOM 1 and DOM 2, respectively (see SI Figure S2a). Moreover, to highlight the different characteristics between DOM 1 and DOM 2, the two sets of Unique Assigned Formulas were also extracted and compared (see SI Figure S2b).

In addition, the two different alkaline extracts of the Blank Membranes (see Figure S2c) and the DOM extracted (see SI Figure S2d) were compared, accordingly.

**Table 1.** Counts of mass peaks as computed from negative electrospray 12T FT-ICR mass spectra for singly charged ions with nitrogen rule check and 500 ppb tolerance for DOM 1 and DOM 2, as well as for the water feeding the NF Membranes (UF effluent after addition of reagents) and the brine effluents (Brine NF 1 and Brine NF 2), analyzed as part of another study. For the water samples as two sampling campaigns were carried out the average value and the standard deviation (SD) are given.

Members of molecular series	Water feeding the NF Membranes <sup>a</sup>		Brine NF 1 <sup>a</sup>		Brine NF 2 <sup>a</sup>		DOM 1		DOM 2	
	Average	SD	Average	SD	Average	SD	NH <sub>4</sub> OH-PPL	NaOH-PPL	NH <sub>4</sub> OH-PPL	NaOH-PPL
CHO compounds	2589 (53 %)	23	2568 (55 %)	151	1936 (51 %)	742	439 (27 %)	474 (33 %)	627 (38 %)	663 (40 %)
CHOS compounds	732 (15 %)	64	756 (16 %)	93	645 (18 %)	211	337 (21 %)	362 (26 %)	216 (13 %)	320 (20 %)
CHNO compounds	1375 (28 %)	236	1254 (27 %)	85	1066 (28 %)	264	566 (35 %)	343 (24 %)	623 (37 %)	474 (29 %)
CHNOS compounds	224 (4 %)	131	111 (2 %)	29	114 (3 %)	7	279 (17 %)	236 (17 %)	206 (12 %)	181 (11 %)
Number of assigned mass peaks	4919	455	4688	56	3761	803	1621	1415	1672	1638
average H [%]	7.39	0.09	7.26	0.04	7.26	0.06	8.0	7.9	8.1	7.7
average C [%]	65.6	0.1	64.8	0.4	65.0	0.3	64	63	63	61
average O [%]	26.1	0.1	26.9	0.3	25.9	1.7	22	23	24	26
average N [%]	0.4	0.1	0.3	0.1	0.4	0.1	2.6	1.9	2.6	2.2
average S [%]	0.65	0.01	0.7	0.1	0.7	0.3	3.1	4.0	2.0	2.4

Members of molecular series	Water feeding the NF Membranes <sup>a</sup>		Brine NF 1 <sup>a</sup>		Brine NF 2 <sup>a</sup>		DOM 1		DOM 2	
	Average	SD	Average	SD	Average	SD	NH <sub>4</sub> OH-PPL	NaOH-PPL	NH <sub>4</sub> OH-PPL	NaOH-PPL
computed H/C ratio from FTICR mass peaks	1.35	0.01	1.35	0.01	1.34	0.01	1.5	1.5	1.5	1.5
computed O/C ratio from FTICR mass peaks	0.30	0.01	0.32	0.01	0.31	0.01	0.26	0.28	0.29	0.32
computed C/N ratio from FTICR mass peaks	16	1	16	1	15	1	13.5	11.6	12.4	11.7
computed C/S ratio from FTICR mass peaks	15.7	0.8	14.5	0.1	16.3	2.3	27.0	19.5	26.6	22.8
Average DBE, intensity weighted	8.0	0.4	7.9	0.1	7.9	0.1	7.4	6.4	6.3	6.6
Average DBE/C, intensity weighted	0.38	0.01	0.38	0.01	0.38	0.01	0.31	0.29	0.29	0.31
Average mass, intensity weighted	388	8	386	1	382	6	435.8	402.1	407.1	419.1

<sup>a</sup> From previous study<sup>13</sup>

**NMR analysis.** All proton detected NMR spectra were acquired immediately after sample preparation with a Bruker Avance III NMR spectrometer operating at 800.13 MHz ( $B_0 = 18.8$  T) and TopSpin 3.0/PL3 software with samples from redissolved solids (0.7-5.8 mg solid DOM in typically 46-75  $\mu$ L methanol- $d_4$  (SI Table S3) in sealed 1.7 mm Bruker Match tubes. Proton spectra were acquired with an inverse geometry 5 mm z-gradient  $^1\text{H}/^{13}\text{C}/^{15}\text{N}/^{31}\text{P}$  QCI cryogenic probe ( $90^\circ$  excitation pulses:  $^1\text{H} \sim 10$   $\mu$ s); NMR chemical shift reference:  $^1\text{H}$  NMR,  $\text{HD}_2\text{OD}$ : 3.30 ppm. All spectra were acquired at 283 K to impede side reactions during NMR acquisitions. 1-D  $^1\text{H}$  NMR spectra were recorded with a spin-echo sequence (10  $\mu$ s delay) to allow for high-Q probe ringdown; classical presaturation “zgpr” and “zgpurge” and solvent suppression with presaturation and 1 ms spin-lock (*noesypr1d*), 5 s acquisition time, 10 s relaxation delay (d1), typically 738 scans, 1 Hz exponential line broadening. For data analysis of the NMR acquisitions, spectra were all normalized to identical areas of total integral from  $\delta_{\text{H}} \sim 0.5$ -9.5 ppm (excluding residual water, methanol and formic acid) and the spectra were divided into 0.001 ppm width buckets and exported using Amix version 3.9.4 (Bruker BioSpin, Rheinstetten, Germany). Bucket-derived  $^1\text{H}$  NMR section integrals were defined in Table 2 based on key substructures from DOM<sup>12</sup>.

**Reproducibility.** Reproducibility of mass spectra was evaluated with replicate injections for two samples of the study within one week. The counts of signals obtained (presence/absence of mass peaks) were compared between those replicates with 1 ppm mass accuracy window<sup>15</sup>. The number of formulas assigned was obtained comparing presence/absence of theoretical exact  $m/z$  (within 0.1 ppm mass accuracy window) of the assigned formulas for each run. For the common molecular compositions assigned, the relative intensity for each pair of replicates was also evaluated. Moreover, based on the formulas assigned, the given computed average values of H, C, N, O and S (atom %) and the H/C, O/C, C/N and C/S ratios as well as DBE and carbon (DBE/C) and mass-to-charge ( $m/z$ ) ratios based upon intensity-weighted averages of mass peaks were calculated and compared between replicates.

**Table 2.**  $^1\text{H}$  NMR section integrals (percent of non-exchangeable protons) and key substructures from DOM 1 and DOM 2, as well as from the water feeding the NF Membranes (UF effluent after addition of reagents) and the brine effluents (Brine NF 1 and Brine NF 2), analyzed as part of another study. For the water samples as two sampling campaigns were carried out the average value and the standard deviation (in brackets) are given (exclusion of residual water, methanol and formic acid).

$\delta(^1\text{H})$ [ppm]	9.5 - 7.0	7.0 - 5.3	4.9 - 3.1	3.1 - 1.9	1.9 - 1.35	1.35-1.25	1.25-0.5	Sum 1.9-0.5	$\text{H}_{\text{olefinic}} / \text{H}_{\text{aromatic}}$	$\text{H}_3\text{C} / (\text{CH}_2)_n$	
Key substructures	$\text{H}_{\text{ar}}$	$\text{H}_\text{C}=\text{C}, \text{H}_\text{C}\text{O}_2$	$\text{H}_\text{CO}$	$\text{H}-\text{C}-\text{C}-\text{O}$	$\text{H}-\text{C}-\text{C}-\text{C}-\text{O}$	$(\text{CH}_2)_n$	$\text{H}_3\text{C}-\text{C}-\text{C}$				
<b>Water feeding the NF Membranes<sup>a</sup></b>	2.8 (0.5)	1.2 (0.1)	11 (4)	20 (2)	22 (3)	17 (3)	27 (3)	66 (3)	0.5 (0.1)	1.7 (0.5)	
<b>Brine NF 1<sup>a</sup></b>	2.0 (0.3)	1.9 (0.5)	9 (3)	25.9 (0.4)	25.2 (0.6)	10 (1)	26 (3)	61 (2)	0.9 (0.1)	2.7 (0.6)	
<b>Brine NF 2<sup>a</sup></b>	2.1 (0.2)	1.5 (0.5)	8.1 (0.4)	24 (2)	24 (1)	12 (3)	28 (1)	64 (3)	0.7 (0.1)	2.6 (0.5)	
<b>DOM 1</b>	NH <sub>4</sub> OH - PPL	4.2	1.1	22.2	19.1	18.6	8.8	25.9	53.4	0.3	2.9
	NaOH - PPL	-0.9	1.7	25.3	19.5	20.0	14.4	20.1	54.4	-1.9	1.4
<b>DOM 2</b>	NH <sub>4</sub> OH - PPL	4.4	-0.1	21.9	21.7	16.1	8.7	27.2	52.1	0.0	3.1
	NaOH - PPL	1.8	1.2	19.2	18.3	18.5	21.6	19.3	59.4	0.7	0.9

<sup>a</sup> From previous study<sup>13</sup>

## RESULTS AND DISCUSSION

**Morphology and Elemental Composition of the Membranes Surface.** The used membranes were sacrificed and analyzed, together with the blanks. Naked eye observation already allowed discrimination between the blank and the used membranes (see Figures 1a-d). More detailed evidence of fouling could be detected in the used membranes by means of SEM-EDX (Table 3, Figures 1e-h).

Regarding the effluent feeding the NF modules, organic fouling may be present on the membrane surface, as shown by the smooth layer visible in the SEM images (Figure 1e-h). As previously shown<sup>2,13,16</sup>, UF treatment has no appreciable effect on DOM rejection and so, not surprisingly, any UF effluent could cause DOM deposition on the membrane layer<sup>10</sup>. Moreover, the used NF membranes showed a lesser percentage of carbon, with respect to blanks, indicating the deposition of inorganic substances and also colloids that are visible, e.g. in Figures 1e and 1g. In this preliminary analysis Si, Al, P and Ca were the most abundant elements. However, only an approximative molecular speciation can

be deduced from here taking into account previous feed water analyses, which determined abundances of silicates, phosphonates and carbonates; however, the overall percentage of oxygen as derived from SEM-EDX characterization has been notably increased. The impossibility to identify and elucidate organic compounds by SEM-EDX, lead to the use of FT-ICR mass spectrometry and NMR spectroscopy for further molecular level characterization of organic compounds.

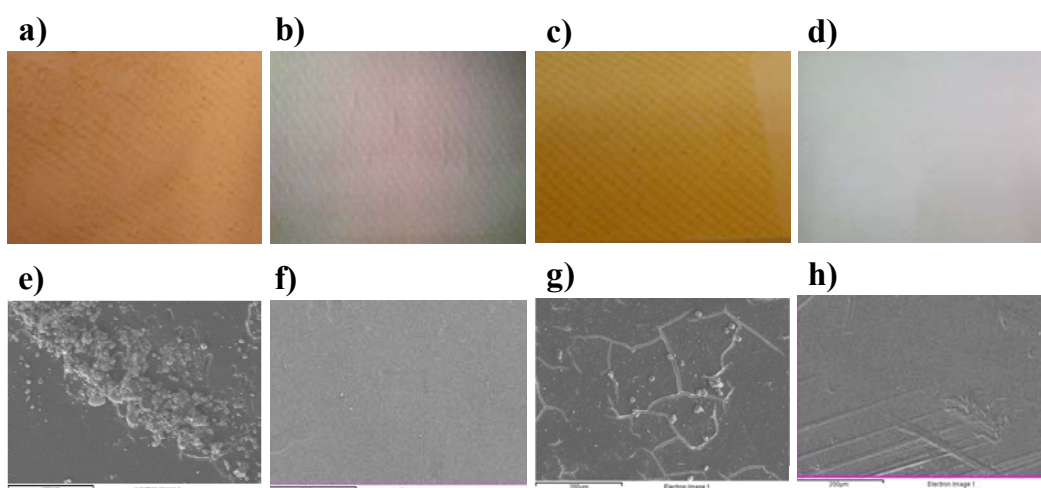


**Figure 1.** Photographs of used and blank membranes: a) Used Membrane 1, b) Blank Membrane 1, c) Used Membrane 2 and d) Blank Membrane 2. SEM images of the same membranes: e) Used Membrane 1, f) Blank Membrane 1, g) Used Membrane 2 and h) Blank Membrane 2.

**Table 3.** Atomic composition of detected elements on the membrane surface by EDX analysis (expressed as percentage by weight of the atomic element).

Samples	Weight (%)						
	C	O	Ca	S	Si	Al	P
<b>Blank Membrane 1</b>	74.8	18.1	n.d.	7.1	n.d.	n.d.	n.d.
<b>Used Membrane 1</b>	46.1	37.2	7.93	3.97	2.42	1.23	0.51
<b>Blank Membrane 2</b>	79.9	12.7	n.d.	7.4	n.d.	n.d.	n.d.
<b>Used Membrane 2</b>	57.4	32.6	2.39	4.31	0.36	1.31	1.03

n.d.: not detected

**Optimization of DOM extraction.** Nanofiltration membranes are extremely delicate and very little is known about their manufacturing process and composition, because it is usually part of the proprietary know-how of membrane producing companies. In some cases the fouling layer is thick enough to be successfully scraped from the membrane. In our study however, the foulants had to be removed by chemical means.

The extraction conditions were optimized in order to improve the recovery of DOM and damage the membranes as little as possible. The following factors were evaluated: proportions of membrane; extraction temperatures (room temperature and slightly warming up to 35 °C) and the use of different alkaline solutions as extraction solvents (NH<sub>4</sub>OH and NaOH). The optimal conditions were chosen based on peak richness and overall amplitude of DOM signatures in FT-ICR mass spectra.

#### *Effects of membrane proportion and temperature*

The sampling on the membrane layer was performed along the membrane. Initially, 3 pieces of 4 cm<sup>2</sup> each were taken along the membrane sheet. After alkaline extraction and SPE, the FT-ICR mass spectra showed insufficient S/N ratio of DOM signatures even after an accumulation time of 20 minutes (500 scans). For this reason, the area of membrane used was continually increased; SI Figure S3 and S4, show the corresponding improvement of S/N ratio of mass peaks. Finally, a membrane area equivalent to DIN A4 size (20 x 30 cm) was used for the extraction of each membrane (M1 and M2) as well as for the blank membranes (B1 and B2).

Although the membranes are extremely delicate and we wanted to extract the DOM on the membrane but damage as less as possible the active layer itself, we compared the extraction at room temperature and slightly warming up to 35°C, to see if there was any improvement on the extraction. As shown in SI Figure S5, there was no improvement on the extraction upon warming and so, the optimal extraction was carried out at room temperature. Moreover, the destruction of membranes is less probable at ambient temperature.

#### *Alkaline solution*

Two different alkaline solutions were tested: NH<sub>4</sub>OH and NaOH. NH<sub>4</sub>OH is frequently used for the initial solubilization of collected secondary organic aerosols from quartz filters<sup>14</sup>. NaOH a stronger base, was chosen because NaOH solution is usually used as cleaning solution of choice when NF or RO membranes are suspected to be affected by

organic fouling; it has been also used to remove NOM for membrane autopsies<sup>17,18</sup>. Three factors were considered to evaluate the appropriateness of the respective extraction method: i) preservation destruction of blank membranes, ii) overall mass peak richness and S/N ratio of DOM signals in the FT-ICR mass spectra and iii) evaluation of DOM properties.

No major destruction was observed when treating the blank membranes (B1 and B2) with either NH<sub>4</sub>OH or NaOH. The mass peaks and assigned formulas obtained from each extraction method are summarized in SI Table S4 and SI Figure S6 and already demonstrate visible differences between the DOM isolated in case of blank and used membranes. NaOH solution extracts a higher proportion of CHO compounds, whereas the extraction with NH<sub>4</sub>OH seems to favor the extraction of compounds containing heteroatoms (N and S). Here, de novo formation of CHNO and CHNOS compounds by reaction of organic matter with NH<sub>3</sub> may contribute in part to the observed discrepancy<sup>19,20</sup> (see SI Table S5). Moreover, the compounds extracted by means of NaOH show a higher degree of unsaturation (DBE: 8.3-9.4 and DBE/C: 0.37-0.41).

The two different alkaline DOM extracts showed also differences in the computed average values of H, C, N, O and S (atom %), the H/C, O/C, C/N and C/S ratios, DBE, DBE/C, *m/z* ratio (based upon intensity-weighted averages of mass peaks) (Table 1). In particular, considering absence/presence of the assigned elemental compositions, more than 58 % were unique when extracted with either NH<sub>4</sub>OH or NaOH (see SI Table S6). Taking into account the satisfactory of mass spectra obtained from the analysis of replicates (see section Reproducibility), we concluded that the molecular composition DOM extracted with either NH<sub>4</sub>OH or NaOH was remarkably different.

Considering these preliminary findings, we conclude that NaOH solution, which is usually also used to remove organic fouling from RO or NF membranes, is more appropriate for DOM extraction. NaOH solution has been used in conjunction with membrane autopsy, but characterization at molecular level has not been carried out before. The advantage of NH<sub>4</sub>OH volatility has to be confronted with the largely unknown extent and selectivity of putative reactions of NH<sub>3</sub> with organic matter constituents, which appears to outweigh the relative ease of operation.

Nevertheless, we have analyzed the Blank Membranes and the Used Membranes with the two alkaline solutions. Analogous DOM extraction selectivity issues in water samples had been observed previously<sup>21,22</sup>.

**Reproducibility.** Reproducibility in mass peak detection (absence/presence of mass peaks) showed that between 68 and 80 % of mass peaks were common in both replicate runs (see SI Table S7). Moreover, the percentages of common formulas were almost the same (67-80%; with better concordance for DOM rather than for blank samples) after setting sensible chemical constraints for the validation of the assigned molecular formula, showing that formulas assignment and filtration was reproducible.

To assess mass peak magnitude reproducibility, the ratios of peak magnitudes (ratio of individual peak magnitude to base peak magnitude) were computed for the common peaks in both runs. The average percent relative standard deviation (RSD) was lower than 20 % and when plotting the ratio of peak magnitudes of run 1 vs those of run 2, they showed fair agreement ( $R^2 \geq 0.92$ ) (see SI Figure S7).

Moreover, the comparison between replicates of the computed average values of H, C, N, O and S (atom %), the H/C, O/C, C/N and C/S ratios, DBE, DBE/C,  $m/z$  ratio (based upon intensity-weighted averages of mass peaks) showed inter-day RSD lower than 7% (see SI Table S8).

This extent of reproducibility is considered acceptable and in accordance with other results available in the literature<sup>15,23-25</sup>.

## **FT-ICR MS membrane characterization**

### ***Analysis of Blanks***

In a first preliminary test, there was evidence of membrane damage during the extraction process led us to extract membrane polymers together with DOM. For that reason it was very important to analyze the blanks and the used membranes under the same conditions. Moreover, both membranes as well as DOM are composed by the same elements carbon, oxygen, nitrogen, hydrogen and sulfur, although in different proportions.

The CHO and CHOS compounds are the major components of B1 and B2 extracts (see SI Table S4 and SI Figure S6) and the high sulfur content is remarkable (S : 3.3-8.9 %); notably, polysulphone is one of the main membrane components.

Both membranes are composed of polysulphone and polyamide and B2 membranes have also a thin active layer of polypiperazine<sup>26</sup> (SI Table S2). Based on the amount of dry sample (SI Table S3) and the number of assigned peaks (SI Table S4), it seems that membrane B2 had suffered from a major destruction no matter which alkaline solution was used. Most likely, not only polyamide and polysulphone are destroyed during alkaline extraction, but also the active layer.

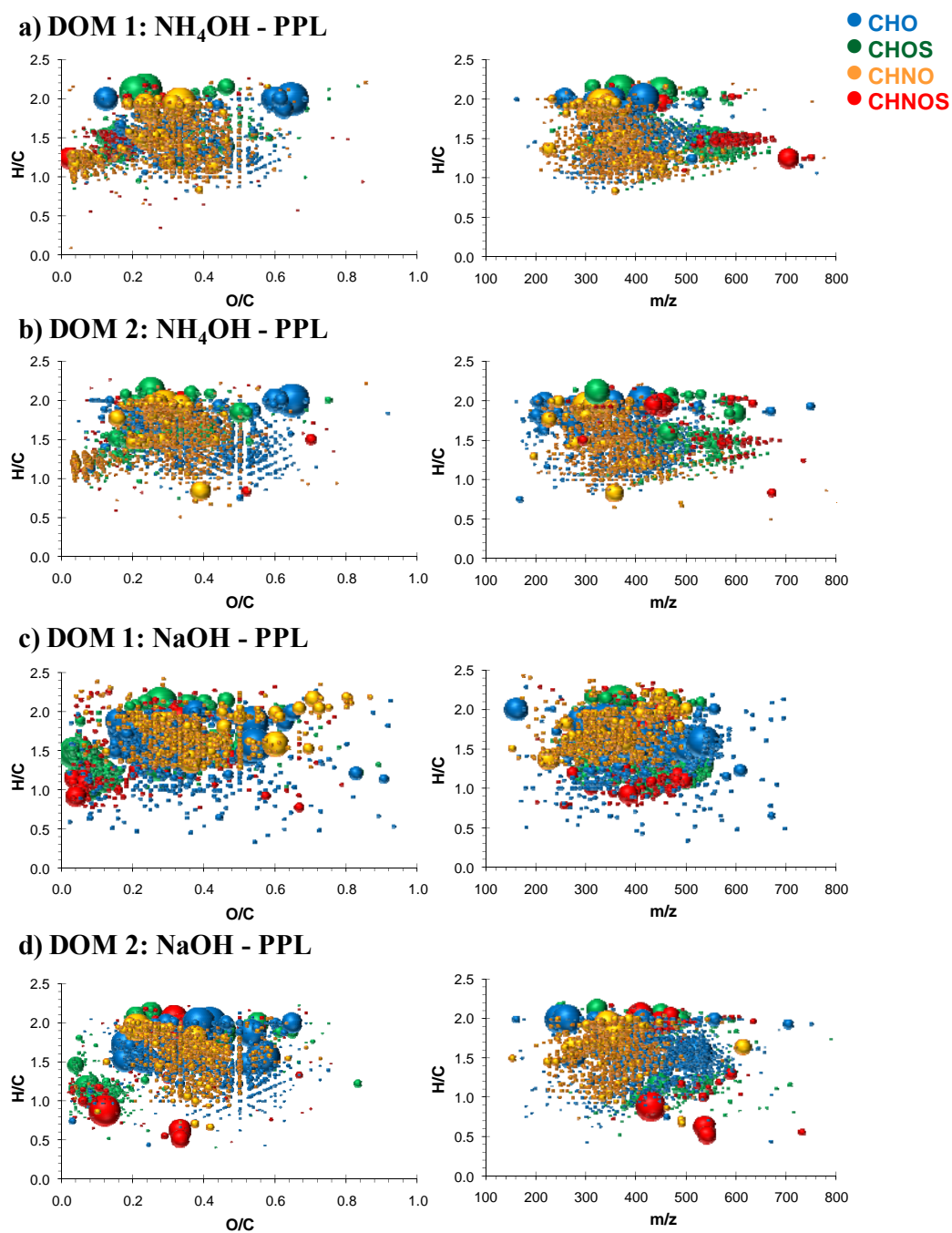


**Figure 2.** Van Krevelen diagrams and H/C ratio vs mass-to-charge ( $m/z$ ) plots for all formulas assigned of DOM extracted from the Used Membranes: a) DOM 1 extracted with  $\text{NH}_4\text{OH}$  alkaline solution and SPE-PPL, b) DOM 2 extracted with  $\text{NH}_4\text{OH}$  alkaline solution and SPE-PPL c) DOM 1 extracted with  $\text{NaOH}$  alkaline solution and SPE-PPL, d) DOM 2 extracted with  $\text{NaOH}$  alkaline solution and SPE-PPL, on color-coded composition: CHO (blue), CHOS (green), CHNO (orange), CHNOS (red). Circular areas indicate relative mass peak intensity.

### ***DOM from fouled Nanofiltration Membranes***

DOM extracted from the Used Membranes was characterized by means of FT-ICR mass spectrometry; respective van Krevelen plots (Figure 2) show the regular patterns of the compositional space, as typically observed in DOM of various origin<sup>27,28</sup>.

With more than 1500 assigned mass peaks between  $m/z$  150–800, the CHO and CHNO compounds were the major components of the DOM extracted from the membranes (57 - 75 % of assigned formulas) (see Table 1, Figure 2) and the fraction of CHOS and CHNOS compounds ranged near 13 and 26 %. As a consequence, the content of nitrogen and sulfur is significant here (around 1.9 - 2.6 % and 2.0 - 4.0 %, respectively). Considering the properties of the feed water (Table 1), the nitrogen and sulfur dissolved molecules containing seemed to be concentrated on the membrane surface.

A similar phenomenon was observed with the Brine samples of the same pilot plant<sup>13</sup>. The Brine samples presented higher content of oxygen and nitrogen in comparison to Permeate samples, leading to the conclusion that the NF process preferentially removed these (more hydrophilic) compounds. Regarding the results obtained in the present study, the DOM molecules that preferentially adsorb onto the membranes, presented a high content of nitrogen, sulfur and oxygen and so they are suspected to be more functionalized. The interaction of these molecules with the negatively charged and hydrophobic membrane is more effective for these compounds, and so they are better removed; but they are also much more strongly adsorbed. Furthermore, the brine effluent interacts for longer time with the membrane surface and so, the brine organic molecules may be more susceptible to membrane adsorption.

The design of the pilot plant allowed comparing the performance of the two NF membranes under the influence of identical feed water. Explicit trends are not easily apparent from the computed average values of H, C, N, O and S (atom %), DBE and the DBE/C, H/C, O/C, C/N and C/S ratios: i) the oxygen content is slightly higher in DOM 2 and ii) the sulfur content is significantly higher in DOM 1. When comparing absence/presence of the assigned formulas for each sample (DOM 1 vs DOM 2, see SI Figure S2b), we observed that only around 30 and 50 % common  $m/z$  (see SI Table S9). The  $m/z$  unique to DOM 1 and DOM 2 have been plotted separately (see SI Figures S8 and S9). The van Krevelen diagram showed that CHOS compounds are more enhanced in DOM 1, as well as compounds with higher DBE values (more unsaturated compounds,

H/C < 1.5). In contrast, the van Krevelen diagram from DOM 2 showed that rather saturated compounds with H/C > 1.5 were more enriched. Moreover, in DOM 2, CHO and CHNO compounds were found more abundant and as a consequence the oxygen and nitrogen contents of DOM were higher. The differences between DOM 1 and DOM 2 reveal that DOM interacts and adsorbs differently depending on the membrane properties. These conclusions have been reached before at bulk level<sup>7,8,10</sup>, but without dependable molecular level information.

**Structural information obtained from <sup>1</sup>H NMR spectra.** Regarding the structural information obtained from <sup>1</sup>H NMR spectra, the extracts obtained from Blank and Used Membranes present smooth bulk envelopes, reflecting intrinsic averaging from massive signal overlap of NMR resonances supposedly derived from membrane polymers and DOM (see SI Figure S10 and S11). In Figure 3, the difference spectra have been normalized to identical areas of total integral from  $\delta_H \sim 0.5$ -9.5 ppm (excluding residual water, methanol and formic acid) (see NMR section integrals in Table 2 and SI Table S10) showing the fundamental substructures from higher to lower field (from right to left): pure aliphatic  $\delta_H \sim 0.5$ -1.25 ppm,  $\underline{\mathbf{H}}_3\mathbf{C}$ -C-C; polymethylene group  $\delta_H \sim 1.25$ -1.35 ppm,  $(\underline{\mathbf{C}}\underline{\mathbf{H}}_2)_n$ ; functionalized aliphatics  $\delta_H \sim 1.35$ -1.9 ppm,  $\underline{\mathbf{H}}\mathbf{C}$ -C-CO and  $\underline{\mathbf{H}}\mathbf{C}$ -CN and  $\underline{\mathbf{H}}\mathbf{C}$ -CS; “acetate-analogue” and carboxyl-rich alicyclic materials (CRAM)  $\delta_H \sim 1.9$ -3.1 ppm,  $\underline{\mathbf{H}}\mathbf{C}$ -C-O; “carbohydrate-like” and methoxy  $\delta_H \sim 3.1$ -4.9 ppm,  $\underline{\mathbf{H}}\mathbf{C}\mathbf{O}$ ; olefins  $\delta_H \sim 5.3$ -7.0 ppm  $\underline{\mathbf{H}}\mathbf{C}=\mathbf{C}$ ,  $\underline{\mathbf{H}}\mathbf{C}\mathbf{O}_2$ ; and aromatic  $\delta_H \sim 7.0$ -9.5 ppm,  $\underline{\mathbf{H}}_{\text{ar}}$  NMR resonances.

The two different alkaline DOM extracts showed notable differences, differences in their <sup>1</sup>H NMR spectra, analogous to respective FT-ICR mass spectra. The main divergence has been observed in the aliphatic section, specially for the pure aliphatic ( $\delta_H \sim 0.5$ -1.25 ppm,  $\underline{\mathbf{H}}_3\mathbf{C}$ -C-C) and the polymethylene regions ( $\delta_H \sim 1.25$ -1.35 ppm,  $(\underline{\mathbf{C}}\underline{\mathbf{H}}_2)_n$ ), although the total integral of the area ( $\delta_H \sim 0.5$ -1.9 ppm) does not present much variation.

Considering both Blank Membranes (B1 and B2), the total aliphatic section ( $\delta_H \sim 0.5$ -1.9 ppm) was most predominant, with more than 60% of total <sup>1</sup>H NMR section integral, followed by the sections for “acetate-analogue” CRAM ( $\delta_H \sim 1.9$ -3.1 ppm) and “carbohydrate-like” methoxy ( $\delta_H \sim 3.1$ -4.9 ppm) in descending abundance (see SI Table S10). Slight differences were detected between the two dissimilar membrane extracts, as expected. For B2, the regions  $\delta_H \sim 1.35$ -1.9 ppm and  $\delta_H \sim 5.3$ -7.0 ppm were enhanced in

comparison to B1, whereas, the region  $\delta_{\text{H}} \sim 1.9\text{-}3.1$  ppm was enhanced for B1. Regarding the FT-ICR mass spectra, the higher proportion of region  $\delta_{\text{H}} \sim 1.35\text{-}1.9$  ppm NMR resonances might indicate presence of heteroatoms in functionalized aliphatic units of the polymers, such as  $\underline{\text{H}}\text{C-C-S}$  and  $\underline{\text{H}}\text{C-C-N}$  functionalities, which is in accordance with the higher content of heteroatoms (nitrogen and sulfur) in B2 as deduced from mass spectra. In contrast, elevated  $^1\text{H}$  NMR-derived nominal unsaturation ( $\delta_{\text{H}} \sim 5.3 - 7.0$  ppm) in B2 at first seems to contradict FTMS-based conclusions; however  $\text{HCO}_2$ -units at  $\delta_{\text{H}} \sim 5.3$  may resonate here (Figure 3).

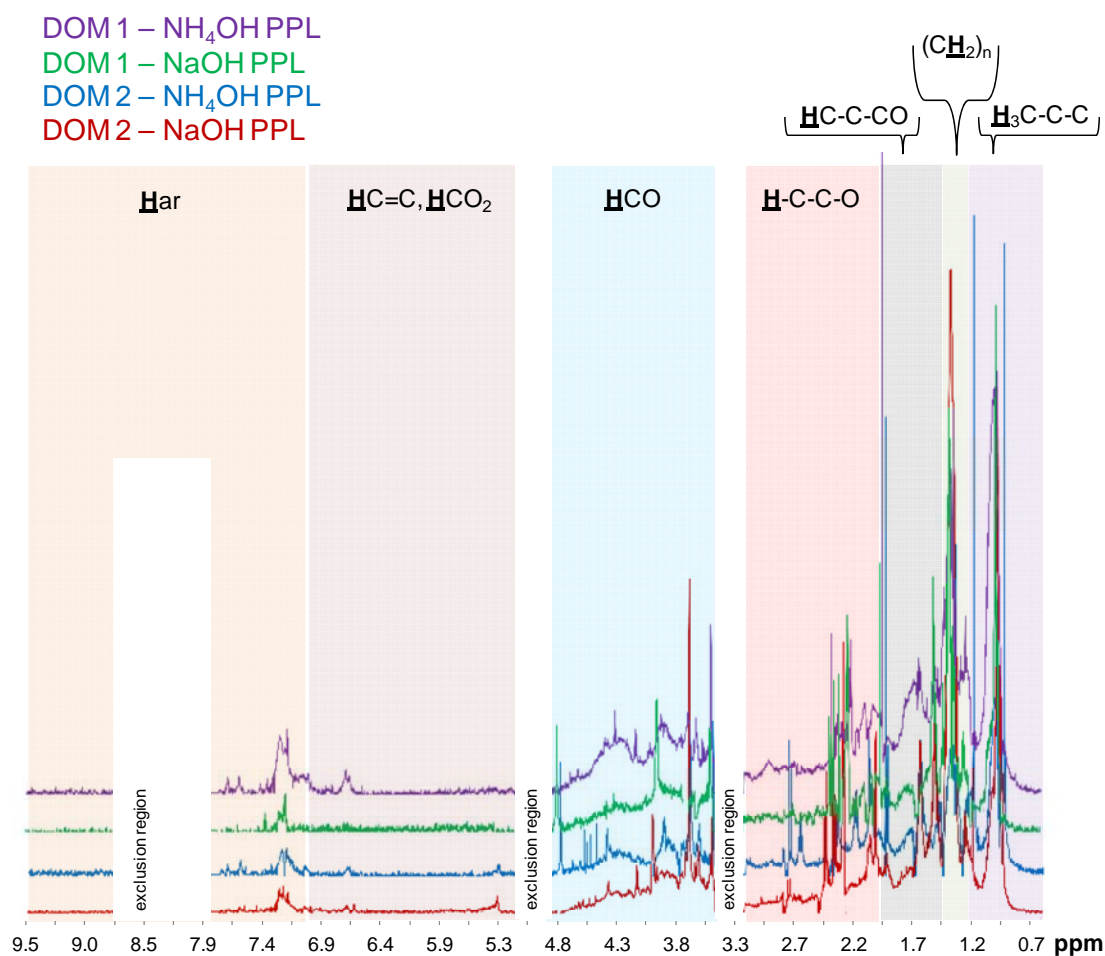


**Figure 3.**  $^1\text{H}$  NMR spectra of (purple): DOM 1 extracted with  $\text{NH}_4\text{OH}$  alkaline solution and SPE-PPL, (blue): DOM 2 extracted with  $\text{NH}_4\text{OH}$  alkaline solution and SPE-PPL, (green): DOM 1 extracted with  $\text{NaOH}$  alkaline solution and SPE-PPL, (red): DOM 2 extracted with  $\text{NaOH}$  alkaline solution and SPE-PPL, plotted as the difference spectra from each Blank (B) and Used Membrane (M), respectively (see SI Figure S10 and S11). The difference spectra have been normalized to identical areas of total integral from  $\delta_{\text{H}} \sim 0.5\text{-}9.5$  ppm (excluding residual water, methanol and formic acid). Fundamental substructures are indicated from higher to lower field (from right to left): pure aliphatic  $\delta_{\text{H}} \sim 0.5\text{-}1.25$  ppm,  $\underline{\text{H}}_3\text{C-C-C}$ ; polymethylene group  $\delta_{\text{H}} \sim 1.25\text{-}1.35$  ppm,  $(\underline{\text{C}}\underline{\text{H}}_2)_n$ ; functionalized aliphatics  $\delta_{\text{H}} \sim 1.35\text{-}1.9$  ppm,  $\underline{\text{H}}\text{C-C-CO}$ ,  $\underline{\text{H}}\text{C-CN}$  and  $\underline{\text{H}}\text{C-CS}$ ; “acetate-analogue” and carboxyl-rich alicyclic materials (CRAM)  $\delta_{\text{H}} \sim 1.9\text{-}3.1$  ppm,  $\underline{\text{H}}\text{C-C-O}$ ; “carbohydrate-like” and methoxy  $\delta_{\text{H}} \sim 3.1\text{-}4.9$  ppm,  $\underline{\text{H}}\text{CO}$ ; olefins  $\delta_{\text{H}} \sim 5.3\text{-}7.0$  ppm  $\underline{\text{H}}\text{C=C}$ ,  $\underline{\text{H}}\text{CO}_2$ ; and aromatic  $\delta_{\text{H}} \sim 7.0\text{-}9.5$  ppm,  $\underline{\text{H}}_{\text{ar}}$  NMR resonances.

$^1\text{H}$  NMR spectra of Blank (B1 and B2) and Used Membrane extracts (M1 and M2), showed abundance variation of the fundamental substructures (see Table S10 and Figures S10 and S11). In M1 and M2, the total aliphatic section is still the most dominant, with more than 50% of total  $^1\text{H}$  NMR section integral (see Table 2). However compared with B1 and B2 extracts it is decreased (especially in polymethylene section) in favour of the “acetate-analogue” and CRAM ( $\delta_{\text{H}} \sim 1.9\text{-}3.1$  ppm) and “carbohydrate-like” and methoxy ( $\delta_{\text{H}} \sim 3.1\text{-}4.9$  ppm) which both contributed about 20 % to the  $^1\text{H}$  NMR section integral. Compared to feed water and brine, the DOM on the NF membranes presented a major contribution in the “carbohydrate-like” and methoxy region ( $\delta_{\text{H}} \sim 3.1\text{-}4.9$  ppm), whereas the total aliphatic region ( $\delta_{\text{H}} \sim 0.5\text{-}1.9$  ppm) was diminished. It seems that in accordance to FT-ICR data, DOM adsorbed on the membranes seemed to be more functionalized, and perhaps represented carbohydrate-rich materials, like cellular exudates.

**Organic Fouling.** Organic fouling remains poorly understood, because it is very specific to the characteristics of the foulant molecules<sup>8</sup>. HRMS and NMR provide the most direct relationship between measured variable and molecular properties and are the most selective technique to characterize DOM with molecular precision. This study provides new insights about DOM molecular features associated with membrane fouling, and enables revised hypotheses about the factors causing organic fouling. It has been shown that the membrane properties and feed water organic matter influence the type of foulant<sup>7,8</sup>, but until now membrane autopsy remains the most effective way to investigate the fouling process. Furthermore, it seems that brine effluents can provide valuable clues of the kind of molecules that might adsorb on the membranes, without the necessity to sacrifice any module. Further studies with different fouling types (different feeding inlets) and membranes should be carried out to further develop these assessments.

## ACKNOWLEDGEMENTS

The authors are grateful to the International Humic Substance Society for the Training Grant that has enabled the collaboration between the Mass Spectrometry Laboratory / Organic Pollutants (IDAEA-CSIC) and Helmholtz Zentrum München, German Research Center for Environmental Health, Research Unit Analytical Biogeochemistry (BGC). The

authors would also like to thank Aigües de Manresa S.A. for providing the facilities required to install and operate the pilot plant.

## AUTHOR CONTRIBUTIONS

N.C.-F. and J.C. designed research. G.R., X.M.-L. and M.R. designed and were in charge of the pilot plant, supplied the membranes and performed most of the complementary analysis. FT-ICR MS and NMR measurements were realized by N.C.-F. under the supervision of M.H., P.S.-K. and N.H. in the Helmholtz Zentrum München, German Research Center for Environmental Health, Research Unit Analytical Biogeochemistry (BGC). M.H. supplied MS mathematical evaluation tools; N.C.-F., M.H. and N.H. analyzed data. N.C.-F. wrote the paper. All the authors contributed significantly in the correction and improvement of the last version of the manuscript.

## SUPPORTING INFORMATION AVAILABLE

Supplementary data as noted in the text can be found in the online version. These include additional materials and methods details, tables and figures. Moreover, a spread sheet data base in excel format includes all the elemental formulas of the samples. This information is available free of charge via the Internet at <http://pubs.acs.org/>.

## REFERENCES

1. Ribera, G.; Clarens, F.; Martínez-Lladó, X.; Jubany, I.; Martí, V.; Rovira, M., Life cycle and human health risk assessments as tools for decision making in the design and implementation of nanofiltration in drinking water treatment plants. *Science of The Total Environment* **2014**, 466-467, (0), 377-386.
2. Verliefde, A. R. D.; Cornelissen, E. R.; Heijman, S. G. J.; Hoek, E. M. V.; Amy, G. L.; Bruggen, B. V. d.; van Dijk, J. C., Influence of Solute–Membrane Affinity on Rejection of Uncharged Organic Solutes by Nanofiltration Membranes. *Environmental Science & Technology* **2009**, 43, (7), 2400-2406.

3. Ates, N.; Yilmaz, L.; Kitis, M.; Yetis, U., Removal of disinfection by-product precursors by UF and NF membranes in low-SUVA waters. *Journal of Membrane Science* **2009**, *328*, 104-112.
4. de la Rubia, À.; Rodríguez, M.; León, V. M.; Prats, D., Removal of natural organic matter and THM formation potential by ultra- and nanofiltration of surface water. *Water Research* **2008**, *42*, (3), 714-722.
5. Bellona, C.; Drewes, J. E.; Xu, P.; Amy, G., Factors affecting the rejection of organic solutes during NF/RO treatment - a literature review. *Water Research* **2004**, *38*, (12), 2795-2809.
6. Verliefde, A.; Cornelissen, E.; Amy, G.; Van der Bruggen, B.; van Dijk, H., Priority organic micropollutants in water sources in Flanders and the Netherlands and assessment of removal possibilities with nanofiltration. *Environmental Pollution* **2007**, *146*, (1), 281-289.
7. Xu, P.; Bellona, C.; Drewes, J. E., Fouling of nanofiltration and reverse osmosis membranes during municipal wastewater reclamation: Membrane autopsy results from pilot-scale investigations. *Journal of Membrane Science* **2010**, *353*, (1-2), 111-121.
8. Schäfer, A. I.; Fane, A. G.; Waite, T. D., *Nanofiltration: Principles and Applications*. Elsevier Advanced Technology, Chapter 8, 2005.
9. Jeong, S.; Kim, S.-J.; Hee Kim, L.; Seop Shin, M.; Vigneswaran, S.; Vinh Nguyen, T.; Kim, I. S., Foulant analysis of a reverse osmosis membrane used pretreated seawater. *Journal of Membrane Science* **2013**, *428*, (0), 434-444.
10. Verliefde, A. R. D.; Cornelissen, E. R.; Heijman, S. G. J.; Petrinic, I.; Luxbacher, T.; Amy, G. L.; Van der Bruggen, B.; van Dijk, J. C., Influence of membrane fouling by (pretreated) surface water on rejection of pharmaceutically active compounds (PhACs) by nanofiltration membranes. *Journal of Membrane Science* **2009**, *330*, 90-103.
11. Matilainen, A.; Gjessing, E. T.; Lahtinen, T.; Hed, L.; Bhatnagar, A.; Sillanpää, M., An overview of the methods used in the characterisation of natural organic matter (NOM) in relation to drinking water treatment. *Chemosphere* **2011**, *83*, (11), 1431-1442.

12. Hertkorn, N.; Harir, M.; Koch, B. P.; Michalke, B.; Schmitt-Kopplin, P., High-field NMR spectroscopy and FTICR mass spectrometry: powerful discovery tools for the molecular level characterization of marine dissolved organic matter. *Biogeosciences* **2013**, *10*, (3), 1583-1624.
13. Cortés-Francisco, N.; Harir, M.; Lucio, M.; Ribera, G.; Martínez-Lladó, X.; Rovira, M.; Schmitt-Kopplin, P.; Hertkorn, N.; Caixach, J., High-field FT-ICR mass spectrometry and NMR spectroscopy to characterize DOM removal through a nanofiltration pilot plant. *Water Research* **2014**, DOI: 10.1016/j.watres.2014.08.046.
14. Schmitt-Kopplin, P.; Gelencsér, A.; Dabek-Zlotorzynska, E.; Kiss, G.; Hertkorn, N.; Harir, M.; Hong, Y.; Gebefügi, I., Analysis of the Unresolved Organic Fraction in Atmospheric Aerosols with Ultrahigh-Resolution Mass Spectrometry and Nuclear Magnetic Resonance Spectroscopy: Organosulfates As Photochemical Smog Constituents. *Analytical Chemistry* **2010**, *82*, (19), 8017-8026.
15. Sleighter, R. L.; Chen, H.; Wozniak, A. S.; Willoughby, A. S.; Caricasole, P.; Hatcher, P. G., Establishing a Measure of Reproducibility of Ultrahigh-Resolution Mass Spectra for Complex Mixtures of Natural Organic Matter. *Analytical Chemistry* **2012**, *84*, (21), 9184-9191.
16. Cortés-Francisco, N.; Caixach, J., Molecular Characterization of Dissolved Organic Matter through a Desalination Process by High Resolution Mass Spectrometry. *Environmental Science & Technology* **2013**, *47*, (17), 9619-9627.
17. Luo, M.; Wang, Z., Complex fouling and cleaning-in-place of a reverse osmosis desalination system. *Desalination* **2001**, *141*, (1), 15-22.
18. Lee, H.; Amy, G.; Cho, J.; Yoon, Y.; Moon, S.-H.; Kim, I. S., Cleaning strategies for flux recovery of an ultrafiltration membrane fouled by natural organic matter. *Water Research* **2001**, *35*, (14), 3301-3308.
19. Amrani, A.; Turner, J. W.; Ma, Q.; Tang, Y.; Hatcher, P. G., Formation of sulfur and nitrogen cross-linked macromolecules under aqueous conditions. *Geochimica et Cosmochimica Acta* **2007**, *71*, (17), 4141-4160.
20. McKee, G. A.; Hatcher, P. G., Alkyl amides in two organic-rich anoxic sediments: A possible new abiotic route for N sequestration. *Geochimica et Cosmochimica Acta* **2010**, *74*, (22), 6436-6450.

21. Gonsior, M.; Zwartjes, M.; Cooper, W. J.; Song, W.; Ishida, K. P.; Tseng, L. Y.; Jeung, M. K.; Rosso, D.; Hertkorn, N.; Schmitt-Kopplin, P., Molecular characterization of effluent organic matter identified by ultrahigh resolution mass spectrometry. *Water Research* **2011**, *45*, (9), 2943-2953.
22. Sleighter, R. L.; McKee, G. A.; Hatcher, P. G., Direct Fourier transform mass spectral analysis of natural waters with low dissolved organic matter. *Organic Geochemistry* **2009**, *40*, (1), 119-125.
23. Mesfioui, R.; Love, N. G.; Bronk, D. A.; Mulholland, M. R.; Hatcher, P. G., Reactivity and chemical characterization of effluent organic nitrogen from wastewater treatment plants determined by Fourier transform ion cyclotron resonance mass spectrometry. *Water Research* **2012**, *46*, (3), 622-634.
24. Kido Soule, M. C.; Longnecker, K.; Giovannoni, S. J.; Kujawinski, E. B., Impact of instrument and experiment parameters on reproducibility of ultrahigh resolution ESI FT-ICR mass spectra of natural organic matter. *Organic Geochemistry* **2010**, *41*, (8), 725-733.
25. Minor, E. C.; Steinbring, C. J.; Longnecker, K.; Kujawinski, E. B., Characterization of dissolved organic matter in Lake Superior and its watershed using ultrahigh resolution mass spectrometry. *Organic Geochemistry* **2012**, *43*, (0), 1-11.
26. Mänttari, M.; Pekuri, T.; Nyström, M., NF270, a new membrane having promising characteristics and being suitable for treatment of dilute effluents from the paper industry. *Journal of Membrane Science* **2004**, *242*, (1-2), 107-116.
27. Hertkorn, N.; Frommberger, M.; Witt, M.; Koch, B. P.; Schmitt-Kopplin, P.; Perdue, E. M., Natural Organic Matter and the Event Horizon of Mass Spectrometry. *Analytical Chemistry* **2008**, *80*, (23), 8908-8919.
28. Sleighter, R. L.; Hatcher, P. G., Molecular characterization of dissolved organic matter (DOM) along a river to ocean transect of the lower Chesapeake Bay by ultrahigh resolution electrospray ionization Fourier transform ion cyclotron resonance mass spectrometry. *Marine Chemistry* **2008**, *110*, (3-4), 140-152.

### 4.3. Discussion

HRMS was used to provide information on a molecular level of marine DOM evolution through a desalination process and freshwater DOM evolution through different NF membranes. Pilot-scale treatment operations were conducted and different sampling campaigns were carried out along the treatment lines. These studies have evaluated the changes in DOM through different treatment stages, which is a critical aspect to better describe the effect of different treatments (UF, NF and RO).

Pretreatment is usually necessary to remove mineral, particulate, organic and biological contaminants that can negatively affect the performance of RO and NF membranes. In both treatment lines UF was used as pretreatment. It was observed that UF had no or little effect on DOM. The high degree of order of DOM in raw water (seawater and pretreated surface water) was still present in UF effluents. An example is shown in Figure 4.7.

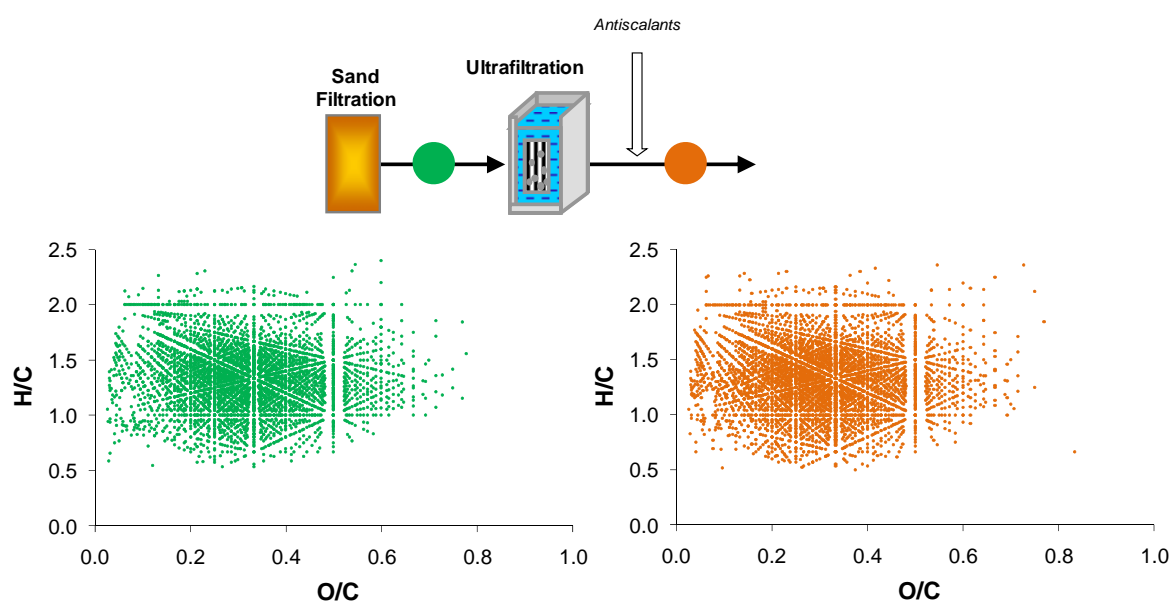


**Figure 4.7.** Van Krevelen diagrams of the pretreated surface water before and after the UF process from the sampling campaign in June for the UF-NF pilot plant.

In addition, no cut-off regarding the mass-to-charge ratio was observed in the UF stage. Regarding other conventional analysis carried out in the same samples (see Table 4.4), parameters more related to particulate (i.e. silt density index - SDI) are the only ones changing significantly.

**Table 4.4.** Summary of some complementary analysis performed on the samples.

Parameters	UF-RO pilot plant <sup>a</sup>			UF-NF pilot plant <sup>b</sup>			
	Raw Seawater	UF effluent	Permeate effluent	Pretreated Surfacewater	UF effluent	UF effluent + antiscalants	Permeate effluent <sup>c</sup>
NPOC (mg C/L)	0.72±0.01	0.71±0.01	0.01±0.01	2.5±0.036	2.5±0.7	3.9±2.2	0.29±0.2
Conductivity (mS/cm)	56.5±0.3	56.4±0.5	0.41±0.03	0.59±0.01	0.59±0.02	0.9±0.4	0.26±0.1
SDI (%/min)	22.7	2.2	N/A	5.2±1.7	< 3	< 3	N/A

N/A: no data available.

<sup>a</sup>The mean value ± standard deviation of n=3 is shown (when available).

<sup>b</sup>The mean value ± standard deviation of the two sampling campaigns is shown.

<sup>c</sup> Permeate effluents from NF membrane 1 and 2 are considered together.

These observations are in accordance with some previous studies (Verliefde et al., 2009b) and it can be concluded that UF is essentially affecting the particulate fraction. In addition, it was shown that antiscalants have no direct effect on DOM, even though they can control calcium and magnesium salts from precipitation and their concentration can affect the organic matter rejection (Her et al., 2000).

On the other hand, it has been shown that the NF and RO membranes have a large effect on DOM. When the water is treated in the NF or RO modules, some of the recurring periodical patterns from DOM are lost, in more extent with the RO process. Generally speaking, NF and RO membranes caused a huge attenuation of DOM.

The main group of compounds found on the Permeates correspond to molecules with less atoms of oxygen and more atoms of hydrogen that could be classified as *lipid-like* (see section 3.1.3. Figura 3.8, page 104). Compared to the water at the inlet of the membranes, these effluents present more aliphatic character with higher H/C ratios (see Table 4.5 below). Not surprisingly, compounds such as fatty-acids and linear alkyl benzene sulfonates (LAS) are found in the Permeates (Figure 4.8). Moreover, from the study of the UF-NF pilot plant additional analyses could be performed. With the NMR measurements, the HRMS data was corroborated and provided more information at structural level. As shown in Table 2 (section 4.2.2., page 187-188) when the water was treated in the NF membranes the integrals from NMR regions involving oxygen atoms (CRAM and functionalized aliphatics) were decreased in some cases by more than 50%.

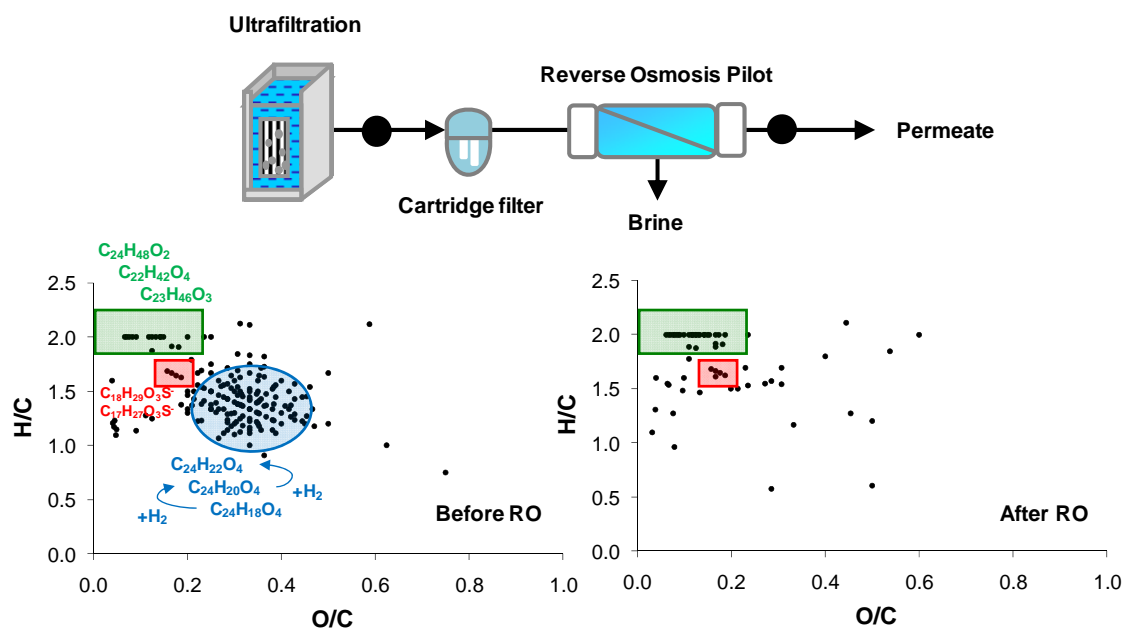


**Figure 4.8.** Van Krevelen diagrams of marine DOM before and after the RO process. In the van Krevelen diagrams the different type of compounds identified are highlighted with different colors and few formulas are given as examples: i) highly saturated structures (high H/C) with low oxygen content (green); ii) anthropogenic compounds identified (LAS) (red); iii) unsaturated compounds with higher number of oxygen atoms (high O/C) (blue).

On the other hand, compounds more functionalized with higher content of oxygen and nitrogen are not capable of going through the membranes and appeared to be slightly concentrated in the brines.

**Table 4.5.** Summary of the main characteristics of the formulas identified by negative ESI-HRMS. For further details see also Table 1 in section 4.2.1. page 164 and Table 1 in section 4.2.2. page 185-186.

Parameters	UF-RO pilot plant			UF-NF pilot plant <sup>a</sup>			
	Seawater	UF effluent	Permeate effluent	Surface water	UF effluent	UF effluent + antiscalants	Permeate effluent <sup>b</sup>
$H/C_{av}$	1.43	1.46	1.72	$1.37\pm 0.01$	$1.36\pm 0.02$	$1.35\pm 0.01$	$1.76\pm 0.06$
$O/C_{av}$	0.32	0.29	0.18	$0.30\pm 0.01$	$0.30\pm 0.02$	$0.30\pm 0.01$	$0.19\pm 0.01$
$DBE_{av}$	6.2	5.8	3.6	$7.7\pm 0.1$	$7.8\pm 0.3$	$8.0\pm 0.4$	$3.3\pm 0.6$
$DBE/C_{av}$	0.35	0.33	0.21	$0.37\pm 0.01$	$0.38\pm 0.01$	$0.38\pm 0.01$	$0.18\pm 0.03$

<sup>a</sup> The mean value  $\pm$  standard deviation of the two sampling campaigns is shown.

<sup>b</sup> Permeate effluents from NF membrane 1 and 2 are considered together.

These studies demonstrate that ESI-HRMS is selective to evaluate the performance of a water treatment plant, characterizing which effects each step treatment in DOM has. Moreover, the selectivity and specificity of HRMS permitted to characterize the slight molecular selectivity of DOM between two dissimilar NF membranes (see Figure A10

and Figure A11 in Appendix B, pages 288-289), which was not so obvious using other techniques (aggregate parameters - UV and TOC,  $^1\text{H}$  NMR).

To some extent, these studies as well as some others (Zhang et al., 2012a; Zhang et al., 2012b; Lavonen et al., 2013) allow the water supply industry to employ more effective water treatment strategies. The impact that these NF or RO treatments can have on drinking water quality has been partially studied with the analysis of DBPs. New DBPs regulations require reduction in water TOC contents which may require enhanced or additional stage treatment. It has been shown in previous studies that molecules with a low degree of oxidation (low O/C) were found to be more reactive towards chlorine. DOM from permeate effluents is mainly characterized by these type of compounds, so although large decrease of DOM (and consequently large diminution of DBPs) is achieved by these treatments, regulated and non-regulated DBPs were still be found (see Table A5 page 278 and Figure A12 page 290 in Appendix B). As NF and RO processes have a large effect on molecules containing more heteroatoms, specially oxygen, the addition of an oxidation pretreatment (for instance, with low ozone doses) may help to oxidize DOM and enhance the effectiveness of RO or NF treatments.

HRMS has been mainly used to characterize DOM from different origins (see section 1.2. pages 9-10) and only in very recent studies has been used for the characterization of DOM in water treatment plants. One of the fields where this technique has not been used before is on the characterization of membrane fouling. If DOM is supposed to cause organic fouling, HRMS would give information at molecular level of these deposits.

In the present study, the extraction protocol was optimized testing different amounts of membrane, temperature and alkaline solutions. Analysis of blanks and used membranes have been carried out. Additional information was available as the water feeding the membranes was very well characterized in a previous study, as well as the permeate and brine effluents. Considering the properties of the feed water, the DOM on the membrane surface seemed to be containing more compounds with sulfur and nitrogen. These compounds with higher content of heteroatoms are suspected to be more functionalized and so it seems that the interaction of these molecules with the membranes is more effective, leading to two consequences: i) these compounds are better rejected which will explain why these compounds are slightly concentrated in the brine; and ii) they are much more adsorbed on membrane surface.

Membrane autopsy using HRMS provided molecular information of organic fouling. This destructive analysis is most of the time necessary to classify the occurring fouling. However, with the data of the studies it has been shown that brine effluents can give an idea of the kind of molecules susceptible of adsorbing on the membrane surfaces.



# **Chapter 5.**

# **Conclusions**

---



The specific conclusions extracted from each one of the three chapters have already been discussed. The general conclusions referred to the overall work are:

- High resolution mass spectrometry has demonstrated to be a very powerful technique for the characterization of target, non-target and unknown compounds in the environment. The studies performed have illustrated the advantages of this technique in front of low resolution tandem mass spectrometry.
- It is difficult to apply a systematic methodology for the characterization of unknowns. In this sense, strict procedures have to be developed in each case to obtain reliable data. Mass accuracy and precision are indispensable parameters that have to be determined.
- The comparative studies of different mass analyzers (QqQ, TOF, FT-ICR and orbitrap) have provided objective information on the advantages and limitations of each technology with regard to: calibration protocols, mass accuracy, resolution, sensitivity and spectral accuracy.
- Due to the complexity of DOM, FT-ICR and FT-Orbitrap are the only mass analyzers capable of resolving individual signals of DOM. Strict protocols in mass measurement and data processing have to be applied to ensure the assignment of the molecular formulas.
- The isolation of DOM without the necessity of filtration step has been successfully applied, using liquid-liquid extraction methodology. This technique has shown to be efficient for DOM concentration in different water bodies.
- New structural information has been obtained, based on a high resolution tandem mass spectrometry method developed. From the results obtained, it can be concluded that coastal marine DOM molecules, although structurally homogeneous, might be richer in diversity of functional groups than previously described.
- Isolation of DOM and structural elucidation experiments are the procedures, where larger improvements should be made.
- High resolution mass spectrometry is a very selective technique that can be used to characterize DOM changes at molecular level through different treatment plants.
- Behavior at molecular level of DOM through advanced treatments based on membrane technology (UF, NF and RO) has been described.

- These studies provide information on the effects that each treatment step has in DOM and may allow the water supply industry to employ more effective water treatment strategies.

- A method for the characterization of DOM adsorbed on membrane surface has been developed and successfully applied. Information on the types of molecules preferably adsorbed on membrane surface has been obtained. With the data of the studies it has been shown that brine effluents can give a clue about the kind of molecules susceptible of adsorbing on the membrane surfaces.

## References

- Aiken, G.R., McKnight, D.M., Thorn, K.A., Thurman, E.M. (1992) Isolation of hydrophilic organic acids from water using nonionic macroporous resins. *Organic Geochemistry* 18 (4), 567-573.
- Allpike, B.P., Heitz, A., Joll, C.A., Kagi, R.I., Abbt-Braun, G., Frimmel, F.H., Brinkmann, T., Her, N., Amy, G. (2005) Size Exclusion Chromatography To Characterize DOC Removal in Drinking Water Treatment. *Environmental Science & Technology* 39 (7): 2334-2342.
- Altieri, K.E., Turpin, B.J., Seitzinger, S.P. (2009) Composition of Dissolved Organic Nitrogen in Continental Precipitation Investigated by Ultra-High Resolution FT-ICR Mass Spectrometry. *Environmental Science & Technology* 43 (18): 6950-6955.
- Amery, F., Degryse, F., Cheyns, K., De Troyer, I., Mertens, J., Merckx, R., Smolders, E. (2008) The UV-absorbance of dissolved organic matter predicts the fivefold variation in its affinity for mobilizing Cu in an agricultural soil horizon. *European Journal of Soil Science* 59 (6) : 1087-1095
- Barco, M., Planas, C., Palacios, O., Ventura, F., Rivera, J., Caixach, J. (2003) Simultaneous Quantitative Analysis of Anionic, Cationic, and Nonionic Surfactants in Water by Electrospray Ionization Mass Spectrometry with Flow Injection Analysis. *Analytical Chemistry* 75 (19), 5129-5136.
- Baruth, E.E. (Ed) (2004) Water Treatment Plant Design. American Water Works Association American Society of Civil Engineers. McGraw-Hill, 4<sup>th</sup> Edition.
- Beckmann, M., Parker, D., Enot, D.P., Duval, E. and Draper, J. (2008) High-throughput, nontargeted metabolite fingerprinting using nominal mass flow injection electrospray mass spectrometry. *Nat. Protocols* 3(3), 486-504.
- Beißmann, S., Reisinger, M., Toelgyesi, L., Klampfl, C. and Buchberger, W. (2013) Fast screening of stabilizers in polymeric materials by flow injection-tandem mass spectrometry. *Analytical and Bioanalytical Chemistry* 405(21), 6879-6884.
- Beynon, J.H. (1954). Qualitative analysis of organic compounds by mass spectrometry. *Nature* 174, 735–37.

- Beynon, J.H. (1960) *Mass Spectrometry and Its Applications to Organic Chemistry*, 1<sup>st</sup> Edition. Elsevier, London.
- Bhandari, D. and Van Berkel, G.J. (2012) Evaluation of Flow-Injection Tandem Mass Spectrometry for Rapid and High-Throughput Quantitative Determination of B Vitamins in Nutritional Supplements. *Journal of Agricultural and Food Chemistry* 60(34), 8356-8362.
- Bijlsma, L., Emke, E., Hernández, F. and De Voogt, P. (2013) Performance of the linear ion trap Orbitrap mass analyzer for qualitative and quantitative analysis of drugs of abuse and relevant metabolites in sewage water. *Analytica Chimica Acta* 768 (1), 102-110.
- Blake, S., Walker, S.H., Muddiman, D., Hinks, D. and Beck, K. (2011) Spectral Accuracy and Sulfur Counting Capabilities of the LTQ-FT-ICR and the LTQ-Orbitrap XL for Small Molecule Analysis. *Journal of the American Society for Mass Spectrometry* 22(12), 2269-2275.
- Blondeau, R. (1986) Comparison of soil humic and fulvic-acids of similar molecular-weight. *Organic Geochemistry* 9 (1): 47-50.
- Boehme, J., Wells, M. (2006) Fluorescence variability of marine and terrestrial colloids: Examining size fractions of chromophoric dissolved organic matter in the Damariscotta River estuary. *Marine Chemistry* 101 (1-2) :95-103
- Borman S., Russell H., Siuzdak G. (2003) *A Mass Spec Timeline*. American Chemical Society.
- Bristow, A.W.T., Webb, K.S. (2003) Intercomparison study on accurate mass measurement of small molecules in mass spectrometry. *Journal of the American Society for Mass Spectrometry* 14, (10), 1086-1098.
- Bruins, A.P. (1998) Mechanistic aspects of electrospray ionization. *Journal of Chromatography A* 794 (1-2), 345-357.
- Brunnée, C. (1987) The ideal mass analyzer: Fact or fiction? *International Journal of Mass Spectrometry and Ion Processes* 76 (2), 125-237.
- Burdige, D.J., Kline, S.W., Chen, W. (2004) Fluorescent dissolved organic matter in marine sediment pore waters. *Marine Chemistry* 89 (1-4) :289-311.

- Cabaleiro, N., de la Calle, I., Bendicho, C. and Lavilla, I. (2013) Current trends in liquid-liquid and solid-liquid extraction for cosmetic analysis: a review. *Analytical Methods* 5 (2), 323-340.
- Camper, A.K. (2004) Involvement of humic substances in regrowth. *International Journal of Food Microbiology* 92 (3), 355-364.
- Cole, R.B. (ed) (2012) *Electrospray and MALDI Mass Spectrometry: Fundamentals, Instrumentation, Practicalities, and Biological Applications*, Second Edition. John Wiley & Sons, Inc. Hoboken, NJ, USA.
- Cooks, R.G., Ouyang, Z., Takáts, Z., Wiseman, J.M. (2006) Ambient mass spectrometry. *Science* 311, 1566.
- D'Andrilli, J., Dittmar, T., Koch, B.P., Purcell, J.M., Marshall, A.G., Cooper, W.T. (2010) Comprehensive characterization of marine dissolved organic matter by Fourier transform ion cyclotron resonance mass spectrometry with electrospray and atmospheric pressure photoionization. *Rapid Communications in Mass Spectrometry* 24 (5): 643-650.
- Dittmar, T., Koch, B., Hertkorn, N. and Kattner, G. (2008) A simple and efficient method for the solid-phase extraction of dissolved organic matter (SPE-DOM) from seawater. *Limnology and Oceanography: Methods*, 6 , pp. 230-235.
- Donegan, M., Browning, M. (2012) A Review: Recent Developments in Sample Ionization Interfaces used in Mass Spectrometry. *Journal of Liquid Chromatography & Related Technologies* 35(16), 2345-2363.
- Draper, J., Lloyd, A., Goodacre, R. and Beckmann, M. (2013) Flow infusion electrospray ionisation mass spectrometry for high throughput, non-targeted metabolite fingerprinting: a review. *Metabolomics* 9 (1), 4-29.
- Eikebrokk, B., Vogt, R. D., Liltved, H. (2004) NOM increase in Northern European source waters: Discussion of possible causes and impacts on coagulation/contact filtration processes. *Water Science and Technology* 4 (4): 47-54.
- Erve, J.C.L., Gu, M., Wang, Y., DeMaio, W. and Talaat, R.E. (2009) Spectral Accuracy of Molecular Ions in an LTQ/Orbitrap Mass Spectrometer and Implications for Elemental Composition Determination. *Journal of the American Society for Mass Spectrometry* 20(11), 2058-2069.

- European Commission, (2002) Decision 2002/657/EC, Off. J. Eur. Commun. 221, 8.
- European Commission, (2012) Directorate General Health and Consumer Protection, SANCO/12495/2011.
- European Communities (Drinking Water) (No. 2) Regulations. SI. No. 278 of 2007. (<http://www.irishstatutebook.ie/2007/en/si/0278.html>) (Accessed 12/12/2013).
- European Union Water Framework Directive 2008/105/CE
- European Union Water Framework Directive 2013/39/UE
- Flerus, R., Koch, B.P., Schmitt-Kopplin, P., Witt, M. and Kattner, G. (2011) Molecular level investigation of reactions between dissolved organic matter and extraction solvents using FT-ICR MS. *Marine Chemistry* 124 (1-4), 100-107.
- Forcisi, S., Moritz, F., Kanawati, B., Tziotis, D., Lehmann, R. and Schmitt-Kopplin, P. (2013) Liquid chromatography-mass spectrometry in metabolomics research: Mass analyzers in ultra high pressure liquid chromatography coupling. *Journal of Chromatography A* 1292(0), 51-65.
- Frimmel, F.H. and Huber, L. (1996) Influence of humic substances on the aquatic adsorption of heavy metals on defined mineral phases. *Environment International* 22 (5), 507-517.
- Gao, B., Lu, Y., Sheng, Y., Chen, P. and Yu, L. (2013) Differentiating Organic and Conventional Sage by Chromatographic and Mass Spectrometry Flow Injection Fingerprints Combined with Principal Component Analysis. *Journal of Agricultural and Food Chemistry* 61 (12), 2957-2963.
- Gelpí E (2008) From large analogical instruments to small digital black boxes: 40 years of progress in mass spectrometry and its role in proteomics. Part I 1965–1984. *Journal of Mass Spectrometry* 43(4), 419–435.
- Gelpí, E. (2009) From large analogical instruments to small digital black boxes: 40 years of progress in mass spectrometry and its role in proteomics. Part II 1985–2000. *Journal of Mass Spectrometry* 44(8), 1137-1161.
- Gerlich, M. and Neumann, S. (2012) MetFusion: integration of compound identification strategies. *Journal of Mass Spectrometry* 48(3), 291-298.

- Gonsior, M., Peake, B.M., Cooper, W.T., Podgorski, D., D'Andrilli, J. and Cooper, W.J. (2009) Photochemically Induced Changes in Dissolved Organic Matter Identified by Ultrahigh Resolution Fourier Transform Ion Cyclotron Resonance Mass Spectrometry. *Environmental Science & Technology* 43 (3), 698-703.
- Gonsior, M., Peake, B.M., Cooper, W.T., Podgorski, D.C., D'Andrilli, J., Dittmar, T. and Cooper, W.J. (2011a) Characterization of dissolved organic matter across the Subtropical Convergence off the South Island, New Zealand. *Marine Chemistry* 123(1-4), 99-110.
- Gonsior, M., Zwartjes, M., Cooper, W.J., Song, W., Ishida, K.P., Tseng, L.Y., Jeung, M.K., Rosso, D., Hertkorn, N. and Schmitt-Kopplin, P. (2011b) Molecular characterization of effluent organic matter identified by ultrahigh resolution mass spectrometry. *Water Research* 45(9), 2943-2953.
- Green, N.W., Perdue, E.M., Aiken, G.R., Butler, K.D., Chen, H., Dittmar, T., Niggemann, J. and Stubbins, A. (2014) An intercomparison of three methods for the large-scale isolation of oceanic dissolved organic matter. *Marine Chemistry* 161 (0), 14-19.
- Greenlee, L.F., Lawler, D.F., Freeman, B.D., Marrot, B. (2009) Moulin, P., Reverse osmosis desalination: Water sources, technology, and today's challenges, *Water Research* 43, 2317-2348.
- Gross, J.H. (2011) *Mass Spectrometry*. 2nd Edition Springer. Heidelberg, Germany.
- Gross, J.H. (2014) Direct analysis in real time-a critical review on DART-MS. *Analytical and Bioanalytical Chemistry* 406(1), 63-80.
- Gure, A., Lara, F.J., Moreno-González, D., Megersa, N., del Olmo-Iruela, M. and García-Campaña, A.M. (2014) Salting-out assisted liquid-liquid extraction combined with capillary HPLC for the determination of sulfonylurea herbicides in environmental water and banana juice samples. *Talanta* 127(0), 51-58.
- Ham, B.M. (2008) *Even Electron Mass Spectrometry with Biomolecule Applications*, 1st edn. Wiley Interscience, United States of America.
- He, H., Emmett, M.R., Nilsson, C.L., Conrad, C.A. and Marshall, A.G. (2011) High mass accuracy and resolution facilitate identification of glycosphingolipids and phospholipids. *International Journal of Mass Spectrometry* 305 (2-3), 116-119.

- Her, N., Amy, G. and Jarusutthirak, C. (2000) Seasonal variations of nanofiltration (NF) foulants: identification and control. *Desalination* 132 (1-3), 143-160.
- Hernández, F., Sancho, J.V., Ibáñez, M., Abad, E., Portolés, T. and Mattioli, L. (2012) Current use of high-resolution mass spectrometry in the environmental sciences. *Analytical and Bioanalytical Chemistry* 403(5), 1251-1264.
- Hertkorn, N., Claus, H., Schmitt-Kopplin, P., Perdue, E.M. and Filip, Z. (2002) Utilization and Transformation of Aquatic Humic Substances by Autochthonous Microorganisms. *Environmental Science & Technology* 36 (20), 4334-4345.
- Hertkorn, N., Benner, R., Frommberger, M., Schmitt-Kopplin, P., Witt, M., Kaiser, K., Kettrup, A. and Hedges, J.I. (2006) Characterization of a major refractory component of marine dissolved organic matter. *Geochimica et Cosmochimica Acta* 70 (12), 2990-3010.
- Hertkorn, N., Ruecker, C., Meringer, M., Gugisch, R., Frommberger, M., Perdue, E., Witt, M. and Schmitt-Kopplin, P. (2007) High-precision frequency measurements: indispensable tools at the core of the molecular-level analysis of complex systems. *Analytical and Bioanalytical Chemistry* 389 (5), 1311-1327.
- Hertkorn, N., Frommberger, M., Witt, M., Koch, B.P., Schmitt-Kopplin, P. and Perdue, E.M. (2008) Natural Organic Matter and the Event Horizon of Mass Spectrometry. *Analytical Chemistry* 80 (23), 8908-8919.
- Hertkorn, N., Harir, M., Koch, B.P., Michalke, B. and Schmitt-Kopplin, P. (2013) High-field NMR spectroscopy and FTICR mass spectrometry: powerful discovery tools for the molecular level characterization of marine dissolved organic matter. *Biogeosciences* 10 (3), 1583-1624.
- Herzprung, P., Hertkorn, N., Friese, K. and Schmitt-Kopplin, P. (2010) Photochemical degradation of natural organic sulfur compounds (CHOS) from iron-rich mine pit lake pore waters – an initial understanding from evaluation of single-elemental formulae using ultra-high-resolution mass spectrometry. *Rapid Communications in Mass Spectrometry* 24 (19), 2909-2924
- Herzprung, P., von Tümpling, W., Hertkorn, N., Harir, M., Büttner, O., Bravidor, J., Friese, K. and Schmitt-Kopplin, P. (2012) Variations of DOM Quality in Inflows of a Drinking Water Reservoir: Linking of van Krevelen Diagrams with EEMF

Spectra by Rank Correlation. *Environmental Science & Technology* 46(10), 5511-5518.

Holčápek, M., Jirásko, R., Lída, M. (2012) Recent developments in liquid chromatography-mass spectrometry and related techniques. *Journal of Chromatography A* 1259(0), 3-15.

<http://masspec.scripps.edu> (Accessed 23/11/2010)

<http://membrane.ces.utexas.edu/2012/08/09/cen-science-technology-waterworks/>  
(Accessed 29/07/2014)

<http://www.aiguesdebarcelona.cat/documents/10540/21743/monografia.pdf>  
(Accessed 05/08/2014)

[http://www.atll.cat/site/unitFiles/1013/ITAM\\_Llobregat\\_ENG+FR.pdf](http://www.atll.cat/site/unitFiles/1013/ITAM_Llobregat_ENG+FR.pdf)  
(Accessed 05/08/2014)

<http://www.eco-web.com/edi/img/090714-1.gif> (Accessed 25/07/2014).

<http://www.grahamscutt.co.uk> (Accessed 21/07/2014)

<http://www.humicsubstances.org/aquatichafa.html> (Accessed 19/08/2014).

<http://www.humicsubstances.org/whatarehs.html> (Accessed 19/08/2014).

<http://www.scopus.com> (Accessed September 2014).

<http://www.thermoscientific.com/en/about-us/videos/iorbi-remote-orbitrap-pairing.html>  
(Accessed 18/08/2014).

<http://www.unep.com> (Accessed 25/07/2014).

Hu, Q., Noll, R.J., Li, H., Makarov, A., Hardman, M. and Graham Cooks, R. (2005) The Orbitrap: a new mass spectrometer. *Journal of Mass Spectrometry* 40(4), 430-443.

Hudson, N., Baker, A., Reynolds, D. (2007) Fluorescence analysis of dissolved organic matter in natural, waste and polluted waters—a review. *River Research and Applications* 23 (6):631-649

- Jaffé, R., McKnight, D., Maie, N., Cory, R., McDowell, W.H. and Campbell, J.L. (2008) Spatial and temporal variations in DOM composition in ecosystems: The importance of long-term monitoring of optical properties. *Journal of Geophysical Research: Biogeosciences* 113 (G4), G04032.
- Jeong, S., Kim, S.-J., Hee Kim, L., Seop Shin, M., Vigneswaran, S., Vinh Nguyen, T., Kim, I. S. (2013) Fouling analysis of a reverse osmosis membrane used pretreated seawater. *Journal of Membrane Science* 428, (0), 434-444.
- Kaiya, Y., Itoh, Y., Fujita, K. and Takizawa, S. (1996) Study on fouling materials in the membrane treatment process for potable water. *Desalination* 106 (1-3), 71-77.
- Kaufmann, A., Widmer, M. and Maden, K. (2010) Post-interface signal suppression, a phenomenon observed in a single-stage Orbitrap mass spectrometer coupled to an electrospray interfaced liquid chromatograph. *Rapid Communications in Mass Spectrometry* 24(14), 2162-2170.
- Kaufmann, A. (2012) The current role of high-resolution mass spectrometry in food analysis. *Analytical and Bioanalytical Chemistry* 403(5), 1233-1249.
- Kim, S., Kramer, R.W., Hatcher, P.G. (2003) Graphical Method for Analysis of Ultrahigh-Resolution Broadband Mass Spectra of Natural Organic Matter, the Van Krevelen Diagram. *Analytical Chemistry* 75, (20), 5336-5344.
- Kingdon, K.H. (1923) A method for the neutralization of electron space charge by positive ionization at very low gas pressures. *Physical Review* 21, 408-418.
- Koch, B.P., Witt, M., Engbrodt, R., Dittmar, T. and Kattner, G. (2005) Molecular formulae of marine and terrigenous dissolved organic matter detected by electrospray ionization Fourier transform ion cyclotron resonance mass spectrometry. *Geochimica et Cosmochimica Acta* 69 (13), 3299-3308.
- Koch, B.P., Ludwichowski, K.-U., Kattner, G., Dittmar, T. and Witt, M. (2008) Advanced characterization of marine dissolved organic matter by combining reversed-phase liquid chromatography and FT-ICR-MS. *Marine Chemistry* 111(3-4), 233-241.
- Koprivnjak, J.F., Pfromm, P.H., Ingall, E., Vetter, T.A., Schmitt-Kopplin, P., Hertkorn, N., Frommberger, M., Knicker, H. and Perdue, E.M. (2009) Chemical and spectroscopic characterization of marine dissolved organic matter isolated using

- coupled reverse osmosis–electrodialysis. *Geochimica et Cosmochimica Acta* 73 (14), 4215-4231.
- Krasner, S. W., Weinberg, H. S., Richardson, S. D., Pastor, S. J., Chinn, R., Sclimenti, M. J., Onstad, G. D., Thruston, A. D. (2006) Occurrence of a New Generation of Disinfection Byproducts. *Environmental Science & Technology* 40, (23), 7175-7185.
- Krauss, M., Singer, H. and Hollender, J. (2010) LC-high resolution MS in environmental analysis: from target screening to the identification of unknowns. *Analytical and Bioanalytical Chemistry* 397(3), 943-951.
- Kujawinski, E.B., Behn, M.D. (2006) Automated Analysis of Electrospray Ionization Fourier Transform Ion Cyclotron Resonance Mass Spectra of Natural Organic Matter. *Analytical Chemistry* 78, (13), 4363-4373.
- Kujawinski, E.B., Longnecker, K., Blough, N.V., Vecchio, R.D., Finlay, L., Kitner, J.B. and Giovannoni, S.J. (2009) Identification of possible source markers in marine dissolved organic matter using ultrahigh resolution mass spectrometry. *Geochimica et Cosmochimica Acta* 73 (15), 4384-4399.
- Kumar, P., Rúbies, A., Centrich, F., Granados, M., Cortés-Francisco, N., Caixach, J., Companyó, R. (2013) Targeted analysis with benchtop quadrupole-orbitrap hybrid mass spectrometer: Application to determination of synthetic hormones in animal urine. *Analytica Chimica Acta* 780, 65-73.
- Lam, B., Baer, A., Alae, M., Lefebvre, B., Moser, A., Williams, A., Simpson, A.J. (2007) Major Structural Components in Freshwater Dissolved Organic Matter. *Environmental Science & Technology* 41 (24):8240-8247.
- Lavonen, E.E., Gonsior, M., Tranvik, L.J., Schmitt-Kopplin, P. and Köhler, S.J. (2013) Selective Chlorination of Natural Organic Matter: Identification of Previously Unknown Disinfection Byproducts. *Environmental Science & Technology* 47 (5), 2264-2271.
- Lechtenfeld, O.J., Koch, B.P., Gašparović, B., Frka, S., Witt, M. and Kattner, G. (2013) The influence of salinity on the molecular and optical properties of surface microlayers in a karstic estuary. *Marine Chemistry* 150(0), 25-38.

- Leenheer, J.A., Rostad, C.E., Gates, P.M., Furlong, E.T. and Ferrer, I. (2001) Molecular Resolution and Fragmentation of Fulvic Acid by Electrospray Ionization/Multistage Tandem Mass Spectrometry. *Analytical Chemistry* 73 (7), 1461-1471.
- Liu, Z., Sleighter, R.L., Zhong, J., Hatcher, P.G. (2011) The chemical changes of DOM from black waters to coastal marine waters by HPLC combined with ultrahigh resolution mass spectrometry. *Estuarine, Coastal and Shelf Science* 92 (2):205-216.
- Makarov, A. (2000) Electrostatic Axially Harmonic Orbital Trapping: A High-Performance Technique of Mass Analysis. *Analytical Chemistry* 72(6), 1156-1162.
- Makarov, A., Denisov, E. and Lange, O. (2009) Performance Evaluation of a High-field Orbitrap Mass Analyzer. *Journal of the American Society for Mass Spectrometry* 20(8), 1391-1396.
- Malaeb, L., Ayoub, G.M. (2011) Reverse Osmosis technology for water treatment: State of the art review. *Desalination* 267, 1-8.
- Marshall, A.G., Grosshans, P.B. (1991) Fourier transform ion cyclotron resonance mass spectrometry: the teenage years. *Analytical Chemistry* 63(4), 215A-229A.
- Marshall, A.G., Hendrickson, C.L. and Jackson, G.S. (1998) Fourier transform ion cyclotron resonance mass spectrometry: A primer. *Mass Spectrometry Reviews* 17(1), 1-35.
- Marshall, A.G. and Hendrickson, C.L. (2008) High-Resolution Mass Spectrometers. *Annual Review of Analytical Chemistry* 1(1), 579-599.
- Mawhinney, D.B., Rosario-Ortiz, F.L., Baik, S., Vanderford, B.J. and Snyder, S.A. (2009) Characterization of fulvic acids by liquid chromatography-quadrupole time-of-flight mass spectrometry. *Journal of Chromatography A* 1216 (9), 1319-1324.
- McIntyre, C., Barry, D.B., Jardine, D.R. (1997) Electrospray Mass Spectrometry of Groundwater Organic Acids. *Journal of Mass Spectrometry* 32, 328-330.
- Miura, D., Tsuji, Y., Takahashi, K., Wariishi, H. and Saito, K. (2010) A Strategy for the Determination of the Elemental Composition by Fourier Transform Ion Cyclotron

- Resonance Mass Spectrometry Based on Isotopic Peak Ratios. *Analytical Chemistry* 82(13), 5887-5891.
- Mopper, K., Stubbins, A., Ritchie, J.D., Bialk, H.M. and Hatcher, P.G. (2007) Advanced Instrumental Approaches for Characterization of Marine Dissolved Organic Matter: Extraction Techniques, Mass Spectrometry, and Nuclear Magnetic Resonance Spectroscopy. *Chemical Reviews* 107 (2), 419-442.
- Murphy, E.M., Zachara, J.M. and Smith, S.C. (1990) Influence of mineral-bound humic substances on the sorption of hydrophobic organic compounds. *Environmental Science & Technology* 24 (10), 1507-1516.
- Nebbioso, A., Piccolo, A. (2013) Molecular characterization of dissolved organic matter (DOM): a critical review. *Analytical and Bioanalytical Chemistry* 405(1), 109-124.
- Perdue, E.M., Ritchie, J.D. (2003) Dissolved Organic Matter in Fresh Waters. Volume 5: Surface and Ground Water, Weathering, Erosion and Soils. Ed. J.I. Drever. Chapter 11. United Kingdom.
- Pérez-González, A., Urtiaga, A.M., Ibañez, R., Ortiz, I. (2012) State of the art and review on the treatment technologies of water reverse osmosis concentrates. *Water Research* 46, 267-283.
- Perry, R.H., Cooks, R.G., Noll, R.J. (2008) Orbitrap mass spectrometry: Instrumentation, ion motion and applications. *Mass Spectrometry Reviews* 27(6), 661-699.
- Persson, L., Alsberg, T., Kiss, G., Odham, G. (2000) On-line size-exclusion chromatography/electrospray ionisation mass spectrometry of aquatic humic and fulvic acids. *Rapid Communications in Mass Spectrometry* 14: 286-292.
- Pressman, J. G., Richardson, S. D., Speth, T. F., Miltner, R. J., Narotsky, M. G., Hunter, I. I. I. E. S., Rice, G. E., Teuschler, L. K., McDonald, A., Parvez, S., Krasner, S. W., Weinberg, H. S., McKague, A. B., Parrett, C. J., Bodin, N., Chinn, R., Lee, C.-F. T., Simmons, J. E. (2010) Concentration, Chlorination, and Chemical Analysis of Drinking Water for Disinfection Byproduct Mixtures Health Effects Research: U.S. EPA's Four Lab Study. *Environmental Science & Technology* 44, (19), 7184-7192.

- Reemtsma, T. (2001) The use of liquid chromatography-atmospheric pressure ionization-mass spectrometry in water analysis - Part II: Obstacles. *Trends in Analytical Chemistry* 20 (10): 533-542.
- Reemtsma, T., These, A., Linscheid, M., Leenheer, J. and Spitzzy, A. (2008) Molecular and Structural Characterization of Dissolved Organic Matter from the Deep Ocean by FTICR-MS, Including Hydrophilic Nitrogenous Organic Molecules. *Environmental Science & Technology* 42 (5), 1430-1437.
- Reemtsma, T. (2009) Determination of molecular formulas of natural organic matter molecules by (ultra-) high-resolution mass spectrometry: Status and needs. *Journal of Chromatography A* 1216 (18), 3687-3701.
- Remucal, C.K., Cory, R.M., Sander, M. and McNeill, K. (2012) Low Molecular Weight Components in an Aquatic Humic Substance As Characterized by Membrane Dialysis and Orbitrap Mass Spectrometry. *Environmental Science & Technology* 46 (17), 9350-9359.
- Ribera, G. (2013) PhD Thesis. Technical and environmental viability of membrane technologies in water treatment: NF drinking water process and MBR for wastewater reuse. Universitat Politècnica de Catalunya.
- Richardson, S.D., Plewa, M.J., Wagner, E.D., Schoeny, R. and DeMarini, D.M. (2007) Occurrence, genotoxicity, and carcinogenicity of regulated and emerging disinfection by-products in drinking water: A review and roadmap for research. *Mutation Research/Reviews in Mutation Research* 636(1-3), 178-242.
- Sánchez-González, J., García-Otero, N., Moreda-Piñeiro, A. and Bermejo-Barrera, P. (2012) Multi-walled carbon nanotubes - Solid phase extraction for isolating marine dissolved organic matter before characterization by size exclusion chromatography. *Microchemical Journal* 102(0), 75-82.
- Schäfer, A. I., Fane, A. G., Waite, T. D. (2005) *Nanofiltration: Principles and Applications*. Elsevier Advanced Technology, Chapter 8.
- Schmidt, F., Elvert, M., Koch, B.P., Witt, M. and Hinrichs, K.-U. (2009) Molecular characterization of dissolved organic matter in pore water of continental shelf sediments. *Geochimica et Cosmochimica Acta* 73(11), 3337-3358.

- Scigelova, M., Hornshaw, M., Giannakopoulos, A., Makarov, A. (2011) Fourier Transform Mass Spectrometry. *Molecular & Cellular Proteomics* 10 (7).
- Senko, M.W., Hendrickson, C.L., Emmett, M.R., Shi, S.D.H., Marshall, A.G. (1997) External Accumulation of Ions for Enhanced Electrospray Ionization Fourier Transform Ion Cyclotron Resonance Mass Spectrometry. *Journal of the American Society for Mass Spectrometry* 8 (9), 970-976.
- Simjouw, J.-P., Minor, E.C. and Mopper, K. (2005) Isolation and characterization of estuarine dissolved organic matter: Comparison of ultrafiltration and C18 solid-phase extraction techniques. *Marine Chemistry* 96 (3-4), 219-235.
- Sleighter, R.L. and Hatcher, P.G. (2008) Molecular characterization of dissolved organic matter (DOM) along a river to ocean transect of the lower Chesapeake Bay by ultrahigh resolution electrospray ionization Fourier transform ion cyclotron resonance mass spectrometry. *Marine Chemistry* 110 (3-4), 140-152.
- Sleighter, R.L., Liu, Z., Xue, J. and Hatcher, P.G. (2010) Multivariate Statistical Approaches for the Characterization of Dissolved Organic Matter Analyzed by Ultrahigh Resolution Mass Spectrometry. *Environmental Science & Technology* 44 (19), 7576-7582.
- Sleighter, R.L. and Hatcher, P. G. (2011) Fourier Transform Mass Spectrometry for the Molecular Level Characterization of Natural Organic Matter. Instrument Capabilities, Applications and Limitations. Fourier Transforms - Approach to Scientific Principles, Prof. Goran Nikolic (Ed.), ISBN: 978-953-307-231-9, InTech, Available from: <http://www.intechopen.com>.
- Sparks D.L. (1995) Environmental Soil Chemistry, Academic Press, San Diego, USA.
- Stenson, A.C., Marshall, A.G. and Cooper, W.T. (2003) Exact Masses and Chemical Formulas of Individual Suwannee River Fulvic Acids from Ultrahigh Resolution Electrospray Ionization Fourier Transform Ion Cyclotron Resonance Mass Spectra. *Analytical Chemistry* 75 (6), 1275-1284.
- Stoll, N., Schmidt, E. and Thurow, K. (2006) Isotope Pattern Evaluation for the Reduction of Elemental Compositions Assigned to High-Resolution Mass Spectral Data from Electrospray Ionization Fourier Transform Ion Cyclotron Resonance Mass Spectrometry. *Journal of the American Society for Mass Spectrometry* 17(12), 1692-1699.

- Tanaka, T., Nagao, S., Ogawa, H. (2001) Attenuated Total Reflection Fourier Transform Infrared (ATR-FTIR) Spectroscopy of Functional Groups of Humic Acid Dissolving in Aqueous Solution. *Analytical Sciences* 17, i1081-i1084.
- Tfaily, M.M., Hamdan, R., Corbett, J.E., Chanton, J.P., Glaser, P.H., Cooper, W.T. (2013) Investigating Dissolved Organic Matter Decomposition in Northern Peatlands using Complimentary Analytical Techniques. *Geochimica et Cosmochimica Acta* 112, 116-129.
- These, A. and Reemtsma, T. (2005) Structure-Dependent Reactivity of Low Molecular Weight Fulvic Acid Molecules during Ozonation. *Environmental Science & Technology* 39 (21), 8382-8387.
- Tipping, E., Corbishley, H.T., Koprivnjak, J., Lapworth, D.J., Miller, M.P., Vincent, C.D., Hamilton-Taylor, J. (2009) Quantification of natural DOM from UV absorption at two wavelengths. *Environmental Chemistry* 6 (6):472-476.
- Tremblay, L.B. (2006) PhD Thesis. The ultrahigh resolution mass spectrometry of natural organic matter from different sources. The Florida State University.
- van Heemst JDH, van Bergen PF, Stankiewicz BA, de Leeuw JW (1999) Multiple sources of alkylphenols produced upon pyrolysis of DOM, POM and recent sediments. *Journal of Analytical and Applied Pyrolysis* 52 (2): 239-256
- Verliefde, A., Cornelissen, E., Amy, G., Van der Bruggen, B. and van Dijk, H. (2007) Priority organic micropollutants in water sources in Flanders and the Netherlands and assessment of removal possibilities with nanofiltration. *Environmental Pollution* 146 (1), 281-289.
- Verliefde, A.R.D., Cornelissen, E.R., Heijman, S.G.J., Hoek, E.M.V., Amy, G.L., Bruggen, B.V.d. and van Dijk, J.C. (2009a) Influence of Solute–Membrane Affinity on Rejection of Uncharged Organic Solutes by Nanofiltration Membranes. *Environmental Science & Technology* 43 (7), 2400-2406.
- Verliefde, A.R.D., Cornelissen, E.R., Heijman, S.G.J., Petrinic, I., Luxbacher, T., Amy, G.L., Van der Bruggen, B. and van Dijk, J.C. (2009b) Influence of membrane fouling by (pretreated) surface water on rejection of pharmaceutically active compounds (PhACs) by nanofiltration membranes. *Journal of Membrane Science* 330, 90-103.

- Vichi, S., Cortés-Francisco, N. and Caixach, J. (2013) Determination of volatile thiols in lipid matrix by simultaneous derivatization/extraction and liquid chromatography-high resolution mass spectrometric analysis. Application to virgin olive oil. *Journal of Chromatography A* 1318(0), 180-188.
- Wei, Y., Lei, H., Wang, L., Zhu, L., Zhang, X., Liu, Y., Chen, S. and Ahring, B. (2014) Liquid-Liquid Extraction of Biomass Pyrolysis Bio-oil. *Energy & Fuels* 28(2), 1207-1212.
- Wershaw, R.L., Pinckney, D.J., Llaguno, E.C., Vicentebecket, V. (1990) NMR characterization of humic-acid fractions from different Philippine soils and sediments. *Analytical Chimica Acta* 232 (1): 31-42.
- Witt, M., Fuchser, J., Koch, B.P. (2009) Fragmentation Studies of Fulvic Acids Using Collision Induced Dissociation Fourier Transform Ion Cyclotron Resonance Mass Spectrometry. *Analytical Chemistry* 81 (7), 2688-2694.
- Wolf, S., Schmidt, S., Muller-Hannemann, M. and Neumann, S. (2010) In silico fragmentation for computer assisted identification of metabolite mass spectra. *BMC Bioinformatics* 11(1), 148.
- Xian, F., Hendrickson, C.L. and Marshall, A.G. (2012) High Resolution Mass Spectrometry. *Analytical Chemistry* 84(2), 708-719.
- Xu, P., Bellona, C., Drewes, J. E. (2010) Fouling of nanofiltration and reverse osmosis membranes during municipal wastewater reclamation: Membrane autopsy results from pilot-scale investigations. *Journal of Membrane Science* 353, (1-2), 111-121.
- Xu, Y. and Goodacre, R. (2012) Multiblock principal component analysis: an efficient tool for analyzing metabolomics data which contain two influential factors. *Metabolomics* 8 (1), 37-51.
- Zhang, H., Zhang, Y., Shi, Q., Ren, S., Yu, J., Ji, F., Luo, W. and Yang, M. (2012a) Characterization of low molecular weight dissolved natural organic matter along the treatment trait of a waterworks using Fourier transform ion cyclotron resonance mass spectrometry. *Water Research* 46 (16), 5197-5204.
- Zhang, H., Zhang, Y., Shi, Q., Hu, J., Chu, M., Yu, J. and Yang, M. (2012b) Study on Transformation of Natural Organic Matter in Source Water during Chlorination

and Its Chlorinated Products using Ultrahigh Resolution Mass Spectrometry. *Environmental Science & Technology* 46 (8), 4396-4402.

Zhang, F., Harir, M., Moritz, F., Zhang, J., Witting, M., Wu, Y., Schmitt-Kopplin, P., Fekete, A., Gaspar, A. and Hertkorn, N. (2014) Molecular and structural characterization of dissolved organic matter during and post cyanobacterial bloom in Taihu by combination of NMR spectroscopy and FTICR mass spectrometry. *Water Research* 57 (0), 280-294.

# Appendix A.

## Supporting Information Research Article N° 3

---

Nuria Cortés-Francisco and Josep Caixach

Molecular Characterization of Dissolved Organic Matter through a Desalination Process by High Resolution Mass Spectrometry.

*Environmental Science & Technology* **2013**, 47, (17), 9619-9627.



Supporting Information:

# Molecular characterization of dissolved organic matter through a desalination process by high resolution mass spectrometry

*Nuria Cortés-Francisco<sup>1</sup> and Josep Caixach<sup>1\*</sup>*

<sup>1</sup>Mass Spectrometry Laboratory / Organic Pollutants, IDAEA-CSIC, Jordi Girona 18,  
08034 Barcelona, Spain. Tel: (+34) 93 400 61 00. Fax: (+34) 93 204 59 04

E-mail address: josep.caixach@idaea.csic.es

**Number of Tables: 2**

**Number of Figures: 7**

**Table of contents:**

Table S1. Summary of some complementary analysis performed on the samples. For pH, conductivity and NPOC the mean value  $\pm$  standard deviation of n:3 is shown.

Table S2. Elemental formulae of the tentatively identified as anthropogenic linear alkyl benzene sulfonates.

Figure S1. a) Mass spectrum of SRFA standard and b) mass spectrum of SRNOM standard, both obtained by negative ESI-LTQ-FT-Orbitrap-MS.

Figure S2. Van Krevelen diagram of RSW sample built taking into account the different composition of the elemental formulae assigned. The degree of alkylation (diagonals), hydrogenation (vertical), oxidation/reduction (horizontal) of DOM is shown in several lines.

Figure S3. Van Krevelen diagrams for all formulae assigned of a) RSW, b) UF effluent, c) Permeate RO and d) Brine RO samples built taking into account the different composition of the elemental formulae assigned.

Figure S4. Van Krevelen diagram for all formulae assigned of SRFA standard, on color-coded analyte relative abundance plots. The colored circles show the theoretical areas to classify substance classes, described in the marine DOM literature.

Figure S5. Number of formulae as a function of DBE-O value for RSW, UF effluent, Permeate RO and Brine RO samples.

Figure S6. Mass resolved atomic H/C ratio of a) RSW and b) UF effluent samples of the assigned formulae.

Figure S7. Van Krevelen diagrams for all formulae assigned of Brine RO sample (blue) and Brine RO sample 100 fold dilution (green).

**Table S1.** Summary of some complementary analysis performed on the samples. For pH, conductivity and NPOC the mean value  $\pm$  standard deviation of n:3 is shown.

Sample	pH	Conductivity (mS/cm)	NPOC (mg C/L)	Salinity (mg NaCl/L)	Enumeration of phytoplankton (cells/mL)	SDI (%/min)
<b>RSW</b>	8.2 $\pm$ 0.05	56.5 $\pm$ 0.3	0.716 $\pm$ 0.006	31200	95	22.7
<b>UF effluent</b>	8.1 $\pm$ 0.1	56.4 $\pm$ 0.5	0.705 $\pm$ 0.005	31000	< 3	2.2
<b>Permeate RO</b>	6.5 $\pm$ 0.1	0.41 $\pm$ 0.3	0.013 $\pm$ 0.007	118	< 3	Not determined
<b>Brine RO</b>	Not determined	Not determined	1.243 $\pm$ 0.006	50200	< 3	Not determined

**Table S2.** Elemental formulae of the tentatively identified as anthropogenic linear alkyl benzene sulfonates.

Linear alkyl benzene sulfonates	Theoretical $m/z$ from single negatively charged molecular ion
$C_{16}H_{25}O_3S^-$	297.1530
$C_{17}H_{27}O_3S^-$	311.1686
$C_{18}H_{29}O_3S^-$	325.1843
$C_{19}H_{31}O_3S^-$	339.1999

**Figure S1.** a) Mass spectrum of SRFA standard and b) mass spectrum of SRNOM standard, both obtained by negative ESI-LTQ-FT-Orbitrap-MS.

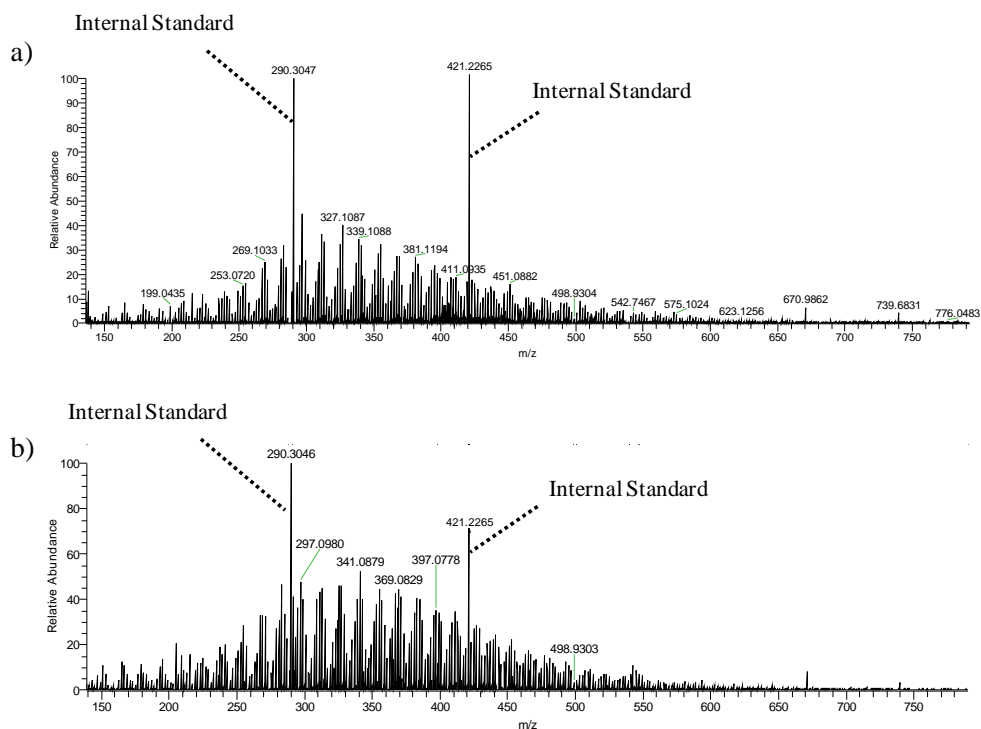


**Figure S2.** Van Krevelen diagram of RSW sample built taking into account the different composition of the elemental formulae assigned. The degree of alkylation (diagonals), hydrogenation (vertical), oxidation/reduction (horizontal) of DOM is shown in several lines.

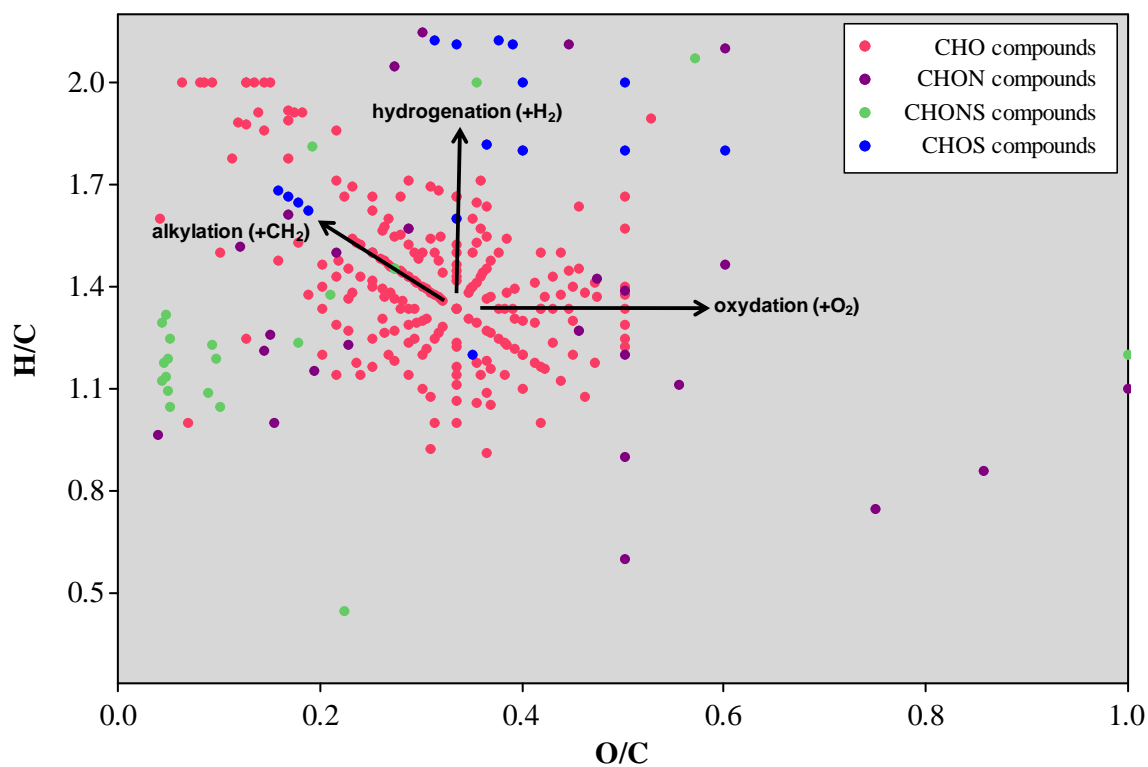


**Figure S3.** Van Krevelen diagrams for all formulae assigned of a) RSW, b) UF effluent, c) Permeate RO and d) Brine RO samples built taking into account the different composition of the elemental formulae assigned.

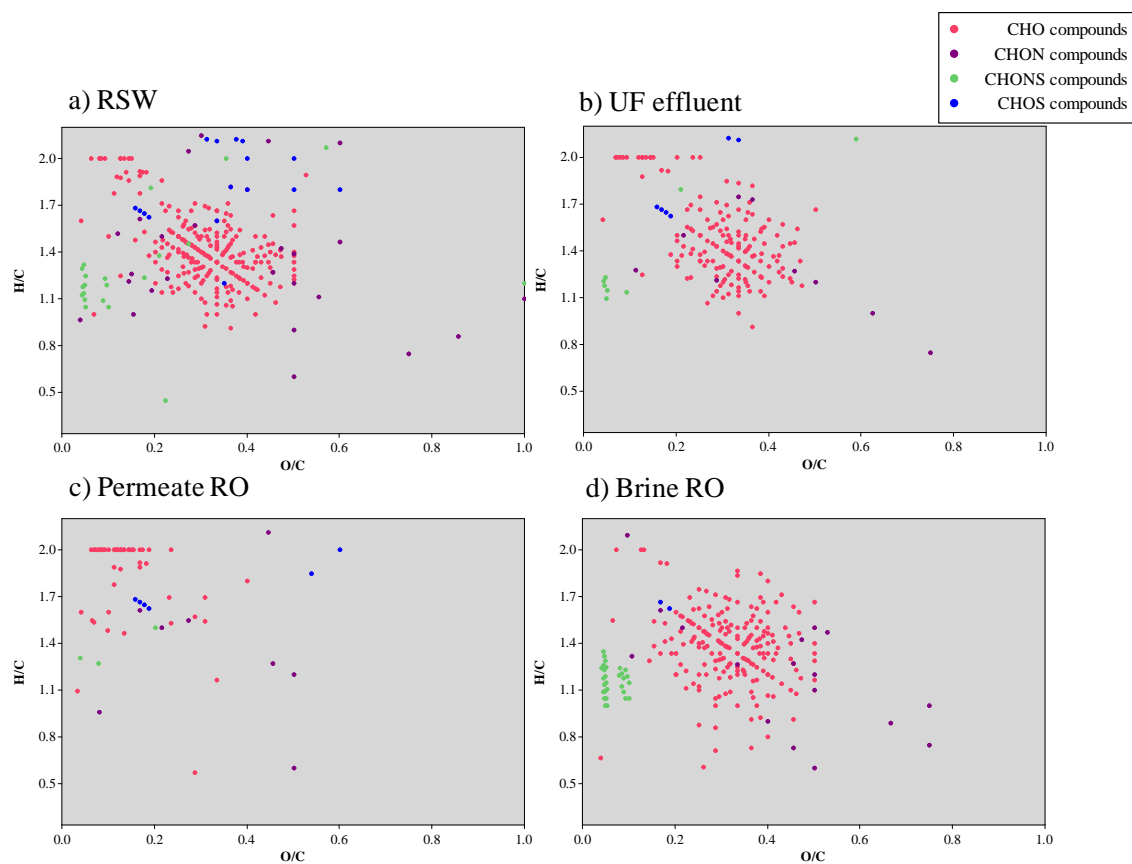


**Figure S4.** Van Krevelen diagram for all formulae assigned of SRFA standard, on color-coded analyte relative abundance plots. The colored circles show the theoretical areas to classify substance classes, described in the DOM literature.

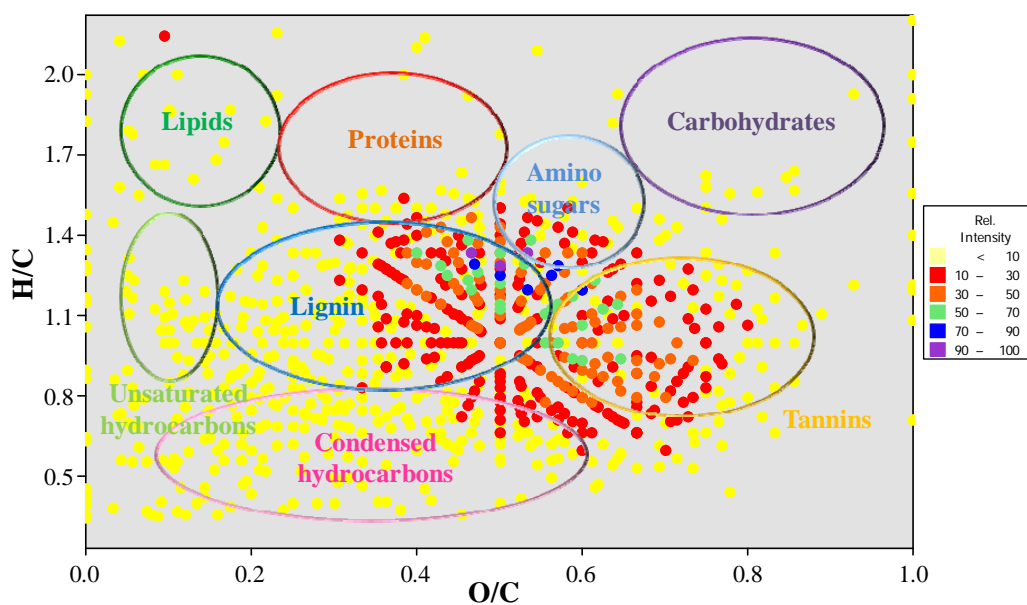


**Figure S5.** Number of formulae as a function of DBE-O value for RSW, UF effluent, Permeate RO and Brine RO samples.

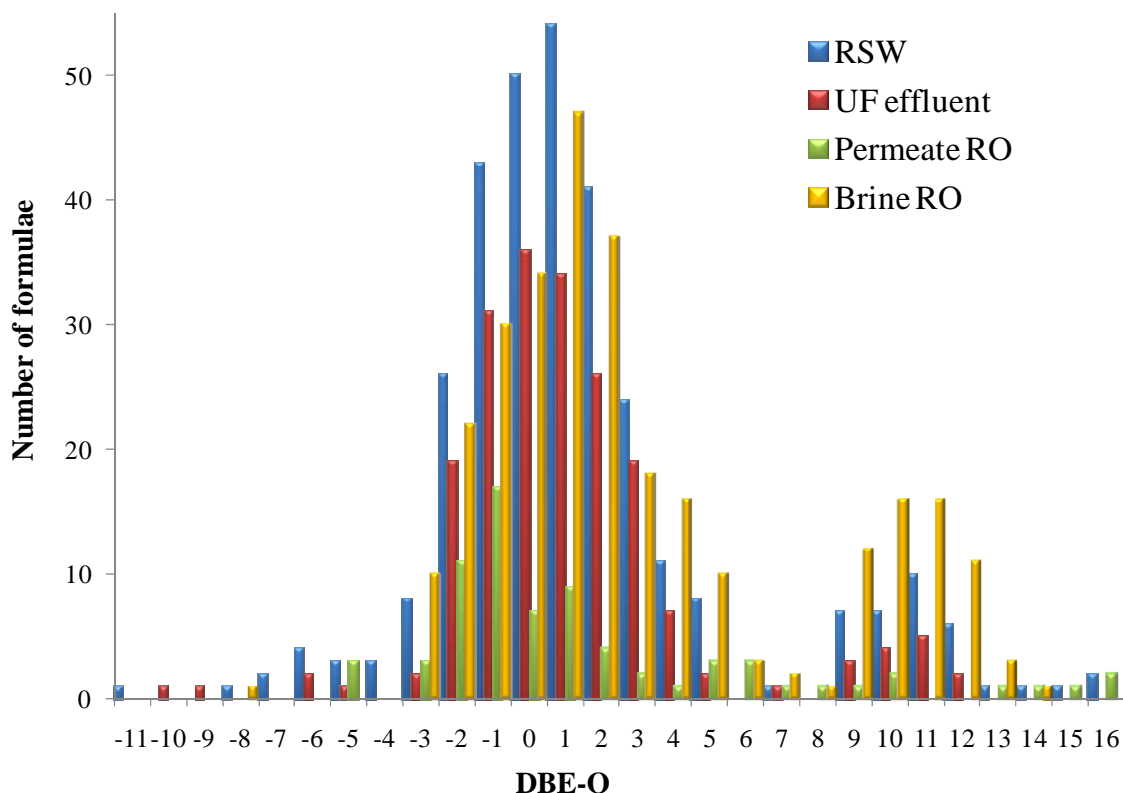


**Figure S6.** Mass resolved atomic H/C ratio of RSW and UF effluent samples of the assigned formulae. Components which are present both in RSW and UF are in black dots, RSW components only in RSW are presented in red and UF components in blue dots.

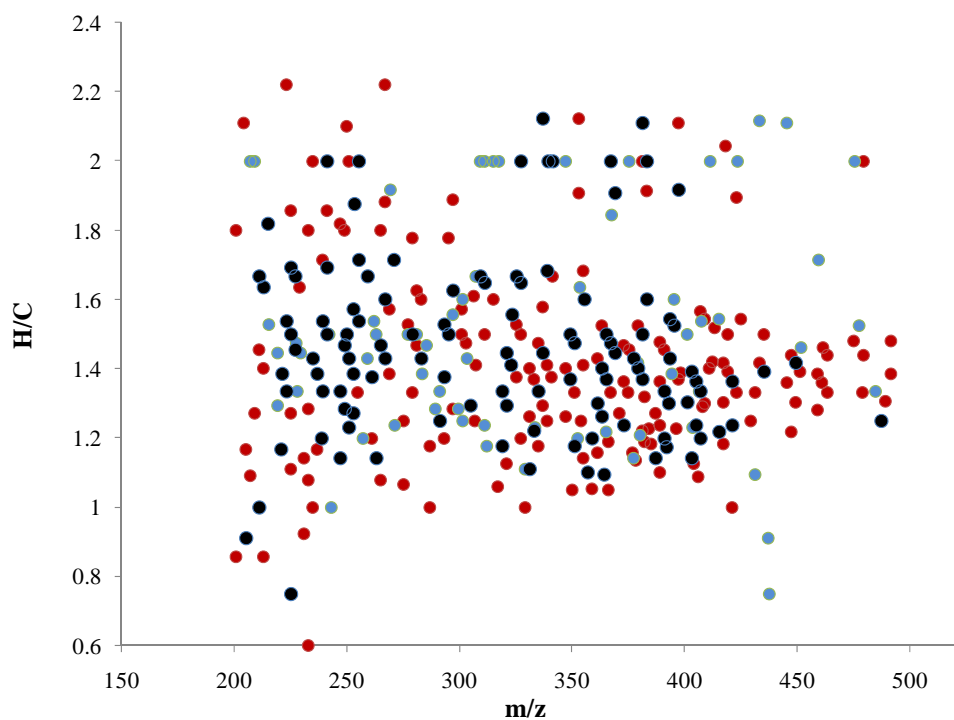
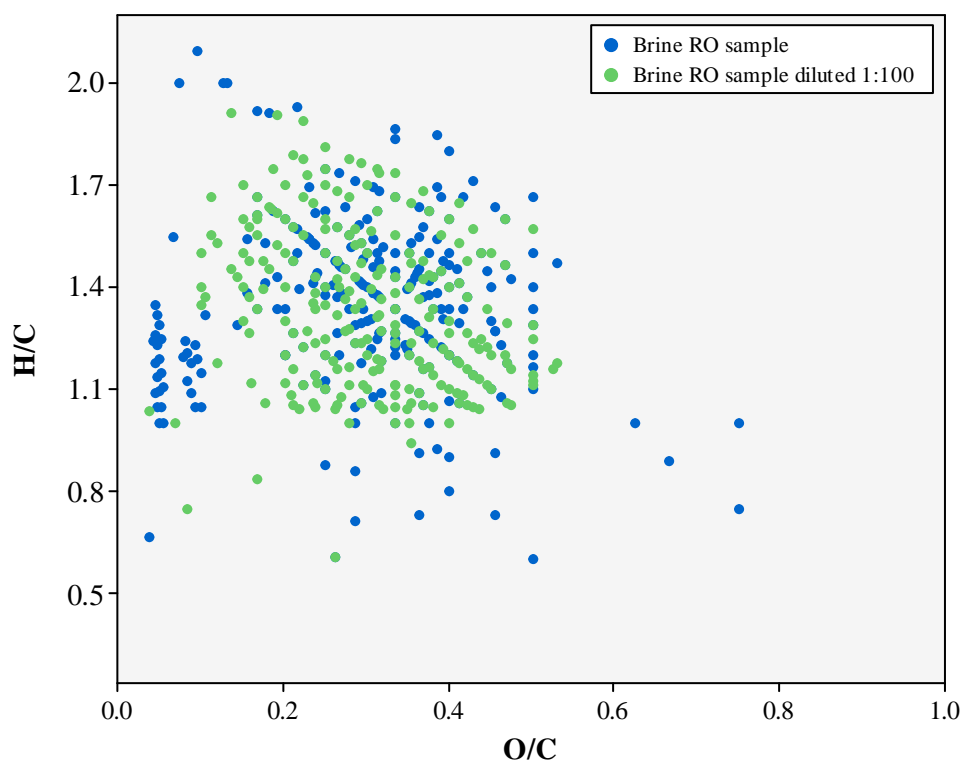


**Figure S7.** Van Krevelen diagrams for all formulae assigned of Brine RO sample (blue) and Brine RO sample 100 fold dilution (green).





## Appendix B.

### Supporting Information Research Article N° 4

---

Nuria Cortés-Francisco, Mourad Harir, Marianna Lucio, Gemma Ribera, Xavier Martinez-Lladó, Miquel Rovira, Philippe Schmitt-Kopplin, Norbert Hertkorn and Josep Caixach.

High-field FT-ICR Mass Spectrometry and NMR Spectroscopy to Characterize DOM Removal through a Nanofiltration Pilot Plant.

*Water Research* **2014**, DOI: 10.1016/j.watres.2014.08.046.



## Supplementary Information:

### **High-field FT-ICR mass spectrometry and NMR spectroscopy to characterize DOM removal through a nanofiltration pilot plant**

Nuria Cortés-Francisco <sup>1\*</sup>, Mourad Harir <sup>2</sup>, Marianna Lucio <sup>2</sup>, Gemma Ribera <sup>3</sup>, Xavier Martínez-Llado <sup>3</sup>, Miquel Rovira <sup>3</sup>, Philippe Schmitt-Kopplin <sup>2,4</sup>, Norbert Hertkorn <sup>2\*</sup> and Josep Caixach <sup>1</sup>

<sup>1</sup> Mass Spectrometry Laboratory / Organic Pollutants, IDAEA-CSIC; Jordi Girona 18-26, 08034 Barcelona, Spain. Tel: (+34) 93 400 61 00. Fax: (+34) 93 204 59 04.

<sup>2</sup> Helmholtz Zentrum Muenchen, German Research Center for Environmental Health, Research Unit Analytical Biogeochemistry (BGC), Ingolstaedter Landstrasse 1, D-85764 Neuherberg, Germany.

<sup>3</sup> Fundació CTM Centre Tecnològic; Plaça de la Ciència, 2, 08243 Manresa, Spain.

<sup>4</sup> Chair of Analytical Food Chemistry, Technische Universität München, Alte Akademie 10, 85354, Freising-Weihenstephan, Germany

E-mail addresses: [nuria.cortes@cid.csic.es](mailto:nuria.cortes@cid.csic.es) & [hertkorn@helmholtz-muenchen.de](mailto:hertkorn@helmholtz-muenchen.de)

Number of Tables: 6

Number of Figures: 14

**Table of contents:****A1. Materials and Methods**

**A1.1.** Pilot plant set-up and membranes used

**A1.2.** DOM extraction

**A1.3.** Fourier transform ion cyclotron mass spectrometry

**A1.4.** NMR analysis

**A1.5.** Complementary analysis

**A1.6.** Statistical analysis

**Table A1.** UF and NF membrane specifications from the suppliers.

**Table A2.** Specific properties of NF membranes.

**Table A3.** Sample volume, extracts final volume, extracts dilution for FT-ICR MS analysis and amount of sample used for NMR analysis of each sample.

**Table A4.** Physico-chemical parameters determined during the six-month pilot plant process in the pretreated water as average values and the standard deviation of n=6 measurements (except for Fe<sub>total</sub>).

**Table A5.** Trihalomethane formation potential (THMFP) and regulated trihalomethanes (THMs) analyzed during the six-month of pilot plant process, in the main sampling points: pretreated water, UF effluent, Permeate NF 1 and Permeate NF 2. The average values of n=6 and the standard deviation (in brackets) are given.

**Table A6.** Physico-chemical parameters determined in the samples of the present study.

**Figure A1.** Dendrograms from HCA of a) FT-ICR MS and b) NMR data, which reveals the different cluster of samples and sampling campaigns: June (yellow) and October (orange).

**Figure A2.** The reconstructed (only assigned mass peaks) negative electrospray 12T FT-ICR mass spectra of DOM samples: pretreated water (PW), ultrafiltration effluent (UF), ultrafiltration effluent after addition of antiscalant (UFS), permeate NF 1 (PER 1) and permeate NF 2 (PER 2). Left: June sampling campaign; Right: October sampling campaign.

**Figure A3.** The nominal mass  $m/z$  361 expansion of negative electrospray 12T FT-ICR MS mass spectra of Pretreated water June (yellow) and October (orange). The depicted elemental formulas represent negative singly charged molecular ions.

**Figure A4.** (Left) Van Krevelen diagrams for all formulas assigned of the October samples: pretreated water (PW), ultrafiltration effluent (UF), ultrafiltration effluent after adding antiscalant (UFS), NF permeate 1 (PER 1), NF permeate 2 (PER 2), on color-coded composition: CHO

(blue), CHOS (green), CHNO (orange), CHNOS (red). (Right) H/C ratio vs mass-to-charge ( $m/z$ ) plot for all formulas assigned of the samples: PW, UF, UFS, PER1, PER2, on same color-coded composition. Circular areas indicate relative mass peak intensity.

**Figure A5.** The reconstructed (only assigned mass peaks) negative electrospray 12T FT-ICR mass spectra of Pretreated water samples from June and October. The spectra are colour-coded taking into account the different composition of the elemental formulas assigned: CHO (blue), CHOS (green), CHNO (orange), CHNOS (red).

**Figure A6.**  $^1\text{H}$  NMR spectra of Pretreated water from June (yellow) and October (orange) acquired with solvent suppression and exclusion regions. Intensities are normalized to 100% intensity for the methylene group ( $\delta_{\text{H}} \sim 1.28$  ppm). Fundamental substructures are indicated from higher to lower field (from right to left): pure aliphatic  $\delta_{\text{H}} \sim 0.5\text{-}1.25$  ppm,  $\text{H}_3\text{C-C-C}$ ; polymethylene group  $\delta_{\text{H}} \sim 1.25\text{-}1.35$  ppm,  $(\text{CH}_2)_n$ ; functionalized aliphatics  $\delta_{\text{H}} \sim 1.35\text{-}1.9$  ppm,  $\text{H-C-C-CO}$ ; “acetate-analogue” and carboxyl-rich alicyclic materials (CRAM)  $\delta_{\text{H}} \sim 1.9\text{-}3.1$  ppm,  $\text{H-C-C-O}$ ; “carbohydrate-like” and methoxy  $\delta_{\text{H}} \sim 3.1\text{-}4.9$  ppm,  $\text{HCO}$ ; olefins  $\delta_{\text{H}} \sim 5.3\text{-}7.0$  ppm  $\text{HC=C}$ ,  $\text{HCO}_2$ ; and aromatic  $\delta_{\text{H}} \sim 7.0\text{-}9.5$  ppm,  $\text{H}_{\text{ar}}$  NMR resonances.

**Figure A7.** Nominal mass  $m/z$  361 expansion of negative electrospray 12T FT-ICR mass spectra of a) Pretreated water (yellow), UF effluent (dark blue) and UF + antiscaling effluent (light blue) from June; b) Zoom from the grey square in a) to see also the peaks that are less intense, but are also present in the three samples; c) UF + antiscaling effluent (light blue), Permeate NF 1 (red) and Permeate NF 2 (green) from June; d) Zoom from the grey square in c) to see that most of the peaks are partially or completely removed after the nanofiltration process.

**Figure A8.**  $^1\text{H}$  NMR spectra of Pretreated water (yellow), UF effluent (dark blue) and UF + antiscaling effluent (light blue) from June acquired with solvent suppression and exclusion regions. Intensities are normalized to 100% intensity for the methylene group ( $\delta_{\text{H}} \sim 1.28$  ppm). Fundamental substructures are indicated from higher to lower field (from right to left): pure aliphatic  $\delta_{\text{H}} \sim 0.5\text{-}1.25$  ppm,  $\text{H}_3\text{C-C-C}$ ; polymethylene group  $\delta_{\text{H}} \sim 1.25\text{-}1.35$  ppm,  $(\text{CH}_2)_n$ ; functionalized aliphatics  $\delta_{\text{H}} \sim 1.35\text{-}1.9$  ppm,  $\text{H-C-C-CO}$ ; “acetate-analogue” and carboxyl-rich alicyclic materials (CRAM)  $\delta_{\text{H}} \sim 1.9\text{-}3.1$  ppm,  $\text{H-C-C-O}$ ; “carbohydrate-like” and methoxy  $\delta_{\text{H}} \sim 3.1\text{-}4.9$  ppm,  $\text{HCO}$ ; olefins  $\delta_{\text{H}} \sim 5.3\text{-}7.0$  ppm  $\text{HC=C}$ ,  $\text{HCO}_2$ ; and aromatic  $\delta_{\text{H}} \sim 7.0\text{-}9.5$  ppm,  $\text{H}_{\text{ar}}$  NMR resonances.

**Figure A9.**  $^1\text{H}$  NMR spectra of UF + antiscaling effluent (light blue), Permeate NF 1 (red) and Permeate NF 2 (green) from June acquired with solvent suppression and exclusion regions. Intensities are normalized to 100% intensity for the methylene group ( $\delta_{\text{H}} \sim 1.28$  ppm). Fundamental substructures are indicated from higher to lower field (from right to left): pure aliphatic  $\delta_{\text{H}} \sim 0.5\text{-}1.25$  ppm,  $\text{H}_3\text{C-C-C}$ ; polymethylene group  $\delta_{\text{H}} \sim 1.25\text{-}1.35$  ppm,  $(\text{CH}_2)_n$ ; functionalized aliphatics  $\delta_{\text{H}} \sim 1.35\text{-}1.9$  ppm,  $\text{H-C-C-CO}$ ; “acetate-analogue” and carboxyl-rich alicyclic materials (CRAM)  $\delta_{\text{H}} \sim 1.9\text{-}3.1$  ppm,  $\text{H-C-C-O}$ ; “carbohydrate-like” and methoxy  $\delta_{\text{H}} \sim 3.1\text{-}4.9$  ppm,  $\text{HCO}$ ; olefins  $\delta_{\text{H}} \sim 5.3\text{-}7.0$  ppm  $\text{HC=C}$ ,  $\text{HCO}_2$ ; and aromatic  $\delta_{\text{H}} \sim 7.0\text{-}9.5$  ppm,  $\text{H}_{\text{ar}}$  NMR resonances.

**Figure A10.** Analysis of common  $m/z$  (within 0.1 ppm mass accuracy window) in PER 1 and PER 2, based on the intensity ratios ( $\text{Ri}_{\text{PER 1/PER 2}}$ ). Differentiation of the  $m/z$  intensity  $\text{Ri}_{\text{PER 1/PER 2}} > 1.5$ , shows that these  $m/z$  are enhanced in PER 1 (red square).

**Figure A11.** Van Krevelen diagram and H/C ratio vs  $m/z$  plot from a) the  $m/z$  unique and the intensity enriched in PER 1 (with respect to PER 2) and  $m/z$  unique in PER 2; b) the  $m/z$  common in PER 1 and PER 2 (considering June and October sampling campaigns together).

**Figure A12.** Unregulated DBPs analyzed in the samples: UF effluent, Permeate NF 1 and Permeate NF 2 (considering June and October together) after strong chlorination (following 5710-B Standard Method (American Public Health Association et al., 1998)).

**Figure A13.** Reconstructed mass spectra (only assigned formulas), van Krevelen diagrams and H/C ratio vs mass-to-charge ( $m/z$ ) plot of the Brine samples from June: Brine NF 1 and Brine NF 2, on color-coded composition: CHO (blue), CHOS (green), CHNO (orange), CHNOS (red). Circular areas indicate relative mass peak intensity.

**Figure A14.**  $^1\text{H}$  NMR spectra of Brine NF 1 (pink) and Brine NF 2 (purple) from June acquired with solvent suppression and exclusion regions. Intensities are normalized to 100% intensity for the methylene group ( $\delta_{\text{H}} \sim 1.28$  ppm). Fundamental substructures are indicated from higher to lower field (from right to left): pure aliphatic  $\delta_{\text{H}} \sim 0.5\text{-}1.25$  ppm,  $\underline{\text{H}}_3\text{C-C-C}$ ; polymethylene group  $\delta_{\text{H}} \sim 1.25\text{-}1.35$  ppm,  $(\underline{\text{C}}\underline{\text{H}}_2)_n$ ; functionalized aliphatics  $\delta_{\text{H}} \sim 1.35\text{-}1.9$  ppm,  $\underline{\text{H}}\text{-C-C-CO}$ ; “acetate-analogue” and carboxyl-rich alicyclic materials (CRAM)  $\delta_{\text{H}} \sim 1.9\text{-}3.1$  ppm,  $\underline{\text{H}}\text{-C-C-O}$ ; “carbohydrate-like” and methoxy  $\delta_{\text{H}} \sim 3.1\text{-}4.9$  ppm,  $\underline{\text{H}}\text{CO}$ ; olefins  $\delta_{\text{H}} \sim 5.3\text{-}7.0$  ppm  $\underline{\text{H}}\text{C}=\text{C}$ ,  $\underline{\text{H}}\text{CO}_2$ ; and aromatic  $\delta_{\text{H}} \sim 7.0\text{-}9.5$  ppm,  $\underline{\text{H}}_{\text{ar}}$  NMR resonances.

## A1. Materials and Methods

### A1.1. Pilot plant set-up and membranes used

A NF pilot plant, which includes a UF module as pretreatment, was designed and installed in the DWTP.

The UF step reduced the silt density index (SDI) by removing particulate and colloidal matter in order to avoid severe permeate flux decline in NF membrane processes. Pretreated water (PW) from sand filters passed through a 500 L tank to feed the UF module. Effluent from UF was stored in a 1000 L tank before the on-line addition of the following chemical products: sodium metabisulfite (1 - 2 ppm) to remove free chlorine and scale inhibitor (1.5 ppm of Genesys LF) to avoid inorganic scaling.

In the NF process step, two different membranes were contained in separated trains of six 4" spiral wound modules each one: ESNA1LF2-4040 (membrane 1) and NF270-4040 (membrane 2). They were operating at the same recovery (50 %) and permeate flux (28 lmh). These parameters were fixed to represent the operational conditions of an industrial full-scale NF plant for the treatment of drinking water.

### A1.2. DOM extraction

The liquid-liquid extraction protocol was chosen in order to manipulate as less as possible the real nature of the water, and analyze the whole water without prior filtration, as well as to eliminate any remaining salts which would suppress the ion generation within electrospray. Any sample pretreatment can cause fractionation of DOM (Perdue et al., 2003; Nebbioso et al., 2013; Reemtsma, 2009). The LLE extraction has been evaluated in front of SPE extraction, with the analysis of the SRFA and SRNOM standards and we have shown that equivalent results can be obtained with both methodologies (Cortés-Francisco, et al., 2013). Moreover, the idea of the study was to look for differences (or lack of differences) along the different treatment stages and this can be done using SPE, LLE or any other methodology as long as all the samples are treated the same way. The extracts were stored at -27°C in the dark until use. For FT-ICR MS, extracts were diluted to obtain concentrations around 10-5  $\mu\text{g}\cdot\text{mL}^{-1}$  in methanol (Table A3). For NMR spectroscopy, aliquots of methanol extracts of the samples were evaporated in vacuo to dryness and methanol-d<sub>4</sub> (100 % <sup>2</sup>H, Aldrich, Steinheim, Germany) was added; this cycle was repeated three times to largely exchange methanol-h<sub>4</sub> by methanol-d<sub>4</sub>.

### A1.3. Fourier transform ion cyclotron mass spectrometry

Diluted DOM extracts (see Table A3) were injected into the electrospray source using a microliter pump at a flow rate of 120  $\mu\text{L}\cdot\text{h}^{-1}$  with a nebulizer gas pressure of 138 kPa and a drying gas pressure of 103 kPa. A source heater temperature of 200°C was maintained to ensure rapid

desolvation in the ionized droplets. Spectra were first externally calibrated on clusters of arginine ( $0.57 \mu\text{mol}\cdot\text{L}^{-1}$  in methanol) and internal calibration was systematically done using appropriate reference mass list reaching accuracy values lower than 500 ppb.

#### **A1.4. NMR analysis**

Proton spectra were acquired with an inverse geometry 5 mm z-gradient  $^1\text{H}/^{13}\text{C}/^{15}\text{N}/^{31}\text{P}$  QCI cryogenic probe ( $90^\circ$  excitation pulses:  $^1\text{H} \sim 10 \mu\text{s}$ ); NMR chemical shift reference:  $^1\text{H}$  NMR,  $\text{HD}_2\text{O}$ : 3.30 ppm. All spectra were acquired at 283 K to impede side reactions during NMR acquisitions. 1-D  $^1\text{H}$  NMR spectra were recorded with a spin-echo sequence (10  $\mu\text{s}$  delay) to allow for high-Q probe ringdown; classical presaturation “zgpr” and “zgpurge” (Simpson et al., 2005) and solvent suppression with presaturation and 1 ms spin-lock (*noesypr1d*), 5 s acquisition time, 10 s relaxation delay (d1), typically 738 scans, 1 Hz exponential line broadening.

#### **A1.5. Complementary analysis**

Inorganic composition, pH, conductivity, ultraviolet light adsorption (UVA), SDI, non-purgable organic carbon (NPOC) and trihalomethane formation potential (THMFP) were determined regularly during the six-months operation of the pilot plant and published as part of another study. In SI Table A4, there are the average results for these parameters in PW (Ribera et al., 2013). Also during the six months of operation of the plant THMFP and regulated THM were regularly determined in the main sampling points: PW, UF effluent, PER 1 and PER 2 (Table A5).

For the samples of the present study, Table A6 summarizes the data for some complementary analysis performed: conductivity, pH, NPOC, UVA, total inorganic carbon (TIC), total nitrogen (TN), major inorganic cations (calcium, magnesium, potassium and sodium) and anions (chloride, nitrates, sulphates).

All these analysis were carried out as described in previous work (Ribera et al., 2013). Briefly: Ion Chromatography (Dionex ICS-2000) was used to analyze anions (chloride, nitrates, sulphates) and cations (calcium, magnesium, potassium and sodium). Total Carbon Analyzer (AnalytikJena Multi NC 3,100) was used to analyze TIC, NPOC and TN. Inductively coupled plasma mass spectrometry (ICP-MS), Agilent 7500cx, was used to analyze trace elements. UVA was measured using a spectrophotometer (Shimadzu UV\_1603). THMFP was determined applying the 5710-B standard method and regulated THM concentrations were analyzed by HS-GC/ECD (Agilent 7694E-Hewlett Packard 6890). Reference materials and spiked samples were analyzed together with samples in each analysis batch, and the recoveries were always between 90 % and 110 %.

Moreover, for the screening of unregulated DBPs 1 L of the samples UF effluent, the Permeate NF 1 and Permeate NF 2 (from both campaigns, June and October 2011) were chlorinated off-line, following the 5710-B Standard Method (American Public Health Association et al., 1998). Each sample after chlorination were extracted by closed-loop stripping analysis and analyzed by

gas chromatography coupled to mass spectrometry, following the 6040-B Standard Method (American Public Health Association et al., 1998).

#### **A1.6. Statistical analysis**

For the statistical analysis the raw data, FT-ICR MS and NMR, were independently preprocessed. The exported FT-ICR mass spectra were aligned over the entire mass range through an in-house software with a mass accuracy window of 1 ppm (Lucio et al., 2010). The NMR spectra were divided into 0.001 ppm width buckets and exported using Amix version 3.9.4 (Bruker BioSpin, Rheinstetten, Germany).

As a result of high dimensionality and complexity of the data sets, different multivariate analyses were applied. These statistical elaborations investigate the possible relations between samples and variables (peaks for FT-ICR MS and integral regions for NMR). Multiple models were built up using SIMCA-P+12 (Umetrics, Umeå, Sweden) for both FT-ICR MS and NMR data. Through unsupervised (principal component analysis - PCA and hierarchical clustering - HCA) and supervised (orthogonal partial least squares - OPLS/O2PLS-DA) analysis, we were able to define trends on the data and discriminate between experimental groups.

FT-ICR MS and NMR data were examined by HCA to measure the relationships between samples. HCA underlines the geometrical distances between different samples and the similarity has been calculated with the Ward method. The output is represented by the dendrogram, which reveals the different cluster of the samples. Moreover, FT-ICR MS data were investigated with PCA and OPLS/O2PLS-DA. The outputs of the models were lists of masses, which represented the chemical properties of each group. These were investigated with van Krevelen diagrams. On the other hand, NMR data was investigated with a multiblock PCA analysis (Xu et al., 2012). In particular, the multiblock analysis was possible to apply because we have information for blocking the different regions of the NMR spectra according into the chemical meaningful (key substructures). These visualizations could at the end summarize the significant differences on DOM along the treatments.

#### **References**

1. American Public Health Association, American Water Works Association and Water Pollution Control Federation. (1998) Standard methods for the examination of water and wastewater (20th ed.): Washington, D.C., variously paged.
2. Lucio M, Fekete A, Schmitt-Kopplin P (2010) High resolution tools offer to follow bacterial growth on a molecular level In: Handbook of Molecular Microbial Ecology I Metagenomics and Complementary Approaches. Hoboken: Wiley-Blackwell.
3. Nebbioso, A. and Piccolo, A. (2013) Molecular characterization of dissolved organic matter (DOM): a critical review. *Analytical and Bioanalytical Chemistry* 405(1), 109-124.

4. Perdue E. M. and Ritchie J. D. (2003) Dissolved organic matter in fresh waters. In: Surface and Ground Water, Weathering, Erosion and Soils, (J. I. Drever, ed.) Vol. 5, Treatise on Geochemistry (H. D. Holland and K. K. Turekian, eds.), Elsevier-Pergamon, Oxford, Chapter 11.
5. Reemtsma, T. (2009) Determination of molecular formulas of natural organic matter molecules by (ultra-) high-resolution mass spectrometry: Status and needs. *Journal of Chromatography A* 1216(18), 3687-3701.
6. Ribera, G., Llenas, L., Rovira, M., de Pablo, J. and Martinez-Llado, X. (2013) Pilot plant comparison study of two commercial nanofiltration membranes in a drinking water treatment plant. *Desalination and Water Treatment* 51(1-3), 448-457.
7. Simpson, A.J. and Brown, S.A. (2005) Purge NMR: Effective and easy solvent suppression. *Journal of Magnetic Resonance* 175(2), 340-346.
8. Xu, Y. and Goodacre, R. (2012) Multiblock principal component analysis: an efficient tool for analyzing metabolomics data which contain two influential factors. *Metabolomics* 8(1), 37-51.

**Table A1.** UF and NF membrane specifications from the suppliers.

	<b>Tripure UF</b>	<b>ESNA1LF2-4040 Membrane 1</b>	<b>NF270-4040 Membrane 2</b>
Supplier	Berghoff	Hydranautics	DOW-Filmtec
Configuration	Dead-end (In-out) Hollow fiber	Cross-flow Spiral-wound	Cross-flow Spiral-wound
Operation TMP (bar)	1-1.5	21 max.	41 max.
Design flux (l/m <sup>2</sup> h)	60-100	--	22-29
Pretreatment	Sand filtered	UF (SDI<3)	UF (SDI<3)
Water recovery	95-100 %	15 %	17 %
Material	Polysulphone (modified PS)	Composite polyamide	Polyamide (polypiperazine)
Membrane Surface (m <sup>2</sup> )	41.5	7.9	7.6
Pressure drop per module (bar)	--	0.7	1.0

**Table A2.** Specific properties of NF membranes.

<b>Property</b>	<b>ESNA1LF2-4040 Membrane 1</b>	<b>NF270-4040 Membrane 2</b>
WCO	200 (Amy et al., 2001)	270 (DOW Water) 175 (Klöpffel et al., 2010)
Clean water permeability (m <sup>3</sup> /(m <sup>2</sup> ·day·kPa))	1.84 (Amy et al., 2001; Park et al., 2005)	3.3 (Sentana et al., 2010) 3.19 (Park et al., 2005)
% conductivity rejection	80 (Ribera et al., 2013)	55 (Ribera et al., 2013)
Contact angle	60 <sup>a</sup> (Yoon et al., 2005) 23-40 <sup>b</sup> (Childress et al., 2012)	28.5 (Klöpffel et al., 2010)
Z-potential	-12 <sup>b</sup> (Sentana et al., 2010) -7 (Oatley, D. 2012)	-19.7 (Klöpffel et al., 2010) -32 (Oatley, D.L. et al., 2012)
Porosity AFM (nm)	0.49 (Llenas et al., 2011)	0.50 (Llenas et al., 2011)
Roughness AFM (nm)	49.7 (Llenas et al., 2011)	5.35 (Llenas et al., 2011)
Isoelectric point	2-3 (Oatley, D. 2012)	3.5 (Oatley, D.L. et al., 2012)

<sup>a</sup>Value for ESNA1 membrane<sup>b</sup>Value for ESNA1LF membranes

## References

1. Amy, G.L., et al (2001) NOM rejection by and fouling of, NF and UF membranes, Denver.

2. Childress, A.E., Brant, J.A., Rempala, P., Phipps, D.W., Kwan, P. (2012) Evaluation of membrane characterization methods, p. 179, Water Research Foundation, Denver.
3. DOW Water & Process Solutions technical manual, Technical manual, FILMTEC Reverse Osmosis Membranes. in: F.N. 609-00071-1009, (Ed.).
4. Klüpfel, A.M. and Frimmel, F.H. (2010) Nanofiltration of river water - fouling, cleaning and micropollutant rejection. *Desalination* 250(3), 1005-1007.
5. Llenas, L., Martínez-Lladó, X., Yaroshchuk, A., Rovira, M. and de Pablo, J. (2011) Nanofiltration as pretreatment for scale prevention in seawater reverse osmosis desalination. *Desalination and Water Treatment* 36(1-3), 310-318.
6. Oatley, D. (2012) Isoelectric point of NF270 and ESNA1LF2 (Personal Communication), Swansea.
7. Oatley, D.L., Llenas, L., Pérez, R., Williams, P.M., Martínez-Lladó, X. and Rovira, M. (2012) Review of the dielectric properties of nanofiltration membranes and verification of the single oriented layer approximation. *Adv. Colloid Interfac. Sci.* 173, 1-11.
8. Park, N., Kwon, B., Sun, M., Ahn, H., Kim, C., Kwoak, C., Lee, D., Chae, S., Hyung, H. and Cho, J. (2005) Application of various membranes to remove NOM typically occurring in Korea with respect to DBP, AOC and transport parameters. *Desalination* 178(1-3), 161-169.
9. Ribera, G., Llenas, L., Rovira, M., de Pablo, J. and Martinez-Llado, X. (2013) Pilot plant comparison study of two commercial nanofiltration membranes in a drinking water treatment plant. *Desalination and Water Treatment* 51(1-3), 448-457.
10. Sentana, I., Puche, R.D.S., Sentana, E. and Prats, D. (2010) Reduction of chlorination byproducts in surface water using ceramic nanofiltration membranes. *Desalination* 277(1-3), 147-155.
11. Yoon, Y., Amy, G., Cho, J. and Her, N. (2005) Effects of retained natural organic matter (NOM) on NOM rejection and membrane flux decline with nanofiltration and ultrafiltration. *Desalination* 173(3), 209-221.

**Table A3.** Sample volume, extracts final volume, extracts dilution for FT-ICR MS analysis and amount of sample used for NMR analysis of each sample.

		Sample Volume (mL)	Final extract ( $\mu\text{L}$ )	Folds diluted for FT-ICR analysis	Sample analyzed in NMR (mg)
Pretreated Water	June	1500	250	1000	N/A
	October	1500	250	1000	N/A
UF effluent	June	1500	250	1000	3.2
	October	1500	250	1000	1.2
Uf effluent + antiscalant	June	1500	250	1000	5.1
	October	1500	250	1000	N/A
Permeate NF 1	June	1500	250	50	3.6
	October	1500	250	50	3.1
Permeate NF 2	June	1500	250	50	3.2
	October	1500	250	50	1.5
Brine NF 1	June	1500	250	2000	6.2
	October	1500	250	2000	5.7
Brine NF 2	June	1500	250	2000	4.3
	October	1500	250	2000	6.2

N/A: no data available

**Table A4.** Physico-chemical parameters determined during the six-month pilot plant process in the pretreated water as average values and the standard deviation of n=6 measurements (except for  $\text{Fe}_{\text{total}}$ ).

Parameter	Average value	Standard deviation	Parameter	Average value	Standard deviation
Conductivity ( $\mu\text{S}\cdot\text{cm}^{-1}$ )	570	30	Sr ( $\text{mg}\cdot\text{L}^{-1}$ )	1.05	0.05
pH	7.8	0.2	Si ( $\text{mg}\cdot\text{L}^{-1}$ )	0.9	0.9
NPOC ( $\mu\text{g}\cdot\text{L}^{-1}$ )	2560	540	$\text{Ca}^{2+}$ ( $\text{mg}\cdot\text{L}^{-1}$ )	82	9
UVA (254 nm)	0.039	0.015	$\text{Mg}^{2+}$ ( $\text{mg}\cdot\text{L}^{-1}$ )	12	2
THMPF ( $\mu\text{g}\cdot\text{L}^{-1}$ )	120	40	$\text{Na}^{+}$ ( $\text{mg}\cdot\text{L}^{-1}$ )	20	6
SDI ( $\%\cdot\text{min}^{-1}$ )	5.2	1.7	$\text{K}^{+}$ ( $\text{mg}\cdot\text{L}^{-1}$ )	2.0	0.5
Al ( $\mu\text{g}\cdot\text{L}^{-1}$ )	51	13	$\text{HCO}_3^{-}$ ( $\text{mg}\cdot\text{L}^{-1}$ )	175	8
Ba ( $\mu\text{g}\cdot\text{L}^{-1}$ )	43	10	$\text{SO}_4^{2-}$ ( $\text{mg}\cdot\text{L}^{-1}$ )	100	23
$\text{Fe}_{\text{total}}$ ( $\mu\text{g}\cdot\text{L}^{-1}$ )	7.5	N/A	$\text{Cl}^{-}$ ( $\text{mg}\cdot\text{L}^{-1}$ )	35	7
B ( $\mu\text{g}\cdot\text{L}^{-1}$ )	27	2	$\text{NO}_3^{-}$ ( $\text{mg}\cdot\text{L}^{-1}$ )	3.0	1.6
Mn ( $\mu\text{g}\cdot\text{L}^{-1}$ )	0.14	0.17	$\text{F}^{-}$ ( $\text{mg}\cdot\text{L}^{-1}$ )	0.16	0.04

N/A: no data available

**Table A5.** Trihalomethane formation potential (THMFP) and regulated trihalomethanes (THMs) analyzed during the six-month of pilot plant process, in the main sampling points: pretreated water, UF effluent, Permeate NF 1 and Permeate NF 2. The average values of n=6 and the standard deviation (in brackets) are given.

	Pretreated Water	UF effluent	Permeate NF 1	Permeate NF 2
	$\mu\text{g} \cdot \text{L}^{-1}$			
<b>THMFP</b>	120 (40)	106 (24)	1 (3)	4 (6)
<b>Chloroform</b>	147 (30)	144 (35)	24 (15)	31 (17)
<b>Bromodichloromethane</b>	12.8 (2)	14 (2)	5 (1)	6 (1)
<b>Chlorodibromomethane</b>	< 2.5	< 2.5	< 2.5	< 2.5
<b>Bromoform</b>	< 2.5	< 2.5	< 2.5	< 2.5

**Table A6.** Physico-chemical parameters determined in the samples of the present study.

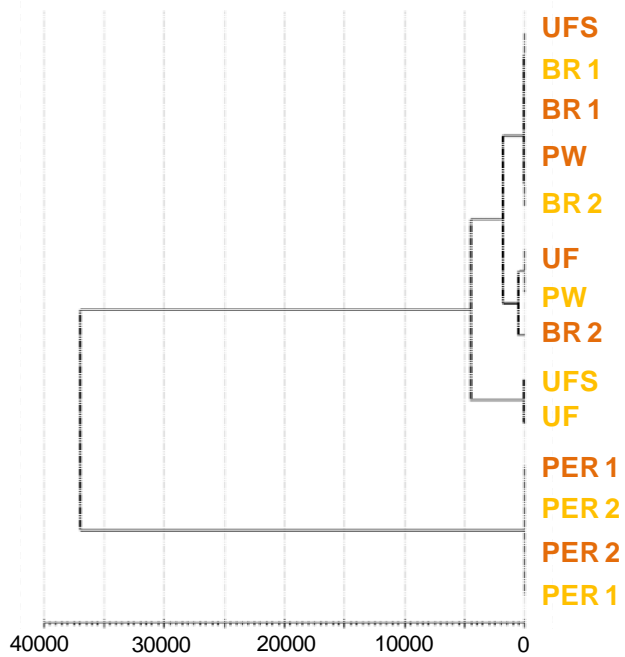
Parameters	Pretreated Water		UF effluent		UF effluent + antiscaling		Permeate NF 1		Permeate NF 2	
	June	Oct	June	Oct	June	Oct	June	Oct	June	Oct
Conductivity ( $\mu\text{S} \cdot \text{cm}^{-1}$ )	596	579	596	574	619	1258	94.7	229	294	422
pH	7.71	7.71	7.19	7.7	7.19	8.0	6.63	7.73	7.00	7.89
NPOC ( $\mu\text{g} \cdot \text{L}^{-1}$ )	2474	2526	2054	3035	2335	5553	110.6	465	79.1	522
UVA (254 nm)	0.03	0.03	0.03	0.03	0.03	0.12	N/A	N/A	N/A	N/A
TIC ( $\text{mg} \cdot \text{L}^{-1}$ )	36.3	36.5	36.2	36.8	32.4	60.1	10.4	20.4	20.7	35.6
TN ( $\text{mg} \cdot \text{L}^{-1}$ )	0.6	0.9	0.5	0.8	0.6	1.1	0.35	0.7	0.44	0.8
Ca <sup>2+</sup> ( $\text{mg} \cdot \text{L}^{-1}$ )	81.3	89.6	82.1	98.9	82.3	228.3	9.4	28.7	35.7	60.9
Mg <sup>2+</sup> ( $\text{mg} \cdot \text{L}^{-1}$ )	11.7	9.6	11.7	9.6	11.7	26.1	1.3	3.5	3.9	5.1
K <sup>+</sup> ( $\text{mg} \cdot \text{L}^{-1}$ )	1.9	2.0	2.0	2.0	1.9	3.2	0.8	1.3	1.4	1.8
Na <sup>+</sup> ( $\text{mg} \cdot \text{L}^{-1}$ )	19.5	17.1	20.8	17.3	23.0	28.1	10.1	12.8	16.7	17.2
Cl <sup>-</sup> ( $\text{mg} \cdot \text{L}^{-1}$ )	32.4	30.4	32.7	30.4	44.4	40.5	17.9	16.3	62.1	37.9
NO <sub>3</sub> <sup>-</sup> ( $\text{mg} \cdot \text{L}^{-1}$ )	1.5	2.8	1.4	2.4	1.4	2.4	0.8	2.0	1.2	2.8
SO <sub>4</sub> <sup>2-</sup> ( $\text{mg} \cdot \text{L}^{-1}$ )	103.2	95.8	103.5	95.6	105.8	408.7	1.5	4.8	4.1	7.5

N/A: no data available

**Figure A1.** Dendrograms from HCA of a) FT-ICR and b) NMR data, which reveals the different cluster of samples and sampling campaigns: June (yellow) and October (orange).

**June sampling Campaign**  
**October sampling Campaign**

**a) FT-ICR**



**b) NMR**

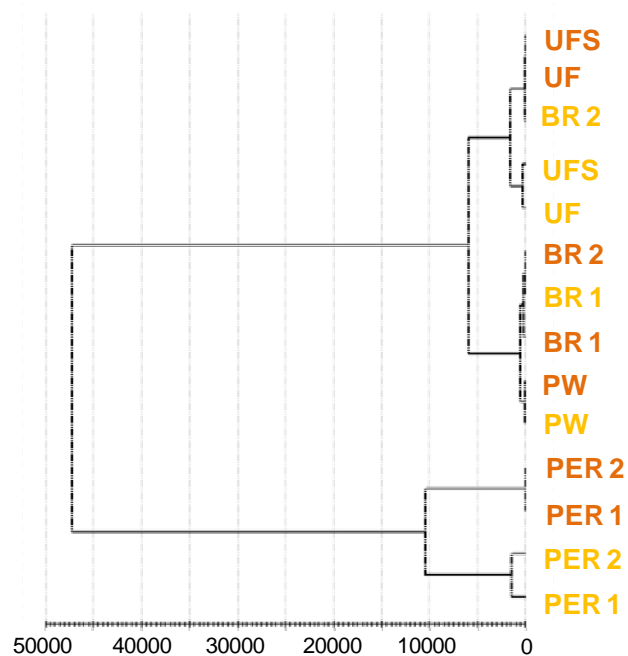


**Figure A2.** The reconstructed (only assigned mass peaks) negative electrospray 12T FT-ICR mass spectra of DOM samples: pretreated water (PW), ultrafiltration effluent (UF), ultrafiltration effluent after addition of antiscaling (UFS), permeate NF 1 (PER 1) and permeate NF 2 (PER 2). Left: June sampling campaign; Right: October sampling campaign.

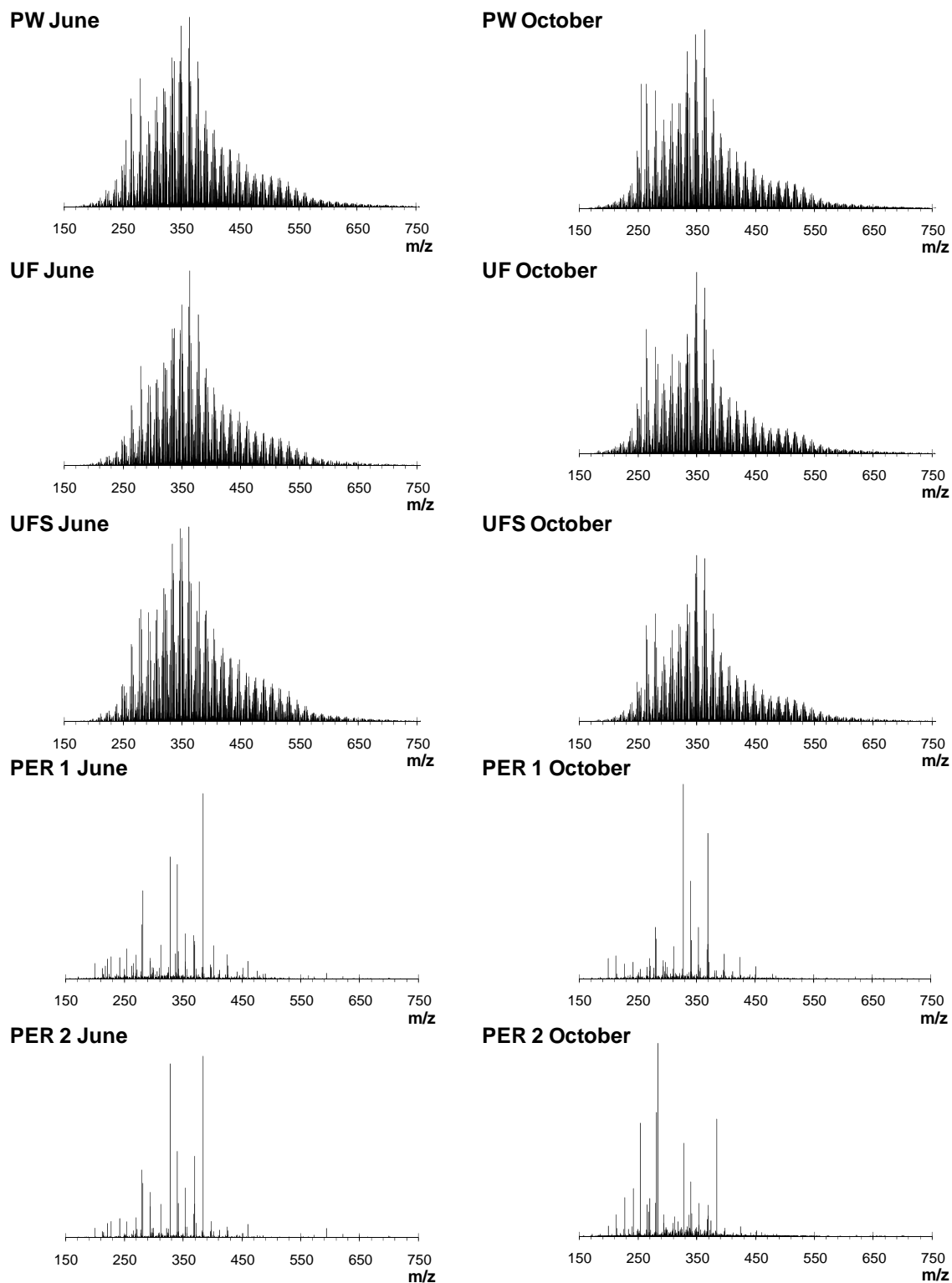


**Figure A3.** The nominal mass  $m/z$  361 expansion of negative electrospray 12T FT-ICR mass spectra of Pretreated water June (yellow) and October (orange). The depicted elemental formulas represent negative singly charged molecular ions.

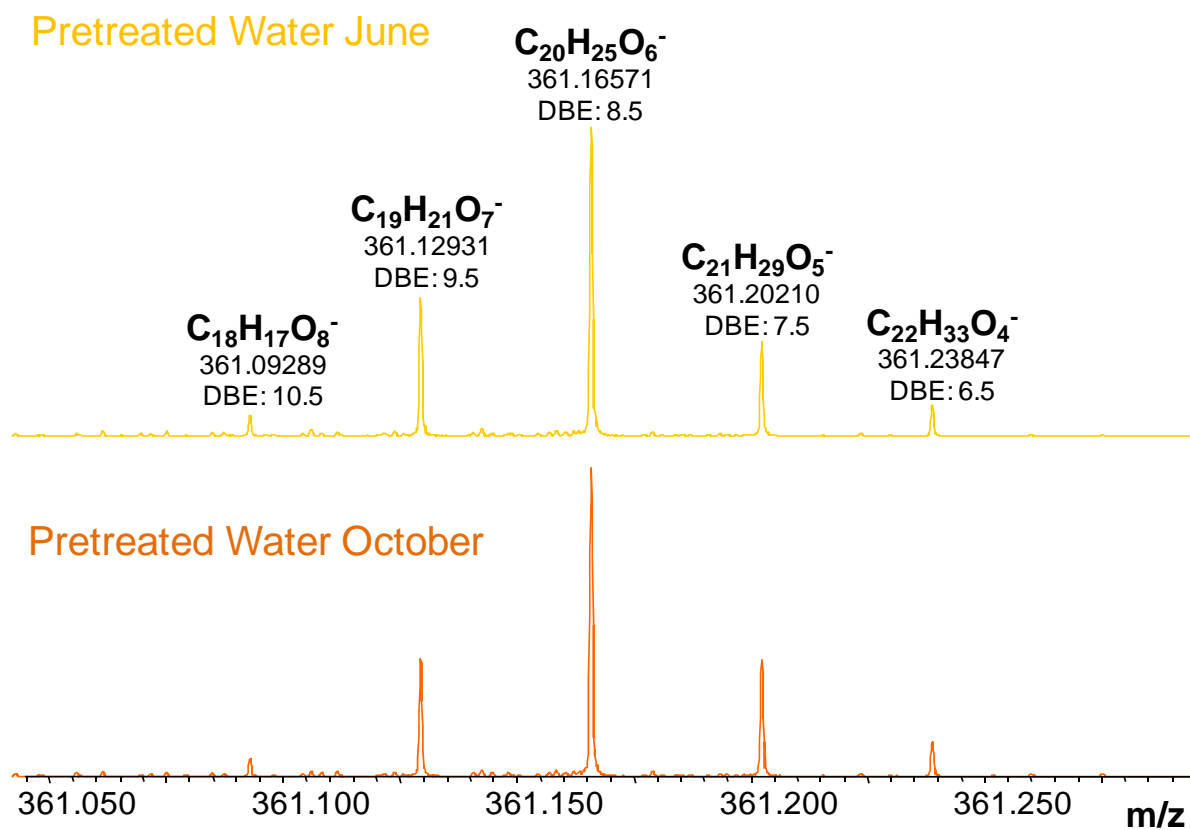


**Figure A4.** (Left) Van Krevelen diagrams for all formulas assigned of the October samples: pretreated water (PW), ultrafiltration effluent (UF), ultrafiltration effluent after adding antiscalant (UFS), NF permeate 1 (PER 1), NF permeate 2 (PER 2), on color-coded composition: CHO (blue), CHOS (green), CHNO (orange), CHNOS (red). (Right) H/C ratio vs mass-to-charge ( $m/z$ ) plot for all formulas assigned of the samples: PW, UF, UFS, PER1, PER2, on same color-coded composition. Circular areas indicate relative mass peak intensity.

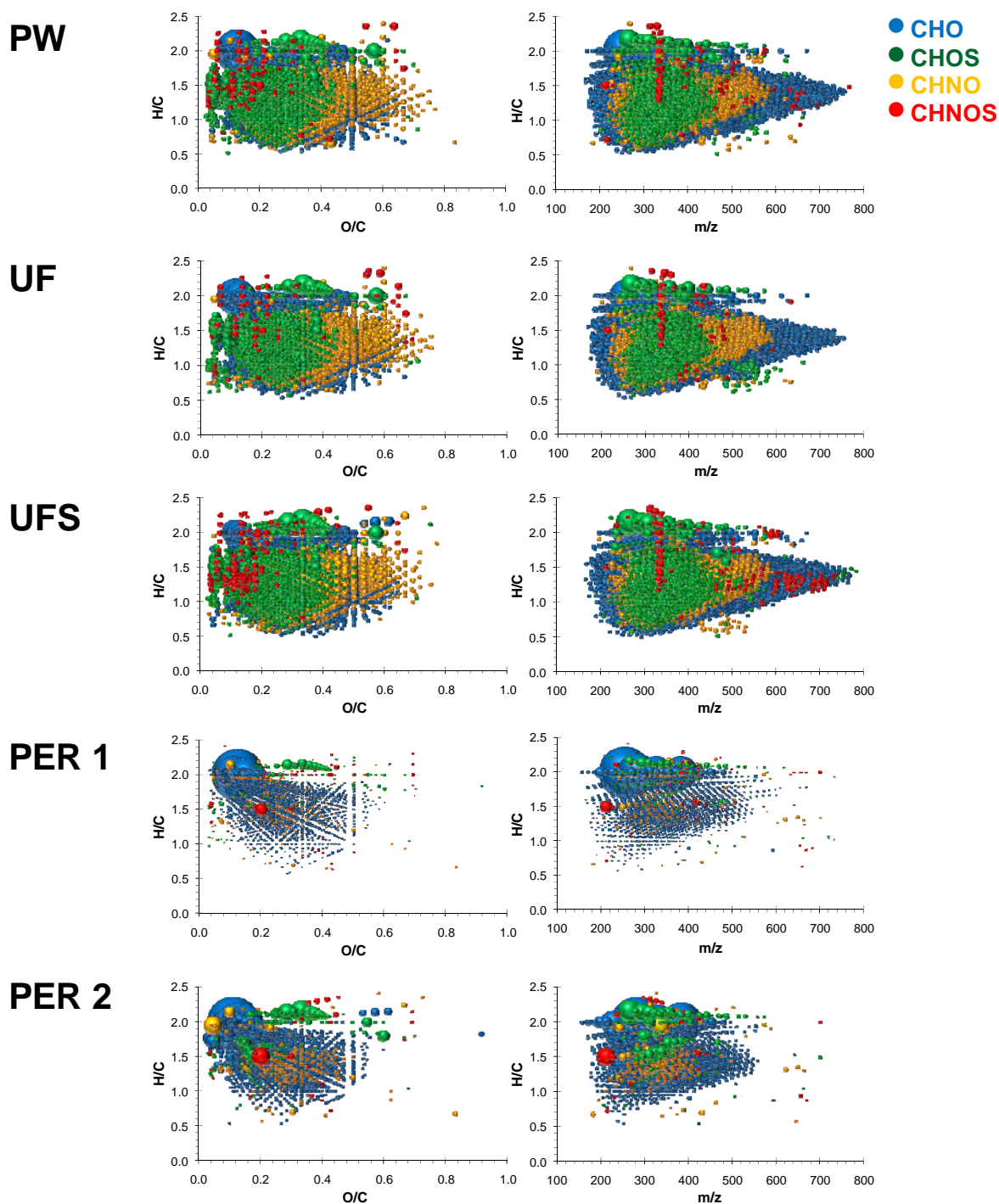
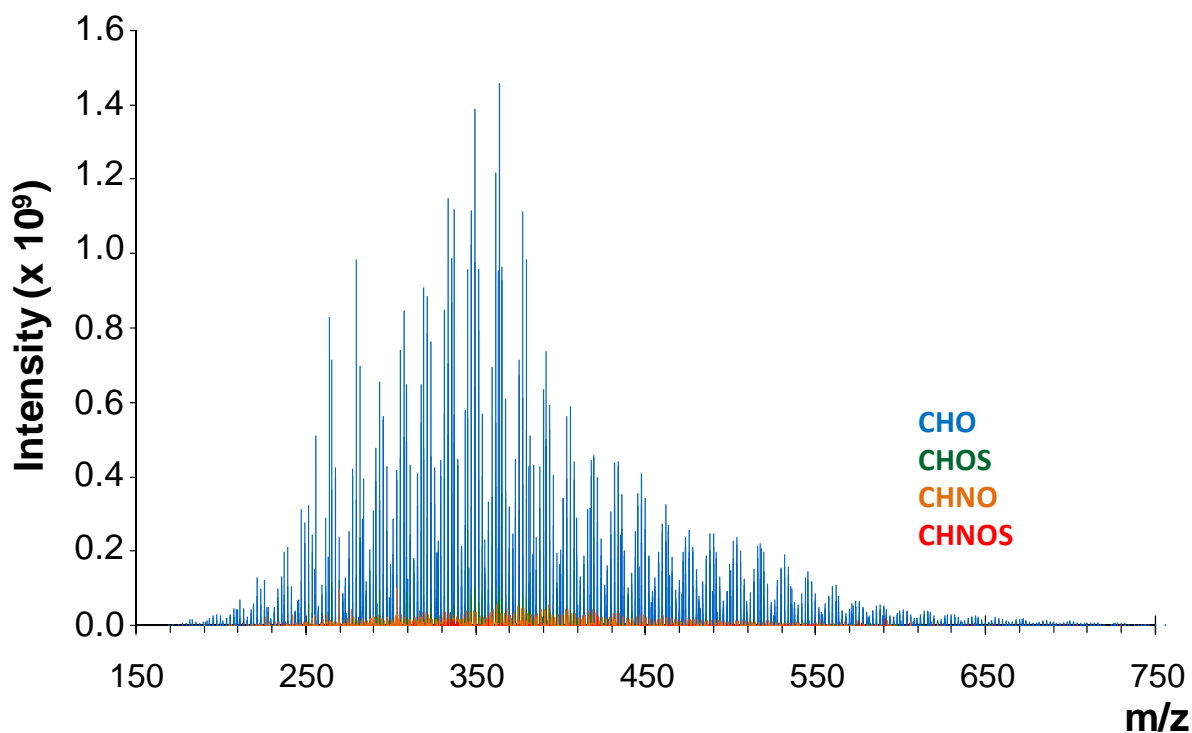


**Figure A5.** The reconstructed (only assigned mass peaks) negative electrospray 12T FT-ICR mass spectra of Pretreated water samples from June and October. The spectra are colour-coded taking into account the different composition of the elemental formulas assigned: CHO (blue), CHOS (green), CHNO (orange), CHNOS (red).

### Pretreated Water June



### Pretreated Water October

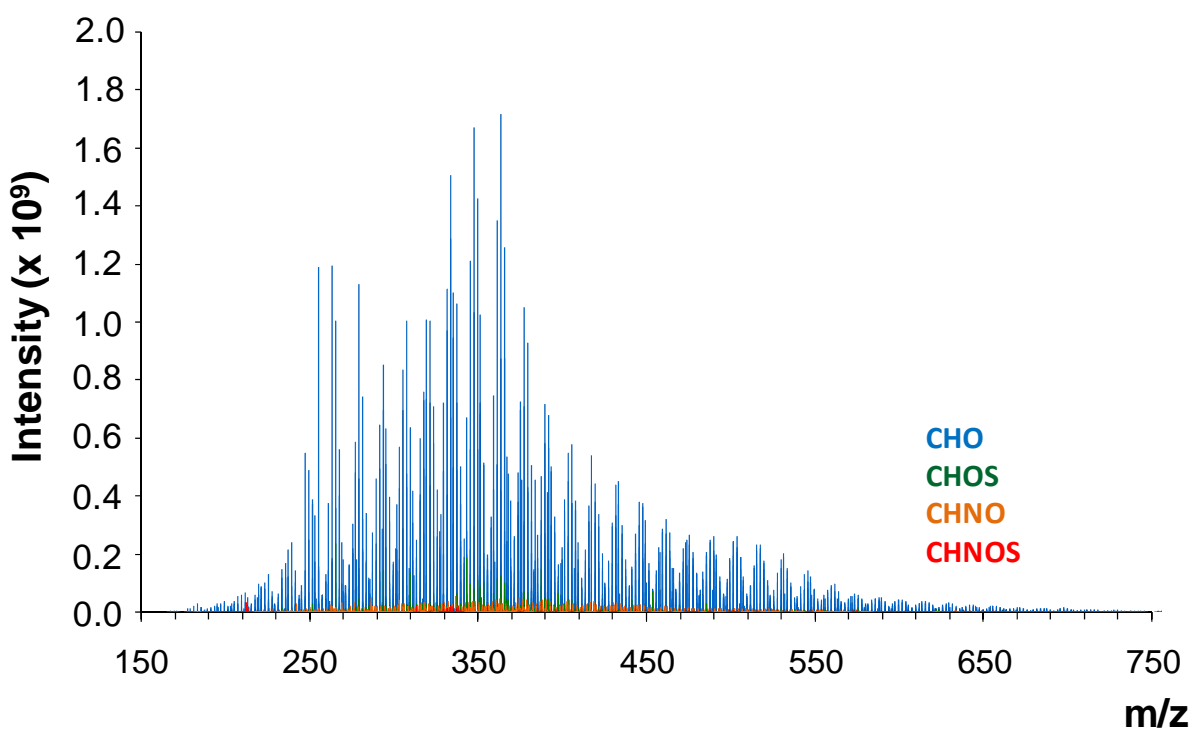


**Figure A6.**  $^1\text{H}$  NMR spectra of Pretreated water from June (yellow) and October (orange) acquired with solvent suppression and exclusion regions. Intensities are normalized to 100% intensity for the methylene group ( $\delta_{\text{H}} \sim 1.28$  ppm). Fundamental substructures are indicated from higher to lower field (from right to left): pure aliphatic  $\delta_{\text{H}} \sim 0.5\text{-}1.25$  ppm,  $\text{H}_3\text{C-C-C}$ ; polymethylene group  $\delta_{\text{H}} \sim 1.25\text{-}1.35$  ppm,  $(\text{CH}_2)_n$ ; functionalized aliphatics  $\delta_{\text{H}} \sim 1.35\text{-}1.9$  ppm,  $\text{H-C-C-CO}$ ; “acetate-analogue” and carboxyl-rich alicyclic materials (CRAM)  $\delta_{\text{H}} \sim 1.9\text{-}3.1$  ppm,  $\text{H-C-C-O}$ ; “carbohydrate-like” and methoxy  $\delta_{\text{H}} \sim 3.1\text{-}4.9$  ppm,  $\text{HCO}$ ; olefins  $\delta_{\text{H}} \sim 5.3\text{-}7.0$  ppm,  $\text{HC=C}$ ,  $\text{HCO}_2$ ; and aromatic  $\delta_{\text{H}} \sim 7.0\text{-}9.5$  ppm,  $\text{H}_{\text{ar}}$  NMR resonances.

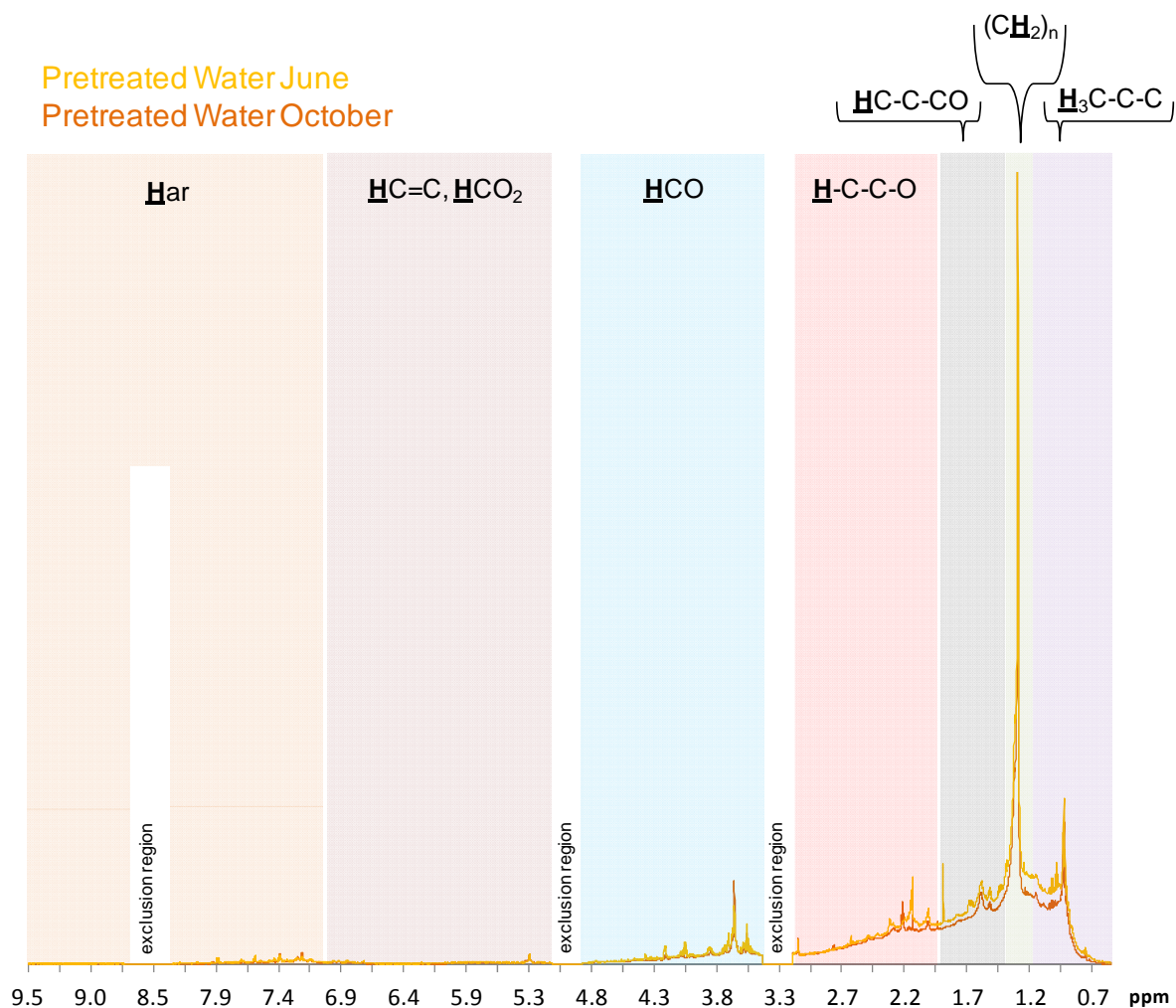


**Figure A7.** Nominal mass  $m/z$  361 expansion of negative electrospray 12T FT-ICR mass spectra of a) Pretreated water (yellow), UF effluent (dark blue) and UF + antiscaling effluent (light blue) from June; b) Zoom from the grey square in a) to see also the peaks that are less intense, but are also present in the three samples; c) UF + antiscaling effluent (light blue), Permeate NF 1 (red) and Permeate NF 2 (green) from June; d) Zoom from the grey square in c) to see that most of the peaks are partially or completely removed after the nanofiltration process.

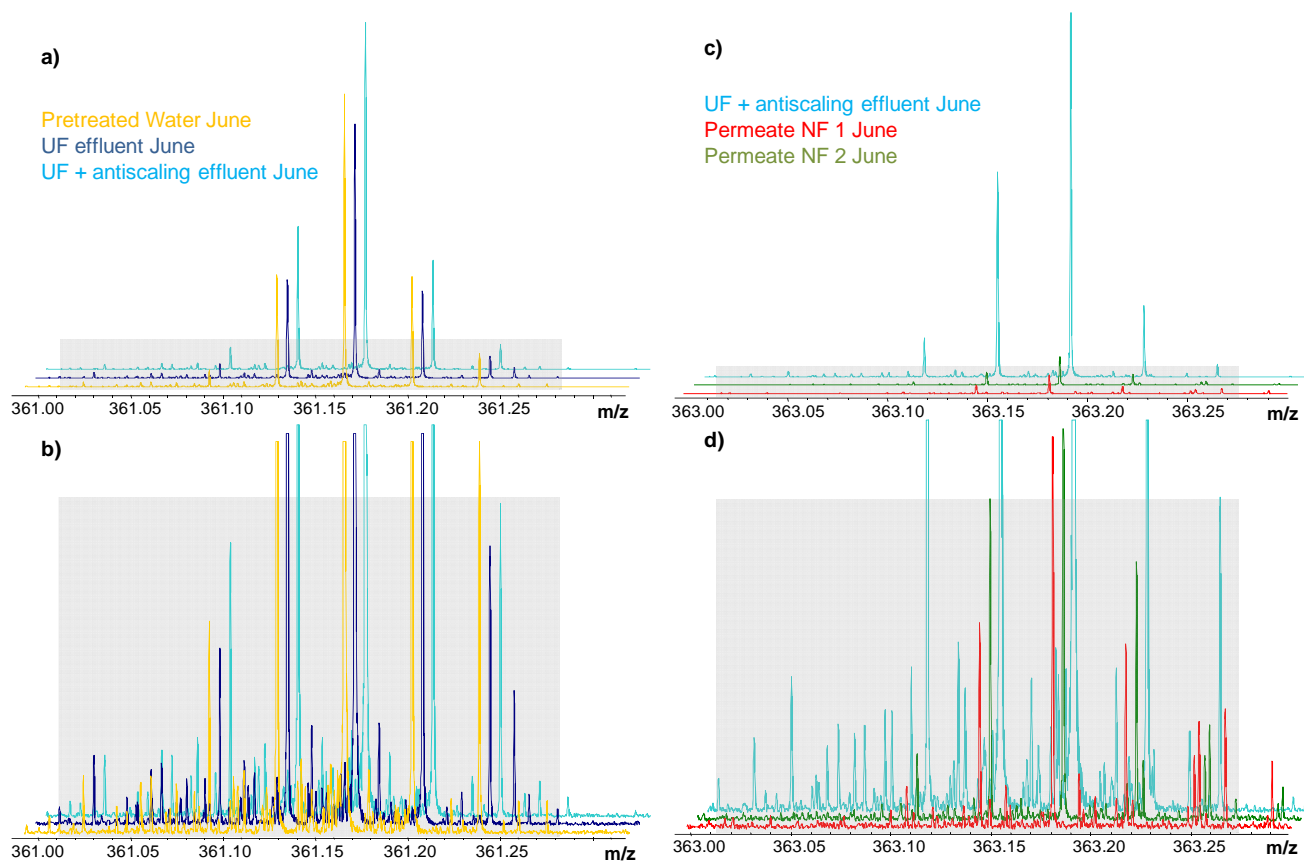


**Figure A8.**  $^1\text{H}$  NMR spectra of Pretreated water (yellow), UF effluent (dark blue) and UF + antiscaling effluent (light blue) from June acquired with solvent suppression and exclusion regions. Intensities are normalized to 100% intensity for the methylene group ( $\delta_{\text{H}} \sim 1.28$  ppm). Fundamental substructures are indicated from higher to lower field (from right to left): pure aliphatic  $\delta_{\text{H}} \sim 0.5\text{-}1.25$  ppm,  $\text{H}_3\text{C-C-C}$ ; polymethylene group  $\delta_{\text{H}} \sim 1.25\text{-}1.35$  ppm,  $(\text{CH}_2)_n$ ; functionalized aliphatics  $\delta_{\text{H}} \sim 1.35\text{-}1.9$  ppm,  $\text{H-C-C-CO}$ ; “acetate-analogue” and carboxyl-rich alicyclic materials (CRAM)  $\delta_{\text{H}} \sim 1.9\text{-}3.1$  ppm,  $\text{H-C-C-O}$ ; “carbohydrate-like” and methoxy  $\delta_{\text{H}} \sim 3.1\text{-}4.9$  ppm,  $\text{HCO}$ ; olefins  $\delta_{\text{H}} \sim 5.3\text{-}7.0$  ppm  $\text{HC=C}$ ,  $\text{HCO}_2$ ; and aromatic  $\delta_{\text{H}} \sim 7.0\text{-}9.5$  ppm,  $\text{H}_{\text{ar}}$  NMR resonances.

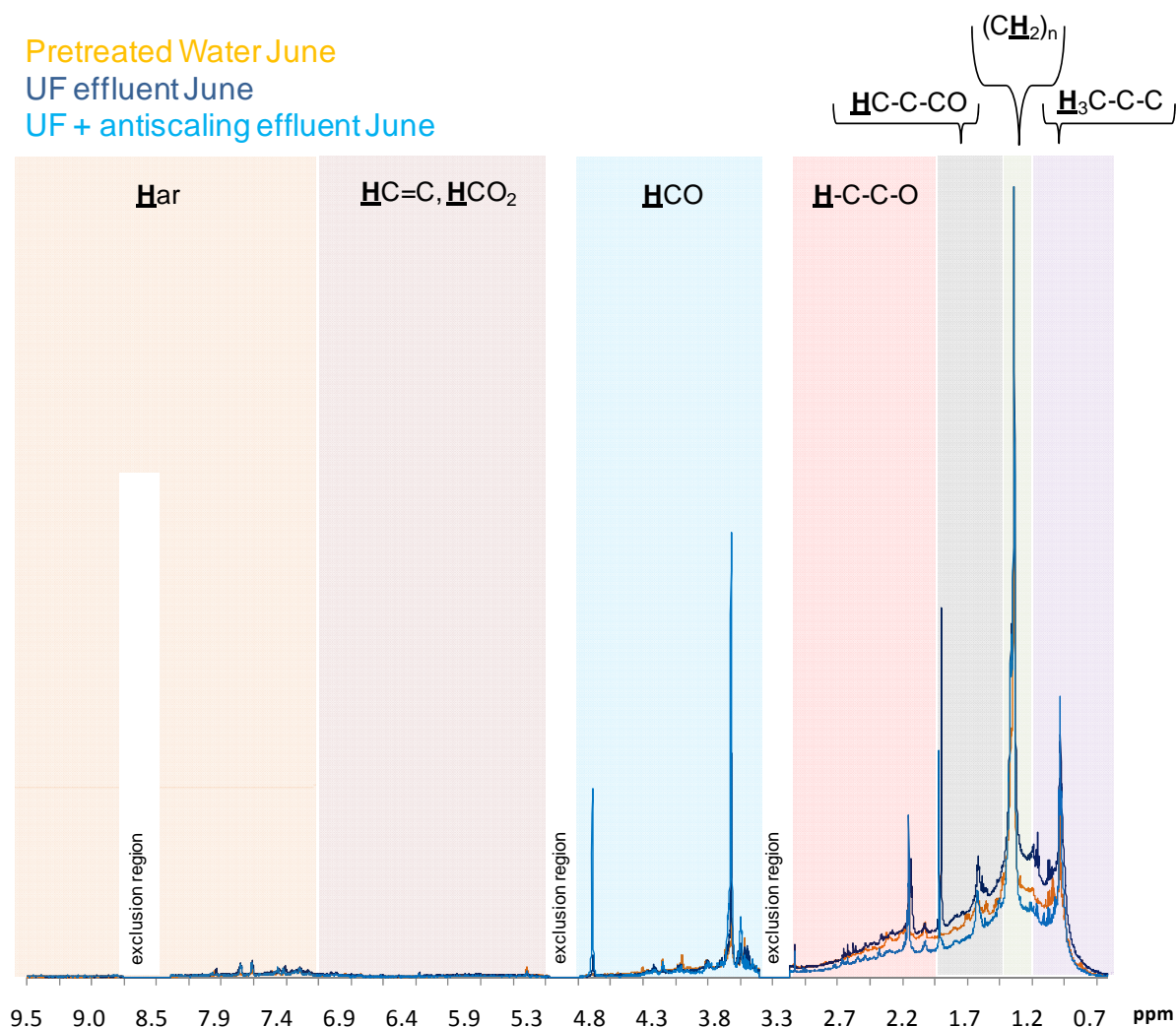


**Figure A9.**  $^1\text{H}$  NMR spectra of UF + antiscaling effluent (light blue), Permeate NF 1 (red) and Permeate NF 2 (green) from June acquired with solvent suppression and exclusion regions. Intensities are normalized to 100% intensity for the methylene group ( $\delta_{\text{H}} \sim 1.28$  ppm). Fundamental substructures are indicated from higher to lower field (from right to left): pure aliphatic  $\delta_{\text{H}} \sim 0.5\text{-}1.25$  ppm,  $\text{H}_3\text{C-C-C}$ ; polymethylene group  $\delta_{\text{H}} \sim 1.25\text{-}1.35$  ppm,  $(\text{CH}_2)_n$ ; functionalized aliphatics  $\delta_{\text{H}} \sim 1.35\text{-}1.9$  ppm,  $\text{H-C-C-CO}$ ; “acetate-analogue” and carboxyl-rich alicyclic materials (CRAM)  $\delta_{\text{H}} \sim 1.9\text{-}3.1$  ppm,  $\text{H-C-C-O}$ ; “carbohydrate-like” and methoxy  $\delta_{\text{H}} \sim 3.1\text{-}4.9$  ppm,  $\text{HCO}$ ; olefins  $\delta_{\text{H}} \sim 5.3\text{-}7.0$  ppm  $\text{HC=C}$ ,  $\text{HCO}_2$ ; and aromatic  $\delta_{\text{H}} \sim 7.0\text{-}9.5$  ppm,  $\text{H}_{\text{ar}}$  NMR resonances.

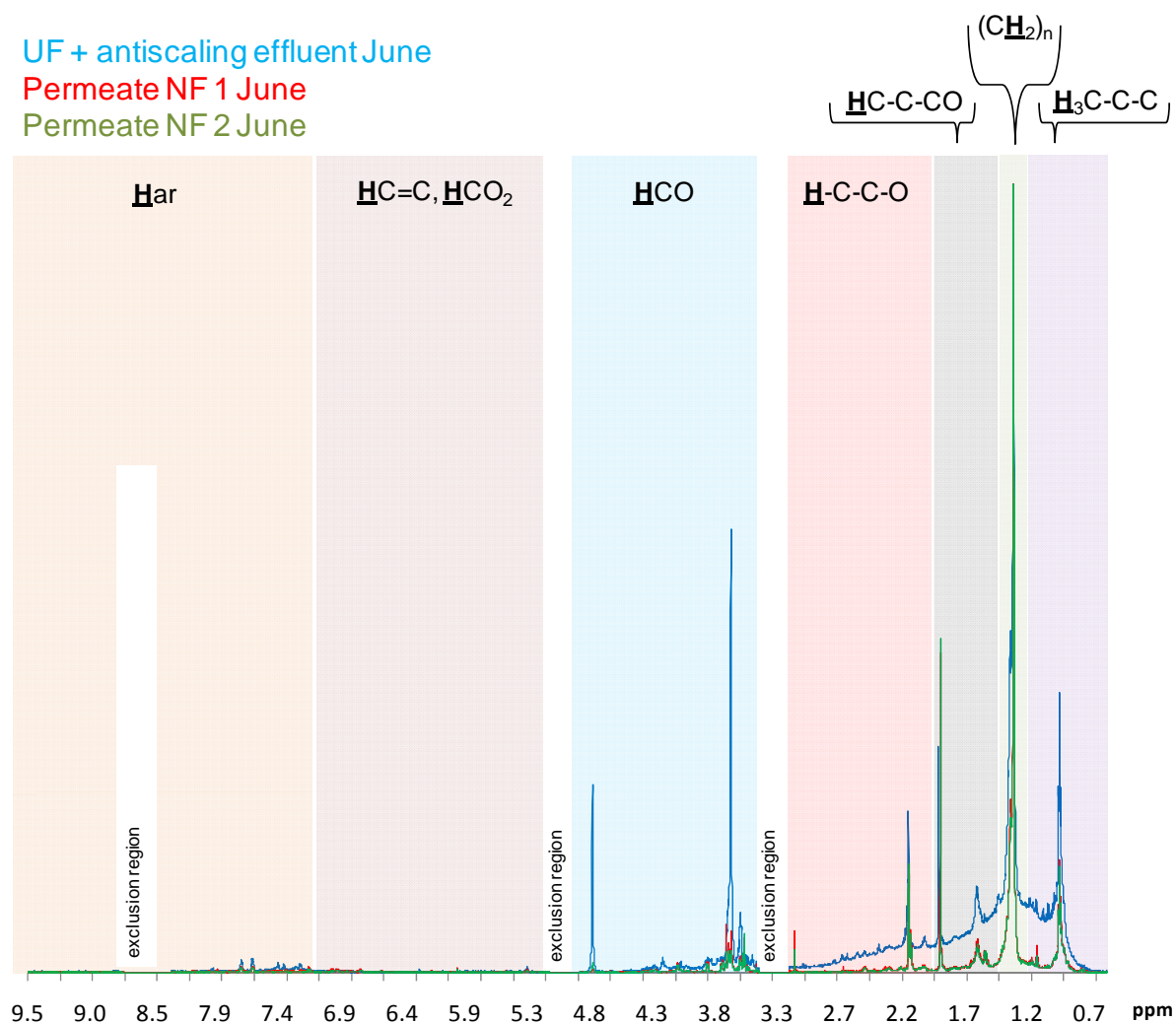


**Figure A10.** Analysis of common  $m/z$  (within 0.1 ppm mass accuracy window) in PER 1 and PER 2 (considering June and October sampling campaigns together), based on the intensity ratios ( $Ri_{PER\ 1/PER\ 2}$ ). Differentiation of the  $m/z$  intensity  $Ri_{PER\ 1/PER\ 2} > 1.5$ , shows that these  $m/z$  are enhanced in PER 1 (red square).

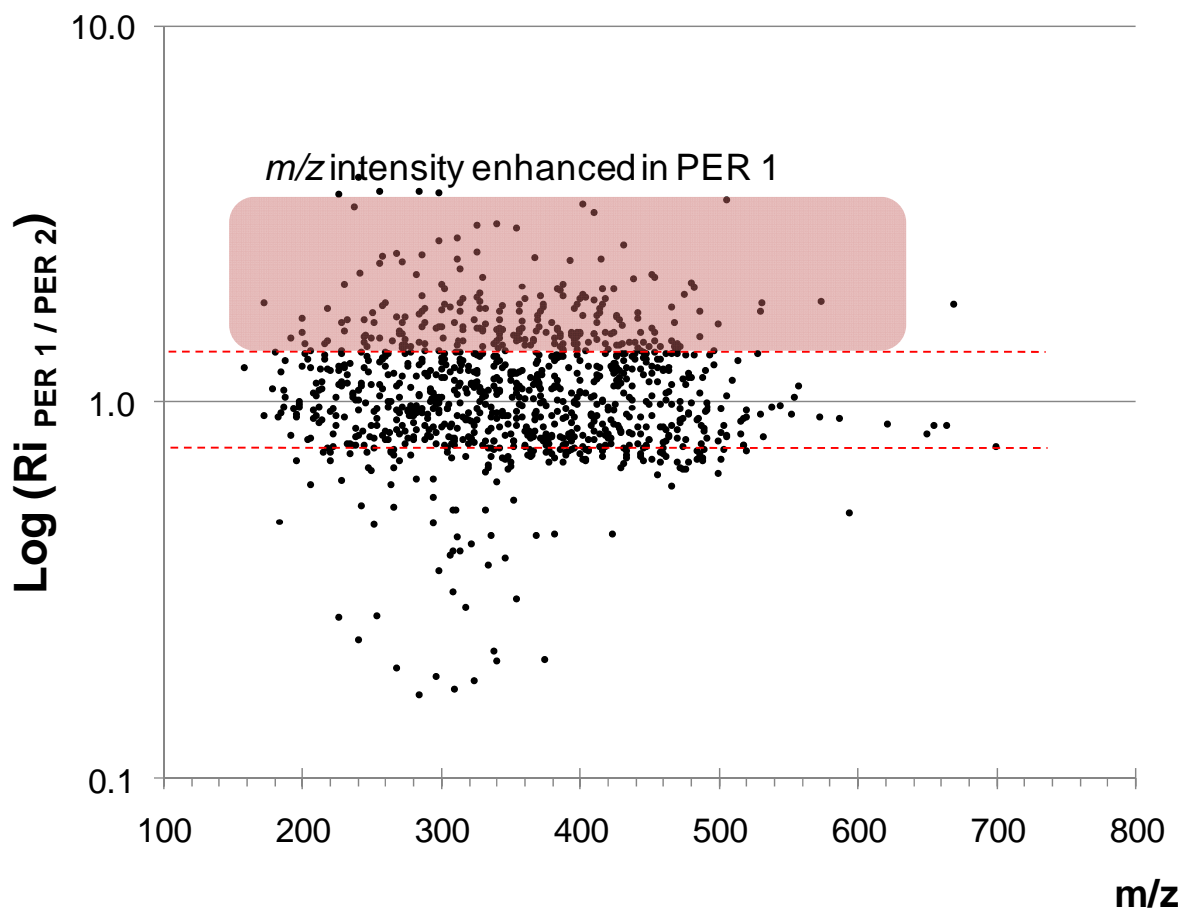
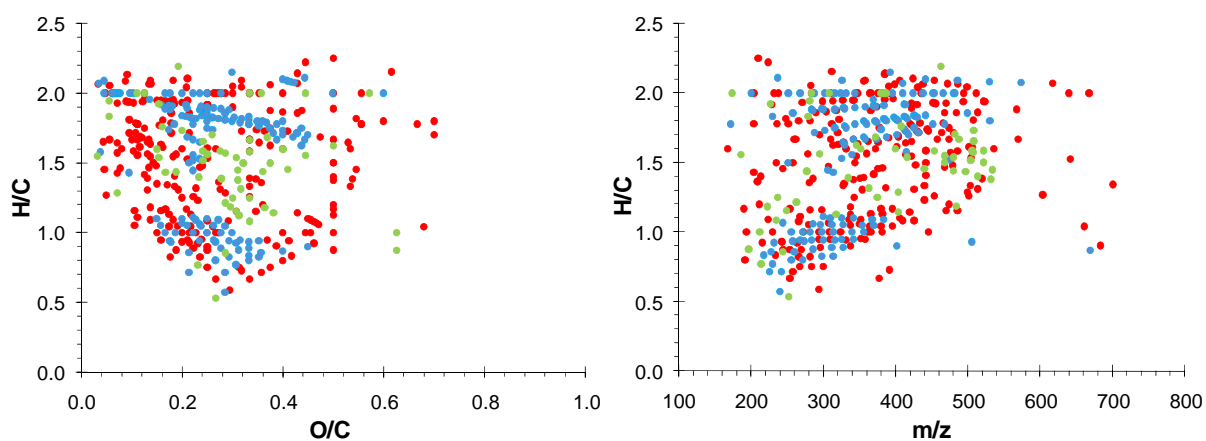


**Figure A11.** Van Krevelen diagram and H/C ratio vs  $m/z$  plot from a) the  $m/z$  unique and the intensity enriched in PER 1 (with respect to PER 2) and  $m/z$  unique in PER 2; b) the  $m/z$  common in PER 1 and PER 2 (considering June and October sampling campaigns together).

- a)  **$m/z$  unique in PER 1**  
 **$m/z$  intensity enhanced in PER 1**  
 **$m/z$  unique in PER 2**



- b)  **$m/z$  common in PER 1 and PER 2**  
 **$m/z$  intensity enhanced in PER 1**

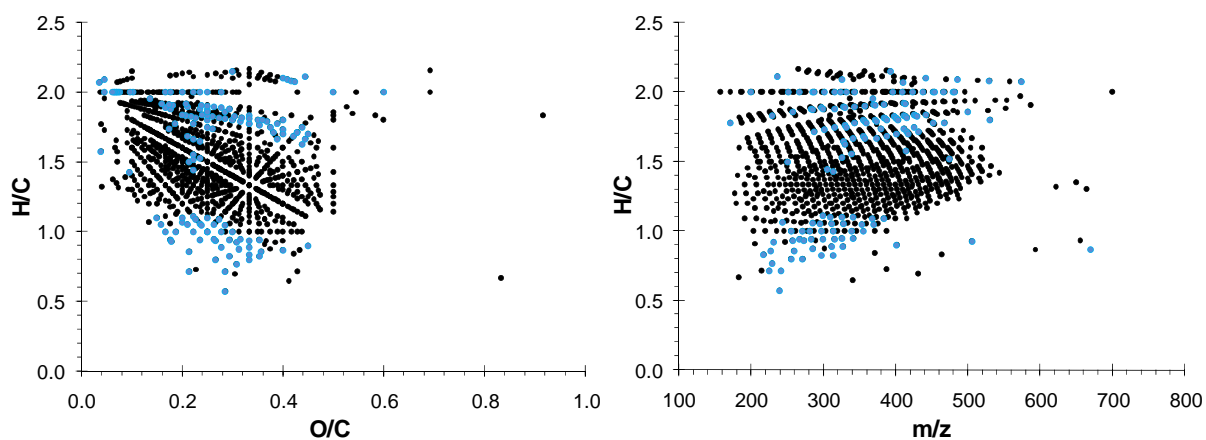


**Figure A12.** Unregulated DBPs analyzed in the samples: UF effluent, Permeate NF 1 and Permeate NF 2 (considering June and October together) after strong chlorination (following 5710-B Standard Method (American Public Health Association et al., 1998).

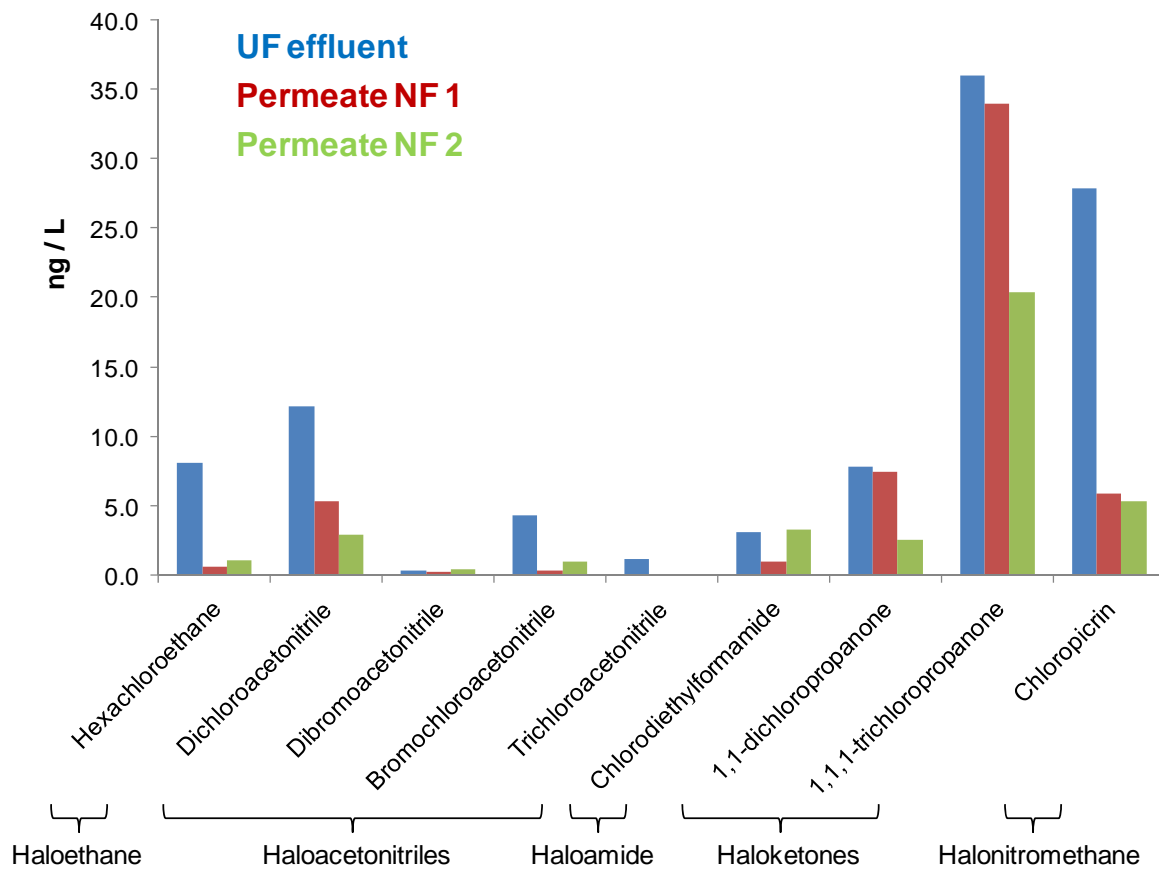
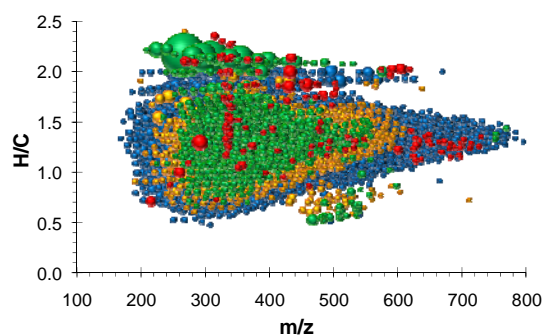
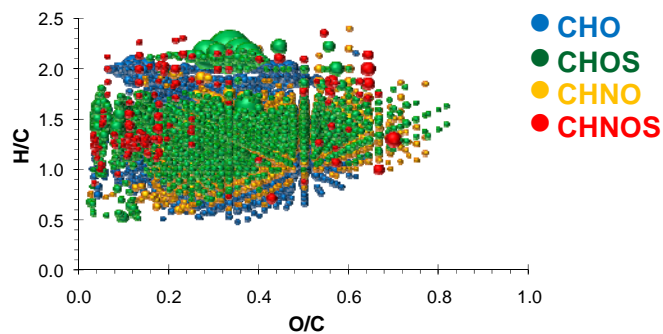
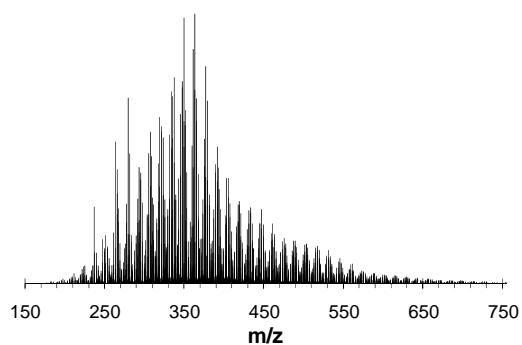


**Figure A13.** Reconstructed mass spectra (only assigned formulas), van Krevelen diagrams and H/C ratio vs mass-to-charge ( $m/z$ ) plot of the Brine samples from June: Brine NF 1 and Brine NF 2, on color-coded composition: CHO (blue), CHOS (green), CHNO (orange), CHNOS (red). Circular areas indicate relative mass peak intensity.

### Brine NF 1 June



### Brine NF 2 June

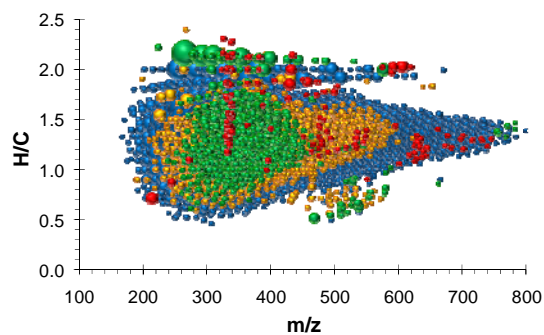
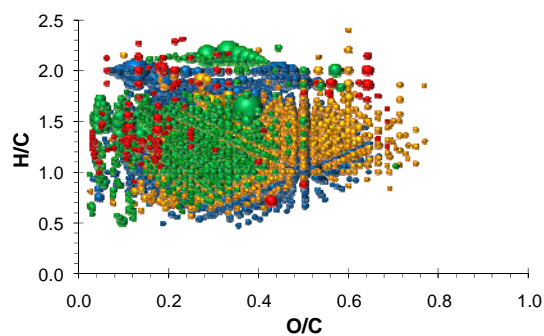
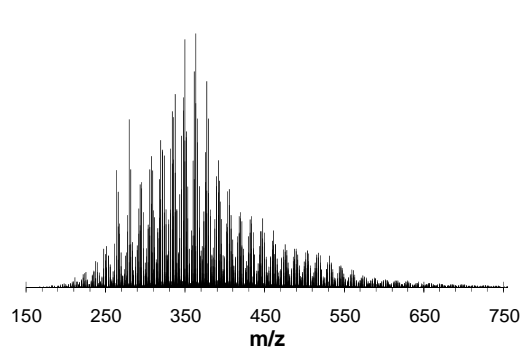
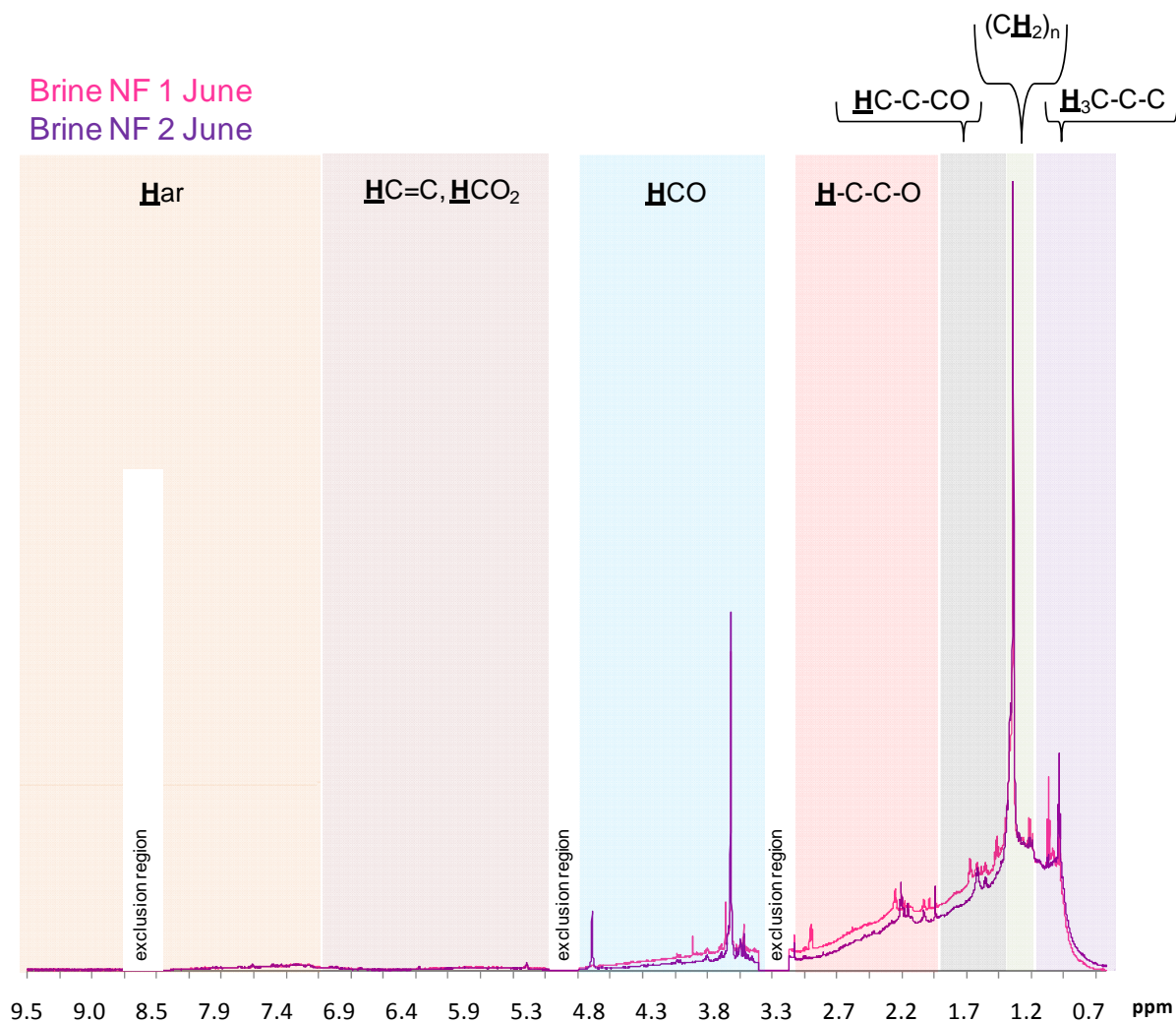


**Figure A14.**  $^1\text{H}$  NMR spectra of Brine NF 1 (pink) and Brine NF 2 (purple) from June acquired with solvent suppression and exclusion regions. Intensities are normalized to 100% intensity for the methylene group ( $\delta_{\text{H}} \sim 1.28$  ppm). Fundamental substructures are indicated from higher to lower field (from right to left): pure aliphatic  $\delta_{\text{H}} \sim 0.5\text{-}1.25$  ppm,  $\text{H}_3\text{C-C-C}$ ; polymethylene group  $\delta_{\text{H}} \sim 1.25\text{-}1.35$  ppm,  $(\text{CH}_2)_n$ ; functionalized aliphatics  $\delta_{\text{H}} \sim 1.35\text{-}1.9$  ppm,  $\text{H-C-C-CO}$ ; “acetate-analogue” and carboxyl-rich alicyclic materials (CRAM)  $\delta_{\text{H}} \sim 1.9\text{-}3.1$  ppm,  $\text{H-C-C-O}$ ; “carbohydrate-like” and methoxy  $\delta_{\text{H}} \sim 3.1\text{-}4.9$  ppm,  $\text{HCO}$ ; olefins  $\delta_{\text{H}} \sim 5.3\text{-}7.0$  ppm  $\text{HC=C}$ ,  $\text{HCO}_2$ ; and aromatic  $\delta_{\text{H}} \sim 7.0\text{-}9.5$  ppm,  $\text{H}_{\text{ar}}$  NMR resonances.



# Appendix C.

## Supporting Information Research Article N° 5

---

Nuria Cortés-Francisco, Mourad Harir, Gemma Ribera, Xavier Martinez-Lladó, Miquel Rovira, Philippe Schmitt-Kopplin, Norbert Hertkorn and Josep Caixach  
Molecular Characterization of DOM causing Fouling to NF Membranes by High-field FT-ICR Mass Spectrometry and NMR Spectroscopy.

*Environmental Science & Technology, (submitted)*



**Supporting Information:****Molecular characterization of DOM causing fouling to NF membranes by high-field FT-ICR mass spectrometry and NMR spectroscopy.**

Nuria Cortés-Francisco <sup>1</sup>, Mourad Harir <sup>2</sup>, Gemma Ribera <sup>3</sup>, Xavier Martinez-Llado <sup>3</sup>, Miquel Rovira <sup>3</sup>, Philippe Schmitt-Kopplin <sup>2,4</sup>, Norbert Hertkorn <sup>\*2</sup>, and Josep Caixach <sup>1</sup>

<sup>1</sup> Mass Spectrometry Laboratory / Organic Pollutants, IDAEA-CSIC; Jordi Girona 18-26, 08034 Barcelona, Spain. Tel: (+34) 93 400 61 00. Fax: (+34) 93 204 59 04.

<sup>2</sup> Helmholtz Zentrum Muenchen, German Research Center for Environmental Health, Research Unit Analytical Biogeochemistry (BGC), Ingolstaedter Landstrasse 1, D-85764 Neuherberg, Germany. Tel: (+49) 089 3187 2834. Fax: (+49) 089 3187 3358.

<sup>3</sup> Fundació CTM Centre Tecnològic; Plaça de la Ciència, 2, 08243 Manresa, Spain.

<sup>4</sup> Chair of Analytical Food Chemistry, Technische Universität München, Alte Akademie 10, 85354, Freising-Weihenstephan, Germany

E-mail address: hertkorn@helmholtz-muenchen.de

Number of Tables: 10

Number of Figures: 11

**Table of contents:**

**Table S1.** Physico-chemical parameters determined in the water feeding the NF membranes (UF effluent after addition of reagents) during the six-month pilot plant process as average values and the standard deviation of n=6 measurements.

**Table S2.** NF membrane specifications and properties.

**Table S3.** Sample amount, extracts final volume and amount of sample used for NMR analysis of each sample.

**Table S4.** Counts of mass peaks as computed from negative electrospray 12T FT-ICR mass spectra for singly charged ions with nitrogen rule check and 500 ppb tolerance for the Blank Membranes of the study, with the two different extraction solutions.

**Table S5.** Counts of unique assigned mass peaks comparing the two alkaline solutions for the Blank Membranes of the study as computed from negative electrospray 12T FT-ICR mass spectra for singly charged ions with nitrogen rule check and 500 ppb tolerance.

**Table S6.** Counts of DOM unique assigned mass peaks comparing the two alkaline solutions for the two used membranes of the study as computed from negative electrospray 12T FT-ICR mass spectra for singly charged ions with nitrogen rule check and 500 ppb tolerance.

**Table S7.** Reproducibility between replicate injections for two samples of the study along one week of work. The reproducibility is evaluated in terms of average of common peaks / formulas and standard deviation of the samples, proportion of common peaks / formulas and average % RSD for peak / formulas magnitude ratios (see also Figure S7 and Table S8).

**Table S8.** Counts of mass peaks for the duplicates of the study as computed from negative electrospray 12T FT-ICR mass spectra for singly charged ions with nitrogen rule check and 500 ppb tolerance. The average value and the standard deviation (SD) have been calculated, as well as the relative standard deviation (RSD).

**Table S9.** Counts of unique assigned mass peaks extracted comparing DOM 1 vs DOM 2, with each alkaline solution of the study as computed from negative electrospray 12T FT-ICR mass spectra for singly charged ions with nitrogen rule check and 500 ppb tolerance.

**Table S10.** <sup>1</sup>H NMR section integrals (percent of non-exchangeable protons) and key substructures from Blank Membranes and Used Membranes (exclusion of residual water, methanol and formic acid).

**Figure S1.** Schematic diagram of the experimental set-up for the NF pilot plant.

**Figure S2.** Scheme of the procedure carried out for data evaluation. The formulas assigned from FT-ICR data of the eight initial extracts (B1 - NaOH PPL; M1 - NaOH PPL; B1 - NH<sub>4</sub>OH PPL; M1 - NH<sub>4</sub>OH PPL; B2 - NaOH PPL; M2 - NaOH PPL; B2 - NH<sub>4</sub>OH PPL; M2 - NH<sub>4</sub>OH PPL) have been compared based on presence/absence (comparison based on the *m/z* theoretical and mass window 0.1ppm) with two main objectives: the DOM characterization from the two

Membranes (a and b; blue rows) and the comparison of alkaline solution extraction (c and d; red rows).

**Figure S3.** The negative electrospray 12T FT-ICR mass spectra (in the mass range  $m/z$  361-371) of Membrane 2 tests performed for the optimization of the amount of membrane to be used. In a) the initial sample of 4 cm<sup>2</sup> (per three pieces of membrane along the membrane sheet = equivalent to 12 cm<sup>2</sup>), b) an increased sampling area equivalent to 36 cm<sup>2</sup> and c) the optimal amount equivalent to an area of DIN-A4. Note the different intensities of the signals in the spectra (see axis y).

**Figure S4.** The nominal mass 365 expansion of the negative electrospray 12T FT-ICR mass spectra of Membrane 2 tests performed for the optimization of the amount of membrane to be used, showing the assigned formulas. In a) a sampling area equivalent to 36 cm<sup>2</sup> and b) the optimal amount equivalent to an area of DIN-A4. The common peak masses obtained when sampling 36 cm<sup>2</sup> and DIN-A4 equivalent area are indicated in boxes, showing that when a smaller amount of membrane is used, some of the signals are not detected, even after 500 scans acquisition. Note the different intensities of the signals in the spectra (see axis y).

**Figure S5.** The nominal mass 343 expansion of the negative electrospray 12T FT-ICR mass spectra of Membrane 2 tests performed for the optimization of the temperature of extraction. a) the extraction was performed at room temperature and b) the extraction was performed slightly heating at 35 °C.

**Figure S6.** Van Krevelen diagrams and H/C ratio vs mass-to-charge ( $m/z$ ) plots for all formulas assigned of the Blank Membranes: a) Blank 1 (B1) extracted with NH<sub>4</sub>OH alkaline solution and SPE-PPL, b) Blank 2 (B2) extracted with NH<sub>4</sub>OH alkaline solution and SPE-PPL c) B1 extracted with NaOH alkaline solution and SPE-PPL and d) B2 extracted with NaOH alkaline solution and SPE-PPL, on color-coded composition: CHO (blue), CHOS (green), CHNO (orange), CHNOS (red). Circular areas indicate relative mass peak intensity.

**Figure S7.** Reproducibility of mass peak magnitude. Ratios of peak magnitudes (the ratio of the peak's magnitude to the magnitude of the base peak) at  $S/N \geq 3$  of Run 1 are plotted against Run 2 for the duplicates of the study: a) Blank 2 (B2) considering mass peaks, b) B2 considering molecular formulas assigned, c) Membrane 1 (M1) considering mass peaks and d) M1 considering molecular formulas assigned. The fit ( $R^2$ ) is specified in each case and the 1:1 line is provided as a reference on each plot.

**Figure S8.** Van Krevelen diagrams and H/C ratio vs mass-to-charge ( $m/z$ ) plots for the Unique formulas assigned when comparing DOM 1 vs DOM 2, for DOM extracted with NH<sub>4</sub>OH alkaline solution and SPE-PPL: a) Unique assigned formulas of DOM 1 and b) Unique assigned formulas of DOM 2, on color-coded composition: CHO (blue), CHOS (green), CHNO (orange), CHNOS (red). Circular areas indicate relative mass peak intensity.

**Figure S9.** Van Krevelen diagrams and H/C ratio vs mass-to-charge ( $m/z$ ) plots for the Unique formulas assigned when comparing DOM 1 vs DOM 2, for DOM extracted with NaOH alkaline solution and SPE-PPL: a) Unique assigned formulas of DOM 1 and b) Unique assigned formulas of DOM 2, on color-coded composition: CHO (blue), CHOS (green), CHNO (orange), CHNOS (red). Circular areas indicate relative mass peak intensity.

**Figure S10.**  $^1\text{H}$  NMR spectra of (purple): Used Membrane 1 extracted with  $\text{NH}_4\text{OH}$  alkaline solution and SPE-PPL, (blue): Used Membrane 2 extracted with  $\text{NH}_4\text{OH}$  alkaline solution and SPE-PPL, (green): Used Membrane 1 extracted with  $\text{NaOH}$  alkaline solution and SPE-PPL, (red): Used Membrane 2 extracted with  $\text{NaOH}$  alkaline solution and SPE-PPL. Intensities are normalized to 100% intensity for the methylene group ( $\delta_{\text{H}} \sim 1.28$  ppm). Fundamental substructures are indicated from higher to lower field (from right to left): pure aliphatic  $\delta_{\text{H}} \sim 0.5$ -1.25 ppm,  $\underline{\text{H}}_3\text{C-C-C}$ ; polymethylene group  $\delta_{\text{H}} \sim 1.25$ -1.35 ppm,  $(\underline{\text{C}}\underline{\text{H}}_2)_n$ ; functionalized aliphatics  $\delta_{\text{H}} \sim 1.35$ -1.9 ppm,  $\underline{\text{H}}\text{C-C-CO}$ ,  $\underline{\text{H}}\text{C-CN}$  and  $\underline{\text{H}}\text{C-CS}$ ; “acetate-analogue” and carboxyl-rich alicyclic materials (CRAM)  $\delta_{\text{H}} \sim 1.9$ -3.1 ppm,  $\underline{\text{H}}\text{C-C-O}$ ; “carbohydrate-like” and methoxy  $\delta_{\text{H}} \sim 3.1$ -4.9 ppm,  $\underline{\text{H}}\text{CO}$ ; olefins  $\delta_{\text{H}} \sim 5.3$ -7.0 ppm  $\underline{\text{H}}\text{C}=\text{C}$ ,  $\underline{\text{H}}\text{CO}_2$ ; and aromatic  $\delta_{\text{H}} \sim 7.0$ -9.5 ppm,  $\underline{\text{H}}_{\text{ar}}$  NMR resonances.

**Figure S11.**  $^1\text{H}$  NMR spectra of (purple): Blank Membrane 1 extracted with  $\text{NH}_4\text{OH}$  alkaline solution and SPE-PPL, (blue): Blank Membrane 2 extracted with  $\text{NH}_4\text{OH}$  alkaline solution and SPE-PPL, (green): Blank Membrane 1 extracted with  $\text{NaOH}$  alkaline solution and SPE-PPL, (red): Blank Membrane 2 extracted with  $\text{NaOH}$  alkaline solution and SPE-PPL. Intensities are normalized to 100% intensity for the methylene group ( $\delta_{\text{H}} \sim 1.28$  ppm). Fundamental substructures are indicated from higher to lower field (from right to left): pure aliphatic  $\delta_{\text{H}} \sim 0.5$ -1.25 ppm,  $\underline{\text{H}}_3\text{C-C-C}$ ; polymethylene group  $\delta_{\text{H}} \sim 1.25$ -1.35 ppm,  $(\underline{\text{C}}\underline{\text{H}}_2)_n$ ; functionalized aliphatics  $\delta_{\text{H}} \sim 1.35$ -1.9 ppm,  $\underline{\text{H}}\text{C-C-CO}$ ,  $\underline{\text{H}}\text{C-CN}$  and  $\underline{\text{H}}\text{C-CS}$ ; “acetate-analogue” and carboxyl-rich alicyclic materials (CRAM)  $\delta_{\text{H}} \sim 1.9$ -3.1 ppm,  $\underline{\text{H}}\text{C-C-O}$ ; “carbohydrate-like” and methoxy  $\delta_{\text{H}} \sim 3.1$ -4.9 ppm,  $\underline{\text{H}}\text{CO}$ ; olefins  $\delta_{\text{H}} \sim 5.3$ -7.0 ppm  $\underline{\text{H}}\text{C}=\text{C}$ ,  $\underline{\text{H}}\text{CO}_2$ ; and aromatic  $\delta_{\text{H}} \sim 7.0$ -9.5 ppm,  $\underline{\text{H}}_{\text{ar}}$  NMR resonances.

**Table S1.** Physico-chemical parameters determined in the water feeding the NF membranes (UF effluent after addition of reagents) during the six-month pilot plant process as average values and the standard deviation of n=6 measurements.

Parameters	Average value	Standard deviation
Conductivity ( $\mu\text{S}\cdot\text{cm}^{-1}$ )	891	330
pH	7.7	0.4
NPOC ( $\mu\text{g}\cdot\text{L}^{-1}$ )	4860	3218
UVA (254 nm)	0.07	0.05
TIC ( $\text{mg}\cdot\text{L}^{-1}$ )	43	14
TN ( $\text{mg}\cdot\text{L}^{-1}$ )	0.8	0.3
$\text{Ca}^{2+}$ ( $\text{mg}\cdot\text{L}^{-1}$ )	140	71
$\text{Mg}^{2+}$ ( $\text{mg}\cdot\text{L}^{-1}$ )	18	8
$\text{K}^{+}$ ( $\text{mg}\cdot\text{L}^{-1}$ )	25	0.7
$\text{Na}^{+}$ ( $\text{mg}\cdot\text{L}^{-1}$ )	20	8
$\text{Cl}^{-}$ ( $\text{mg}\cdot\text{L}^{-1}$ )	42	2
$\text{NO}_3^{-}$ ( $\text{mg}\cdot\text{L}^{-1}$ )	1.7	0.5
$\text{SO}_4^{2-}$ ( $\text{mg}\cdot\text{L}^{-1}$ )	238	154

**Table S2.** NF membrane specifications and properties.

Property	ESNA1LF2-4040 Membrane 1		NF270-4040 Membrane 2	
Supplier	Hydranautics		DOW-Filmtec	
Configuration	Cross-flow Spiral-wound			
Operation TMP (bar)	21 max.		41 max.	
Design flux (l/m <sup>2</sup> h)	N/A		22-29	
Pretreatment	UF (SDI<3)			
Water recovery	15 %		17 %	
Material	Polyamide layer on top of a polysulphone support		Piperazine-based polyamide layer on top of a polysulphone support	
Membrane Surface (m <sup>2</sup> )	7.9		7.6	
Pressure drop per module (bar)	0.7		1.0	
WCO	200	Amy et al. <sup>1</sup>	270 175	DOW Water <sup>9</sup> Klöpffel et al. <sup>10</sup>
Clean water permeability (m <sup>3</sup> /(m <sup>2</sup> ·day·kPa))	1.84	Amy et al. <sup>1</sup> Park et al. <sup>2</sup>	3.3 3.19	Sentana et al. <sup>6</sup> Park et al. <sup>2</sup>
% conductivity rejection	80	Ribera et al. <sup>3</sup>	55	Ribera et al. <sup>3</sup>
Contact angle	60 <sup>a</sup> 23-40 <sup>b</sup>	Yoon et al. <sup>4</sup> Childress et al. <sup>5</sup>	28.5	Klöpffel et al. <sup>10</sup>
Z-potential	-12 <sup>b</sup> -7	Sentana et al. <sup>6</sup> Oatley, D. <sup>7</sup>	-19.7 -32	Klöpffel et al. <sup>10</sup> Oatley, D.L. et al. <sup>11</sup>
Porosity AFM (nm)	0.49	Llenas et al. <sup>8</sup>	0.50	Llenas et al. <sup>8</sup>
Roughness AFM (nm)	49.7	Llenas et al. <sup>8</sup>	5.35	Llenas et al. <sup>8</sup>
Isoelectric point	2-3	Oatley, D. <sup>7</sup>	3.5	Oatley, D.L. et al. <sup>11</sup>

<sup>a</sup>Value for ESNA1 membrane<sup>b</sup>Value for ESNA1LF membranes

N/A: no data available

## References

1. Amy, G.L. *NOM rejection by and fouling of, NF and UF membranes*, AWWA Research Foundation and American Water Works Association, Denver, 2001.
2. Park, N.; Kwon, B.; Sun, M.; Ahn, H.; Kim, C.; Kwoak, C.; Lee, D.; Chae, S.; Hyung, H.; Cho, J., Application of various membranes to remove NOM typically occurring in Korea with respect to DBP, AOC and transport parameters. *Desalination* **2005**, *178*, (1-3), 161-169.
3. Ribera, G.; Llenas, L.; Rovira, M.; de Pablo, J.; Martinez-Llado, X., Pilot plant comparison study of two commercial nanofiltration membranes in a drinking water treatment plant. *Desalination and Water Treatment* **2013**, *51*, (1-3), 448-457.

4. Yoon, Y.; Amy, G.; Cho, J.; Her, N., Effects of retained natural organic matter (NOM) on NOM rejection and membrane flux decline with nanofiltration and ultrafiltration. *Desalination* **2005**, *173*, (3), 209-221.
5. Childress, A.E.; Brant, J.A.; Rempala, P.; Phipps, D.W.; Kwan, P., *Evaluation of membrane characterization methods*, Water Research Foundation, Denver, 2012, p.179
6. Sentana, I.; Puche, R.D.S.; Sentana, E.; Prats, D., Reduction of chlorination byproducts in surface water using ceramic nanofiltration membranes. *Desalination* **2010**, *277*, (1-3), 147-155.
7. Oatley, D. Isoelectric point of NF270 and ESNA1LF2 (Personal Communication), Swansea, 2012.
8. Llenas, L.; Martínez-Lladó, X.; Yaroshchuk, A.; Rovira, M.; de Pablo, J., Nanofiltration as pretreatment for scale prevention in seawater reverse osmosis desalination. *Desalination and Water Treatment* **2011**, *36*, (1-3), 310-318.
9. DOW Water & Process Solutions technical manual, Technical manual, FILMTEC Reverse Osmosis Membranes. in: F.N. 609-00071-1009.
10. Klüpfel, A.M.; Frimmel, F.H., Nanofiltration of river water - fouling, cleaning and micropollutant rejection. *Desalination* **2010**, *250*, (3), 1005-1007.
11. Oatley, D.L.; Llenas, L.; Pérez, R.; Williams, P.M.; Martínez-Lladó, X.; Rovira, M., Review of the dielectric properties of nanofiltration membranes and verification of the single oriented layer approximation. *Adv. Colloid Interfac. Sci.* **2012**, *173*, 1-11.

**Table S3.** Sample amount, extracts final volume and amount of sample used for NMR analysis of each sample.

<b>Samples</b>	<b>Extraction</b>	<b>Sample amount (cm<sup>2</sup>)</b>	<b>Final extract (μL)</b>	<b>Sample analyzed in NMR (mg)</b>
Blank 1	NH <sub>4</sub> OH PPL	DIN - A4	1000	1.4
	NaOH PPL	DIN - A4	1000	0.9
Membrane 1	NH <sub>4</sub> OH PPL	DIN - A4	1000	1.3
	NaOH PPL	DIN - A4	1000	0.7
Blank 2	NH <sub>4</sub> OH PPL	DIN - A4	1000	3.7
	NaOH PPL	DIN - A4	1000	5.8
Membrane 2	NH <sub>4</sub> OH PPL	DIN - A4	1000	3.6
	NaOH PPL	DIN - A4	1000	4.3

**Table S4.** Counts of mass peaks as computed from negative electrospray 12T FT-ICR mass spectra for singly charged ions with nitrogen rule check and 500 ppb tolerance for the Blank Membranes of the study, with the two different extraction solutions.

Members of molecular series	Blank 1		Blank 2	
	NH <sub>4</sub> OH-PPL	NaOH-PPL	NH <sub>4</sub> OH-PPL	NaOH-PPL
CHO compounds	357 (43 %)	508 (57 %)	325 (24 %)	638 (44 %)
CHOS compounds	259 (31 %)	215 (24 %)	674 (49 %)	542 (37 %)
CHNO compounds	120 (14 %)	91 (10 %)	132 (10 %)	125 (9 %)
CHNOS compounds	92 (11 %)	80 (9 %)	250 (18 %)	142 (10 %)
Number of assigned mass peaks	828	894	1381	1447
average H [%]	8.4	7.4	7.8	8.0
average C [%]	61	60	55	60
average O [%]	25	28	28	26
average N [%]	1.1	1.0	0.7	0.6
average S [%]	4.5	3.3	8.9	5.1
computed H/C ratio from FTICR mass peaks	1.6	1.5	1.7	1.6
computed O/C ratio from FTICR mass peaks	0.30	0.36	0.39	0.33
computed C/N ratio from FTICR mass peaks	13	13	14	16
computed C/S ratio from FTICR mass peaks	15	16	13	15
Average DBE, intensity weighted	4.1	5.5	3.4	4.5
Average DBE/C, intensity weighted	0.24	0.30	0.21	0.25
Average mass, intensity weighted	324.8	343.5	343.9	333.4

**Table S5.** Counts of unique assigned mass peaks comparing the two alkaline solutions for the Blank Membranes of the study as computed from negative electrospray 12T FT-ICR mass spectra for singly charged ions with nitrogen rule check and 500 ppb tolerance.

Members of molecular series	Blank 1		Blank 2	
	NH <sub>4</sub> OH-PPL	NaOH-PPL	NH <sub>4</sub> OH-PPL	NaOH-PPL
Unique assigned mass peaks extracted with:				
Unique assigned mass peaks	40 %	44 %	40 %	43 %
CHO compounds	61 (18 %)	212 (54 %)	37 (7 %)	348 (56 %)
CHOS compounds	130 (39 %)	82 (21 %)	245 (44 %)	115 (18 %)
CHNO compounds	82 (25 %)	53 (13 %)	78 (14 %)	73 (12 %)
CHNOS compounds	59 (18 %)	47 (12 %)	197 (35 %)	90 (14 %)
Number of unique assigned mass peaks	332	394	557	626
average H [%]	7.8	6.2	7.1	6.9
average C [%]	62	59	56	62
average O [%]	23	30	27	26
average N [%]	2.3	1.2	2.5	1.5
average S [%]	4.8	3.6	7.5	3.7
computed H/C ratio from FTICR mass peaks	1.5	1.3	1.5	1.3
computed O/C ratio from FTICR mass peaks	0.29	0.38	0.36	0.31
computed C/N ratio from FTICR mass peaks	14.3	17.4	12.2	16.3
computed C/S ratio from FTICR mass peaks	15.8	17.9	14.8	18.8
Average DBE, intensity weighted	6.0	9.4	5.8	8.3
Average DBE/C, intensity weighted	0.29	0.41	0.30	0.37
Average mass, intensity weighted	379.4	446.2	404.9	412.1

**Table S6.** Counts of DOM unique assigned mass peaks comparing the two alkaline solutions for the two used membranes of the study as computed from negative electrospray 12T FT-ICR mass spectra for singly charged ions with nitrogen rule check and 500 ppb tolerance.

Members of molecular series	DOM 1		DOM 2	
	NH <sub>4</sub> OH-PPL	NaOH-PPL	NH <sub>4</sub> OH-PPL	NaOH-PPL
Unique assigned mass peaks extracted with:				
Unique assigned mass peaks	75 %	71 %	61 %	58 %
CHO compounds	266 (22 %)	298 (30 %)	354 (35 %)	386 (40 %)
CHOS compounds	255 (21 %)	279 (28 %)	156 (15 %)	257 (26 %)
CHNO compounds	433 (36 %)	211 (21 %)	330 (33 %)	180 (18 %)
CHNOS compounds	264 (22 %)	220 (22 %)	175 (17 %)	151 (16 %)
Number of unique assigned mass peaks	1218	1008	1015	974
average H [%]	8.0	7.8	8.4	7.4
average C [%]	65	64	63	62
average O [%]	22	22	24	26
average N [%]	2.3	2.0	1.9	1.8
average S [%]	3.0	4.8	2.4	3.6
computed H/C ratio from FTICR mass peaks	1.5	1.5	1.6	1.4
computed O/C ratio from FTICR mass peaks	0.26	0.26	0.28	0.31
computed C/N ratio from FTICR mass peaks	14.8	11.8	14.7	13.3
computed C/S ratio from FTICR mass peaks	28.8	19.5	25.8	22.5
Average DBE, intensity weighted	7.5	7.0	7.0	7.8
Average DBE/C, intensity weighted	0.31	0.31	0.29	0.32
Average mass, intensity weighted	437.8	410.0	418.9	452.8

**Table S7.** Reproducibility between replicate injections for two samples of the study along one week of work. The reproducibility is evaluated in terms of average of common peaks / formulas and standard deviation of the samples, proportion of common peaks / formulas and average % RSD for peak / formulas magnitude ratios (see also Figure S7 and Table S8).

<b>Sample</b>		<b>Average of common peaks / formulas (SD)</b>	<b>% of common peaks / formulas</b>	<b>Average % RSD for peak / formulas magnitude ratios</b>
Blank 2 NaOH- PPL	Peaks	3004 (764)	68	20 %
	Assigned Formulas	1270 (182)	67	18 %
Membrane 1 NH <sub>4</sub> OH-PPL	Peaks	4443 (233)	80	14 %
	Assigned Formulas	2374 (77)	80	12 %

**Table S8.** Counts of mass peaks for the duplicates of the study as computed from negative electrospray 12T FT-ICR mass spectra for singly charged ions with nitrogen rule check and 500 ppb tolerance. The average value and the standard deviation (SD) have been calculated, as well as the relative standard deviation (RSD).

Members of molecular series	Blank 2 NaOH PPL		Average (SD)	RSD (%)	Membrane 1 NH <sub>4</sub> OH PPL		Average (SD)	RSD (%)
average H [%]	7.9	8.0	7.9 (0.1)	1	8.5	8.5	8.5 (0.0)	0.0
average C [%]	62	60	61 (2)	3	62	62	62 (0.1)	0.2
average O [%]	24	26	25 (2)	7	25	25	25 (0.05)	0.2
average N [%]	0.6	0.6	0.6 (0.01)	2	1.5	1.5	1.5 (0.02)	1
average S [%]	5.4	5.1	5.2 (0.2)	4	3.2	3.2	3.2 (0.01)	0.2
computed H/C ratio from FTICR mass peaks	1.5	1.6	1.6 (0.05)	3	1.6	1.6	1.6 (0.0)	0.0
computed O/C ratio from FTICR mass peaks	0.30	0.33	0.32 (0.02)	7	0.30	0.30	0.30 (0.0)	0.0
computed C/N ratio from FTICR mass peaks	14.5	16.0	15.2 (1.1)	7	13.0	12.9	13.0 (0.08)	0.7
computed C/S ratio from FTICR mass peaks	15.8	14.9	15.3 (0.7)	4	20.8	21.0	20.9 (0.1)	0.7
Average DBE, intensity weighted	4.9	4.5	4.7 (0.3)	6	4.6	4.5	4.6 (0.07)	2
Average DBE/C, intensity weighted	0.27	0.25	0.26 (0.01)	5	0.23	0.23	0.23 (0.0)	0.0
Average mass, intensity weighted	351.2	333.4	342 (13)	4	364.7	358.7	361.7 (4)	1

**Table S9.** Counts of unique assigned mass peaks extracted comparing DOM 1 vs DOM 2, with each alkaline solution of the study as computed from negative electrospray 12T FT-ICR mass spectra for singly charged ions with nitrogen rule check and 500 ppb tolerance.

Members of molecular series	NH <sub>4</sub> OH-PPL		NaOH-PPL	
	DOM 1	DOM 2	DOM 1	DOM 2
Unique assigned mass peaks in:				
Unique assigned mass peaks	48 %	50 %	66 %	69 %
CHO compounds	130 (17 %)	316 (38 %)	255 (27 %)	444 (38 %)
CHOS compounds	243 (31 %)	123 (15 %)	288 (31 %)	246 (21 %)
CHNO compounds	216 (27 %)	273 (33 %)	183 (20 %)	314 (27 %)
CHNOS compounds	197 (25 %)	122 (15 %)	208 (22 %)	152 (13 %)
Number of unique assigned mass peaks	786	834	934	1156
average H [%]	7.8	8.2	6.9	7.4
average C [%]	65	63	63	62
average O [%]	21	25	22	26
average N [%]	1.9	2.3	1.9	2.2
average S [%]	4.6	2.3	5.0	2.8
computed H/C ratio from FTICR mass peaks	1.5	1.6	1.5	1.4
computed O/C ratio from FTICR mass peaks	0.24	0.30	0.26	0.32
computed C/N ratio from FTICR mass peaks	17.8	13.0	18.7	12.3
computed C/S ratio from FTICR mass peaks	26.0	25.2	23.9	23.1
Average DBE, intensity weighted	8.3	5.9	12.3	7.5
Average DBE/C, intensity weighted	0.32	0.27	0.37	0.34
Average mass, intensity weighted	466.3	404.0	400.5	426.8

**Table S10.**  $^1\text{H}$  NMR section integrals (percent of non-exchangeable protons) and key substructures from Blank Membranes and Used Membranes (exclusion of residual water, methanol and formic acid).

$\delta(^1\text{H})$ [ppm]		9.5 - 7.0	7.0 - 5.3	4.9 - 3.1	3.1 - 1.9	1.9 - 1.35	1.35-1.25	1.25-0.5	Sum 1.9-0.5	$\frac{\text{H}_{\text{olefinic}}}{\text{H}_{\text{aromatic}}}$	$\frac{\text{H}_3\text{C}}{(\text{CH}_2)_n}$
Key substructures		$\underline{\text{H}}_{\text{ar}}$	$\underline{\text{H}}\text{C}=\text{C},$ $\underline{\text{H}}\text{CO}_2$	$\underline{\text{H}}\text{CO}$	$\underline{\text{H}}\text{-C-C-O}$	$\underline{\text{H}}\text{-C-C-C-O}$	$(\underline{\text{C}}\text{H}_2)_n$	$\underline{\text{H}}_3\text{C-C-C}$			
<b>Blank 1</b>	NH <sub>4</sub> OH - PPL	3.8	1.3	10.7	19.7	15.4	29.4	19.7	64.5	0.3	0.7
	NaOH - PPL	5.6	1.5	12.4	17.9	18.6	25.5	18.5	62.6	0.3	0.7
<b>Blank 2</b>	NH <sub>4</sub> OH - PPL	3.4	2.5	10.2	9.5	22.8	29.7	21.9	74.3	0.7	0.7
	NaOH - PPL	4.4	3.2	10.3	11.4	22.6	30.5	17.6	70.7	0.7	0.6
<b>Membrane 1</b>	NH <sub>4</sub> OH - PPL	4.1	1.1	19.8	19.2	18.0	13.1	24.6	55.7	0.3	1.9
	NaOH - PPL	2.6	1.6	18.5	18.6	19.2	20.2	19.3	58.7	0.6	1.0
<b>Membrane 2</b>	NH <sub>4</sub> OH - PPL	4.1	0.6	18.4	18.1	18.1	15.0	25.6	58.7	0.2	1.7
	NaOH - PPL	2.2	1.5	17.8	17.3	19.1	23.0	19.1	61.1	0.7	0.8

**Figure S1.** Schematic diagram of the experimental set-up for the NF pilot plant.

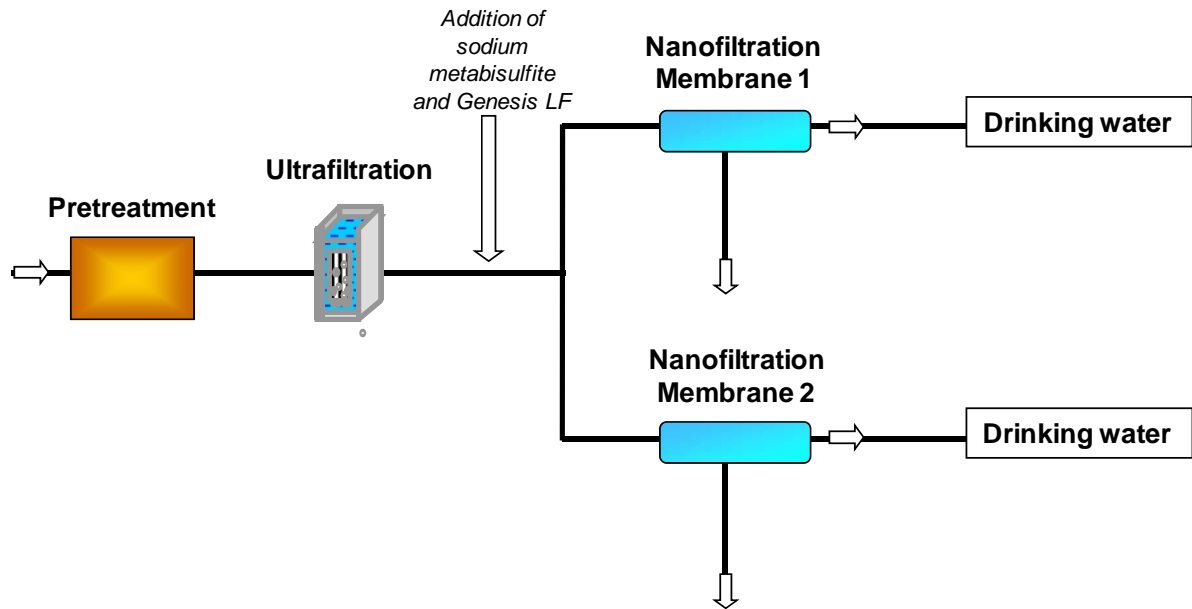
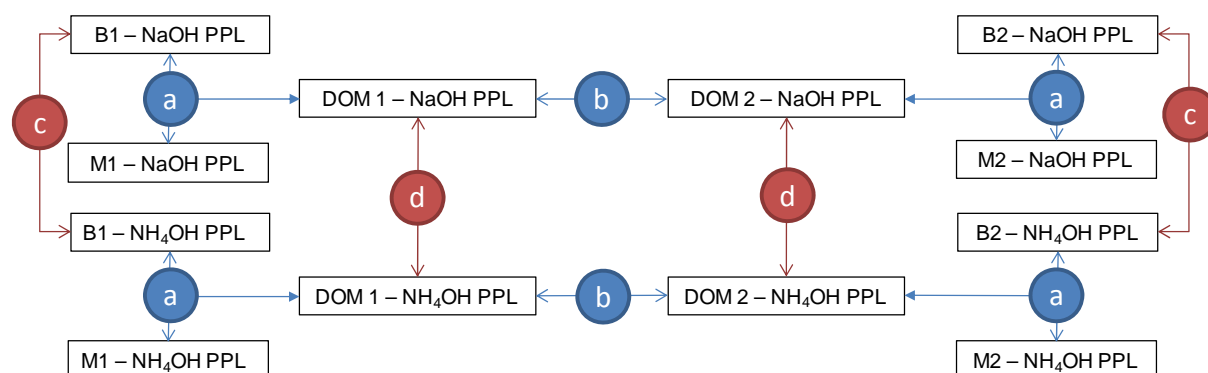


**Figure S2.** Scheme of the procedure carried out for data evaluation. The formulas assigned from FT-ICR data of the eight initial extracts (B1 - NaOH PPL; M1 - NaOH PPL; B1 - NH<sub>4</sub>OH PPL; M1 - NH<sub>4</sub>OH PPL; B2 - NaOH PPL; M2 - NaOH PPL; B2 - NH<sub>4</sub>OH PPL; M2 - NH<sub>4</sub>OH PPL) have been compared based on presence/absence (comparison based on the *m/z* theoretical and mass window 0.1ppm) with two main objectives: the DOM characterization from the two Membranes (a and b; blue rows) and the comparison of alkaline solution extraction (c and d; red rows).



#### DOM characterization from the two different Membranes

- a** Comparison the Blank Membranes (B) vs Used Membranes (M) to extract only the unique formulas of M which correspond to the dissolved organic matter (DOM) extracted from each membrane with the two different alkaline solutions (NH<sub>4</sub>OH and NaOH).
- b** Comparison of the DOM extracted from the two different Membranes (DOM 1 vs DOM 2). The comparison has been carried out with the two different alkaline solutions used.

#### Comparison of Alkaline Solution Extraction

- c** Comparison between the Blank Membranes extracted with the two different alkaline solutions (NH<sub>4</sub>OH and NaOH) to evaluate differences on the destruction of the membranes.
- d** Comparison between the Used Membranes extracted with the two different alkaline solutions (NH<sub>4</sub>OH and NaOH) to evaluate differences on the DOM extracted.

**Figure S3.** The negative electrospray 12T FT-ICR mass spectra (in the mass range  $m/z$  361-371) of Membrane 2 tests performed for the optimization of the amount of membrane to be used. In a) the initial sample of 4 cm<sup>2</sup> (per three pieces of membrane along the membrane sheet = equivalent to 12 cm<sup>2</sup>), b) an increased sampling area equivalent to 36 cm<sup>2</sup> and c) the optimal amount equivalent to an area of DIN-A4. Note the different intensities of the signals in the spectra (see axis y).

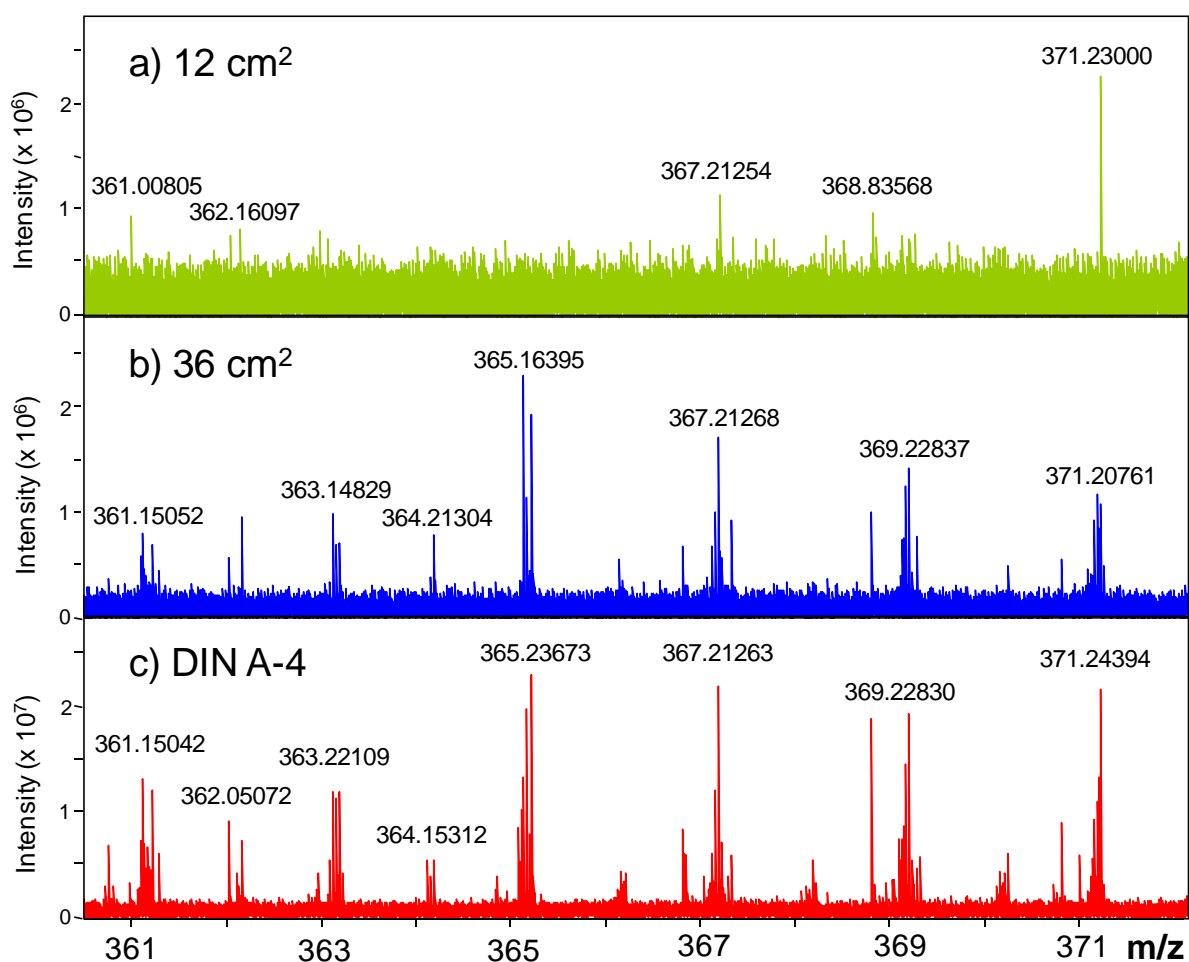


**Figure S4.** The nominal mass 365 expansion of the negative electrospray 12T FT-ICR mass spectra of Membrane 2 tests performed for the optimization of the amount of membrane to be used, showing the assigned formulas. In a) a sampling area equivalent to 36 cm<sup>2</sup> and b) the optimal amount equivalent to an area of DIN-A4. The common peak masses obtained when sampling 36 cm<sup>2</sup> and DIN-A4 equivalent area are indicated in boxes, showing that when a smaller amount of membrane is used, some of the signals are not detected, even after 500 scans acquisition. Note the different intensities of the signals in the spectra (see axis y).

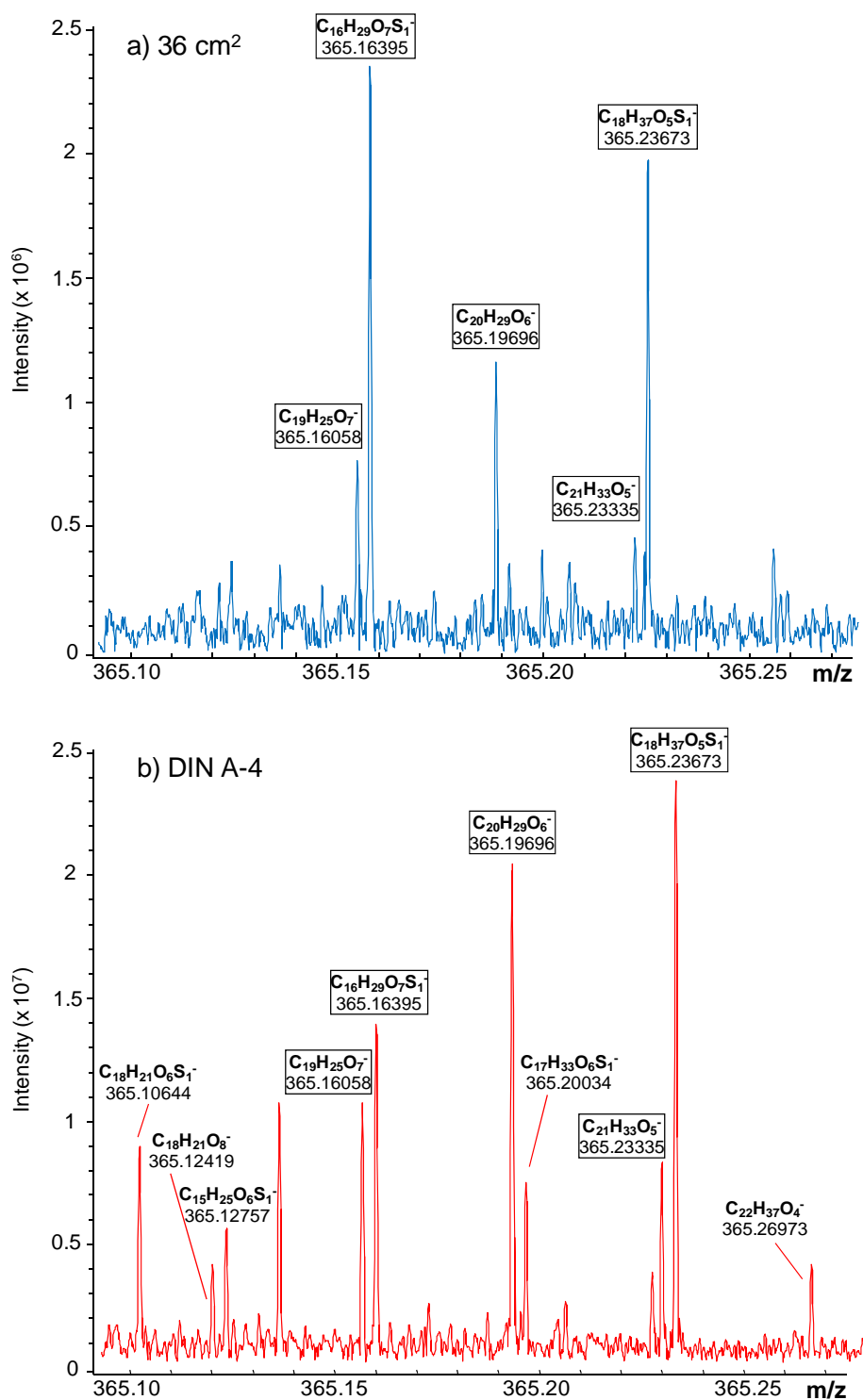


**Figure S5.** The nominal mass 343 expansion of the negative electrospray 12T FT-ICR mass spectra of Membrane 2 tests performed for the optimization of the temperature of extraction. a) the extraction was performed at room temperature and b) the extraction was performed slightly heating at 35 °C.

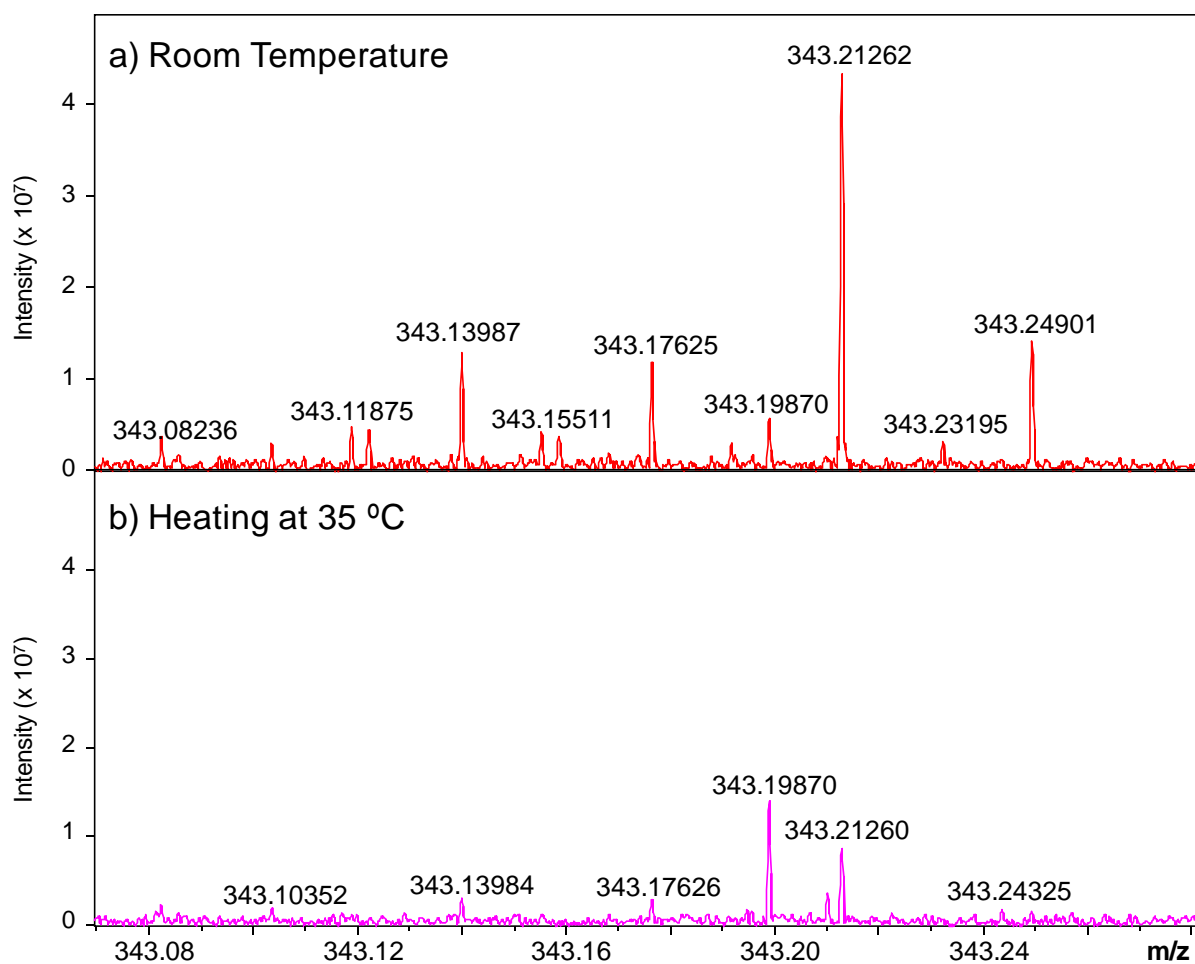
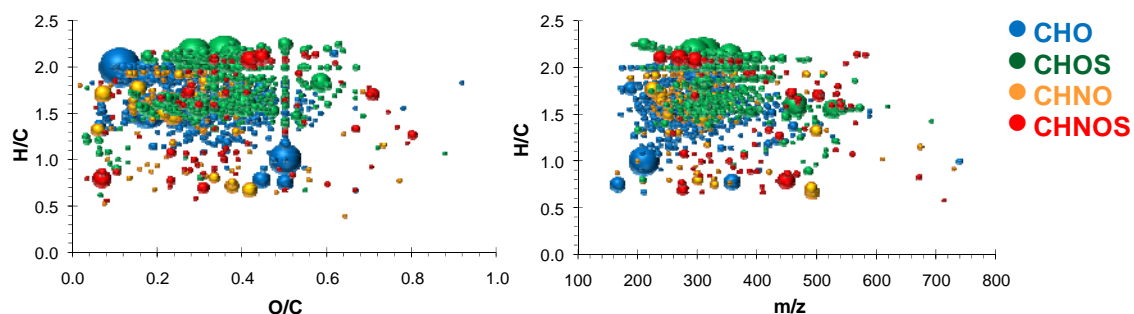
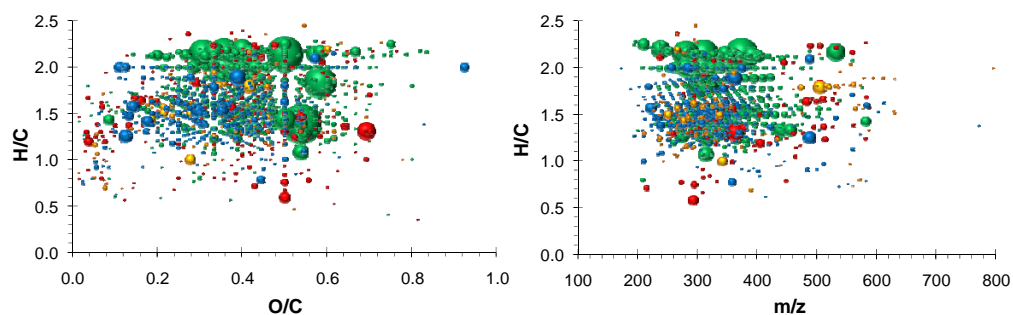


**Figure S6.** Van Krevelen diagrams and H/C ratio vs mass-to-charge ( $m/z$ ) plots for all formulas assigned of the Blank Membranes: a) Blank 1 (B1) extracted with  $\text{NH}_4\text{OH}$  alkaline solution and SPE-PPL, b) Blank 2 (B2) extracted with  $\text{NH}_4\text{OH}$  alkaline solution and SPE-PPL c) B1 extracted with  $\text{NaOH}$  alkaline solution and SPE-PPL and d) B2 extracted with  $\text{NaOH}$  alkaline solution and SPE-PPL, on color-coded composition: CHO (blue), CHOS (green), CHNO (orange), CHNOS (red). Circular areas indicate relative mass peak intensity.

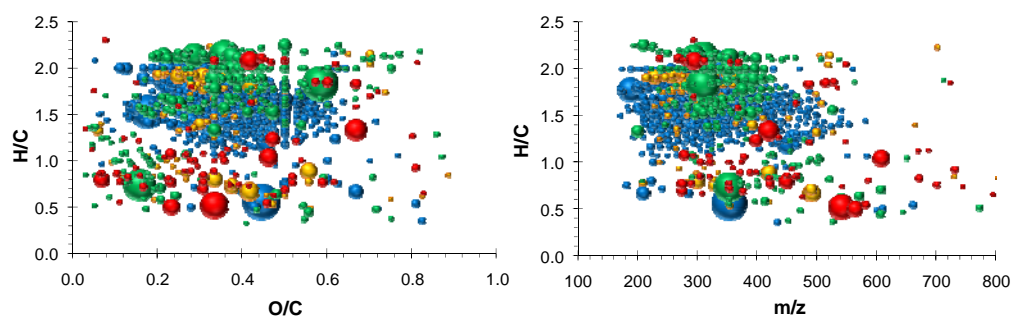
**a) B1:  $\text{NH}_4\text{OH}$  - PPL**



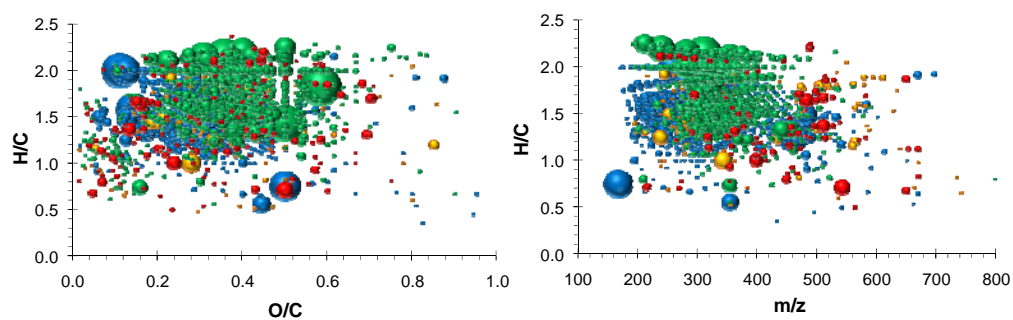
**b) B2:  $\text{NH}_4\text{OH}$  - PPL**



**c) B1:  $\text{NaOH}$  - PPL**

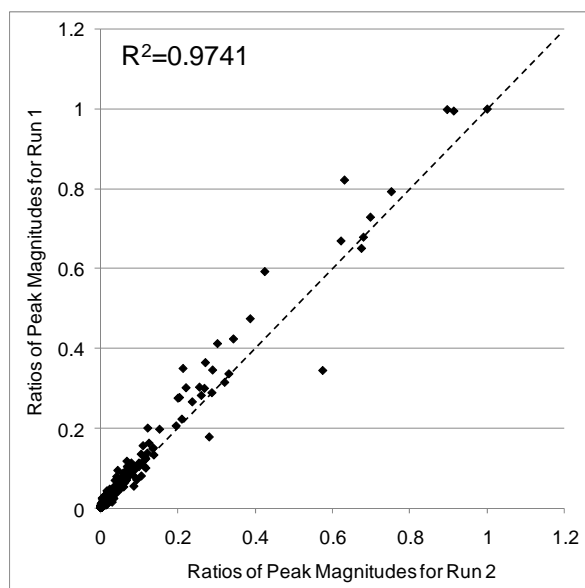


**d) B2:  $\text{NaOH}$  - PPL**

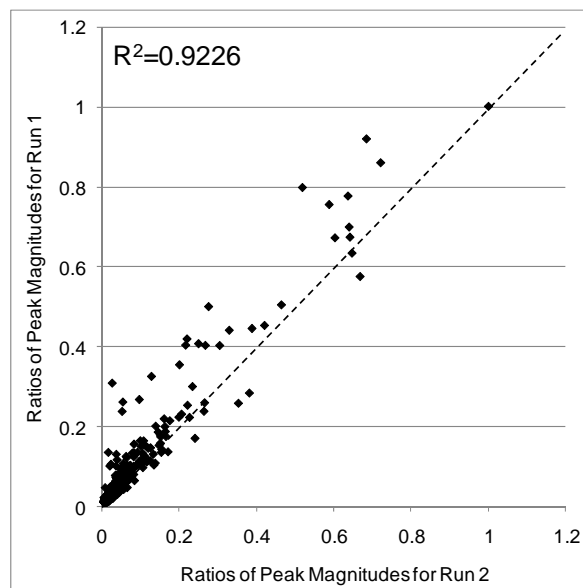
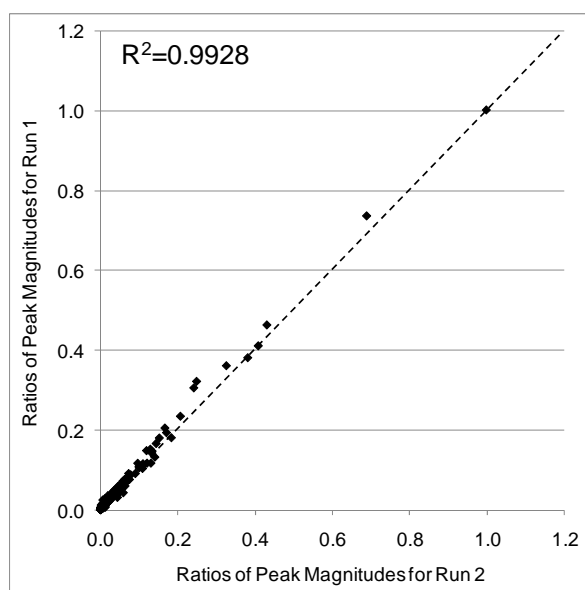
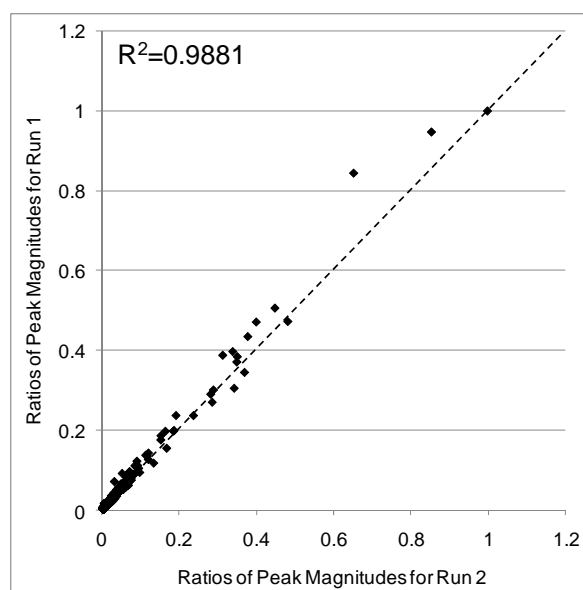


**Figure S7.** Reproducibility of mass peak magnitude. Ratios of peak magnitudes (the ratio of the peak's magnitude to the magnitude of the base peak) at  $S/N \geq 3$  of Run 1 are plotted against Run 2 for the duplicates of the study: a) Blank 2 (B2) considering mass peaks, b) B2 considering molecular formulas assigned, c) Membrane 1 (M1) considering mass peaks and d) M1 considering molecular formulas assigned. The fit ( $R^2$ ) is specified in each case and the 1:1 line is provided as a reference on each plot.

a) B2 NaOH PPL S/N=3 Peaks



b) B2 NaOH PPL S/N=3 Formulas

c) M1 NH<sub>4</sub>OH PPL S/N=3 Peaksd) M1 NH<sub>4</sub>OH PPL S/N=3 Formulas

**Figure S8.** Van Krevelen diagrams and H/C ratio vs mass-to-charge ( $m/z$ ) plots for the Unique formulas assigned when comparing DOM 1 vs DOM 2, for DOM extracted with  $\text{NH}_4\text{OH}$  alkaline solution and SPE-PPL: a) Unique assigned formulas of DOM 1 and b) Unique assigned formulas of DOM 2, on color-coded composition: CHO (blue), CHOS (green), CHNO (orange), CHNOS (red). Circular areas indicate relative mass peak intensity.

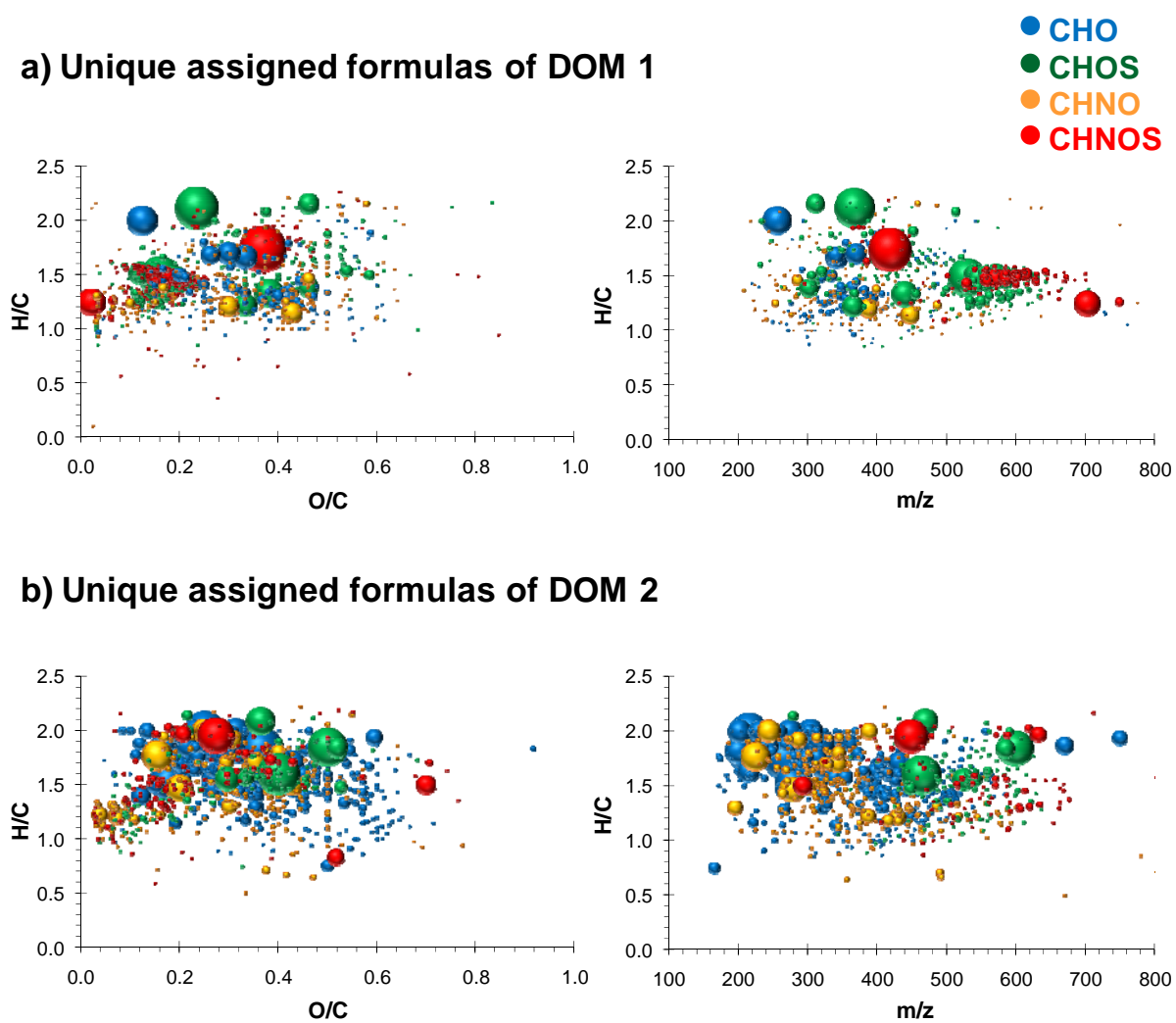


**Figure S9.** Van Krevelen diagrams and H/C ratio vs mass-to-charge ( $m/z$ ) plots for the Unique formulas assigned when comparing DOM 1 vs DOM 2, for DOM extracted with NaOH alkaline solution and SPE-PPL: a) Unique assigned formulas of DOM 1 and b) Unique assigned formulas of DOM 2, on color-coded composition: CHO (blue), CHOS (green), CHNO (orange), CHNOS (red). Circular areas indicate relative mass peak intensity.

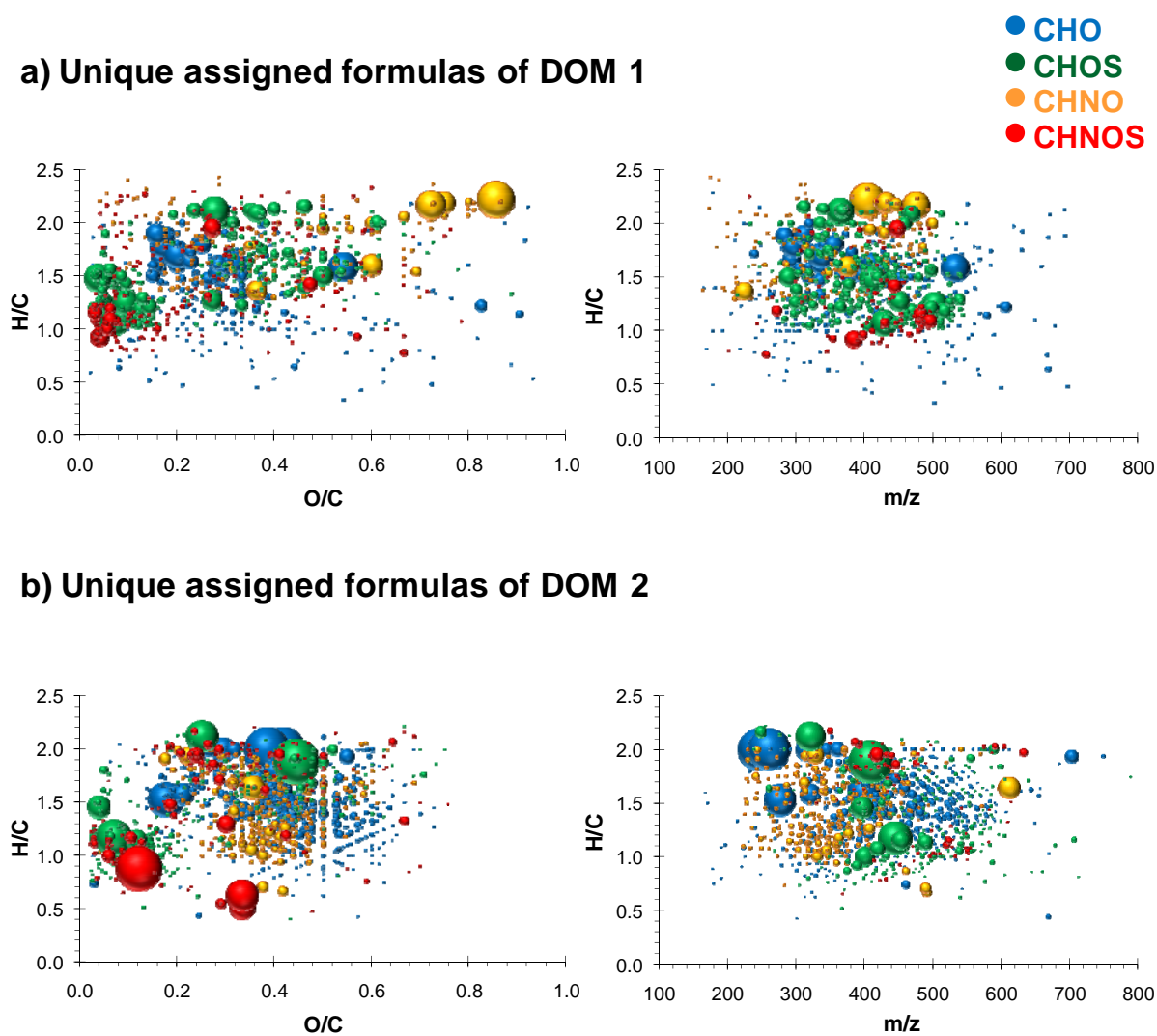


**Figure S10.**  $^1\text{H}$  NMR spectra of (purple): Used Membrane 1 extracted with  $\text{NH}_4\text{OH}$  alkaline solution and SPE-PPL, (blue): Used Membrane 2 extracted with  $\text{NH}_4\text{OH}$  alkaline solution and SPE-PPL, (green): Used Membrane 1 extracted with  $\text{NaOH}$  alkaline solution and SPE-PPL, (red): Used Membrane 2 extracted with  $\text{NaOH}$  alkaline solution and SPE-PPL. Intensities are normalized to 100% intensity for the methylene group ( $\delta_{\text{H}} \sim 1.28$  ppm). Fundamental substructures are indicated from higher to lower field (from right to left): pure aliphatic  $\delta_{\text{H}} \sim 0.5$ -1.25 ppm,  $\text{H}_3\text{C-C-C}$ ; polymethylene group  $\delta_{\text{H}} \sim 1.25$ -1.35 ppm,  $(\text{CH}_2)_n$ ; functionalized aliphatics  $\delta_{\text{H}} \sim 1.35$ -1.9 ppm,  $\text{HC-C-CO}$ ,  $\text{HC-CN}$  and  $\text{HC-CS}$ ; “acetate-analogue” and carboxyl-rich alicyclic materials (CRAM)  $\delta_{\text{H}} \sim 1.9$ -3.1 ppm,  $\text{HC-C-O}$ ; “carbohydrate-like” and methoxy  $\delta_{\text{H}} \sim 3.1$ -4.9 ppm,  $\text{HCO}$ ; olefins  $\delta_{\text{H}} \sim 5.3$ -7.0 ppm  $\text{HC=C}$ ,  $\text{HCO}_2$ ; and aromatic  $\delta_{\text{H}} \sim 7.0$ -9.5 ppm,  $\text{H}_{\text{ar}}$  NMR resonances.

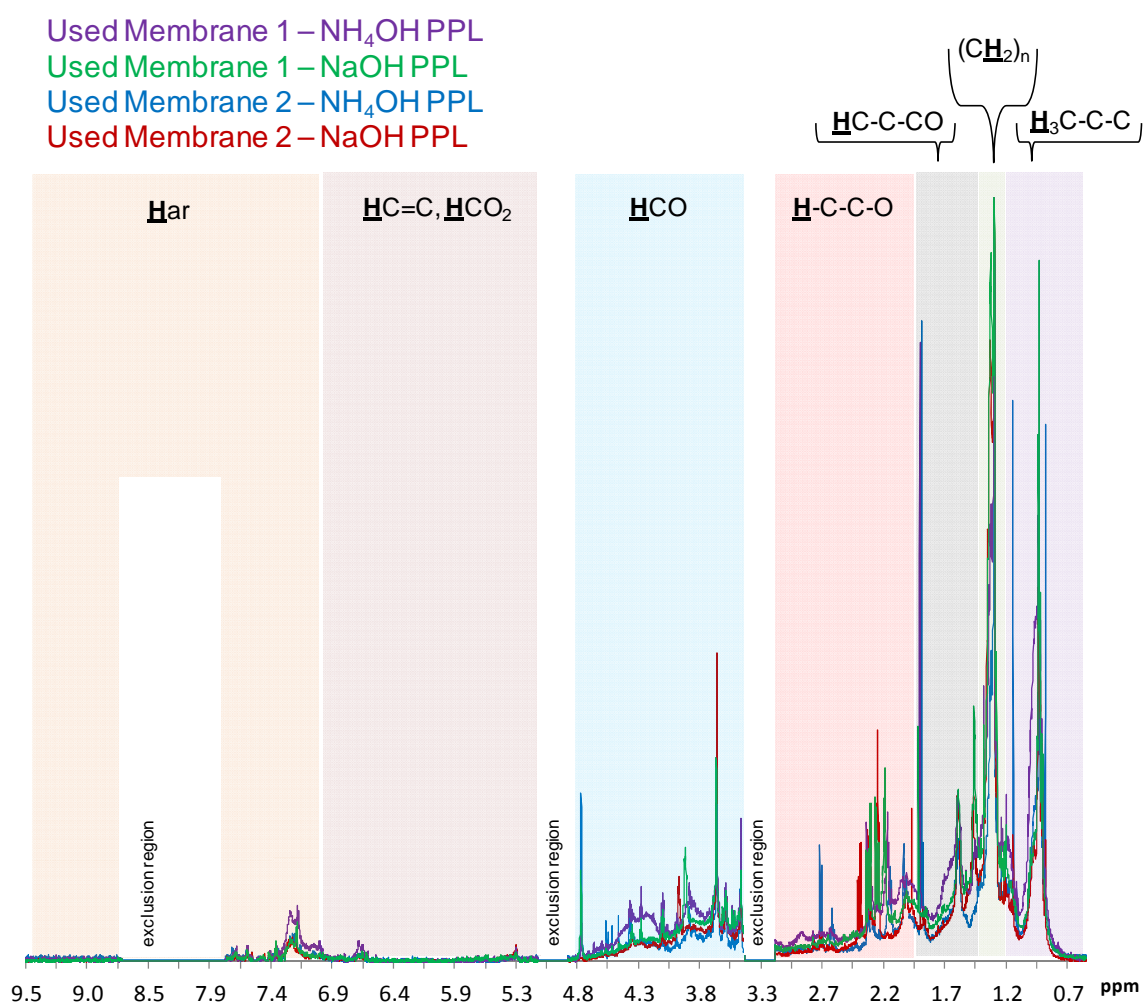
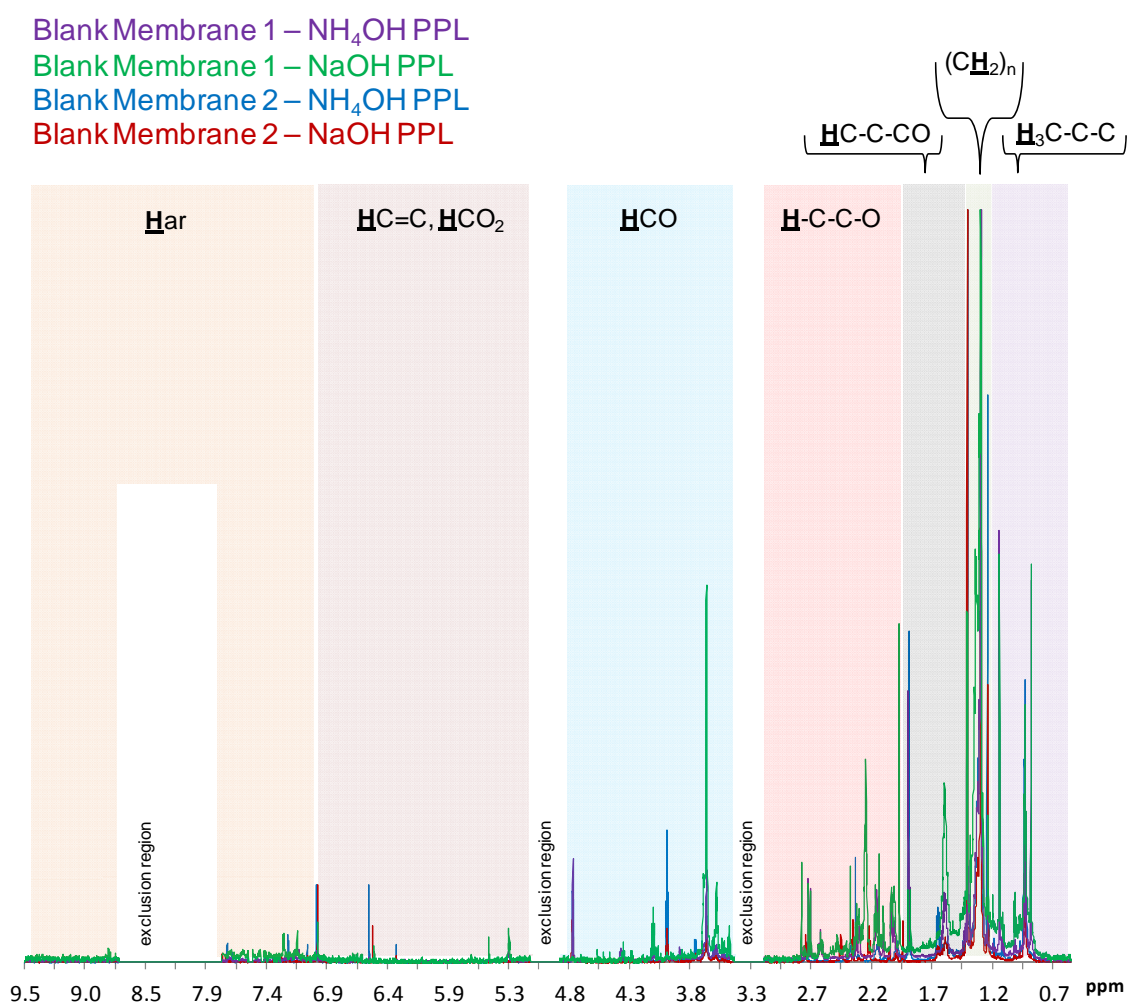


**Figure S11.**  $^1\text{H}$  NMR spectra of (purple): Blank Membrane 1 extracted with  $\text{NH}_4\text{OH}$  alkaline solution and SPE-PPL, (blue): Blank Membrane 2 extracted with  $\text{NH}_4\text{OH}$  alkaline solution and SPE-PPL, (green): Blank Membrane 1 extracted with  $\text{NaOH}$  alkaline solution and SPE-PPL, (red): Blank Membrane 2 extracted with  $\text{NaOH}$  alkaline solution and SPE-PPL. Intensities are normalized to 100% intensity for the methylene group ( $\delta_{\text{H}} \sim 1.28$  ppm). Fundamental substructures are indicated from higher to lower field (from right to left): pure aliphatic  $\delta_{\text{H}} \sim 0.5$ -1.25 ppm,  $\text{H}_3\text{C-C-C}$ ; polymethylene group  $\delta_{\text{H}} \sim 1.25$ -1.35 ppm,  $(\text{CH}_2)_n$ ; functionalized aliphatics  $\delta_{\text{H}} \sim 1.35$ -1.9 ppm,  $\text{HC-C-CO}$ ,  $\text{HC-CN}$  and  $\text{HC-CS}$ ; “acetate-analogue” and carboxyl-rich alicyclic materials (CRAM)  $\delta_{\text{H}} \sim 1.9$ -3.1 ppm,  $\text{HC-C-O}$ ; “carbohydrate-like” and methoxy  $\delta_{\text{H}} \sim 3.1$ -4.9 ppm,  $\text{HCO}$ ; olefins  $\delta_{\text{H}} \sim 5.3$ -7.0 ppm  $\text{HC=C}$ ,  $\text{HCO}_2$ ; and aromatic  $\delta_{\text{H}} \sim 7.0$ -9.5 ppm,  $\text{H}_{\text{ar}}$  NMR resonances.



# **Appendix D.**

## **Summary in Catalan - Resum en Català**

---



## OBJECTIUS DE LA TESI I ORGANITZACIÓ DE LA MEMÒRIA

L'objectiu principal d'aquesta tesi és l'ús de l'espectrometria de masses d'alta resolució per a la caracterització de la matèria orgànica dissolta en masses d'aigua naturals i tractades. L'alta resolució és una de les tècniques que ha contribuït d'una manera significativa a conèixer la matèria orgànica dissolta, aportant informació de les fórmules dels compostos que formen part d'aquestes mesclures tan complexes.

Els objectius específics d'aquesta tesi són:

- Investigar els avantatges de l'espectrometria de masses d'alta resolució per a la identificació i caracterització dels compostos en el medi ambient. L'estudi busca concloure quins paràmetres poden afectar la determinació de la fórmula elemental, amb especial atenció a l'exactitud de massa i la resolució, amb l'objectiu de dissenyar un procediment per a la caracterització de compostos desconeguts en mostres complexes.
- Avaluar diferents analitzadors de masses capaços de fer mesures de massa exacta i de treballar en alta resolució: el triple quadrupol, el temps de vol, el transformada de Fourier ressonància ciclotrònica d'ions i l'orbitrap. En els últims anys s'han desenvolupat nous analitzadors i s'han dut a terme avenços molt importants i per aquesta motiu ha estat necessari avaluar: el protocols de calibratge, l'exactitud de massa, la resolució, la sensibilitat i l'exactitud espectral.
- Utilitzar l'espectrometria de masses d'alta resolució per a la caracterització de la matèria orgànica dissolta en el medi aquàtic. L'interès principal és avaluar els canvis que experimenta la matèria orgànica dissolta al llarg de diferents plantes de tractament. Es vol estudiar quin efecte té cada tractament i principalment ens hem centrat en tractaments avançats de membrana.

La tesi s'ha estructurat en 5 capítols. El capítol 1 consisteix en una breu introducció sobre la matèria orgànica natural i dissolta, així com els diferents mètodes d'anàlisi que s'han utilitzat. El capítol 2, consta de dues publicacions científiques. En primer lloc un capítol de llibre que introdueix els principals conceptes d'espectrometria de masses i mesura de massa exacta i posa de manifest les estratègies per la determinació estructural de compostos orgànics en el medi ambient. S'han il·lustrat diferents exemples per demostrar l'avantatge d'utilitzar l'espectrometria de masses d'alta

resolució, en front de l'espectrometria de masses en tàndem. En segon lloc, es recull la comparativa de diferents analitzadors de massa capaços d'adquirir dades en alta resolució i dur a terme mesures de massa exacta. En el capítol 3, es mostra la metodologia analítica que s'ha utilitzat per a l'anàlisi de la matèria orgànica dissolta en el medi aquàtic. Els analitzadors de massa de transformada de Fourier ressonància ciclòrica d'ions i de transformada de Fourier-orbitrap s'han avaluat. A més a més, s'ha procedit a posar a punt una metodologia analítica basada en l'espectrometria de masses d'alta resolució en tàndem per a la caracterització estructural de la matèria orgànica dissolta de l'aigua de mar. En el capítol 4, tres articles científics mostren l'ús principalment de l'espectrometria de masses d'alta resolució per a avaluar els canvis de la matèria orgànica dissolta al llarg de diferents plantes de tractament. A més s'ha desenvolupat un mètode per a caracteritzar la matèria orgànica adherida a la superfície de les membranes de tractament, per poder caracteritzar l'embrutiment de les mateixes. Finalment, en el capítol 5, s'han resumit les principals conclusions del treball.

# 1. INTRODUCCIÓ

## 1.1. La Matèria Orgànica Natural

Tots els éssers vius quan moren es descomponen i formen el que es coneix com matèria orgànica natural. La seva formació és deguda a la degradació i transformació de les restes de plantes i microorganismes, on intervenen multitud de reaccions químiques i bioquímiques donant lloc a una mescla complexa i heterogènia de material divers. Els principals elements que la constitueixen són: C, H, O, N, S i P, però se'n sap ben poc a nivell molecular i estructural.

La matèria orgànica natural es pot classificar en dues parts: la fracció no-húmica i les substàncies húmiques. La matèria orgànica natural també es pot dividir en tres fraccions principals: els humins, els àcids húmics i els àcids fúlvics. Aquesta divisió es basa en la solubilitat en l'aigua de cada una de les fraccions a diferents pHs: la fracció soluble en aigua a qualsevol pH són els àcids fúlvics, els àcids húmics són insolubles a pH=1 i la fracció humina és insoluble en aigua, a qualsevol pH. La fracció de la matèria orgànica natural que es troba en els medis aquàtics es defineix com la matèria orgànica dissolta. Alguns estudis la defineixen com la part de la matèria orgànica natural capaç de passar a través d'un filtre de 0.45 µm. Hi ha molts altres estudis que la filtració la fan a través de filtres de diferents mida de porus, des de 0.2 µm a 0.7 µm. Al llarg de la tesi ens referirem a la matèria orgànica dissolta d'una manera més genèrica, com a la matèria orgànica que es troba en el medi aquàtic.

La matèria orgànica dissolta es tracta doncs d'una mescla complexa i la seva composició i estructura encara no es coneix del tot. Com que es tracta d'una mescla natural, no existeixen patrons sintètics i només l' *International Humic Substance Society* subministra patrons i materials de referència de matèria orgànica dissolta de diferents orígens. La matèria orgànica dissolta no és tòxica per definició, però hi ha estudis que demostren que poden afectar la solubilitat i el transport de contaminants orgànics en el medi. A més, s'ha descrit la matèria orgànica dissolta com a la matèria precursora en la formació de productes de desinfecció en processos de cloració. També hi ha estudis que demostren que afecta el bon funcionament dels tractaments a les plantes de tractament d'aigües i per tant la qualitat final de l'aigua que s'obté. Per exemple, pot afectar severament el procés de coagulació i encara de manera més greu pot afectar els diferents tractaments de membrana, provocant el que es coneix com a "embrutiment" o *fouling*.

## 1.2. Mètodes per a l' Anàlisi de la Matèria Orgànica Dissolta

Degut a que la matèria orgànica dissolta és una mescla heterogènia calen diferents tècniques combinades entre elles per al seu anàlisi. Si ens centrem en l'anàlisi de la matèria orgànica dissolta en matrius aquàtiques, cal tenir en compte la baixa concentració d'aquests compostos en aquest medi. És per això que calen tècniques molt potents amb una alta sensibilitat. A la Taula 1, es resumeixen les principals tècniques analítiques utilitzades, l'informació que se n'obté, així com els principals descobriments i les principals referències bibliogràfiques.

Algunes tècniques de separació (cromatografia de gasos, cromatografia de líquids, cromatografia d'exclusió molecular, electroforesis capil·lar) i de degradació tèrmica (ex. piròlisis) s'han acoblat a diferents tipus de detectors (per ex: detectors de flama, detectors de carboni orgànic, fotodíode array) i diferents tipus d'analitzadors (per ex., triple quadrupol, quadrupol-temps de vol, transformada de Fourier ressonància ciclòtrònica d'ions). La cromatografia líquida d'exclusió molecular ha estat la tècnica de separació més emprada en l'anàlisi de la matèria orgànica i s'ha acoblat a diferents tipus de detectors, com per exemple detectors d'espectroscòpia d'ultravioleta-visible i analitzadors de carboni orgànic total. Aquesta tècnica de separació, però presenta alguns problemes, com que per exemple depenen del detector al que estigui acoblada s'obtenen respostes i distribucions moleculars molt diferents. Per exemple, quan s'ha acoblat a un analitzador de masses de transformada de Fourier ressonància ciclòtrònica d'ions, la resolució de treball a de ser inferior a 100,000 per tenir suficient sensibilitat i per tant les senyals a l'espectre no estan del tot resoltes. A més a més, no existeixen patrons adequats per al calibratge de les columnes necessàries (Reemtsma i col., 2001).

En quan a la estructura de la matèria orgànica dissolta, la principal tècnica que s'ha utilitzat fins ara ha estat la ressonància magnètica nuclear. Els espectres de ressonància magnètica nuclear de protó i de carboni 13, mostren embolcalls i no s'intueixen pics definits, degut a la gran complexitat estructural de la matèria orgànica dissolta. De totes maneres, l'àrea que queda dibuixada sota l'espectre de ressonància magnètica nuclear es pot dividir en diferents àrees de manera que es pot semi-quantificar la influència de cada estructura predominant (per exemple, protó de cadena alquíllica o protó aromàtic) en front del total d'àrea.

**Taula 1.** Principals tècniques analítiques utilitzades per a la caracterització de la matèria orgànica dissolta. Per a cada una de les tècniques, la informació que se'n pot obtenir així com els principals descobriments aconseguits estan també resumits.

<b>Tècnica analítica</b>	<b>Informació obtinguda</b>	<b>Principals descobriments</b>	<b>Referències</b>
Anàlisi elemental	Composició elemental	Diferent composició dels àcids fúlvics i dels àcids húmics.	Sparks i col., 1995
Espectroscòpia d'ultravioleta-visible	Aromaticitat	Procés de degradació de la matèria orgànica. Matèria orgànica cromòfora.	Amery i col., 2008 Jaffé i col., 2008 Tipping i col., 2009
Fluorescència	Aromaticitat	Anells aromàtics condensats. Cadenes alifàtiques insaturades. Components minoritaris de la matèria orgànica natural.	Hudson i col., 2007
<i>Excitation-Emission Matrix Fluorescence</i>	Aromaticitat	Distingir entre matèria orgànica cromòfora semblant a les proteïnes, húmics i fúlvics. Propietats òptiques de la matèria orgànica dissolta.	Boheme i col., 2006 Burdige i col., 2004 Herzprung i col., 2012
Espectroscòpia infraroja de Transformada de Fourier	Grups funcionals	Presència de grups funcionals aromàtics, alifàtics i carboxílics.	Tanaka i col., 2001
Ressonància magnètica nuclear	Grups funcionals	La matèria orgànica natural està formada per productes de degradació de plantes. Diferències entre els àcids húmics i fúlvics. Els grups fenòlics no són el component majoritari dels húmics.	Blondeau 1986 Wershaw i col., 1990 Hertkorn i col., 2006 Lam i col., 2007 Hertkorn i col., 2013
2D- Ressonància magnètica nuclear	Informació estructural	Relacionar la matèria orgànica natural amb biopolímers de classes conegudes.	
Espectrometria de masses	Distribució de senyals en l'espectre de masses	Ions mono carregats cada 2 Da Series de pic separades per 14 Da	McIntyre i col., 1997 Persson i col., 2000
Espectrometria de masses d'alta resolució	Resolució i identificació de composicions individuals de compostos de la matèria orgànica dissolta	Perfils regulars amb una separació de 0.0364 Da. Fórmules elementals de la matèria orgànica dissolta.	Stenson i col., 2003 Altieri i col., 2009 D'Andrilli i col., 2010
Espectrometria de masses en tàndem	Informació estructural	Pèrdues neutres de 44 Da i 18 Da. Grups funcionals carboxil i hidroxil.	Leenheer i col., 2001 Witt i col., 2009

Els avenços en espectrometria de masses d'alta resolució i en les fonts d'ionització a pressió atmosfèrica han revolucionat l'anàlisi de la matèria orgànica dissolta. Amb aquesta tècnica s'han pogut determinar detalls de la seva composició per separar els diferents constituents. Altres espectròmetres de masses s'han utilitzat per l'anàlisi de la matèria orgànica dissolta, com per exemple els quadrupols, les trampes d'ions i els analitzadors de temps de vol o algunes combinacions entre ells. De totes maneres, l'analitzador de transformada de Fourier ressonància ciclòtrica d'ions i més recentment el de transformada de Fourier-orbitrap, presenten diversos avantatges en front els altres sistemes.

Degut a la seva complexitat, hi ha diversos factors que s'han de tenir en compte:

- i) l'alta resolució és indispensable per poder separar totes les senyals a l'espectre
- ii) calen mesures de massa molt exactes per poder assignar la fórmula elemental d'una manera fiable
- iii) calen mètodes molt sensibles i/o un pas previ per extreure i concentrar la matèria orgànica dissolta
- iv) calen procediments estrictes per el tractament de les dades
- v) calen estratègies basades en l'espectrometria de masses (o altres tècniques) per obtenir informació estructural de la matèria orgànica dissolta

## 2. ESPECTROMETRIA DE MASSES D'ALTA RESOLUCIÓ I MASSA EXACTA

### 2.1. Introducció

Les primeres referències sobre l'espectrometria de masses daten del 1897 a càrrec de Joseph John Thomson de la Universitat de Cambridge, Anglaterra i el descobriment de l'existència de l'electró arrel dels seus experiments sobre la conductivitat elèctrica dels gasos. J.J. Thomson va construir el que es pot considerar el primer espectròmetre de masses de la història, que rebia el nom de *Parabola Spectrograph* (Borman S. i col, 2003). Des d'aleshores, s'han desenvolupat molts analitzadors de massa i fonts d'ionització (veure Taula 2).

**Taula 2.** Desenvolupaments històrics en l'espectrometria de masses principalment relacionats amb l'espectrometria de masses d'alta resolució i l'anàlisi del medi ambient (adaptat Borman S. i col, 2003; <http://masspec.scripps.edu> )

Científics	Any	Contribució
J. J. Thomson	1897	Primer espectròmetre de masses ( <i>Parabola Spectrograph</i> )
F. W. Aston	1919	Observació dels isòtops utilitzant l'espectrometria de masses
A. J. Dempster	1920	Font d'ionització d'impacte d'electrons
J. Mattauch i F.K. Herzog	1934	Analitzador de doble enfocament
W. E. Stephens	1946	Analitzador de temps de vol
J.A. Hipple i col·laboradors	1949	Ressonància Ciclotrònica d'Ions
A.O. Nier i E.G. Johnson	1953	Sectors magnètic de doble enfocament de geometria inversa
W. Paul	1953	Analitzador tipus Quadrupol senzill
J.H. Beynon	1956	Identificació de compostos orgànics a partir de la mesura de massa exacta
J.H. Futrell i C.D. Miller	1966	Espectrometria de masses en tàndem
M. Dole / J.B. Fenn	1968	Font d'ionització electrospray
M. B. Comisarow i A. G. Marshall	1974	Transformada de Fourier Ressonància Ciclotrònica d'Ions
R.A. Yost i C.G. Enke	1978	Analitzador tipus Triple Quadrupol
G.L. Glish i D.E. Goeringer	1984	Analitzador híbrid tipus quadrupol-temps de vol
A. Makarov	2000	Transformada de Fourier Orbitrap
Z. Takats i col. (R.G. Cooks)	2004	DESI (Desorption Electrospray Ionization)
R.D. Cody i col.	2005	DART (Direct Analysis in Real Time)

Durant l'últim segle els analitzadors de massa que utilitzem i coneixem avui en dia ja estaven inventats: quadrupol, temps de vol, transformada de Fourier ressonància ciclòtrica d'ions, sector magnètic i qualsevol combinació d'aquests. Tal i com il·lustra Brunnée en el seu mapa de L'Illa del Tresor (Brunnée 1987), ja des dels anys 50 els sectors magnètics dominaven el panorama de l'espectrometria de masses i més concretament de l'alta resolució i l'exactitud de massa. Des d'aleshores el panorama ha canviat una mica, com il·lustrava Makarov (Figura 1.).

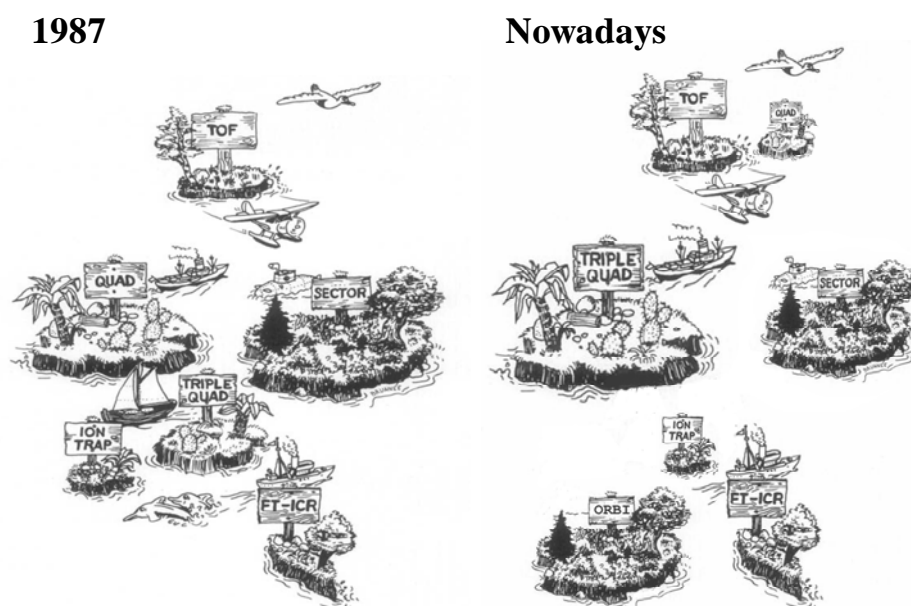


**Figura 1.** (Esquerra) L'Illa del Tresor de Brunnée que il·lustra els diferents analitzadors de massa que s'utilitzaven en el 1987. (Dreta) L'Illa del Tresor proposada per Makarov (adaptada de la que Makarov va presentar a l' *International Mass Spectrometry Conference* a Bremen el 2009), que correspondria a la situació avui en dia.

J.H. Beynon va ser el primer en utilitzar els sectors magnètics per a la identificació de molècules orgàniques a partir de la seva mesura de massa exacta. En la seva obra "Mass Spectrometry and its applications to organic chemistry" Beynon defineix el concepte de resolució com el coneixem avui en dia, i posa èmfasi en la necessitat de dur a terme mesures de massa el més exactes possibles per tal de reduir les possibles fórmules moleculars a l'hora d'identificar un compost. Insisteix en la necessitat d'obtenir mesures sense interferències i en obtenir impureses ben resoltes, a la vegada que elogia les capacitats d'anàlisi d'aquesta tècnica en front d'altres tècniques existents. També defineix eines per poder reduir el nombre de possibles fórmules moleculars, observant els isòtops més pesants i el nombre d'insaturacions de la molècula (Beynon

1960). Aquestes consideracions encara es tenen en compte avui en dia a l'hora de realitzar mesures de massa exacta.

De fet, en aquest capítol l'estudi de l'espectrometria de masses d'alta resolució per a la caracterització estructural i determinació de compostos orgànics en el medi ambient es presenta en un capítol de llibre.

A més a més, degut a les noves tecnologies i avenços científics duts a terme en el camp de l'espectrometria de masses s'ha volgut avaluar la capacitat de diferents analitzadors de masses per a la realització de mesures de massa exacta i treballant en alta resolució.

## 2.2. Procediment Experimental i Resultats

### 2.2.1. Treball científic: Capítol de Llibre

*High resolution mass spectrometric techniques for structural characterization and determination of organic pollutants in the environment.*

Nuria Cortés-Francisco i Josep Caixach

Capítol 6 en el llibre: *Chromatographic Analysis of the Environment: Mass Spectrometry Based Approaches, 4th edition.*

Editors: Leo M.L. Nollet & D. Lambropoulou.

CRC Press Boca Raton, Florida, USA (Taylor and Francis Group).

L'espectrometria de masses d'alta resolució presenta diversos avantatges respecte l'espectrometria de masses de baixa resolució o espectrometria de masses en tàndem. En el medi ambient, el número de compostos a determinar pot ser molt gran. A més a més, aquests compostos poden trobar-se a concentracions molt baixes i poden ser desconeguts o productes de transformació / degradació dels contaminants originals (Hernández i col., 2012). L'espectrometria de masses d'alta resolució permet identificar i determinar contaminants coneguts, així com identificar compostos dels quals no tenim patró (Krauss i col., 2012). Aquest apartat conté en primer lloc un petit resum de la terminologia utilitzada en l'espectrometria de masses d'alta resolució, seguit de la discussió de com afecten diferents paràmetres a la determinació de la fórmula elemental i a la identificació de compostos.

## **Terminologia**

Es defineix la massa nominal d'un ió amb una fórmula molecular coneguda com el resultat de calcular la massa del ió tenint en compte la massa en nombre enter del ió més abundant.

Per altra banda, la massa exacta teòrica es defineix com la massa d'un ió amb una fórmula molecular coneguda calculada utilitzant la massa exacta de d'isòtop més abundant de cada element (Ham 2008). Cal considerar que en un espectròmetre de masses es detecten i mesuren masses de molècules amb càrrega (anions, cations o radicals) i que per tant, la massa exacta haurà de tenir en compte el guany d'un protó en el cas d'un ió molecular de la forma  $[M+H]^+$ , la pèrdua d'un protó i la massa de l'electró en el cas d'ions moleculars tipus  $[M-H]^-$  (Gross 2004).

La massa exacta experimental és la massa mesurada d'una ió amb un cert grau d'exactitud i precisió

L'exactitud en la mesura de massa d'un ió es pot expressar com la diferència entre la massa exacta teòrica de l'ió i la massa exacta experimental de l'ió en unitats de massa atòmica o Da. Una altra manera d'avaluar l'exactitud de la mesura de massa és amb unitats de ppm d'error:

**Equació 1.** 
$$ppm = \frac{massa_{calculada} - massa_{mesurada}}{massa_{calculada}} \times 10^6 = \frac{\Delta m}{m} \times 10^6$$

La precisió en la mesura de massa d'un ió s'expressa com la repetibilitat de la mesura de massa exacta com a desviació estàndard.

La resolució (R) és la capacitat de l'espectròmetre de masses de separar dos ions de relació massa-càrrega ( $m/z$ ) diferents. Es defineix com la massa observada dividida entre la diferència entre dues masses properes.

Pels instruments amb analitzadors tipus quadrupol, transformada de Fourier-ressonància ciclotrònica d'ions, trampa d' ions i temps de vol la diferència de massa es mesura al 50% de l' alçada del pic (FWHM).

### **Factor que influeixen en l'exactitud de la mesura de massa**

#### **- Resolució**

La resolució jugarà un paper important en la mesura de massa exacta, ja que les interferències han d'estar ben resoltes, per una bona exactitud en la mesura. Cal destacar, que una resolució adequada és una condició necessària, però no suficient per dur a terme mesures de massa exacta.

#### **- *Tuning*, Forma del pic i Abundància de l'ió**

Cal que el pic sigui simètric perquè el punt màxim del pic correspongui a la centroide. La forma del pic es pot veure afectada per diferents factors com: mala optimització de l'instrument, senyal molt baixa dels ions, insuficient resolució per poder distingir interferències, etc. Tenir molta senyal de l'ió del qual volem fer la mesura de massa pot arribar a saturar el detector i per tant que la mesura de massa no sigui prou exacta. Si per contra es té poca senyal podem tenir problemes de mesura de massa deguts a que la poca intensitat de senyal afecti a la forma del pic.

#### **- Calibratge**

El calibratge dels espectròmetres de massa es duu a terme utilitzant un o més compostos de referència amb massa exacta coneguda. Un bon calibratge és vital per aconseguir bons resultats amb un nivell d'exactitud adequat i aquest cal que englobi tot l' interval de masses de treball.

En general, en mesures de massa exacta cal un primer calibratge extern de l'equip i en alguns instruments un segon calibratge intern que farà assolir millors nivells d'exactitud.

### **Determinació de la Fórmula Molecular**

Un cop realitzades les mesures de massa exacta l'objectiu és poder establir la identitat dels compostos desconeguts i per això, cal assignar una fórmula molecular a la massa mesurada.

Els instruments de massa i els softwares de tractament de dades tenen incorporats programes per calcular masses monoisotòpiques exactes, obtenir possibles fórmules moleculars i distribucions isotòpiques a partir de la massa d'un ió. S'han de definir diferents paràmetres per elaborar un nombre limitat de fórmules de les quals haurem de poder decidir quina és la més probable.

### **Factors que influeixen en la determinació de la fórmula molecular**

#### **- Exactitud i precisió**

S'haurà de considerar l'exactitud i la precisió en la mesura de massa per poder triar en una primera etapa quines fórmules moleculars acceptem i quines rebutgem.

Per exemple, si l'exactitud en la mesura de massa exacta que s'assoleix de mitjana amb un instrument concret és de 5ppm ( $\pm 2$ ppm precisió), mesures de massa exacta de fins a 7ppm cal que es considerin en una primera avaluació de la informació. Aquest criteri és millor que triar un nombre concret de les primeres fórmules moleculars que proposa l'instrument.

A més a més, depenent de la massa de l'ió que vulguem identificar s'haurà de fixar una exactitud de massa o un altre. No és recomanable fixar una exactitud de massa fixa per tot l'interval de masses, ja que amb un valor fix d'exactitud expressat en ppm d'error el número de possibles fórmules moleculars augmenta estrepitosament en augmentar la relació massa càrrega de l'ió problema.

#### **- Elements químics a considerar**

Si no tenim informació addicional del tipus de compost que estem buscant, s'haurien de considerar tots els elements que es poden trobar en un compost orgànic. Això voldria dir considerar molts elements i en realitat ningú ho fa així, sinó que s'assumeixen hipòtesis i en base a això es restringeixen els elements a considerar.

### - Restriccions del nombre d'àtoms de cada element

Restringir quants àtoms de cada element considerem per construir la llista de possibles candidats és important per obtenir una llista no massa extensa. Per exemple el nombre màxim de carbonis es pot restringir dividint la massa nominal de l'ió per el nombre atòmic del carboni (12).

### - Tipus d'ió, Formació d'adductes i càrrega, nombre d'insaturacions, regla del nitrogen

Si es coneix la naturalesa de l'ió que es forma (depenent per exemple de la font d'ionització) podrem eliminar de la llista les fórmules moleculars que no corresponen a la forma ionitzada real.

El nombre d' insaturacions d'una molècula amb una fórmula molecular com  $C_aH_bN_cO_d$  està definit per:

$$R + DB = a - \frac{1}{2}b + \frac{1}{2}c + 1$$

Quan hi ha altres elements presents aquests es contenen com si es tractés de C, H, N o O tenint en compte el seu nombre d'oxidació: C  $\approx$  Si; H  $\approx$  Heteroàtoms; N  $\approx$  P

**Taula 3.** Valors possibles de RDBE

Valor de RDBE	Informació sobre la fórmula molecular
<1.5	La fórmula no és possible teòricament
Nombre decimal	L'ió format té nombre parell d'electrons (anió o catió)
Nombre enter	L'ió format té nombre imparell d' electrons (ió radical)

NOTA: En ESI-MS no obtenim ions radical

A més a més, per compostos amb  $m/z < 500$  es pot utilitzar la regla del nitrogen per veure si la molècula té nombre parell o imparell de nitrògens, depenent de si té  $m/z$  parell o imparell.

Taula 4. Regla del nitrogen

Número de nitrògens	m/z Imparell	m/z Parell
N <sub>0</sub> , N <sub>2</sub> , N <sub>4</sub> ...	EE <sup>+</sup>	OE <sup>+</sup>
N <sub>1</sub> , N <sub>3</sub> , N <sub>5</sub> ...	OE <sup>+</sup>	EE <sup>+</sup>

#### - Distribució Isotòpica i Ion ratio

Alguns elements com el Cl o el Br tenen un perfil isotòpic molt particular per l'abundància relativa dels seus isòtops en la natura. Observar el perfil isotòpic de l'ió pot aportar informació sobre si la molècula conté algun d'aquests heteroàtoms o no. Per altra banda, observar la relació entre el pic molecular corresponen al <sup>12</sup>C (M) i el senyal (M+1) del <sup>13</sup>C pot aportar informació del nombre de carbonis presents en una molècula de fórmula molecular C<sub>n</sub>H<sub>2n+2</sub>.

Altres estratègies per restringir el nombre de candidats de la llista de possibles fórmules i identificar el compost mesurat són:

- L'estudi de les Valències (Normes de LEWIS i SENIOR)
- Ràtio d'elements i probabilitats dels elements
- Tècniques complementàries per obtenir informació estructural
- Qualsevol informació addicional
- Bases de dades i processament automàtic de les dades

### 2.2.2. Treball científic: Article N° 1

*Accurate mass measurements and ultrahigh-resolution: evaluation of different mass spectrometers for daily routine analysis of small molecules in negative electrospray ionization modes*

Nuria Cortés-Francisco, Cintia Flores, Encarna Moyano i Josep Caixach.

*Analytical and Bioanalytical Chemistry* **2011**, 400, (10), 3595-3606.

La mesura de massa exacta i l'espectrometria de masses d'alta resolució s'ha utilitzat per determinar la composició elemental de compostos orgànics desconeguts i per

confirmar la identitat de compostos orgànics coneguts. El creixent ús d'aquesta tècnica ha estat possible gràcies al desenvolupament de noves tecnologies, que engloben: l'evolució dels analitzadors de temps de vol, els analitzadors tipus quadrupol-temps de vol i triples quadrupols; la introducció dels nous analitzadors orbitrap; així com els espectròmetres de masses amb analitzadors tipus transformada de Fourier ressonància ciclòrica d'ions cada vegada més accessibles.

Un protocol de treball estricte i minuciós és necessari per assolir mesures de massa amb prou exactitud per poder proposar fórmules moleculars de compostos encara avui desconeguts. La manera en que es realitza la mesura de massa exacta és crítica per assolir una millor exactitud i precisió, que definiran la incertesa de la mesura. Amb aquest treball s'han pogut avaluar alguns aspectes que són crítics en la mesura de massa i en la posterior determinació de la fórmula elemental:

- l'exactitud de la mesura de massa
- la precisió de la mesura de massa
- el procés de calibratge
- la resolució
- el tractament de les dades per obtenir les fórmules moleculars candidates

S'ha avaluat i comparat la mesura de massa exacta amb instruments de massa exacta i alta resolució, per tal de dissenyar un protocol de treball adequat, per poder assegurar la qualitat en les mesures de massa i l'adjudicació inequívoca de la identitat de compostos "desconeguts". S'ha analitzat una mescla de compostos coneguts de  $m/z$  100 a 600 en els diferents espectròmetres de masses, obtenint mesures de massa exacta durant tot un dia de treball per poder obtenir l'exactitud i la precisió de la mesura de massa.

Les principals conclusions del treball són:

- Tant l'exactitud com la precisió de la mesura de massa són claus per conèixer l'incertesa de la mesura de massa que es produeix en cada cas.
- L'alta resolució és una condició necessària però no imprescindible per a la mesura de massa exacta. Quan no hi ha interferències properes a la nostra  $m/z$  equips que a priori no definiríem com a "alta resolució" poden donar bones mesures de massa. Ara bé en mesclades complexes, com la matèria orgànica dissolta, l'alta resolució serà imprescindible.

- S'observa pitjor exactitud de massa i precisió a les  $m/z$  altes que a les  $m/z$  baixes. Contràriament, necessitarem sempre una millor exactitud i precisió de massa a les  $m/z$  altes, ja que sinó no obtindrem una assignació inequívoca de la fórmula elemental del compost en qüestió.
- El calibratge extern és imprescindible per a garantir una bona mesura de massa exacta. En alguns casos, la deriva de la mesura farà necessari l'ús d'altres estratègies de calibratge (calibratge intern i/o *post-processing*).
- El recalibratge o calibratge *post-processing* proporciona resultats fins a 2 o 3 vegades més exactes i precisos, i per tant es presenta com una bona alternativa al calibratge intern habitual.

A mode de resum a la Figura 2 es mostra l'error en la mesura de massa i la desviació estàndard de les  $n=10$  mesures realitzades al llarg d'un dia de treball per els diferents analitzadors de massa, treballant en calibratge extern.

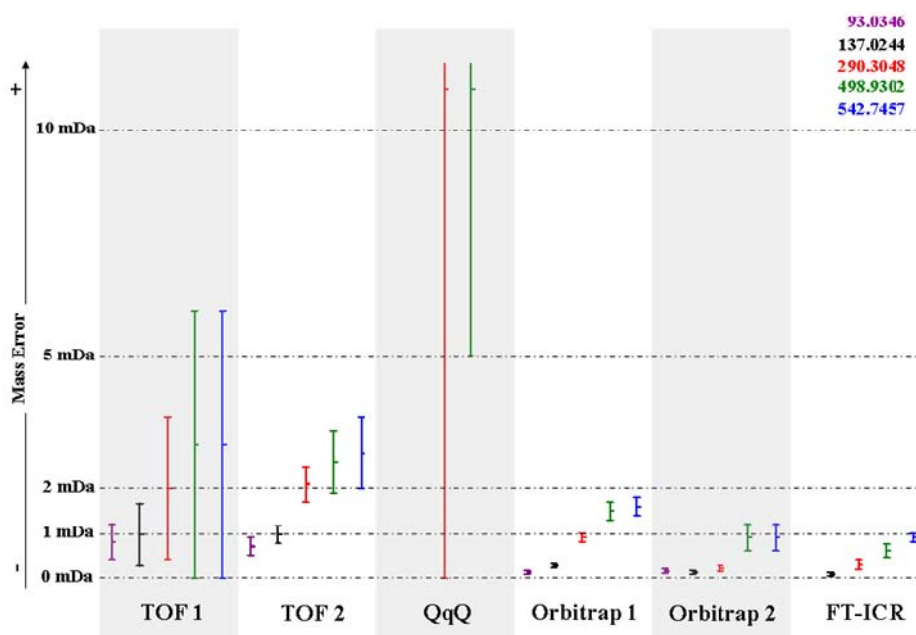


**Figura 2.** Exactitud de massa i precisió de les mesures realitzades en els diferents espectròmetres de masses de l'estudi: temps de vols (TOF), triple quadrupol (QqQ), orbitrap i transformada de Fourier ressonància ciclòtrica d'ions (FT-ICR).

### 3. ESPECTROMETRIA DE MASSES D'ALTA RESOLUCIÓ PER A LA CARACTERITZACIÓ DE LA MATERIA ORGANICA DISSOLTA

#### 3.1. Introducció

##### Mètodes d'extracció

Actualment s'utilitzen molts mètodes diferents per a l'extracció de la matèria orgànica dissolta del medi aquàtic. Principalment les tècniques que més s'utilitzen són l'extracció en fase sòlida amb diferents rebliments, l' ultrafiltració i la osmosis inversa. L'extracció en fase sòlida és la més utilitzada ja que és la més senzilla i barata, però requereix d'un pas previ de filtració, per a que el mètode funcioni correctament. Per tal d'evitar aquest pas previ en la filtració en la present tesi doctoral s'ha procedit a utilitzar el mètode d'extracció líquid-líquid.

##### Espectrometria de masses d'alta resolució

L'espectrometria de masses d'alta resolució ha revolucionat l'anàlisi de la matèria orgànica dissolta. Gràcies a aquesta tècnica s'ha pogut concloure que tot i ser una barreja heterogènia, els compostos que formen la matèria orgànica segueixen un perfil que es repeteix al llarg de tot l'espectre de masses.

S'observen:

- Diferències de masses 14.0156 Da corresponents a la metilació.
- Diferències de masses de 0.00364 Da corresponents a canvis estructurals de grups CH<sub>4</sub> per O.
- Diferències de masses de 2.0157 degudes a canvis de grups H<sub>2</sub> per dobles enllaços o anells.
- Que els pics a l'espectre estan monocarregats.
- En una mateixa massa nominal hi ha fins a 7 pics diferents.

Aquesta tècnica s'ha fet servir per identificar i comparar matèria orgànica dissolta de diferents orígens (Koch i col, 2005) en base a les seves fórmules moleculars, així com

també per estudiar els seus diferents processos de degradació (Kujawinski E.B. i col, 2004).

### **Determinació de la fórmula elemental, anàlisi de les dades i representació gràfica**

La proporció de H/C i de O/C és molt útil per indicar la presència de diferents estructures en la matèria orgànica dissolta. Proporcions de H/C que s'aproximin a la unitat implica estructures químiques aromàtiques amb grups carboxils o quinones. Per contra, proporcions de H/C més gran que la unitat fa pensar en estructures alifàtiques amb grups amino. La proporció de O/C reflecteix el contingut de carbohidrats: com més gran sigui la proporció de O/C més gran ha de ser el contingut en carbohidrats en aquell compost (Kim J. I. i col, 1990). Una representació gràfica habitual de les proporcions de H/C i O/C de molècules és el diagrama de van Krevelen (Figura 3). La zona del diagrama on se situïn les fórmules moleculars proposades aporta una idea del tipus de substància que és. En el present estudi s'ha utilitzat aquesta eina per a poder analitzar millor les estructures proposades (Kim S. i col, 2003).

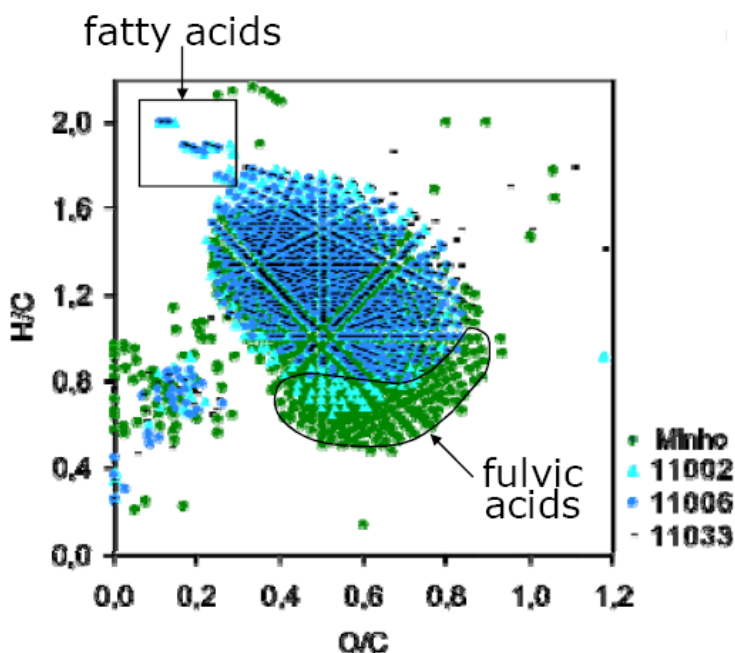


**Figura 3.** Si es representa la proporció H/C respecte la proporció O/C s'obté el diagrama de van Krevelen. (extret Schmidt i col, 2009).

Una altra manera de poder analitzar les masses exactes mesurades és fer l'anàlisi de les dades per Kendrick mass defect (Figure 4). Els diagrames de Kendrick mass defect

serveixen per observar diferències característiques en la fórmula molecular d' un conjunt de compostos i així observar línies de tendència de la composició d'aquestes substàncies.

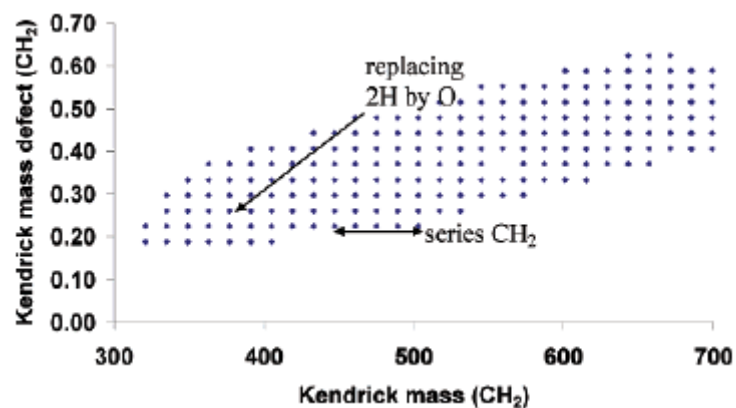


**Figura 4.** Anàlisi de Kendrick mass defect per el grup funcional CH<sub>2</sub> (extret de Kim S. i col, 2003)

### Analitzador de Transformada de Fourier - Ressonància Ciclotrònica d'Ions i Analitzador de Transformada de Fourier - Orbitrap

Els espectròmetres de masses amb analitzadors transformada de Fourier ressonància ciclotrònica d'ions i transformada de Fourier-Orbitrap són analitzadors d'emmagatzematge d'ions. En el cas de l'analitzador transformada de Fourier ressonància ciclotrònica d'ions el seu funcionament es basa en el fenomen de la ressonància ciclotrònica d'ions en presència d'un camp magnètic. D'una manera similar, en el transformada de Fourier-Orbitrap els ions orbiten al voltant d'un elèctrode central en presència d'un camp elèctric. Tots dos analitzadors de masses apliquen la transformada de Fourier.

La freqüència ciclotrònica i la freqüència orbital són independents de la posició inicial en que comenci el moviment i de la seva velocitat. És per això que aquests analitzadors són capaços de proporcionar una resolució molt elevada, sense haver de fer cap correcció de temps o d'energies, a diferència del que passa amb altres analitzadors.

El principal avantatge dels analitzador de transformada de Fourier és que la relació massa-càrrega dels ions s'obté per la mesura de freqüències. Les freqüències es poden mesurar amb més exactitud que altres paràmetres experimentals, i per això els

analitzadors transformada de Fourier ressonància ciclòtica d'ions i transformada de Fourier-Orbitrap són els analitzadors que proporcionen més exactitud de massa i resolució.

En la Figura 5, a mode d'exemple es mostra les diferents etapes de medició dels ions en l'analitzador de transformada de Fourier ressonància ciclòtica d'ions.

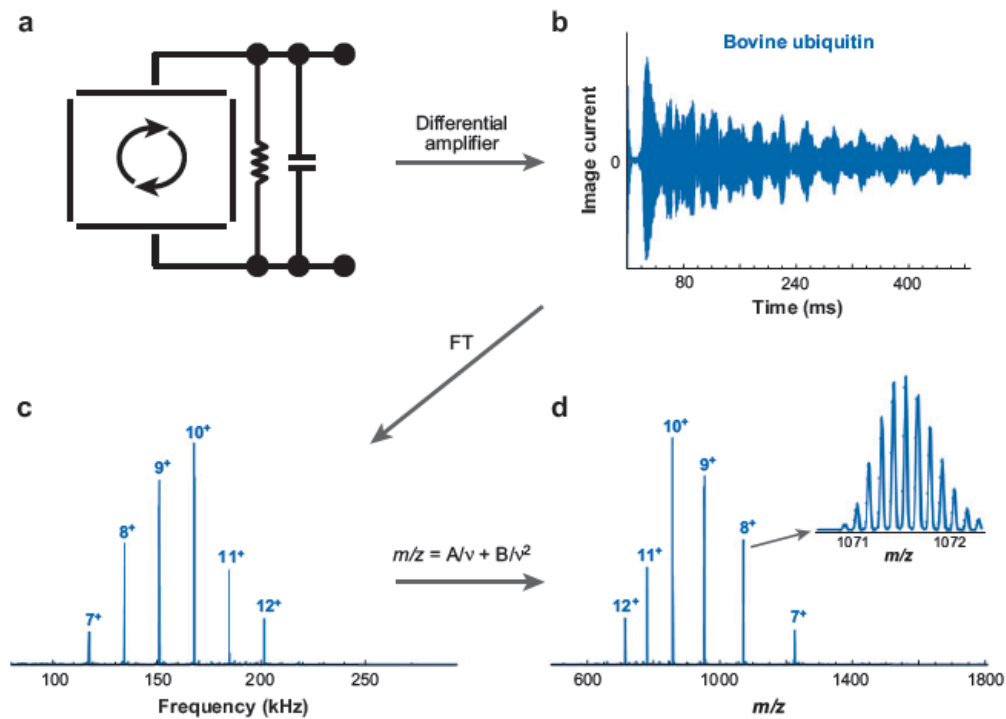


**Figura 5.** a) Representació esquemàtica d'un ió excitat b) time-domain senyal que es produeix en detectar els ions en la cel·la ICR c) espectre de frequency-domain obtingut per FT a partir de la senyal time-domain d) espectre de masses resultant després de la conversió de freqüències en m/z a partir del calibratge (extret Marshall A.G. i col, 2008).

## 3.2. Procediment experimental i Resultats

### 3.2.1. Anàlisi Directe de la Matèria Orgànica Dissolta

#### Extracció de la Matèria Orgànica Dissolta de diferents masses d'aigües

L'extracció líquid-líquid s'utilitza en moltes aplicacions, tot hi que existeix una tendència a substituir-la per l'extracció en fase sòlida, per tal d'utilitzar menys quantitat de dissolvent i a més poder automatitzar el procés d'extracció. Com ja s'ha comentat anteriorment per tal d'evitar el pas previ de filtració de la matèria orgànica dissolta hem volgut comprovar l'eficàcia de l'extracció líquid-líquid per a l'extracció en diferents masses d'aigua. S'han extret set mostres d'aigua de diferents procedències:

- aigua ultra pura
- patró d'àcids fúlvics dissolts en aigua ultra pura
- aigua de mar de la costa
- aigua superficial
- aigua d'un llac d'alta muntanya
- aigua residual (entrada d'una planta depuradora)
- aigua de mar (profunditat)

Cada una de les mostres s'ha extret mitjançant l'extracció líquid-líquid i l'extracció en fase sòlida, per poder comparar-les. Cada extracció s'ha fet per duplicat.

Els resultats de l'estudi mostren que l'extracció líquid-líquid presenta recuperacions de la matèria orgànica dissolta respecte l'extracció en fase sòlida acceptables. De fet per la majoria de les mostres l'extracció líquid-líquid resulta igual d'eficaç que l'extracció en fase sòlida. Només en el cas de l'aigua de mar, sembla que l'eficàcia de l'extracció disminueix respecte a l'extracció en fase sòlida al voltant del 60 %. Per contra, en el cas de l'aigua residual, l'extracció utilitzant el mètode d'extracció líquid-líquid és molt més eficaç (> 200%).

Calen dur a terme més estudis per comprovar com canvia la naturalesa de la matèria orgànica dissolta extreta amb una tècnica o amb l'altre. De fet existeixen pocs estudis on es conegui a nivell molecular, utilitzant l'espectrometria de masses, quines

característiques tenen els diferents extractes obtinguts per a cada una de les tècniques que hi ha a la literatura. Les primeres proves inicials en el cas de l'extracció líquid-líquid, demostren que no hi ha canvis significatius en quan a la ràtio H/C i O/C, però les mostres extretes utilitzant l'extracció líquid-líquid si que presenten valors una mica més baixos que en quan al nombre d'insaturacions.

### **Rendiment dels espectròmetres de masses de Transformada de Fourier**

Amb l'anàlisi dels patrons de matèria orgànica de la *International Humic Substance Society* s'han pogut avaluar alguns aspectes que són crítics en la caracterització de la matèria orgànica: exactitud de massa, resolució, sensibilitat i exactitud espectral. S'han utilitzat diferents models comercial dels analitzadors de transformada de Fourier ressonància ciclòtrònica d'ions i transformada de Fourier-Orbitrap:

**Taula 5.** Espectròmetres de massa utilitzats en l'estudi.

Analitzador de Massa	Instrument, fabricant	Resolució, $m/\Delta m$ (FWHM)	Exactitud de massa		Interval de masses	Velocitat d'escombratge
			Externa	Interna		
Q-ICR	<b>Solarix 12T, Bruker Daltonics</b>	1,000,000 ( $m/z$ 400)	< 0.6	< 0.25	100-10,000	-
LIT-ICR	<b>LTQ FT Ultra 7T, Thermo Scientific</b>	1,000,000 ( $m/z$ 400)	< 1.2	< 1	50-4000	1 Hz at R: 100,000
LIT-Orbitrap	<b>LTQ Orbitrap XL, Thermo Scientific</b>	100,000 ( $m/z$ 400)	< 3	< 1	50-2000; 200-4000	1 Hz at R: 60,000 0.6 Hz at R: 100,000
Orbitrap	<b>Exactive, Thermo Scientific</b>	100,000 ( $m/z$ 200)	< 5	< 2	50-4000	1 Hz at R: 100,000

Els resultats obtinguts amb la utilització de l'analitzador de transformada de Fourier-Orbitrap han estat satisfactoris i equivalents als resultats publicats a la literatura sobre la caracterització d'aquests mateixos materials de referència. El analitzador de masses de transformada de Fourier-Orbitrap per tant tot hi que no arriba a igualar totes les especificacions tècniques de l'analitzador de transformada de Fourier ressonància ciclòtrònica d'ions, presenta un gran potencial com a tecnologia alternativa per a la caracterització de la matèria orgànica dissolta.

### 3.2.2. Treball científic: Article N° 2

*Structural characterization of marine dissolved organic matter. Fragmentation studies.*

Nuria Cortés-Francisco and Josep Caixach

Enviat a *Analytical and Bioanalytical Chemistry*.

Encara no es coneix l'estructura de la matèria orgànica dissolta. Com s'ha comentat anteriorment la tècnica més emprada ha estat la ressonància magnètica nuclear, però també s'ha abordat aquest problema des del punt de vista de l'espectrometria de masses en tàndem.

Els estudis realitzats amb espectròmetres de masses amb analitzadors de trampa d'ions han permès conèixer els models de fragmentació dels àcids fúlvics, on es revelen pèrdues consecutives de grups CO<sub>2</sub> (fins a 6) així com pèrdues de molècules d'H<sub>2</sub>O (Leenheer J.A i col, 2001). Aquests resultats coincideixen amb els estudis realitzats amb els espectròmetres de masses híbrids tipus quadrupol-temps de vol (Plancque i col, 2001) i triple quadrupol (Reemtsma T. i col, 2003). També s'han utilitzat triples quadrupols, actuant com a quadrupols senzills en un intent de quantificar els àcids fúlvics i els àcids húmics (Persson L. i col, 2000). S'han comparat els espectres de masses i els espectres de masses/masses dels àcids fúlvics i àcids húmics amb espectres de molècules conegudes per intentar adjudicar les fórmules moleculars a estructures concretes (McIntyre C. i col, 2002).

Per tal de tenir informació estructural de la matèria orgànica dissolta caracteritzada s'han dut a terme anàlisis d'espectrometria de masses d'alta resolució en tàndem. S'han realitzat experiments d'una mostra de matèria orgànica dissolta procedent de l'aigua de mar i s'han analitzat també el patró d'àcids fúlvics per comparar si obteníem perfils de fragmentació similars. Els experiments s'han realitzat a un seguit de masses compreses entre  $m/z$  359-375. Com que la selecció de l'ió precursor s'ha realitzat en una trampa d'ions per cada ió precursor seleccionat en realitat hem seleccionat diversos ions. Després en base a la massa teòrica de diferents pèrdues identificades a la bibliografia i en base a altres possibles pèrdues que es poden donar en compostos orgànics multifuncionals s'ha procedit a analitzar un per un els espectres de masses de productes.

A partir d'aquests anàlisis s'han observat diverses pèrdues corresponents a grups CO<sub>2</sub> així com pèrdues de molècules d'H<sub>2</sub>O. A més a més s'han observat algunes pèrdues que correspondrien a la una pèrdua de C<sub>2</sub>H<sub>4</sub>O. Aquesta nova informació estructural

significaria que la matèria orgànica dissolta de l'aigua de mar és més rica estructuralment del que s'havia observat fins ara i que probablement existeixen altres grups funcionals a part del carboxil i l' hidroxil, que s'havia descrit fins ara.

De totes maneres aquesta metodologia presenta el principal inconvenient que el processament de les dades és molt lent i per tant només es pot aplicar a determinats pics a l'espectre, ja que l'extracció de tota la informació dels espectre de productes de fragmentació sinó pot ser etern. Per això altres tècniques com la ressonància magnètica nuclear són més adequades quan es tracta d'analitzar grups de mostres per veure diferències entre elles. Per això, la ressonància magnètica nuclear s'ha utilitzat a continuació a l'estudi de la matèria orgànica dissolta al llarg de les plantes de tractament.

## 4. CARACTERITZACIÓ DE LA MATERIA ORGANICA AL LLARG DE LES PLANTES DE TRACTAMENT.

### 4.1. Introducció

Durant els últims anys la importància de trobar noves fonts de subministrament d'aigua potable està agafant cada vegada més pes. Això esdevé a partir de que les demandes d'aigua cada vegada són més altes i les reserves naturals d'aigua no són capaces de mantenir el nivell de demanda actual. L'augment de la demanda obliguen a considerar com a possibles fonts de subministrament d'aigua potable l'aigua salada i les aigües residuals.

Davant de la complexitat tècnica que això comporta, les empreses subministradores comencen a dedicar esforços i recursos en la possibilitat d'obtenir aigua potable de fonts que fins fa pocs anys es descartava la possibilitat degut a la manca tecnològica i a les grans inversions que això suposava.

A mida que hi ha hagut cada vegada més coneixement sobre la importància i els riscos que deriva de no tenir un aigua potable de qualitat s'han anat millorant els tractaments tant físics com químics.

Amb aquests processos es dissenyen les plantes de tractament d'aigua de manera que actualment una planta convencional pot tenir quatre etapes principals: Predesinfecció, coagulació, filtració i desinfecció final.

En la predesinfecció considerada com una etapa química poden arribar a intervenir compostos com son l'ozó o el clor i tenen com a objectiu eliminar els microorganismes.

En l'etapa de coagulació intervenen tant processos químics com físics. En aquesta etapa es fan servir compostos químics per tal d'alterar les propietats físiques de la matèria en suspensió i d'aquesta manera fer sedimentar aquests compostos.

En la filtració s'eliminen compostos d'una mida en particular i com a última etapa en la desinfecció final s'aconsegueix un aigua amb garanties per al subministrament.

Alternativament a aquestes etapes existeixen unes altres etapes més complexes com poden ser l'utilització del carbó actiu o la tecnologia de membranes que poden ajudar a eliminar compostos concrets en les aigües a tractar com poden ser els trihalometans.

Com a plantes de tractament més complexes també es poden trobar les que tracten l'aigua salada per a obtenir aigua potable. Aquestes utilitzen la tecnologia de membranes amb les quals arriben a una eficiència del 45%. És a dir que per cada 100

litres d'aigua de mar es poden arribar a aconseguir 45 litres d'aigua potable. L' utilització de membranes d'osmosis és una tecnologia utilitzada àmpliament en la indústria i s'utilitza per a separar molècules tenint en compte la seva mida, forma, estructura química o càrregues elèctriques.

Depenent de l'objectiu que es vulgui aconseguir amb el tractament, es poden utilitzar una ampla gama de membranes. Totes elles tenen en comú en que els pretactaments són necessaris per tal de guanyar eficiència de procés ja que un pretractament dolent pot afectar tant a la vida útil de la membrana com al procés. Els principals problemes que ens podem trobar amb les membranes és l'anomenat *fouling*. Aquest fenomen consisteix en deposicions de compostos sobre les membranes. Això pot desencadenar en interaccions químiques entre compostos de la membrana o el desenvolupament del biofilm que acaba provocant un augment de l'energia necessària i/o una baixada de cabal de permeat.

Per aquests motius que poden fer viable o no aquest tractament i per motius de qualitat de l'aigua és molt important determinar la naturalesa de la matèria orgànica dissolta en l'aigua abans del tractament. La matèria orgànica dissolta pot arribar a ocasionar reaccions no desitjades quan reacciona amb el clor durant el procés de desinfecció i donar productes perillosos per a la salut com són els trihalometans.

## **4.2. Procediment Experimental i Resultats**

### **4.2.1. Treball Científic: Article N° 4**

*Molecular Characterization of Dissolved Organic Matter through a Desalination Process by High Resolution Mass Spectrometry.*

Nuria Cortés-Francisco and Josep Caixach

*Environmental Science & Technology* **2013**, *47*, (17), 9619-9627.

S'ha procedit a analitzar els patrons de matèria orgànica, àcids fúlvics i àcids húmics procedents de la *International Humic Substance Society*, i les mostres procedents de la planta pilot Dessaladora (*Raw Water*, Ultrafiltració, Osmosis Inversa), per tal d'analitzar la naturalesa de la matèria orgànica d'aigua de mar i veure com afecten els tractaments (ultrafiltració, osmosis inversa) a la matèria orgànica.

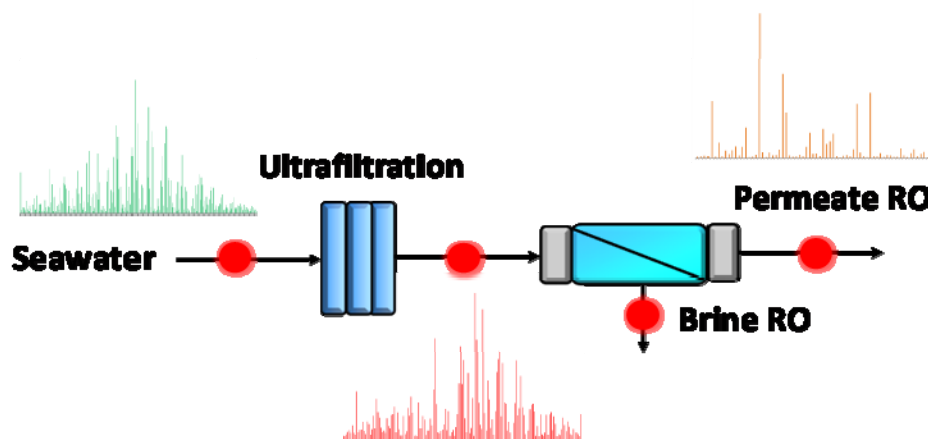


**Figura 6.** Esquema de la planta pilot de RO que s'ha utilitzat en l'estudi on es mostren els diferents punts de mostreig i s'observa el canvi en l'espectre de masses de la matèria orgànica dissolta, al llarg de la planta de tractament.

S'ha observat com canvia la naturalesa de la matèria orgànica, obtenint informació a nivell molecular de com afecta l'osmosi inversa (Figura 5). S'observa que hi ha l'eliminació casi completa de compostos amb estructures amb més alt contingut en oxigen ( $O/C: 0.3-0.4$ ) i que els compostos menys funcionalitats amb composicions elementals més semblants a estructures lipídiques ( $H/C \geq 1.6$  i  $O/C \leq 0.2$ ) passen les membranes d'osmosi i queden en el Permeat (*Permeate RO*).

#### 4.2.2. Treball Científic: Article N° 5

High-field FT-ICR mass spectrometry and NMR spectroscopy to characterize DOM removal through a nanofiltration pilot plant.

Nuria Cortés-Francisco, Mourad Harir, Marianna Lucio, Gemma Ribera, Xavier Martínez-Llado, Miquel Rovira, Philippe Schmitt-Kopplin, Norbert Hertkorn i Josep Caixach.

*Water Research* **2014**, DOI: 10.1016/j.watres.2014.08.046.

Un dels objectius d'utilitzar tractaments de membrana a les plantes potabilitzadores ve de la necessitat de reduir el contingut de matèria orgànica per evitar la formació de productes de desinfecció en la post-cloració. Una planta pilot instal·lada com a tractament terciari de la potabilitzadora de Manresa va servir per poder obtenir aigua tractada amb dues membranes comercials de nanofiltració. L'estudi neix arrel de la col·laboració amb el Centre Tecnològic de Manresa.

Es van realitzar diferents campanyes de mostreig (Juny i Octubre) i es va procedir a mostrejar i analitzar les mostres dels diferents punts: aigua de l'entrada (només ha rebut un pretractament), l' efluent de la UF, l' efluent de la UF + antiqelants (és l'aigua que alimenta les membranes), el permeat de la membrana 1, el permeat de la membrana 2, el concentrat de la membrana 1 i el concentrat de la membrana 2.

En aquest cas es van realitzar anàlisis utilitzant l'espectrometria de masses d'alta resolució i la ressonància magnètica nuclear, per tal de obtenir informació complementària. A més a més, es van utilitzar tècniques estadístiques per extreure l' informació de les mostres i veure quines semblances i diferències presentaven les mostres.

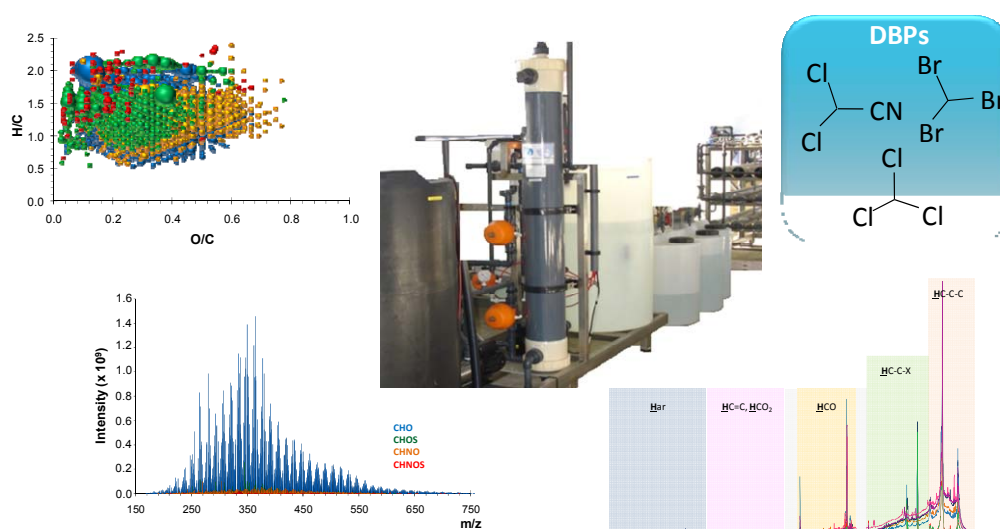


**Figura 7.** Esquema dels diferents anàlisis que es van realitzar per a l'estudi de la planta pilot UF-NF.

Utilitzant l'espectrometria de masses d'alta resolució s'ha pogut determinar com canvia la naturalesa de la matèria orgànica al llarg dels tractaments. Com ja s'havia observat en els estudis anteriors, la ultrafiltració té poc efecte sobre la matèria orgànica dissolta. En canvi, la tècnica és prou selectiva i s'han pogut observar diferent eliminació quan l'aigua es tracta amb la membrana 1 o la membrana 2, sobretot pel que fa als compostos que contenen nitrogen.

A partir de l'anàlisi dels espectres de ressonància magnètica nuclear de protó (<sup>1</sup>H-RMN) es pot quantificar la naturalesa de la matèria orgànica de les mostres, per identificar quins són els grups funcionals més importants. En el cas de les mostres d'aigua tenim majoritàriament estructures alifàtiques (regió 1.9-0.5 de <sup>1</sup>H-RMN). Veiem com en els Permeats (*Permeate NF 1* i *Permeate NF 2*) hi ha un cert enriquiment d'aquest grup de

compostos en detriment de compostos que contenen oxigen (regió 3.1-1.9 de  $^1\text{H}$ -RMN), que s'eliminen millor en els concentrats (*Brine* NF 1 i *Brine* NF 2).

#### 4.2.3. Treball Científic: Article N° 6

Molecular characterization of DOM causing fouling to NF membranes by high-field FT-ICR mass spectrometry and NMR spectroscopy.

Nuria Cortés-Francisco, Mourad Harir, Gemma Ribera, Xavier Martínez-Llado, Miquel Rovira, Philippe Schmitt-Kopplin, Norbert Hertkorn and Josep Caixach.

Enviat a *Environmental Science & Technology*

Un dels principals inconvenients dels tractaments de membrana (osmosis inversa i nanofiltració) és el manteniment d'aquestes. Degut a l'activitat biològica i a la presència de matèria orgànica en l'aigua, les membranes pateixen el que s'anomena "embrutiment" o fouling.

Per conèixer com es pot eliminar i/o prevenir aquest embrutiment cal conèixer la naturalesa del dipòsit de les membranes. Fins al moment, l'autòpsia de les membranes s'ha dut a terme amb metodologies com l'espectroscòpia d'infraroig per transformada de Fourier en mode de reflectància total atenuada, la microscòpia electrònica d'escombratge, la inspecció visual, per combustió del dipòsit, etc. però mai a nivell molecular utilitzant l'espectrometria de masses d'alta resolució i la ressonància magnètica nuclear.

Per aquesta raó, s'ha desenvolupat un mètode d'extracció i anàlisi de la matèria orgànica retinguda en les membranes en els processos de tractament de membranes de nanofiltració.

Degut a la naturalesa de les membranes, ha estat crític optimitzar els següents paràmetres:

- Quantitat de membrana: es va haver d'optimitzar la quantitat de membrana que s'havia d'extreure, ja que tot hi que s'havia observat principi de fouling en la membrana, aquestes no contenien quantitats de dipòsit molt importants.
- Temperatura d'extracció: es va provar fent l'extracció a temperatura ambient i escalfant suaument a 35°C.

- Solució alcalina per a l'extracció: es van haver de provar dues solucions alcalines: 0.1 % NaOH de pH = 12.9; 0.35 M NH<sub>4</sub>OH de pH = 11.7). L'objectiu era minimitzar durant l'extracció la destrucció de la pròpia capa activa de la membrana, que dificultaria l'anàlisi de la matèria retinguda, veure quina de les dues solucions extreia més matèria orgànica dissolta i veure si la naturalesa de la matèria orgànica dissolta era la mateixa.

Els resultats de l'estudi mostren que els compostos que tenen més tendència a adherir-se a la superfície de les membranes tenen un alt contingut en heteroàtoms, com l'oxigen, nitrogen i el sofre. A més aquests compostos són més similars als compostos caracteritzats en els Concentrats (*Brines*) de les membranes. Sembla ser que els compostos que tenen més tendència a interaccionar amb la membrana i per tant són rebutjats més eficaçment, a l'hora són adsorbits més fàcilment, provocant l'embrutiment de la membrana.

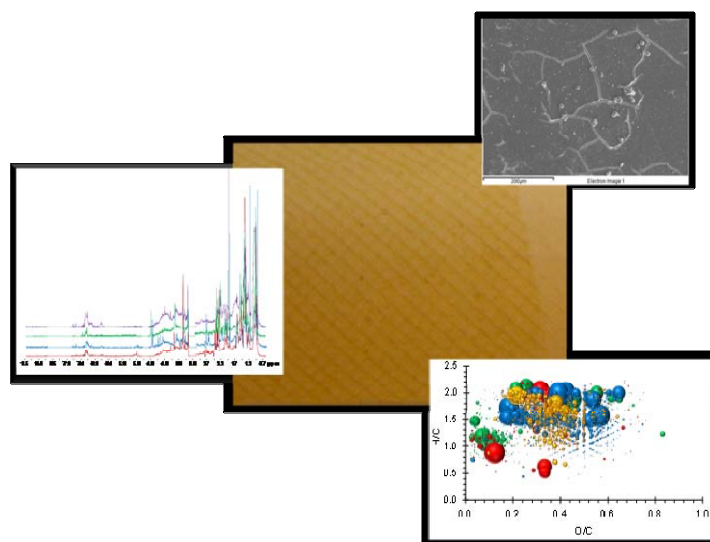


**Figura 8.** Imatge de la membrana "bruta" i de les diferents tècniques que s'han utilitzat per a l'anàlisi de la matèria orgànica dissolta adherida a la superfície: la resonància magnètica nuclear, l'espectrometria de masses d'alta resolució i la microscòpia electrònica d'escombratge.

## 5. CONCLUSIONS

Les conclusions específiques de cada un dels tres capítols ja s'han comentat anteriorment. Les conclusions generals del treball global es presenten a continuació:

- L'espectrometria de masses d'alta resolució ha demostrat ser una tècnica molt potent per a la caracterització de compostos que coneixem i que buscàvem d'entrada, de compostos que no buscàvem a priori però que són susceptibles de torbar-se a les mostres i que se'n coneix l'existència i compostos desconeguts en el medi ambient. S'ha utilitzat en molts estudis per il·lustrar els avantatges d'aquesta tècnica en front de l'espectrometria de baixa resolució en tàndem.
- Una metodologia sistemàtica és difícil d'aplicar per a la caracterització de desconeguts. En aquest sentit, s'han de dissenyar procediments de treball molt estrictes per obtenir dades fiables. L'exactitud de massa i la precisió de massa són paràmetres imprescindibles que s'han de determinar.
- Amb l'estudi comparatiu dut a terme amb diferents espectròmetres de masses, s'ha pogut concloure d'una manera objectiva quins són els avantatges i inconvenients de cada tecnologia pel que fa a: protocols de calibratge, exactitud de massa, resolució, sensibilitat i exactitud espectral.
- Degut a la complexitat de la matèria orgànica dissolta, els analitzadors de massa transformada de Fourier ressonància ciclotrònica d'ions i transformada de Fourier-Orbitrap són els únics capaços de resoldre les senyals d'un espectre de masses de matèria orgànica dissolta. Protocols de mesura i de processament de dades són necessaris per tal d'assegurar una correcta assignació molecular.
- L'extracció de la matèria orgànica dissolta sense la necessitat de filtrar la mostra s'ha dut a terme aplicant l'extracció líquid-líquid. Aquesta tècnica ha demostrat ser eficient per concentrar la matèria orgànica dissolta de diferents masses d'aigua.
- S'ha obtingut nova informació estructural de la matèria orgànica dissolta de l'aigua de mar, gràcies al desenvolupament d'un mètode basat en l'espectrometria de masses d'alta resolució en tàndem. Dels resultats obtinguts es pot concloure que la matèria orgànica dissolta de l'aigua de mar costera, tot hi

que és homogènia, és més rica estructuralment del que s'havia descrit anteriorment.

- Mètodes per extreure la matèria orgànica dissolta i mètodes per obtenir informació estructural són els passos que cal millorar en quan a caracterització de la matèria orgànica dissolta. Cal dur a terme més recerca en aquests dos camps.
- L'espectrometria de masses d'alta resolució és una tècnica molt selectiva que es pot utilitzar per caracteritzar el canvis que experimenta la matèria orgànica dissolta al llarg de les plantes de tractament.
- S'ha descrit el comportament de la matèria orgànica dissolta a nivell molecular al llarg de tractaments avançats de membrana: ultrafiltració, nanofiltració i osmosis inversa.
- Aquests estudis han aportat informació dels efectes que té cada pas del tractament en la matèria orgànica dissolta i pot ser útil per l'industria del tractament d'aigües per utilitzar estratègies de tractament més eficients.
- S'ha desenvolupat un mètode per a la caracterització de la matèria orgànica dissolta adsorbida en la superfície de les membranes. S'ha aplicat amb èxit per caracteritzar quin tipus de compostos s'adsorbeixen preferentment. Amb les dades de l'estudi, s'ha pogut veure que el tipus de compostos caracteritzats als concentrats, són també els més susceptibles d'adsorbir-se a la membrana.



